METAMORPHIC AND GEOCHRONOLOGICAL EVOLUTION OF MID- AND UPPER-CRUSTAL ROCKS IN THE NEPALESE HIMALAYA

by

Iva Lihter

M.Sc., University of Zagreb, 2015

A THESIS SUBMITTED IN PARTIAL FULFILLMENT OF
THE REQUIREMENTS FOR THE DEGREE OF

DOCTOR OF PHILOSOPHY

In

THE COLLEGE OF GRADUATE STUDIES

(Earth and Environmental Sciences)

THE UNIVERSITY OF BRITISH COLUMBIA

(Okanagan)

December 2020

© Iva Lihter, 2020

The following individuals certify that they have read, and recommend to the College of Graduate Studies for acceptance, a thesis/dissertation entitled:

Metamorphic and geochronological evolution of mid- and upper-crustal rocks in the Nepalese Himalaya

submitted by Iva Lihter in partial fulfillment of the requirements of

the degree of Doctor of Philosophy

Dr. Kyle Larson, I. K. Barber Faculty of Science, UBC Okanagan

Supervisor

Dr. John Greenough, I. K. Barber Faculty of Science, UBC Okanagan

Supervisory Committee Member

Dr. Yuan Chen, I. K. Barber Faculty of Science, UBC Okanagan

Supervisory Committee Member

Dr. Susan Murch, I. K. Barber Faculty of Science, UBC Okanagan

University Examiner

Dr. Kathryn Bethune, Department of Geology, University of Regina

External Examiner

Abstract

As a young, active collisional orogen, the Himalaya has been a common target for studying collisional dynamics and metamorphic processes. Despite this targeted investigation, there remain unresolved issues that hinder our understanding of the mountain belt formation. For example, while the Himalayan metamorphic core (HMC), a package of exhumed mid-crustal rocks that record Cenozoic metamorphism and deformation in the Himalaya, was previously thought to be a laterally continuous unit, recent research has documented evidence of a complex structural and metamorphic evolution not accounted for in previous tectonic models. In addition, parts of the Himalaya remain understudied due to geographic isolation and/or political obstacles potentially holding back new discoveries.

This study works to elucidate the metamorphic and geochronologic evolution of mid- and upper-crustal rocks from three different locations in the Nepalese Himalaya. The results from high-precision Lu-Hf garnet geochronology and U-Th-Pb accessory geochronology in the Kanchenjunga region outline new evidence of pre-Himalayan garnets within the HMC. It is argued that these ca. 290 - 230 Ma garnets reflect either two-stage growth during Cambro-Ordovician and Cenozoic times, or growth during the early Permian opening of the Neo-Tethys, unrelated to Himalayan metamorphism. A similar multidisciplinary approach with mineral geochemistry, monazite petrochronology and phase equilibria modelling on mid-crustal rocks from the Makalu-Arun region outlines at least three late Oligocene to mid-Miocene tectonometamorphic discontinuities within the HMC, with one of these inferred as an out-of-sequence thrust. The dataset obtained is consistent with a structural model driven by thrust wedge kinematics. Finally, garnet trace element geochemistry, monazite petrochronology and classical (conventional) thermobarometry carried out on metamorphic rocks in the vicinity of a Miocene pluton in the Upper Mustang region resolved contrasting interpretations on the origin of these rocks. This work provides evidence that metamorphism in the area was driven by time-resolved heat transfer away from the pluton.

The dataset and interpretations produced as part of this thesis provide critical information for our understanding of the development of the Himalayan mid-crust and the development of new tectonic models explaining orogenic processes in general.

Lay Summary

The collision of and continued convergence between the Indian and Eurasian tectonic plates is the driving force responsible for the development of the Himalaya and the Tibetan plateau. While much has been learned about the processes responsible for the present structure and geological evolution of the mountain belt there remain significant knowledge gaps that hinder the understanding of not only the Himalaya, but also mountain belts in general. This thesis investigates deeply exhumed rocks from three locations across the Himalaya using a variety of analytical techniques to characterize the pressure, temperature and time histories these rocks record. The results obtained from this work help fill existing knowledge gaps and elucidate the geological complexity of the ongoing Himalayan collisional system. These findings also have critical implications for our understanding of older/ancient mountain belts around the globe.

Preface

This PhD program started in January 2017 and consists of three projects. Fieldwork associated with one of the projects was conducted during September-October of 2016. This thesis, the overall research and the published journal articles are my original work and were supervised by Dr. Kyle Larson. All research analyses, data processing, interpretation and writing are my own work with the contributions of other researchers (see below).

Dr. Kyle Larson was a fieldwork team leader for the Mustang project and provided supervision, guidance, and feedback throughout my research. He significantly contributed during discussions for data interpretations and editorial assistance for all three projects. Work in Chapter 3, the Kanchenjunga project, was performed in collaboration with Dr. Matthijs Smit from the University of British Columbia, Vancouver who performed and processed Lu-Hf garnet geochronological analysis. I provided laboratory assistance for the analysis under his supervision. Specimens for the same project were collected by Dr. Larson and his past students. Dr. John Cottle from the University of California, Santa Barbara performed U-Th-Pb geochronological analysis and processed the data. Dr. Kyle Ashley from the University of Pittsburgh performed Raman spectroscopy on quartz inclusions and data processing. Dr. Sudip Shrestha from the University of British Columbia Okanagan assisted with electron microscopy and initial phase equilibria modelling. All researchers provided feedback and Dr. Smit contributed significantly towards data interpretation and outline of the manuscript. This chapter is being prepared for submission as:

Lihter, I., Larson, K.P., Smit, M.A, Cottle, J.M., Ashley, K.T., Shrestha, S. Decrypting the polymetamorphic record of the Himalaya. In preparation.

Chapter 4, the Makalu project, was developed in collaboration with Dr. John Cottle, who provided specimens for this project including the thin sections with original data collected by a former student, such as whole-rock X-Ray fluorescence data and GPS sampling locations. Dr. Cottle also performed monazite U-Th-Pb petrochronology analysis. Dr. Sudip Shrestha assisted with phase equilibria modelling, electron microscopy and provided feedback on interpretation. This chapter is being prepared for submission as:

Lihter, I., Larson, K.P., Cottle, J.M., Shrestha, S. Tectonometamorphic evolution of the Himalayan metamorphic core across the Makalu-Arun region, eastern Nepal. In preparation.

Work in Chapter 5, the Mustang project, was also performed in collaboration with Dr. John Cottle, who supervised me during U-Th-Pb petrochronological analysis and provided processed data. Dr. Sudip Shrestha provided assistance with initial phase equilibria modelling, guidance for electron microscopy and feedback on the manuscript. Geochronological data on igneous rocks and fieldwork assistance were provided by M.Sc. Alex Brubacher. This chapter benefited from the reviews of Dr. Clare Warren, Dr. Zoe Braden and two anonymous reviewers and has been published as:

Lihter, I., Larson, K.P., Shrestha, S., Cottle, J.M., Brubacher, A.D., 2020. Contact metamorphism of the Tethyan Sedimentary Sequence, Upper Mustang region, west-central Nepal. Geological Magazine 1–16.

Table of Contents

Abstract iii

Lay Summary iv

Preface v

Table of Contents vii

List of Tables xi

List of Figures xii

Acknowledgements xiv

Chapter 1 Introduction 1

1.1 Background 1

1.2 Research rationale 4

1.3 Objectives and approach 6

1.1.1 Kanchenjunga 6

1.1.2 Makalu-Arun 7

1.1.3 Upper Mustang 8

Chapter 2 Methodology 9

2.1 Geochemistry 9

2.2 Thermobarometry 11

2.2.1 Conventional thermobarometry 11

2.2.2 Trace element thermometry 12

2.2.3 Elastic barometry 13

2.2.4 Thermodynamic modelling 14

2.3 Geochronology 15

2.3.1 U-Th-Pb geochronology 15

2.3.2 Lu-Hf geochronology 17

2.4 Pressure-Temperature-time (P-T-t) paths 17

Chapter 3 Decrypting the polymetamorphic record of the Himalaya 19

3.1 Background 19

3.2 Geology of Kanchenjunga region 20

3.3 Analytical methods..... 22

3.3.1 Major and trace element geochemistry 22

3.3.2 Garnet geochronology..... 23

3.3.3 Monazite geochronology 23

3.3.4 Trace element thermometry 24

3.3.5 Elastic barometry 24

3.4 Results and interpretation..... 25

3.5 Discussion..... 30

3.6 Summary..... 32

Chapter 4 Tectonometamorphic evolution of the Himalayan metamorphic core across the Makalu-Arun region, eastern Nepal 33

4.1 Background 33

4.2 Geological setting 34

4.2.1 Lithotectonic units..... 34

4.2.2 Metamorphic and geochronologic history 36

4.3 Analytical methods..... 39

4.3.1 Geochemistry 39

4.3.2 Petrochronology 40

4.4 Petrography 40

4.5 Monazite petrochronology 44

4.6 Mineral geochemistry 50

4.6.1 Garnet geochemistry 51

4.6.2 Biotite geochemistry 52

4.7 Phase equilibria modelling..... 53

4.7.1 Phase diagrams 54

4.8 Interpretation 61

4.8.1 Garnet geochemistry 61

4.8.2 Timing of metamorphism 61

4.8.3 Tectonometamorphic evolution 63

4.9 Discussion 64

4.9.1 Tectonometamorphic discontinuities 64

4.9.2 Tectonic interpretation 66

4.9.3 Implications and regional comparison 68

4.10 Summary 69

Chapter 5 Contact metamorphism of the Tethyan Sedimentary Sequence, Upper Mustang region, west-central Nepal 70

5.1 Background 70

5.2 Local geological setting 71

5.3 Analytical methods 74

5.3.1 Petrography and mineral geochemistry 74

5.3.2 Monazite (petro)chronology 75

5.4 Petrography 76

5.4.1 Igneous specimens 76

5.4.2 Metamorphic specimens 77

5.5 Mineral geochemistry 80

5.5.1 Major-element geochemistry 80

5.5.2 Garnet trace-element geochemistry 81

5.6 Thermobarometry 84

5.6.1 Ti-in-biotite thermometry 84

5.6.2 Garnet-biotite and garnet-biotite-muscovite-plagioclase thermobarometry 86

5.7 Monazite (petro)chronology 87

5.7.1 Igneous specimens 88

5.7.2 Metamorphic specimens 89

5.8 Interpretation 91

5.8.1 Textural relationships and mineral chemistry 91

5.8.2 Trace-element partitioning 92

5.8.3 Timing of metamorphism 93

5.9 Discussion 94

5.9.1 Regional comparisons 98

5.10 Summary 99

Chapter 6 Conclusions 101

6.1 Conclusions 101

6.2 Future work 102

References 104

APPENDIX 134

APPENDIX A 135

Appendix A1. Lu-weighted garnet age calculation 136

APPENDIX B 168

APPENDIX C 221

Appendix C1. Heat diffusion parameters 222

List of Tables

Table 3.1. Lu-Hf isotopic data for five metamorphic specimens. 27
Table 5.1. Temperature estimates derived from thermal diffusion model. 97
Table A1. Major element geochemistry for garnet and biotite 143
Table A2. Garnet trace element geochemistry 155
Table A3. Monazite and xenotime geochronology data..... 158
Table A4. Quartz trace element geochemistry 160
Table A5. Temperature estimates for quartz and biotite inclusions..... 165
Table A6. Raman spectroscopy data for quartz inclusions 166
Table A7. Lu budget calculation for garnet geochronology..... 167
Table B1. Petrochronological data for monazite grains 178
Table B2. Garnet geochemistry 214
Table B3. Biotite geochemistry 215
Table B4. Effective bulk rock composition used for phase equilibria modelling..... 220
Table C1. Compositional mineral analysis for garnet, biotite, muscovite and feldspar 226
Table C2. Trace element composition of garnet 233
Table C3. Monazite U-Th-Pb geochronology data and trace elements 236
Table C4. Modal proportions (%) of minerals 245
Table C5. Temperature and pressure estimates for metamorphic specimens 246
Table C6. Whole rock XRF analysis (wt. %)..... 249

List of Figures

Figure 1.1. Geological Map of the Nepalese Himalaya 2
Figure 1.2. Simplified cross-section of the Himalaya displaying major structures 4
Figure 3.1. Simplified geological map of Kanchenjunga region with sampling locations 21
Figure 3.2. Garnet end-member profiles for five metamorphic specimens 26
Figure 3.3. Garnet and accessory mineral trace element and geochronology data 28
Figure 3.4. Temperature and pressure estimates derived from garnet inclusions 30
Figure 4.1. Geological map of the study area..... 35
Figure 4.2. Simplified geological map of the investigated transect 38
Figure 4.3. Photomicrographs and back-scatter electron images of analysed thin-sections.. 43
Figure 4.4. Concordia diagrams for analysed monazite in eight specimens. 46
Figure 4.5. Monazite age probability diagram for all eight specimens. 47
Figure 4.6. Y vs. age diagram for monazite. 49
Figure 4.7. Gd/Yb vs. age diagram for monazite. 50
Figure 4.8. Garnet end-member profiles for four metamorphic specimens. 52
Figure 4.9. Ti vs XMg diagram for biotite in four specimens. 53
Figure 4.10. Phase diagram for MK256. 57
Figure 4.11. Phase diagram for MK258. 58
Figure 4.12. Phase diagram for MK262. 59
Figure 4.13. Phase diagram for MK268. 60
Figure 4.14. Summary diagram with timing of prograde and retrograde metamorphism 65
Figure 4.15. Proposed tectonic model for the Makalu-Arun region. 67
Figure 5.1. Geological map of the study area..... 73
Figure 5.2. Thin-section photomicrographs of metamorphic specimens 79
Figure 5.3. Element distribution maps of Mn and garnet end-member profiles 81
Figure 5.4. Compositional diagram of Y and Gd/Yb for garnet 83
Figure 5.5. Garnet and monazite trace element geochemistry 84
Figure 5.6. Thermobarometry results 85
Figure 5.7. Garnet-biotite-muscovite-plagioclase pressure estimates..... 87
Figure 5.8. Monazite petrochronology results..... 89
Figure 5.9. Monazite trace element data 91

Figure 5.10. Age probability plot for igneous and metamorphic specimens. 93
Figure 5.11. Thermal diffusion model of a sheet-like intrusion..... 96
Figure A1. Garnet trace element profiles 137
Figure A2. Concordia diagram for monazite and xenotime..... 138
Figure A3. BSE images of analysed monazite and xenotime grains 139
Figure A4. BSE image of excluded xenotime grains in specimens KA031 and KA064..... 140
Figure A5. Locations of spot analyses for titanium in quartz thermometry 140
Figure A6. Pressure-temperature estimates of garnet inclusions 142
Figure B1. μ-XRF maps of analysed thin sections..... 169
Figure B2. Yttrium X-ray maps of analysed monazite grains..... 170
Figure B3. Phase equillibria modelling results for MK256 174
Figure B4. Phase equillibria modelling results for MK258 175
Figure B5. Phase equillibria modelling results for MK262 176
Figure B6. Phase equillibria modelling results for MK268 177
Figure C1. Monazite X-ray maps and BSE images for metamorphic specimens..... 223
Figure C2. BSE images of accessory minerals in metamorphic specimens 225

Acknowledgements

Firstly, I want to thank my supervisor, Dr. Kyle Larson, for offering me this PhD project. The invaluable amount of guidance, help and push I have got through these four years form the foundation of this thesis, and, without it, it would be very difficult to achieve what I did.

I also want to thank Dr. Yuan Chen and Dr. John Greenough, my graduate committee members, for wonderful conversations and tracking my progress.

Dr. Matthijs Smit and Dr. John Cottle, thank you for hosting me in your Lu-Hf and U-Pb geochron labs. I learned a lot during those visits which also strengthened this thesis. I would also like to thank Dr. Mark Button and David Arkinstall for their support and assistance during the analyses.

Sudip, thank you for many, many dedicated hours you spent on teaching me advanced phase equilibria modelling, and lab analysis. It shortened my path drastically!

My labmates and friends - Nicky, Ricky, Kat, Sudip, Kumar, Isa, Alex, Lutfi. I guess it is my time to leave the lab now but thank you guys for everything. I will remember our awesome trips and conferences, and of course, beer nights at the Well.

Former EESCGS members - Erica, Zhen, Sudip, Kumar, Upama, Alex. It has been a while, but forming the EESCGS, planning of the amazing trips and first poster symposium will always have a special place in my heart.

Pia and Marko, bez vas dvoje se ne bih usudila na ovaj put. Hvala na svemu!

To all my friends, who waited patiently for me to return texts and calls. Who always supported me and knew how to comfort me during bad days, Thank YOU! I guess we did it.

Mojoj familiji, sekama, i posebno mami! Fala na strpljenju, pusa!

And lastly, I would like to thank Teke Tamang and his Nepalese team for taking care of us during our fieldtrips in Khumbu, Mustang and Tsum Valley. Huge thank you goes to Pradap Tamang, our humble guide and the cook, for keeping an eye on me and making sure I stay healthy and alive throughout the trek! धन्यवाद

Chapter 1 Introduction

1.1 Background

The Himalaya is a present-day example of a young, "hot" orogen formed in response to the collision of two continental plates (Jamieson and Beaumont, 2013; Hu et al., 2016). Its current structure provides exposure and accessibility to exhumed, former mid-crustal rocks that hold key information about the processes responsible for the development of the mountain belt. Over the past 30 years, many different studies have been conducted in the Himalaya culminating in a variety of different orogen-scale kinematic models (see Harris, 2007; He et al., 2015). These models have commonly been exported to explain the development of other, older orogens across the world, including the Canadian Cordillera (e.g. Brown and Daniel Gibson, 2006), the Appalachians (e.g. Merschat et al., 2005), the Trans-Hudson (e.g. Rivers, 2008; Darbyshire et al., 2017), the Andes (e.g. Husson and Sempere, 2003), and many others. The models currently proposed to explain the development of the Himalaya vary significantly from end-member "channel flow" (e.g. Beaumont et al., 2001, 2004; Jamieson et al., 2004), and "critical taper" (e.g. Bollinger et al., 2006; Kohn, 2008) models, to "tectonic wedging" (e.g. Webb et al., 2007), and/or a combination and variations of these (e.g. Larson et al., 2010a; Yakymchuk and Godin, 2012; He et al., 2015; Shrestha et al., 2017). Central to all models is explaining the tectonometamorphic evolution of the Himalayan metamorphic core, a package of medium- to high-metamorphic grade former mid-crustal rocks that record Cenozoic metamorphism and deformation (Cottle et al., 2015). Because of its importance, many geological studies have targeted the exhumed metamorphic core and compared geological data extracted with those predicted by the various models. Interestingly, these detailed studies have outlined significant complexity within the orogen not necessarily explained by major models, such as cryptic structures within the Himalayan metamorphic core, that necessitate the re-examination of orogen kinematics (see Larson et al., 2015; Montomoli et al., 2015).

The Himalaya is an NW-SE oriented curved mountain belt that extends over 2500 km along strike (Fig. 1.1a). The formation of this mountain belt initiated ca. 55 Myr ago when the Indian and Eurasian continental plates began colliding (Le Fort, 1975; Yin and Harrison, 2000; Hu et al., 2016) resulting in the subduction of the Indian plate under the Eurasian plate and the rise of the Tibetan Plateau north of the Himalaya. The Indus-Yarlung Tsangpo suture zone

marks the boundary between rocks of Indian and Asian affinity (Yin and Harrison, 2000). This orogen can be broadly divided into four orogen-parallel lithotectonic units bounded by four major north-dipping structures (Figs 1.1b, 1.2) (Upreti, 1999; Yin and Harrison, 2000; Kohn, 2014a).

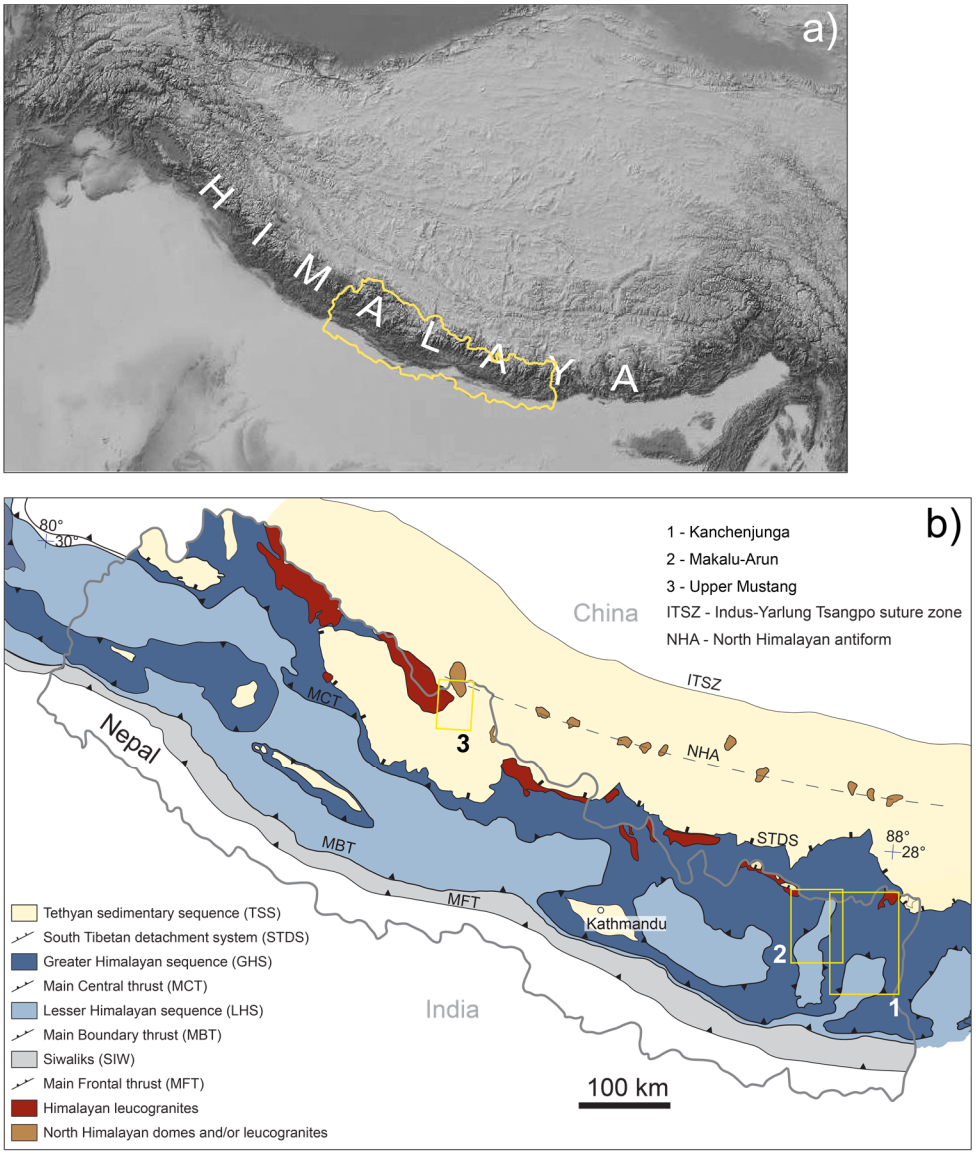

Figure 1.1. Geological Map of the Nepalese Himalaya. a) Digital elevation model of the Himalaya (DEM AW3D30 was obtained from Japan Aerospace Exploration Agency - JAXA). Nepal boundary is outlined in yellow. b) Simplified geological map displaying major lithotectonic units and structures (modified after Yin, 2006; Guo and Wilson, 2012; McQuarrie et al., 2014). A thick grey outline marks the boundary of Nepal. Yellow rectangles show the location area of three research projects; 1) Kanchenjunga region, 2) Makalu-Arun region, and 3) Upper Mustang region.

Starting from the south, the lowermost tectonic unit is the Siwaliks (or Sub-Himalayan Sequence) which comprises Miocene-Pleistocene unmetamorphosed fluvial molasses and sediments (Nakayama and Ulak, 1999; Goswami and Deopa, 2018). The Siwaliks is bounded in the south, by the Main Frontal Thrust (MFT) which separates it from the foreland basins of Indo Gangetic plains, and on the top, by the top-to-the south sense Main Boundary Thrust (MBT), which carries the structurally higher Lesser Himalayan Sequence (LHS) in its hanging wall. The LHS comprises Precambrian to late Paleozoic, and late Mesozoic to early-mid Cenozoic low- to medium-grade metasedimentary and sedimentary rocks and is bounded on top by the top-to-the south sense Main Central Thrust (MCT). The MCT is a shear zone that marks the base of the Greater Himalayan Sequence (GHS) (Gansser, 1964; Schelling, 1992; Goscombe et al., 2006; Searle et al., 2008), and together with the GHS forms the Himalayan metamorphic core. The exact position of the MCT in different sections of the Himalaya has long been debated (e.g. Searle et al., 2008; Martin, 2017a). Its location has been inferred based on different datasets including lithology, geochronology, or isograds, which has resulted in drastic variation in its interpreted structural position (e.g. Searle et al., 2008).

The GHS represents the major portion of the exhumed, former metamorphic core of the orogen and comprises medium- to high-grade metamorphic rocks and migmatites. It is characterized by an inverted-metamorphic sequence of mineral isograds (i.e. garnet - staurolite - kyanite - sillimanite) with low-metamorphic grade upper greenschist rocks at its base and high-grade granulite facies rocks and migmatites near its top (Arita, 1983; Harrison et al., 1999; Goscombe and Hand, 2000; Searle et al., 2008). These rocks, especially at high structural levels, are often intruded by leucogranite plutons, sills and dykes (e.g. Harris and Massey, 1994; Searle, 1999). The top of the GHS is bounded by the South Tibetan Detachment System (STDS), a system of north dipping, normal-sense shear zones, which juxtaposes the overlying Tethyan Sedimentary Sequence (TSS), an Early Paleozoic to Cretaceous low metamorphic grade metasedimentary and sedimentary rocks, atop the GHS rocks (Fort et al., 1982; Upreti, 1999). Structural windows through the TSS expose metamorphic rocks in domal culminations across southern Tibet. These domes primarily crop out along a common E-W axis typically referred to as the North Himalayan antiform (Figs 1.1a, 1.2) (see Jessup et al., 2019). Most of these exposures are considered to be the lateral extension of the GHS (Cottle et al., 2009;

Jessup et al., 2019), and are often associated with abundant leucogranites (e.g. Lee et al., 2004, 2006; Aoya et al., 2006; Quigley et al., 2006; Zeng et al., 2008; Langille et al., 2010; Larson et al., 2010b; Fu et al., 2017).

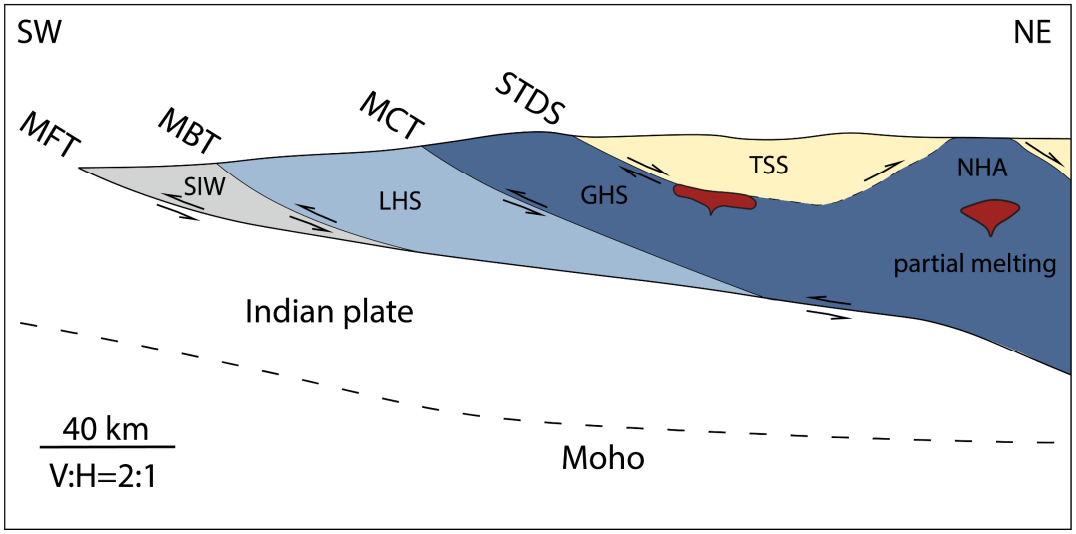

Figure 1.2. Simplified cross-section of the Himalaya displaying major structures(modified after Beaumont et al., 2001; Wagner et al., 2010). MFT - Main Frontal thrust, MBT - Main Boundary thrust, MCT - Main Central thrust, STDS - South Tibetan Detachment system. SIW - Siwaliks, LHS - Lesser Himalayan sequence, GHS - Greater Himalayan sequence, TSS - Tethyan Sedimentary sequence, NHA - North Himalayan antiform.

1.2 Research rationale

The Himalaya is a natural laboratory for studying orogenesis. It preserves an entire orogenic wedge from undeformed foreland sediments in the south, through a thrust and fold belt and exposure of high metamorphic grade, former mid-crustal rocks, to the upper crustal carapace atop the metamorphic rocks to the north (Kohn, 2014a; Martin, 2017b). This structural framework, which can be traversed across a distance of only ~ 200 km in some areas, preserves critical spatial relationships that are typically lost when mountain belts are eroded away.

The Himalayan metamorphic core was thought to be a semi-uniform, continuous unit bounded by two opposite sense faults until the first decade of the 21st century (e.g. Hodges, 2000; Searle et al., 2006). A series of studies published in the past decade, however, have identified numerous local to regional scale, structures that separate this unit into unique rock packages with distinct tectonometamorphic histories (e.g. Goscombe et al., 2006; Carosi et al.,

2010; Imayama et al., 2010; Yakymchuk and Godin, 2012; Larson et al., 2013; Wang et al., 2013; Warren et al., 2014; Ambrose et al., 2015; Iaccarino et al., 2017; Shrestha et al., 2017). These tectonometamorphic discontinuities (as they have been colloquially termed) within the Himalayan metamorphic core are often cryptic and nearly impossible to recognize in the field (see Carosi et al., 2018; Waters, 2019). Because of that, they are generally identified based on markedly different pressure-temperature-time-deformation (P-T-t-D) signatures in closely adjacent rock packages (e.g. Groppo et al., 2009; Carosi et al., 2010; Larson et al., 2013; Montomoli et al., 2013; Wang et al., 2013; Warren et al., 2014; Ambrose et al., 2015; Iaccarino et al., 2017; Shrestha et al., 2017). The identification of similar structures/discontinuities in various regions in the Himalaya has triggered attempts to correlate some of these structures along the strike of the orogen (Goscombe et al., 2006) and re-cast their potential importance as regional features (see Montomoli et al., 2015; Waters, 2019). While most studies that have identified discontinuities have reported one or two structures from across-strike transects (Hodges et al., 1996; Grujic et al., 2002; Goscombe et al., 2006; Montomoli et al., 2013; Wang et al., 2013; From and Larson, 2014; Larson and Cottle, 2014;), some studies have documented the existence of up to five different structures (Ambrose et al., 2015; Larson et al., 2015; Shrestha et al., 2020), which indicates that the exhumed metamorphic core of the Himalaya orogen may have a far more complex structure than previously thought. The occurrence of these discontinuities requires rethinking of the internal structure of the Himalayan metamorphic core and our perspective on mid-crustal convergence accommodation, extrusion and emplacement processes within the Himalaya and continent-continent collisions in general.

The Himalaya provides good exposure and reasonable accessibility through a series of river valleys that transect much of the mountain range. However, there remain remote areas that are severely understudied due to their geographic location, difficult access and political sensitivity. Many of these places are located in Nepal or India close to the Tibetan border, or in southern Tibet where exhumed metamorphic rocks crop out within structural windows through the (meta)sedimentary rocks (see Kohn, 2014a, Jessup et al., 2019 and references therein). These domal outcrops are sometimes characterized as the lateral extensions of the metamorphic core (Nelson et al., 1996) and often contain abundant plutonic rocks. Due to a lack of studies in these areas, the spatial distribution of these metamorphic rocks, and associated plutons, still needs to be explored. Moreover, contrasting interpretations have been

proposed to explain the generation of the metamorphic rocks therein: 1) do they reflect regional metamorphism (i.e. are equivalent to the Himalayan metamorphic core (Hurtado, 2002), or 2) are they the result of contact metamorphism between the plutonic rocks and sedimentary rocks (Guillot et al., 1995a). As such, these areas represent a significant knowledge gap in the overall evolution of the Himalaya.

1.3 Objectives and approach

The main objective of this research is to apply an integrated multi-method approach in to examine the metamorphic and tectonic evolution of the exhumed metamorphic rocks exposed within the Nepalese Himalaya. The detailed information gained from this type of study will provide the data necessary to understand the nature of metamorphic rocks, delineate potential cryptic structures therein and provide insight into the tectonic processes that have controlled the evolution of the Himalaya and formation of other similar mountain belts. The first part of this thesis examines the timing of prograde metamorphism of the mid-crustal rocks exposed in the Kanchenjunga region in easternmost Nepal, where multiple cryptic structures have been previously inferred within the metamorphic core. The second part of the thesis investigates the existence of cryptic structures in rocks from the metamorphic core across a transect through the Makalu-Arun region in eastern Nepal and explores potential correlation with similar structures along strike in adjacent regions. The third part of this thesis characterizes the metamorphic history of the metamorphic rocks surrounding a pluton exposed within a disputed domal culmination in the Upper Mustang region of northernmost west-central Nepal.

1.1.1 Kanchenjunga

The objective of this project was to examine mid-crustal rocks collected from a transect through the Kanchenjunga region in eastern Nepal (Fig. 1.1b). This transect has been investigated previously, and based on differences in U-Th-Pb monazite petrochronology and phase equilibria modelling, has been interpreted to host multiple cryptic thrust-sense geological structures (Ambrose et al., 2015). The findings of that study make specific predictions about the timing of prograde metamorphic histories recorded in the now juxtaposed crustal blocks. The present work tested those predictions by directly dating prograde

metamorphism using garnet Lu-Hf geochronology coupled with trace element analysis across the Kanchenjunga region.

As the currently proposed model is strongly based on the differences in timing and duration of prograde metamorphism inferred from the monazite data, Lu-Hf garnet geochronology can provide means to test this tectonic model by dating prograde metamorphism directly. Because garnet strongly fractionates Lu during its growth, Lu is generally concentrated in the core resulting in Lu-Hf dates weighted towards the earlier portion of garnet growth (e.g. Lapen et al., 2003; Kellett et al., 2014; Smit et al., 2014; Cutts and Smit, 2018). Combined with the garnet geochemistry, this timing of garnet growth can provide more information into conditions of the early prograde metamorphism recorded in the rocks, which can be used to distinguish distinct rock packages with different prograde history. Additional U-Th-Pb geochronology on monazite and xenotime inclusions from garnet grain separates are also used to help refine garnet growth timelines, while trace element thermometry on quartz and biotite inclusions are integrated with elastic barometry on quartz inclusions within garnet grains to investigate the changes in pressure and temperature (P-T) conditions during the garnet growth. This information delivers more insight into the timing and conditions of the growth of specific garnet domains during the metamorphism and helps better quantify the tectonometamorphic history of the region.

1.1.2 Makalu-Arun

The objective of this study was to investigate the existence and characteristics of cryptic structures in the mid-crustal rocks that are exposed along the Makalu-Arun transect in eastern Nepal (Fig. 1.1b). Previous studies in the neighbouring Kanchenjunga region have identified up to five such structures (Ambrose et al. 2015), but it is not clear if they are local or regional in scale. This project examined the metamorphic and geochronological evolution of the exhumed mid-crustal rocks across a transect through the Makalu-Arun area using phase equilibria modelling and mineral geochemistry to quantify differences in peak metamorphic conditions. Moreover, monazite U-Th-Pb petrochronology is used to inform the timing (t) of monazite (re)crystallization. Because monazite and garnet are the two main reservoirs of heavy rare earth elements (HREE) in the specimens examined, changes in the chemical composition of monazite through time can be correlated with the composition of garnet to infer various

stages of garnet growth and of coexisting phases (Pyle and Spear, 1999; Hermann and Rubatto, 2003; Kohn et al., 2005). Such a relationship between garnet and monazite helps provide the timing component to the changes in P-T conditions detailing a metamorphic history of the rocks. A distinct change in timing of prograde and retrograde metamorphism between adjacent rock packages can help outline the discontinuities. Therefore, the peak P-T estimates and timing of a series of specimens collected across the GHS in the region are used to characterize the metamorphic rocks along the transect and identify the presence of such discontinuities.

1.1.3 Upper Mustang

The objective of this project was to investigate the occurrence and characteristics of the metamorphic rocks in the vicinity of a large leucogranite pluton in the remote Upper Mustang region in west-central Nepal (Fig. 1.1b). This study aimed to resolve the contrasting interpretations proposed by the two previous studies, which have argued that the metamorphism in these rocks is a result of either contact metamorphism (Guillot et al., 1995a) or regional metamorphism (Hurtado, 2002).

This project employed conventional and trace element thermobarometry on metamorphic rocks to reflect the chemical changes in garnet growth and to provide the P-T conditions during the metamorphism. The differences in temperature estimates from the metamorphic rocks collected at various distances from the pluton can be used as the major indicator of heat dissipation away from the pluton (Jaeger, 1968, 1964; Annen, 2017). The change in temperature with an increase in distance from the pluton helps evaluate whether the rocks show evidence of heat transfer as a result of pluton intrusion. Moreover, the monazite geochronology on plutonic rocks is used to inform the crystallization age of the pluton, while monazite petrochronology on metamorphic rocks are used to inform the timing of the metamorphism. The differences in the timing of emplacement of pluton vs metamorphism in the surrounding rocks, combined with P-T estimates for the metamorphic rocks are used to characterize the nature of metamorphic rocks and provide interpretation for the metamorphic evolution of the rocks in this region.

Chapter 2 Methodology

The characterization of metamorphic rock packages requires an extensive evaluation of the P-T conditions and the timing of metamorphism recorded in the rocks. The changes in P-T conditions are typically inferred using major mineral thermobarometry (Spear, 1993; Holdaway, 2000; Henry et al., 2005; Wu, 2015), and the time component is often informed through accessory mineral geochronology (see Engi et al., 2017). When age data from accessory mineral geochronometers, such as monazite and xenotime, are combined with thermobarometry to elucidate metamorphic and geochronological history, it provides a complete picture of evolution for the rocks. This thesis utilizes a combination of different methodological approaches, including geochemistry (major and trace element), thermobarometry (conventional, trace element, elastic and thermodynamic modelling) and geochronology (U-Th-Pb and Lu-Hf) to decipher project-specific tectonometamorphic problems. A short description of each method used in this thesis is summarized below.

2.1 Geochemistry

Mineral and whole-rock geochemistry are widely used to investigate the metamorphic processes that the rocks have experienced (Tracy et al., 1976; Muecke et al., 1979; Spear, 1993). This type of data can offer an insight into the origin/protolith of the rocks (e.g. Rollinson, 1993), crystallization and/or breakdown of (dis)equilibrium mineral phases (e.g. Hermann and Rubatto, 2003; Regis et al., 2016; Shrestha et al., 2019) and quantification of P-T conditions during metamorphism (see Kohn, 2016 and references therein).

The major element geochemistry in this thesis is primarily focused on the changes in mineral composition across major, rock-forming minerals such as garnet, biotite, plagioclase and muscovite. Compositional variation, especially within garnet grains, are commonly used to inform the P-T conditions of the metamorphic rocks (Tracy et al., 1976; Woodsworth, 1977; Spear, 1993; Caddick and Kohn, 2013; Baxter et al., 2017). These are primarily looked at through the relative garnet end-member compositions of almandine [$Fe^{2+}/(Fe^{2+}+Ca^{2+}+Mg^{2+}+Mn^{2+})$], grossular [$Ca^{2+}/(Fe^{2+}+Ca^{2+}+Mg^{2+}+Mn^{2+})$], pyrope [$Mg^{2+}/(Fe^{2+}+Ca^{2+}+Mg^{2+}+Mn^{2+})$], and spessartine [$Mn^{2+}/(Fe^{2+}+Ca^{2+}+Mg^{2+}+Mn^{2+})$]. Changes

in the pattern of the compositional profile of a specific element also help to understand the resorption (Mn) and relative changes in pressure (Ca) and temperature (Fe-Mg) during the growth of the mineral itself (Florence and Spear, 1991; Kohn and Spear, 2000; Kohn, 2004; Caddick and Kohn, 2013). The variations in the relative concentrations of these endmembers may inform diffusional processes within the grain, as well as with and outside the grain in the matrix (Caddick et al., 2010; Carlson, 2012; Carlson et al., 2015). The qualitative and quantitative assessment of the major elements is primarily achieved through the use of a Scanning Electron Microscope (SEM) and Electron Probe MicroAnalyser (EPMA). While SEM equipped with energy-dispersive spectrometry (EDS) provides quicker mineral identification and quantification, EPMA equipped with wavelength-dispersive spectrometry (WDS) provides higher accuracy and precision, in the range of 10 - 1000 parts per million. For this reason, SEM is primarily used for identifying minerals and semi-quantitative analysis, while EPMA is preferred for mapping and quantitative major elemental analysis.

The trace element geochemistry used in this research is mainly focused on rare earth elements (REE) and yttrium (Y) concentrations in the minerals garnet and monazite. The chemical changes in monazite, especially in Heavy(H) REE, are often paired with garnet trace element chemistry to understand the relative growth and breakdown of the coexisting minerals (Pyle et al., 2001). For example, the behaviour of garnet and monazite during metamorphic processes can be tracked through the changes in Y content (as a proxy for HREEs), as they both share the same Y budget (Larson et al., 2019; Warren et al., 2019). While garnet strongly incorporates Y during its growth due to its high affinity towards HREEs, monazite, being a light REE phosphate mineral, does not incorporate HREEs or Y as readily. If garnet breaks down, however, any Y released can be incorporated into monazite that happens to be growing/recrystallizing at the time (e.g. Pyle and Spear, 1999; Hermann and Rubatto, 2003; Kohn et al., 2005). Given this relationship, the variations in HREEs in monazite and garnet can provide information critical to the interpretation of the prograde and retrograde history of the rocks (Foster et al., 2000, 2002; Larson et al., 2013; Mottram et al., 2014; Ambrose et al., 2015; Regis et al., 2016; Shrestha et al., 2017). Furthermore, additional changes in monazite chemistry with age can be used to indicate the crystallization or breakdown of other minerals during its growth. For example, as feldspar incorporates Eu as a common substitution for Ca, a positive Eu anomaly in monazite trace elements may indicate the breakdown of feldspars

during its growth (e.g. Rubatto et al., 2006). The quantification of trace elements in minerals, such as garnet, can be carried out using a Laser Ablation system connected to an Inductively Coupled Plasma-Mass Spectrometer (LA ICP-MS) (e.g. Regis et al., 2016; Shrestha et al., 2017). This is a destructive method where materials from the minerals are ablated with the laser, ionized with plasma and analysed through the spectrometer. This setup can provide higher precision in trace element composition, with detection limits < 0.1 parts per million. Trace elements in chronometers are typically collected coevally with geochronological information (see Section 2.3.1 below).

2.2 Thermobarometry

While looking at the chemical variations in major and/or trace elements within minerals can be informing, these data can also be used to quantitatively assess metamorphic conditions (e.g. Holdaway, 2000; Pyle et al., 2001; Henry et al., 2005;). The quantification of the metamorphic conditions under which the minerals in rock specimens (re)crystallized can be estimated by applying thermobarometry tools. The major contributing factors on the resulting P-T estimates and their meaning include the presence of accessory minerals and activity of endmembers (e.g. Ghent and Stout, 1984; Pyle and Spear, 2000; Pyle et al., 2001; Henry et al., 2005), the textural relationship of the minerals (Holdaway, 2000; Wu et al., 2004), calibration setting of thermobarometers (Holdaway, 2000; Kohn, 2014b; Wu, 2015), and/or bulk rock compositions (Powell and Holland, 1988; Holland and Powell, 1998; Zuluaga, 2005). Thermobarometry tools used in this research are divided into conventional thermobarometry, trace element thermometry, elastic barometry and thermodynamic modelling below.

2.2.1 Conventional thermobarometry

Conventional (or classical) thermobarometry is historically the most commonly used thermobarometric method. It involves reaction-based quantification of pressure and temperature between mineral endmembers that are interpreted to be in chemical equilibrium (e.g. Powell and Holland, 2008). The reactions for thermometric estimation involve temperature-driven cation exchange between minerals with the minimal volume change, while those involved in barometric estimation are typically based on the net transfer of cations that result in a significant volume change (e.g. Spear, 1989). Two conventional measures are used

in this research: 1) the garnet-biotite thermometer (Holdaway, 2000) and 2) the garnet-biotite-muscovite-plagioclase barometer (Hodges and Crowley, 1985; Hoisch, 1990; Wu, 2015).

The garnet-biotite (GB) thermometer works on the principle of Fe- Mg cation exchange reaction between mineral endmembers of garnet and biotite (Eq. 2.1).

$$Fe_3Al_2Si_3O_{12} + KMg_3AlSi_3O_{10}(OH)_2 = Mg_3Al_2Si_3O_{12} + KFe_3AlSi_3O_{10}(OH)_2 \quad \text{(eq. 2.1)}$$

almandine phlogopite pyrope annite

With an increase in temperature, the reaction progresses towards the right side, producing pyrope-rich garnet and Fe-rich biotite, while a decrease in temperature results in almandine-rich garnet and Mg-rich biotite.

The garnet-biotite-muscovite-plagioclase (GBMP) barometer involves the net transfer of cations between mineral endmembers with breakdown/crystallization of mineral phases (Spear, 1989) (Eqs. 2.2, 2.3).

$$3CaAl_2Si_2O_8 + KFe_3AlSi_3O_{10}(OH)_2 = Fe_3Al_2Si_3O_{12} + Ca_3Al_2Si_3O_{12} + KAl_3Si_3O_{10}(OH)_2 \quad \text{(eq. 2.2)}$$

anorthite annite almandine grossular muscovite

$$3CaAl_2Si_2O_8 + KMg_3AlSi_3O_{10}(OH)_2 = Mg_3Al_2Si_3O_{12} + Ca_3Al_2Si_3O_{12} + KAl_3Si_3O_{10}(OH)_2 \quad \text{(eq. 2.3)}$$

anorthite phlogopite pyrope grossular muscovite

With an increase in pressure, only the minerals with lower volume are stable, and both reactions progress towards the right creating almandine- and grossular-rich garnet and muscovite from anorthite and Fe-rich biotite. Similarly, pyrope- and grossular-rich garnet and muscovite will form from anorthite and Mg-rich biotite. In contrast, a decrease of pressure will favour high volume minerals and the reactions reverse back to the left.

2.2.2 Trace element thermometry

Trace element thermometers use temperature-dependent trace element concentration in a mineral to provide a temperature estimate of mineral (re)crystallization (see Cruz-Uribe et al., 2018). In contrast to conventional thermobarometry, which is based on major elements,

trace element thermometers utilize trace elements that have more limited mobility and are typically less affected by diffusional processes (e.g. Chernoff and Carlson, 1999; Otamendi et al., 2002; Kelsey and Hand, 2015). Trace element thermometers may, therefore, preserve a more reliable thermal record at higher temperatures in certain situations.

Two titanium (Ti) based trace element thermometers are used in this thesis: 1) the titanium-in-biotite thermometer (Ti-in-Bt, Henry et al., 2005) and, 2) the titanium-in-quartz thermometer (Ti-in-Qtz, Thomas et al., 2010). Both of these thermometers are based on the solubility of Ti in biotite and quartz that increases with temperature and has only a minor dependence on pressure (e.g. Patino Douce et al., 1993; Henry et al., 2005; Wark and Watson, 2006; Thomas et al., 2010; Nachlas et al., 2014; Ashley and Law, 2015). These thermometers are most readily applied to Ti saturated systems but can also be applied to those under saturated if the Ti activity can be quantified or estimated. The determination of activity is the greatest assumption when using trace element thermometry, and if not estimated correctly, it can result in underestimated or overestimated temperatures (Ashley and Law, 2015). While LA ICP-MS is a widely used instrument for analysing trace elements, the advancements in electron microscopy, especially EPMA, combined with its spatial resolution have provided alternative techniques to acquire trace element data. Besides having a very small spot size (<1 μm) suitable for inclusion based thermobarometry, the EPMA also provides a non-destructive analytical approach that has shown to yield high precision trace element data, as low as 1-10 ppm (e.g. Nachlas et al., 2018). As such, EPMA technique has been utilized in this study to obtain trace element data from inclusions in garnet.

2.2.3 Elastic barometry

While the conventional and trace element thermobarometry are dependent on the chemical composition of minerals and/or activities of components (e.g. Ghent and Stout, 1984), Elastic barometry is based on the physical properties of minerals. These allow the estimation of pressure at the time of inclusion entrapment within the mineral when the entrapped inclusion and host have different elastic properties (Enami et al., 2007; Ashley et al., 2014, 2016; Kohn, 2014b; Spear et al., 2014).

The quartz-in-garnet (QuiG) barometry works on the principle where an entrapment pressure of quartz in garnet is quantified by measuring the residual pressure in quartz

inclusions within garnet grains. The quartz grains are included in garnet at a certain pressure, where the pressure on inclusions is equal to the external pressure. As the rock undergoes changes in pressure, such as that experienced on a retrograde path during exhumation, the expansion of an included quartz grain is restricted by the garnet host because of differences in thermal expansion coefficients (e.g. Angel et al., 2019). This in turn is reflected as the residual pressure of the inclusion (Kohn, 2014b; Ferrero and Angel, 2018). Quantification of the residual pressure in quartz is achieved through Raman spectroscopy, which measures frequency shifts in the Raman spectrum. The shift in the Raman band of quartz at 464 cm^{-1} is best correlated to residual pressure and can then be utilized to calculate the entrapment pressure using the elastic models of quartz and garnet (including adjustments for end-member compositions). These calculations can be carried out using a computer-based program such as EosFit-Pinc (Angel et al., 2017a), which uses a user-defined elastic model and garnet composition to calculate the pressure. The greater independence from chemical equilibrium and diffusional changes in grain chemistries compared to conventional thermobarometry and thermodynamic modelling can make QuiG a more reliable barometer for minerals, such as garnet, which is subject to diffusion-driven chemical homogenization at high-temperatures. Using QuiG may allow the quantification of pressure across larger P-T conditions than through net transfer reactions alone (Enami et al., 2007; Ashley et al., 2014; Spear et al., 2014; Baxter et al., 2017).

2.2.4 Thermodynamic modelling

Thermodynamic modelling is the most computationally advanced form of thermobarometry currently in use to derive P-T information of the rocks. It is based on the thermodynamic equilibrium of minerals in a selected P-T range for a given bulk rock composition as predicted by mineral thermodynamic datasets (Powell and Holland, 1988, 2008, 2010; Spear, 1993; Holland and Powell, 1998). The thermodynamic datasets consist of thermodynamic parameters and properties of the mineral phases which are utilized to output a phase diagram (i.e. pseudosection), the calculated fields with assemblages of stable phases across the selected P-T range. This type of modelling is done using computer programs, such as Theriak Domino (de Capitani and Brown, 1987; de Capitani and Petrakakis, 2010), PerpleX (Connolly, 1990), or Thermocalc (Powell and Holland, 1994; Holland and Powell, 1998).

In addition to calculating P-T fields, phase equilibria modelling can also be used to calculate the composition of minerals in a phase diagram to help quantify the P-T conditions of the rock. The measured composition of minerals can be tied to the calculated composition of the minerals in a phase diagram, to get an insight into the P-T condition of the rocks. Based on the variation in mineral composition across different domains, a P-T path can be inferred that can be utilized to track the changes in conditions and processes during the metamorphism (e.g. Palin et al., 2012; Larson et al., 2013; Iaccarino et al., 2015; Weller et al., 2015; Shrestha et al., 2017, 2019). Furthermore, while informing on the changes in P-T conditions, the P-T paths may be used to observe changes in mineral assemblage during the metamorphism, which may provide insight into the assemblage and textures observed in the rock thin section. The most common minerals used to construct P-T paths in medium- to high-grade metamorphic rocks are garnet, biotite and plagioclase (Spear, 1993), which has been widely used to develop the P-T paths for rocks from the Himalaya (e.g. Ambrose et al., 2015; Iaccarino et al., 2017; Wang et al., 2017; Larson et al., 2020a).

2.3 Geochronology

To understand the metamorphic history of a rock, the timing record of different stages of metamorphism must be obtained. This is primarily achieved through the dating of mineral geochronometers, such as monazite, zircon, garnet, xenotime, in the rocks through the use of geochronology. This information is preserved through radioactive decay of isotopes in a mineral, which can be quantified by measuring the isotopic ratios. Based on the mineral type and isotopic systems, two geochronology methods have been used in this thesis. U-Th-Pb geochronology is used with accessory minerals such as monazite and xenotime, while Lu-Hf geochronology is used with major metamorphic mineral garnet.

2.3.1 U-Th-Pb geochronology

The U-Th-Pb geochronology is the most widely used geochronology method to date minerals. It is based on three decay chains, from radioactive parent isotopes ^{238}U, ^{235}U and ^{232}Th, to daughter isotopes ^{206}Pb, ^{207}Pb and ^{208}Pb, respectively. As such, minerals with a high abundance of U and Th are suitable candidates for this method, for example, accessory zircon, monazite, xenotime, titanite, rutile and apatite (see Engi et al., 2017). However, in reality, the

choice of geochronometer from which to extract age data is limited to the presence and size of the accessory minerals within the specimen of interest.

When the age data and composition of the geochronometer are interpreted together, it is collectively referred to as petrochronology (Kylander-Clark et al., 2013; Cottle and Stearns, 2018; Kohn et al., 2019). With the advancement in data acquisition techniques and instrumentation, it is now possible to collect information from accessory minerals on both trace element geochemistry and geochronology at the same time. At present, one of the most effective ways to achieve this is through a split stream system (e.g. Yuan et al., 2008; Kylander-Clark et al., 2013; Viete et al., 2015 Kylander-Clark, 2017) where isotopic ratios and trace elements are simultaneously collected and analysed through two mass spectrometers. Such simultaneous data acquisition from the same part of the accessory grain can be used to understand the conditions of growth of different domains across the analysed mineral (e.g. Kohn and Malloy, 2004; Cottle et al., 2018; Shrestha et al., 2019). The U-Th-Pb petrochronology in this thesis is performed using a similar setup where the Laser Ablation Split Stream (LASS) system is integrated with two Inductively Coupled Plasma Mass Spectrometers (ICP-MS). The Multi Collector (MC) ICP-MS is used to measure U-Th-Pb isotopic ratios, while quadrupole is used for quantification of trace elemental abundance (Kylander-Clark et al., 2013).

In Himalayan metamorphic rocks, monazite and xenotime are often abundant and, therefore, commonly used as geochronometers. Because of the abundance of Th in monazite, and associated problems with excess radiogenic ^{206}Pb from unsupported ^{230}Th that can affect the ^{206}Pb/^{238}U system (Schärer et al., 1984), the ^{208}Pb/^{232}Th dates from the monazite grains are the preferred isotopic system for the young Himalayan rocks, as the uncertainty on the Th decay constant gives issues at older ages. However, the timing information extracted from the monazite in the Himalaya is often incomplete because of (partial) resorption and recrystallization of metamorphic monazite due to high-temperature metamorphism and anatexis (Kohn et al., 2005; Kelsey et al., 2008). As a result, the Himalayan metamorphic monazite often records only the final stages of metamorphism, i.e. the retrograde portion of the P-T path (e.g. Kohn et al., 2005; Larson et al., 2011; From and Larson, 2014; Iaccarino et al., 2015; Regis et al., 2016; Warren et al., 2019), which hinders the access to the complete history of the studied rocks.

2.3.2 Lu-Hf geochronology

The Lu-Hf geochronology is based on radioactive decay of parent isotope ^{176}Lu to daughter isotope ^{176}Hf (e.g. Duchêne et al., 1997; Scherer et al., 2000). This method can be used to date the mineral phases that incorporate Lu and Hf elements, such as zircon, amphibole, rutile and garnet. Advancements in laboratory techniques and analytical precision have made it possible to date minerals with lower concentrations of Hf with high precision (see Baxter et al., 2017), which has led to the increasing use of Lu-Hf geochronology for dating garnets in magmatic and metamorphic rocks. The typical preparation for this method involves the separation of garnet grains from the rock, washing and dissolution through multiple cycles of acid mixtures involving HCl, HNO_3 and HF, to isolate Lu and Hf isotopes. Finally, the isotopic concentrations of Lu and Hf are measured through MC ICP-MS to obtain the dates.

Both Lu and Hf are relatively incompatible and immobile elements, however during its growth, garnet has a much higher affinity towards incorporating Lu due to its lower ionic charge (Baxter and Scherer, 2013). This results in a higher abundance of Lu and other heavy rare earth elements (HREE) of the same charge in garnet than Hf and is reflected through Rayleigh's fractionation pattern, i.e. Lu-rich garnet cores (e.g. Lapen et al., 2003). Such distributions of Lu in garnet grains may result in Lu-Hf dates being biased towards garnet core growth, which in turn reflects the minimum ages of garnet growth. Because of this, Lu-Hf garnet dates often provide the earliest record of prograde metamorphism (e.g. Kellett et al., 2014; Smit et al., 2014; Cutts and Smit, 2018) and can be used to fill out the missing gap in the timing of prograde metamorphic history of the Himalayan rocks, which is often erased from the monazite geochronologic record.

2.4 Pressure-Temperature-time (P-T-t) paths

While P-T paths provide insight into the P-T evolution of the rock, it lacks timing (t) information for different stages of metamorphic evolution. The timing component can be extracted from accessory geochronometers (e.g. monazite) or major metamorphic minerals (e.g. garnet). When time is tied to a P-T path, it is collectively called P-T-t path and as such provides an insight into metamorphic processes that the rock has experienced (e.g. Palin et al., 2012; Larson et al., 2013; Ambrose et al., 2015; Iaccarino et al., 2015, 2017; Weller et al.,

2015; Shrestha et al., 2017, 2019). Because of the HREE chemical relationship between monazite and garnet that enables prediction of the garnet behaviour (growth/stability/breakdown) during monazite growth, dates (U-Th-Pb) extracted from monazite domains can be linked to specific portions, especially the retrograde portion, of the garnet-based P-T path. Moreover, garnet ages (e.g. Lu-Hf, Sm-Nd) can also be used to provide timing information to the prograde part of the P-T path, complementing the timing information obtained from monazite. Each P-T-t path reflects changes or continuation of P-T conditions through time and defines a unique metamorphic signature for each rock (Larson et al., 2013; Shrestha et al., 2017). The comparison of these signatures from different rock packages helps delineate the differences in metamorphic histories, structures and processes during metamorphism, on a small and large orogenic scale.

Chapter 3 Decrypting the polymetamorphic record of the Himalaya

3.1 Background

Tectonic models for the development of the Himalaya (e.g. Jamieson et al., 2004; Kohn, 2008; Larson et al., 2015), Earth's largest active mountain belt, were developed and tested through pressure, temperature and time (P-T-t) information collected from exposed metamorphic rocks. This information is typically obtained through a combination of thermobarometry using garnet compositions, and chronology using high U/Pb accessory minerals such as monazite and zircon (see Larson et al., 2015; Montomoli et al., 2015). The overwhelming majority of accessory mineral dates are Himalayan in age (<55 Ma) and, by merit of textural relationships, garnet, and its chemical and P-T records, are typically inferred to also be of Himalayan origin (Goscombe et al., 2018; Waters, 2019). Drastic changes in regional trends of such data can help trace important tectonic boundaries that are difficult to recognize or altogether unexposed (e.g. Larson et al., 2013, Wang et al., 2013; Ambrose et al., 2015; Iaccarino et al., 2015; Shrestha et al., 2017). However, such changes may also result from disequilibrium among the analysed phases, specifically with relict garnet providing P-T data that do not represent the specific stage dated by accessory minerals.

Garnet Lu-Hf and Sm-Nd garnet geochronology (Griffin and Brueckner, 1980; Duchêne et al., 1997) provides a means to circumvent this issue by providing P-T-t estimates from a single phase. Likewise, these techniques allow testing of the assumption of cogenesis and the models that rely on these. Supporting the validity of this assumption in most cases, most Lu-Hf and Sm-Nd garnet data yield Himalayan ages (e.g. Harris et al., 2004; Kohn, 2009; Anczkiewicz et al., 2014; Kellett et al., 2014; Smit et al., 2014; Shrestha et al., 2017), with only a few studies reporting non-Himalayan (>55 Ma) dates (Argles et al., 1999; Kohn, 2009; Thöni et al., 2012). Still, these studies are very few in number and represent only a small sampling of the metamorphic rocks exposed across the Himalaya. The older ages could arguably be interpreted to represent local anomalies; low-strain or otherwise un-equilibrated rock enclaves in otherwise dominantly Himalayan tectonic units. The prevalence of inherited garnet in metamorphic rocks that are structurally concordant with Himalayan fabrics and

appear, on the basis of their accessory mineral chronometric record, entirely Himalayan is unexplored. To address this potentially important issue in Himalayan geology, we performed an integrated study involving garnet Lu-Hf chronology, and monazite and xenotime U-Th-Pb chronology on typical presumed-Himalayan garnet- to sillimanite-grade rocks from the Kanchenjunga region, east Nepal.

3.2 Geology of Kanchenjunga region

The Himalayan metamorphic core (HMC) is a package of pervasively deformed rocks that record Cenozoic metamorphism and deformation (Cottle et al., 2015). In the Kanchenjunga region of eastern Nepal, it comprises greenschist-facies phyllite and quartzite of the Lesser Himalayan sequence (LHS) in the south, through granulite-facies mylonitic orthogneiss, para-schist and -gneiss, and migmatite of the Greater Himalayan sequence (GHS) farther north (Goscombe et al., 2006; Ambrose et al., 2015). The HMC in this region exhibits an inverted metamorphic sequence with the progressive appearance of kyanite, and sillimanite, and disappearance of muscovite upwards through the structural levels from south to north (Ambrose et al., 2015) (Fig. 3.1). A number of in- and out-of-sequence thrust-sense structures are recognized within the HMC in the Kanchenjunga region (Goscombe et al., 2006; Imayama et al., 2010; Ambrose et al., 2015). These are typically inferred from contrasting timing of prograde and retrograde metamorphism interpreted from garnet-based P-T paths and interpreted links with geochronometers based on trace element chemistry (Imayama et al., 2012; Ambrose et al., 2015).

Five specimens, KA007, KA014, KA031, KA044 and KA064 (see Ambrose et al., 2015) were selected for this study which represent different structural levels within the HMC (Fig.3.1). Specimen KA014, a Grt + Bt + Ms schist (mineral abbreviations after Whitney and Evans, 2010), is the structurally lowest specimen examined. Specimen KA007 is a Grt + Bt + Ms + Ky gneiss sampled SW of KA014 (Fig. 3.1). North of KA014, and structurally higher, gneissic specimens KA031 (Grt + Bt + Ms + Ky + Sil), and gneissic migmatites KA044 (Grt + Bt + Ky + Sil + Kfs), and KA064 (Grt + Bt + Ms + Ky + Sil + Kfs) were investigated (Fig. 3.1). Published monazite U-Th-Pb dates from these specimens, dominantly from matrix grains, are ca. 31 - 19 Ma (KA007), ca. 24 - 14 Ma (KA031), ca. 40 - 16 Ma (KA044) and ca. 42 - 19 Ma (KA064) (Ambrose et al., 2015). Dates from monazite inclusions in garnets range from

24.1 ± 0.5 Ma to 18.4 ± 0.5 Ma (six analyses) in KA031, and from 38.5 ± 0.9 Ma to 25.1 ± 0.6 Ma (four analyses) with two older dates of ca. 106 Ma and ca. 495 Ma in KA064. On the basis of these data, the rocks, and its garnet and P-T record, were inferred to be Himalayan in age and to inform of the Cenozoic tectonics in the region (Ambrose et al., 2015).

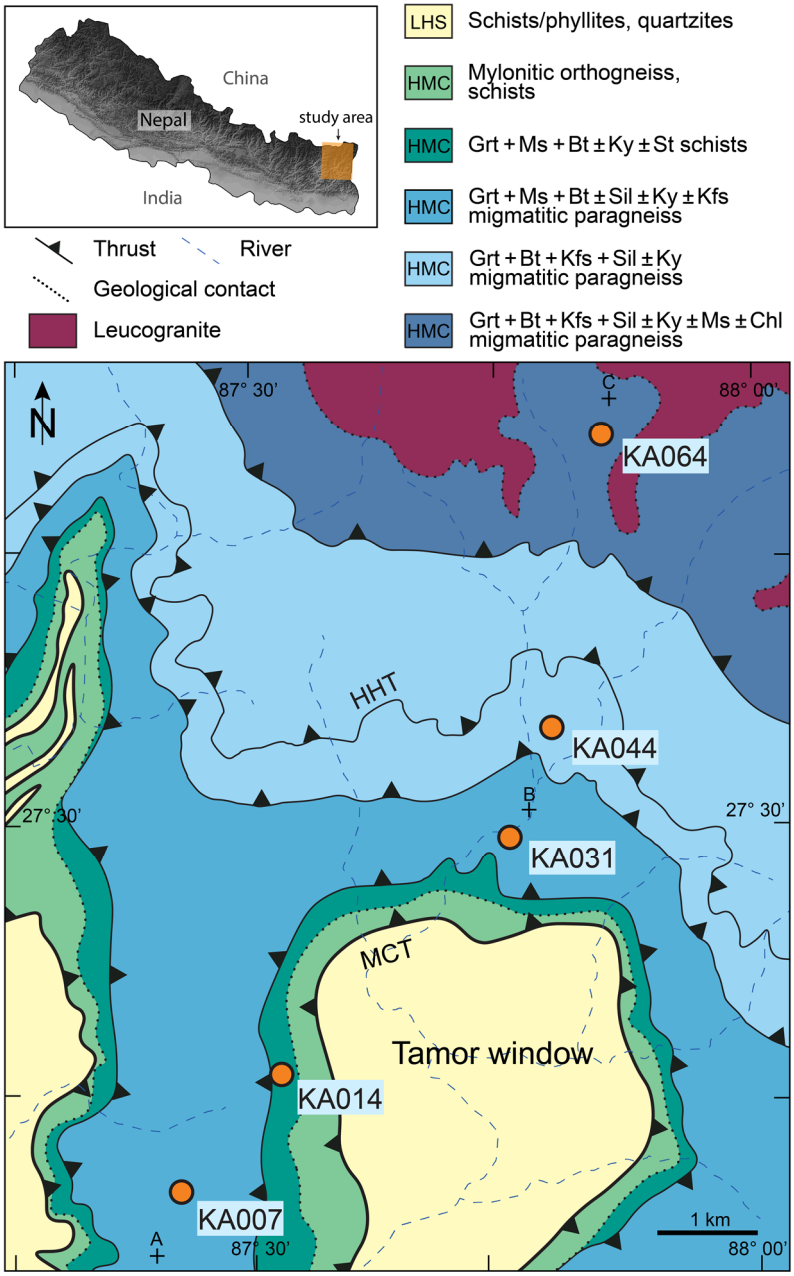

Figure 3.1. Simplified geological map of Kanchenjunga region with sampling locations (after Goscombe et al., 2006; Ambrose et al., 2015) digital elevation model AW3D30 was obtained from Japan Aerospace Exploration Agency - JAXA. The placement of MCT follows Ambrose et al., (2015). HHT = High Himalayan thrust (Goscombe et al., 2006), MCT = Main Central thrust zone. A-B-C marks the transect.

The present analysis of these rocks used Lu-Hf garnet chronology, in combination with U-Th-Pb dating of monazite and xenotime inclusions exclusively in the garnet grains. The P-T conditions of garnet growth are estimated through quartz-in-garnet (QuiG) barometry coupled with titanium-in-biotite (Ti-in-Bt) and titanium-in-quartz (Ti-in-Qtz) thermometry, all from inclusions in garnet. These approaches were favoured over conventional thermometry because 1) Ti is more retentive in garnet than common major elements used for conventional methods (e.g. Kelsey and Hand, 2015), and 2) QuiG does not require chemical equilibrium assumptions and is reliable over large P-T conditions (Ashley et al., 2014; Spear et al., 2014).

3.3 Analytical methods

3.3.1 Major and trace element geochemistry

Major element geochemistry of garnet and biotite, and trace element geochemistry of quartz were acquired using Cameca SXFiveFE electron probe microanalyzer (EPMA) housed in the Fipke Laboratory for Trace Element Research (FiLTER) at the University of British Columbia, Okanagan (UBCO). Operating conditions for major element acquisition were 15 kV, 20 nA, dwell time of 30 s for peak and 15 s for background, with beam size of 0 µm on garnet, and 5 and 10 µm on biotite. Operating conditions for trace element acquisition are following (Nachlas et al., 2018), with 15 kV and beam size of 2 µm. The data obtained from these analyses were regressed and applied to the unknowns as secondary calibration to the method and to account for instrumental drift. Oxide weight percent obtained from EPMA was converted to atom per formula unit (a.p.f.u.) based on the stoichiometric atoms of oxygens in mineral formula (12O - garnet and 22O - biotite). Almandine, grossular, pyrope and spessartine garnet endmembers, and Mg content of garnet and biotite grains were calculated using formulas: almandine = $Fe^{2+}/(Fe^{2+}+Ca+Mg+Mn)$; grossular = $Ca/(Fe^{2+}+Ca+Mg+Mn)$; pyrope = $Mg/(Fe^{2+}+Ca+Mg+Mn)$; spessartine = $Mn/(Fe^{2+}+Ca+Mg+Mn)$; XMg = $Mg/(Fe^{2+}+Mg)$.

Trace element geochemistry and mapping of garnet were acquired using Photon Machines Analyte 193 Excimer laser coupled with Agilent 8900 Triple Quadrupole Inductively Coupled Plasma-Mass Spectrometer (ICP-MS) also housed in FiLTER at UBCO. Garnet mapping and spot analysis were performed on grains mounted in epoxy resin (Struers Epofix kit). Operating conditions for garnet mapping and spot analysis were 100% laser

energy, 8 Hz repetition rate and 6.78 Jcm^{-2} fluence. Mapping line scan spot size of 29.6 µm was used for KA007 and KA064 specimens, 39.4 µm for KA031, 49.3 µm for KA044 and 64.1 µm in KA014 with selected analytes Y, Zr, La, Ce, Gd, Yb and Lu. Garnet spot analysis used spot size of 29.6 µm, 30 s ablation and 30 s background analysis, with selected analytes P, Y and rare earth elements (La, Ce, Pr, Nd, Sm, Eu, Gd, Tb, Dy, Ho, Er, Tm, Yb, Lu). For garnet mapping, NIST SRM 610 was used as an external reference material, while for trace element spot analysis, NIST SRM 612 and 610 were used as external primary and secondary reference material respectively. For both mapping and spot analysis, ^{29}Si was used as an internal standard. Raw data was processed, and maps were visualized using Iolite v.4.3 (Paton et al., 2011).

3.3.2 Garnet geochronology

Each rock specimen was crushed using a Rocklabs hydraulic press to enable individual picking of garnet grains. Complete, whole grains without cracks and fractures were selected for dissolution. Detailed process and analysis are described in (Smit et al., 2010; Cutts and Smit, 2018). The isotopes were analysed using Nu Instruments Nu Plasma Multicollector ICP-MS housed at the University of British Columbia, Vancouver.

3.3.3 Monazite geochronology

Monazite and xenotime inclusions were analysed using a Photon Machines Analyte 193 Excimer laser coupled with Nu Instruments Nu Plasma Multicollector ICP-MS housed at University of California, Santa Barbara. Operating conditions were 4 Hz repetition rate, 1.7 Jcm^{-2} laser fluence for 25 s, and 8 µm spot size, with details described in (Cottle et al., 2013). The isotopes were normalized to '44069', while 'Bananeira' and 'Trebilcock' served as secondary reference materials. Geochronology plots were made using ChrontouR (Larson, 2020).

Nine repeat analyses of 'Bananeira' yielded a weighted mean $^{206}Pb/^{238}U$ age of 522.6 ± 5.7 Ma; mean square weighted deviation (MSWD) = 0.1 (511.7 ± 1.2 Ma ID-TIMS age; Horstwood et al., 2016) and a weighted mean $^{208}Pb/^{232}Th$ age of 500.0 ± 6.3 Ma, MSWD = 0.1 (497.6 ± 1.6 Ma LA ICP-MS age; Kylander-Clark et al., 2013). Eight repeat analyses of 'Trebilcock' yielded a weighted mean $^{206}Pb/^{238}U$ age of 279.8 ± 3.2 Ma, MSWD = 0.8 (ca.

279–285 Ma; Tomascak et al., 1996) and a weighted mean $^{208}Pb/^{232}Th$ age of 261.4 ± 3.5 Ma, MSWD = 0.2 (263.7 ± 1.0 Ma LA ICP-MS age; Kylander-Clark et al., 2013). With monazite and xenotime inclusions being extremely small in size, generally ~ 10 µm, most of the grains were ablated only partially. However, due to lack of signal (and output dates) when spots missed the target and ablated fully garnet, we use dates of all ablated monazite and xenotime grains. As the aim is to constrain the portions based on Cenozoic dates, monazite dates are reported as $^{208}Pb/^{232}Th$.

3.3.4 Trace element thermometry

All specimens selected for this study are garnet-bearing metapelites, and contain quartz, biotite, and Ti-bearing mineral inclusions within garnets, which satisfy the requirement of these thermometers. Both rutile and ilmenite are present as inclusions in garnets from all specimens except for KA014 which only contains ilmenite. The Ti-in-Bt thermometer (Henry et al., 2005) is used to reflect changes in temperature from different garnet domains and is applicable for metapelites in the range of ~ 4 - 6 kbar, while the absolute uncertainty for this method is estimated as ± 24 °C below 600 °C and ± 12 °C above 700 °C. As Ti-in-Bt was used for pressures higher than 6 kbar, the uncertainty on the temperature estimate was doubled from 12 °C to 24 °C. Although the Ti-in-Bt thermometer has only been calibrated to 6 kbar (Henry et al., 2005), it has been successfully applied to higher pressures in previous studies (Mottram et al., 2014; Warren et al., 2014; Carosi et al., 2016). For specimens that contain rutile, the activity of TiO_2 is set as 1 to reflect TiO_2 saturation, while for one specimen without rutile, the activity of TiO_2 is set at 0.85, as metapelites typically show TiO_2 saturation of 0.8 - 1.0 (e.g. Ghent and Stout, 1984; Wark and Watson, 2006). Uncertainty of this pressure-dependent method including analytical uncertainty is 20 - 35 °C.

3.3.5 Elastic barometry

Unpolarized Raman spectra of quartz inclusions in garnet were obtained on a JY Horiba LabRAM HR800 Raman microprobe at Virginia Tech, using a high-resolution 800 mm focal-length spectrometer (1800 lines/mm grating) with a 100 mW, 514.57 nm argon laser. High spatial (~1 µm) resolution was achieved using a 100x objective (NA = 0.90) and a confocal aperture set to 400, with a slit width of 150 µm. Spectra were centered on 360 cm^{-1} for quartz

to allow for the collection of the three main Raman bands for quartz (~ 464, 206 and 127 cm^{-1}) and simultaneous collection of three Ar plasma lines (520.30, 266.29 and 116.04 cm^{-1}), which allows for drift correction. All spectra were collected for 30 - 45 s over 3 accumulations. All Raman lines were fitted using Peakfit v. 4.12 from SYSTAT Software Inc., using a symmetric Gaussian-Loren model for fitting the calibration lines and the asymmetric Pearson IV model for fitting quartz bands.

Inclusion pressure (P_{incl}) was determined by measuring the frequency shift in the 464 cm^{-1} bands for quartz. A Herkimer quartz standard was used for the ambient peak position. Inclusion pressures were calculated using polynomial regressions based on experimental data for the P-dependent Raman peak shifts (Schmidt and Ziemann, 2000). Stress anisotropy was evaluated for each inclusion by using the program stRAinMAN (Angel et al., 2019) with the Grüneisen tensor components for quartz (Murri et al., 2018). Almost every inclusion resulted in calculated $\varepsilon_1+\varepsilon_2$ and ε_3 that were within uncertainty of zero (i.e., inclusions are not under anisotropic stress), with strain-based P_{incl} estimates statistically indistinguishable from those calculated using the 464 cm^{-1} band hydrostatic polynomial. Therefore, only the 464 cm^{-1} band was used for P_{incl} estimation, given the difficulties and high uncertainties with fitting the 206 cm^{-1} quartz band (see Ashley et al., 2015; 2016). Entrapment pressure was calculated using the program EoSFit-Pinc (Angel et al., 2017a), using a modified formulation of the isotropic elastic model (Guiraud and Powell, 2006). The equations of state (EoS) and host shear moduli used in the elastic modelling include: quartz including elastic softening of alpha and beta quartz due to lambda phase transition and a curved α-β boundary (Angel et al., 2017b), almandine (Arimoto et al., 2015; Milani et al., 2015), pyrope (Anderson and Isaak, 1995; Sinogeikin and Bass, 2000; Milani et al., 2015), spessartine (Gréaux and Yamada, 2014), and grossular (Gwanmesia et al., 2014; Milani et al., 2017). Entrapment conditions were refined by assuming ideal mixing between garnet endmembers.

3.4 Results and interpretation

Major element profiles across garnet grains in KA014 from the lowest grade zone at lowest structural level (Fig. 3.1) increase in Fe and Mg towards rims compensated by a decrease in Mn and Ca content. The zoning reflects typical prograde zonation (Tracy et al., 1976). In contrast, garnet grains in KA007, KA031, KA044 and KA064 specimens show

homogeneous major element compositions, with minor changes only at grain rims (Fig. 3.2, Table A1), indicative of intra-granular homogenization and retrograde diffusion at the rims (Florence and Spear, 1991; Kohn and Spear, 2000).

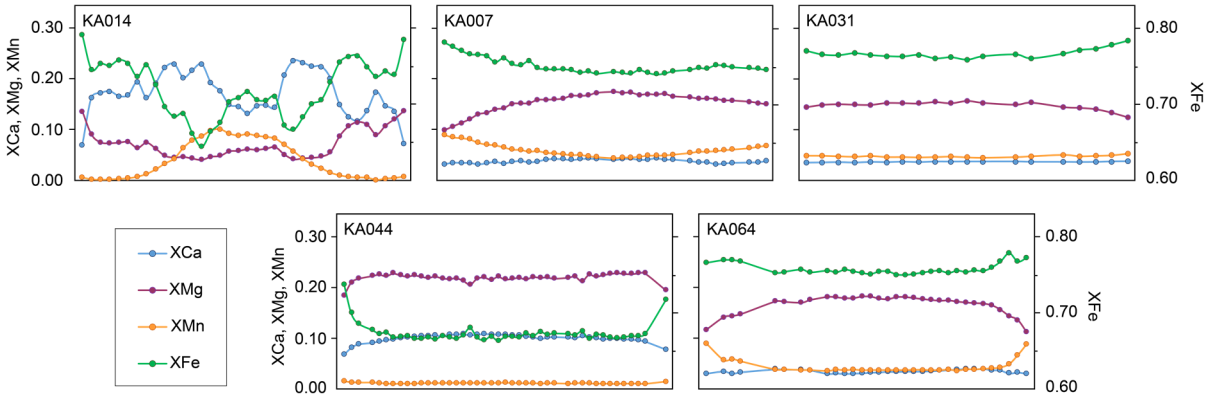

Figure 3.2. Garnet end-member profiles for five metamorphic specimens. Alm - almandine, Grs - grossular, Prp - pyrope, Sps - spessartine.

Garnet heavy rare earth element (HREE) concentrations (Table A2) for specimens KA014, KA031, KA044 and KA064 generally show a core to rim decrease (Fig. 3.3a, c-e) which is consistent with Rayleigh fractionation during growth (Otamendi et al., 2002). Among these specimens, only KA014 shows minor rim HREE-enrichment. In other specimens, the strongest drop in HREE concentrations coincides with a textural boundary that separates cores from rims. This boundary is either marked by circular patterns of quartz and biotite inclusions around inclusion-poor outer cores (KA031, KA044, KA064; Fig. 3.3c-e) or a switch from syn- to post-tectonic inclusion patterns (KA014; Fig. 3.3a). In KA007 garnet, such a boundary is lacking; HREE concentrations are homogeneous across the core and show patchy enrichment along rims. Enrichment in the rims of KA014 and KA007 garnets indicate growth during breakdown of other HREE-rich minerals, such as xenotime, which is consistent with re-integration of yttrium (Y) and phosphorus (P) into garnet (Pyle and Spear, 1999) (Fig. A1). The considerable HREE enrichment in KA007 rims is likely a secondary feature, reflecting diffusive HREE re-uptake as a result of garnet resorption (Kelly et al., 2011).

The Lu-Hf garnet geochronology of the five specimens yielded dates of 49.7 ± 0.9 Ma, 230.9 ± 2.1 Ma, 293.3 ± 0.5 Ma, 51.6 ± 3.2 Ma and 291.3 ± 0.7 Ma for specimens KA014, KA007, KA031, KA044 and KA064, respectively (Fig. 3.3a-e, Table 3.1).

Table 3.1. Lu-Hf isotopic data for five metamorphic specimens.

	Lu (ppm)	Hf (ppm)	$^{176}Lu/^{177}Hf$	2SD	$^{176}Hf/^{177}Hf$	2SD	Lu-Hf age (Ma)	MSWD	Initial $^{176}Hf/^{177}Hf$
KA007									
Grt-1	5.53	0.978	0.802	0.002	0.286	0.000035			
Grt-2	3.48	0.607	0.812	0.002	0.286	0.000037			
Grt-3	6.32	0.980	0.915	0.002	0.286	0.000041			
Wr-1	0.724	7.37	0.014	0.000	0.282	0.000025			
							230.9 ± 2.1	1.3	0.282185 ± 0.000025
KA014									
Grt-1	6.49	0.528	1.740	0.004	0.283	0.000041			
Grt-2	2.43	0.728	0.473	0.001	0.282	0.000038			
Grt-3	6.11	0.373	2.326	0.006	0.284	0.000045			
Wr-1	0.628	4.53	0.020	0.000	0.282	0.000018			
							49.7 ± 0.9	1.3	0.281726 ± 0.000017
KA031									
Grt-1	4.86	0.529	1.302	0.003	0.289	0.000044			
Grt-2	5.44	0.173	4.471	0.011	0.307	0.000034			
Grt-3	5.47	0.142	5.472	0.014	0.312	0.000047			
Grt-4	5.55	0.164	4.801	0.012	0.308	0.000041			
Wr-1	0.675	4.76	0.020	0.000	0.282	0.000018			
							293.3 ± 0.5	0.7	0.282017 ± 0.000017
KA044									
Grt-1	1.52	0.677	0.318	0.001	0.282	0.000027			
Grt-2	1.85	0.729	0.361	0.001	0.283	0.000020			
Grt-4	1.62	0.683	0.336	0.001	0.282	0.000029			
Wr-1	0.119	7.29	0.002	0.000	0.282	0.000015			
							51.6 ± 3.2	0.3	0.282151 ± 0.000015
KA064									
Grt-1	8.31	0.862	1.367	0.003	0.289	0.000027			
Grt-2	4.41	0.216	2.902	0.007	0.298	0.000044			
Grt-3	4.96	0.209	3.364	0.008	0.300	0.000046			
Grt-4	5.89	0.295	2.832	0.007	0.297	0.000045			
Wr-1	0.93	8.53	0.015	0.000	0.282	0.000018			
							291.3 ± 0.7	1.6	0.281996 ± 0.000017

All analysed monazite and xenotime inclusions in garnet are small (mostly ~10 μm, Figs. A2, A3; Table A3). Two monazite inclusions in the garnet rim of specimen KA007 yielded pre-Himalayan dates of 564 ± 43 Ma and 287 ± 19 Ma. In specimen KA031, spot analyses on two monazite inclusions located in the garnet rim yielded 32.2 ± 1.5 Ma and 14.5 ± 0.8 Ma, while three xenotime grains in the garnet core yielded 16.0 ± 0.6 Ma, 14.1 ± 1.5 Ma and 13.4 ± 0.8 Ma. These xenotime core inclusions are located in a crack or cavity (Fig. A4). In specimen KA064, monazite and xenotime inclusions yielded 713 ± 39 Ma to 408 ± 21 Ma. A monazite inclusion in the rim yielded 48.3 ± 2.4 Ma, and a xenotime inclusion in the core yielded a date of 35.9 ± 2.1 Ma. This Himalayan-age xenotime occurs in close proximity to quartz and P-rich alteration (Fig. A4). Dates obtained from inclusions in cracks or cavities, or associated with fluid alterations are excluded from interpretation.

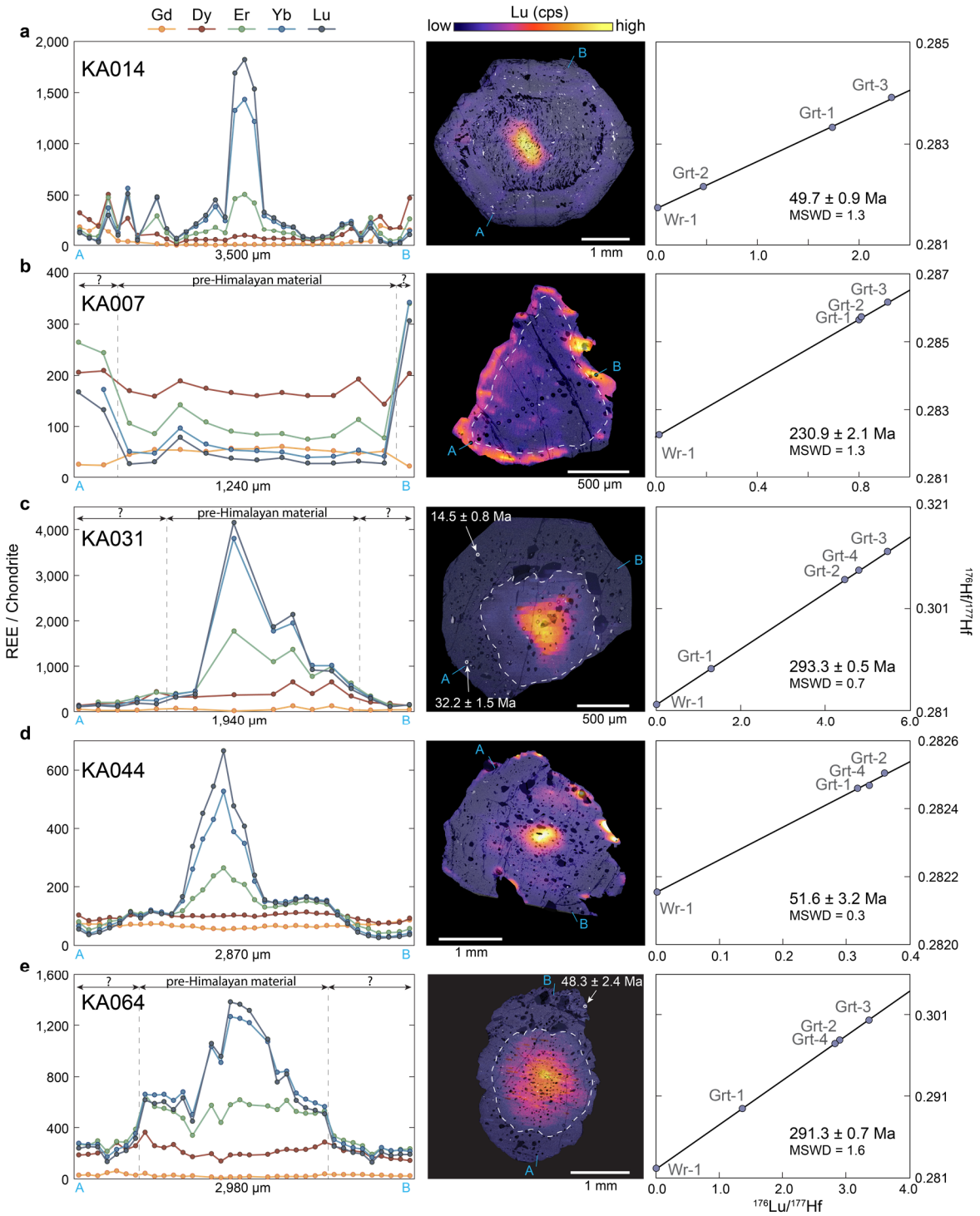

Figure 3.3. Garnet and accessory mineral trace element and geochronology data. Left panel: Garnet trace element profiles. Middle panel: Garnet back-scattered electron image overlaid by Lu trace element heat map. Locations of Cenozoic monazite and xenotime inclusion dates are marked on the image. Letters A and B mark the trace element profile transect. Right panel: Lu-Hf isochron diagrams. White dashed lines separate different interpreted garnet domains.

Based on the spatial distribution of Cenozoic monazite, as well as textural and chemical zonation preserved in garnet, pre-Himalayan garnet grains are divided into core and rim domains (Fig. 3.3), while Himalayan grains are separated into core, mantle and rim (Fig. A5). Titanium concentrations in quartz inclusions measured for Ti-in-Qtz thermometry are relatively homogeneous across garnet grains in all specimens, with only minor variation unrelated to their spatial distribution (Fig. A5, Table A4). As such, they provide no evidence that quartz (re)equilibrated with Ti-reservoir (e.g. rutile) during garnet growth. Biotite inclusions analysed for Ti-in-Bt thermometry are primarily restricted to the mantles and rims in Himalayan garnets (KA014 and KA044), while in pre-Himalayan garnets (KA007, KA031 and KA064) they occur only within rims in a circular pattern together with quartz (Fig. 3.3). Temperature and pressure estimates from the Ti-in-Qtz thermometer (Thomas et al., 2010), Ti-in-Bt thermometer (Henry et al., 2005) and QuiG barometers are shown in Figs. 3.4, A6 and Tables A5, A6. The scarcity of biotite inclusions in some garnets or localized biotite inclusions in others, as well as incomplete re-equilibration of Ti in quartz hinders the comparison of P-T results between specimens. Furthermore, in absence of significant difference in limited P-T estimates obtained from available inclusions in pre-Himalayan and Himalayan specimens, they are not discussed any further.

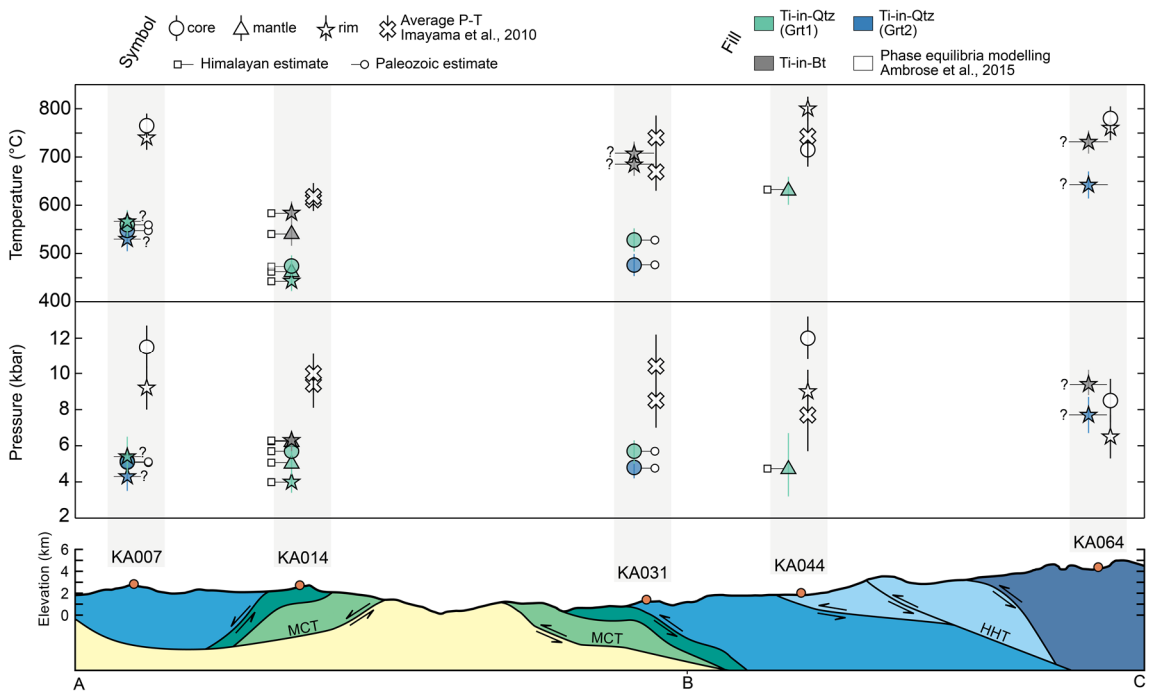

Figure 3.4. Temperature and pressure estimates derived from garnet inclusions in respect to sampling locations. The vertical line reflects uncertainty. The same specimens were used as in Ambrose et al., (2015) while following equivalents based on sampling location and mineral assemblage was used from Imayama et al., (2010): KA014 - M1904, M3104; KA031 - H1301, H2101; KA044 - H1404. The cross-section is modified after Ambrose et al., (2015).

3.5 Discussion

For two of the five specimens (KA014, KA044), Lu-Hf garnet ages correspond to the timing of the initial Himalayan collision (~55 Ma; Hu et al., 2016) and are essentially identical to Lu-Hf ages obtained in isolated HMC exposures in the northern Himalaya (Smit et al., 2014). Strikingly, much older garnet is still present in the other specimens, even though they are texturally not necessarily very different and are structurally interspersed with the other specimens. The recognition of this material opens a new window into Himalayan history and principally could provide an explanation for seemingly anomalous garnet occurrences or compositions, which do not follow regional field gradients or structure. Although the pre-Himalayan garnet in this study is characterized by flat major element profiles, this is not always the case (specimen 31a in Kohn, 2009), indicating that garnet chronology may be necessary to identify relict material that may lead to erroneous tectonic models when used to inform

Himalayan tectonics.

The exact age of the relict garnet is not necessarily self-evident. The presence of Cenozoic monazite grains armoured within the rims of garnet in specimens KA031 and KA064 (this study and Ambrose et al., 2015) could be taken to indicate that at least the rim material is still of Himalayan age. This would imply strong age heterogeneity in these grains, with the ca. 290 Ma dates being the result of mixing between ca. 50 Ma rims and much older cores. The possible age of garnet cores in this multi-growth scenario can be modelled by quantifying the relative Lu contribution of specific grain domains to the bulk-grain Lu budget and, by extension, the contribution of these domains to the bulk-grain Lu-Hf age (e.g. Smit et al., 2010; Kellett et al., 2014, Appendix A1). Using the core-rim distinction (Fig. 3.3) and assuming rim ages defined by the youngest armoured inclusions in the rims of KA031 and KA064, ca. 15 Ma (this study) and ca. 25 Ma (Ambrose et al., 2015), respectively, the modelled 'core dates' for these specimens would be ca. 382 Ma (KA031) and ca. 417 Ma (KA064) (Table A7).

There are several limitations to this approach. The calculations are based on spot analysis data on a 2D garnet surface profile, which may not include the compositional core or capture the full compositional complexity of grains. Estimates of the Lu contribution of each domain can significantly affect the age calculations; an increase of only 0.05 mm in radius of the garnet core in KA064 would reduce the estimated core age by 30 Ma (387 Ma). Still, any of these results are quite far departed from any previously recognized metamorphic events in the HMC or elsewhere in the Himalaya, the closest having occurred ca. 480 Ma (Gehrels et al., 2003; Martin et al., 2007). Moreover, the level of coincidence needed to produce very precise and almost identical Lu-Hf dates by mixing of two very different age components for two specimens in which garnet shows different grain size and HREE zoning, would be extreme; any such interpretation cannot be relied upon. The possibility is therefore entertained that garnet in specimens KA031 and KA064 is actually 293 - 291 Ma and that the monazite inclusions in grain rims have re-equilibrated; the garnet host is poikiloblastic, and potentially permeable along microscopic cracks and interconnected porosity. Analogously, it is possible that KA007 garnet represents ca. 290 Ma garnet that shows a younger age as a result of resorption and late diffusive Lu re-uptake (Kelly et al., 2011). The HREE map and profiles reflect this process and do so only for this specimen (Fig. 3.3). The early Permian age obtained from relict garnet in gneisses of the Kangchenjunga HMC does not represent a component that

is widely recognized in rocks within this or other parts of the Himalaya. It is nevertheless not the first time that it has been recognized; similar Lu-Hf dates of 280 - 250 Ma (Permian) were obtained for the HMC in Langtang, north-central Nepal (Kohn, 2009). This stage coincides with the opening of the Neo-Tethys basin between then Laurasia and Gondwanan terranes that would develop to become Greater India (Stampfli, 2000). The data thus could indicate that garnet within the HMC may date back to the thermally anomalous state of the proto-Himalayan lithosphere during this time, rather than to the pervasive deformation and metamorphism that the rocks would be subjected to ca. 240 Myr later. The Kangchenjunga HMC thus may provide the youngest example of high-grade rocks where the Lu-Hf system in garnet dates both the birth and closure of a large oceanic basin (e.g. Cutts and Smit, 2018; Thiessen et al., 2019).

3.6 Summary

The results of garnet geochronology, thermobarometry and monazite/xenotime geochronology from exhumed, mid-crustal metamorphic rocks exposed in the Kanchenjunga region of the eastern Nepalese Himalaya yielded two populations of garnets. Garnets in two specimens showed Himalayan Lu-Hf dates of ca. 55 Ma, while garnets in three specimens showed pre-Himalayan Lu-Hf dates of ca. 290 - 230 Ma. Pre-Himalayan garnets are interpreted to have grown entirely during the early Permian opening of the Neo-Tethys ocean basin, or during both Cambro-Ordovician orogenesis and Cenozoic metamorphism. The recognition of pre-Himalayan garnet in the Himalayan mid-crust calls into question the interpretations of previous studies which used garnets to interpret Himalayan history without dating the garnet itself and models based on these.

Chapter 4 Tectonometamorphic evolution of the Himalayan metamorphic core across the Makalu-Arun region, eastern Nepal

4.1 Background

The Himalayan metamorphic core (HMC) is a suite of rocks exposed along the Himalayan orogen that have undergone Cenozoic metamorphism, deformation and cooling related to the ongoing convergence between the Indian and the Eurasian continental plates (Cottle et al., 2015). As such, it holds information critical to our understanding of the processes active during the evolution of the orogen. The apparent incompatibility of orogen-wide, coeval, opposite sense structures that bound the Greater Himalayan sequence (GHS) within the HMC, the Main Central thrust below and the South Tibetan detachment system above, triggered extensive research to understand structural framework, kinematics, and the convergence accommodation processes that governed development of the Himalayan mid-crust (see Kohn, 2014a; Waters, 2019). This detailed work resulted in the identification of numerous localized, tectonometamorphic structures (i.e. discontinuities) within the HMC throughout the orogen, which divide it into multiple distinct packages of rocks with unique metamorphic and kinematic histories (Cottle et al., 2015; Larson et al., 2015; Montomoli et al., 2015). These discontinuities are often cryptic, nearly impossible to identify in the field (Larson et al., 2015; Waters, 2019). Instead, these structures have been most commonly recognized through abrupt breaks in the metamorphic history, pressure-temperature-time paths, of adjacent rock packages (Groppo et al., 2009; Corrie and Kohn, 2011; Larson et al., 2013; Montomoli et al., 2013; Shrestha et al., 2017, 2020; Warren et al., 2014).

Known discontinuities have been loosely categorized as late Oligocene - early Miocene in-sequence, and late/middle Miocene out-of-sequence thrust sense structures (see Larson et al., 2015; Montomoli et al., 2015). Some of these structures, however, have also been reported to have accommodated late-stage normal-sense reactivation (Goscombe et al., 2006; Imayama et al., 2012; Martin et al., 2015; Shrestha et al., 2020). Attempts are underway to determine if these thrust-sense structures can be correlated along the strike as regional features (see Larson et al., 2015; Montomoli et al., 2015; Goscombe et al., 2018;), such as with High Himal Thrust/ High Himalayan Discontinuity (HHT/HHD - Goscombe et al., 2006; Montomoli et al., 2013).

The widespread occurrence of these structures indicates that the HMC records a more complex metamorphic and kinematic history than previously thought.

The metamorphic rocks from the Makalu-Arun region were examined using mineral geochemistry, monazite petrochronology and phase equilibria modelling to investigate and characterize the occurrence of structural discontinuities in eastern Nepal. The findings of this work will provide insight into the potentially complex metamorphic evolution of the HMC and examine potential correlations with structures delineated in adjacent regions. Characterization of unique rock packages and quantification of the discontinuities that separate them both locally and regionally will help evaluate their role in the overall evolution of the Himalaya and provide the critical information necessary to test and develop new tectonic models.

4.2 Geological setting

4.2.1 Lithotectonic units

The HMC in the Makalu-Arun region, eastern Nepal, comprises rocks of the GHS and the Lesser Himalayan sequence (LHS) that exhibit Himalayan metamorphism and anatexis (Fig. 4.1a, b). It is characterized by an inverted regional metamorphic gradient, typical of the Himalayan system, with Grt-in, St-in, Ky-in and Sil-in isograds that record increasing metamorphic grade up structural section, towards the north (mineral abbreviations throughout are after Whitney and Evans, 2010). The GHS in this region is composed of schist, paragneiss, orthogneiss, migmatite, interbedded with calc-silicate rocks and local leucogranite (Goscombe and Hand, 2000; Goscombe et al., 2006, 2018). The GHS is bound at its base by the north-dipping top-to-the-south Main Central thrust (MCT) (Goscombe et al., 2006; Streule et al., 2010), which separates it from the lower metamorphic grade rocks of the LHS, and along its top by the north-dipping, normal sense South Tibetan Detachment system (STDS), which separates it from the sedimentary to low- metamorphic grade metasediments of the Tethyan Sedimentary Sequence (TSS) (Fig. 4.1a).

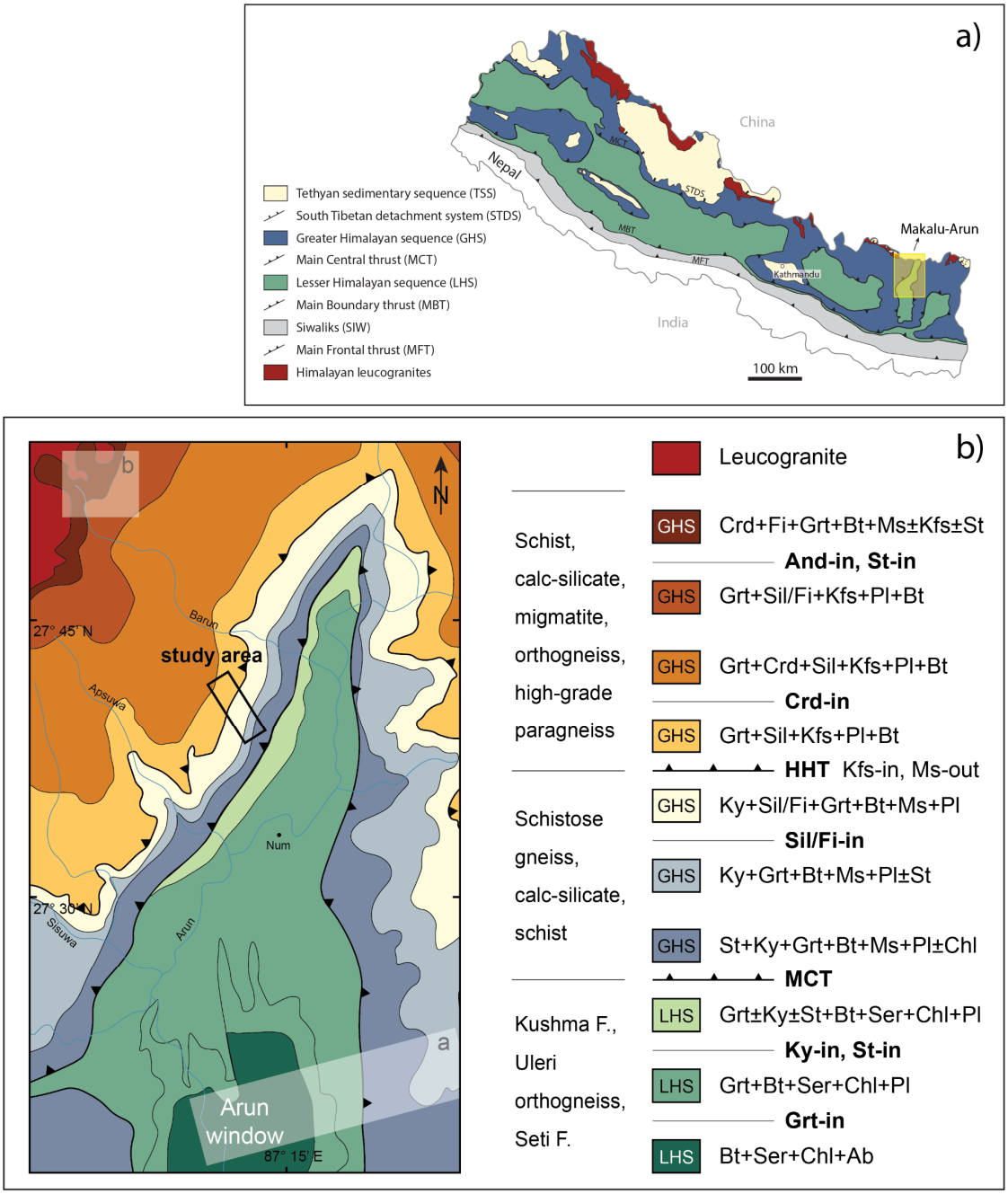

Figure 4.1. Geological map of the study area. a) Simplified geological map of Nepal with major lithotectonic units and bounding structures (modified after Yin, 2006; Guo and Wilson, 2012; McQuarrie et al., 2014). Yellow rectangle shows the location of the Makalu-Arun region. b) Geological map of the Makalu-Arun region (modified after Goscombe et al., 2018). Black outline marks the location of the transect in this study. Shaded rectangles represent study area of Groppo et al., (2009) (a), and Streule et al., (2010) (b). MCT - Main Central thrust, HHT - High Himalayan thrust (position inferred by Goscombe et al., 2018).

The study area is located in the Makalu-Arun region (Fig. 4.1a, b). Herein we follow the detailed lithological work of Goscombe et al., (2006, 2018) for the local geology. Schist and calc-silicate rocks of the Seti Formation comprise the lowermost unit of the LHS in the area and are bounded on the top by the MCT zone. The Ulleri orthogneiss and schist of Kushma Formation are the highest unit of the LHS and bounded on top by the MCT zone. The MCT zone consists of staurolite to kyanite to sillimanite zone metapelite schists, schistose gneisses with carbonate/calc-silicate lenses (Goscombe et al., 2006). The MCT zone is marked on top by the High Himalayan thrust (HHT) which coincides with mylonitic biotite/fibrolite schist (Goscombe et al., 2006, 2018). The HHT in this region was inferred in Goscombe at al. (2006, 2018) based on lithological observations and P-T estimates compiled and summarized across eastern Nepal. The exact location of the HHT in the Makalu area, however has not yet been defined. The HHT is structurally overlain by the Ms-absent, high-grade Grt-Sil-Kfs paragneiss, migmatite, calc-silicate and marble with biotite-sillimanite schist and quartzite. The uppermost unit of the GHS includes biotite-muscovite schists and a Cambrian granitic orthogneiss (Goscombe et al., 2006, 2018). These rocks are variably intruded by Miocene plutons and sills at the highest structural level just below the South Tibetan detachment system.

4.2.2 Metamorphic and geochronologic history

Groppo et al., (2009) documented two distinct structural discontinuities in the eastern side of the Arun window (Fig. 4.1b) based on the differences in P-T paths. One is interpreted as a thrust between Ms + Bt + Grt schists below that record metamorphic conditions of ~ 545 °C and 6.5 kbar and Ms + Bt + Grt + St schists above that record P-T conditions of ~ 600 °C and 8.5 kbar. The other, structurally higher discontinuity is inferred in the Ky zone as a normal-sense structure within Ms + Bt + Grt + St + Ky schists where rocks in the footwall record P-T conditions of ~ 645 °C, 9.5 kbar while rocks in the hanging wall record ~ 655 °C and 7.5 kbar. No geochronological information, however, was published with any of these P-T conditions.

In the area coinciding with the transect investigated in this study (Fig. 4.1b), Groppo et al., (2010) reported apparent decompression and cooling after peak metamorphism at ~ 820 °C and 13 kbar at ca. 31 Ma in Kfs + Grt + Ky + Sil paragneiss. Structurally higher specimens, Grt + Kfs + Ky + Sil migmatites recorded isothermal decompression after peak metamorphism

of ~ 800 °C and 11-10 kbar, and evidence of peritectic garnet growth recording isobaric heating and peak metamorphism at ~ 800 °C and 8 kbar (Groppo et al., 2012).

Structurally higher and NW from transect in this study (Fig. 4.1b), Streule et al. (2010) investigated Sil + Crd paragneiss and leucogranites, and reported peak metamorphism in the Sil stability field at ~ 715 °C and 6 kbar, with a second melting phase in the cordierite stability field at ~ 700 °C and 4 kbar at ca. 16 and 15 Ma.

Goscombe et al. (2018) summarized all previous work in the region. The pooled peak P-T conditions for the Grt + Bt + Ms + Ky gneisses immediately above the MCT in the Makalu-Arun region averages ~ 700 °C and 7.6 kbar. The structurally higher, Grt + Bt + Kfs + Sil paragneises record average conditions of ~ 685 °C and 7.2 kbar. At the highest structural level, in the Crd-in zone, Grt + Bt + Kfs + Sil + Crd gneisses yield average P-T conditions of ~ 740 °C and 6.7 kbar, but with no published geochronological information.

The previous work in the Makalu-Arun region has produced some high-quality P-T data. With few exceptions, however, these datasets generally lack integrated geochronological information making comparisons both within region and with adjacent areas largely speculative. Assessing metamorphic conditions and geochronologic data across the HMC is fundamental to investigate the metamorphic history of this region and potential occurrences of tectonometamorphic discontinuities. In this study, eight high-grade gneiss specimens (MK256, MK257, MK258, MK260, MK262, MK263, MK266 and MK268) from the transect in the western side of the Arun window (Figs 4.1b, 4.2) were selected for phase equilibria modelling paired with high resolution, *in situ*, monazite petrochronology.

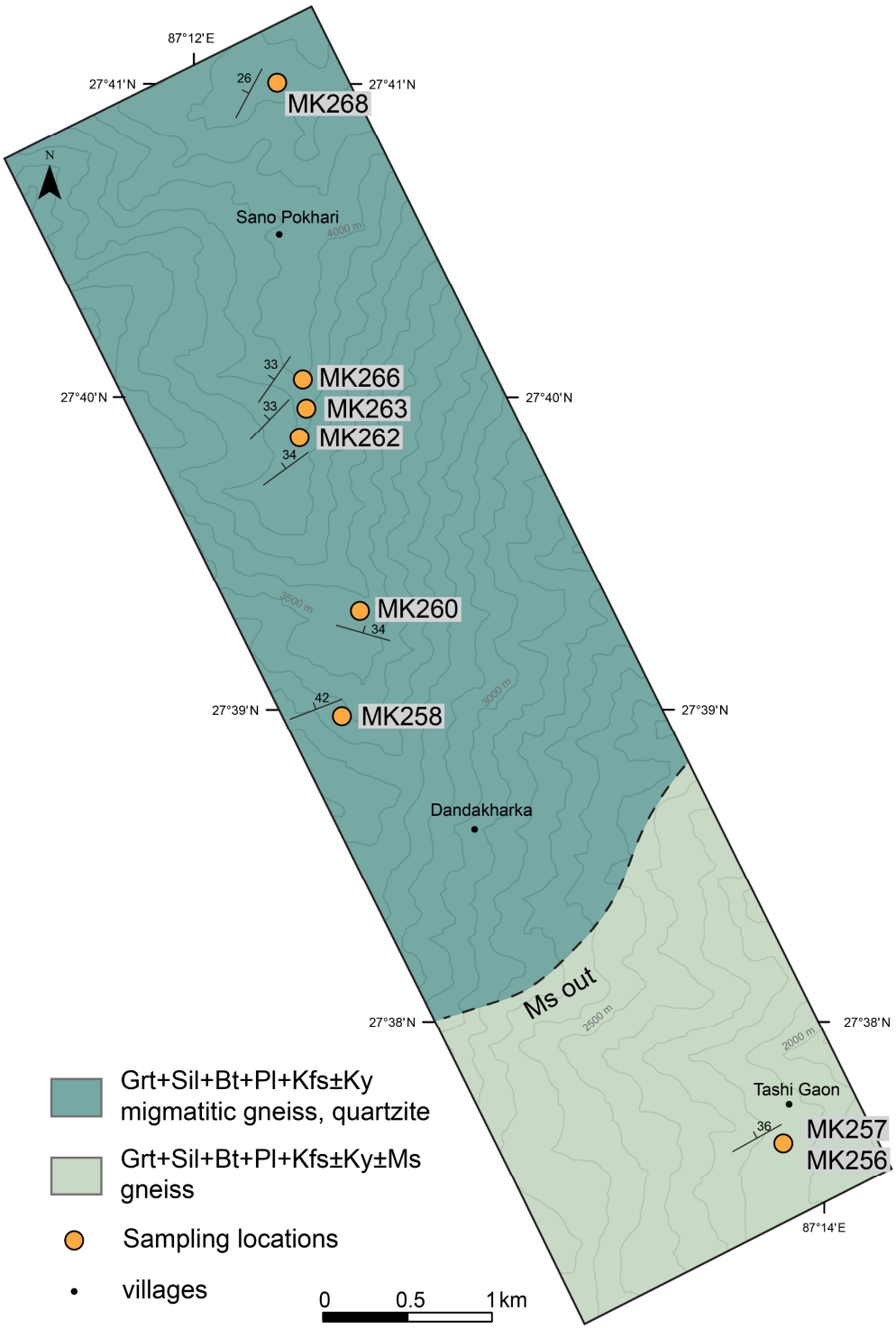

Figure 4.2. Simplified geological map of the investigated transect with sampling locations. Elevation contours are produced using digital elevation model AW3D30 obtained from Japan Aerospace Exploration Agency (JAXA). Ms out marks inferred muscovite isograd.

4.3 Analytical methods

4.3.1 Geochemistry

The whole-rock major element concentration in each of the specimens analysed was obtained through X-ray fluorescence (XRF) for use in thermodynamic modelling. Whole-rock XRF was performed at Pomona College using PanAnalytical Axios wavelength-dispersive X-ray fluorescence instrument following the method as outlined in Johnson et al., (1999).

µXRF maps of thin sections were used for identification and quantification of major mineral phases. Maps were acquired using Bruker M4 Tornado at the University of Laval with an accelerating voltage of 50 kV, a beam current of 600 mA, a step size of 20 µm with 5 ms dwell time.

Elemental X-ray maps of full thin sections and monazite grains, and quantitative elemental analysis on garnet and biotite were obtained using a Cameca SXFiveFE electron microprobe housed in the FiLTER facility at the University of British Columbia Okanagan (UBC-O). Elemental maps (Ce, Ca, P, Ti, and Y) were used to identify accessory minerals (primarily monazite) in thin sections. Thin section maps were obtained using an accelerating voltage of 15 kV, a beam current of 200 nA, a beam size of 40 µm, step size of 40 µm, and a dwell time of 20 ms. Monazite elemental maps of Ca, Si, Th, U, and Y were acquired using an accelerating voltage of 15 kV, a beam current of 200 nA, a beam size of 1 µm, step size of 1 µm, and a dwell time of 100 ms.

Quantitative elemental analysis on garnet and biotite was used to investigate major elemental changes across garnet grains, which was then incorporated into phase equilibria modelling. The analyses were acquired using an accelerating voltage of 15 kV, a beam current of 20 nA, a beam size of 0 µm (garnet) and 5 µm (biotite) with a dwell time of 30 s on the peak and 15 s on the background. The concentrations in oxide weight percent were converted to atom per formula unit (a.p.f.u) based on the stoichiometric atoms of oxygen in garnet (12O) and biotite (22O). Garnet endmembers, almandine (Alm), grossular (Grs), pyrope (Prp), and spessartine (Sps) were calculated as the following: Alm = $Fe^{2+}/(Fe^{2+}+Ca+Mg+Mn)$, Grs = $Ca/(Fe^{2+}+Ca+Mg+Mn)$, Prp = $Mg/(Fe^{2+}+Ca+Mg+Mn)$, Sps = $Mn/(Fe^{2+}+Ca+Mg+Mn)$, while garnet Mg# and biotite Mg# were calculated as Mg# = $Mg/(Fe^{2+}+Mg)$.

4.3.2 Petrochronology

Monazite grains in eight specimens were analyzed using the Laser Ablation Split Stream (LASS) system housed at the University of California, Santa Barbara, with Nu Plasma Multi Collector used for isotopic data collection, and Agilent ICP MS that collected trace element data. Laser settings include a beam size of 8 μm spot, a repetition rate of 3 Hz with 45 shots, and a laser fluence of 1.5 Jcm^{-2}. The method follows Kylander-Clark et al., (2013) with modifications as outlined in McKinney et al., (2015).

Isotopic data were normalized to primary reference material "44069" (424.9 ± 0.4 Ma $^{206}Pb/^{238}U$ ID-TIMS age; Aleinikoff et al., 2006), while "Bananeira" and "Trebilcock" were used as secondary reference material. A hundred and one analyses of "Bananeira" yielded a $^{206}Pb/^{238}U$ weighted mean of 512.4 ± 1.6 Ma, MSWD = 1.1 (511.7 ± 1.2 Ma ID-TIMS age; Horstwood et al., 2016), and a $^{208}Pb/^{232}Th$ weighted mean of 496.6 ± 1.5 Ma, MSWD = 1.49 (497.6 ± 1.6 Ma LA ICP-MS age; Kylander-Clark et al., 2013). Fifty-one analyses of Trebilcock yielded a $^{206}Pb/^{238}U$ weighted mean of 274.7 ± 1.2 Ma, MSWD = 1.60 (c. 279–285 Ma; Tomascak et al., 1996) and $^{208}Pb/^{232}Th$ weighted mean of 256.3 ± 1.1 Ma, MSWD = 1.64 (263.7 ± 1.0 Ma LA CP-MS age; Kylander-Clark et al., 2013). Trace element data were normalized to "Bananeira" and, based on repeat analyses of multiple secondary reference materials, are accurate to within 5% (2 SE, Cottle et al., 2018). Isotopic and trace element data were both processed using Iolite v.4 (Paton et al., 2011). Uncertainty propagation and concordia diagrams were produced using open source R-script ChrontouR (Larson, 2020), while histograms were produced using IsoplotR (Vermeesch, 2018). Dates older than Himalayan orogenesis (55 Ma) and/or dates associated with 2SE greater than 5 Ma are excluded from interpretation (Table B1). $^{208}Pb/^{232}Th$ dates are used for geochronological interpretations due to the problems in the $^{206}Pb/^{238}U$ system associated with excess radiogenic ^{206}Pb from unsupported ^{230}Th (Schärer, 1984).

4.4 Petrography

Identification of minerals and their textural relationship was performed using an optical polarizing microscope with an aid of μXRF maps. The specimens throughout the study (below) are described, analysed and interpreted in order from the structurally lowest specimen (MK256) to the structurally highest (MK268), with increasing specimen number.

All specimens analysed are garnet-sillimanite gneisses with a common assemblage of Qz, Kfs, Pl, Bt, Grt and Sil, where the amount of migmatite increases up the structural level.

The two structurally lowest specimens, MK256 (Grt + Bt + Kfs + Pl + Sil + Ky + Ms + Chl + Rt + Ilm + Ap + Mnz) and MK257 (Grt + Bt + Kfs + Pl + Sil + Ky + Ms + Chl + Rt + Ilm + Ap + Mnz) (Fig. 4.2) are the only specimens that contain muscovite, marking the upper limit of muscovite stability in this transect. Although they are both sampled from the same location, MK256 contains only sparse, small grains of muscovite (Fig. 4.3a), while muscovite in MK257 is more abundant. MK257 also shows distinct signs of chloritization of biotite and sericitization of feldspars indicating potential late hydrothermal alteration (Fig 4.3b, c). Both specimens have a schistose/gneissic texture, defined primarily by preferentially oriented mica. Garnet porphyroblasts are generally subhedral to anhedral. Most of the garnet has polymineralic inclusions (Fig. 4.3d) in addition to monomineralic inclusions of biotite, plagioclase and lobate quartz. Garnet are often replaced by biotite at the rims (Fig. 4.3e). Both MK256 and MK257 contain rare kyanite and both prismatic and fibrolite sillimanite (Fig. 4.3f). The sillimanite is commonly associated with biotite and quartz.

In specimen MK258 (Grt + Bt + Kfs + Pl + Sil + Rt + Ilm + Ap + Mnz) (Fig 4.2), foliation is defined by oriented biotite laths, which form alternating bands with quartz and plagioclase-rich layers. Garnet porphyroblasts are mostly anhedral and contain inclusions of biotite, lobate quartz, plagioclase and apatite as inclusions. The inclusions are generally restricted within cores and mantles and are commonly polymineralic (Fig. 4.3g). Garnet rims are typically replaced by biotite, especially in strain shadows (Fig. 4.3g). Sillimanite occurs as prismatic grains throughout the specimen (Fig. 4.3h), while K-feldspar are rare.

The foliation in specimen MK260 (Grt + Bt + Kfs + Pl + Sil + Ky + Rt + Ilm + Ap + Mnz) (Fig. 4.2) is defined by aligned biotite and sillimanite layers alternating with quartz-rich bands. K-feldspar and rare garnet, often fragmented and partially replaced by biotite and plagioclase, occur as augen/porphyroblasts. Garnet porphyroblasts contain inclusions of plagioclase, biotite and lobate quartz (Fig. 4.3i). Both prismatic and fibrolite sillimanite occur in the specimen, typically replacing biotite (Fig 4.3j). A single relict grain of kyanite was observed in the specimen and appears to be breaking down into plagioclase and minor biotite (Fig. 4.3k).

Specimens MK262 (Grt + Bt + Kfs + Pl + Sil + Ky + Chl + Rt + Ilm + Ap + Mnz) and MK263 (Grt + Bt + Kfs + Pl + Sil + Ky + Rt + Ilm + Mnz) (Fig 4.2) show distinct migmatitic textures with leucosomes at the hand specimen and outcrop scales. K-feldspar, quartz and plagioclase bands alternate with thin layers of biotite and sillimanite. Similar to previous specimens, garnet porphyroblasts contain polymineralic inclusions, typically quartz, plagioclase and an Al-rich material, as well as monomineralic plagioclase and lobate quartz (Fig.4.3l). Rare kyanite inclusions also occur in both specimens (Fig.4.3m). Garnet grains are often replaced by the biotite and sillimanite at the rims (Fig. 4.3m, n).

The structurally highest specimens examined in this study, MK266 (Grt + Bt + Kfs + Pl + Sil + Ky + Rt + Ilm + Ap + Mnz) and MK268 (Grt + Bt + Kfs + Pl + Sil + Ky + Rt + Ilm + Ap + Mnz) (Fig 4.2) are also migmatitic. K-feldspar, plagioclase and quartz layers alternate with preferentially oriented biotite and sillimanite, which together define the foliation. Both specimens contain kyanite grains in the matrix, while in MK266 kyanite also occurs as inclusions in garnet (Fig 4.3o). In addition, garnet porphyroblasts contain plagioclase, biotite, K-feldspar, quartz, and rutile as inclusions, which are often polymineralic. In MK268, garnet grains typically form aggregates, which are texturally indistinguishable from individual porphyroblasts, but recognisable in chemical μXRF maps (Fig. B1).

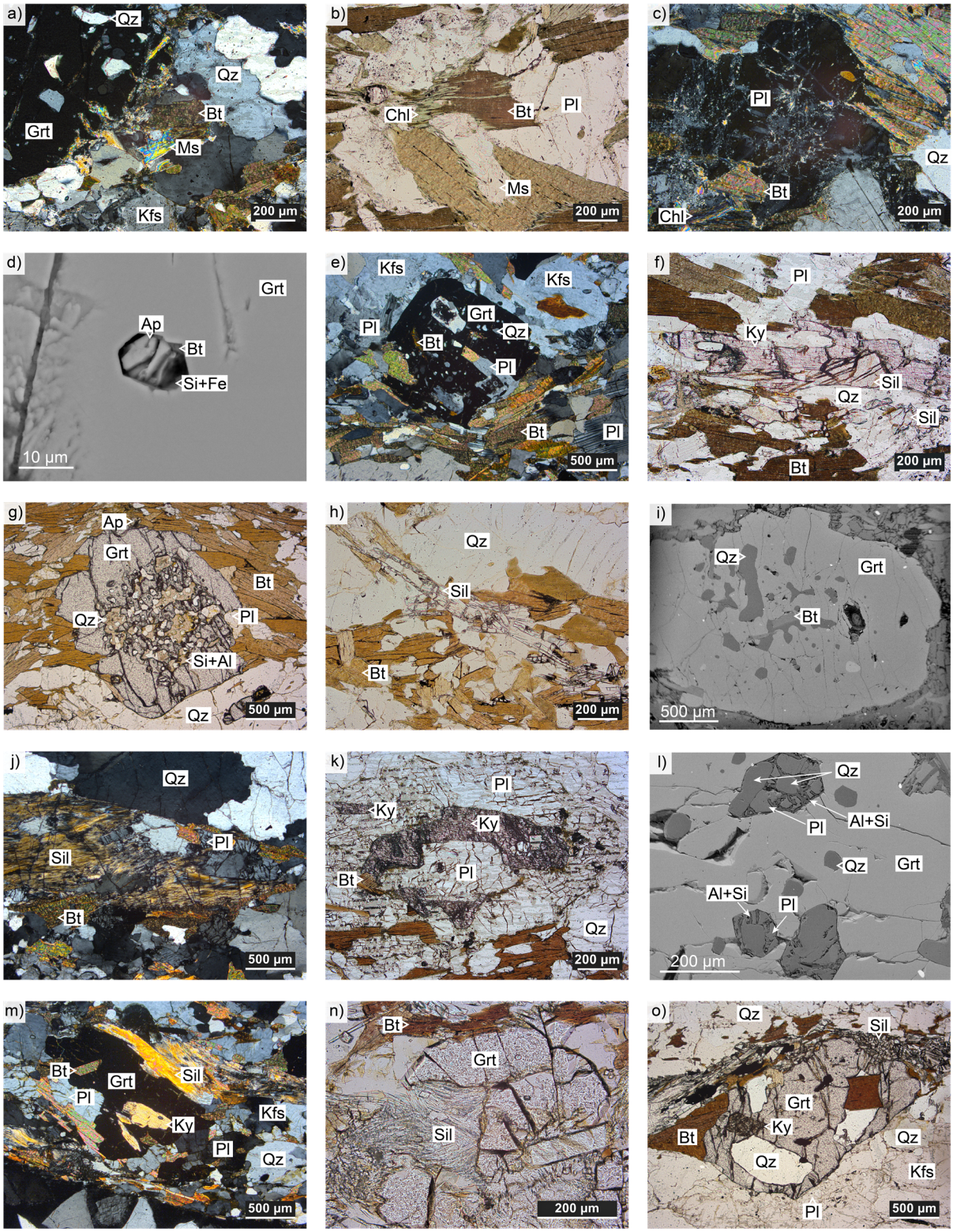

Figure 4.3. Photomicrographs and back-scatter electron images of analysed thin-sections; a) Sparse muscovite grains in the structurally lowest specimen (MK256). b) Hydrothermal alteration of biotite into chlorite (MK257). c) Sericitization of plagioclase and chloritization of

biotite (MK257). d) Polymineralic inclusions in garnet comprising apatite, biotite and Si, Fe - rich material (MK257). e) Breakdown of inclusion-rich, euhedral/subhedral garnet into biotite and plagioclase (MK256). f) Relict kyanite transitioning into sillimanite (MK256). g) Garnet containing inclusions of quartz, plagioclase and Al-rich material. Garnet rims are replaced by biotite and plagioclase (MK258). h) Prismatic sillimanite growing on top of the biotite (MK258). i) Garnet grain with biotite and lobate quartz inclusions (MK260). j) Fibrolite and prismatic sillimanite replacing biotite (MK260). k) Relict kyanite replaced by plagioclase and minor biotite (MK260). l) Inclusions of quartz, plagioclase in garnet, with Al-rich material filling the gaps (MK262). m) Biotite and kyanite inclusions in garnet, with sillimanite rimming the garnet (MK263). n) Garnet grain being replaced by sillimanite (Waters, 2001) (MK263), o) Kyanite and quartz inclusions in garnet. Garnet rims are being replaced by biotite and sillimanite (MK266).

4.5 Monazite petrochronology

Monazite petrochronological analysis is performed on all specimens. This enables the collection of age data and paired chemical composition from spatially distinct portions of the multiple grains in each specimen.

Specimen MK256

A total of 62 spot analyses were carried out on ten monazite grains including 53 spot analyses on eight monazite grains located in the matrix and nine spot analyses from two monazites in garnets. Analysed monazite grains range in size (long axis) from 35 - 115 μm (Fig. B2). Dates range from 33.2 ± 3.1 Ma to 13.9 ± 0.5 Ma (Fig. 4.4a, Table B1), with a dominant population at ca. 15.5 Ma (Fig. 4.5). Dates from monazites located in garnet are more restricted, ranging from 17.5 ± 0.9 Ma to 15.2 ± 0.5 Ma. Yttrium concentrations are generally lower in monazite domains that yielded older dates (>16 Ma) while it is higher in relatively younger monazite domains (ca. 16 Ma to 14 Ma) (Fig. 4.6a). The $(Gd/Yb)_N$ ratio is also lower in monazite domains that yielded older dates (>16 Ma), peaking at ca. 16 Ma and then decreasing towards ca. 14 Ma (Fig. 4.7a).

Specimen MK257

A total of 91 spot analyses were carried out on ten monazite grains. Analysed monazite grains range in size from 35 - 195 μm (long axis) and are all located in the matrix (Fig. B2). The majority of dates extracted range from 37.3 ± 2.8 Ma to 13.8 ± 0.2 Ma (Fig. 4.4b, Table B1). Only four spot analyses from one monazite grain yielded lower dates that range from 7.7

± 0.3 Ma to 5.7 ± 0.2 Ma (Table B1). The monazite dates form a dominant population at ca. 19 Ma, with a secondary population at ca. 16 Ma (Fig. 4.5). Monazite domains that yielded older dates (>23 Ma) are generally associated with low Y concentrations, while domains with dates between ca. 23 Ma and 14 Ma contain variable concentrations (Fig. 4.6b). The $(Gd/Yb)_N$ ratio is also relatively low in monazite domains with older dates (>23 Ma), and similarly varies from ca. 23 Ma to 14 Ma; however, there may be a minor weak decrease in this ratio from ca. 19 Ma to 14 Ma (Fig. 4.7b).

Specimen MK258

Nine monazite grains located in the matrix were analysed with a total of 144 spots. Analysed monazite grains range in size (long axis) from 60 - 250 µm (Fig. B2) yielding dates from 35.3 ± 2.7 Ma to 16.0 ± 0.6 Ma (Fig.4.4c, Table B1) with a dominant population ca. 21.5 Ma (Fig. 4.5). Yttrium concentrations in this specimen show a negative correlation with dates (i.e. the younger the date, the higher the Y concentration, Fig. 4.6c), while $(Gd/Yb)_N$ ratios are scattered for older dates, with a peak at ca. 21 Ma decreasing towards ca. 16 Ma (Fig. 4.7c).

Specimen MK260

A total of 147 spot analyses were carried out on eight monazite grains. Of those 145 spots were sampled in seven monazite grains in the matrix, and two spots were placed in one monazite inclusion in garnet. Analysed monazite grains range in size (long axis) from 20 - 470 µm (Fig. B2). The dates range from 34.7 ± 1.3 Ma to 13.9 ± 0.6 Ma (Fig.4.4d, Table B1), with a dominant population at ca. 18.5 Ma (Fig. 4.5). The analyses from the monazite inclusion in the garnet grain yield dates of 34.7 ± 1.3 Ma and 34.0 ± 1.0 Ma. Monazite domains that yielded older dates (>20 Ma) are associated with low Y concentrations, while from ca. 20 Ma to 14 Ma Y concentrations generally increase (Fig. 4.6d). $(Gd/Yb)_N$ ratios are also low in domains with older dates, with ratios peaking at ca. 19 Ma and decreasing towards ca. 14 Ma (Fig. 4.7d).

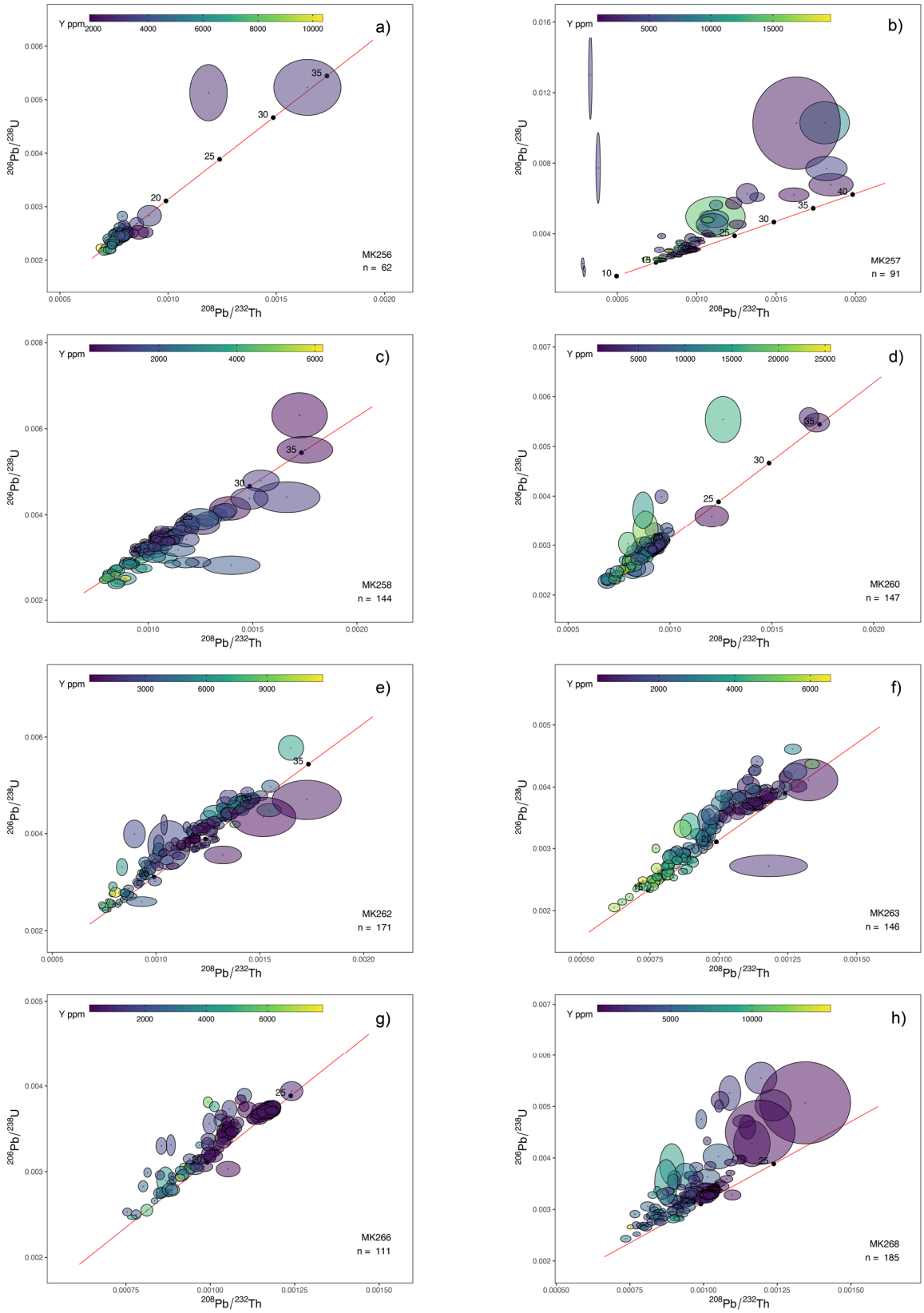

Figure 4.4. Concordia diagrams for analysed monazite in eight specimens.

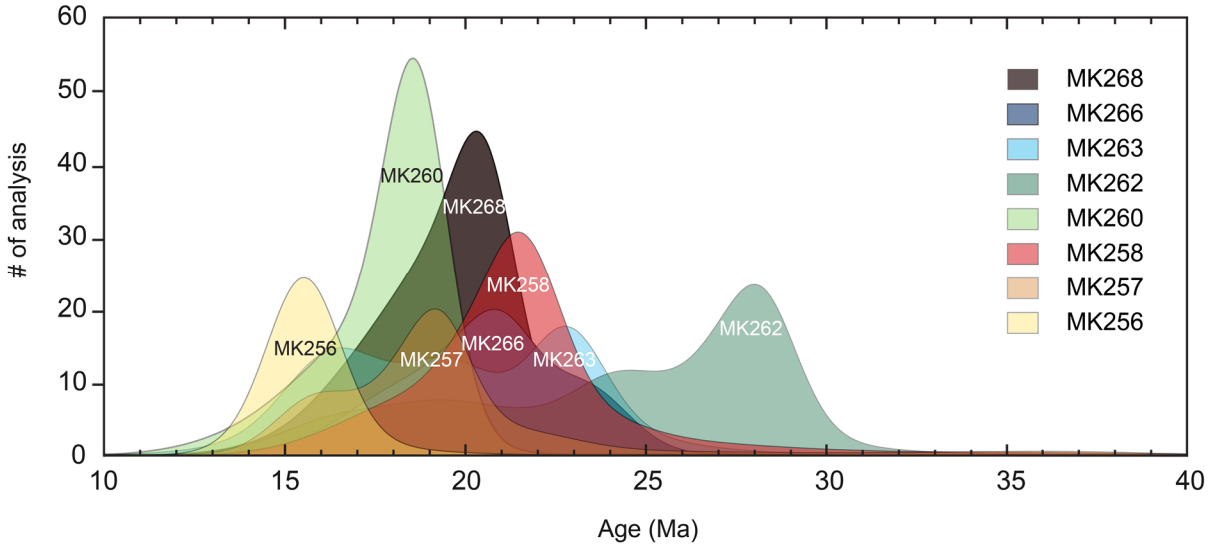

Figure 4.5. Monazite age probability diagram for all eight specimens.

Specimen MK262

Analyses were carried out on ten monazite grains with a total of 171 spots, out of which 147 spots were on six matrix monazite grains and 24 spots were on four monazite inclusions in garnet grains. Analysed monazite grains range in size (long axis) from 30 - 100 µm (Fig. B2). The dates returned span from 34.8 ± 3.4 Ma to 14.9 ± 0.4 Ma (Fig. 4.4e, Table B1), with a dominant population at ca. 28 Ma, and minor peaks at ca. 24 Ma and ca. 19.5 Ma (Fig. 4.5). Dates from the monazite grains in garnets range from 34.8 ± 3.4 Ma to 23.4 ± 0.4 Ma. Yttrium concentrations in monazite domains decrease from ca. 29 Ma to a low at ca. 23 Ma. Concentrations in monazite domains then increase until ca. 15 Ma, forming an overall "V" shape pattern (Fig. 4.6e). In contrast, the $(Gd/Yb)_N$ ratios mirror Y with low values associated with older dates, broadly increasing to ca. 24 Ma, and then decreasing until ca. 15 Ma (Fig. 4.7e).

Specimen MK263

A total of 146 spot analyses were carried out on ten monazite grains, with 34 of those spot analyses on three monazite grains located in garnet grains. Analysed monazite grains range in size (long axis) from 25 - 120 µm (Fig. B2). The dates returned range from 27.0 ± 0.5 Ma to 12.5 ± 0.4 Ma (Fig. 4.4f, Table B1), with three dominant peaks at ca. 23 Ma, 19.5 Ma, and 16 Ma (Fig. 4.5). Dates from monazite grains in garnets range from 26.8 ± 2.1 Ma to 20.8

± 0.4 Ma, with two younger dates of 17.0 ± 0.4 and 16.7 Ma ± 0.5 Ma. With the exception of two outliers, Y concentrations associated with the older dates are high and generally decrease until ca. 21 Ma, after which Y increases in monazite domains with younger dates (Fig. 4.6f). The $(Gd/Yb)_N$ ratios are variable, with the highest ratios at ca. 24 Ma followed by a general decrease towards monazite domains with younger dates, which are associated with the lowest ratios (Fig. 4.7f).

Specimen MK266

Seven monazite grains were analysed with a total of 111 spots. Out of those, 109 spot analyses were conducted on six matrix monazite grains and two spots on a single monazite grain located within the garnet. Analysed monazite grains range in size (long axis) from 30 - 210 µm (Fig. B2). $^{232}Th/^{208}Pb$ dates range from 25.1 ± 0.7 Ma to 15.2 ± 0.3 Ma (Fig. 4.4g, Table B1), with a dominant peak at ca. 21 Ma (Fig. 4.5). Dates from the monazite inclusions in garnet are 21.3 ± 0.7 Ma and 19.8 ± 0.5 Ma. Monazite domains with older dates generally have low Y concentrations, however, concentrations increase toward domains with younger dates after ca. 20 Ma (Fig. 4.6g). The $(Gd/Yb)_N$ ratios are variable but record a general decreasing trend towards domains that yielded younger dates (Fig. 4.7g).

Specimen MK268

A total of 185 spot analyses were carried out on ten monazite grains, out of which 151 spots were conducted in six matrix monazite grains and 34 spots analyses were carried out in four monazite inclusions in garnet. Analysed monazite grains range in size from 45 - 350 µm (long axis) (Fig. B2). The dates range from 27.2 ± 3.1 Ma to 14.9 ± 0.4 Ma (Fig. 4.4h, Table B1), with a dominant peak at ca. 20.5 Ma (Fig. 4.5). The dates from monazite inclusions range from 27.2 ± 3.1 Ma to 15.6 ± 0.3 Ma. Y concentrations record an increasing trend towards domains with younger dates (Fig. 4.6h), while the $(Gd/Yb)_N$ shows variability in domains with older dates, but generally decreases from ca. 20 Ma towards younger dates (Fig. 4.7h).

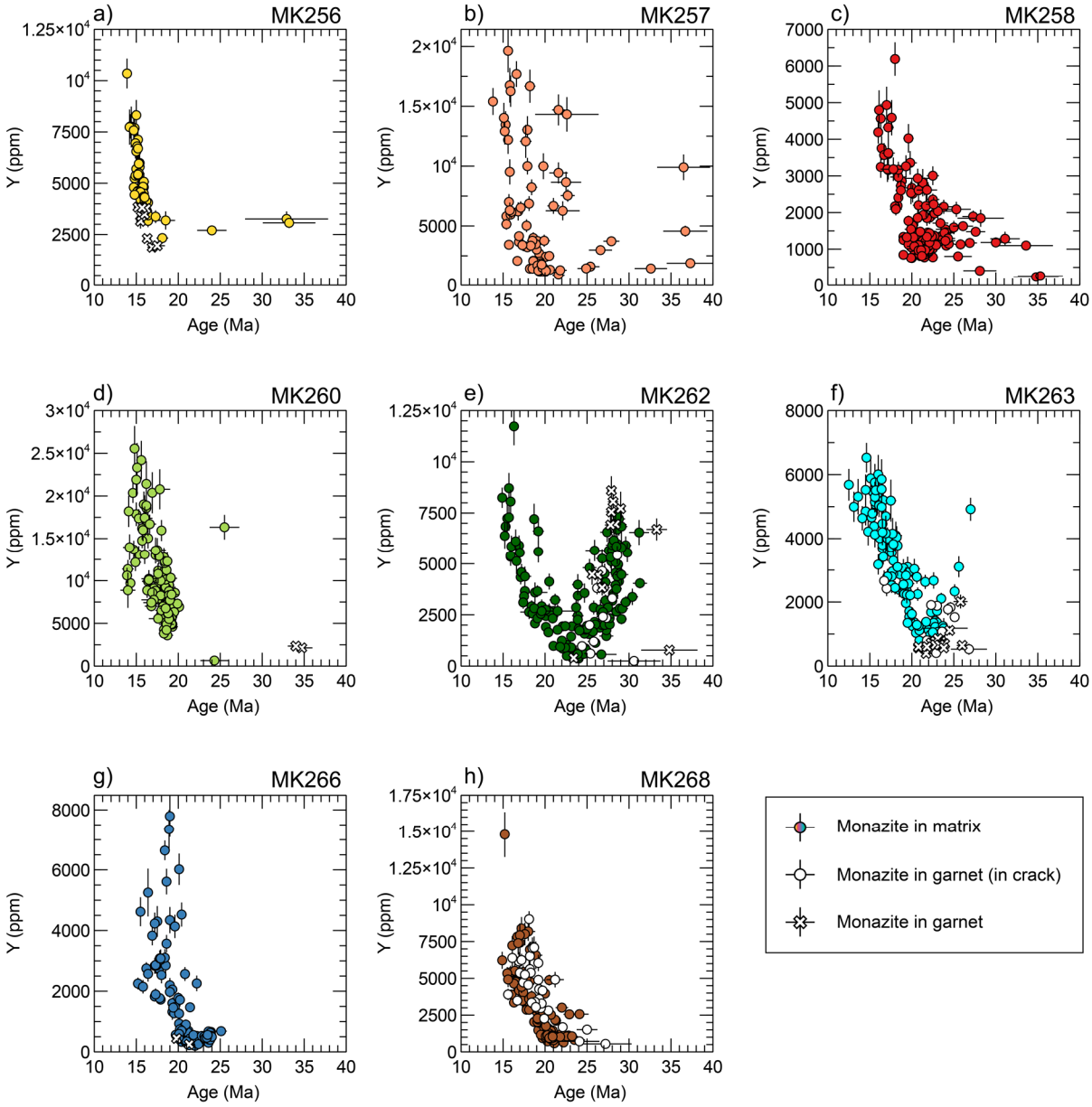

Figure 4.6. Y vs. age diagram for monazite.

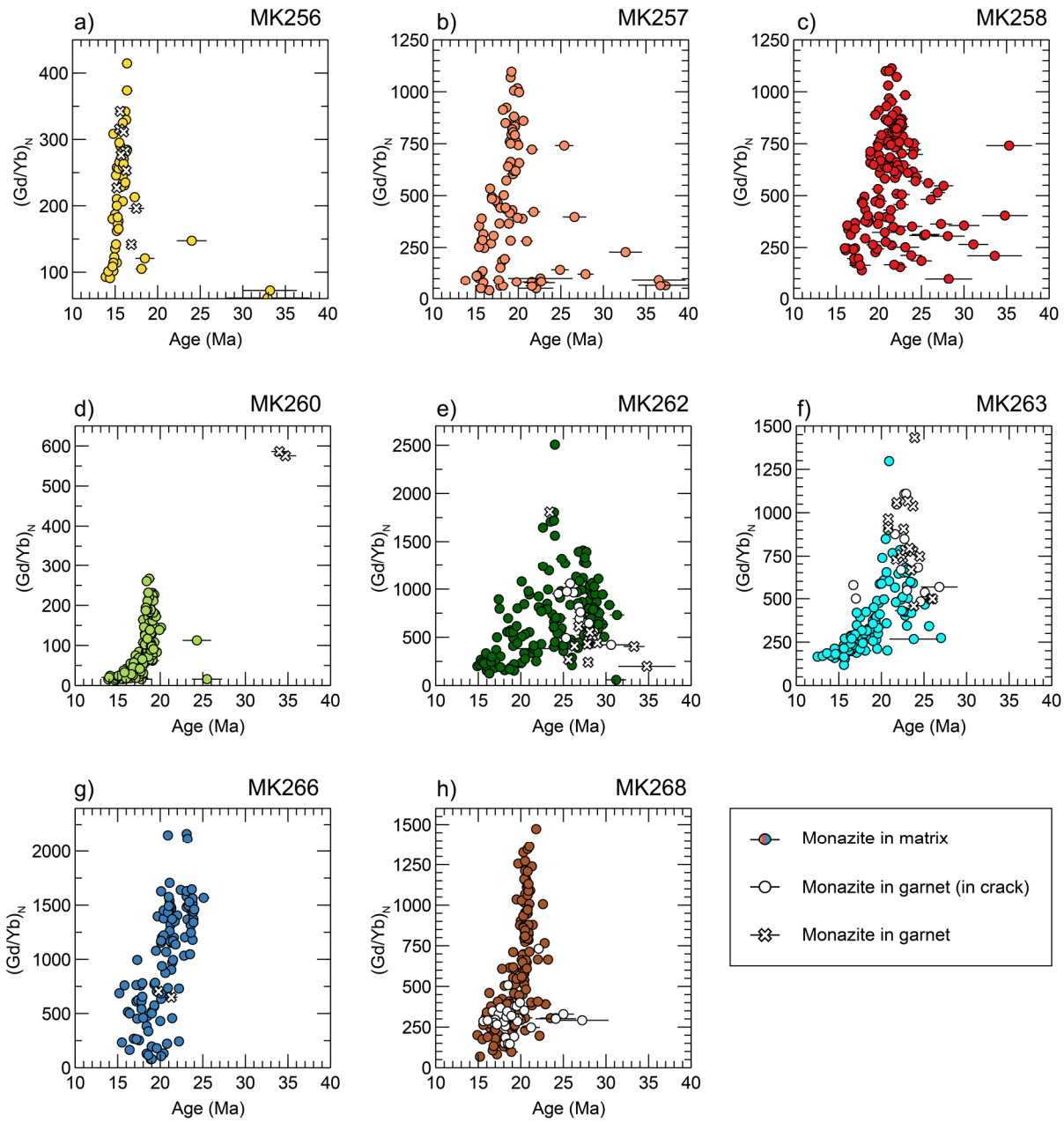

Figure 4.7. Gd/Yb vs. age diagram for monazite.

4.6 Mineral geochemistry

Four specimens (MK256, MK258, MK262 and MK268) were selected based on their spatial positioning and differences in geochronological data for further analysis using garnet and biotite mineral geochemistry, thermobarometry and phase equilibria modelling.

4.6.1 Garnet geochemistry

Garnet in specimen MK256 show flat or homogenized major element profiles with a composition of $Alm_{0.62-0.65}$, $Grs_{0.10-0.12}$, $Prp_{0.22-0.26}$, $Sps_{0.02}$, with upticks of $Alm_{0.66-0.71}$ and $Sps_{0.03-0.04}$, and downticks of $Grs_{0.09-0.11}$ and $Prp_{0.17-0.21}$ at the rims (Fig. 4.8, Table B2).

Specimen MK258 shows distinct chemical zonation in garnet, with the highest $Grs_{0.18-0.23}$ in cores decreasing towards rims ($Grs_{0.07-0.18}$) (Fig. 4.8, Table B2). In contrast, $Alm_{0.48-0.50}$ and $Prp_{0.26-0.30}$ record the lowest contents in garnet cores and increase towards rims ($Alm_{0.50-0.62}$, $Prp_{0.30-0.36}$). $Prp_{0.28-0.30}$ is also characterised by minor downticks at rims. $Sps_{0.02-0.03}$ in garnet from this specimen is flat across the grains.

Garnet investigated in specimen MK262 show similar flat profiles as those in MK256 with a composition of $Alm_{0.68-0.72}$ $Grs_{0.04-0.07}$ $Prp_{0.22-0.24}$ $Sps_{0.02}$, with a gradual uptick of $Alm_{0.71-0.75}$ and $Sps_{0.02-0.03}$, and downticks of $Grs_{0.04-0.05}$ and $Prp_{0.19-0.22}$ at the rims (Fig. 4.8, Table B2).

Garnet in specimen MK268 have well-preserved chemical zonation similar to the grains in MK258. $Grs_{0.16}$ is highest in cores and decreases towards rims ($Grs_{0.03-0.15}$) (Fig. 4.8, Table B2). $Alm_{0.61-0.62}$ shows the lowest concentration in grain cores and increases towards rims ($Alm_{0.62-0.79}$) while $Prp_{0.15-0.24}$ shows decreasing trend from one side of the garnet to the other. $Sps_{0.02-0.03}$ is flat across garnet grains, with minor uptick on one side of the garnet.

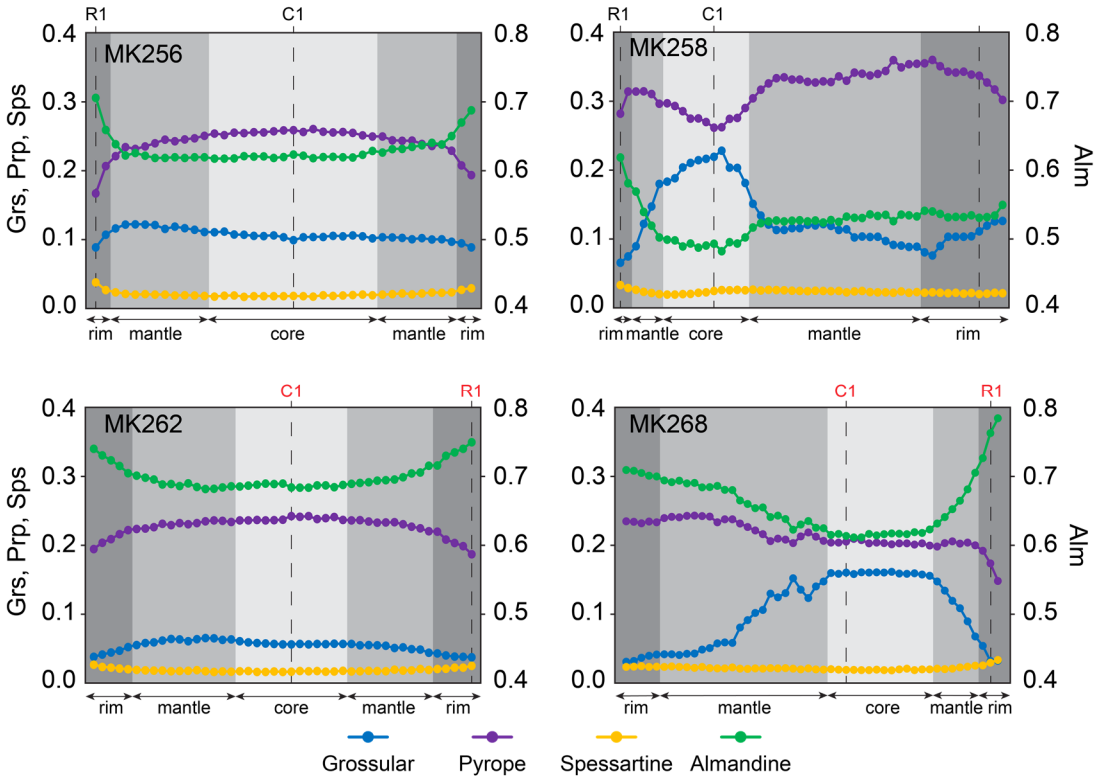

Figure 4.8. Garnet end-member profiles for four metamorphic specimens. C - core, R - rim.

4.6.2 Biotite geochemistry

Biotite grains are divided into two groups based on their textural position; 1) inclusions in the garnet, and 2) matrix, to explore potential differences in mineral geochemistry.

In specimen MK256, the chemical composition of biotite grains ranges in $XMg_{0.48-0.62}$ and $Ti_{0.22-0.43}$ a.p.f.u (Fig. 4.9, Table B3). Biotite inclusions in garnet generally have higher XMg and Ti a.p.f.u than those in the matrix (0.61-0.62 and 0.37-0.43 versus 0.48-0.51 and 0.31-0.38, respectively). Two spots from a single biotite inclusion in one garnet returned lower $XMg_{0.53-0.54}$ and lower of $Ti_{0.22}$.

In specimen MK258, biotite composition ranges in $XMg_{0.66-0.72}$ and $Ti_{0.25-0.33}$ a.p.f.u (Fig. 4.9, Table B3). Inclusions in garnet have higher $XMg_{0.70-0.72}$, and lower $Ti_{0.27-0.28}$ a.p.f.u., when compared to grains in matrix with $XMg_{0.66-0.69}$, and $Ti_{0.29-0.33}$ a.p.f.u.

The biotite in MK262 ranges in composition in $XMg_{0.49-0.55}$ and $Ti_{0.31-0.59}$ a.p.f.u (Fig. 4.9, Table B3). Two analyses on biotite inclusions in garnet have XMg of 0.51, and low $Ti_{0.45}$

$_{-0.46}$ a.p.f.u. The composition of matrix grains overlaps with the inclusions with a $XMg_{0.49-0.55}$, and $Ti_{0.31-0.59}$ a.p.f.u.

The composition of biotite in the structurally highest specimen, MK268, ranges in $XMg_{0.50-0.67}$ and $Ti_{0.38-0.66}$ a.p.f.u (Fig. 4.9, Table B3). Biotite inclusions in garnet have generally higher $XMg_{0.66-0.67}$, and lower $Ti_{0.38-0.54}$ a.p.f.u., than grains in the matrix $XMg_{0.50-0.54}$, and $Ti_{0.54-0.66}$ a.p.f.u.

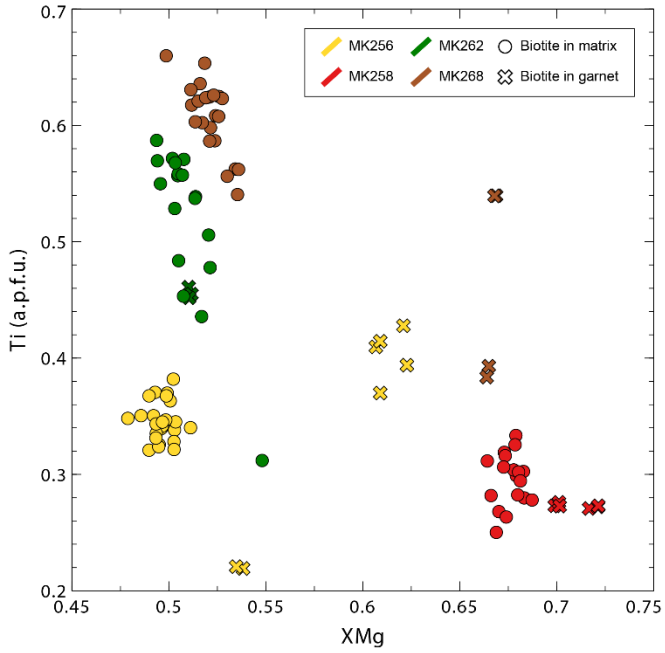

Figure 4.9. Ti vs XMg diagram for biotite in four specimens.

4.7 Phase equilibria modelling

Phase equilibria modelling was performed using the computer program Theriak Domino (de Capitani and Brown, 1987; de Capitani and Petrakakis, 2010) with the thermodynamic dataset of (Holland and Powell, 1998; updated in 2004) in the MnO - Na_2O - CaO - K_2O - FeO - MgO - Al_2O_3 - SiO_2 - H_2O - TiO_2 - Fe_2O_3 (MnNCKFMASHTO) system. Quartz, aluminosilicates, rutile and H_2O were modelled as pure phases, while solid solution models for plagioclase and K-feldspar (Holland and Powell, 1996, 2003), garnet and biotite (Mn - bearing model; White et al., 2005), muscovite (Coggan and Holland, 2002), chlorite (Mn - bearing model; Mahar et al., 1997; Holland and Powell, 1998) , magnetite-spinel (White et

al., 2000, 2005), ilmenite (White et al., 2002, 2005), cordierite, chloritoid, staurolite, talc and epidote (Holland and Powell, 1998) were used for the phase equilibria calculations.

4.7.1 Phase diagrams

As all specimens show evidence of partial melting (e.g. Shrestha et al., 2017), phase diagrams were constructed using bulk rock XRF composition with saturated solidus for garnet cores to replicate conditions during garnet core growth (e.g. Indares et al., 2008; Guilmette et al., 2011). Additional phase diagrams with calculated water contents (e.g. Indares et al., 2008; Guilmette et al., 2011) were generated and used to investigate garnet rims (Figs. 4.10-4.13, Table B4). To display both conditions, each diagram consists of two parts, one representing core growth and other rim growth (Figs. 4.10-4.13). P-T estimates were interpreted based on the intersection of garnet endmember isopleths taken from garnet domains. Garnet Mg# and Grs isopleths are primarily used to quantify the intersections, supported by Mg# of biotite where available. Garnet intersections within the phase diagrams are related to its within grain spatial position where C is used for garnet cores, and R for garnet rims (Figs. 4.8, 4.10). The assemblage where garnet core isopleths intersect represents the equilibrium assemblage for the initial bulk rock composition. To account for changes in equilibrium composition during each step of garnet growth, the effective bulk calculated by a step-by-step garnet fractionation is required (e.g. Gaidies et al., 2008). Moreover, due to intragranular diffusion within garnet grains at high temperatures, which affects the garnet endmember composition differently (e.g. Carlson, 2006; Vielzeuf et al., 2007), the isopleth intersection of compositions taken from intermediate domains in garnet would not reflect meaningful P-T conditions. Therefore, as garnet composition is at least partially homogenized in all specimens, garnet core intersections are taken as a minimum estimate of peak P-T conditions experienced by the rock (e.g. Shrestha et al., 2017; Warren et al., 2019). Rim intersections, however, may reflect equilibration of garnet with the final assemblage, providing the P-T information of the melt crystallization at or nearby the solidus (e.g. Indares et al., 2008; Guilmette et al., 2011; Groppo et al., 2012), especially when in agreement with biotite Mg# isopleths. Because of these recognized issues, the typical P-T path interpretations are avoided, and instead the P-T conditions are herein interpreted in the form of P-T estimates for cores and rims.

Specimen MK256

The observed assemblage in specimen MK256 is Grt + Bt + Kfs + Pl + Sil + Ky + Ms + Chl + Rt + Ilm + Ap + Mnz. Garnet core isopleths in specimen MK256 intersect at ~ 9.5 ± 0.5 kbar and 770 ± 25 °C in the Qz + Pl + Kfs + Grt + Bt + Sil + Rt + melt field (Figs. 4.10, B3), and is also consistent with Mg# of biotite inclusions in garnet (Fig. B3). This intersection plots at the assemblage which is at lower pressure than the observed assemblage containing kyanite, therefore, the P-T estimate is interpreted as a minimum peak estimate. Garnet rim isopleths intersect at ~ 9.0 ± 0.5 kbar and 760 ± 25 °C within uncertainty of the core composition, in the Qz + Pl + Kfs + Grt + Bt + Sil + Rt + melt field, and is consistent with the presence of sillimanite in the final assemblage (Figs. 4.10, B3).

Specimen MK258

The observed assemblage in specimen MK258 consists of Grt + Bt + Kfs + Pl + Sil + Rt + Ilm + Ap + Mnz. Garnet core isopleths in specimen MK258 intersect at ~ 12.5 ± 0.5 kbar and 680 ± 25 °C in the Qz + Pl + Grt + Bt + Ms + Rt + melt field (Figs. 4.11, B4). The field is inconsistent with the observed assemblage which contains K-feldspar grains, indicating that the peak assemblage should be at a higher temperature (Fig. 4.11). Therefore, these conditions are interpreted as a minimum peak P-T estimate. Garnet rim isopleths plot at ~ 8.0 ± 0.5 kbar and 730 ± 25 °C in Qz + Pl + Grt+ Bt + Sil/Ky + Rt + melt fields and intersect with Mg# of biotite in matrix. The lower, sillimanite field, is consistent with the presence of sillimanite in the assemblage (Figs. 4.11, B4).

Specimen MK262

The observed assemblage in specimen MK262 is Grt + Bt + Kfs + Pl + Sil + Ky + Chl + Rt + Ilm + Ap + Mnz. Garnet core isopleths in MK262 cross at ~ 10.0 ± 0.5 kbar and 750 ± 25 °C, mostly within the peak observed assemblage of Qz + Pl + Kfs + Grt + Bt + Ms ± Ky + Rt + melt (Figs. 4.12, B5) and consistent with the occurrence of relict kyanite in this specimen. Garnet rim isopleths intersect at ~ 7.0 ± 0.5 kbar and 740 ± 25 °C in the Qz + Pl + Kfs + Grt + Bt + Ilm + Sil + melt field at the solidus. Intersection in that field is compatible with the presence of sillimanite in the specimen and Mg# of biotite in matrix (Figs. 4.12, B5).

Specimen MK268

In specimen MK268, the observed assemblage is Grt + Bt + Kfs + Pl + Sil + Ky + Rt + Ilm + Ap + Mnz. Core isopleths from two garnets in MK268 plot at ~ 14.0 ± 0.5 kbar and 760 ± 25 °C in the peak assemblage field of Qz + Pl + Kfs + Grt + Bt + Ms + Rt + melt (Figs. 4.13, B6) and overlap with Mg# from biotite inclusions in garnet (Fig. B6). The observed assemblage consists of kyanite grains in the matrix, and therefore the intersected field may reflect either peak or minimum peak P-T conditions (Fig. 4.13). The rim isopleths plot at ~ 5.5 ± 0.5 kbar and 730 ± 25 °C in the Qz + Pl + Kfs + Grt + Bt + Ilm + Sil + melt field, which is compatible with the presence of sillimanite in the specimen and is consistent with the Mg# of biotite in matrix (Figs. 4.13, B6).

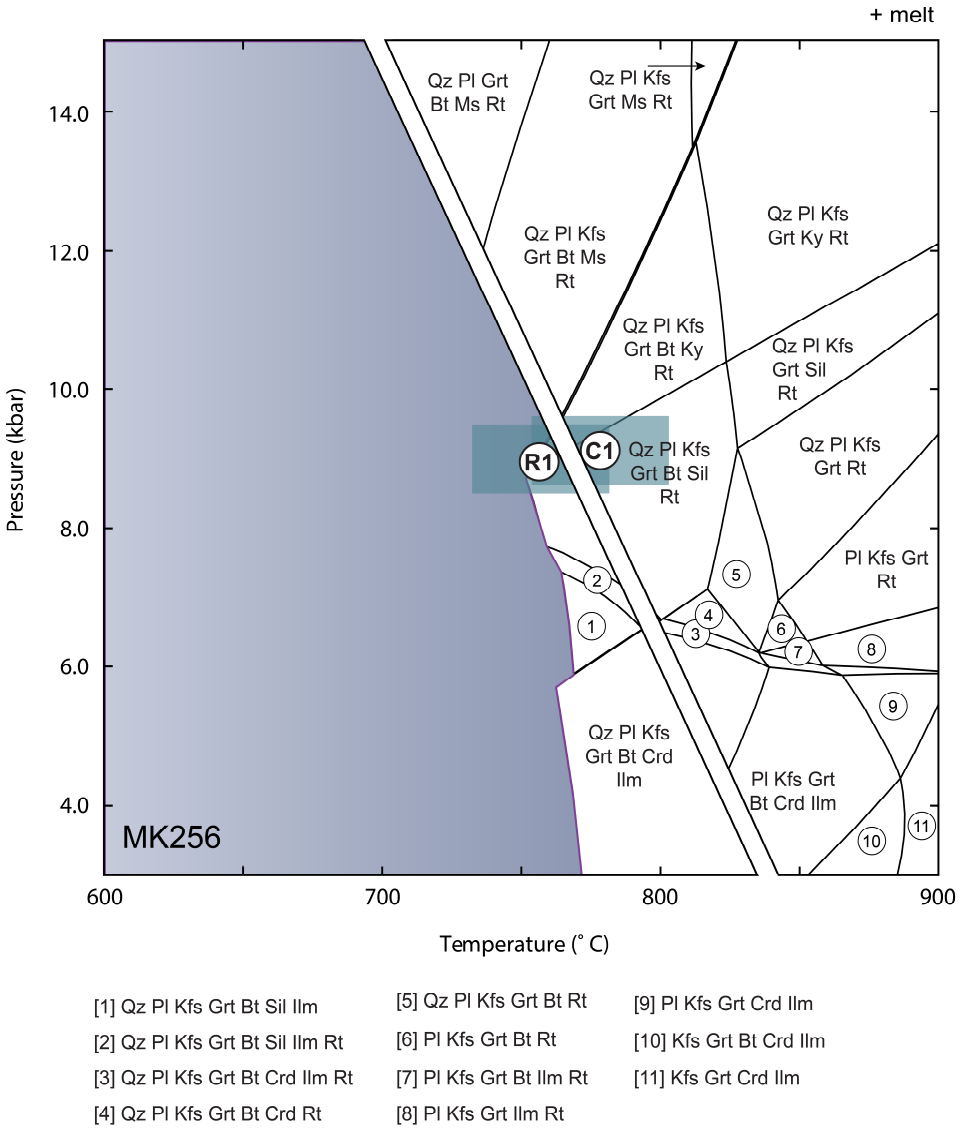

[1] Qz Pl Kfs Grt Bt Sil Ilm
[2] Qz Pl Kfs Grt Bt Sil Ilm Rt
[3] Qz Pl Kfs Grt Bt Crd Ilm Rt
[4] Qz Pl Kfs Grt Bt Crd Rt
[5] Qz Pl Kfs Grt Bt Rt
[6] Pl Kfs Grt Bt Rt
[7] Pl Kfs Grt Bt Ilm Rt
[8] Pl Kfs Grt Ilm Rt
[9] Pl Kfs Grt Crd Ilm
[10] Kfs Grt Bt Crd Ilm
[11] Kfs Grt Crd Ilm

Figure 4.10. Phase diagram for MK256. The phase diagram shows stability fields calculated with saturated solidus for garnet core (right), and calculated water for garnet rim (left). The saturated solidus is calculated at 14 kbar and 631.61 °C. The sub-solidus region is shaded. C - core, R - rim.

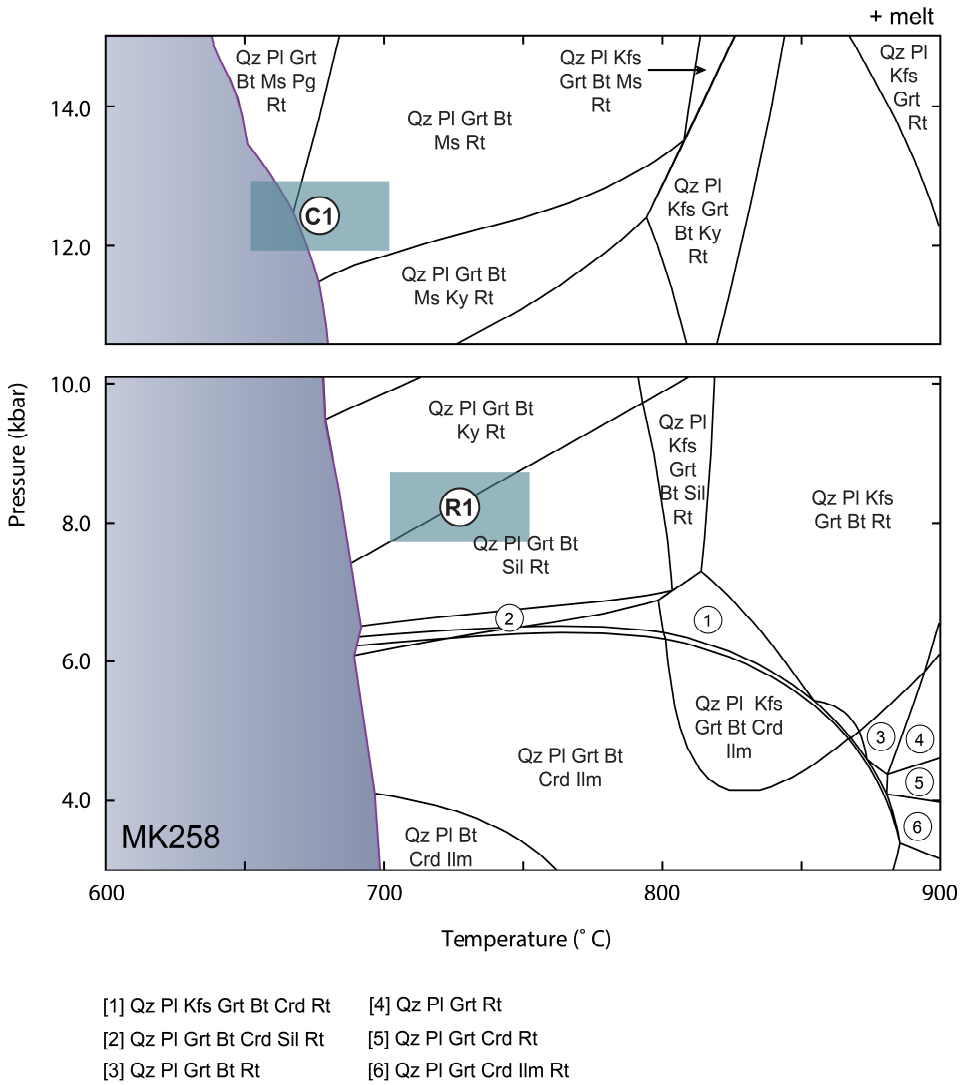

Figure 4.111. Phase diagram for MK258. The phase diagram shows stability fields calculated with saturated solidus for garnet core (top), and calculated water for garnet rim (bottom). The saturated solidus is calculated at 14 kbar and 639.81 °C. The sub-solidus region is shaded. C - core, R - rim.

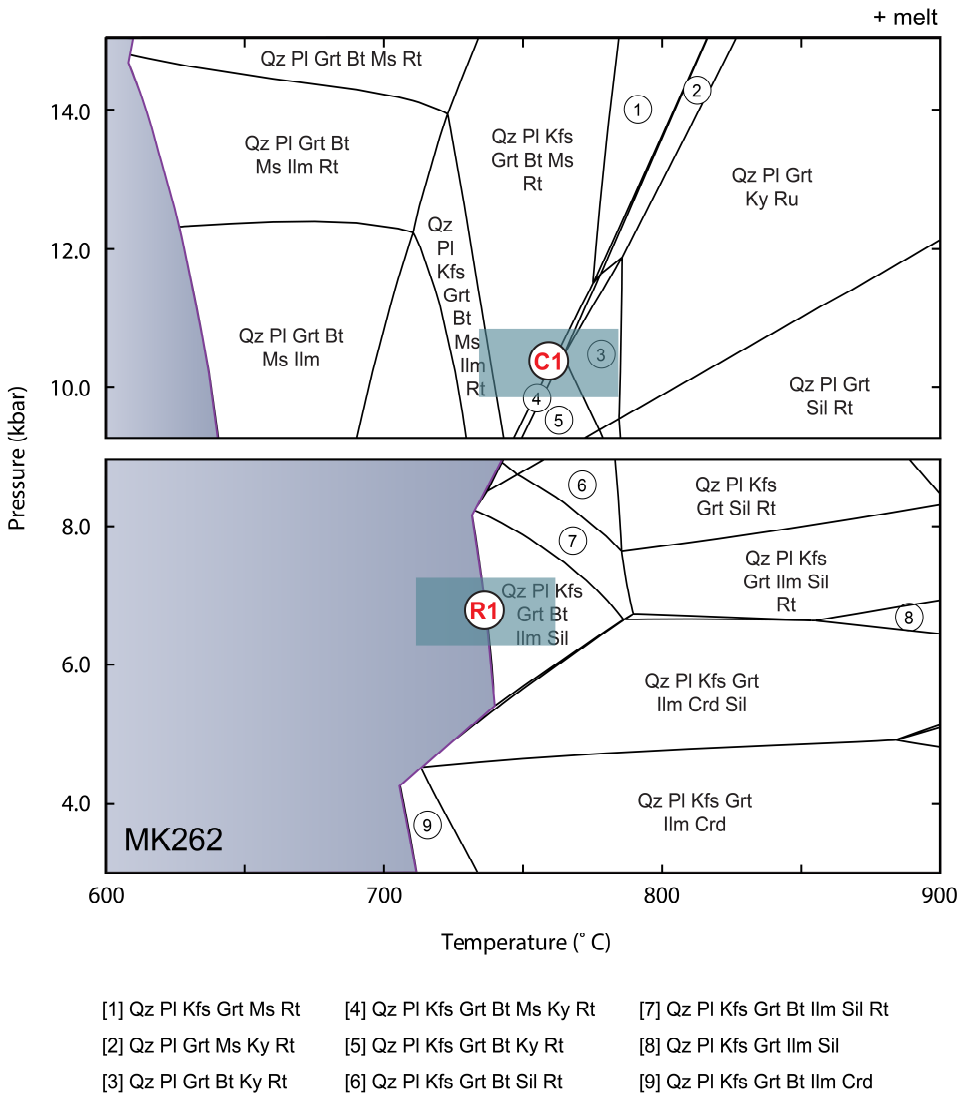

Figure 4.122. Phase diagram for MK262. The phase diagram shows stability fields calculated with saturated solidus for garnet core (top), and calculated water for garnet rim (bottom). The saturated solidus is calculated at 14 kbar and 614.09 °C. The sub-solidus region is shaded. C - core, R - rim.

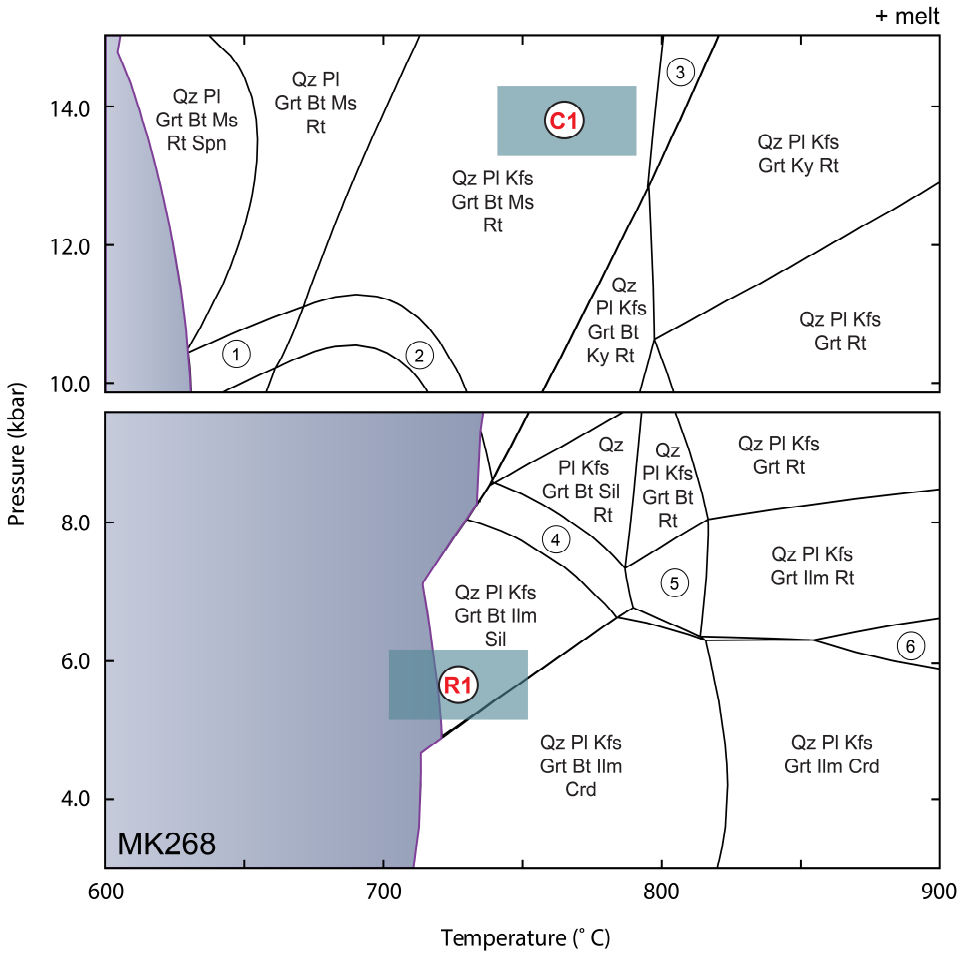

[1] Qz Pl Grt Bt Ms Ilm Rt
[2] Qz Pl Kfs Grt Bt Ms Ilm Rt
[3] Qz Pl Kfs Grt Ms Rt
[4] Qz Pl Kfs Grt Bt Ilm Sil Rt
[5] Qz Pl Kfs Grt Bt Ilm Rt
[6] Qz Pl Kfs Grt Ilm

Figure 4.133. Phase diagram for MK268. The phase diagram shows stability fields calculated with saturated solidus for garnet core (top), and calculated water for garnet rim (bottom). The saturated solidus is calculated at 14 kbar and 611.44 °C. The sub-solidus region is shaded. C - core, R - rim.

4.8 Interpretation

4.8.1 Garnet geochemistry

Flat or homogenized major element profiles from garnet in specimens MK256 and MK262 indicate intra-granular diffusion (Florence and Spear, 1991), while upticks of Alm and Sps are an indicator of retrograde diffusion (Kohn and Spear, 2000) (Fig. 4.8). In contrast, garnet grains in MK258 and 268 show distinct chemical zonation, although flat Sps may indicate intra-granular diffusion to some extent. Garnet in MK258 shows evidence of retrograde diffusion on one side (Kohn and Spear, 2000) (Fig. 4.8)

4.8.2 Timing of metamorphism

The garnet-monazite Rare Earth Element (REE) partitioning is often used to correlate the timing of garnet growth or breakdown with geochronological data obtained from monazite. In a rock where garnet and monazite are the main Heavy REE (HREE) sinks, HREE behaviour in these two minerals is expected to follow a general partitioning pattern (Hermann and Rubatto, 2003; Rubatto et al., 2006; Shrestha et al., 2017; Larson et al., 2019). During garnet growth, HREE in the system will preferentially incorporate into the garnet, resulting in increased HREE, and low $(Gd/Yb)_N$ ratio. In contrast, such behaviour leaves monazite low in HREE, and with a high $(Gd/Yb)_N$ ratio. When garnet ceases to grow and becomes stable, the HREE that are left in the system can incorporate into monazite. Similarly, if garnet breaks down, the HREE released from garnet may also be incorporated into any (re)crystallizing monazite. This results in increased HREE, and a decreased $(Gd/Yb)_N$ ratio in the monazite. Based on this relationship, the trace element geochemistry of monazite can serve as a link to garnet behaviour and may provide direct information on the timing of prograde and retrograde metamorphism (e.g. Foster et al., 2000, 2002; Larson et al., 2013; Regis et al., 2016).

In specimen MK256 the increase in $(Gd/Yb)_N$ in monazite from ca. 19 Ma indicates ongoing prograde metamorphism (correlated with garnet growth), which may have started as early as ca. 33 Ma based on older dates obtained from monazite in the matrix (Fig. 4.7a). The $(Gd/Yb)_N$ ratio starts to decrease after ca. 16 Ma indicating the beginning of retrograde metamorphism (garnet breakdown), however, the youngest monazite inclusion in garnet is dated at ca. 15 Ma, indicating that garnet was still growing at that time (Fig. 4.7a). Therefore, ca. 15 Ma is interpreted as a minimum estimate for the beginning of retrograde metamorphism

for this specimen. The last crystallization of monazite in this specimen is at ca. 14 Ma which is interpreted to record the timing of melt crystallization at the solidus (e.g. Kohn et al., 2005).

In MK257, an increase of $(Gd/Yb)_N$ ratio from ca. 37 Ma is interpreted to reflect ongoing prograde metamorphism during which garnet was growing (Fig. 4.7b). The decrease of the ratio after ca. 19 Ma indicates initiation of retrograde metamorphism, which continued until ca. 15 Ma when final monazite crystallization occurred (Fig. 4.7b). The four of very young monazite dates, ca. 8 - 6 Ma from a single monazite (Table B1) is interpreted to indicate monzite (re)crystallization during late-stage hydrothermal activity (Bollinger and Janots, 2006; Martin et al., 2015), which is consistent with the observation of sericitized feldspar and biotite chloritization in the specimen (Fig. 4.3b, c).

In MK258 a general trend of $(Gd/Yb)_N$ ratio increase is notable from ca. 35 Ma, which indicates that the prograde metamorphism was ongoing during that time (Fig. 4.7c). The $(Gd/Yb)_N$ ratio peaks and starts to decrease at ca. 21 Ma, indicating the beginning of retrograde metamorphism (Fig. 4.7c). The youngest monazite dates of ca. 16 Ma are interpreted to record the timing of final melt crystallization.

Monazite inclusions in garnet in MK260 provide the minimum estimate for ongoing prograde metamorphism for this specimen at ca. 35 Ma. Monazite of this age in MK260 are also characterized by high $(Gd/Yb)_N$ ratios (Fig. 4.7d). Peak $(Gd/Yb)_N$ ratios occur at ca. 18 Ma after which they decrease until ca. 14 Ma (Fig. 4.7d). The decrease in $(Gd/Yb)_N$ ratios is consistent with retrograde metamorphism from 18 to until final melt crystallization at ca. 14 Ma (Fig. 4.7d).

Monazite inclusions in garnet from MK262, show a gradual increase in $(Gd/Yb)_N$ ratio starting at ca. 35 Ma and extending to younger dates reflecting garnet growth and ongoing prograde metamorphism (Fig. 4.7e). The $(Gd/Yb)_N$ ratios decrease after ca. 24 Ma indicating that retrograde metamorphism started at ca. 24 Ma, which is consistent with the youngest date recorded in monazite inclusion in garnet (Fig. 4.7e). The youngest monazite dates extracted from this specimen are ca. 15 Ma, which are interpreted to reflect the timing of final melt crystallization.

The monazite $(Gd/Yb)_N$ ratio in MK263 increases from ca. 27 Ma until 21 Ma, indicating ongoing prograde metamorphism, which overlaps with the dates from monazite inclusions in the garnet (Fig. 4.7f). The youngest date from a monazite inclusion in the garnet

is ca. 20 Ma which broadly coincides with a decrease in $(Gd/Yb)_N$ and therefore the initiation of retrograde metamorphism (Fig. 4.7f). The youngest monazite population occurs at ca. 14 Ma, which is interpreted as the timing of final melt crystallization.

In MK266, the $(Gd/Yb)_N$ ratio in monazite is high from ca. 25 to ca. 20 Ma, which indicates ongoing prograde metamorphism during that time (Fig. 4.7g). The youngest monazite inclusion in garnet is dated at ca. 20 Ma, placing a maximum age for the initiation of retrograde metamorphism. The youngest population of monazite dates occurs at ca. 16 Ma and, as with the previous specimens, is interpreted to reflect the timing of final melt crystallization as the specimen crossed the solidus.

The oldest monazite dates from MK268, ca. 27 to 24 Ma, can be interpreted to reflect ongoing prograde metamorphism (Fig. 4.7h). The $(Gd/Yb)_N$ ratio in monazite reaches its highest value between ca. 23 and 20 Ma after which it decreases, indicating the initiation of retrograde metamorphism (Fig. 4.7h). The youngest population of monazite dates occurs at ca. 15 Ma and are interpreted to reflect final melt crystallization.

4.8.3 Tectonometamorphic evolution

Most specimens used for phase equilibria modelling (MK256, MK258, MK262 and MK268) contain polymineralic inclusions with various combinations of quartz, biotite, feldspar, apatite, rutile and Al-rich material indicating peritectic garnet growth (e.g. Indares et al., 2008; Guilmette et al., 2011). Specimen MK260, however, does not contain obvious polymineralic inclusions. Garnet porphyroblasts are sparse and those that are present are typically cracked. Garnet grains do, however, contain lobate quartz inclusions, which are often an indicator of coeval growth of garnet and quartz in the presence of melt (Waters, 2001). In all four specimens, therefore, at least some portions of garnet grew in suprasolidus conditions, which is consistent with the phase equilibria modelling results for each specimen.

Specimen MK256 records minimum estimate of peak metamorphism at ~ 9.5 ± 0.5 kbar and 770 ± 25 °C. While the geochemical evidence of prograde history in garnet in this specimen has been erased at high temperature, older ages of ca. 20 - 15 Ma and single dates of ca. 25 and 33 Ma obtained from monazite may indicate timing for prograde metamorphism. Based on the interpretation of $(Gd/Yb)_N$ ratios in monazite and the age of monazite included in garnet rims, the age of ca. 15 Ma with peak $(Gd/Yb)_N$ ratios can be interpreted as the timing

for peak metamorphism for this specimen. The 14 Ma indicates the timing of final melt crystallization at the solidus.

Specimen MK258 records minimum peak P-T estimate at ~ 12.5 ± 0.5 kbar and 680 ± 25 °C, however, based on the presence of Kfs in the observed assemblage, the peak P-T must have been in the higher temperature range. The monazite dates from this specimen record a protracted growth. Based on the increasing $(Gd/Yb)_N$ ratios in the monazite, the prograde metamorphism is interpreted to occur between ca. 35 and 21 Ma, where ca. 21 Ma marks the time of peak metamorphism. The younger ages, ca. 21-16 Ma, are interpreted to reflect the retrograde metamorphism where ca. 16 Ma indicates the final melt crystallization.

Specimen MK262 records minimum peak P-T conditions of ~ 10.0 ± 0.5 kbar and 750 ± 25 °C. The increasing $(Gd/Yb)_N$ ratios in monazite dated from ca. 35 - 24 Ma may indicate ongoing prograde metamorphism. The ca. 24 Ma associated with the highest $(Gd/Y)b_N$ ratios is taken as the minimum estimate for the timing of peak metamorphism and the beginning of the retrograde metamorphism. The youngest dates, ca. 15 Ma, are interpreted to reflect final melt crystallization at the solidus.

Specimen MK268 records minimum peak P-T estimate of ~ 14.0 ± 0.5 kbar and 760 ± 25 °C. Due to the scarce prograde record in monazites, the older age of ca. 27 - 20 Ma can be interpreted as minimum timing for prograde metamorphism in this specimen. Peak monazite $(Gd/Yb)_N$ ratios at ca. 20 Ma are interpreted as the minimum age for the peak metamorphism and the beginning of the retrograde metamorphism. $(Gd/Yb)_N$ ratios decrease between ca. 20 Ma and 15 Ma indicating ongoing retrograde metamorphism with the final melt crystallization at ca. 15 Ma at the solidus.

4.9 Discussion

4.9.1 Tectonometamorphic discontinuities

Phase equilibria modelling and monazite petrochronology in this study help outline the differences in metamorphic P-T conditions and the timing of metamorphism across the investigated transect. Distinct differences in metamorphic and geochronologic history between specimens are consistent with the existence of tectonometamorphic discontinuities within the HMC in the Makalu region. Based on petrochronological interpretation of monazite and phase equilibria modelling obtained from this study, the rock specimens can be broadly divided into

four rock packages (Fig. 4.14). From south to north, structurally upwards, Package I includes specimen MK256, Package II includes specimens MK257, MK258 and MK260, Package III includes specimen MK262, and Package IV consists of specimens MK263, MK266 and MK268.

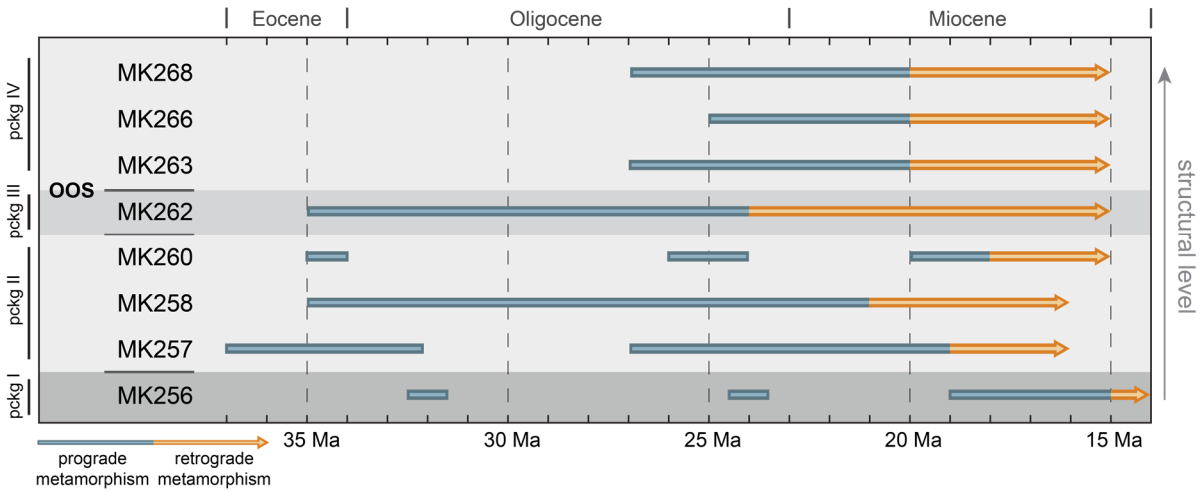

Figure 4.144. Summary diagram with timing of prograde and retrograde metamorphism. Shades of grey represent different rock packages with inferred discontinuities between them.

Each package of rocks records a distinct metamorphic and geochronological history. In Package I, early to late Oligocene ages record prograde metamorphism followed by mid-Miocene decompression and/or cooling starting at ca. 15 Ma (Fig. 4.14). Package II rocks show a protracted record of prograde metamorphism during the early Eocene to early Miocene (Fig. 4.14). The decompression and/or cooling in Package II occurred during the early Miocene starting at ca. 21 - 18 Ma. Package III also records protracted prograde metamorphism during the early Eocene and Oligocene (Fig. 4.14). The retrograde evolution for this package started significantly earlier, at ca. 24 Ma (Fig. 4.14). Lastly, Package IV, comprising the structurally highest rocks evaluated, preserves attenuated prograde metamorphism in the late Oligocene to early Miocene (Fig. 4.14). This is followed by the retrograde metamorphism during early- to mid-Miocene time starting at ca. 20 Ma (Fig. 4.14).

Based on the above observations, it can be argued that each package records unique metamorphic evolution with differences in the timing of their retrograde metamorphic

histories. As indicated above, these data require at least three metamorphic discontinuities in the Makalu-Arun region (Fig. 4.14).

4.9.2 Tectonic interpretation

Most of the rock packages in the Makalu-Arun have a variably preserved record of old monazite dates (Figs. 4.6, 4.7, 4.14), consistent with dissolution and recrystallization of monazite at higher temperatures (e.g. Kohn et al., 2005). The earliest record of prograde metamorphism is preserved within Packages II and III, which indicate prograde metamorphism was ongoing at ca. 35 Ma (Fig. 4.14). Prograde metamorphism continued in these packages until at least ca. 20 Ma and ca. 24 Ma respectively. Package IV does not appear to preserve a complete prograde history, however it does record the transition from prograde to retrograde metamorphism at ca. 20 Ma. Package I is significantly different from the rest of the transect, recording prograde metamorphism until ca. 15 Ma.

Based on the similarities in the timing of prograde metamorphism and the initiation of retrograde metamorphism, we argue that the rocks from Package II and IV may have been part of a single rock package during at least ca. 27 - 20 Ma (Fig. 4.15). The initiation of retrograde metamorphism and exhumation of Package III rocks that started ca. 24 Ma is interpreted to reflect overthrusting (and associated erosion) of Packages II and IV (Fig. 4.15), helping drive prograde metamorphism in those rocks. The present configuration with Package IV rocks structurally above the Package III rocks, however, is not compatible with that interpretation. The juxtaposition of Package IV above Package III, therefore, most likely reflects the occurrence of an out-of-sequence thrust (Figs. 4.14, 4.15). Similar out-of-sequence thrusts have been recognized in the adjacent Kanchenjunga region (Imayama et al., 2010, 2012; Ambrose et al., 2015;) and elsewhere along the orogen (e.g. Grujic et al., 2002; Warren et al., 2011; Larson et al., 2016, 2020a; Larson, 2018). The timing of retrograde metamorphism in Packages II, III and IV was ongoing between 20 - 15 Ma indicating that all three packages were being exhumed at this time. This retrograde metamorphism overlaps with prograde metamorphism of Package I and is consistent with over thrusting of the composite Package II, III, IV thrust sheet driving crustal thickening. Implicit in this interpretation is that the out-of-sequence juxtaposition of Packages III and IV likely post-dates overthrusting of Package I.

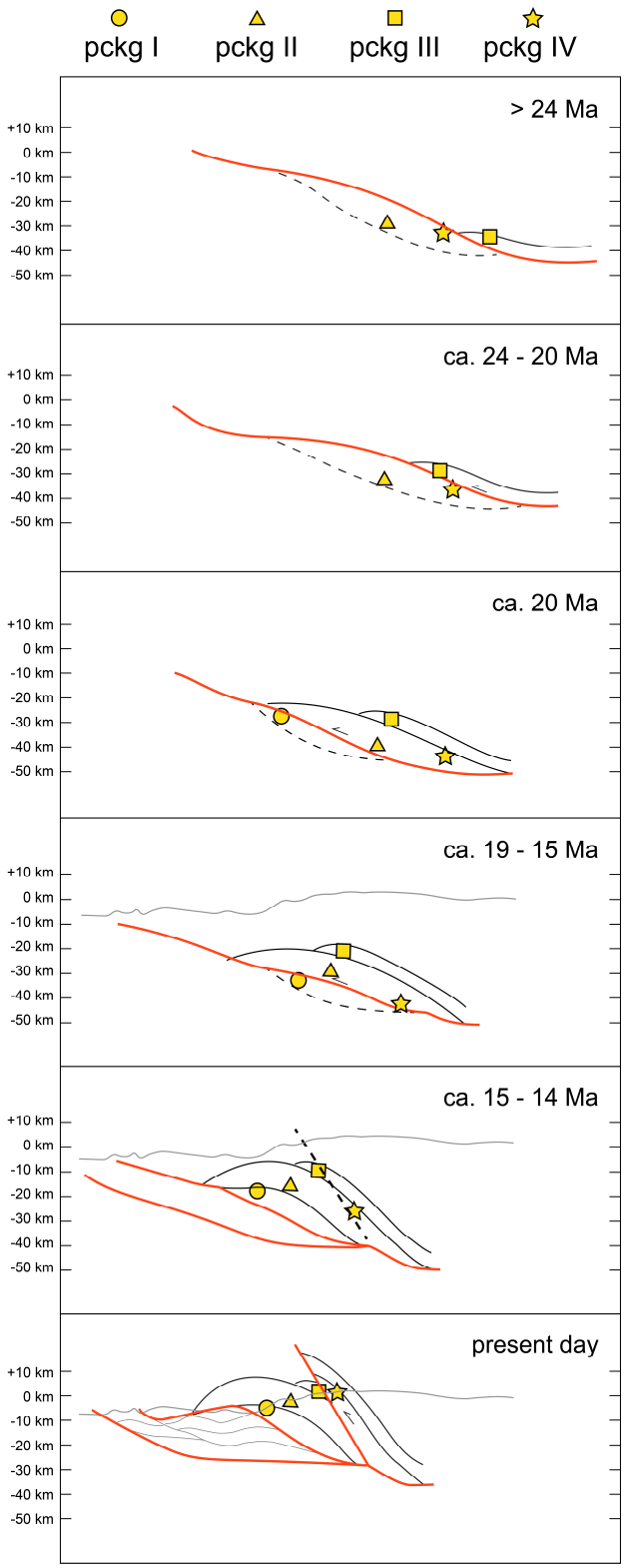

Figure 4.155. Proposed tectonic model for the Makalu-Arun region. Package I - MK256, Package II - MK257, MK258, MK260, Package III - MK262, Package IV - MK263, MK266, MK268.

4.9.3 Implications and regional comparison

At least three discontinuities are inferred within the Sil-zone of the HMC in the Makalu-Arun region. The identification of these discontinuities demonstrates the complexity of the metamorphic history and assembly of the HMC. The foreland migration and juxtaposition of thrusts as interpreted in this study are consistent with models that show underplating, metamorphism and exhumation of materials through the orogenic cycle (He et al., 2015; Larson et al., 2015). It is also broadly consistent with the thermomechanical models (HT111, Jamieson et al., 2006) of the Himalaya, which shows juxtaposition of vertical slices towards foreland during the evolution of the Himalaya, though such models do not explicitly predict out-of-sequence structures.

Similar studies on the opposite side of the Arun window and farther east in the Kanchenjunga region, have also inferred multiple discontinuities along those transects. In the Arun window, Groppo et al., (2009) inferred two discontinuities within structurally lower, St- and Ky-zones, however the lack of geochronological data in that study hinders the comparison with our study. In the Kanchenjunga region, Ambrose et al., (2015) inferred five thrust sense discontinuities primarily based on geochronological data. The out-of-sequence thrust from current study, however, is not comparable to the out-of-sequence thrust in Ambrose et al., (2015), which was identified as the High Himalayan thrust (HHT), structurally equivalent to the HHT thrust in Goscombe et al., (2006). The HHT in Ambrose et al., (2015) was inferred based on the differences in the timing of prograde metamorphism where the prograde metamorphism of footwall and hanging wall initiated in the middle Eocene and late Oligocene, respectively. The thrust activity was, therefore, inferred at ca. 20 - 18 Ma, where the retrograde metamorphism in the hanging wall initiated earlier than in the footwall. However, herein, the thrust activity is inferred at ca. 14 Ma.

In the same area in the Kanchenjunga region, (Imayama et al., 2010) inferred the HHT within Sil zone (Ms-absent), just below Crd-in isograd, based on decreasing pressure from inferred footwall rocks relative to the hanging wall, which display petrographic evidence of isothermal decompression and contain cordierite. The timing of the inferred HHT is, however, interpreted based on the zircon geochronology between structurally lower footwall migmatite in Sil+Ms zone and migmatite in Sil-zone, just below Crd-in isograd, but still interpreted as representative migmatite of HHT shear zone (Imayama et al., 2012). The activity of HHT was

interpreted to be from ca. 27 - 19 Ma as a thrust, and ca. 18 - 6 Ma as normal fault reactivation, however, the same thrust was interpreted in (Larson et al., 2017) as equivalent to the structurally highest in-sequence thrust in Ambrose et al., (2015), rather than the HHT.

The record of the HHT from across the Himalaya includes movement on the HHT in the western Himalaya as an early in-sequence thrust (late Oligocene - early Miocene), while in the eastern Himalaya it has been interpreted recognized as a late out-of-sequence thrust (late/middle Miocene) (see Larson et al., 2015; Montomoli et al., 2015). Furthermore, throughout the Himalaya, this position of the HHT itself is inconsistent, inferred to occur at different structural levels and between rock packages of variable P-T conditions and timing. The along-strike variability in how the HHT is interpreted prevents meaningful lateral correlations. It is possible, even likely, that the HHT is not a single structure and as such attempting to correlate it across hundreds or thousands of kilometers may not be possible. The structural complexity outlined in this study and many other similar works seems to indicate the development of discontinuities may reflect local factors more-so than regional factors.

4.10 Summary

Mineral geochemistry, monazite petrochronology and phase equilibria modelling highlighted differences in tectonometamorphic history within the Sil-zone gneisses in the HMC of the Makalu-Arun region. At least three thrust-sense discontinuities, separating four rock packages, have been identified based on distinct geochronologic and metamorphic history. The oldest inferred thrust was active from ca. 24 - 20 Ma, followed by in-sequence thrusting at ca. 20 - 15 Ma. A late out-of-sequence thrust cross-cuts the older thrust slices and post-dates retrograde metamorphism on all rock packages. Foreland propagation of in-sequence thrusts in this study is consistent with thermomechanical “channel flow” and duplexing models.

Chapter 5 Contact metamorphism of the Tethyan Sedimentary Sequence, Upper Mustang region, west-central Nepal

5.1 Background

The Himalayan orogen is the result of the ongoing collision between the Indian and Asian continental plates, which initiated at ca. 55 Ma (e.g. Klootwijk et al., 1992; Hu et al., 2016). The processes that have governed the evolution of this collisional system have been studied intensively for the past four decades, resulting in a myriad of different tectonic models (e.g. Jamieson et al., 2004, 2006; Kohn, 2008; Larson et al., 2010a, 2015; Cottle et al., 2015; He et al., 2015 and references therein). The vast majority of Indian-affinity rocks exposed in the southern portion of the Himalaya, even those from the highest summits (e.g. Corthouts et al., 2016), have been extensively investigated (e.g. Kohn, 2014a; Martin, 2017b; Kellett et al., 2019). Previous work has resulted in an improved understanding of the processes responsible for the assembly of the Himalaya and the evolution of large, hot orogens in general (e.g. Law et al., 2006). Yet, despite the effort made to examine the Himalaya, some parts of the mountain belt remain understudied as a result of inaccessibility or past political obstacles. These under-explored regions represent knowledge gaps that hinder the evolving knowledgebase of the Himalaya and potentially hold new discoveries to be made.

One such area is the Upper Mustang region, situated in west-central Nepal (Fig. 5.1a, b). Access to this border area has long been restricted to foreigners, making it one of the most scientifically isolated regions of Nepal. One of the few studies to have been completed in the Upper Mustang outlined the 'Upper Mustang massif' (UMM; Hurtado, 2002), an inferred domal culmination comprising two plutonic bodies locally flanked by amphibolite-facies metamorphic rocks (Fig. 5.1c), and interpreted to reflect regional metamorphism correlative to exhumed, former mid-crustal rocks exposed in structural windows in southern Tibet and along the Himalayan front. A second study that examined the same rocks yielded a contrasting interpretation. Based largely on thermobarometry, Guillot et al., (1995a) argued that metamorphism of rocks surrounding the Mugu leucogranite resulted from contact metamorphism.

Erroneous association of metamorphic conditions to inferred processes may impact not only basic interpretations, such as the structural position of the rocks within the crust, but also models that describe the geological evolution of an area or the broader orogen. Fortunately, the Upper Mustang area has recently become more accessible, enabling a targeted investigation of the igneous and metamorphic rocks in this area. In this study, we examine the crystallization of the Mugu pluton and employ classical thermobarometry, trace-element analysis and monazite petrochronology on the surrounding metamorphic rocks to assess the conditions and timing of metamorphism, to test whether these rocks formed under contact or regional metamorphic conditions, and to provide meaningful comparisons with potentially similar features elsewhere within the orogen.

5.2 Local geological setting

The Upper Mustang region is situated in the northern part of west-central Nepal (Fig. 5.1a–c). The area is primarily underlain by the Tethyan Sedimentary Sequence (TSS), which comprises Permo-Carboniferous (meta)shale, limestones and quartzites along with leucogranite plutons and local exposures of amphibolite-facies metamorphic rocks (e.g. Fort et al., 1982; Colchen, 1999; Guillot et al., 1995a; Hurtado, 2002; Le Fort and France-Lanord, 1995). The TSS is separated from the structurally lower, medium to high-grade metamorphic rocks of the Greater Himalayan Sequence by the South Tibetan detachment system (STDS), a system of top-to-the-north-sense, N-dipping faults (Kellett et al., 2019). The Annapurna detachment, the local ductile manifestation of the STDS, has been mapped along the southern boundary of the region (Fig. 5.1c, Godin et al., 2001). The Upper Mustang region is host to a series of N - S striking, high-angle normal faults including the SE-dipping Dangardzong fault (Fig. 5.1c), which is the master fault to the Thakkhola graben. The graben extends from the STDS in the south almost to the Indus-Tsangpo suture zone in the north (e.g. Hurtado et al., 2001; Searle, 2010) and has accommodated E - W extension since at least middle Miocene time (e.g. Coleman and Hodges, 1995; Hurtado, 2002; Larson et al., 2020b).

The Upper Mustang region hosts two adjacent plutonic bodies, the Mugu and the Mustang granites (Le Fort and France-Lanord, 1995). While the Mustang pluton is located entirely within the Upper Mustang, the Mugu pluton extends laterally over 150 km to the NW, into the adjacent Dolpo region. In previous studies, Mugu intrusive rocks have been described

as K-feldspar + plagioclase + muscovite + tourmaline ± garnet ± biotite ± sillimanite leucogranite with local diopside xenocrysts (Le Fort and France-Lanord, 1995; Hurtado, 2002). Reported crystallization ages of the Mugu pluton range from 20.8 ± 0.7 Ma to 17.6 ± 0.3 Ma (Harrison et al., 1999; Hurtado, 2002).

Guillot et al., (1995a) reported thermobarometric constraints from garnet + staurolite + sillimanite schists in the vicinity of the Mugu pluton yielding garnet–biotite thermometry temperatures of 440 ± 30 °C to 575 ± 20 °C and pressures of 3.1 ± 0.8 kbar based on garnet - biotite - muscovite - plagioclase and garnet - plagioclase - aluminium silicate - quartz barometry. These conditions were interpreted to reflect contact metamorphism at a depth of 12 ± 2 km.

In the present work, the timing and conditions of metamorphism of metasedimentary rocks in the vicinity of the Mugu pluton were examined to test previous interpretations about their affinity. Five specimens of garnet ± sillimanite ± staurolite mica schists, UM04, UM05, UM07, UM08 and UM09 were sampled at distances of 476, 445, 361, 296 and 22 m, respectively, from the contact of the Mugu pluton (Fig. 5.1d, e). The geometry of the Mugu pluton beneath the surface is unknown and therefore aerial distances to the nearest observed contact were used for data interpretation. At the contact, the Mugu pluton intrudes and crosscuts the schists with no evidence of a shear zone in the vicinity (Larson et al., 2020b). Foliation in the schist dips moderately to steeply to the SE or SW, while lineations plunge shallowly to moderately to the east (Fig. 5.1d), defined by macroscopic quartz tails around porphyroblasts. Further away from the pluton, the exposed country rock is phyllitic; however, the lithologic transition is obscured by ground cover. In addition to the metamorphic specimens, two leucogranite specimens, GG10 and GG12, collected from the Mugu pluton were also analysed. Petrography, major- and trace-element geochemistry, classical thermobarometry and monazite petrochronology were performed on metamorphic specimens, while basic petrography and monazite geochronology are reported for the igneous specimens.

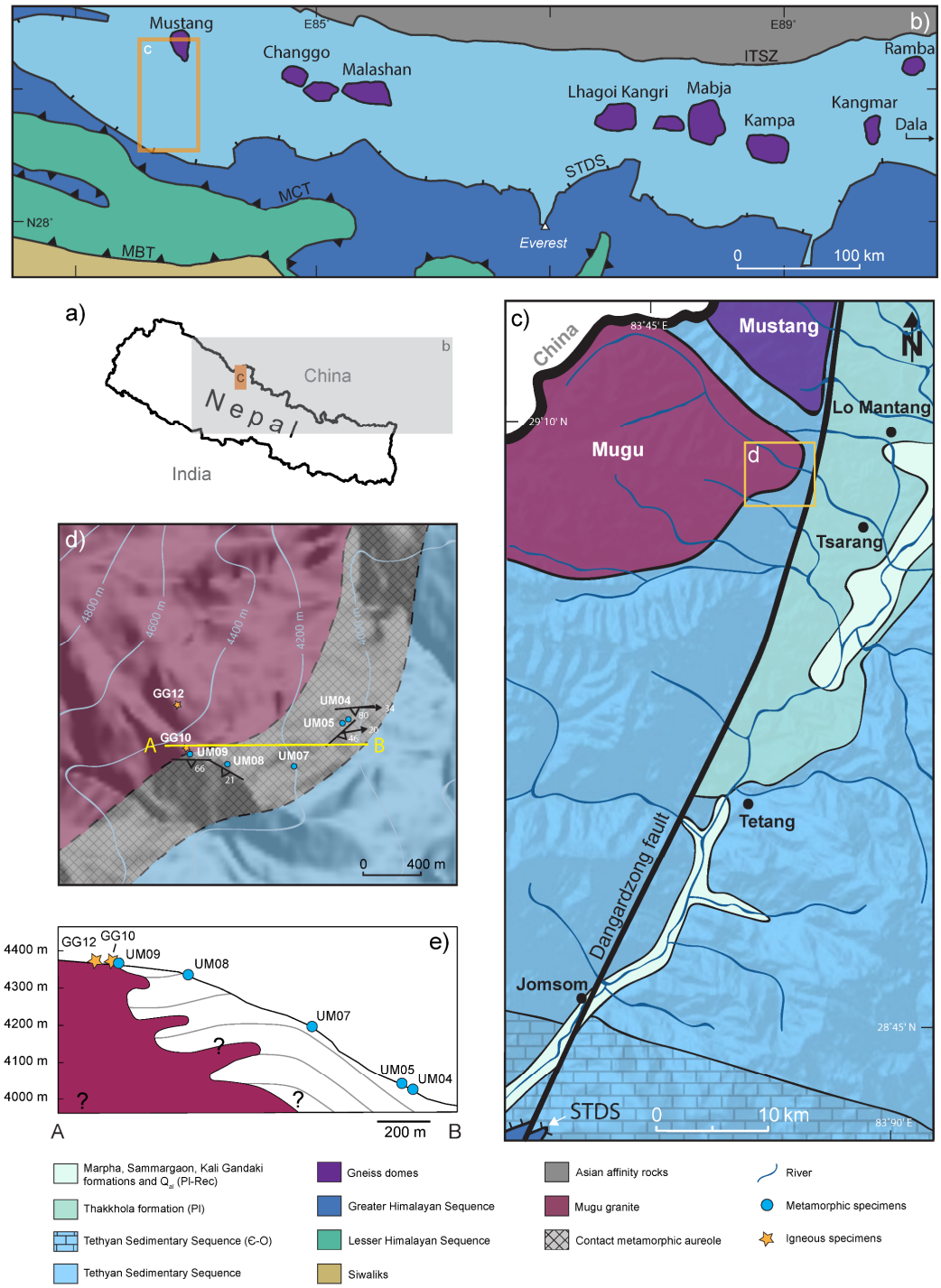

Figure 5.1. Geological map of the study area. a) Location of the study area on the map of Nepal. b) Simplified geological map with the locations of the North Himalayan domes and leucogranites (modified from Larson et al., 2020b after Burchfiel et al., 1992; Lee et al., 2011, 2004; Guo et al., 2008; Quigley et al., 2008; Larson et al., 2010b; Carosi et al., 2013;). c) Simplified geological map of study area (modified after Hurtado et al., 2001); elevation model was provided by Japan Aerospace Exploration Agency. STDS – South Tibetan Detachment

System. d) Sampling locations of igneous and metamorphic rocks. e) Cross-section of the study area.

5.3 Analytical methods

5.3.1 Petrography and mineral geochemistry

All specimens were examined optically using a polarizing microscope in thin-sections cut parallel to the lineation and perpendicular to the foliation.

High-resolution X-ray thin-section maps (Si, Al, Fe, Mg, Ca, Na, K, Mn, Ce, P, Y) were acquired using a Cameca SXFiveFE electron microprobe housed in the FiLTER facility at the University of British Columbia Okanagan (UBCO) using an accelerating voltage of 15 kV, a beam current of 200 nA, a beam size of 20 µm and a step size of 20 µm with a dwell time of 15 ms.

Quantitative major-element geochemistry was measured using the same instrument, with an accelerating voltage of 15 kV, a beam current of 20 nA, a beam size of 5 µm and a dwell time of 30 s on the peak and 15 s on background. Spot data were collected for garnet, biotite, muscovite and plagioclase (Table C1). In addition, qualitative elemental distribution maps of Fe, Ca, Mg and Mn were also generated for selected garnet porphyroblasts with an acceleration voltage of 15 kV, a beam current of 200 nA, a beam size of 5 µm and a step size of 5 µm with a dwell time of 15 ms.

Elemental concentrations were converted from oxide weight percent (wt %) to atom per formula unit (a.p.f.u.) based on the stoichiometric atoms of oxygen in each mineral: garnet, 12O; biotite and muscovite, 22O; and feldspar, 8O. Garnet and feldspar end-members were calculated as almandine (Alm) = Fe^{2+} / (Fe^{2+} + Ca + Mg + Mn), grossular (Grs) = Ca / (Fe^{2+} + Ca + Mg + Mn), pyrope (Prp) = Mg / (Fe^{2+} + Ca + Mg + Mn), spessartine (Sps) = Mn / (Fe^{2+} + Ca + Mg + Mn), anorthite (An) = Ca / (Ca + Na + K), albite (Ab) = Na / (Ca + Na + K) and orthoclase (Or) = K / (Ca + Na + K). The Mg content (XMg) in biotite and muscovite was calculated as XMg = Mg / (Mg + Fe^{2+}).

Garnet trace-element data for two specimens, UM07 and UM09, were obtained in situ using a Photon Machines Analyte 193 Excimer laser paired with a ThermoScientific Element XR inductively coupled plasma – mass spectrometer (ICP-MS), while garnet trace-element data for three specimens, UM04, UM05 and UM08, were obtained using the same laser, but a

Thermo X-series2 quadrupole ICP-MS. The analytes included rare earth elements (REEs; La, Ce, Pr, Nd, Sm, Eu, Gd, Tb, Dy, Ho, Er, Tm, Yb, Lu) and Y. ^{29}Si was used as an internal standard. NIST SRM 612 was used as a primary reference material, while NIST SRM 610 was used as a secondary control. Spot analysis was performed with a spot size of 29.6 µm, a repetition rate of 8 Hz, and laser fluence of 6.78 Jcm^{-2}. Background analysis was set to 60 s, in addition to ablation of 50 s and a 10 s washout. Data reduction for specimens UM07 and UM09 was carried out using Glitter (v.4.4.2, Macquarie University), while Iolite (v.2.5, Paton et al., 2011) was used for specimens UM04, UM05 and UM08. Uncertainties are reported at 1 standard error (SE) (Table C2).

5.3.2 Monazite (petro)chronology

Monazite grains from igneous specimens were separated using standard crushing, hydrodynamic, magnetic and density separation, then mounted in epoxy resin (Struers Epofix kit) and polished to expose grain centres at the University of California Santa Barbara (UCSB), while monazite grains from metamorphic specimens were analysed directly in polished thin sections. X-ray monazite maps (Y, Ca, La, Th, U) from metamorphic specimens were acquired using a Cameca SX-100 electron microprobe housed at UCSB using an accelerating voltage of 20 kV, a beam current of 200 nA and a dwell time of 100 ms. Monazite grains were analysed with a spot size of 8 µm, a repetition rate of 4 Hz and a laser fluence of 1.7 Jcm^{-2} for 25 s using the Laser Ablation Split Stream (LASS) system at UCSB. The detailed methodology is described in Cottle et al., (2012, 2013) and Kylander-Clark et al., (2013) with modifications as outlined in McKinney et al., (2015).

The igneous and metamorphic monazite were analysed in two separate sessions. Isotopic data of monazite in igneous rocks were normalized to '44069' (424.9 ± 0.4 Ma ^{206}Pb/^{238}U isotope dilution – thermal ionization mass spectrometer (ID-TIMS) age; Aleinikoff et al., 2006), while 'Bananeira' and 'Trebilcock' were used as secondary reference materials. A total of 26 repeat analyses of 'Bananeira' yielded a weighted mean ^{206}Pb/^{238}U date of 507.3 ± 1.3 Ma, mean square weighted deviation (MSWD) = 0.7 (511.7 ± 1.2 Ma ID-TIMS age; Horstwood et al., 2016) and a weighted mean ^{208}Pb/^{232}Th date of 508.2 ± 1.4 Ma, MSWD = 2.3 (497.6 ± 1.6 Ma LA ICP-MS age; Kylander-Clark et al., 2013). Seven repeat analyses of 'Trebilcock' yielded a weighted mean ^{206}Pb/^{238}U date of 278.4 ± 1.2 Ma (ca. 279 – 285 Ma;

Tomascak et al., 1996) and a weighted mean $^{208}Pb/^{232}Th$ date of 263.3 ± 1.3 Ma, MSWD = 7.6 (263.7 ± 1.0 Ma LA ICP-MS age; Kylander-Clark et al., 2013).

Isotopic data of monazite in metamorphic rocks were also normalized to '44069', while 'Bananeira' and 'FC-1' were used as secondary reference materials. A total of 27 repeat analyses of 'Bananeira' yielded a weighted mean $^{206}Pb/^{238}U$ date of 506.2 ± 1.3 Ma, MSWD = 2.6 and a weighted mean $^{208}Pb/^{232}$ date of 490.9 ± 1.5 Ma, MSWD = 1.9. A total of 15 repeat analyses of 'FC1' yielded a weighted mean $^{206}Pb/^{238}U$ date of 56.4 ± 0.2 Ma, MSWD = 9.8 (55.7 ± 0.7 Ma ID-TIMS age; Horstwood et al., 2003) and a weighted mean $^{208}Pb/^{232}$ date of 52.7 ± 0.2 Ma, MSWD = 1.3 (54.5 ± 0.2 Ma LA ICP-MS age; Kylander-Clark et al., 2013). Trace elements were normalized to 'Bananeira' and, based on repeat analyses of multiple secondary reference materials, are accurate to within 5% (2 SE, Cottle and Stearns, 2018) (Table C3).

5.4 Petrography

Optical characterization and high-resolution X-ray elemental maps of thin-sections from metamorphic specimens were used for textural analysis, to estimate modal mineral proportions and to identify prospective mineral targets (e.g. monazite) for further analysis. Modal proportions of minerals in each metamorphic specimen are provided in Table C4. All mineral abbreviations used below follow those of Whitney and Evans, (2010).

5.4.1 Igneous specimens

Specimens GG10 and GG12 (Fig. 5.1d) are undeformed leucogranites. Both contain the mineral assemblage Qtz + Pl + Kfs + Ms + Tur + Mnz ± Grt ± Ap ± Rt with only minor differences in mineral size (fine and fine to medium, respectively). GG10 was collected at the contact with the metamorphic assemblage while GG12 was collected ca. 350–400 m further into the pluton (Fig. 5.1d).

5.4.2 Metamorphic specimens

Specimen UM04

This specimen is a staurolite-bearing garnet–mica schist (Fig. 5.2a) with an observed assemblage of Qz + Pl + Bt + Ms + Grt + St + Gr with trace Ilm, Ap, Aln, Tur, Xtm, Zr and Chl. Fine- grained muscovite, graphite and biotite define the main foliation and, together with quartz and plagioclase, form the matrix mineralogy. Garnet porphyroblasts, up to 0.70 mm in diameter, are characterized by euhedral to subhedral forms, with rare inclusions of quartz (Fig. 5.2b). Staurolite occurs as large porphyroblasts up to 4.8 mm in size across the long axis and contain quartz and graphite inclusions in the outer rim. Most occurrences of staurolite are flanked by quartz-filled strain shadows and are partially fragmented and rotated (Fig. 5.2c). Recrystallized quartz and biotite fill the space between broken fragments of staurolite, with no evidence of staurolite overgrowth.

Specimen UM05

UM05 is a staurolite-bearing garnet–mica schist (Fig. 5.2d) with an observed assemblage of Qz + Pl + Bt + Ms + Grt + St + Gr with trace Ilm, Aln, Ap, Zr, Tur and Chl. Fine-grained muscovite, graphite and biotite define the main foliation and, in combination with quartz and plagioclase, are the major constituents of the matrix. Muscovite is most abundant in the pressure shadows of staurolite and garnet porphyroblasts. Garnet, up to ~ 1.2 mm diameter, are subhedral to anhedral, commonly show sector zoning (Fig. 5.2e) and are locally intergrown with staurolite rims. Staurolite porphyroblasts occur as occasionally fragmented, euhedral crystals, with outer portions that contain inclusions of quartz and graphite (Fig. 5.2f).

Specimen UM07

UM07 is a staurolite-bearing garnet–mica schist (Fig. 5.2g) with an observed assemblage of Qz + Pl + Bt + Ms + Grt + St + Gr with trace Ilm, Ap, Tur and Chl. The main foliation is defined

by aligned graphite, muscovite and biotite grains, which, along with quartz and plagioclase, comprise the matrix mineralogy (Fig. 5.2h). In addition to the matrix, muscovite is concentrated in strain caps around staurolite and garnet porphyroblasts (Fig. 5.2i). Garnet occurs as euhedral to subhedral crystals that vary in size with a maximum diameter of ~ 1.6

mm. Larger garnet grains are commonly fractured and contain rare inclusions of quartz, whereas smaller grains are well preserved and mostly inclusion free (Fig. 5.2i). Staurolite porphyroblasts are euhedral with either blocky or elongate habit parallel to the foliation. Staurolite is locally fractured with no staurolite overgrowth present between fragments. Both quartz and graphite occur as inclusions in staurolite, as does garnet in the outer parts of some grains. In addition, quartz fringes form in the pressure shadows adjacent to the porphyroblasts.

Specimen UM08

UM08 is a garnet–mica schist (Fig. 5.2j) with an observed assemblage of Qz + Pl + Bt + Ms + Grt + Gr with trace Aln, Ilm, Ap, Tur, Xtm, Zr and Chl. As in the other specimens, aligned graphite, biotite and muscovite define the matrix foliation, which also includes quartz and plagioclase. Euhedral to subhedral garnet porphyroblasts, up to ~ 1.6 mm in diameter, have weak sector zoning (Fig. 5.2k) with larger grains containing fractures at a high angle to the foliation (Fig. 5.2l).

Specimen UM09

UM09 is a staurolite- and sillimanite-bearing garnet–mica schist (Fig. 5.2m), with an observed assemblage of Qz + Pl + Bt + Ms + Grt + St + Sil + Gr and trace Ilm, Tur and Chl. Laths of biotite, graphite grains and rare muscovite define the main foliation and, together with quartz and plagioclase, comprise the matrix. The few muscovite grains that are present in the specimen occur as very small grains (< 100 μm on the longest axis). Sillimanite (fibrolite) occurs as clustered needles associated with quartz and biotite (Fig. 5.2n), and may reflect the metamorphic reaction Ms = Sil + Bt + Qtz (Foster, 1991), consistent with the apparent disappearance of muscovite in the specimen. As in the other specimens, garnet and staurolite in UM09 occur as porphyroblasts. Garnet porphyroblasts, up to ~ 2.1mm in diameter, are anhedral, commonly fractured and generally characterized by inclusion-rich mantles. Mantle inclusions consist of quartz and graphite (Fig. 5.2o), while rare monazite grains occur locally in rims (Fig. 5.2p). Staurolite porphyroblasts occur mainly as broken and fragmented grains, with biotite occasionally occurring between broken pieces (Fig. 5.2q).

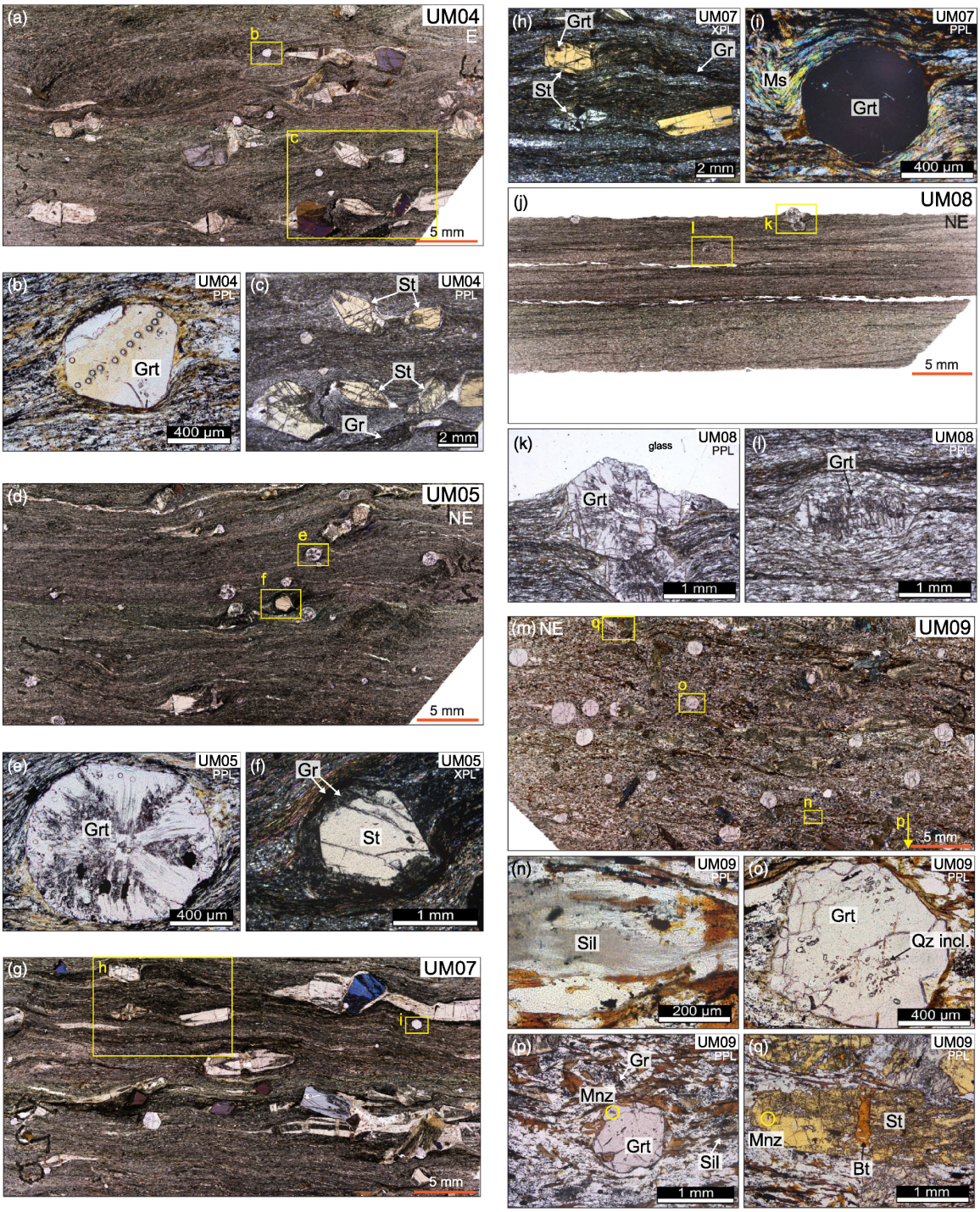

Figure 5.2. Thin-section photomicrographs of metamorphic specimens. Specimen orientation is indicated in the top corner. a) Full thin-section photomicrograph of specimen UM04. b) Subhedral garnet porphyroblast with few quartz inclusions. Laser ablation spots used for trace-element geochemistry are visible throughout the garnet. c) Partially fragmented staurolite porphyroblasts. d) Full thin-section photomicrograph of specimen UM05. e) Garnet porphyroblast with sector zoning. f) Staurolite porphyroblast with graphite inclusions in its

rim. g) Full thin-section photomicrograph of specimen UM07. h) Main foliation defined mainly by graphite, biotite and quartz. Larger, staurolite porphyroblasts are aligned parallel to the foliation. i) Garnet porphyroblast with muscovite in strain caps. j) Full thin-section photomicrograph of specimen UM08. k) Garnet porphyroblast showing weak sector zoning. l) Garnet fragmented perpendicular to the main foliation. m) Full thin-section photomicrograph of specimen UM09. n) Clustered needles of sillimanite formed on top of quartz grains. o) Garnet porphyroblast with quartz inclusions. p) Garnet porphyroblast with monazite inclusion in its rim (yellow circle). q) Biotite formed within the gaps of broken staurolite. Monazite is included in the rim of the staurolite (yellow circle). PPL – plane polarized light; XPL – crossed polarized light.

5.5 Mineral geochemistry

Major- and trace-element geochemistry was obtained from various mineral phases in collected metamorphic specimens. The results presented below were used to investigate the variation both within grains and in different textural positions within the specimens.

5.5.1 Major-element geochemistry

Garnets in this study are dominantly almandine with end-member profiles for all five specimens recording the highest content of Sps and Grs in their cores, which gradually decreases outwards towards the rims (Fig. 5.3a–e). In contrast, Alm and Prp record the opposite trend with the lowest content in the cores that increases at the rims. Garnet compositional maps of Mn for all specimens outline this gradational zonation from core to rim (Fig. 5.3a–e).

Chemical composition of biotite is in the range: 0.12–0.23 a.p.f.u. in Ti and 0.44–0.54 in XMg for UM04; 0.12–0.20 a.p.f.u. in Ti and 0.44–0.47 in XMg for UM05; 0.14–0.25 a.p.f.u. in Ti and 0.42–0.47 in XMg for UM07; 0.15–0.27 a.p.f.u. in Ti and 0.40–0.43 in XMg for UM08; and 0.19–0.32 a.p.f.u. in Ti and 0.32–0.38 in XMg for UM09.

All measured muscovite grains are from the matrix. Muscovite composition is in the range: 6.23–6.34 a.p.f.u. in Si and 0.48–0.59 in XMg in UM04; 5.97–6.05 a.p.f.u. in Si and 0.50–0.56 in XMg in UM05; 6.16–6.25 a.p.f.u. in Si and 0.44–0.58 in XMg in UM07; 6.27–6.45 a.p.f.u. in Si and 0.50–0.59 in XMg in UM08; and 5.93 – 5.95 a.p.f.u. in Si and 0.36–0.41 in XMg in UM09.

Anorthite content in feldspars is in the range 0.26–0.37 in UM04, 0.25–0.35 in UM05, 0.29–0.32 in UM07, 0.30–0.33 in UM08 and 0.15–0.28 in UM09.

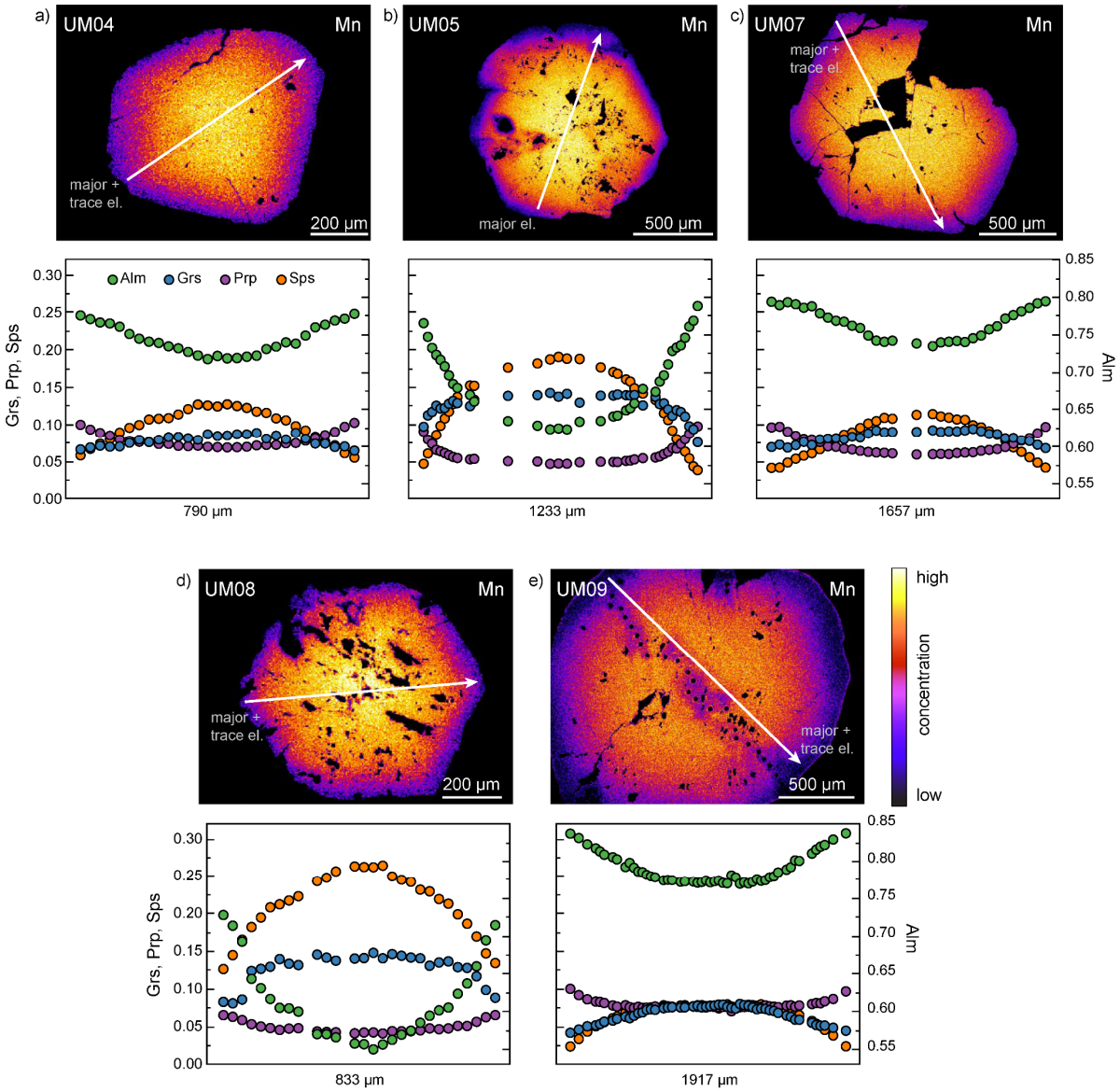

Figure 5.3. Element distribution maps of Mn and garnet end-member profiles for five metamorphic specimens. Arrow indicates direction and profile of major- and/or trace-element analysis. Slight colour change along the profile line (e) is due to laser drilling prior to mapping. Alm – almandine; Grs – grossular; Prp – pyrope; Sps – spessartine.

5.5.2 Garnet trace-element geochemistry

Specimen UM04

The highest Y concentration in UM04 is recorded in the garnet core, which decreases towards the rim (Fig. 5.4a). Gd/Yb records the opposite pattern, with the lowest ratio in the core reflecting the highest concentration of heavy REEs (HREEs) relative to middle REEs

(MREEs) (Fig. 5.4a). A spider plot of REE normalized to chondrite values (from McDonough and Sun, 1995) shows the highest content of HREE in garnet cores, followed by mantle and rims with the lowest content (Fig. 5.5a). A negative Eu anomaly is recorded in all three garnet domains.

Specimen UM05

Garnet in UM05 records a maximum Y concentration in the core, which decreases towards the mantle and increases slightly at the rim (Fig. 5.4b). Gd/Yb ratios record an inverse trend across the grain, increasing sharply away from the core before a slight decrease at the rim (Fig. 5.4b). A spider plot of REE normalized to chondrite values shows that garnet cores have the highest HREE contents, followed by lower values from rim material and mantle analyses with the lowest HREE concentrations (Fig. 5.5b). Trace-element data from the core and mantle outline positive Eu anomalies, while rim data are associated with a negative anomaly.

Specimen UM07

The highest Y concentration measured in garnet in UM07 is recorded in the core and decreases sharply towards the mantle (Fig. 5.4c). A minor increase in Y is recorded only on one side of the garnet rim. The lowest Gd/Yb ratio is recorded in the core of the garnet, which increases sharply throughout the mantle and rim (Fig. 5.4c) with one side recording a decrease at the rim. A spider diagram of chondrite-normalized REEs (Fig. 5.5c) shows the highest relative values of HREE in the core, while the mantle and rims show the lowest. A negative Eu anomaly is consistent throughout the garnet profile.

Specimen UM08

Garnet in UM08 records the lowest Y concentrations in its core, which increase outwards through the mantle to maximal concentrations in the rim regions (Fig. 5.4d). Gd/Yb ratios show the opposite pattern, with the highest ratios in garnet cores and lowest ratios at the rims (Fig. 5.4d). Chondrite-normalized plots of garnet REE shows the highest content of HREE recorded in the rims, followed by mantle and rims that recorded lower content (Fig. 5.5d). All

garnet domains show no distinctive Eu anomaly, except one mantle profile with a strong positive anomaly.

Specimen UM09

Garnet from specimen UM09 has the highest concentration of Y in its core, which decreases towards the mantle (Fig. 5.4e). On each side of the garnet in the mantle, there is a slight increase of Y, after which concentrations decrease again at the rim. Garnet core material has the lowest Gd/Yb ratios, which increase towards the mantle and then fluctuate with alternate increases and decreases across the mantle (Fig. 5.4e). Garnet rim material on one side shows the highest ratio of Gd/Yb recorded; however, the opposite side of the rim shows an asymmetric decrease in the ratio. Similar to UM04 and UM07, chondrite-normalized REE plots show the highest relative values in HREE in the core, followed by mantle and rim material with the lowest values (Fig. 5.5e). A negative Eu anomaly is present across the whole garnet, but is less prominent at the rim.

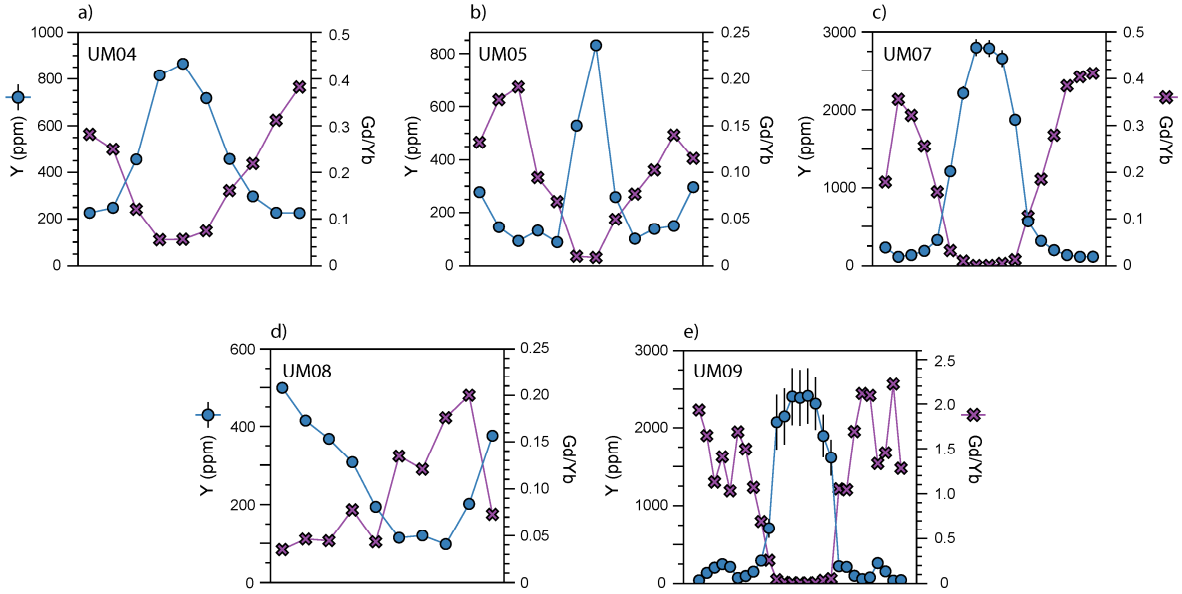

Figure 5.4. Compositional diagram of Y and Gd/Yb for garnet in metamorphic specimens. Vertical line represents 1 standard error.

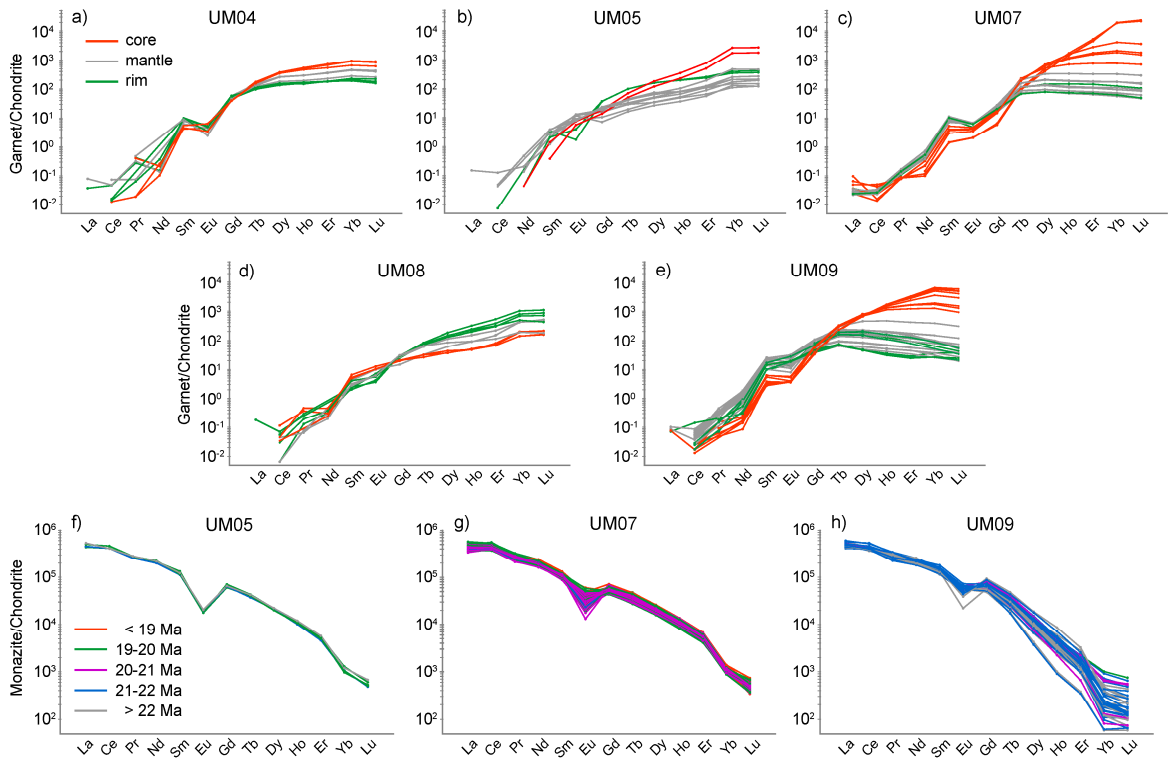

Figure 5.5. Garnet and monazite trace element geochemistry. a–e) Chondrite-normalized garnet trace-element data. f–h) Chondrite-normalized monazite trace-element data. Chondrite values used are from McDonough & Sun (1995).

5.6 Thermobarometry

Classical thermobarometry was used to obtain information on the pressure - temperature (P-T) conditions under which the metasedimentary rocks were formed. Two thermometers, Ti-in-biotite (calibration of Henry et al., 2005) and the garnet - biotite Fe-Mg exchange (calibration of Holdaway, 2000), were used to estimate metamorphic temperature, while the garnet - biotite - muscovite - plagioclase (GBMP) barometer of Wu, (2015) was used to estimate pressure.

5.6.1 Ti-in-biotite thermometry

All specimens examined are peraluminous graphitic metapelites that contain ilmenite or rutile, thereby satisfying the mineral assemblage requirements of the Ti-in-biotite thermometer (Henry et al., 2005). Biotite grains used for this thermometer were analysed from two different locations including the matrix and near garnet. Uncertainties associated with the

resulting temperatures using this thermometer are estimated to be ± 24 °C (Henry et al., 2005). Full results are presented in Fig. 5.6a, b and Table C5.

The majority of Ti-in-biotite temperatures from specimen UM04 range from 567 to 608 °C, with the highest temperatures recorded from the biotite positioned next to garnet rims. The maximum temperature from grains in the matrix is 599 °C, within uncertainty of those near garnet (Fig. 5.6a). Temperatures obtained from both matrix and near-garnet biotite in UM05 cluster in the range of 540 - 578 °C (Fig. 5.6a). In specimen UM07, most temperatures fall into the range of 515 - 587 °C, with no consistent spatial association (Fig. 5.6a). Matrix and near-garnet biotite grains in specimen UM08 yield Ti-in-biotite temperatures in the range 540 - 592 °C, with one matrix analysis yielding the highest temperature of 625 °C (Fig. 5.6a). Finally, a majority of Ti-in-biotite temperatures for UM09 extend from 610 to 648 °C for matrix and near-garnet grains; temperature maximums from grains near garnet and in the matrix are within uncertainty (Fig. 5.6a).

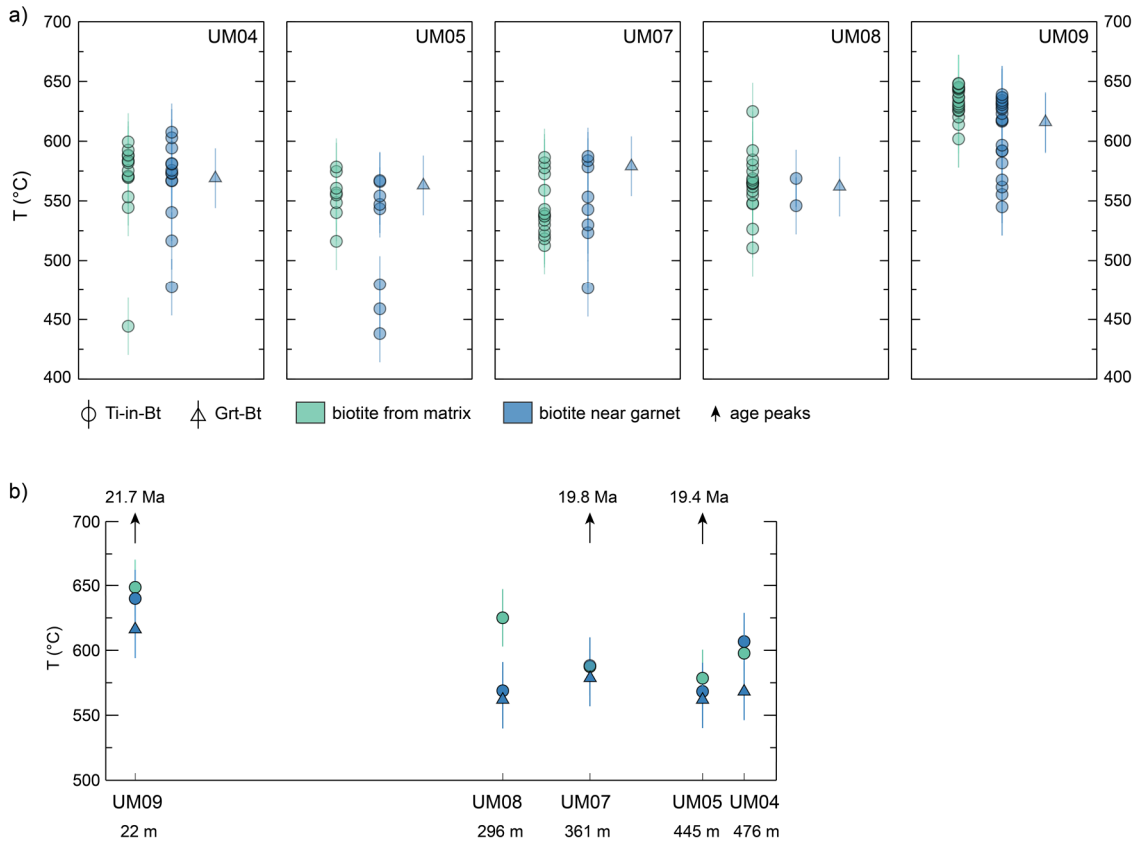

Figure 5.6. Thermobarometry results. a) Ti-in-biotite (Henry et al. 2005) and garnet - biotite (Holdaway, 2000) temperature estimates for biotite from matrix and near garnet. Vertical line represents the uncertainty. b) Summary diagram of recorded peak temperatures. Specimens are positioned relative to their distance from the pluton.

5.6.2 Garnet-biotite and garnet-biotite-muscovite-plagioclase thermobarometry

The garnet - biotite - muscovite - plagioclase (GBMP) barometer of (Wu, 2015) was used to obtain pressures for each specimen together with the garnet–biotite thermometry calibration of Holdaway, (2000), model 6AV. Ferric iron content of biotite and garnet were assumed to be 11.6 mol% for biotite and 3 mol% for garnet, as recommended in Wu, (2015). Absolute uncertainties for the garnet - biotite thermometer are estimated at ± 25°C (Holdaway, 2000), while those for the GBMP barometer are ± 1.2 kbar (Wu, 2015).

Grains were carefully selected, based on their textural relationship and location of data points within that grain, to obtain texturally constrained temperature and pressure estimates. For example, inner rim data from garnet grains were used for calculations, to avoid data points potentially affected by retrograde reactions with surrounding minerals (e.g. biotite reacting with garnet rims). Furthermore, biotite, muscovite and plagioclase grains near garnet were selected to satisfy the requirements of local equilibrium for this thermobarometer (Holdaway, 2000; Wu, 2015). As per Wu, (2015), only plagioclase with XAn > 0.17 were used. Results for temperatures and pressures calculated using the garnet - biotite thermometer and GBMP barometer are presented in Figs. 5.6, 5.7 and Table C5.

The thermobarometer yielded temperature and pressure estimates of 569 °C and 4.4 kbar for UM04, 563 °C and 5.2 kbar for UM05, 579 °C and 5.2 kbar for UM07, 562 °C and 5.0 kbar for UM08, and 615 °C and 5.3 kbar for UM09.

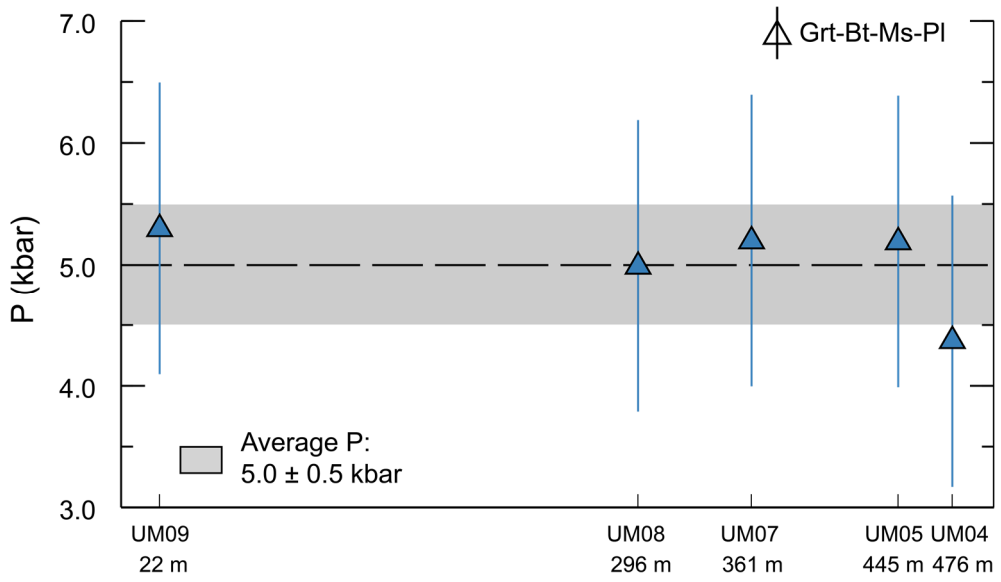

Figure 5.7. Garnet-biotite-muscovite-plagioclase pressure estimates using calibrations of Wu (2015). Specimens are positioned relative to their distance from the pluton. Vertical line represents the uncertainty. Dashed horizontal line represents the average pressure, while grey shaded area represents the uncertainty.

5.7 Monazite (petro)chronology

Monazite U–Th–Pb dates (chronology) were obtained from two igneous specimens GG10 and GG12, while U–Th–Pb dates and trace-element data (petrochronology) were obtained from three metamorphic specimens: UM05, UM07 and UM09. Specimens UM04 and UM08 did not contain monazites that were large enough to target. Monazite grains selected for dating had sizes (long axis) in the range 17–50 µm, 17–80 µm and 15–80 µm for UM05, UM07 and UM09, respectively. Grains from all three specimens are elongate or lobate in shape and are often associated with quartz, mica or allanite locally (Figs. C1, C2). All reported monazite dates are based on the $^{208}Pb/^{232}Th$ isotopic system, the preferred system for Cenozoic monazite, as it avoids potential problems associated with unsupported ^{206}Pb from ^{230}Th decay (Schärer, 1984).

All geochronological and petrochronological data for igneous and metamorphic specimens are presented in Figs 5.8, 5.9 and Table C3. For igneous specimens, a weighted mean age was calculated when the data defined a single dominant age population. For more normally distributed data, the median provides a more meaningful estimate for the actual timing of pluton crystallization (Fig. 5.8a, b). For metamorphic specimens, all monazite dates,

including those discarded from the final age interpretation, are presented on a U - Pb versus Th - Pb concordia diagram (Fig. 5.8c–e). Only monazite isotopic data from ablation spots completely within monazite grains (i.e. spots that did not ablate the matrix, as determined through post-laser analysis scanning electron microscopy) were used for interpretation of metamorphic ages (Fig. 5.8f–h). The age peaks for each metamorphic specimen were determined through Gaussian deconvolution as implemented in Isoplot v.4.15 (Ludwig, 2003; Vermeesch, 2018).

5.7.1 Igneous specimens

A total of 40 spot analyses on monazite from specimen GG10 yield a weighted mean age of 21.3 Ma, with excess scatter (MSWD = 5.7). We therefore take a conservative approach and interpret the median age of 21.3 ± 0.5 Ma (Fig. 8a) to reflect the main crystallization of the pluton. Of the 40 spot analyses of monazite from specimen GG12, 31 combine to yield a coherent population at 21.3 ± 0.1 Ma (MSWD = 1.5) (Fig. 8b), which is taken to be representative of the main crystallization phase of this specimen.

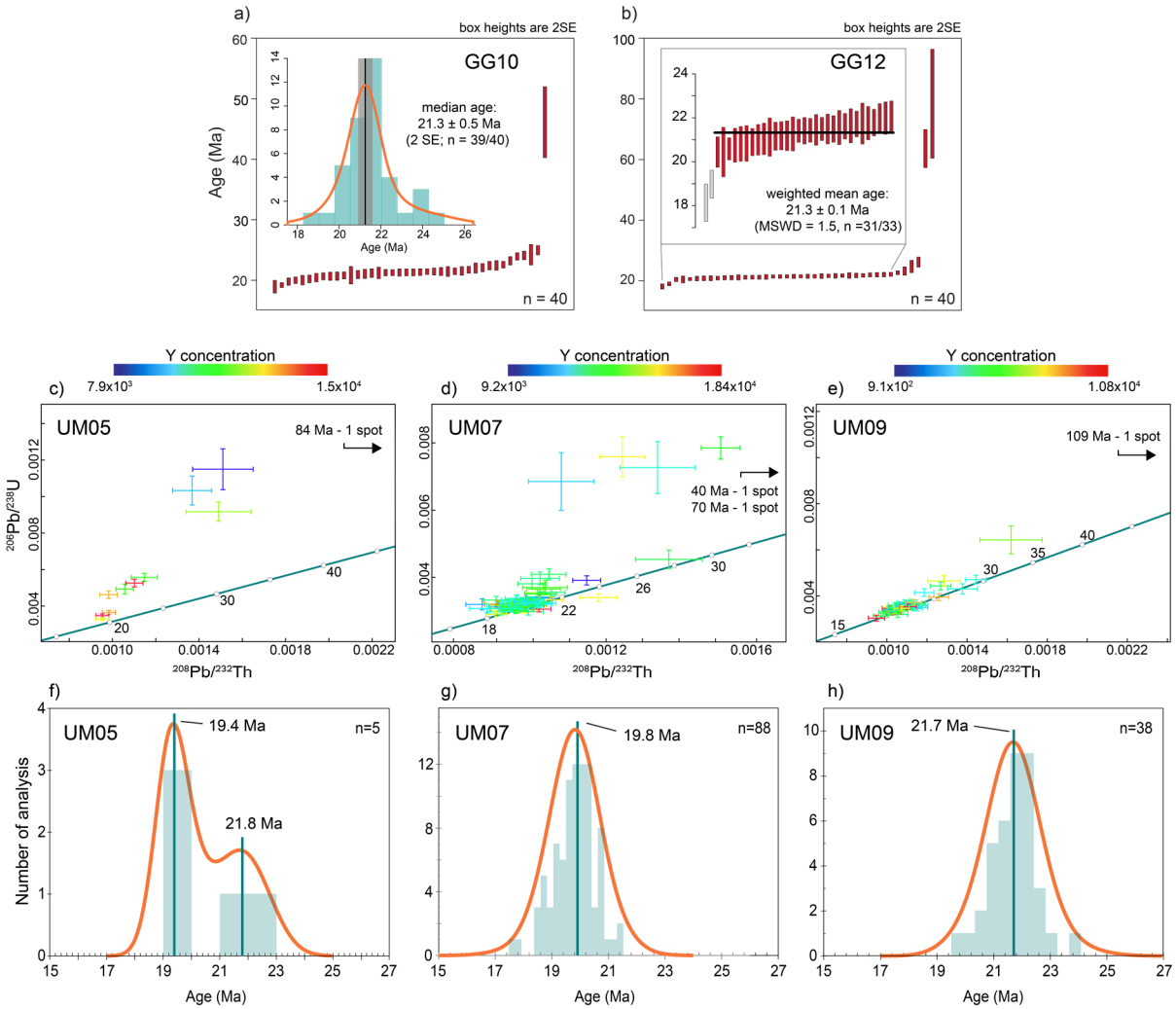

Figure 5.8. Monazite petrochronology results. a, b) Monazite median and weighted mean age for two igneous specimens. c–e) Monazite $^{206}Pb/^{238}U$ vs. $^{208}Pb/^{232}Th$ concordia diagram for all monazite analysis in metamorphic rocks. (f–h) Gaussian deconvolution diagrams for analyses that ablated monazite exclusively.

5.7.2 Metamorphic specimens

Specimen UM05

A total of 11 spot analyses were carried out across six monazite grains in specimen UM05 (Fig. 5.8c), of which five spots in three grains ablated monazite exclusively. All monazite grains in this specimen were located in the matrix. Monazite dates from UM05 range from 22.2 ± 0.8 Ma to 19.2 ± 0.6 Ma, with a main peak at ca. 19.4 Ma and secondary peak at ca. 21.8 Ma (Fig. 5.8f). Neither Gd/Yb ratios (Fig. 5.9a) nor Y concentrations (Fig. 5.9b) show a significant correlation with date. Moreover, chondrite-normalized REE values of monazite

show a relatively invariant pattern of enriched LREE and less enrichment towards HREE, regardless of date (Fig. 5.5f).

Specimen UM07

In specimen UM07, 105 spot analyses were performed on 15 monazite grains (Fig. 5.8d), of which 88 spot analyses from 13 grains ablated monazite exclusively. All monazite grains in this specimen occurred in the matrix. Monazite dates range from 21.4 ± 0.6Ma to 17.7 ± 0.9 Ma. The dates form a unimodal distribution with an age peak at ca. 19.8 Ma (Fig. 5.8g). Monazite Gd/Yb ratios (Fig. 5.9a) and Y concentrations (Fig. 5.9b) do not appear to systematically change with date. As in UM05, chondrite-normalized REE show little variation across the data. All analyses record significant enrichment in LREE with decreasing enrichment in MREE and HREE, with no correlation to date (Fig. 5.5g).

Specimen UM09

In specimen UM09, 58 monazite analyses were performed on 13 monazite grains (Fig. 5.8e), with one monazite grain located in the rim of garnet porphyroblast and one monazite grain in the rim of staurolite. Out of 58 analyses, only 38 spots from 11 monazite grains ablated monazite exclusively. Dates from monazites located in matrix range from 24.0 ± 1.0 Ma to 19.6 ± 0.8 Ma. Six monazite analyses from within garnet (Fig. 5.2p) range from 22.0 ± 0.8 Ma to 20.6 ± 0.7 Ma, while a single monazite analysis from within staurolite (Fig. 5.2q) yielded a 22.6 ± 0.7 Ma date. The age peak defined by the monazite dates is ca. 21.7 Ma (Fig. 5.8h). As for the other specimens described, the Gd/Yb ratios (Fig. 5.9a) and Y concentrations (Fig. 5.9b) recorded in monazite from UM09 do not vary with date and do not show significant variation on chondrite-normalized REE plots (Fig. 5.5h).

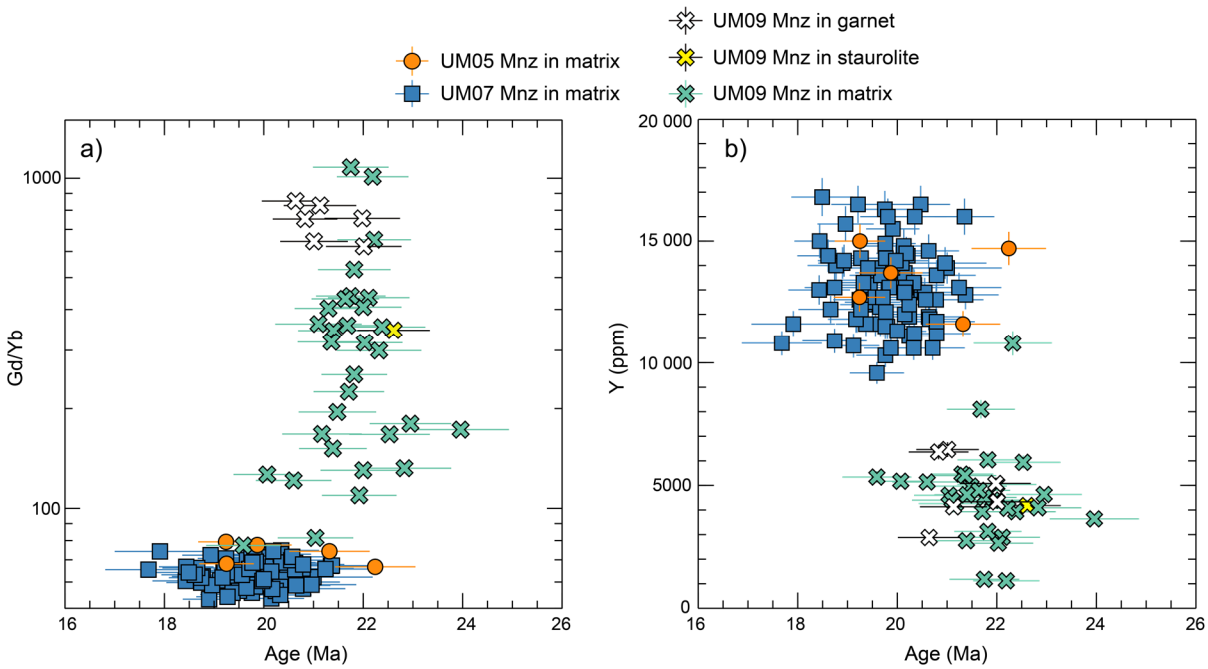

Figure 5.9. Monazite trace element data. a) Gd/Yb v. age diagram for monazite. b) Y v. age diagram for monazite. Horizontal lines represent 2 standard errors of each $^{208}Pb/^{232}Th$ date, while vertical lines represent 2 standard errors of each Y concentration.

5.8 Interpretation

5.8.1 Textural relationships and mineral chemistry

All metamorphic specimens examined in this study have a similar mineral assemblage, but record key differences in chemical compositions that help distinguish the metamorphic conditions at which they formed. With the exception of UM08, all metamorphic specimens contain staurolite. The absence of staurolite in UM08 may be linked to its bulk composition, which has lower Al compared to the other specimens (Table C6). Specimen UM09, collected closest to the contact with the Mugu granite, is the only specimen that contains sillimanite and has the highest percentage of staurolite (16%). Moreover, while the rest of the specimens contain 14 - 26 % muscovite, UM09 contains <1% muscovite, interpreted to be relics largely consumed during the production of sillimanite (Foster, 1991). All these observations are consistent with UM09 recording higher-grade metamorphic conditions than the other specimens in the area located further away from the pluton. Garnet porphyroblasts in UM05 and UM08 contain quartz and graphite inclusions that define sector zoning. Textural sector zoning typically occurs in pelitic rocks abundant with graphite (Andersen, 1984; Burton, 1986;

Rice, 1987, 1993; Rice and Mitchell, 1991), and is often interpreted to reflect rapid growth (Andersen, 1984).

Garnet major-element profiles show bell-shaped patterns indicative of prograde growth zonation in all five specimens, with Sps and Grs enrichment in the cores while Alm and Prp show the opposite pattern (Hollister, 1966). None of the garnets analysed contain evidence of retrograde diffusion at the rims, such as a marked increase in Grs and Sps or a decrease in Alm and Prp (Tracy et al., 1976; Kohn and Spear, 2000). Peak temperatures are estimated from the highest obtained temperatures calculated in each specimen. Temperatures estimated from Ti-in-biotite and garnet - biotite thermometers are highest in the specimen closest to the pluton (Fig. 5.6b). Pressures obtained from the garnet - biotite - muscovite - plagioclase barometer are within uncertainty across all specimens (Fig. 5.7). When averaged, they define a pressure of 5.0 ± 0.5 kbar (Fig. 5.7) which corresponds to a depth of 18 ± 2 km, assuming an average crustal density of 2.83 gcm^{-3}.

5.8.2 Trace-element partitioning

Trace-element profiles of garnet from four specimens (UM04, UM05, UM07 and UM09) show high Y concentrations in the cores (Fig. 5.4a–c, e), which generally decrease towards the mantle and rim. This observation is consistent with Rayleigh fractionation of garnet during prograde growth (Otamendi et al., 2002). The increase in Y concentration in the rim of UM05 and, to a lesser degree in the rim of UM07 and the mantle of UM09, may represent breakdown of another Y-bearing mineral, such xenotime or allanite during rim growth (Pyle and Spear, 1999) Completely different trace-element behaviour is recorded in garnet from specimen UM08 (Fig. 5.4d). An increase in Y concentration towards the garnet rims may indicate breakdown of a Y + HREE -bearing mineral such as xenotime. If xenotime provided the Y + HREE that was incorporated into the garnet, it would have released P into the system. This P was likely partitioned into apatite and allanite, rather than monazite (e.g. Spear and Pyle, 2002, 2010; Wing et al., 2003; Shrestha et al., 2019), favoured by the high CaO content of the specimen. This inference is consistent with the lack of xenotime and sparse, small monazite grains observed in UM08 (Fig. C2). Specimen UM05 is the only specimen to record a distinctive positive Eu anomaly in the cores and mantles of garnet, while specimen UM08 yielded a single spot with a positive anomaly (Fig. 5.5b, d). Such a positive anomaly

may indicate growth of garnet during the breakdown of the Eu-bearing phase (e.g. plagioclase, apatite), most probably by the substitution of Eu^{2+} for Ca^{2+} (Taylor and McLennan, 1988).

5.8.3 Timing of metamorphism

The specimens of the Mugu pluton, UM10 and UM12, yield indistinguishable crystallization ages of 21.3 ± 0.5 Ma and 21.3 ± 0.1 Ma, respectively. Monazite from the metamorphic specimen closest to the exposure of the pluton UM09 define an age peak at ca. 21.7 Ma, while specimens further away returned peaks at ca. 19.8 Ma (UM07) and ca. 19.4 Ma (UM05). As these rocks do not show evidence of partial melting, the rims of garnet and/or staurolite should record peak/near-peak temperature metamorphic conditions. Dates from monazite included in garnet and staurolite rims in UM09 range from 22.6 ± 0.7 Ma to 20.6 ± 0.7 Ma, which overlap with the majority of monazite analyses from the matrix, consistent with coeval growth of matrix monazite and porphyroblasts. For that reason, we interpret the age peak at ca. 21.7 Ma as the age of peak metamorphism in specimen UM09. Specimens UM07 and UM05 do not contain any monazite inclusions in garnet and/or staurolite. However, in the absence of any evidence of partial melting, we interpret that the monazite grains in these specimens grew across prograde and peak metamorphic (temperature) conditions (e.g. Pyle and Spear, 2003; Kohn and Malloy, 2004; Buick et al., 2006) and that the age peaks in each represent the timing of peak metamorphism in the specimens.

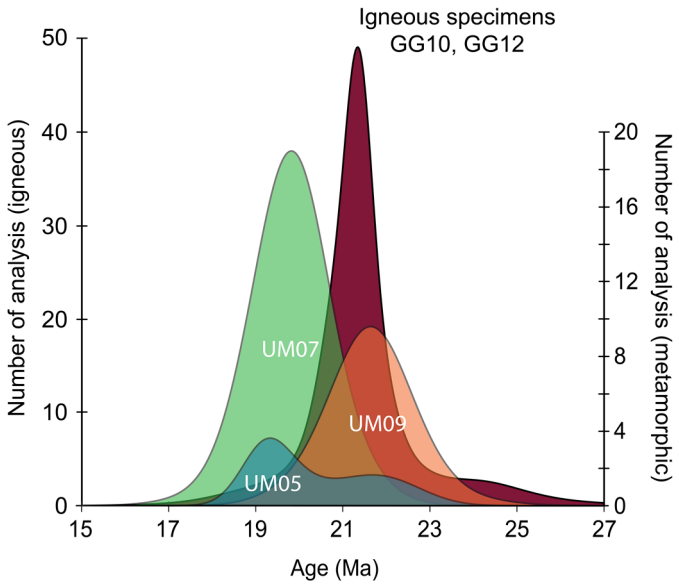

Figure 5.10. Age probability plot for igneous and metamorphic specimens.

5.9 Discussion

Metamorphism in different parts of the Himalaya has been linked to various heat sources. In addition to primary crustal geothermal heat controlled by radioactive decay (e.g. Jamieson et al., 2004), other potential heat sources include heating associated with shear zones (e.g. Hubbard, 1996), the post-thrusting relaxation of disturbed geotherms (e.g. Groppo et al., 2013) and contact/conductive heating linked primarily to the intrusion of igneous bodies (e.g. Kawakami et al., 2007; Mahéo et al., 2007; Aikman et al., 2008).

Metamorphism of the rocks examined in this study, enhanced through conductive heat transfer away from the Mugu pluton, is broadly consistent with: (1) the interpreted decrease in metamorphic grade away from the pluton observed in the field, from medium- to fine-grained schist with garnet and staurolite porphyroblasts to fine-grained phyllite; (2) differences in mineral assemblages across the specimens with proximity to the pluton (e.g. appearance of sillimanite, disappearance of muscovite); (3) invariant pressure estimates; and (4) the results of Ti-in-biotite and garnet - biotite thermometry, in which the specimen closest to the exposure of the pluton records the highest temperature.

Monazite dates from metamorphic specimens examined in this study overlap with both those from the Mugu pluton presented here (Fig. 5.10) and those previously reported (ca. 26.2 – 17.6 Ma; Harrison et al., 1999; Hurtado, 2002). Furthermore, the metamorphic peak age (~ 21.7 Ma) in the specimen closest to the pluton, UM09, is within uncertainty of the crystallization age of the pluton (21.3 ± 0.5 Ma). The main age peaks from the metamorphic specimens are younger with increasing distance from the pluton (Fig. 5.10), which we interpret to reflect monazite growth associated with time integrated heat transfer away from the pluton. The general lack of monazite in specimen UM04 and the few, small grains present in UM05, the two specimens interpreted to be furthest from the pluton, may also reflect differential heating away from the Mugu pluton in which the thermal pulse experienced may not have provided enough time to nucleate and grow much monazite.

A simple thermal diffusion model for sheet-like intrusions (Jaeger, 1968, 1964) was constructed to compare predicted temperatures in specimens with respect to time and position relative to the pluton (Appendix C1, Table 5.1). The Mugu pluton is elongate in shape and covers 1600 km^2 in the Mustang–Dolpo area (Le Fort and France-Lanord, 1995); the present model uses a radius of 10 km to approximate the local width of the pluton in the study area

(Fig. 5.1c) (Le Fort and France-Lanord, 1995). While the three-dimensional shape of the pluton is not known, the modelling results for long cylindrical plutons are similar to those for sheet-like intrusions (Jaeger, 1964).

In order to reproduce the temperature estimates recorded by classical thermometry in specimens UM05 and UM07, this model requires that the Mustang region had a geothermal gradient of ca. 25 °C km^{-1} (background heat of ca. 450 °C) at the time of intrusion of the Mugu pluton (Fig. 5.11, see Jaeger, 1968, 1964). While the model matches well with the temperatures recorded by UM05 and UM07 (Fig. 5.11, Table 5.1), it underestimates the temperature recorded in UM09, the specimen closest to the pluton. Problems with temperatures estimated at the contact are a known issue for this type of modelling (Jaeger, 1964; Yardley, 1990), as such, this underestimation in temperature is not considered significant. If the time when pluton intrudes is set to 0, conductive modelling predicts that specimen UM09 would reach peak temperature (peak metamorphism) after ca. 100 - 500 ka. Specimens further away, UM07 and UM05, would reach peak temperature after ca. 1 Ma, while rocks at 1500 m from the pluton would reach peak temperature at ca. 1 - 2 Ma (Fig. 5.11; Table 5.1). The spatially distinct timing of peak temperature with distance from the contact in the model is consistent with younger monazite age peaks further away from the Mugu pluton. These results further confirm that conductive heating from the pluton provided the additional heat required to metamorphose the studied rocks to their peak temperature conditions. Moreover, the results outline the potentially important contribution that pluton emplacement can have in developing the metamorphic assemblages found nearby, which should be acknowledged.

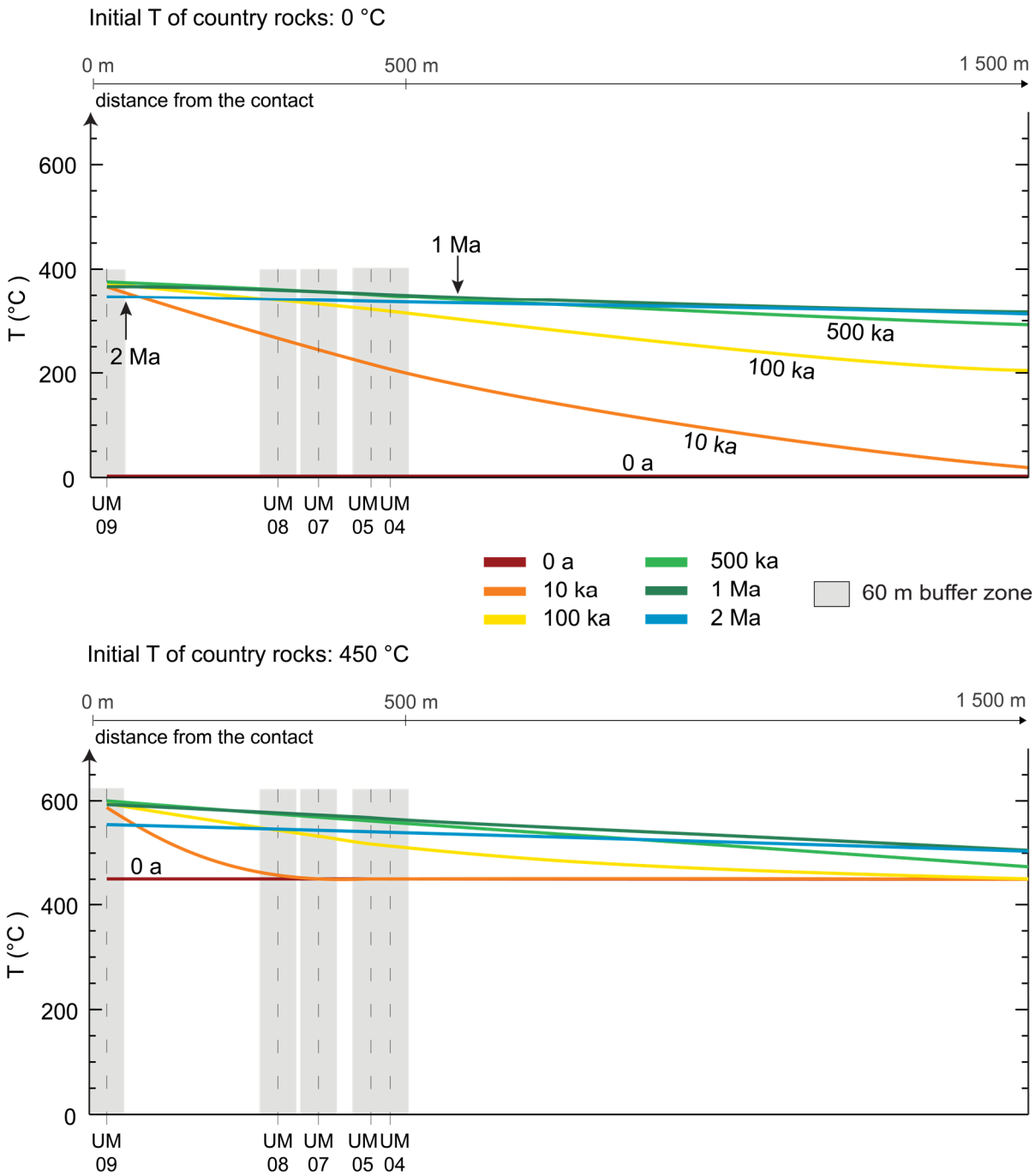

Figure 5.11. Thermal diffusion model of a sheet-like intrusion based on Jaeger (1964, 1968). Detailed temperature estimates are provided in Table 5.1.

Table 5.1. Temperature estimates derived from thermal diffusion model.

Initial temperature of country rocks set as 0 °C

	0 yr	10 000 yr	100 000 yr	500 000 yr	1 Myr	2 My
UM09 (22 m)	0 °C	367 °C	372 °C	374 °C	370 °C	346 °C
UM07 (361 m)	0 °C	243 °C	332 °C	356 °C	358 °C	339 °C
UM05 (445 m)	0 °C	216 °C	322 °C	351 °C	354 °C	337 °C
at 1500 m	0 °C	22 °C	206 °C	296 °C	316 °C	314 °C

Initial temperature of country rocks set as 450 °C (25 °C/km gradient)

	0 yr	10 000 yr	100 000 yr	500 000 yr	1 Myr	2 My
UM09 (22 m)	450 °C	587 °C	596 °C	598 °C	592 °C	554 °C
UM07 (361 m)	450 °C	450 °C	531 °C	569 °C	572 °C	543 °C
UM05 (445 m)	450 °C	450 °C	516 °C	562 °C	567 °C	540 °C
at 1500 m	450 °C	450 °C	450 °C	473 °C	506 °C	503 °C

Microtextural observations within the metapelites, such as the rotation and fragmentation of porphyroblasts, indicate that deformation in these rocks occurred after peak metamorphism, ca. 19.4 Ma, for the youngest specimen. This deformation is interpreted to be related to the E - W extension across the adjacent Thakkhola graben (see Larson et al., 2020b), which initiated as early as ca. 17 Ma (Guillot et al., 1999; Hurtado, 2002; Larson et al., 2020b). However, the igneous specimens do not record extension-related deformation, which may reflect the strong rheological contrast between the graphite-rich pelitic schists and the leucogranite (e.g. Treagus and Treagus, 2002). Deformations recorded in the metamorphic rocks are unlikely to be related to movement on the STDS as there is no such fault documented in the area (Guillot et al., 1995a; Hurtado, 2002; Larson et al., 2020b) and the closest documented exposure is nearly 50 km south of the present study area in the Annapurna region. There, Godin et al., (2001) argue that final movement on the STDS occurred at ca. 22.5 Ma based on the ages of weakly deformed dykes that intrude across the shear zone. Pressure estimates from the contact metamorphic assemblages that formed around leucogranite bodies can be used to gain a rough estimate of the depth of emplacement. In combination with the age of the intrusion, this can be used to outline the thickness of the TSS during that time. The results of the present study indicate that the TSS was at least 18 ± 2 km thick at the time of

emplacement of the Mugu granite. This is consistent with a previous estimate of ca. 17 km based on restored sections in the hanging wall of the Annapurna detachment immediately south of the Upper Mustang region (Kellett and Godin, 2009).

5.9.1 Regional comparisons

The P-T estimates from this study are similar to those previously reported by Guillot et al., (1995a), who also interpreted the metamorphic rocks in the vicinity of the Mugu pluton as reflecting contact metamorphism. While rocks in the Mugu aureole have characteristics consistent with contact metamorphism, they also require a minor component of regional background heating as discussed above. These findings contrast with the interpretations of Hurtado, (2002), who suggested that the same rocks reflect entirely regional metamorphism structurally below the STDS. It is possible, however, that high-grade regional metamorphism is exposed further north in the vicinity of Mustang pluton where Le Fort and France-Lanord, (1995) reported orthogneiss and local anatexis.

Metamorphic rocks around the Manaslu granite, ca. 90 km SE of the current study area, that have a similar assemblage to those studied here also have different interpretations. Based on the pressure - temperature conditions of ~ 550 °C and ~ 5.5 kbar near the base of the pluton, Guillot et al., (1994, 1995b) interpreted those rocks as contact metamorphic rocks, while Searle and Godin, (2003) interpreted metamorphic rocks in the vicinity of the pluton as a part of the exhumed mid-crust in the footwall of the STDS and the product of regional metamorphism, much like the pluton itself (Cottle et al., 2019).

Contact metamorphic rocks surrounding granitic intrusions have also been reported from several locations in southern Tibet, both within the TSS and in exhumed former mid-crustal rocks exposed in structural windows, commonly referred to as the North Himalayan domes. Some of these domes and/or plutonic bodies include, from east to west, the ca. 44 Ma Dala granitoid (Aikman et al., 2008), the ca. 44 Ma and ca. 28 Ma Ramba leucogranite in the Ramba dome (Guo et al., 2008; Liu et al., 2014), the ca. 14.5 - 14 Ma Kouwu leucogranite in the Mabja dome (Lee et al., 2004), the ca. 22 Ma Kung Co granite of the Kung Co half-graben (Mahéo et al., 2007), the ca. 22 - 16 Ma Paiku and ca. 18 - 15.5 Ma Cuobu leucogranites in the Malashan dome (Aoya et al., 2005; Kawakami et al., 2007), and the High Himalayan ca. 25 – 23 Ma Bura Buri leucogranite (Carosi et al., 2013) (Fig. 5.1d). Contact metamorphism reported

in the studies referenced above occurs either structurally above STDS-related faults and/or shear zones, or post-dates movement on such structures.

The contact metamorphic rocks associated with igneous intrusions typically consist of metasedimentary schist with similar garnet ± staurolite ± andalusite assemblages to those investigated here, with overlapping temperatures of ~ 520 - 575 °C and slightly lower pressures of ~ 3.0 - 4.1 kbar (e.g. Kawakami et al., 2007; Mahéo et al., 2007; Aikman et al., 2008). The higher pressure in the present study area, compared with the previously mentioned studies, probably favoured sillimanite over andalusite in Upper Mustang. Similar mineral textures, such as garnet sector zonation, have also been reported in contact metamorphic rocks in the Malashan dome (Kawakami et al., 2007) and the Kung Co granite (Mahéo et al., 2007).

The identification and investigation of contact metamorphic rocks in the TSS can help to improve our understanding of the internal structure of the Himalaya through time. The present geometry of orogen-scale structures such as the STDS at depth is largely based on geophysical data (e.g. Nelson et al., 1996). However, there is little information about how that geometry may have changed through time. Moreover, the contrasting interpretations of the orientation of the STDS are a first-order difference between various orogenic models (see summary in Webb et al., 2011). Study of contact metamorphism within the TSS structurally above the STDS may allow for quantification of minimum upper crustal thicknesses through time across the orogen. As an example, if we take the presently available crustal thickness data as translated from calculated pressures, the minimum thickness of the TSS above the STDS is generally greater in the south than it is further north. While it is acknowledged that the thicknesses are minimums, this type of data, paired with further information about proximity to the STDS, may provide critical insights into the geometry of the structures and help inform orogen-scale kinematic reconstructions.

5.10 Summary

The results obtained from this study provide new, robust information on the timing of the crystallization of the Mugu pluton and the timing of contact metamorphism in the surrounding metasedimentary rocks. The monazite crystallization age of the Mugu granite exposed in the study area is ca. 21.3 Ma, while the dominant monazite age peaks obtained from metamorphic rocks in the area are ca. 21.7, ca. 19.8 and ca. 19.4 Ma, decreasing with increasing

distance from the pluton. Field observations of apparent decreasing metamorphic grade away from the pluton, changes in mineral assemblage, a noted decrease in metamorphic temperatures further away from the pluton, and constant pressure estimates are all consistent with the interpretation of heat diffusion into surrounding rocks during emplacement of the Mugu pluton driving metamorphism. Simple thermal modelling confirms that the Mugu pluton provided the additional heat required (above background) for time-integrated contact metamorphism and monazite growth away from the leucogranite.

Chapter 6 Conclusions

6.1 Conclusions

The results of the integrated, multi-method approach in this thesis provide new findings on the characteristics of the mid- and upper-crustal rocks exposed in the Himalaya and the processes active during the evolution of the orogen. The dataset produced through this work improves our understanding of the convergence accommodation in general, which can be applied to the other orogenic systems around the world.

Three different aspects of Himalayan orogen were investigated herein with a primary focus on the metamorphic and geochronological records in three different areas of the Nepalese Himalaya. The first project (Chapter 3) investigated the geochronological and metamorphic record to provide insight into the prograde evolution of the exhumed, mid-crustal rocks where multiple discontinuities have been inferred previously. The second project (Chapter 4) looked into the geochronological record and metamorphic characteristics of exhumed, mid-crustal rocks to identify previously unrecognized structural discontinuities and assess potential regional correlations. The final project (Chapter 5) explored the metamorphic history of upper-crustal rocks in the vicinity of a Miocene pluton to provide more insight into their origin and potential assessment of metamorphic and exhumation processes.

In the Kanchenjunga region, the Lu-Hf geochronology carried out on garnets that were used in previous studies for tectonometamorphic interpretation returned variable ages. Garnet grains in some rocks yielded dates that are older than Himalayan orogen. This provides evidence for pre-Himalayan garnet within the rocks that typically record Himalayan metamorphism. Combined with accessory U-Th-Pb geochronology, the results show that garnet grains in some rocks grew during the early Permian or Cambrian/Ordovician, while in other garnet grew during Cenozoic reflecting Himalayan metamorphism. This calls into question the interpretations of previous studies that have used garnets to interpret Himalayan evolution without dating the garnet itself and, potentially, the models based on those works.

The investigation of rocks within the transect across the Makalu-Arun region with a combination of mineral geochemistry, monazite U-Th-Pb petrochronology and phase equilibria modelling highlighted sharp differences in geochronologic and metamorphic

histories. Those differences outlined different rock packages separated by at least three tectonometamorphic discontinuities active between the late Oligocene to middle Miocene. Both in-sequence and out-of-sequence thrusts were recognized to be responsible for the development of the mid-crust in that region based on the timing of inferred movement across them. The 'assembly' of the mid-crust, through the propagation of the in-sequence thrust and late out-of-sequence thrust by underplating and duplexing, is consistent with duplexing models proposed for the development of the Himalaya.

The research carried out in the Upper Mustang region involved characterizing the metamorphic rocks surrounding a pluton in the Tethyan Himalaya to resolve contrasting interpretations of the origin and metamorphism of those rocks. The results of a multi-method approach, including geochemistry, igneous and metamorphic monazite U-Th-Pb petrochronology and thermobarometry, supported by heat dissipation modelling, confirm that the metamorphism in these rocks was contact-related during early Miocene pluton emplacement. The overall results support time-integrated heat transfer from the pluton driving metamorphism in the upper crust, rather than regional metamorphism associated with middle-crust.

The results from these three projects provide a new metamorphic and geochronologic record to understand processes active in the mid-crust and the upper-crust of the Himalayan orogen and form a crucial dataset for the development of new tectonic models for the evolution of the Himalaya and similar hot orogens around the world.

6.2 Future work

To complement this thesis and to investigate further aspects of the evolution of the rocks in these study areas, the following work is recommended:

1. The geochronologic data obtained through monazite and garnet geochronology in the Kanchenjunga region provided two possible interpretations for the timing of the pre-Himalayan garnet growth. To help resolve this dichotomy, Sm-Nd garnet geochronology should be performed on garnets that returned pre-Himalayan Lu-Hf age. As Sm-Nd dates are often weighted towards the rim growth, it would offer more

insight into the final stage of garnet growth, resolving whether garnets are entirely Permian in age or Cambrian/Ordovician with Himalayan rims.

2. Garnet trace element geochemistry and phase equilibria modelling with phosphate phases for the gneisses in the Makalu-Arun region may provide further insight into the garnet-monazite heavy rare earth element partitioning relationship and help better inform the timing of garnet growth. Furthermore, similar to the Kanchenjunga project, carrying out Lu-Hf garnet geochronology will provide additional information on the prograde evolution of these rocks. In addition, ^{40}Ar-^{39}Ar dating of micas may offer further insight into the late retrograde stage which, when coupled with quartz petrofabrics, would help characterize the sense of movement across each structure. This would help identify any late-stage normal fault activity, if present on some of these structures, as identified in similar studies of other regions in Nepal.

3. To complement methods that provided the evidence of time-integrated metamorphism, and to investigate the garnet growth history, Lu-Hf garnet geochronology in metamorphic rocks from the Upper Mustang region is recommended. This method will provide direct information on the minimum timing of garnet growth and prograde metamorphism. Furthermore, Lu-Hf geochronology could also be used on the plutonic rocks in the area, which are locally garnet-bearing.

4. New thermo-mechanical models that take into account the new information generated herein and other studies should be developed, as these have confirmed the HMC is significantly more complicated than previously thought when previous models were developed.

References

Aikman, A.B., Harrison, T.M., Lin, D., 2008. Evidence for Early (> 44 Ma) Himalayan Crustal Thickening, Tethyan Himalaya, southeastern Tibet. Earth Planet. Sci. Lett. 274, 14–23.

Aleinikoff, J.N., Schenck, W.S., Plank, M.O., Srogi, L., Fanning, C.M., Kamo, S.L., Bosbyshell, H., 2006. Deciphering igneous and metamorphic events in high-grade rocks of the Wilmington Complex, Delaware: Morphology, cathodoluminescence and backscattered electron zoning, and SHRIMP U-Pb geochronology of zircon and monazite. Geol. Soc. Am. Bull. 118, 39–64.

Ambrose, T.K., Larson, K.P., Guilmette, C., Cottle, J.M., Buckingham, H., Rai, S., 2015. Lateral extrusion, underplating, and out-of-sequence thrusting within the Himalayan metamorphic core, Kanchenjunga, Nepal. Lithosphere 7, 441–464.

Anczkiewicz, R., Chakraborty, S., Dasgupta, S., Mukhopadhyay, D., Kołtonik, K., 2014. Timing, duration and inversion of prograde Barrovian metamorphism constrained by high resolution Lu–Hf garnet dating: A case study from the Sikkim Himalaya, NE India. Earth Planet. Sci. Lett. 407, 70–81.

Andersen, T.B., 1984. Inclusion patterns in zoned garnets from Magerøy, north Norway. Mineral. Mag. 48, 21–26.

Anderson, O.L., Isaak, D.G., 1995. Elastic Constants of Mantle Minerals at High Temperature: A Handbook of Physical Constants, in: Ahrens, T.J. (Ed.), Mineral Physics & Crystallography, AGU Reference Shelf. American Geophysical Union, Washington, D. C., pp. 64–97.

Angel, R.J., Mazzucchelli, M.L., Alvaro, M., Nestola, F., 2017a. EosFit-Pinc: A simple GUI for host-inclusion elastic thermobarometry. Am. Mineral. 102, 1957–1960.

Angel, R.J., Alvaro, M., Miletich, R., Nestola, F., 2017b. A simple and generalised P–T–V EoS for continuous phase transitions, implemented in EosFit and applied to quartz. Contrib. Mineral. Petrol. 172, 29.

Angel, R.J., Murri, M., Mihailova, B., Alvaro, M., 2019. Stress, strain and Raman shifts. Zeitschrift für Kristallographie - Crystalline Materials 234, 129–140.

Annen, C., 2017. Factors Affecting the Thickness of Thermal Aureoles. Front. Earth Sci. 5, 1614.

Aoya, M., Wallis, S.R., Terada, K., Lee, J., Kawakami, T., Wang, Y., Heizler, M., 2005. North-south extension in the Tibetan crust triggered by granite emplacement. Geology 33, 853–856.

Aoya, M., Wallis, S.R., Kawakami, T., Lee, J., Wang, Y., Maeda, H., 2006. The Malashan gneiss dome in south Tibet: comparative study with the Kangmar dome with special reference to kinematics of deformation and origin of associated granites. Geological Society, London, Special Publications 268, 471–495.

Argles, T.W., Prince, C.I., Foster, G.L., Vance, D., 1999. New garnets for old? Cautionary tales from young mountain belts. Earth Planet. Sci. Lett. 172, 301–309.

Arimoto, T., Gréaux, S., Irifune, T., Zhou, C., Higo, Y., 2015. Sound velocities of Fe3Al2Si3O12 almandine up to 19GPa and 1700K. Phys. Earth Planet. Inter. 246, 1–8.

Arita, K., 1983. Origin of the inverted metamorphism of the lower Himalayas, central Nepal. Tectonophysics 95, 43–60.

Ashley, K.T., Caddick, M.J., Steele-MacInnis, M., Bodnar, R.J., Dragovic, B., 2014. Geothermobarometric history of subduction recorded by quartz inclusions in garnet. Geochem. Geophys. Geosyst. 15, 350–360.

Ashley, K.T., Law, R.D., 2015. Modeling prograde TiO2 activity and its significance for Ti-in-quartz thermobarometry of pelitic metamorphic rocks. Contrib. Mineral. Petrol. 169, 23.

Ashley, K.T., Darling, R.S., Bodnar, R.J., Law, R.D., 2015. Significance of "stretched" mineral inclusions for reconstructing P–T exhumation history. Contrib. Mineral. Petrol. 169, 55.

Ashley, K.T., Steele-MacInnis, M., Bodnar, R.J., Darling, R.S., 2016. Quartz-in-garnet inclusion barometry under fire: Reducing uncertainty from model estimates. Geology G38211.1–4.

Baxter, E.F., Scherer, E.E., 2013. Garnet Geochronology: Timekeeper of Tectonometamorphic Processes. Elements 9, 433–438.

Baxter, E.F., Caddick, M.J., Dragovic, B., 2017. Garnet: A Rock-Forming Mineral Petrochronometer. Rev. Mineral. Geochem. 83, 469–533.

Beaumont, C., Jamieson, R.A., Nguyen, M.H., Lee, B., 2001. Himalayan tectonics explained by extrusion of a low-viscosity crustal channel coupled to focused surface denudation. Nature 414, 738–742.

Beaumont, C., Jamieson, R.A., Nguyen, M.H., Medvedev, S., 2004. Crustal channel flows: 1. Numerical models with applications to the tectonics of the Himalayan-Tibetan orogen: Himalayan-Tibetan crustal channel flows. Geophys. Res., Geol. Soc. Spec. Publ. 109, 112.

Bollinger, L., Janots, E., 2006. Evidence for Mio-Pliocene retrograde monazite in the Lesser Himalaya, far western Nepal. Eur. J. Mineral. 18, 289–297.

Bollinger, L., Henry, Avouac, J.-P., 2006. Mountain building in the Nepal Himalaya: Thermal and kinematic model. Earth and Planetary Sciences Letters 244.

Brown, R.L., Daniel Gibson, H., 2006. An argument for channel flow in the southern Canadian Cordillera and comparison with Himalayan tectonics. Geological Society, London, Special Publications 268, 543–559.

Buick, I.S., Hermann, J., Williams, I.S., Gibson, R.L., Rubatto, D., 2006. A SHRIMP U–Pb and LA-ICP-MS trace element study of the petrogenesis of garnet–cordierite–orthoamphibole gneisses from the Central Zone of the Limpopo Belt, South Africa. Lithos 88, 150–172.

Burchfiel, B.C., Chen, Z., Hodges, K.V., Liu, Y.P., Royden, L.H., Deng, C., Xu, J., 1992. The South Tibetan Detachment System, Himalayan Orogen: Extension Contemporaneous With and Parallel to Shortening in a Collisional Mountain Belt, Geological Society of America Special Paper. Geological Society of America.

Burton, K.W., 1986. Garnet-quartz intergrowths in graphitic pelites: the role of the fluid phase. Mineral. Mag. 50, 611–620.

Caddick, M.J., Konopasek, J., Thompson, A.B., 2010. Preservation of Garnet Growth Zoning and the Duration of Prograde Metamorphism. J. Petrol. 51, 2327–2347.

Caddick, M.J., Kohn, M.J., 2013. Garnet: Witness to the Evolution of Destructive Plate Boundaries. Elements 9, 427–432.

Carlson, W.D., 2006. Rates of Fe, Mg, Mn, and Ca diffusion in garnet. Am. Mineral. 91, 1–11.

Carlson, W.D., 2012. Rates and mechanism of Y, REE, and Cr diffusion in garnet. Am. Mineral. 97, 1598–1618.

Carlson, W.D., Hixon, J.D., Garber, J.M., Bodnar, R.J., 2015. Controls on metamorphic equilibration: the importance of intergranular solubilities mediated by fluid composition. J. Metamorph. Geol. 33, 123–146.

Carosi, R., Montomoli, C., Rubatto, D., Visonà, D., 2010. Late Oligocene high-temperature shear zones in the core of the Higher Himalayan Crystallines (Lower Dolpo, western Nepal). Tectonics, Geol. Soc. Spec. Publ. 29.

Carosi, R., Montomoli, C., Rubatto, D., Visonà, D., 2013. Leucogranite intruding the South Tibetan Detachment in western Nepal: implications for exhumation models in the Himalayas. Terra Nova 25, 478–489.

Carosi, R., Montomoli, C., Iaccarino, S., Massonne, H.-J., Rubatto, D., Langone, A., Gemignani, L., Visonà, D., 2016. Middle to late Eocene exhumation of the Greater Himalayan Sequence in the Central Himalayas: Progressive accretion from the Indian plate. GSA Bulletin 128, 1571–1592.

Carosi, R., Montomoli, C., Iaccarino, S., 2018. 20 years of geological mapping of the metamorphic core across Central and Eastern Himalayas. Earth-Sci. Rev. 177, 124–138.

Chernoff, C.B., Carlson, W.D., 1999. Trace element zoning as a record of chemical disequilibrium during garnet growth. Geology 27, 555–558.

Coggan, R., Holland, T.J.B., 2002. Mixing properties of phengitic micas and revised garnet--phengite thermometers. J. Metamorph. Geol. 20, 683–696.

Colchen, M., 1999. The Thakkhola–Mustang graben in Nepal and the late Cenozoic extension in the Higher Himalayas. J. Asian Earth Sci. 17, 683–702.

Coleman, M., Hodges, K., 1995. Evidence for Tibetan plateau uplift before 14 Myr ago from a new minimum age for east--west extension. Nature 374, 49–52.

Connolly, J.A.D., 1990. Multivariable phase diagrams; an algorithm based on generalized thermodynamics. Am. J. Sci. 290, 666–718.

Corrie, S.L., Kohn, M.J., 2011. Metamorphic history of the central Himalaya, Annapurna region, Nepal, and implications for tectonic models. Geol. Soc. Am. Bull. 123, 1863–1879.

Corthouts, T.L., Lageson, D.R., Shaw, C.A., 2016. Polyphase deformation, dynamic metamorphism, and metasomatism of Mount Everest's summit limestone, east central Himalaya, Nepal/Tibet. Lithosphere 8, 38–57.

Cottle, J., Searle, M., Horstwood, M., Waters, D., 2009. Timing of Midcrustal Metamorphism, Melting, and Deformation in the Mount Everest Region of Southern Tibet Revealed by U(-Th)-Pb Geochronology. J. Geol. 117, 643–664.

Cottle, J.M., Kylander-Clark, A.R., Vrijmoed, J.C., 2012. U–Th/Pb geochronology of detrital zircon and monazite by single shot laser ablation inductively coupled plasma mass spectrometry (SS-LA-ICPMS). Chem. Geol. 332-333, 136–147.

Cottle, J.M., Burrows, A.J., Kylander-Clark, A., Freedman, P.A., Cohen, R.S., 2013. Enhanced sensitivity in laser ablation multi-collector inductively coupled plasma mass spectrometry. J. Anal. At. Spectrom. 28, 1700–1706.

Cottle, J.M., Larson, K.P., Kellett, D.A., 2015. How does the mid-crust accommodate deformation in large, hot collisional orogens? A review of recent research in the Himalayan orogen. J. Struct. Geol. 78, 119–133.

Cottle, J.M., Stearns, M.A., 2018. Application of Single-Shot Laser Ablation Split-Stream Inductively Coupled Plasma Mass Spectrometry to Accessory Phase Petrochronology: Planetary Records Down to Atom Scale, in: Moser, D.E., Corfu, F., Darling, J.R., Reddy, S.M., Tait, K. (Eds.), Microstructural Geochronology, Geophysical Monograph Series. John Wiley & Sons, Inc., Hoboken, NJ, USA, pp. 91–111.

Cottle, J.M., Larson, K.P., Yakymchuk, C., 2018. Contrasting accessory mineral behavior in minimum-temperature melts: Empirical constraints from the Himalayan metamorphic core. Lithos 312-313, 57–71.

Cottle, J., Lederer, G., Larson, K., 2019. The monazite record of pluton assembly: Mapping manaslu using petrochronology. Chem. Geol. 530, 119309.

Cruz-Uribe, A.M., Feineman, M.D., Zack, T., Jacob, D.E., 2018. Assessing trace element (dis)equilibrium and the application of single element thermometers in metamorphic rocks. Lithos 314-315, 1–15.

Cutts, J.A., Smit, M.A., 2018. Rates of Deep Continental Burial From Lu-Hf Garnet Chronology and Zr-in-Rutile Thermometry on (Ultra)high-Pressure Rocks: Lu-Hf garnet chronology of UHP eclogites. Tectonics 37, 71–88.

Darbyshire, F.A., Bastow, I.D., Petrescu, L., Gilligan, A., Thompson, D.A., 2017. A tale of two orogens: Crustal processes in the Proterozoic Trans-Hudson and Grenville Orogens, eastern Canada. Tectonics 36, 1633–1659.

de Capitani, C., Brown, T.H., 1987. The computation of chemical equilibrium in complex systems containing non-ideal solutions. Geochim. Cosmochim. Acta 51, 2639–2652.

de Capitani, C., Petrakakis, K., 2010. The computation of equilibrium assemblage diagrams with Theriak/Domino software. Am. Mineral. 95, 1006–1016.

Duchêne, S., Blichert-Toft, J., Luais, B., Télouk, P., Lardeaux, J.-M., Albarède, F., 1997. The Lu–Hf dating of garnets and the ages of the Alpine high-pressure metamorphism. Nature 387, 586–589.

Enami, M., Nishiyama, T., Mouri, T., 2007. Laser Raman microspectrometry of metamorphic quartz: A simple method for comparison of metamorphic pressures. Am. Mineral. 92, 1303–1315.

Engi, M., Lanari, P., Kohn, M.J., 2017. Significant Ages—An Introduction to Petrochronology. Rev. Mineral. Geochem. 83, 1–12.

Ferrero, S., Angel, R.J., 2018. Micropetrology: Are Inclusions Grains of Truth? J. Petrol. 59, 1671–1700.

Florence, F.P., Spear, F.S., 1991. Effects of diffusional modification of garnet growth zoning on P-T path calculations. Contrib. Mineral. Petrol. 107, 487–500.

Fort, M., Freytet, P., Colchen, M., 1982. Structural and sedimentological evolution of the Thakkhola Mustang graben (Nepal Himalayas). Zeitschrift für Geomorphologie 42, 75–98.

Foster, C.T., 1991. The role of biotite as a catalyst in reaction mechanisms that form sillimanite. Can. Mineral. 29, 943–963.

Foster, G., Kinny, P., Vance, D., Prince, C., Harris, N., 2000. The significance of monazite U–Th–Pb age data in metamorphic assemblages; a combined study of monazite and garnet chronometry. Earth Planet. Sci. Lett. 181, 327–340.

Foster, G., Gibson, H.D., Parrish, R., Horstwood, M., Fraser, J., Tindle, A., 2002. Textural, chemical and isotopic insights into the nature and behaviour of metamorphic monazite. Chem. Geol. 191, 183–207.

From, R., Larson, K., 2014. Tectonostratigraphy, deformation, and metamorphism of the Himalayan mid-crust exposed in the Likhu Khola region, east-central Nepal. Geosphere 10, 292–307.

Fu, J., Li, G., Wang, G., Huang, Y., Zhang, L., Dong, S., Liang, W., 2017. First field identification of the Cuonadong dome in southern Tibet: implications for EW extension of the North Himalayan gneiss dome. Int. J. Earth Sci. 106, 1581–1596.

Gaidies, F., de Capitani, C., Abart, R., 2008. THERIA_G: a software program to numerically model prograde garnet growth. Contrib. Mineral. Petrol. 155, 657–671.

Gansser, A., 1964. Geology of the Himalayas. Interscience.

Gehrels, G.E., DeCelles, P.G., Martin, A., Ojha, T.P., Pinhassi, G., Upreti, B.N., 2003. Initiation of the Himalayan orogen as an early Paleozoic thin-skinned thrust belt. GSA Today 13, 4–9.

Ghent, E.D., Stout, M.Z., 1984. TiO2 activity in metamorphosed pelitic and basic rocks: principles and applications to metamorphism in southeastern Canadian Cordillera. Contrib. Mineral. Petrol. 86, 248–255.

Godin, L., Parrish, R.R., Brown, R.L., Hodges, K.V., 2001. Crustal thickening leading to exhumation of the Himalayan Metamorphic core of central Nepal: Insight from U-Pb Geochronology and 40Ar/39Ar Thermochronology. Tectonics 20, 729–747.

Goscombe, B., Hand, M., 2000. Contrasting P–T Paths in the Eastern Himalaya, Nepal: Inverted Isograds in a Paired Metamorphic Mountain Belt. J. Petrol. 41, 1673–1719.

Goscombe, B., Gray, D., Hand, M., 2006. Crustal architecture of the Himalayan metamorphic front in eastern Nepal. Gondwana Res. 10, 232–255.

Goscombe, B., Gray, D., Foster, D.A., 2018. Metamorphic response to collision in the Central Himalayan Orogen. Gondwana Res. 57, 191–265.

Goswami, P.K., Deopa, T., 2018. Petrotectonic setting of the provenance of Lower Siwalik sandstones of the Himalayan foreland basin, southeastern Kumaun Himalaya, India. Island Arc, North Atlantic Treaty Organization, Advanced Study Institute Series, 148 27, e12242.

Gréaux, S., Yamada, A., 2014. P–V–T equation of state of Mn3Al2Si3O12 spessartine garnet. Phys. Chem. Miner. 41, 141–149.

Griffin, W.L., Brueckner, H.K., 1980. Caledonian Sm–Nd ages and a crustal origin for Norwegian eclogites. Nature 285, 319–321.

Groppo, C., Rolfo, F., Lombardo, B., 2009. P-T Evolution across the Main Central Thrust Zone (Eastern Nepal): Hidden Discontinuities Revealed by Petrology. J. Petrol. 50, 1149–1180.

Groppo, C., Rubatto, D., Rolfo, F., Lombardo, B., 2010. Early Oligocene partial melting in the Main Central Thrust Zone (Arun valley, eastern Nepal Himalaya). Lithos 118, 287–301.

Groppo, C., Rolfo, F., Indares, A., 2012. Partial Melting in the Higher Himalayan Crystallines of Eastern Nepal: the Effect of Decompression and Implications for the "Channel Flow" Model. J. Petrol. 53, 1057–1088.

Groppo, C., Rolfo, F., Mosca, P., 2013. The cordierite-bearing anatectic rocks of the higher Himalayan crystallines (eastern Nepal): low-pressure anatexis, melt productivity, melt loss and the preservation of cordierite. J. Metamorph. Geol. 31, 187–204.

Grujic, D., Hollister, L.S., Parrish, R.R., 2002. Himalayan metamorphic sequence as an orogenic channel: insight from Bhutan. Earth Planet. Sci. Lett. 198, 177–191.

Guillot, S., Hodges, K.V., Le Fort, P., Pêcher, A., 1994. New constraints of the age of the Manaslu leucogranite: evidence for episodic tectonic denudation in the central Himalayas. Geology 22, 559–562.

Guillot, S., Pêcher, A., Le Fort, P., 1995a. Contrôles tectoniques et thermiques de la mise en place des leucogranites himalayens. C. R. Acad. Sci. 320, 55–61.

Guillot, S., Le Fort, P., Pêcher, A., Barman, M.R., Aprahamian, J., 1995b. Contact metamorphism and depth of emplacement of the Manaslu granite (central Nepal). Implications for Himalayan orogenesis. Tectonophysics 241, 99–119.

Guillot, S., Cosca, M., Allemand, P., Le Fort, P., 1999. Contrasting metamorphic and geochronologic evolution along the Himalayan belt, in: Macfarlane, A., Sorkhabi, R.B., Quade, J. (Eds.), Himalaya and Tibet: Mountain Roots to Mountain Tops, 328. Geological Society of America.

Guilmette, C., Indares, A., Hébert, R., 2011. High-pressure anatectic paragneisses from the Namche Barwa, Eastern Himalayan Syntaxis: Textural evidence for partial melting, phase equilibria modeling and tectonic implications. Lithos 124, 66–81.

Guiraud, M., Powell, R., 2006. P V T relationships and mineral equilibria in inclusions in minerals. Earth Planet. Sci. Lett. 244, 683–694.

Guo, L., Zhang, J., Zhang, B., 2008. Structures, kinematics, thermochronology and tectonic evolution of the Ramba gneiss dome in the northern Himalaya. Prog. Nat. Sci. 18, 851–860.

Guo, Z., Wilson, M., 2012. The Himalayan leucogranites: Constraints on the nature of their crustal source region and geodynamic setting. Gondwana Res. 22, 360–376.

Gwanmesia, G.D., Wang, L., Heady, A., Liebermann, R.C., 2014. Elasticity and sound velocities of polycrystalline grossular garnet (Ca3Al2Si3O12) at simultaneous high pressures and high temperatures. Phys. Earth Planet. Inter. 228, 80–87.

Harris, N., Massey, J., 1994. Decompression and anatexis of Himalayan metapelites. Tectonics 13, 1537–1546.

Harris, N.B.W., Caddick, M., Kosler, J., Goswami, S., Vance, D., Tindle, A.G., 2004. The pressure-temperature-time path of migmatites from the Sikkim Himalaya. J. Metamorph. Geol. 22, 249–264.

Harris, N., 2007. Channel flow and the Himalayan–Tibetan orogen: a critical review. J. Geol. Soc. London 164, 511–523.

Harrison, T.M., Grove, M., Lovera, O.M., Catlos, E.J., D'Andrea, J., 1999. The origin of Himalayan anatexis and inverted metamorphism: Models and constraints. J. Asian Earth Sci. 17, 755–772.

He, D., Webb, A.A.G., Larson, K.P., Martin, A.J., Schmitt, A.K., 2015. Extrusion vs. duplexing models of Himalayan mountain building 3: duplexing dominates from the Oligocene to Present. Int. Geol. Rev. 57, 1–27.

Henry, D.J., Guidotti, C.V., Thomson, J.A., 2005. The Ti-saturation surface for low-to-medium pressure metapelitic biotites: Implications for geothermometry and Ti-substitution mechanisms. Am. Mineral. 90, 316–328.

Hermann, J., Rubatto, D., 2003. Relating zircon and monazite domains to garnet growth zones: age and duration of granulite facies metamorphism in the Val Malenco lower crust. J. Metamorph. Geol. 21, 833–852.

Hodges, K.V., Crowley, J.L., 1985. Error estimation and empirical geothermobarometry for pelitic systems. Am. Mineral.

Hodges, K.V., Parrish, R.R., Searle, M.P., 1996. Tectonic evolution of the central Annapurna Range, Nepalese Himalayas. Tectonics 15, 1264–1291.

Hodges, K.V., 2000. Tectonics of the Himalaya and southern Tibet from two perspectives. GSA Bulletin 112, 324–350.

Hoisch, T.D., 1990. Empirical calibration of six geobarometers for the mineral assemblage quartz+muscovite+biotite+plagioclase+garnet. Contrib. Mineral. Petrol. 104, 225–234.

Holdaway, M.J., 2000. Application of new experimental and garnet Margules data to the garnet-biotite geothermometer. Am. Mineral. 85, 881–892.

Holland, T., Powell, R., 1996. Thermodynamics of order-disorder in minerals; II, Symmetric formalism applied to solid solutions. Am. Mineral. 81, 1425–1437.

Holland, T., Powell, R., 1998. An internally consistent thermodynamic data set for phases of petrological interest. J. Metamorph. Geol. 16, 309–343.

Holland, T., Powell, R., 2003. Activity–composition relations for phases in petrological calculations: an asymmetric multicomponent formulation. Contrib. Mineral. Petrol. 145, 492–501.

Hollister, L.S., 1966. Garnet Zoning: An Interpretation Based on the Rayleigh Fractionation Model. Science 154, 1647–1651.

Horstwood, M.S.A., Foster, G.L., Parrish, R.R., Noble, S.R., Nowell, G.M., 2003. Common-Pb corrected in situ U–Pb accessory mineral geochronology by LA-MC-ICP-MS. J. Anal. At. Spectrom. 18, 837–846.

Horstwood, M.S.A., Košler, J., Gehrels, G., Jackson, S.E., McLean, N.M., Paton, C., Pearson, N.J., Sircombe, K., Sylvester, P., Vermeesch, P., Bowring, J.F., Condon, D.J., Schoene, B., 2016. Community-Derived Standards for LA-ICP-MS U-(Th-)Pb Geochronology - Uncertainty Propagation, Age Interpretation and Data Reporting. Geostand. Geoanal. Res. 40, 311–332.

Hubbard, M., 1996. Ductile shear as a cause of inverted metamorphism: Example from the Nepal Himalaya. J. Geol. 104, 493–499.

Hurtado, J.M., Hodges, K.V., Whipple, K.X., 2001. Neotectonics of the Thakkhola graben and implications for recent activity on the South Tibetan fault system in the central Nepal Himalaya. GSA Bulletin 113, 222–240.

Hurtado, J.M., 2002. Tectonic Evolution of the Thakkhola Graben and Dhaulagiri Himalaya, Central Nepal (PhD Dissertation). Massachusetts Institute of Technology.

Hu, X., Garzanti, E., Wang, J., Huang, W., An, W., Webb, A., 2016. The timing of India-Asia collision onset – Facts, theories, controversies. Earth-Sci. Rev. 160, 264–299.

Husson, L., Sempere, T., 2003. Thickening the Altiplano crust by gravity-driven crustal channel flow. Geophys. Res. Lett. 30, 1243.

Iaccarino, S., Montomoli, C., Carosi, R., Massonne, H.-J., Langone, A., Visonà, D., 2015. Pressure–temperature–time–deformation path of kyanite-bearing migmatitic paragneiss in the Kali Gandaki valley (Central Nepal): Investigation of Late Eocene–Early Oligocene melting processes. Lithos 231, 103–121.

Iaccarino, S., Montomoli, C., Carosi, R., Massonne, H.-J., Visonà, D., 2017. Geology and tectono-metamorphic evolution of the Himalayan metamorphic core: insights from the Mugu Karnali transect, Western Nepal (Central Himalaya). J. Metamorph. Geol. 35, 301–325.

Imayama, T., Takeshita, T., Arita, K., 2010. Metamorphic P-T profile and P-T path discontinuity across the far-eastern Nepal Himalaya: investigation of channel flow models. J. Metamorph. Geol. 28, 527–549.

Imayama, T., Takeshita, T., Yi, K., Cho, D.-L., Kitajima, K., Tsutsumi, Y., Kayama, M., Nishido, H., Okumura, T., Yagi, K., Itaya, T., Sano, Y., 2012. Two-stage partial melting and contrasting cooling history within the Higher Himalayan Crystalline Sequence in the far-eastern Nepal Himalaya. Lithos 134-135, 1–22.

Indares, A., White, R.W., Powell, R., 2008. Phase equilibria modelling of kyanite-bearing anatectic paragneisses from the central Grenville Province. J. Metamorph. Geol. 26, 815–836.

Jaeger, J.C., 1964. Thermal effects of intrusions. Rev. Geophys. 2, 443.

Jaeger, J.C., 1968. Cooling and solidification of igneous rocks, in: Hess, H.H., Poldervaart, A. (Eds.), Basalts, the Poldervaart Treatise on Rocks of Basaltic Composition. Wiley, New York-London-Sidney, pp. 503–536.

Jamieson, R.A., Beaumont, C., Medvedev, S., Nguyen, M.H., 2004. Crustal channel flows: 2. Numerical models with implications for metamorphism in the Himalayan-Tibetan orogen. J. Geophys. Res., Geol. Soc. Spec. Publ. 109, 364.

Jamieson, R.A., Beaumont, C., Nguyen, M.H., Grujic, D., 2006. Provenance of the Greater Himalayan Sequence and associated rocks: predictions of channel flow models. Geological Society, London, Special Publications 268, 165–182.

Jamieson, R.A., Beaumont, C., 2013. On the origin of orogens. GSA Bulletin 125, 1671–1702.

Jessup, M.J., Langille, J.M., Diedesch, T.F., Cottle, J.M., 2019. Gneiss Dome Formation in the Himalaya and southern Tibet. Geological Society, London, Special Publications 483, 401–422.

Johnson, D.M., Hooper, P.R., M, C.R., 1999. GeoAnalytical Lab, Washington State University. Adv. X-Ray Anal. 41, 843–867.

Kawakami, T., Aoya, M., Wallis, S.R., Lee, J., 2007. Contact metamorphism in the Malashan dome, North Himalayan gneiss domes, southern Tibet: an example of shallow extensional tectonics in the Tethys Himalaya. Journal of Metamorphic Geology 25, 831–853.

Kellett, D.A., Godin, L., 2009. Pre-Miocene deformation of the Himalayan superstructure, Hidden valley, central Nepal. J. Geol. Soc. London 166, 261–275.

Kellett, D.A., Cottle, J.M., Smit, M., 2014. Eocene deep crust at Ama Drime, Tibet: Early evolution of the Himalayan orogen. Lithosphere 6, 220–229.

Kellett, D.A., Cottle, J.M., Larson, K.P., 2019. The South Tibetan Detachment System: history, advances, definition and future directions. Geological Society, London, Special Publications 483, 377–400.

Kelly, E.D., Carlson, W.D., Connelly, J.N., 2011. Implications of garnet resorption for the Lu-Hf garnet geochronometer: an example from the contact aureole of the Makhavinekh Lake Pluton, Labrador. J. Metamorph. Geol. 29, 901–916.

Kelsey, D.E., Clark, C., Hand, M., 2008. Thermobarometric modelling of zircon and monazite growth in melt-bearing systems: examples using model metapelitic and metapsammitic granulites. J. Metamorph. Geol. 26, 199–212.

Kelsey, D.E., Hand, M., 2015. On ultrahigh temperature crustal metamorphism: Phase equilibria, trace element thermometry, bulk composition, heat sources, timescales and tectonic settings. Geoscience Frontiers 6, 311–356.

Klootwijk, C.T., Gee, J.S., Peirce, J.W., Smith, G.M., 1992. An early India-Asia contact; paleomagnetic constraints from Ninetyeast Ridge, ODP Leg 121. Geology 20, 395–398.

Kohn, M.J., Spear, F., 2000. Retrograde net transfer reaction insurance for pressure-temperature estimates. Geology 28, 1127–1130.

Kohn, M.J., 2004. Oscillatory- and sector-zoned garnets record cyclic (?) rapid thrusting in central Nepal. Geochem. Geophys. Geosyst. 5.

Kohn, M.J., Malloy, M.A., 2004. Formation of monazite via prograde metamorphic reactions among common silicates: implications for age determinations. Geochim. Cosmochim. Acta 68, 101–113.

Kohn, M.J., Wieland, M.S., Parkinson, C.D., Upreti, B.N., 2005. Five generations of monazite in Langtang gneisses: implications for chronology of the Himalayan metamorphic core. J. Metamorph. Geol. 23, 399–406.

Kohn, M.J., 2008. P-T-t data from central Nepal support critical taper and repudiate large-scale channel flow of the Greater Himalayan Sequence. GSA Bulletin 120, 259–273.

Kohn, M.J., 2009. Models of garnet differential geochronology. Geochim. Cosmochim. Acta 73, 170–182.

Kohn, M.J., 2014a. Himalayan Metamorphism and Its Tectonic Implications. Annu. Rev. Earth Planet. Sci. 42, 381–419.

Kohn, M.J., 2014b. "Thermoba-Raman-try": Calibration of spectroscopic barometers and thermometers for mineral inclusions. Earth Planet. Sci. Lett. 388, 187–196.

Kohn, M.J., 2016. Metamorphic chronology—a tool for all ages: Past achievements and future prospects. Am. Mineral. 101, 25–42.

Kohn, M.J., Engi, M., Lanari, P. (Eds.), 2019. Petrochronology: Methods and Applications. Mineralogical Society of America.

Kylander-Clark, A.R.C., Hacker, B.R., Cottle, J.M., 2013. Laser-ablation split-stream ICP petrochronology. Chem. Geol. 345, 99–112.

Kylander-Clark, A.R.C., 2017. Petrochronology by Laser-Ablation Inductively Coupled Plasma Mass Spectrometry. Rev. Mineral. Geochem. 83, 183–198.

Langille, J., Lee, J., Hacker, B., Seward, G., 2010. Middle crustal ductile deformation patterns in southern Tibet: Insights from vorticity studies in Mabja Dome. J. Struct. Geol. 32, 70–85.

Lapen, T.J., Johnson, C.M., Baumgartner, L.P., Mahlen, N.J., Beard, B.L., Amato, J.M., 2003. Burial rates during prograde metamorphism of an ultra-high-pressure terrane: an

example from Lago di Cignana, western Alps, Italy. Earth Planet. Sci. Lett. 215, 57–72.

Larson, K.P., Godin, L., Price, R.A., 2010a. Relationships between displacement and distortion in orogens: Linking the Himalayan foreland and hinterland in central Nepal. GSA Bulletin 122, 1116–1134.

Larson, K.P., Godin, L., Davis, W.J., Davis, D.W., 2010b. Out-of-sequence deformation and expansion of the Himalayan orogenic wedge: insight from the Changgo culmination, south central Tibet. Tectonics, Geol. Soc. Spec. Publ. 29.

Larson, K.P., Cottle, J.M., Godin, L., 2011. Petrochronologic record of metamorphism and melting in the upper Greater Himalayan sequence, Manaslu-Himal Chuli Himalaya, west-central Nepal. Lithosphere 3, 379–392.

Larson, K.P., Gervais, F., Kellett, D.A., 2013. A P–T–t–D discontinuity in east-central Nepal: Implications for the evolution of the Himalayan mid-crust. Lithos 179, 275–292.

Larson, K.P., Cottle, J.M., 2014. Midcrustal discontinuities and the assembly of the Himalayan midcrust. Tectonics, Geol. Soc. London Spec. Publ. 33, 718–740.

Larson, K.P., Ambrose, T.K., Webb, A.A.G., Cottle, J.M., Shrestha, S., 2015. Reconciling Himalayan midcrustal discontinuities: The Main Central thrust system. Earth Planet. Sci. Lett. 429, 139–146.

Larson, K.P., Kellett, D.A., Cottle, J.M., King, J., Lederer, G., Rai, S.M., 2016. Anatexis, cooling, and kinematics during orogenesis: Miocene development of the Himalayan metamorphic core, east-central Nepal. Geosphere 12, 1575–1595.

Larson, K.P., Camacho, A., Cottle, J.M., Coutand, I., Buckingham, H.M., Ambrose, T.K., Rai, S.M., 2017. Cooling, exhumation, and kinematics of the Kanchenjunga Himal, far east Nepal: Exhumation of the Kanchenjunga Himal. Tectonics 36, 1037–1052.

Larson, K.P., 2018. Refining the structural framework of the Khimti Khola region, east-central Nepal Himalaya, using quartz textures and c-axis fabrics. J. Struct. Geol. 107, 142–152.

Larson, K.P., Ali, A., Shrestha, S., Soret, M., Cottle, J.M., Ahmad, R., 2019. Timing of metamorphism and deformation in the Swat valley, northern Pakistan: Insight into garnet-monazite HREE partitioning. Geoscience Frontiers 10, 849–861.

Larson, K.P., 2020. Geochronology Plotting Scripts in R. OSF. https://doi.org/10.17605/OSF.IO/P46MB

Larson, K.P., Shrestha, S., Soret, M., Smit, M., 2020a. The P-T-t-D evolution of the Mahabharat, east-central Nepal: The out-of-sequence development of the Himalaya. Geoscience Frontiers.

Larson, K.P., Kellett, D.A., Cottle, J.M., Camacho, A., Brubacher, A.D., 2020b. Mid-Miocene initiation of E-W extension and recoupling of the Himalaya. Terra Nova 32, 151–158.

Law, R.D., Searle, M.P., Godin, L., 2006. Channel Flow, Ductile Extrusion and Exhumation in Continental Collision Zones. Geological Society.

Lee, J., Hacker, B.R., Wang, Y., 2004. Evolution of North Himalayan gneiss does: structural and metamorphic studies in Mabja Dome, southern Tibet. J. Struct. Geol. 26, 2297–2316.

Lee, J., McClelland, W., Wang, Y., Blythe, A., McWilliams, M., 2006. Oligocene-Miocene middle crustal flow in southern Tibet: geochronology of Mabja Dome. Geological Society, London, Special Publications 268, 445–469.

Lee, J., Hager, C., Wallis, S.R., Stockli, D.F., Whitehouse, M.J., Aoya, M., Wang, Y., 2011. Middle to late Miocene extremely rapid exhumation and thermal reequilibration in the Kung Co rift, southern Tibet. Tectonics, Rev. Mineral. Geochem. 30, TC2007.

Le Fort, P., 1975. Himalayas: The Collided Range. Present knowledge of the continental arc. Am. J. Sci. 275-A, 1–44.

Le Fort, P., France-Lanord, C., 1995. Granites from Mustang and surrounding regions (Central Nepal). Journal of Nepal Geological Society 11, 53–58.

Liu, Z.-C., Wu, F.-Y., Ji, W.-Q., Wang, J.-G., Liu, C.-Z., 2014. Petrogenesis of the Ramba leucogranite in the Tethyan Himalaya and constraints on the channel flow model. Lithos 208-209, 118–136.

Ludwig, K.R., 2003. Isoplot 3.00. Berkeley Geochronology Center Special Publication 4.

Mahar, E.M., Baker, J.M., Powell, R., Holland, T.J.B., Howell, N., 1997. The effect of Mn on mineral stability in metapelites. J. Metamorph. Geol. 15, 223–238.

Mahéo, G., Leloup, P.H., Valli, F., Lacassin, R., Arnaud, N., Paquette, J.-L., Fernandez, A., Haibing, L., Farley, K.A., Tapponnier, P., 2007. Post 4 Ma initiation of normal faulting in southern Tibet. Constraints from the Kung Co half graben. Earth Planet. Sci. Lett. 256, 233–243.

Martin, A.J., Gehrels, G.E., DeCelles, P.G., 2007. The tectonic significance of (U,Th)/Pb ages of monazite inclusions in garnet from the Himalaya of central Nepal. Chem. Geol. 244, 1–24.

Martin, A.J., Copeland, P., Benowitz, J.A., 2015. Muscovite 40Ar/39Ar ages help reveal the Neogene tectonic evolution of the southern Annapurna Range, central Nepal. Geological Society, London, Special Publications 412, 199–220.

Martin, A.J., 2017a. A review of definitions of the Himalayan Main Central Thrust. Int. J. Earth Sci. 106, 2131–2145.

Martin, A.J., 2017b. A review of Himalayan stratigraphy, magmatism, and structure. Gondwana Res. 49, 42–80.

McDonough, W.F., Sun, S.-S., 1995. The composition of the Earth. Chem. Geol. 120, 223–253.

McKinney, S.T., Cottle, J.M., Lederer, G.W., 2015. Evaluating rare earth element (REE) mineralization mechanisms in Proterozoic gneiss, Music Valley, California.

McQuarrie, N., Tobgay, T., Long, S.P., Reiners, P.W., Cosca, M.A., 2014. Variable exhumation rates and variable displacement rates: Documenting recent slowing of Himalayan shortening in western Bhutan. Earth Planet. Sci. Lett. 386, 161–174.

Merschat, A.J., Hatcher, R.D., Davis, T.L., 2005. The northern Inner Piedmont, southern Appalachians, USA: kinematics of transpression and SW-directed mid-crustal flow. J. Struct. Geol. 27, 1252.

Milani, S., Nestola, F., Alvaro, M., Pasqual, D., Mazzucchelli, M.L., Domeneghetti, M.C., Geiger, C.A., 2015. Diamond–garnet geobarometry: The role of garnet compressibility and expansivity. Lithos 227, 140–147.

Milani, S., Angel, R.J., Scandolo, L., Mazzucchelli, M.L., Ballaran, T.B., Klemme, S., Domeneghetti, M.C., Miletich, R., Scheidl, K.S., Derzsi, M., Tokár, K., Prencipe, M., Alvaro, M., Nestola, F., 2017. Thermo-elastic behavior of grossular garnet at high pressures and temperatures. Am. Mineral. 102, 851–859.

Montomoli, C., Iaccarino, S., Carosi, R., Langone, A., Visonà, D., 2013. Tectonometamorphic discontinuities within the Greater Himalayan Sequence in Western Nepal (Central Himalaya): Insights on the exhumation of crystalline rocks. Tectonophysics 608, 1349–1370.

Montomoli, C., Carosi, R., Iaccarino, S., 2015. Tectonometamorphic discontinuities in the Greater Himalayan Sequence: a local or a regional feature? Geological Society, London, Special Publications 412, 25–41.

Mottram, C.M., Argles, T.W., Harris, N.B., 2014. Tectonic interleaving along the Main Central Thrust, Sikkim Himalaya. J. Geol. Soc. London 171, 255–268.

Muecke, G.K., Pride, C., Sarkar, P., 1979. Rare-earth element geochemistry of regional metamorphic rocks. Phys. Chem. Earth. 11, 449–464.

Murri, M., Mazzucchelli, M.L., Campomenosi, N., Korsakov, A.V., Prencipe, M., Mihailova, B.D., Scambelluri, M., Angel, R.J., Alvaro, M., 2018. Raman elastic geobarometry for anisotropic mineral inclusions. Am. Mineral. 103, 1869–1872.

Nachlas, W.O., Whitney, D.L., Teyssier, C., Bagley, B., Mulch, A., 2014. Titanium concentration in quartz as a record of multiple deformation mechanisms in an extensional shear zone. Geochem. Geophys. Geosyst. 15, 1374–1397.

Nachlas, W.O., Thomas, J.B., Hirth, G., 2018. TitaniQ deformed: Experimental deformation of out-of-equilibrium quartz porphyroclasts. J. Struct. Geol. 116, 207–222.

Nakayama, K., Ulak, P.D., 1999. Evolution of fluvial style in the Siwalik Group in the foothills of the Nepal Himalaya. Sediment. Geol. 125, 205–224.

Nelson, K.D., Zhao, W., Brown, L.D., Kuo, J., Che, J., Liu, X., Klemperer, S.L., Makovsky, Y., Meissner, R., Mechie, J., Kind, R., Wenzel, F., Ni, J., Nabelek, J., Leshou, C., Tan, H., Wei, W., Jones, A.G., Booker, J., Unsworth, M., Kidd, W.S.F., Hauck, M., Alsdorf, D., Ross, A., Cogan, M., Wu, C., Sandvol, E., Edwards, M., 1996. Partially Molten Middle Crust Beneath Southern Tibet: Synthesis of Project INDEPTH Results. Science 274, 1684–1688.

Otamendi, J.E., de la Rosa, J.D., Patino Douce, A.E., Castro, A., 2002. Rayleigh fractionation of heavy rare earths and yttrium during metamorphic garnet growth. Geology 30, 159–162.

Palin, R.M., Searle, M.P., Waters, D.J., Horstwood, M.S.A., Parrish, R.R., 2012. Combined thermobarometry and geochronology of peraluminous metapelites from the Karakoram metamorphic complex, North Pakistan; New insight into the tectonothermal evolution of the Baltoro and Hunza Valley regions. J. Metamorph. Geol. 30, 793–820.

Patino Douce, A.E., Dana Johnston, A., Rice, J.M., 1993. Octahedral excess mixing properties in biotite: A working model with applications to geobarometry and geothermometry. Am. Mineral. 78, 113–131.

Paton, C., Hellstrom, J., Paul, B., Woodhead, J., Hergt, J., 2011. Iolite: Freeware for the visualisation and processing of mass spectrometric data. J. Anal. At. Spectrom. 26, 2508–2518.

Powell, R., Holland, T.J.B., 1988. An internally consistent dataset with uncertainties and correlations: 3. Applications to geobarometry, worked examples and a computer program. J. Metamorph. Geol. 6, 173–204.

Powell, R., Holland, T., 1994. Optimal geothermometry and geobarometry. Am. Mineral. 79, 120–133.

Powell, R., Holland, T.J.B., 2008. On thermobarometry. J. Metamorph. Geol. 26, 155–179.

Powell, R., Holland, T., 2010. Using Equilibrium Thermodynamics to Understand Metamorphism and Metamorphic Rocks. Elements 6, 309–314.

Pyle, J.M., Spear, F.S., 1999. Yttrium zoning in garnet: coupling of major and accessory phases during metamorphic reactions. Geological Materials Research 1, 1–49.

Pyle, J.M., Spear, F.S., 2000. An empirical garnet (YAG) – xenotime thermometer. Contrib. Mineral. Petrol. 138, 51–58.

Pyle, J.M., Spear, F.S., Rudnick, R.L., McDonough, W.F., 2001. Monazite-xenotime-garnet equilibrium in metapelites and a new monazite-garnet thermometer. J. Petrol. 42, 2083–2107.

Pyle, J.M., Spear, F.S., 2003. Four generations of accessory-phase growth in low-pressure migmatites from SW New Hampshire. Am. Mineral. 88, 338–351.

Quigley, M.C., Liangjun, Y., Xiaohan, L., Wilson, C.J.L., Sandiford, M., Phillips, D., 2006. 40Ar/39Ar thermochronology of the Kampa Dome, southern Tibet: Implications for tectonic evolution of the North Himalayan gneiss domes. Tectonophysics 421.

Quigley, M.C., Liangjun, Y., Gregory, C., Corvino, Sandiford, M., Wilson, C.J.L., Xiaohan, L., 2008. U-Pb SHRIMP zircon geochronology and T-t-d history of the Kampa Dome, southern Tibet. Tectonophysics 446, 97–113.

Regis, D., Warren, C.J., Mottram, C.M., 2016. Using monazite and zircon petrochronology to constrain the P–T–t evolution of the middle crust in the Bhutan Himalaya. Journal of 34, 617–639.

Rice, A.H.N., 1987. Continuous out-of-sequence ductile thrusting in the Norwegian Caledonides. Geol. Mag. 124, 249–260.

Rice, A.H.N., Mitchell, J.I., 1991. Porphyroblast textural sector-zoning and matrix displacement. Mineral. Mag. 55, 379–396.

Rice, A.H.N., 1993. Textural and twin sector-zoning and displacement of graphite in chiastolite and pyralspite and grandite garnets in the Variscides of south-west England. Proceedings-Ussher Society 8, 124–124.

Rivers, T., 2008. Assembly and preservation of lower, mid, and upper orogenic crust in the Grenville Province—Implications for the evolution of large hot long-duration orogens. Precambrian Res. 167, 237–259.

Rollinson, H.R., 1993. Using Geochemical Data: Evaluation, Presentation, Interpretation. Routledge.

Rubatto, D., Hermann, J., Buick, I.S., 2006. Temperature and bulk composition control on the growth of monazite and zircon during low-pressure anatexis (Mount Stafford, Central Australia). J. Petrol. 47, 1973–1996.

Schärer, U., 1984. The effect of inital 230 Th disequilibrium on young U-Pb ages: the Makalu case, Himalaya. Earth and Planetary Sciences Letters 67, 191–204.

Schärer, U., Hamet, J., Allegre, C., 1984. The Transhimlaya (Gangdese) plutonsim in the Ladakh region: a U-Pb and Rb-Sr study. Earth Planet. Sci. Lett. 67, 327–339.

Schelling, D., 1992. The tectonostratigraphy and structure of the eastern Nepal Himalaya. Tectonics 11, 925–943.

Scherer, E.E., Cameron, K.L., Blichert-Toft, J., 2000. Lu–hf garnet geochronology: closure temperature relative to the Sm–Nd system and the effects of trace mineral inclusions. Geochim. Cosmochim. Acta 64, 3413–3432.

Schmidt, C., Ziemann, M.A., 2000. In-situ Raman spectroscopy of quartz: A pressure sensor for hydrothermal diamond-anvil cell experiments at elevated temperatures. Am. Mineral. 85, 1725–1734.

Searle, M.P., 1999. Emplacement of Himalayan leucogranites by magma injection along giant sill complexes: examples from Cho Oyu, Gyachung Kang and Everest leucogranites (Nepal Himalaya). J. Asian Earth Sci.

Searle, M.P., Godin, L., 2003. The South Tibetan Detachment and the Manalsu Leucogranite: A Structural Reinterpretation and Restoration of the Annapurna-Manaslu Himalaya, Nepal. J. Geol. 111.

Searle, M.P., Law, R.D., Jessup, M.J., 2006. Crustal structure, restoration and evolution of the Greater Himalaya in Nepal-South Tibet: implications for channel flow and ductile extrusion of the middle crust, in: Law, R.D., Searle, M.P., Godin, L. (Eds.), Channel Flow, Ductile Exrusion and Exhumation in Continental Collision Zones. pp. 355–378.

Searle, M.P., Law, R.D., Godin, L., Larson, K.P., Streule, M.J., Cottle, J.M., Jessup, M.J., 2008. Defining the Himalayan Main Central Thrust in Nepal. J. Geol. Soc. London 165, 523–534.

Searle, M.P., 2010. Low-angle normal faults in the compressional Himalayan orogen; Evidence from the Annapurna–Dhaulagiri Himalaya, Nepal. Geosphere 6, 296–315.

Shrestha, S., Larson, K.P., Guilmette, C., Smit, M.A., 2017. The P-T-t evolution of the exhumed Himalayan metamorphic core in the Likhu Khola region, East Central Nepal. J. Metamorph. Geol. 35, 663–693.

Shrestha, S., Larson, K.P., Duesterhoeft, E., Soret, M., Cottle, J.M., 2019. Thermodynamic modelling of phosphate minerals and its implications for the development of P-T-t histories: A case study in garnet - monazite bearing metapelites. Lithos 334-335, 141–160.

Shrestha, S., Larson, K.P., Martin, A.J., Guilmette, C., Smit, M.A., Cottle, J.M., 2020. The Greater Himalayan Thrust Belt: Insight Into the Assembly of the Exhumed Himalayan Metamorphic Core, Modi Khola Valley, Central Nepal. Tectonics 39, 295.

Sinogeikin, S.V., Bass, J.D., 2000. Single-crystal elasticity of pyrope and MgO to 20 GPa by Brillouin scattering in the diamond cell. Phys. Earth Planet. Inter. 120, 43–62.

Smit, M.A., Scherer, E.E., Bröcker, M., van Roermund, H.L.M., 2010. Timing of eclogite facies metamorphism in the southernmost Scandinavian Caledonides by Lu–Hf and Sm–Nd geochronology. Contrib. Mineral. Petrol. 159, 521–539.

Smit, M.A., Hacker, B.R., Lee, J., 2014. Tibetan garnet records early Eocene initiation of thickening in the Himalaya. Geology 42, 591–594.

Spear, F.S., 1989. Metamorphic pressure-temperature-time paths. American Geophysical Union, Washington, D.C.

Spear, F.S., 1993. Metamorphic Phase Equilibria and Pressure-temperature-time Paths. Mineralogical Society of America.

Spear, F.S., Pyle, J.M., 2002. Apatite, Monazite, and Xenotime in Metamorphic Rocks. Rev. Mineral. Geochem. 48, 293–335.

Spear, F.S., Pyle, J.M., 2010. Theoretical modeling of monazite growth in a low-Ca metapelite. Chem. Geol. 273, 111–119.

Spear, F.S., Thomas, J.B., Hallett, B.W., 2014. Overstepping the garnet isograd: a comparison of QuiG barometry and thermodynamic modeling. Contrib. Mineral. Petrol. 168, 1059.

Stampfli, G.M., 2000. Tethyan oceans. Geological Society, London, Special Publications 173, 1–23.

Streule, M.J., Searle, M.P., Waters, D.J., Horstwood, M.S.A., 2010. Metamorphism, melting, and channel flow in the Greater Himalayan Sequence and Makalu leucogranite: Constraints from thermobarometry, metamorphic modeling, and U-Pb geochronology. Tectonics 29, TC5011.

Taylor, S.R., McLennan, S.M., 1988. The significance of the rare earths in geochemistry and cosmochemistry, in: Handbook on the Physics and Chemistry of Rare Earths. Elsevier, pp. 485–578.

Thiessen, E.J., Daniel Gibson, H., Regis, D., Pehrsson, S.J., Cutts, J.A., Smit, M.A., 2019. High-grade metamorphism flying under the radar of accessory minerals. Geology 47, 568–572.

Thomas, J.B., Bruce Watson, E., Spear, F.S., Shemella, P.T., Nayak, S.K., Lanzirotti, A., 2010. TitaniQ under pressure: the effect of pressure and temperature on the solubility of Ti in quartz. Contrib. Mineral. Petrol. 160, 743–759.

Thöni, M., Miller, C., Hager, C., Grasemann, B., Horschinegg, M., 2012. New geochronological constraints on the thermal and exhumation history of the Lesser and Higher Himalayan Crystalline Units in the Kullu–Kinnaur area of Himachal Pradesh (India). J. Asian Earth Sci. 52, 98–116.

Tomascak, P.B., Krogstad, E.J., Walker, R.J., 1996. U-Pb Monazite Geochronology of Granitic Rocks from Maine: Implications for Late Paleozoic Tectonics in the Northern Appalachians. J. Geol. 104, 185–195.

Tracy, R.J., Robinson, P., Thompson, A.B., 1976. Garnet composition and zoning in the determination of temperature and pressure of metamorphism, central Massachusetts. Am. Mineral. 61, 762–775.

Treagus, S.H., Treagus, J.E., 2002. Studies of strain and rheology of conglomerates. J. Struct. Geol. 24, 1541–1567.

Upreti, B.N., 1999. An overview of the stratigraphy and tectonics of the Nepal Himalaya. J. Asian Earth Sci. 17, 577–606.

Vermeesch, P., 2018. IsoplotR: A free and open toolbox for geochronology. Geoscience Frontiers 9, 1479–1493.

Vielzeuf, D., Baronnet, A., Perchuk, A.L., Laporte, D., Baker, M.B., 2007. Calcium diffusivity in alumino-silicate garnets: an experimental and ATEM study. Contrib. Mineral. Petrol. 154, 153–170.

Viete, D.R., Kylander-Clark, A.R.C., Hacker, B.R., 2015. Single-shot laser ablation split stream (SS-LASS) petrochronology deciphers multiple, short-duration metamorphic events. Chem. Geol. 415, 70–86.

Wagner, T., Lee, J., Hacker, B.R., Seward, G., 2010. Kinematics and vorticity in Kangmar Dome, southern Tibet: Testing midcrustal channel flow models for the Himalaya. Tectonics, Geol. Soc. Spec. Publ. 29.

Wang, J.M., Zhang, J.J., Wang, X.X., 2013. Structural kinematics, metamorphic P-T profiles and zircon geochronology across the Greater Himalayan Crystalline Complex in south-central Tibet: implication for a revised channel flow. J. Metamorph. Geol. 31, 607–628.

Wang, J.-M., Wu, F.-Y., Rubatto, D., Liu, S.-R., Zhang, J.-J., Liu, X.-C., Yang, L., 2017. Monazite behaviour during isothermal decompression in pelitic granulites: a case study from Dinggye, Tibetan Himalaya. Contrib. Mineral. Petrol. 172, 81.

Wark, D.A., Watson, E.B., 2006. TitaniQ: a titanium-in-quartz geothermometer. Contrib. Mineral. Petrol. 152, 743–754.

Warren, C.J., Grujic, D., Kellett, D.A., Cottle, J.M., Jamieson, R.A., Ghalley, K.S., 2011. Probing the depths of the India-Asia collision: U-Th-Pb monazite chronology of granulites from NW Bhutan. Tectonics 30.

Warren, C.J., Singh, A.K., Roberts, N.M.W., Regis, D., Halton, A.M., Singh, R.B., 2014. Timing and conditions of peak metamorphism and cooling across the Zimithang Thrust, Arunachal Pradesh, India. Lithos 200-201, 94–110.

Warren, C.J., Greenwood, L.V., Argles, T.W., Roberts, N.M.W., Parrish, R.R., Harris, N.B.W., 2019. Garnet–monazite rare earth element relationships in sub-solidus metapelites: a case study from Bhutan. Geological Society, London, Special Publications 478, 145–166.

Waters, D.J., 2001. The significance of prograde and retrograde quartz-bearing intergrowth microstructures in partially melted granulite-facies rocks. Lithos 56, 97–110.

Waters, D.J., 2019. Metamorphic constraints on the tectonic evolution of the High Himalaya in Nepal: the art of the possible. Geological Society, London, Special Publications 483, 325–375.

Webb, A.A.G., Yin, A., Mark Harrison, T., Célérier, J., Paul Burgess, W., 2007. The leading edge of the Greater Himalayan Crystalline complex revealed in the NW Indian Himalaya: Implications for the evolution of the Himalayan orogen. Geology 35, 955–958.

Webb, A.A.G., Schmitt, A.K., He, D., Weigand, E.L., 2011. Structural and geochronological evidence for the leading edge of the Greater Himalayan Crystalline complex in the central Nepal Himalaya. Earth Planet. Sci. Lett. 304, 483–495.

Weller, O.M., St-Onge, M.R., Searle, M.P., Waters, D.J., Rayner, N., Chen, S., Chung, S.-L., Palin, R.M., 2015. Quantifying the P-T-t conditions of north-south Lhasa terrane accretion: new insight into the pre-Himalayan architecture of the Tibetan plateau. J. Metamorph. Geol. 33, 91–113.

White, R.W., Powell, R., Clarke, G.L., 2002. The interpretation of reaction textures in Fe-rich metapelitic granulites of the Musgrave Block, central Australia: constraints from mineral equilibria calculations in the system K2O--FeO--MgO--Al2O3--SiO2--H2O--TiO2--Fe2O3. J. Metamorph. Geol. 20, 41–55.

White, R.W, Powell, R., Holland, T. J. B, Worley, A., 2000. The effect of TiO2 and Fe2O3 on metapelitic assemblages at greenschist and amphibolite facies conditions: mineral equilibria calculations in the system K2O-FeO-MgO-Al2O3-SiO2-H2O-TiO2-Fe2O3. Journal of Metamorphic Geology.

White, R.W., Pomroy, N.E., Powell, R., 2005. An in situ metatexite-diatexite transition in upper amphibolite facies rocks from Broken Hill, Australia. J. Metamorph. Geol. 23, 579–602.

Whitney, D.L., Evans, B.W., 2010. Abbreviations for names of rock-forming minerals. Am. Mineral. 95, 185–187.

Wing, B.A., Ferry, J.M., Harrison, T.M., 2003. Prograde destruction and formation of monazite and allanite during contact and regional metamorphism of pelites: petrology and geochronology. Contrib. Mineral. Petrol. 145, 228–250.

Woodsworth, G.J., 1977. Homogenization of Zoned Garnets From Pelitic Schists. Can. Mineral. 15, 230–242.

Wu, C.M., 2015. Revised empirical garnet-biotite-muscovite-plagioclase geobarometer in metapelites. J. Metamorph. Geol. 33, 167–176.

Wu, C.-M., Zhang, J.J., Ren, L.D., 2004. Empirical garnet-biotite-plagioclase-quartz (GBPQ) geobarometry in medium- to high-grade metapelites. J. Petrol. 45, 1907–1921.

Yakymchuk, C., Godin, L., 2012. Coupled role of deformation and metamorphism in the construction of inverted metamorphic sequences: an example from far-northwest Nepal. J. Metamorph. Geol. 30, 513–535.

Yardley, B.W.D., 1990. An Introduction to Metamorphic Petrology. Cambridge University Press.

Yin, A., 2006. Cenozoic tectonic evolution of the Himalayan orogen as constrained by along-strike variation of structural geometry, exhumation history, and foreland sedimentation. Earth Science Reviews 76, 1–131.

Yin, A., Harrison, T.M., 2000. Geologic Evolution of the Himalayan-Tibetan Orogen. Annu. Rev. Earth Planet. Sci. 28, 211–280.

Yuan, H.-L., Gao, S., Dai, M.-N., Zong, C.-L., Günther, D., Fontaine, G.H., Liu, X.-M., Diwu, C., 2008. Simultaneous determinations of U–Pb age, Hf isotopes and trace element compositions of zircon by excimer laser-ablation quadrupole and multiple-collector ICP-MS. Chem. Geol. 247, 100–118.

Zeng, L., Liu, J., Gao, L., Xie, K., Wen, L., 2008. Early Oligocene anatexis in the Yardoi gneiss dome, southern Tibet and geological implications. Chin. Sci. Bull. 54, 104.

Zuluaga, C.A., 2005. The effect of zoned garnet on metapelite pseudosection topology and calculated metamorphic P-T paths. Am. Mineral. 90, 1619–1628.

APPENDIX

APPENDIX A

Supporting materials for Chapter 3

Chapter 3 Decrypting the polymetamorphic record of the Himalaya

Appendix A1. Lu-weighted garnet age calculation

Figure A1. Garnet trace element profiles

Figure A2. Concordia diagrams for monazite and xenotime

Figure A3. Monazite and xenotime BSE images

Figure A4. BSE images of excluded xenotime grains in specimens KA031 and KA064

Figure A5. Locations of spot analyses for titanium in quartz thermometry

Figure A6. P-T estimates of garnet inclusions obtained using Ti-in-Qtz, Ti-in-Bt and QuiG

Table A1. Major element geochemistry for garnet and biotite

Table A2. Garnet trace element geochemistry

Table A3. Monazite and xenotime geochronology data

Table A4. Quartz trace element geochemistry

Table A5. Temperature estimates for quartz and biotite inclusions

Table A6. Raman spectroscopy data for quartz inclusions

Table A7. Lu budget calculation for garnet geochronology

APPENDIX

A1. Lu-weighted garnet age calculation

Due to the varying garnet grain shapes, the shape of each garnet was also considered. The surface area of each garnet was measured to obtained average radius, which was then used to calculate volume of each domain.

A - surface area (mm^2)

R - radius (mm)

V - volume (mm^3)

V (rim, mm^3)

AvLu - average Lu (ppm)

Lu core - Lu in the core (%)

Lu rim - Lu in the rim (%)

Est. core age - estimated age of garnet core

$R = \text{sqrt}(A/\pi)$

$V = (R^3) \times \pi \times (4/3)$

V rim = V (grain) - V (core)

Lu core = 100 x ((AvLu x V1)/(AvLu1 x V1+AvLu2 x V2))

Lu rim = 100 - Lu core

Est. core age = (Lu-Hf age - (Lu rim / 100 x Rim age)) / (Lu core / 100)

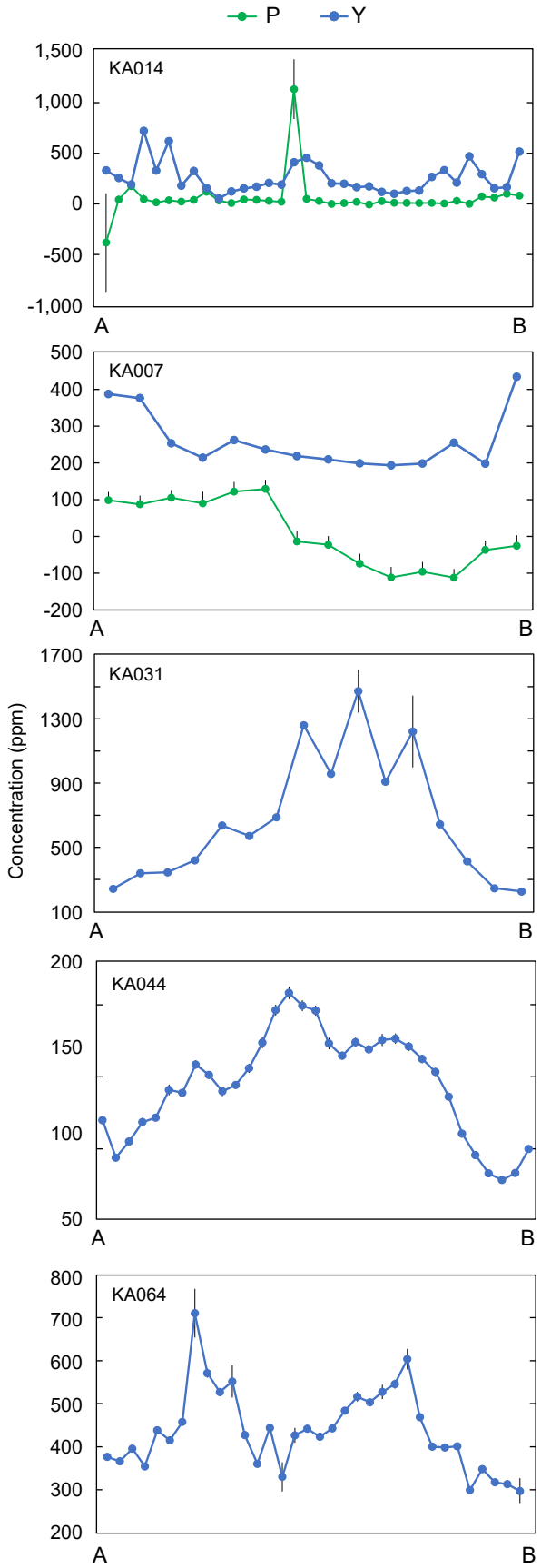

Figure A1. Garnet trace element profiles.

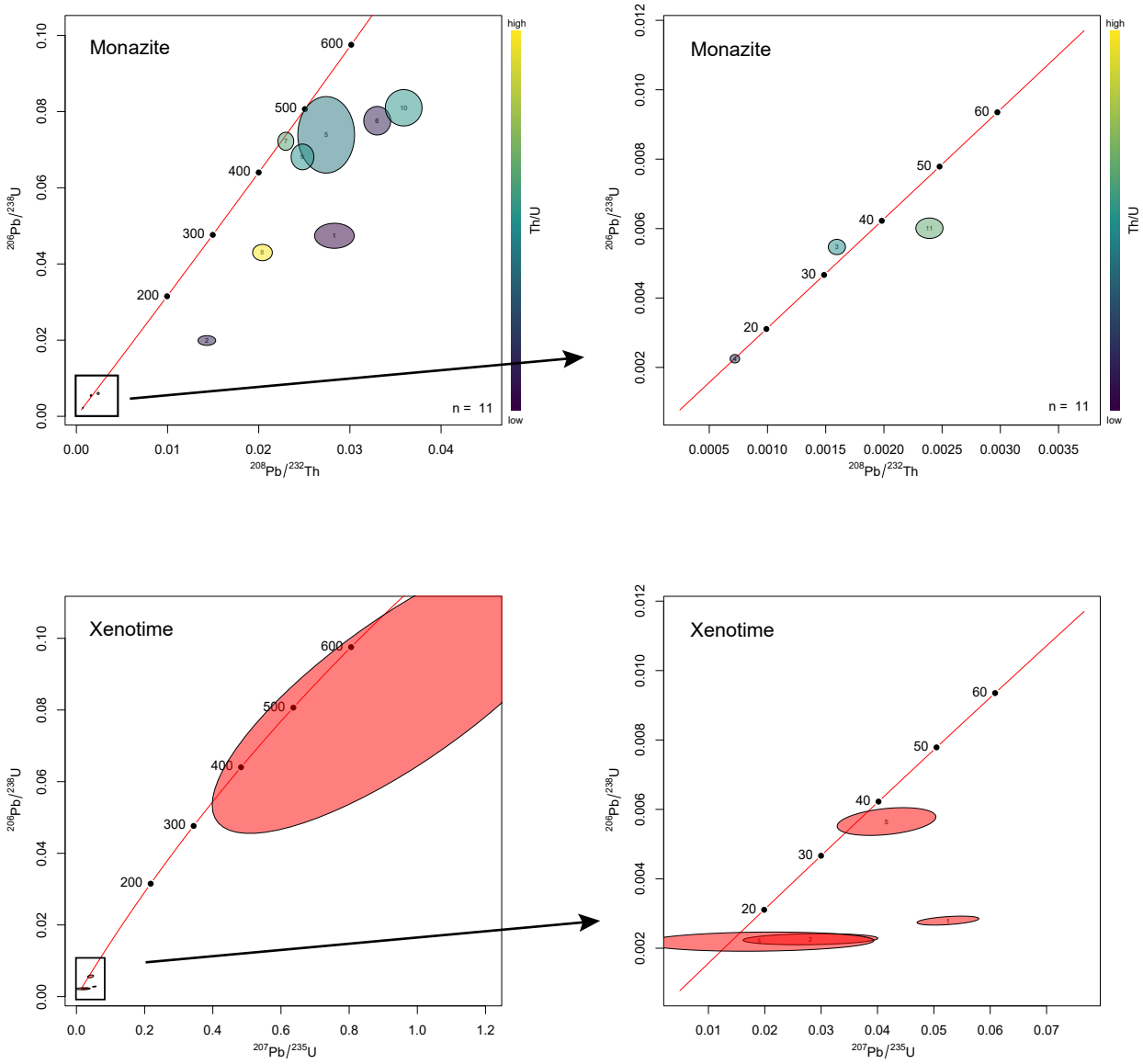

Figure A2. Concordia diagram for monazite and xenotime.

KA007 M1

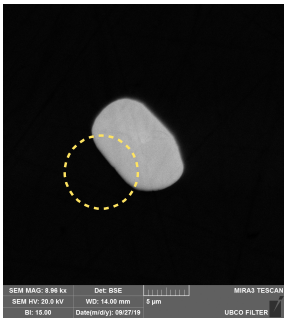

KA007 M2

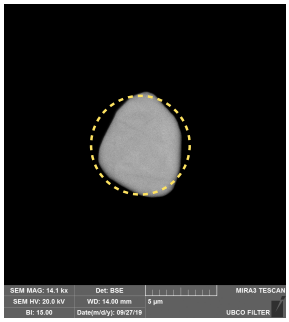

KA031 M2

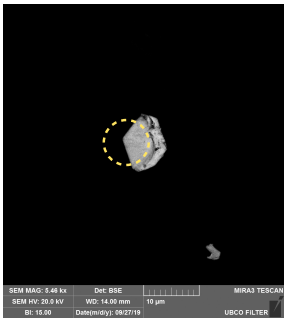

KA031 M3

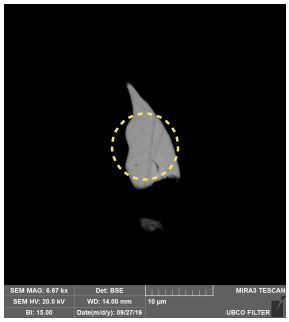

KA031 X1

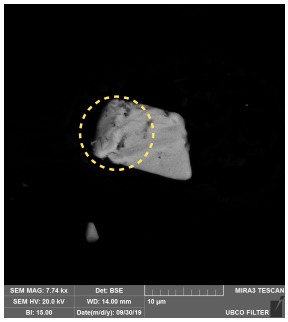

KA031 X2

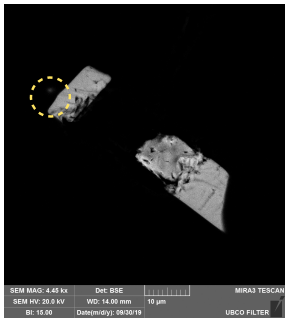

KA063 M2

KA064 M3

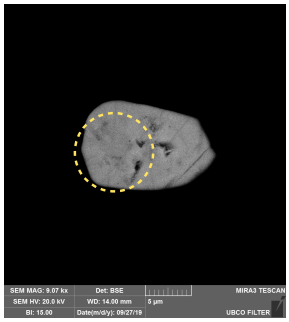

KA064 M4

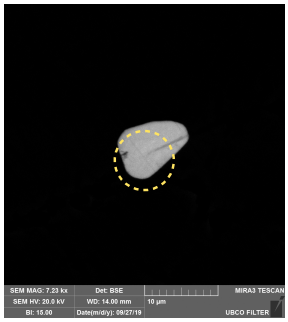

KA064 M5

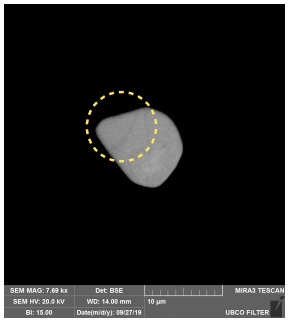

KA064 M6

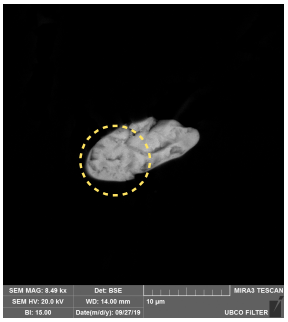

KA064 M7

KA064 X1

KA064 X2

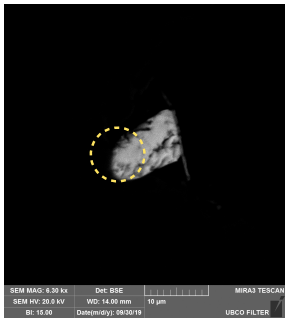

Figure A3. BSE images of analyzed monazites and xenotime grains.

KA031 Xenotime X1

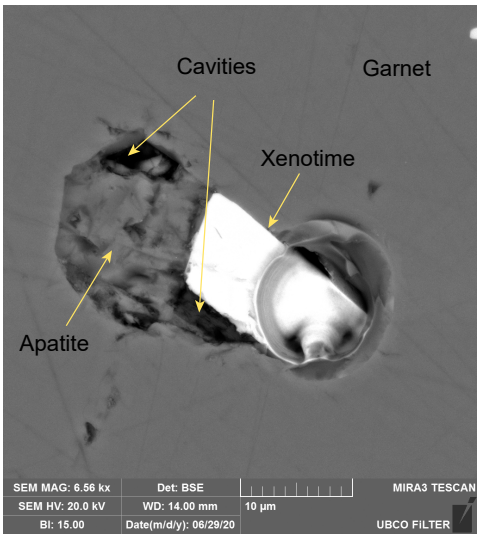

KA064 Xenotime X2

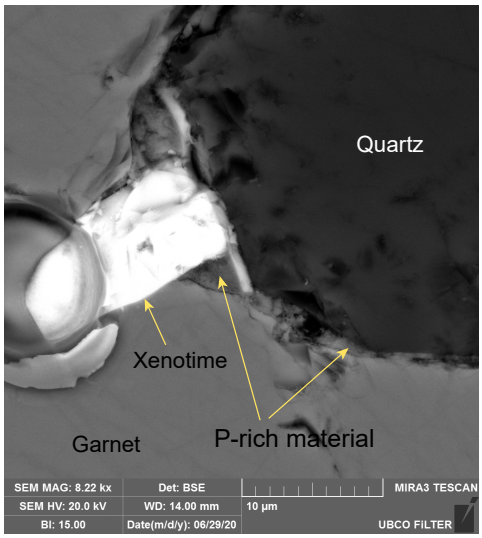

KA064 Xenotime X2

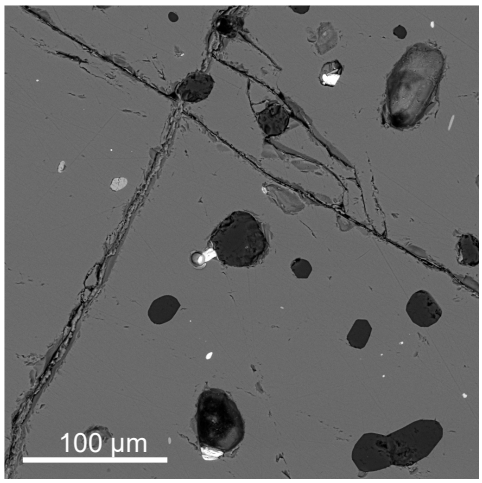

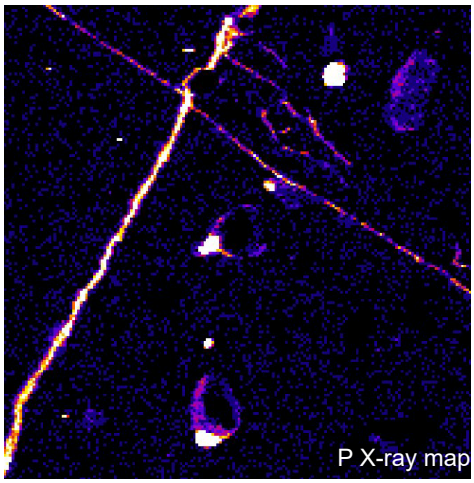

Figure A4. BSE images of excluded xenotime grains in specimens KA031 and KA064.

KA007 - Grt1

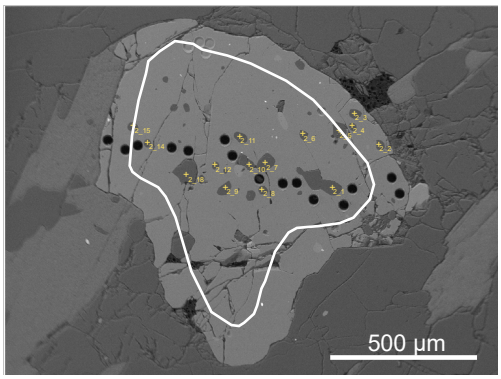

KA007 - Grt2

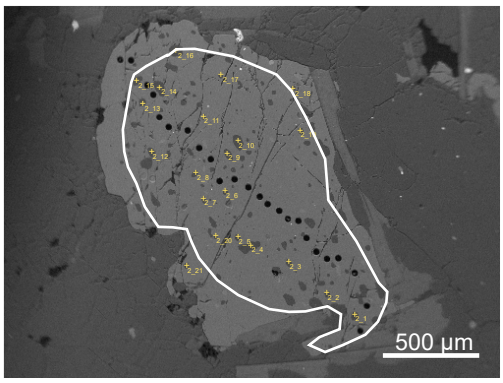

Figure A5. Locations of spot analyses for titanium in quartz thermometry.

KA014 - Grt1

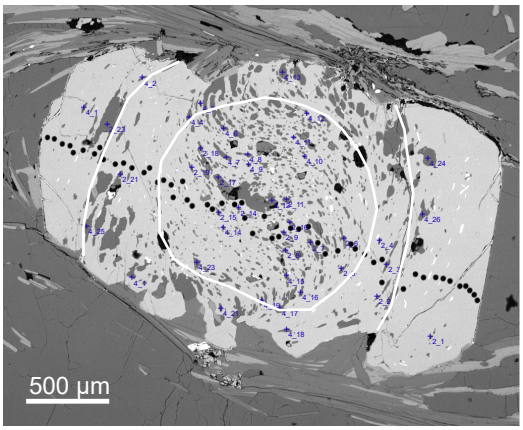

KA031 - Grt1

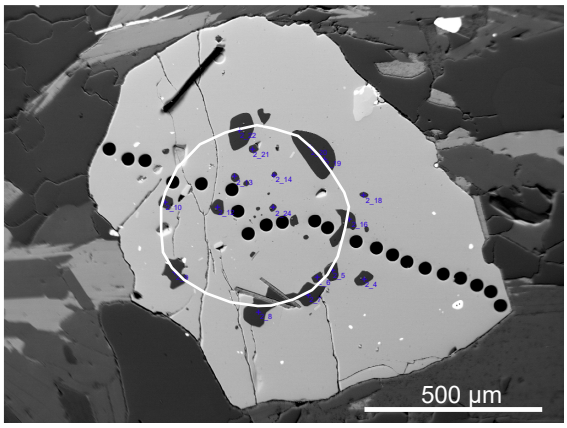

KA031 - Grt2

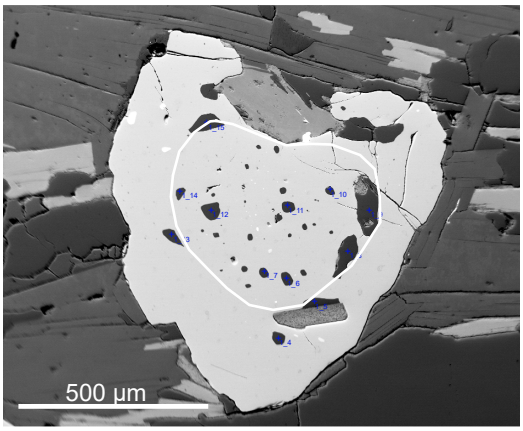

KA044 - Grt1

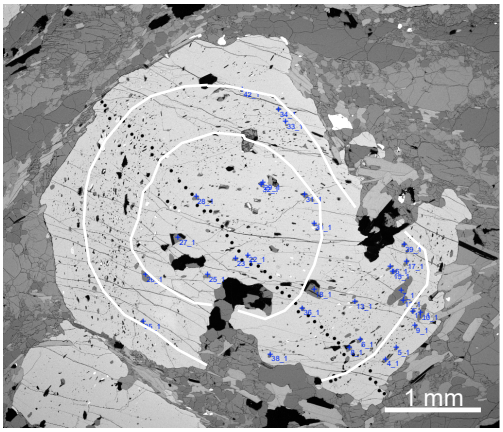

KA064 - Grt2

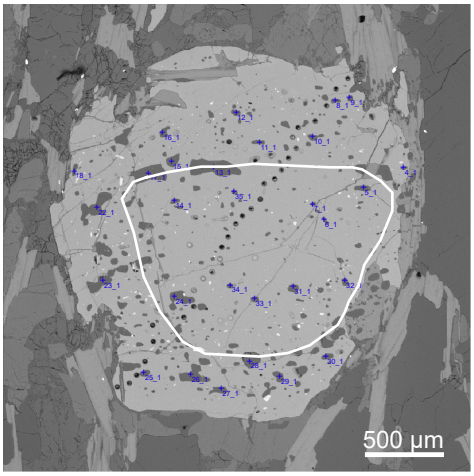

Figure A5. Continued.

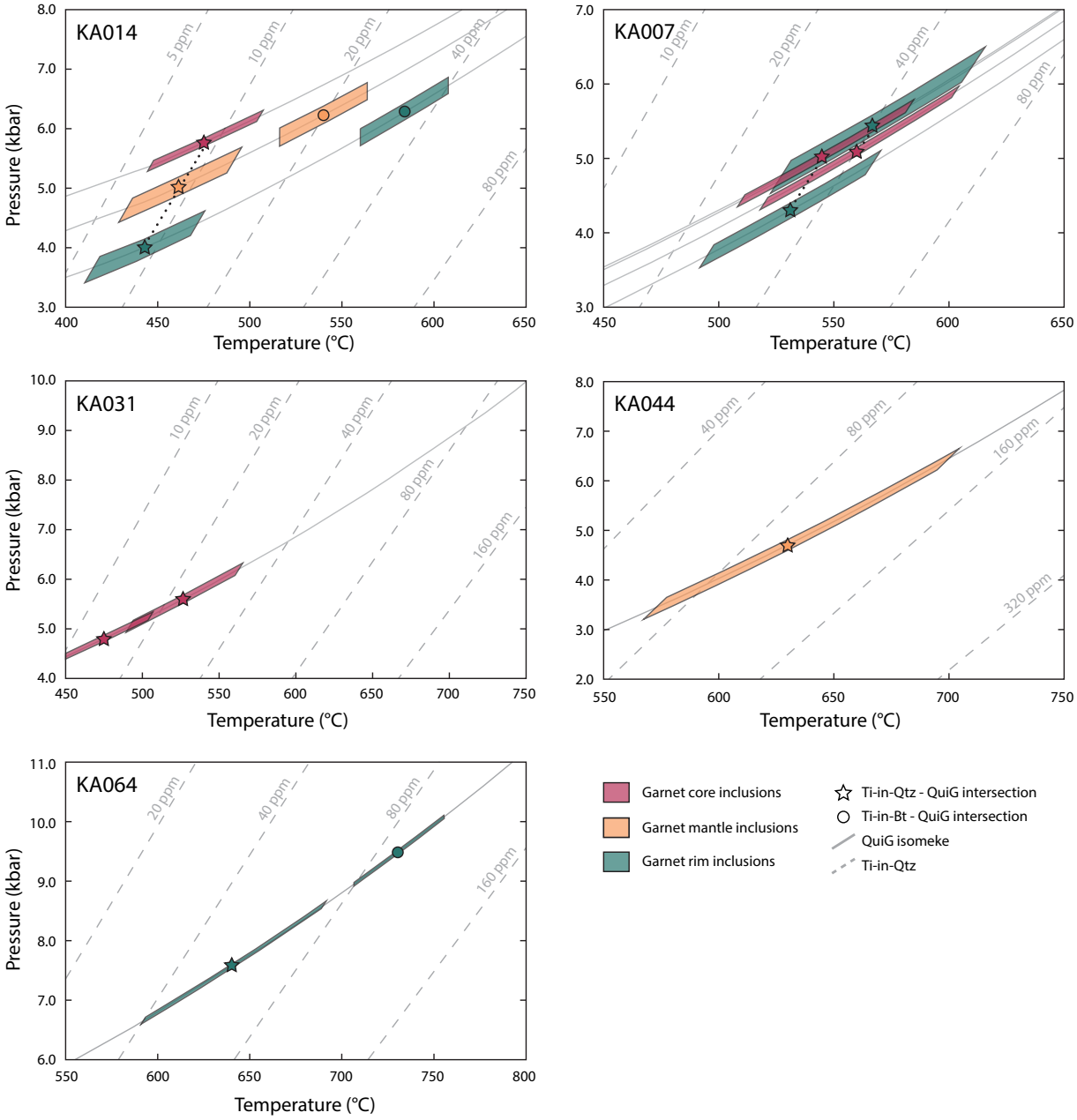

Figure A6. Pressure-temperature estimates of garnet inclusions obtained using Ti-in-Qtz, Ti-in-Bt and QuiG.

Table A1. Major element geochemistry for garnet and biotite

Biotite	**KA014 (in Grt1)**							**KA031**					
Location	in Grt1 mantle	in Grt1 mantle	in Grt1 mantle	in Grt1 mantle	in Grt1 rim	in Grt1 rim	in Grt1 rim	in Grt1 core	in Grt1 core	in Grt2 mantle	in Grt2 mantle	in Grt2 mantle	in Grt2 mantle
An. #	1 / 1 .	1 / 3 .	1 / 4 .	1 / 5 .	3 / 1 .	3 / 2 .	3 / 4 .	4 / 3 .	4 / 4 .	2 / 2 .	2 / 3 .	2 / 4 .	2 / 5 .
SiO2	36.18	35.14	35.59	36.39	35.94	36.04	35.30	35.32	35.96	35.67	35.22	35.62	34.78
TiO2	1.44	1.28	1.42	1.42	1.68	1.67	1.65	2.89	2.06	3.45	3.62	3.57	3.58
Al2O3	19.08	19.36	19.37	19.99	19.24	19.75	19.73	20.01	20.32	19.76	19.54	19.73	18.97
FeO	18.73	19.18	18.87	18.61	17.74	17.82	17.80	15.94	15.42	17.68	17.80	17.65	17.68
MnO	0.01	0.02	0.03	0.01	0.02	0.02	0.00	0.06	0.07	0.04	0.04	0.04	0.02
MgO	9.53	10.15	10.00	9.54	10.79	10.74	10.53	0.11	0.05	9.87	9.78	9.57	9.90
CaO	0.27	0.17	0.22	0.28	0.26	0.20	0.22	0.41	0.38	0.07	0.06	0.08	0.06
Na2O	0.39	0.40	0.37	0.41	0.48	0.44	0.47	10.93	10.91	0.40	0.38	0.33	0.40
K2O	8.76	8.83	8.79	8.70	8.70	8.87	8.90	9.30	9.40	9.35	9.40	9.31	9.33
F	0.73	0.74	0.72	0.65	0.69	0.80	0.65	0.56	0.38	0.59	0.56	0.63	0.51
Cl	0.09	0.09	0.06	0.10	0.06	0.04	0.05	0.12	0.12	0.15	0.14	0.16	0.14
H2O*	3.57	3.55	3.58	3.65	3.63	3.61	3.63	3.70	3.78	3.70	3.69	3.66	3.66
Total	98.78	98.92	99.02	99.76	99.23	100.00	98.93	99.33	98.84	100.72	100.24	100.34	99.03
Si	5.51	5.38	5.42	5.47	5.43	5.40	5.36	5.30	5.40	5.32	5.29	5.34	5.30
Al iv	2.49	2.62	2.58	2.53	2.57	2.60	2.64	2.70	2.60	2.68	2.71	2.66	2.70
Al vi	0.94	0.86	0.90	1.01	0.85	0.89	0.89	0.85	0.99	0.80	0.76	0.82	0.70
Ti	0.17	0.15	0.16	0.16	0.19	0.19	0.19	0.33	0.23	0.39	0.41	0.40	0.41
Fe	2.39	2.45	2.40	2.34	2.24	2.23	2.26	2.00	1.94	2.21	2.24	2.21	2.25
Mn	0.00	0.00	0.00	0.00	0.00	0.00	0.00	0.01	0.01	0.00	0.01	0.01	0.00
Mg	2.16	2.32	2.27	2.14	2.43	2.40	2.38	2.45	2.44	2.20	2.19	2.14	2.25
Ca	0.04	0.03	0.04	0.05	0.04	0.03	0.04	0.02	0.01	0.01	0.01	0.01	0.01
Na	0.11	0.12	0.11	0.12	0.14	0.13	0.14	0.12	0.11	0.12	0.11	0.10	0.12
K	1.70	1.72	1.71	1.67	1.68	1.70	1.72	1.78	1.80	1.78	1.80	1.78	1.81
OH*	3.62	3.62	3.64	3.66	3.65	3.61	3.67	3.70	3.79	3.69	3.70	3.66	3.72
F	0.35	0.36	0.35	0.31	0.33	0.38	0.31	0.27	0.18	0.28	0.27	0.30	0.25
Cl	0.02	0.02	0.02	0.03	0.02	0.01	0.01	0.03	0.03	0.04	0.04	0.04	0.04
TOTAL	19.52	19.65	19.59	19.49	19.58	19.58	19.62	19.55	19.53	19.50	19.52	19.46	19.56
Al total	3.43	3.49	3.48	3.54	3.43	3.49	3.53	3.54	3.60	3.48	3.46	3.48	3.41
XMg	0.48	0.49	0.49	0.48	0.52	0.52	0.51	0.55	0.56	0.50	0.49	0.49	0.50

Table A1. Major element geochemistry for garnet and biotite

Biotite	**KA044**			**KA064**								
Location	in Grt1 core	in Grt1 core	in Grt1 core	in Grt1 mantle	in Grt1 mantle	in Grt1 mantle	in Grt1 mantle	in Grt1 mantle	in Grt1 mantle	in Grt2 rim	in Grt2 rim	in Grt2 rim
An. #	1 / 1 .	1 / 2 .	1 / 3 .	2 / 1 .	2 / 2 .	2 / 3 .	2 / 4 .	2 / 5 .	2 / 6 .	1 / 2 .	1 / 4 .	2 / 1 .
SiO2	36.73	36.72	36.44	34.81	35.11	34.44	34.01	34.24	34.41	34.94	34.47	34.77
TiO2	0.13	0.12	0.12	3.85	3.82	3.83	3.83	3.78	3.81	4.33	4.40	3.24
Al2O3	19.65	19.83	19.79	19.53	19.71	19.49	19.06	19.10	18.99	19.95	19.64	19.69
FeO	12.13	12.22	11.90	21.82	21.48	21.79	21.95	21.37	21.15	17.44	17.46	18.62
MnO	0.00	0.00	0.00	0.07	0.09	0.08	0.06	0.08	0.06	0.03	0.05	0.06
MgO	15.95	15.32	15.87	6.80	6.93	7.04	6.99	7.46	7.62	8.34	8.56	8.73
CaO	0.03	0.03	0.02	0.02	0.02	0.00	0.01	0.02	0.01	0.03	0.06	0.07
Na2O	0.28	0.25	0.31	0.27	0.29	0.29	0.31	0.32	0.31	0.32	0.33	0.26
K2O	9.31	9.47	9.37	9.55	9.64	9.59	9.55	9.42	9.47	9.60	9.43	9.55
F	1.52	1.79	1.60	0.46	0.50	0.59	0.53	0.47	0.59	0.53	0.54	0.70
Cl	0.07	0.06	0.07	0.04	0.04	0.04	0.04	0.05	0.04	0.08	0.09	0.09
H2O*	3.31	3.17	3.26	3.72	3.72	3.64	3.63	3.67	3.62	3.68	3.65	3.58
Total	99.09	98.99	98.74	100.92	101.36	100.82	99.95	99.97	100.08	99.28	98.66	99.36
Si	5.44	5.46	5.42	5.29	5.30	5.25	5.24	5.26	5.27	5.29	5.26	5.30
Al iv	2.56	2.54	2.58	2.71	2.70	2.75	2.76	2.74	2.73	2.71	2.74	2.70
Al vi	0.87	0.93	0.89	0.79	0.81	0.75	0.71	0.71	0.70	0.86	0.80	0.84
Ti	0.01	0.01	0.01	0.44	0.43	0.44	0.44	0.44	0.44	0.49	0.51	0.37
Fe	1.50	1.52	1.48	2.77	2.71	2.78	2.83	2.74	2.71	2.21	2.23	2.37
Mn	0.00	0.00	0.00	0.01	0.01	0.01	0.01	0.01	0.01	0.00	0.01	0.01
Mg	3.52	3.39	3.52	1.54	1.56	1.60	1.61	1.71	1.74	1.88	1.95	1.99
Ca	0.00	0.00	0.00	0.00	0.00	0.00	0.00	0.00	0.00	0.01	0.01	0.01
Na	0.08	0.07	0.09	0.08	0.09	0.09	0.09	0.10	0.09	0.09	0.10	0.08
K	1.76	1.79	1.78	1.85	1.86	1.87	1.88	1.84	1.85	1.86	1.84	1.86
OH*	3.27	3.14	3.23	3.77	3.75	3.71	3.73	3.76	3.70	3.72	3.71	3.64
F	0.71	0.84	0.75	0.22	0.24	0.28	0.26	0.23	0.29	0.26	0.26	0.34
Cl	0.02	0.02	0.02	0.01	0.01	0.01	0.01	0.01	0.01	0.02	0.02	0.02
TOTAL	19.75	19.73	19.77	19.48	19.48	19.53	19.57	19.55	19.55	19.41	19.43	19.53
Al total	3.43	3.47	3.47	3.50	3.51	3.50	3.46	3.46	3.43	3.56	3.53	3.54
XMg	0.70	0.69	0.70	0.36	0.37	0.37	0.36	0.38	0.39	0.46	0.47	0.46

Table A1. Major element geochemistry for garnet and biotite

KA007 (Grt2)																		
Location	rim	rim	rim	rim	rim	rim	rim	rim	mantle	mantle	mantle	mantle	mantle	mantle	mantle	mantle	mantle	mantle
An. #	1 / 1 .	2 / 1 .	3 / 1 .	4 / 1 .	5 / 1 .	6 / 1 .	7 / 1 .	8 / 1 .	9 / 1 .	10 / 1 .	11 / 1 .	12 / 1 .	13 / 1 .	14 / 1 .	15 / 1 .	16 / 1 .	17 / 1 .	18 / 1 .
SiO2	36.65	36.71	36.65	36.67	36.57	36.66	36.69	36.60	36.83	36.81	36.77	36.92	36.86	37.03	37.04	37.03	36.96	37.11
TiO2	0.03	0.05	0.05	0.03	0.06	0.03	0.02	0.03	0.09	0.06	0.02	0.15	0.02	0.04	0.03	0.02	0.02	0.03
Al2O3	21.72	21.61	21.84	21.85	21.73	21.78	21.76	21.78	21.88	21.88	21.77	21.84	21.92	21.92	21.93	21.94	21.85	22.01
FeO	35.02	35.05	35.09	34.67	34.77	34.81	34.85	34.85	34.55	34.53	34.46	34.26	34.25	34.21	34.39	34.27	34.08	34.28
MnO	3.99	3.78	3.74	3.61	3.31	3.16	3.11	2.92	2.73	2.70	2.53	2.59	2.44	2.40	2.33	2.23	2.25	2.14
MgO	2.48	2.67	2.87	3.05	3.29	3.38	3.58	3.62	3.85	3.87	3.86	4.05	4.06	4.08	4.13	4.27	4.26	4.30
CaO	1.09	1.21	1.20	1.19	1.10	1.17	1.29	1.16	1.29	1.35	1.25	1.31	1.46	1.50	1.49	1.42	1.50	1.53
Na2O	0.01	0.01	0.01	0.02	0.00	0.00	0.01	0.03	0.00	0.01	0.01	0.02	0.01	0.00	0.01	0.02	0.00	0.02
K2O	0.02	0.01	0.01	0.00	0.00	0.00	0.00	0.00	0.00	0.00	0.00	0.00	0.00	0.00	0.00	0.00	0.00	0.00
Total	101.00	101.10	101.46	101.09	100.83	100.99	101.32	100.99	101.22	101.21	100.68	101.13	101.02	101.17	101.34	101.18	100.92	101.43
Si	2.95	2.95	2.93	2.94	2.93	2.93	2.92	2.93	2.93	2.93	2.94	2.93	2.93	2.94	2.93	2.94	2.94	2.93
Al iv	0.05	0.05	0.07	0.06	0.07	0.07	0.08	0.07	0.07	0.07	0.06	0.07	0.07	0.06	0.07	0.06	0.06	0.07
Al vi	2.00	1.99	1.99	2.00	1.99	1.99	1.97	1.98	1.98	1.98	1.99	1.98	1.99	1.99	1.98	1.99	1.98	1.99
Ti	0.00	0.00	0.00	0.00	0.00	0.00	0.00	0.00	0.01	0.00	0.00	0.01	0.00	0.00	0.00	0.00	0.00	0.00
Fe3+	0.00	0.01	0.01	0.00	0.01	0.01	0.02	0.02	0.01	0.01	0.01	0.01	0.01	0.01	0.01	0.01	0.01	0.01
Fe2+	2.36	2.35	2.34	2.32	2.32	2.32	2.30	2.31	2.29	2.28	2.29	2.27	2.27	2.26	2.27	2.26	2.25	2.26
Mn	0.27	0.26	0.25	0.24	0.22	0.21	0.21	0.20	0.18	0.18	0.17	0.17	0.16	0.16	0.16	0.15	0.15	0.14
Mg	0.30	0.32	0.34	0.36	0.39	0.40	0.42	0.43	0.46	0.46	0.46	0.48	0.48	0.48	0.49	0.50	0.50	0.51
Ca	0.09	0.10	0.10	0.10	0.09	0.10	0.11	0.10	0.11	0.12	0.11	0.11	0.12	0.13	0.13	0.12	0.13	0.13
Total	8.03	8.03	8.04	8.03	8.03	8.03	8.04	8.04	8.03	8.04	8.03	8.03	8.04	8.03	8.03	8.03	8.03	8.03
spot #	1	2	3	4	5	6	7	8	9	10	11	12	13	14	15	16	17	18
Almandine	0.78	0.78	0.77	0.77	0.77	0.76	0.76	0.76	0.75	0.75	0.76	0.75	0.75	0.75	0.75	0.74	0.74	0.74
Grossular	0.03	0.03	0.03	0.03	0.03	0.03	0.04	0.03	0.04	0.04	0.04	0.04	0.04	0.04	0.04	0.04	0.04	0.04
Pyrope	0.10	0.11	0.11	0.12	0.13	0.13	0.14	0.14	0.15	0.15	0.15	0.16	0.16	0.16	0.16	0.17	0.17	0.17
Spessartine	0.09	0.08	0.08	0.08	0.07	0.07	0.07	0.06	0.06	0.06	0.06	0.06	0.05	0.05	0.05	0.05	0.05	0.05
XMg	0.11	0.12	0.13	0.14	0.14	0.15	0.16	0.16	0.17	0.17	0.17	0.17	0.18	0.18	0.18	0.18	0.18	0.18

Table A1. Major element geochemistry for garnet and biotite

KA007 (Grt2)																		
Location	core	core	core	core	core	core	core	core	mantle	mantle	mantle	mantle	mantle	mantle	mantle	rim	rim	rim
An. #	19 / 1 .	21 / 1 .	22 / 1 .	23 / 1 .	24 / 1 .	25 / 1 .	26 / 1 .	27 / 1 .	28 / 1 .	30 / 1 .	31 / 1 .	32 / 1 .	33 / 1 .	34 / 1 .	35 / 1 .	37 / 1 .	38 / 1 .	39 / 1 .
SiO2	37.11	36.99	37.03	36.92	37.13	37.12	37.04	37.03	37.06	37.01	36.89	36.93	36.90	37.04	36.93	36.99	36.91	36.94
TiO2	0.02	0.01	0.03	0.02	0.04	0.02	0.03	0.13	0.08	0.05	0.03	0.01	0.01	0.03	0.02	0.02	0.03	0.00
Al2O3	22.03	22.07	22.13	21.93	22.00	22.03	22.02	21.95	22.00	22.04	21.93	21.93	21.93	21.91	21.93	21.97	21.90	21.95
FeO	34.22	34.32	34.12	34.33	34.29	34.09	34.24	34.19	34.17	34.22	34.51	34.36	34.50	34.24	34.28	34.34	34.21	34.04
MnO	2.06	1.97	2.03	2.03	2.09	2.18	2.20	2.21	2.28	2.43	2.54	2.55	2.59	2.66	2.72	2.86	2.97	3.07
MgO	4.43	4.48	4.43	4.44	4.33	4.36	4.35	4.38	4.25	4.19	4.13	4.13	4.11	4.02	4.01	3.97	3.89	3.82
CaO	1.51	1.43	1.50	1.53	1.45	1.46	1.57	1.45	1.46	1.34	1.27	1.27	1.11	1.16	1.21	1.24	1.25	1.34
Na2O	0.01	0.00	0.04	0.00	0.01	0.00	0.01	0.01	0.00	0.01	0.00	0.03	0.01	0.00	0.02	0.01	0.01	0.01
K2O	0.01	0.00	0.00	0.00	0.00	0.00	0.00	0.01	0.00	0.00	0.00	0.00	0.00	0.00	0.00	0.00	0.01	0.00
Total	101.41	101.28	101.31	101.20	101.34	101.26	101.45	101.36	101.29	101.29	101.29	101.20	101.16	101.07	101.13	101.40	101.17	101.16
Si	2.93	2.93	2.93	2.93	2.94	2.94	2.93	2.93	2.93	2.93	2.93	2.93	2.93	2.94	2.94	2.93	2.93	2.94
Al iv	0.07	0.07	0.07	0.07	0.06	0.06	0.07	0.07	0.07	0.07	0.07	0.07	0.07	0.06	0.06	0.07	0.07	0.06
Al vi	1.98	1.99	1.99	1.97	1.99	1.99	1.98	1.98	1.99	1.99	1.98	1.99	1.99	2.00	1.99	1.99	1.99	1.99
Ti	0.00	0.00	0.00	0.00	0.00	0.00	0.00	0.01	0.00	0.00	0.00	0.00	0.00	0.00	0.00	0.00	0.00	0.00
Fe3+	0.01	0.01	0.01	0.02	0.01	0.01	0.02	0.01	0.01	0.01	0.02	0.01	0.01	0.00	0.01	0.01	0.01	0.00
Fe2+	2.25	2.26	2.25	2.25	2.26	2.25	2.25	2.25	2.26	2.26	2.27	2.27	2.28	2.27	2.27	2.27	2.27	2.26
Mn	0.14	0.13	0.14	0.14	0.14	0.15	0.15	0.15	0.15	0.16	0.17	0.17	0.17	0.18	0.18	0.19	0.20	0.21
Mg	0.52	0.53	0.52	0.52	0.51	0.51	0.51	0.52	0.50	0.49	0.49	0.49	0.49	0.48	0.48	0.47	0.46	0.45
Ca	0.13	0.12	0.13	0.13	0.12	0.12	0.13	0.12	0.12	0.11	0.11	0.11	0.09	0.10	0.10	0.11	0.11	0.11
Total	8.04	8.04	8.04	8.04	8.03	8.03	8.04	8.03	8.03	8.03	8.04	8.04	8.04	8.03	8.03	8.03	8.03	8.03
spot #	19	21	22	23	24	25	26	27	28	30	31	32	33	34	35	37	38	39
Almandine	0.74	0.74	0.74	0.74	0.75	0.74	0.74	0.74	0.74	0.75	0.75	0.75	0.75	0.75	0.75	0.75	0.75	0.74
Grossular	0.04	0.04	0.04	0.04	0.04	0.04	0.04	0.04	0.04	0.04	0.04	0.04	0.03	0.03	0.03	0.03	0.04	0.04
Pyrope	0.17	0.17	0.17	0.17	0.17	0.17	0.17	0.17	0.17	0.16	0.16	0.16	0.16	0.16	0.16	0.15	0.15	0.15
Spessartine	0.05	0.04	0.04	0.04	0.05	0.05	0.05	0.05	0.05	0.05	0.06	0.06	0.06	0.06	0.06	0.06	0.07	0.07
XMg	0.19	0.19	0.19	0.19	0.18	0.19	0.19	0.19	0.18	0.18	0.18	0.18	0.18	0.17	0.17	0.17	0.17	0.17

Table A1. Major element geochemistry for garnet and biotite

KA014 (Grt1)																		
Location	rim	rim	rim	rim	rim	rim	mantle	mantle	mantle	mantle	mantle	core	core	core	core	core	core	core
An. #	1 / 2 .	1 / 3 .	1 / 4 .	1 / 5 .	1 / 6 .	1 / 7 .	1 / 8 .	1 / 9 .	1 / 10 .	1 / 11 .	1 / 12 .	1 / 13 .	1 / 14 .	1 / 15 .	1 / 16 .	1 / 17 .	1 / 18 .	1 / 19 .
SiO2	36.64	36.63	36.40	36.51	36.54	36.10	36.85	36.56	36.59	36.58	36.43	36.46	36.45	36.62	36.43	36.42	36.36	36.26
TiO2	0.01	0.08	0.11	0.11	0.09	0.05	0.11	0.09	0.07	0.16	0.12	0.16	0.17	0.11	0.12	0.10	0.12	0.06
Al2O3	21.94	21.76	21.67	21.65	21.69	21.32	21.84	21.64	21.71	21.62	21.57	21.51	21.57	21.78	21.51	21.54	21.48	21.56
FeO	35.75	33.41	33.51	33.55	33.74	33.69	32.84	33.53	32.36	30.85	30.35	30.30	29.23	28.32	29.34	29.69	31.17	31.09
MnO	0.23	0.07	0.02	0.05	0.10	0.16	0.29	0.54	0.94	1.45	1.87	2.80	3.47	3.82	4.30	4.41	4.03	3.87
MgO	3.44	2.27	1.87	1.83	1.86	1.88	1.61	1.86	1.56	1.21	1.13	1.15	1.07	1.01	1.16	1.20	1.42	1.44
CaO	2.42	5.72	5.99	6.13	5.79	5.83	6.79	5.68	6.69	7.73	7.97	7.02	7.54	7.96	6.66	6.07	5.16	5.01
Na2O	0.02	0.02	0.03	0.00	0.02	0.00	0.01	0.01	0.01	0.03	0.04	0.03	0.01	0.02	0.03	0.01	0.02	0.02
K2O	0.00	0.01	0.00	0.00	0.00	0.00	0.00	0.00	0.00	0.00	0.00	0.00	0.00	0.00	0.00	0.00	0.00	0.00
Total	100.43	99.96	99.60	99.84	99.82	99.04	100.34	99.89	99.94	99.62	99.48	99.42	99.51	99.65	99.56	99.45	99.77	99.31
Si	2.93	2.94	2.94	2.94	2.94	2.94	2.95	2.94	2.94	2.95	2.94	2.95	2.94	2.94	2.95	2.95	2.95	2.94
Al iv	0.07	0.06	0.06	0.06	0.06	0.06	0.05	0.06	0.06	0.05	0.06	0.05	0.06	0.06	0.05	0.05	0.05	0.06
Al vi	2.00	2.00	2.00	2.00	2.00	1.99	2.01	2.00	2.00	2.00	2.00	2.00	2.00	2.01	2.00	2.01	2.00	2.01
Ti	0.00	0.00	0.01	0.01	0.01	0.00	0.01	0.01	0.00	0.01	0.01	0.01	0.01	0.01	0.01	0.01	0.01	0.00
Fe3+	0.00	0.00	0.00	0.00	0.00	0.01	0.00	0.00	0.00	0.00	0.00	0.00	0.00	0.00	0.00	0.00	0.00	0.00
Fe2+	2.40	2.25	2.27	2.27	2.29	2.28	2.21	2.27	2.19	2.10	2.06	2.07	1.99	1.93	2.00	2.03	2.12	2.13
Mn	0.02	0.00	0.00	0.00	0.01	0.01	0.02	0.04	0.06	0.10	0.13	0.19	0.24	0.26	0.29	0.30	0.28	0.27
Mg	0.41	0.27	0.22	0.22	0.22	0.23	0.19	0.22	0.19	0.15	0.14	0.14	0.13	0.12	0.14	0.14	0.17	0.17
Ca	0.21	0.49	0.52	0.53	0.50	0.51	0.58	0.49	0.58	0.67	0.69	0.61	0.65	0.69	0.58	0.53	0.45	0.44
Total	8.03	8.03	8.03	8.03	8.02	8.03	8.02	8.02	8.02	8.02	8.02	8.02	8.02	8.02	8.02	8.02	8.02	8.02
#	2	3	4	5	6	7	8	9	10	11	12	13	14	15	16	17	18	19
Almandine	0.79	0.75	0.75	0.75	0.76	0.75	0.74	0.75	0.73	0.70	0.68	0.69	0.66	0.64	0.66	0.68	0.70	0.71
Grossular	0.07	0.16	0.17	0.18	0.17	0.17	0.19	0.16	0.19	0.22	0.23	0.20	0.22	0.23	0.19	0.18	0.15	0.14
Pyrope	0.14	0.09	0.07	0.07	0.07	0.08	0.06	0.07	0.06	0.05	0.04	0.05	0.04	0.04	0.05	0.05	0.06	0.06
Spessartine	0.01	0.00	0.00	0.00	0.00	0.00	0.01	0.01	0.02	0.03	0.04	0.06	0.08	0.09	0.10	0.10	0.09	0.09
XMg	0.15	0.11	0.09	0.09	0.09	0.09	0.08	0.09	0.08	0.06	0.06	0.06	0.06	0.06	0.07	0.07	0.08	0.08

Table A1. Major element geochemistry for garnet and biotite

KA014 (Grt1)																		
Location	core	core	core	core	core	core	core	core	core	core	mantle	mantle	mantle	mantle	rim	rim	rim	rim
An. #	1 / 20 .	1 / 21 .	1 / 22 .	1 / 23 .	1 / 24 .	1 / 25 .	1 / 26 .	1 / 27 .	1 / 28 .	1 / 29 .	1 / 30 .	1 / 31 .	1 / 32 .	1 / 33 .	1 / 34 .	1 / 35 .	1 / 36 .	1 / 37 .
SiO2	36.34	36.47	36.45	36.33	36.49	36.58	36.53	36.54	36.49	36.50	36.87	36.64	36.52	36.89	36.67	36.70	37.01	36.37
TiO2	0.03	0.07	0.04	0.04	0.13	0.14	0.10	0.12	0.14	0.07	0.02	0.07	0.04	0.05	0.08	0.05	0.03	0.02
Al2O3	21.52	21.40	21.64	21.48	21.63	21.69	21.61	21.60	21.63	21.68	21.92	21.68	21.67	21.91	21.74	21.81	22.00	21.61
FeO	31.52	31.10	31.14	31.43	29.58	29.58	30.10	31.14	31.30	32.53	33.65	34.25	34.32	33.63	33.15	33.39	33.22	35.36
MnO	3.99	3.83	3.75	3.60	3.06	2.51	1.86	1.37	1.03	0.64	0.42	0.28	0.24	0.21	0.01	0.13	0.20	0.30
MgO	1.52	1.49	1.55	1.62	1.26	1.04	1.08	1.11	1.17	1.39	2.19	2.68	2.88	2.77	2.28	2.72	3.06	3.43
CaO	4.56	5.08	5.12	4.97	7.22	8.21	8.05	7.82	7.81	7.01	5.22	4.38	4.09	4.84	6.11	5.15	4.79	2.52
Na2O	0.01	0.03	0.01	0.00	0.02	0.02	0.04	0.04	0.02	0.02	0.00	0.00	0.00	0.00	0.03	0.02	0.01	0.02
K2O	0.00	0.00	0.00	0.00	0.00	0.00	0.00	0.00	0.00	0.00	0.00	0.00	0.00	0.00	0.00	0.00	0.00	0.00
Total	99.49	99.47	99.72	99.47	99.39	99.77	99.37	99.74	99.59	99.86	100.29	99.98	99.77	100.31	100.06	99.98	100.32	99.62
Si	2.95	2.96	2.95	2.95	2.95	2.94	2.95	2.95	2.94	2.94	2.95	2.94	2.94	2.94	2.94	2.94	2.94	2.94
Al iv	0.05	0.04	0.05	0.05	0.05	0.06	0.05	0.05	0.06	0.06	0.05	0.06	0.06	0.06	0.06	0.06	0.06	0.06
Al vi	2.01	2.01	2.01	2.00	2.01	2.00	2.01	2.00	2.00	2.00	2.02	2.00	2.00	2.01	2.00	2.00	2.01	1.99
Ti	0.00	0.00	0.00	0.00	0.01	0.01	0.01	0.01	0.01	0.00	0.00	0.00	0.00	0.00	0.00	0.00	0.00	0.00
Fe3+	0.00	0.00	0.00	0.00	0.00	0.00	0.00	0.00	0.00	0.00	0.00	0.00	0.00	0.00	0.00	0.00	0.00	0.01
Fe2+	2.16	2.12	2.12	2.14	2.02	2.01	2.05	2.11	2.13	2.20	2.27	2.31	2.31	2.26	2.23	2.25	2.23	2.38
Mn	0.27	0.26	0.26	0.25	0.21	0.17	0.13	0.09	0.07	0.04	0.03	0.02	0.02	0.01	0.00	0.01	0.01	0.02
Mg	0.18	0.18	0.19	0.20	0.15	0.12	0.13	0.13	0.14	0.17	0.26	0.32	0.35	0.33	0.27	0.33	0.36	0.41
Ca	0.40	0.44	0.44	0.43	0.62	0.71	0.70	0.68	0.68	0.61	0.45	0.38	0.35	0.41	0.53	0.44	0.41	0.22
Total	8.02	8.02	8.02	8.02	8.02	8.02	8.02	8.02	8.02	8.03	8.02	8.03	8.03	8.02	8.03	8.03	8.02	8.03
#	20	21	22	23	24	25	26	27	28	29	30	31	32	33	34	35	36	37
Almandine	0.72	0.71	0.70	0.71	0.67	0.67	0.68	0.70	0.71	0.73	0.76	0.76	0.76	0.75	0.74	0.74	0.74	0.79
Grossular	0.13	0.15	0.15	0.14	0.21	0.24	0.23	0.22	0.22	0.20	0.15	0.12	0.12	0.14	0.17	0.15	0.14	0.07
Pyrope	0.06	0.06	0.06	0.07	0.05	0.04	0.04	0.04	0.05	0.06	0.09	0.11	0.11	0.11	0.09	0.11	0.12	0.14
Spessartine	0.09	0.09	0.09	0.08	0.07	0.06	0.04	0.03	0.02	0.01	0.01	0.01	0.01	0.00	0.00	0.00	0.00	0.01
XMg	0.08	0.08	0.08	0.08	0.07	0.06	0.06	0.06	0.06	0.07	0.10	0.12	0.13	0.13	0.11	0.13	0.14	0.15

Table A1. Major element geochemistry for garnet and biotite

KA031 (Grt1)																			
Location	rim	mantle	mantle	mantle	mantle	mantle	mantle	core	core	core	core	core	core	core	mantle	mantle	rim	rim	rim
An. #	1 / 4 .	1 / 5 .	1 / 6 .	1 / 7 .	1 / 8 .	1 / 9 .	1 / 10 .	1 / 11 .	1 / 12 .	1 / 13 .	1 / 14 .	1 / 15 .	1 / 17 .	1 / 18 .	1 / 20 .	1 / 21 .	1 / 22 .	1 / 23 .	1 / 24 .
SiO2	37.04	37.09	36.98	37.09	37.20	37.21	37.25	37.18	37.13	37.09	36.84	36.85	37.15	37.00	36.97	37.26	37.18	37.19	36.82
TiO2	0.01	0.02	0.01	0.01	0.02	0.02	0.03	0.02	0.04	0.03	0.05	0.02	0.03	0.02	0.02	0.01	0.03	0.00	0.00
Al2O3	22.12	22.08	22.10	22.05	22.04	21.97	22.02	22.20	22.09	22.04	21.88	21.91	22.09	21.88	22.09	22.14	22.06	22.04	21.96
FeO	34.73	34.53	34.78	34.79	34.62	34.66	34.82	34.59	34.42	34.34	34.39	34.74	34.71	34.69	34.61	34.84	34.83	35.14	35.22
MnO	2.21	2.20	2.16	2.11	2.18	2.09	2.09	2.06	2.08	2.12	2.05	2.02	2.08	2.16	2.28	2.16	2.19	2.24	2.38
MgO	3.70	3.82	3.86	3.84	3.82	3.92	3.93	3.90	3.97	3.90	4.01	3.92	3.84	3.94	3.70	3.67	3.59	3.41	3.17
CaO	1.23	1.25	1.27	1.24	1.29	1.28	1.31	1.28	1.32	1.31	1.32	1.32	1.33	1.30	1.29	1.29	1.29	1.33	1.33
Na2O	0.01	0.04	0.04	0.02	0.02	0.00	0.01	0.00	0.02	0.04	0.02	0.02	0.03	0.03	0.00	0.02	0.02	0.00	0.00
K2O	0.00	0.00	0.00	0.00	0.00	0.00	0.00	0.00	0.00	0.00	0.00	0.01	0.00	0.00	0.00	0.00	0.00	0.00	0.00
Total	101.04	101.01	101.20	101.16	101.19	101.16	101.46	101.23	101.09	100.88	100.56	100.81	101.26	101.01	100.97	101.39	101.18	101.36	100.87
Si	2.94	2.94	2.94	2.94	2.95	2.95	2.95	2.94	2.94	2.94	2.94	2.94	2.94	2.94	2.94	2.95	2.95	2.95	2.94
Al iv	0.06	0.06	0.06	0.06	0.05	0.05	0.05	0.06	0.06	0.06	0.06	0.06	0.06	0.06	0.06	0.05	0.05	0.05	0.06
Al vi	2.01	2.01	2.00	2.01	2.01	2.00	2.00	2.01	2.01	2.01	2.00	2.00	2.01	2.00	2.01	2.01	2.01	2.01	2.01
Ti	0.00	0.00	0.00	0.00	0.00	0.00	0.00	0.00	0.00	0.00	0.00	0.00	0.00	0.00	0.00	0.00	0.00	0.00	0.00
Fe3+	0.00	0.00	0.00	0.00	0.00	0.00	0.00	0.00	0.00	0.00	0.00	0.00	0.00	0.00	0.00	0.00	0.00	0.00	0.00
Fe2+	2.32	2.31	2.32	2.32	2.31	2.31	2.31	2.31	2.30	2.30	2.30	2.31	2.31	2.31	2.32	2.32	2.33	2.35	2.37
Mn	0.15	0.15	0.15	0.14	0.15	0.14	0.14	0.14	0.14	0.14	0.14	0.14	0.14	0.15	0.15	0.14	0.15	0.15	0.16
Mg	0.44	0.45	0.46	0.45	0.45	0.46	0.46	0.46	0.47	0.46	0.48	0.47	0.45	0.47	0.44	0.43	0.42	0.40	0.38
Ca	0.10	0.11	0.11	0.11	0.11	0.11	0.11	0.11	0.11	0.11	0.11	0.11	0.11	0.11	0.11	0.11	0.11	0.11	0.11
Total	8.03	8.03	8.03	8.03	8.02	8.02	8.03	8.03	8.03	8.02	8.03	8.03	8.03	8.03	8.03	8.02	8.02	8.02	8.03
#	4	5	6	7	8	9	10	11	12	13	14	15	17	18	20	21	22	23	24
Almandine	0.77	0.77	0.77	0.77	0.77	0.76	0.76	0.77	0.76	0.76	0.76	0.76	0.77	0.76	0.77	0.77	0.77	0.78	0.78
Grossular	0.03	0.04	0.04	0.03	0.04	0.04	0.04	0.04	0.04	0.04	0.04	0.04	0.04	0.04	0.04	0.04	0.04	0.04	0.04
Pyrope	0.15	0.15	0.15	0.15	0.15	0.15	0.15	0.15	0.16	0.15	0.16	0.15	0.15	0.15	0.15	0.14	0.14	0.13	0.12
Spessartine	0.05	0.05	0.05	0.05	0.05	0.05	0.05	0.05	0.05	0.05	0.05	0.05	0.05	0.05	0.05	0.05	0.05	0.05	0.05
XMg	0.16	0.16	0.16	0.16	0.16	0.17	0.17	0.17	0.17	0.17	0.17	0.17	0.16	0.17	0.16	0.16	0.15	0.15	0.14

Table A1. Major element geochemistry for garnet and biotite

KA044 (Grt3)															
Location	rim	rim	rim	rim	mantle	mantle	mantle	mantle	mantle	mantle	mantle	mantle	mantle	core	core
An. #	1 / 2 .	1 / 3 .	1 / 4 .	1 / 6 .	1 / 7 .	1 / 8 .	1 / 9 .	1 / 10 .	1 / 11 .	1 / 12 .	1 / 13 .	1 / 14 .	1 / 15 .	1 / 16 .	1 / 17 .
SiO2	37.14	37.58	37.62	37.61	37.68	37.58	37.58	37.77	37.81	37.50	37.92	37.65	37.56	37.63	37.67
TiO2	0.05	0.03	0.05	0.04	0.05	0.07	0.07	0.05	0.07	0.06	0.05	0.08	0.16	0.04	0.07
Al2O3	21.97	22.25	22.36	22.46	22.25	22.29	22.30	22.35	22.32	22.20	22.24	22.08	22.29	22.29	22.28
FeO	33.92	32.55	31.91	31.55	31.33	31.27	31.26	31.26	31.27	31.25	31.01	31.06	31.00	31.15	30.97
MnO	0.60	0.54	0.50	0.50	0.46	0.42	0.38	0.41	0.41	0.42	0.43	0.45	0.45	0.45	0.47
MgO	4.71	5.44	5.65	5.81	5.87	5.77	5.94	5.86	5.78	5.84	5.77	5.68	5.77	5.67	5.63
CaO	2.39	2.89	3.14	3.27	3.36	3.44	3.53	3.61	3.65	3.68	3.77	3.76	3.79	3.74	3.83
Na2O	0.00	0.01	0.01	0.01	0.00	0.00	0.01	0.02	0.03	0.00	0.01	0.02	0.01	0.00	0.00
K2O	0.00	0.01	0.00	0.01	0.00	0.01	0.00	0.00	0.00	0.00	0.00	0.00	0.00	0.00	0.00
Total	100.79	101.29	101.23	101.26	101.00	100.85	101.06	101.32	101.34	100.94	101.20	100.78	101.04	100.98	100.91
Si	2.94	2.94	2.94	2.93	2.94	2.94	2.93	2.94	2.94	2.93	2.95	2.95	2.93	2.94	2.94
Al iv	0.06	0.06	0.06	0.07	0.06	0.06	0.07	0.06	0.06	0.07	0.05	0.05	0.07	0.06	0.06
Al vi	1.99	1.99	1.99	1.99	1.99	1.99	1.98	1.99	1.99	1.98	1.99	1.98	1.98	1.99	1.99
Ti	0.00	0.00	0.00	0.00	0.00	0.00	0.00	0.00	0.00	0.00	0.00	0.00	0.01	0.00	0.00
Fe3+	0.01	0.01	0.00	0.00	0.01	0.00	0.01	0.01	0.01	0.02	0.01	0.01	0.01	0.01	0.00
Fe2+	2.23	2.12	2.08	2.05	2.04	2.04	2.03	2.03	2.03	2.02	2.01	2.02	2.01	2.03	2.02
Mn	0.04	0.04	0.03	0.03	0.03	0.03	0.02	0.03	0.03	0.03	0.03	0.03	0.03	0.03	0.03
Mg	0.55	0.63	0.66	0.67	0.68	0.67	0.69	0.68	0.67	0.68	0.67	0.66	0.67	0.66	0.66
Ca	0.20	0.24	0.26	0.27	0.28	0.29	0.29	0.30	0.30	0.31	0.31	0.32	0.32	0.31	0.32
Total	8.03	8.03	8.03	8.03	8.03	8.03	8.03	8.03	8.03	8.04	8.02	8.03	8.03	8.03	8.03
#	2	3	4	6	7	8	9	10	11	12	13	14	15	16	17
Almandine	0.74	0.70	0.69	0.68	0.67	0.67	0.67	0.67	0.67	0.67	0.67	0.67	0.66	0.67	0.67
Grossular	0.07	0.08	0.09	0.09	0.09	0.10	0.10	0.10	0.10	0.10	0.10	0.10	0.10	0.10	0.11
Pyrope	0.18	0.21	0.22	0.22	0.23	0.22	0.23	0.22	0.22	0.22	0.22	0.22	0.22	0.22	0.22
Spessartine	0.01	0.01	0.01	0.01	0.01	0.01	0.01	0.01	0.01	0.01	0.01	0.01	0.01	0.01	0.01
XMg	0.20	0.23	0.24	0.25	0.25	0.25	0.25	0.25	0.25	0.25	0.25	0.25	0.25	0.25	0.24

Table A1. Major element geochemistry for garnet and biotite

KA044 (Grt3)														
Location	core	core	core	core	core	core	core	core	core	core	core	core	core	core
An. #	1 / 18 .	1 / 19 .	1 / 20 .	1 / 21 .	1 / 22 .	1 / 23 .	1 / 24 .	1 / 25 .	1 / 26 .	1 / 27 .	1 / 28 .	1 / 29 .	1 / 30 .	1 / 31 .
SiO2	37.58	37.69	37.53	37.72	37.91	37.85	37.59	37.88	37.78	37.78	37.78	37.77	37.65	37.54
TiO2	0.17	0.10	0.05	0.05	0.06	0.07	0.03	0.04	0.05	0.02	0.05	0.04	0.17	0.03
Al2O3	22.25	22.26	23.37	22.28	22.39	22.33	22.15	22.30	22.20	22.26	22.20	22.27	22.25	22.36
FeO	31.24	31.15	30.67	31.24	30.88	31.20	31.17	31.24	31.26	31.20	31.41	31.19	31.31	31.47
MnO	0.48	0.46	0.48	0.46	0.46	0.45	0.48	0.49	0.47	0.44	0.43	0.44	0.42	0.43
MgO	5.69	5.55	5.34	5.67	5.73	5.62	5.77	5.64	5.66	5.72	5.63	5.75	5.69	5.74
CaO	3.86	3.87	3.80	3.85	3.90	3.88	3.86	3.85	3.81	3.79	3.71	3.67	3.53	3.64
Na2O	0.01	0.03	0.00	0.01	0.02	0.03	0.01	0.02	0.01	0.00	0.00	0.01	0.01	0.00
K2O	0.00	0.00	0.00	0.00	0.00	0.00	0.00	0.01	0.00	0.01	0.00	0.00	0.00	0.00
Total	101.27	101.11	101.24	101.28	101.35	101.42	101.05	101.47	101.23	101.23	101.22	101.15	101.03	101.22
Si	2.93	2.94	2.90	2.94	2.95	2.94	2.93	2.94	2.94	2.94	2.94	2.94	2.94	2.93
Al iv	0.07	0.06	0.10	0.06	0.05	0.06	0.07	0.06	0.06	0.06	0.06	0.06	0.06	0.07
Al vi	1.97	1.99	2.04	1.98	2.00	1.99	1.97	1.99	1.98	1.99	1.99	1.99	1.99	1.98
Ti	0.01	0.01	0.00	0.00	0.00	0.00	0.00	0.00	0.00	0.00	0.00	0.00	0.01	0.00
Fe3+	0.02	0.00	0.00	0.01	0.00	0.01	0.02	0.01	0.01	0.01	0.01	0.01	0.00	0.01
Fe2+	2.02	2.03	2.04	2.02	2.01	2.02	2.01	2.02	2.02	2.02	2.04	2.03	2.04	2.04
Mn	0.03	0.03	0.03	0.03	0.03	0.03	0.03	0.03	0.03	0.03	0.03	0.03	0.03	0.03
Mg	0.66	0.65	0.62	0.66	0.66	0.65	0.67	0.65	0.66	0.66	0.65	0.67	0.66	0.67
Ca	0.32	0.32	0.31	0.32	0.32	0.32	0.32	0.32	0.32	0.32	0.31	0.31	0.30	0.30
Total	8.03	8.03	8.04	8.03	8.03	8.03	8.04	8.03	8.03	8.03	8.03	8.03	8.03	8.04
#	18	19	20	21	22	23	24	25	26	27	28	29	30	31
Almandine	0.67	0.67	0.68	0.67	0.66	0.67	0.66	0.67	0.67	0.67	0.67	0.67	0.67	0.67
Grossular	0.11	0.11	0.10	0.11	0.11	0.11	0.11	0.11	0.10	0.10	0.10	0.10	0.10	0.10
Pyrope	0.22	0.21	0.21	0.22	0.22	0.22	0.22	0.22	0.22	0.22	0.22	0.22	0.22	0.22
Spessartine	0.01	0.01	0.01	0.01	0.01	0.01	0.01	0.01	0.01	0.01	0.01	0.01	0.01	0.01
XMg	0.25	0.24	0.23	0.25	0.25	0.24	0.25	0.24	0.24	0.25	0.24	0.25	0.25	0.25

Table A1. Major element geochemistry for garnet and biotite

KA044 (Grt3)														
Location	core	core	core	core	core	core	core	mantle	mantle	mantle	mantle	mantle	mantle	rim
An. #	1 / 32 .	1 / 34 .	1 / 35 .	1 / 36 .	1 / 37 .	1 / 38 .	1 / 39 .	1 / 40 .	1 / 41 .	1 / 42 .	1 / 43 .	1 / 44 .	1 / 45 .	1 / 48 .
SiO2	37.79	37.77	37.89	37.54	37.68	37.54	37.63	37.76	37.99	37.73	37.75	37.64	37.77	37.61
TiO2	0.05	0.05	0.05	0.05	0.06	0.05	0.06	0.05	0.05	0.04	0.05	0.05	0.05	0.02
Al2O3	22.22	22.33	22.36	22.49	22.26	22.35	22.33	22.14	22.33	22.36	22.30	22.30	22.35	22.31
FeO	31.26	31.30	31.11	30.77	31.36	31.32	31.22	31.15	31.14	31.35	31.30	31.38	31.28	32.97
MnO	0.43	0.41	0.42	0.47	0.43	0.40	0.41	0.39	0.38	0.42	0.40	0.42	0.39	0.59
MgO	5.65	5.72	5.78	5.47	5.89	5.76	5.85	5.90	5.97	5.94	5.91	5.95	5.94	5.02
CaO	3.67	3.64	3.59	3.70	3.66	3.61	3.51	3.55	3.55	3.52	3.50	3.44	3.36	2.76
Na2O	0.01	0.00	0.00	0.01	0.01	0.02	0.00	0.01	0.02	0.00	0.01	0.01	0.01	0.01
K2O	0.00	0.00	0.00	0.00	0.00	0.00	0.00	0.00	0.00	0.00	0.00	0.00	0.00	0.01
Total	101.08	101.21	101.21	100.50	101.35	101.05	101.01	100.94	101.43	101.37	101.22	101.19	101.15	101.28
Si	2.95	2.94	2.95	2.94	2.93	2.93	2.94	2.95	2.95	2.93	2.94	2.93	2.94	2.94
Al iv	0.05	0.06	0.05	0.06	0.07	0.07	0.06	0.05	0.05	0.07	0.06	0.07	0.06	0.06
Al vi	1.99	1.99	2.00	2.01	1.98	1.99	1.99	1.98	1.99	1.98	1.99	1.98	1.99	2.00
Ti	0.00	0.00	0.00	0.00	0.00	0.00	0.00	0.00	0.00	0.00	0.00	0.00	0.00	0.00
Fe3+	0.01	0.00	0.00	0.00	0.02	0.01	0.01	0.01	0.01	0.01	0.01	0.01	0.00	0.00
Fe2+	2.03	2.03	2.03	2.03	2.02	2.04	2.03	2.02	2.01	2.03	2.03	2.03	2.03	2.17
Mn	0.03	0.03	0.03	0.03	0.03	0.03	0.03	0.03	0.03	0.03	0.03	0.03	0.03	0.04
Mg	0.66	0.66	0.67	0.64	0.68	0.67	0.68	0.69	0.69	0.69	0.69	0.69	0.69	0.59
Ca	0.31	0.30	0.30	0.31	0.31	0.30	0.29	0.30	0.30	0.29	0.29	0.29	0.28	0.23
Total	8.03	8.03	8.02	8.03	8.04	8.03	8.03	8.03	8.03	8.03	8.03	8.03	8.03	8.03
#	32	34	35	36	37	38	39	40	41	42	43	44	45	48
Almandine	0.67	0.67	0.67	0.67	0.67	0.67	0.67	0.67	0.67	0.67	0.67	0.67	0.67	0.72
Grossular	0.10	0.10	0.10	0.10	0.10	0.10	0.10	0.10	0.10	0.10	0.10	0.09	0.09	0.08
Pyrope	0.22	0.22	0.22	0.21	0.22	0.22	0.22	0.23	0.23	0.23	0.23	0.23	0.23	0.19
Spessartine	0.01	0.01	0.01	0.01	0.01	0.01	0.01	0.01	0.01	0.01	0.01	0.01	0.01	0.01
XMg	0.24	0.25	0.25	0.24	0.25	0.25	0.25	0.25	0.26	0.25	0.25	0.25	0.25	0.21

Table A1. Major element geochemistry for garnet and biotite

KA064 (Grt2)

Location	rim	rim	rim	rim	mantle	mantle	mantle	core	core	core	core	core	core	core	core	core
An. #	1 / 2 .	1 / 4 .	1 / 5 .	1 / 6 .	1 / 10 .	1 / 11 .	1 / 13 .	1 / 14 .	1 / 16 .	1 / 17 .	1 / 18 .	1 / 19 .	1 / 20 .	1 / 21 .	1 / 22 .	1 / 23 .
SiO2	37.22	37.36	37.44	37.39	37.47	37.42	37.44	37.41	37.47	37.47	37.39	37.42	37.50	37.33	37.43	37.38
TiO2	0.02	0.00	0.03	0.02	0.03	0.02	0.02	0.02	0.01	0.02	0.02	0.01	0.02	0.04	0.02	0.01
Al2O3	21.85	21.92	21.94	21.91	22.03	21.99	22.04	22.04	22.00	22.01	21.98	22.07	21.99	22.03	21.99	22.01
FeO	34.20	34.65	34.74	34.69	34.35	34.51	34.53	33.98	34.60	34.47	34.61	34.53	34.52	34.42	34.58	34.31
MnO	3.95	2.50	2.62	2.39	1.67	1.68	1.63	1.61	1.55	1.66	1.61	1.67	1.61	1.63	1.63	1.61
MgO	2.94	3.59	3.66	3.75	4.43	4.40	4.36	4.47	4.66	4.64	4.59	4.60	4.69	4.68	4.57	4.53
CaO	1.04	1.20	1.03	1.15	1.37	1.35	1.33	1.29	1.04	1.07	1.04	1.07	1.08	1.13	1.15	1.19
Na2O	0.02	0.02	0.01	0.01	0.00	0.00	0.00	0.01	0.00	0.00	0.02	0.00	0.01	0.01	0.01	0.01
K2O	0.01	0.00	0.01	0.00	0.00	0.01	0.00	0.00	0.00	0.00	0.00	0.00	0.00	0.01	0.00	0.00
Total	101.25	101.24	101.47	101.30	101.35	101.38	101.35	100.81	101.35	101.35	101.25	101.37	101.43	101.28	101.39	101.05
Si	2.96	2.96	2.96	2.96	2.95	2.95	2.95	2.96	2.95	2.95	2.95	2.95	2.95	2.95	2.95	2.95
Al iv	0.04	0.04	0.04	0.04	0.05	0.05	0.05	0.04	0.05	0.05	0.05	0.05	0.05	0.05	0.05	0.05
Al vi	2.01	2.01	2.01	2.01	2.00	2.00	2.00	2.01	2.00	2.00	2.00	2.00	2.00	2.00	2.00	2.01
Ti	0.00	0.00	0.00	0.00	0.00	0.00	0.00	0.00	0.00	0.00	0.00	0.00	0.00	0.00	0.00	0.00
Fe3+	0.00	0.00	0.00	0.00	0.00	0.00	0.00	0.00	0.00	0.00	0.00	0.00	0.00	0.00	0.00	0.00
Fe2+	2.30	2.31	2.31	2.31	2.27	2.28	2.28	2.26	2.28	2.27	2.29	2.28	2.27	2.27	2.28	2.27
Mn	0.27	0.17	0.18	0.16	0.11	0.11	0.11	0.11	0.10	0.11	0.11	0.11	0.11	0.11	0.11	0.11
Mg	0.35	0.42	0.43	0.44	0.52	0.52	0.51	0.53	0.55	0.55	0.54	0.54	0.55	0.55	0.54	0.53
Ca	0.09	0.10	0.09	0.10	0.12	0.11	0.11	0.11	0.09	0.09	0.09	0.09	0.09	0.10	0.10	0.10
Total	8.02	8.02	8.02	8.02	8.02	8.02	8.02	8.02	8.02	8.02	8.02	8.02	8.02	8.03	8.02	8.02
#	2	4	5	6	10	11	13	14	16	17	18	19	20	21	22	23
Almandine	0.77	0.77	0.77	0.77	0.75	0.75	0.76	0.75	0.76	0.75	0.76	0.75	0.75	0.75	0.75	0.75
Grossular	0.03	0.03	0.03	0.03	0.04	0.04	0.04	0.04	0.03	0.03	0.03	0.03	0.03	0.03	0.03	0.03
Pyrope	0.12	0.14	0.14	0.15	0.17	0.17	0.17	0.18	0.18	0.18	0.18	0.18	0.18	0.18	0.18	0.18
Spessartine	0.09	0.06	0.06	0.05	0.04	0.04	0.04	0.04	0.03	0.04	0.04	0.04	0.04	0.04	0.04	0.04
XMg	0.13	0.15	0.16	0.16	0.19	0.19	0.18	0.19	0.19	0.19	0.19	0.19	0.19	0.20	0.19	0.19

Table A1. Major element geochemistry for garnet and biotite

KA064 (Grt2)

Location	core	core	core	mantle	mantle	mantle	mantle	mantle	mantle	mantle	mantle	rim	rim	rim	rim	rim
An. #	1 / 24 .	1 / 25 .	1 / 26 .	1 / 27 .	1 / 28 .	1 / 29 .	1 / 30 .	1 / 31 .	1 / 32 .	1 / 33 .	1 / 34 .	1 / 35 .	1 / 36 .	1 / 37 .	1 / 38 .	1 / 39 .
SiO2	37.42	37.39	37.37	37.37	37.42	37.45	37.31	37.41	37.41	37.35	37.35	37.40	37.35	37.18	37.10	36.90
TiO2	0.01	0.03	0.03	0.01	0.01	0.01	0.00	0.00	0.00	0.03	0.02	0.00	0.01	0.02	0.00	0.00
Al2O3	22.03	22.00	21.97	21.97	22.02	22.06	21.98	21.94	22.07	21.98	21.95	22.02	22.00	21.90	21.80	21.70
FeO	34.31	34.24	34.62	34.47	34.50	34.23	34.25	34.27	34.55	34.37	34.30	34.70	34.94	35.20	34.57	34.57
MnO	1.63	1.62	1.66	1.65	1.62	1.62	1.66	1.58	1.70	1.68	1.72	1.78	1.86	2.15	2.94	3.87
MgO	4.65	4.64	4.61	4.55	4.50	4.45	4.46	4.39	4.38	4.33	4.30	4.22	3.99	3.65	3.43	2.81
CaO	1.18	1.21	1.20	1.21	1.23	1.26	1.31	1.34	1.39	1.36	1.39	1.30	1.27	1.06	1.12	1.03
Na2O	0.01	0.02	0.02	0.02	0.02	0.02	0.02	0.01	0.00	0.00	0.04	0.02	0.01	0.01	0.00	0.00
K2O	0.00	0.00	0.00	0.01	0.00	0.00	0.00	0.00	0.00	0.00	0.00	0.00	0.00	0.00	0.00	0.00
Total	101.25	101.15	101.48	101.26	101.32	101.10	101.01	100.95	101.49	101.10	101.07	101.45	101.43	101.19	100.95	100.87
Si	2.95	2.95	2.95	2.95	2.95	2.96	2.95	2.96	2.95	2.95	2.96	2.95	2.95	2.95	2.96	2.96
Al iv	0.05	0.05	0.05	0.05	0.05	0.04	0.05	0.04	0.05	0.05	0.04	0.05	0.05	0.05	0.04	0.04
Al vi	2.00	2.00	1.99	2.00	2.00	2.01	2.00	2.01	2.00	2.00	2.00	2.00	2.00	2.01	2.01	2.01
Ti	0.00	0.00	0.00	0.00	0.00	0.00	0.00	0.00	0.00	0.00	0.00	0.00	0.00	0.00	0.00	0.00
Fe3+	0.00	0.00	0.01	0.00	0.00	0.00	0.00	0.00	0.00	0.00	0.00	0.00	0.00	0.00	0.00	0.00
Fe2+	2.27	2.26	2.27	2.28	2.28	2.27	2.27	2.28	2.28	2.28	2.28	2.29	2.32	2.35	2.31	2.33
Mn	0.11	0.11	0.11	0.11	0.11	0.11	0.11	0.11	0.11	0.11	0.12	0.12	0.12	0.14	0.20	0.26
Mg	0.55	0.55	0.54	0.54	0.53	0.52	0.53	0.52	0.51	0.51	0.51	0.50	0.47	0.43	0.41	0.34
Ca	0.10	0.10	0.10	0.10	0.10	0.11	0.11	0.11	0.12	0.11	0.12	0.11	0.11	0.09	0.10	0.09
Total	8.02	8.02	8.03	8.02	8.02	8.02	8.02	8.02	8.03	8.02	8.02	8.02	8.02	8.02	8.02	8.02
#	24	25	26	27	28	29	30	31	32	33	34	35	36	37	38	39
Almandine	0.75	0.75	0.75	0.75	0.75	0.76	0.75	0.76	0.75	0.76	0.75	0.76	0.77	0.78	0.77	0.77
Grossular	0.03	0.03	0.03	0.03	0.03	0.04	0.04	0.04	0.04	0.04	0.04	0.04	0.04	0.03	0.03	0.03
Pyrope	0.18	0.18	0.18	0.18	0.18	0.17	0.17	0.17	0.17	0.17	0.17	0.16	0.16	0.14	0.14	0.11
Spessartine	0.04	0.04	0.04	0.04	0.04	0.04	0.04	0.04	0.04	0.04	0.04	0.04	0.04	0.05	0.07	0.09
XMg	0.19	0.19	0.19	0.19	0.19	0.19	0.19	0.19	0.18	0.18	0.18	0.18	0.17	0.16	0.15	0.13

Table A2. Garnet trace element geochemistry

Analysis #	P	2SE	Y	2SE	La	2SE	Ce	2SE	Pr	2SE	Nd	2SE	Sm	2SE	Eu	2SE	Gd	2SE	Tb	2SE	Dy	2SE	Ho	2SE	Er	2SE	Tm	2SE	Yb	2SE	Lu	2SE
KA007-2	98	22	387	9	0.0	0.0	0.1	0.0	0.0	0.0	0.0	0.0	0.3	0.1	0.1	0.0	4.9	0.4	3.6	0.2	50.4	2.1	14.0	0.5	42.2	1.5	5.6	0.2	33.8	0.9	4.1	0.1
KA007-3	87	24	376	8	0.0	0.0	0.1	0.0	0.0	0.0	0.0	0.0	0.3	0.1	0.1	0.0	4.7	0.4	3.7	0.1	51.2	1.7	13.4	0.4	38.9	1.3	4.8	0.2	27.6	1.2	3.2	0.1
KA007-4	105	21	253	7	0.0	0.0	0.1	0.0	0.0	0.0	0.0	0.0	0.8	0.1	0.1	0.0	8.8	0.4	4.3	0.2	41.6	1.5	7.8	0.3	16.7	0.6	1.7	0.1	8.1	0.4	0.7	0.0
KA007-5	90	32	214	6	0.0	0.0	0.1	0.0	0.0	0.0	0.1	0.1	1.0	0.1	0.2	0.0	10.6	0.6	5.0	0.2	39.0	1.7	6.6	0.3	13.5	0.7	1.4	0.1	7.4	0.4	0.7	0.1
KA007-6	122	26	262	7	0.0	0.0	0.1	0.0	0.0	0.0	0.0	0.1	0.8	0.1	0.1	0.0	10.6	0.5	5.2	0.2	46.3	1.9	9.2	0.3	22.5	1.0	2.6	0.1	15.3	1.0	1.9	0.1
KA007-7	129	25	236	8	0.0	0.0	0.1	0.0	0.1	0.0	0.0	0.1	0.8	0.1	0.1	0.0	10.0	0.6	5.1	0.2	42.7	1.8	7.8	0.4	17.2	0.9	2.0	0.1	10.3	0.7	1.2	0.1
KA007-8	-14	30	219	6	0.0	0.0	0.0	0.0	0.0	0.0	-0.1	0.1	1.0	0.2	0.2	0.0	11.1	0.5	5.2	0.2	40.7	1.6	6.8	0.2	14.4	0.7	1.6	0.1	8.6	0.4	0.9	0.1
KA007-9	-23	24	209	5	0.0	0.0	-0.1	0.0	0.0	0.0	-0.2	0.1	0.9	0.2	0.2	0.0	11.1	0.5	4.9	0.2	39.2	1.2	6.4	0.3	13.3	0.7	1.5	0.1	8.3	0.5	0.8	0.1
KA007-10	-75	27	198	6	0.0	0.0	-0.1	0.0	0.0	0.0	-0.2	0.1	0.9	0.2	0.2	0.0	11.9	0.6	5.2	0.2	40.7	1.4	6.4	0.3	13.5	0.6	1.4	0.1	7.9	0.5	0.9	0.1
KA007-11	-112	29	193	3	0.0	0.0	-0.1	0.0	0.0	0.0	-0.2	0.1	0.9	0.2	0.2	0.0	10.8	0.7	5.1	0.2	39.0	1.4	6.0	0.2	11.8	0.6	1.3	0.1	6.4	0.3	0.7	0.0
KA007-12	-96	27	198	5	0.0	0.0	0.0	0.0	0.0	0.0	-0.1	0.0	0.6	0.1	0.1	0.0	10.1	0.6	5.0	0.3	39.1	1.5	6.2	0.3	12.8	0.7	1.3	0.1	6.6	0.3	0.7	0.0
KA007-13	-112	23	255	4	0.0	0.0	-0.1	0.0	0.0	0.0	-0.1	0.1	0.8	0.2	0.1	0.0	9.2	0.5	5.0	0.2	47.1	1.4	8.6	0.2	18.0	0.6	1.8	0.1	8.4	0.4	0.8	0.1
KA007-14	-37	25	198	4	0.0	0.0	0.0	0.0	0.0	0.0	0.0	0.0	1.0	0.1	0.3	0.0	10.3	0.5	4.3	0.2	35.1	1.4	5.9	0.2	12.3	0.5	1.2	0.1	6.5	0.3	0.7	0.0
KA007-15	-26	29	434	11	0.0	0.0	0.0	0.0	0.0	0.0	0.0	0.0	0.4	0.1	0.1	0.0	4.2	0.4	3.3	0.2	49.7	1.6	15.9	0.7	54.3	2.0	8.3	0.4	54.9	2.4	7.5	0.4
KA014-2	-384	478	318	32	3.6	1.1	5.8	1.4	1.0	0.5	5.0	1.4	4.7	1.6	1.5	0.4	37.0	4.7	12.3	1.3	79.6	8.5	11.9	1.4	25.1	3.7	3.2	0.7	21.2	4.2	3.0	0.4
KA014-3	35	37	245	8	0.2	0.1	1.8	2.1	0.2	0.1	0.6	0.2	2.7	0.5	1.3	0.1	29.5	1.3	10.4	0.4	64.0	2.2	8.6	0.5	14.4	0.8	1.5	0.1	11.2	0.8	1.9	0.2
KA014-4	165	31	181	10	0.1	0.0	0.1	0.0	0.0	0.0	0.6	0.1	4.7	0.4	2.4	0.1	40.9	2.6	10.0	0.7	48.0	3.1	7.0	0.6	14.0	1.0	1.5	0.1	8.6	0.8	0.8	0.1
KA014-5	39	42	702	22	0.0	0.0	0.0	0.0	0.0	0.0	0.2	0.1	1.7	0.3	0.9	0.1	28.5	0.9	14.1	0.5	124.0	4.0	27.5	1.2	76.1	4.0	10.0	0.7	59.8	3.6	7.4	0.5
KA014-6	7	34	317	8	0.0	0.0	0.1	0.0	0.0	0.0	0.0	0.0	0.6	0.1	0.4	0.1	8.5	0.6	4.4	0.2	45.2	2.1	9.8	0.4	26.7	1.0	3.4	0.2	20.2	0.9	2.4	0.1
KA014-7	27	34	601	14	0.0	0.0	0.1	0.0	0.0	0.0	0.1	0.0	0.4	0.1	0.3	0.1	8.1	0.5	5.1	0.2	66.4	2.2	21.3	0.9	77.3	2.6	12.6	0.4	90.9	2.8	12.6	0.4
KA014-8	14	22	170	4	0.1	0.0	0.3	0.1	0.0	0.0	0.1	0.1	0.5	0.1	0.4	0.1	6.7	0.6	3.0	0.1	24.1	0.8	4.7	0.2	12.2	0.4	1.7	0.1	10.4	0.6	1.2	0.1
KA014-9	32	30	312	5	0.1	0.0	0.1	0.0	0.1	0.0	0.1	0.0	0.3	0.1	0.2	0.0	2.6	0.3	1.7	0.1	27.5	0.9	10.6	0.3	47.8	1.5	9.1	0.3	75.9	2.5	11.9	0.4
KA014-10	111	34	149	8	0.1	0.0	0.1	0.0	0.0	0.0	0.0	0.0	0.1	0.1	0.1	0.0	2.2	0.2	1.3	0.1	16.0	1.0	5.1	0.4	19.3	1.4	3.4	0.2	27.0	2.2	4.2	0.3
KA014-11	25	11	45	2	0.1	0.0	0.2	0.1	0.0	0.0	0.1	0.1	0.0	0.0	0.0	0.0	0.4	0.1	0.2	0.0	4.2	0.2	1.5	0.1	6.4	0.4	1.3	0.1	10.1	0.6	1.7	0.1
KA014-12	0	22	113	5	0.0	0.0	0.1	0.0	0.0	0.0	0.3	0.5	0.1	0.0	0.1	0.0	2.1	0.2	1.1	0.1	12.9	0.7	3.6	0.2	13.5	0.9	2.5	0.2	20.7	1.4	3.4	0.2
KA014-13	36	25	143	3	0.0	0.0	0.1	0.0	0.0	0.0	0.0	0.0	0.1	0.0	0.1	0.0	1.7	0.2	1.0	0.1	13.5	0.5	4.6	0.2	18.8	0.7	3.4	0.1	31.4	1.6	5.4	0.2
KA014-14	31	20	160	5	0.0	0.0	0.1	0.0	0.0	0.0	0.0	0.0	0.1	0.0	0.1	0.0	1.3	0.2	0.9	0.0	13.7	0.6	4.9	0.2	21.3	0.9	4.4	0.2	41.1	2.0	7.5	0.4
KA014-15	21	22	196	5	0.0	0.0	0.0	0.0	0.0	0.0	0.0	0.0	0.0	0.0	0.1	0.0	1.1	0.2	0.8	0.1	14.0	0.5	5.8	0.2	28.9	0.7	6.2	0.2	62.1	1.7	11.2	0.3
KA014-16	12	30	180	12	0.0	0.0	0.1	0.0	0.0	0.0	0.1	0.1	0.1	0.1	0.1	0.0	1.3	0.2	0.9	0.1	12.4	0.9	4.5	0.5	19.5	2.2	4.3	0.5	40.4	4.8	7.0	0.9
KA014-17	1107	290	398	7	0.0	0.0	0.1	0.0	0.0	0.0	0.2	0.1	0.1	0.0	0.1	0.0	1.2	0.1	1.0	0.1	21.9	0.7	11.8	0.3	74.6	1.6	19.7	0.4	213.7	4.5	41.7	0.9
KA014-18	41	20	441	18	0.0	0.0	0.1	0.0	0.0	0.0	0.1	0.0	0.1	0.0	0.1	0.0	1.2	0.2	1.1	0.1	24.9	1.4	13.0	0.8	81.2	4.8	21.5	1.3	231.1	14.0	44.9	2.7
KA014-19	20	21	366	10	0.1	0.1	0.3	0.2	0.0	0.0	0.2	0.1	0.1	0.0	0.0	0.0	1.1	0.1	1.0	0.1	20.6	0.7	10.9	0.5	67.3	2.7	17.9	0.9	196.0	9.1	37.8	1.7
KA014-20	-8	21	193	3	0.0	0.0	0.1	0.0	0.0	0.0	0.0	0.0	0.1	0.0	0.1	0.0	1.3	0.1	1.0	0.1	14.7	0.4	5.7	0.2	25.5	0.8	5.1	0.2	47.2	1.3	8.2	0.2
KA014-21	0	16	188	3	0.0	0.0	0.1	0.0	0.0	0.0	0.1	0.0	0.1	0.0	0.1	0.0	1.7	0.2	1.1	0.1	16.4	0.4	5.8	0.2	23.6	0.6	4.4	0.1	39.3	1.3	6.9	0.2
KA014-22	12	31	155	11	0.0	0.0	0.1	0.0	0.0	0.0	0.0	0.0	0.1	0.1	0.1	0.0	1.9	0.2	1.2	0.1	15.9	1.4	5.2	0.4	19.3	1.7	3.6	0.4	30.7	3.0	5.1	0.5
KA014-23	-14	28	163	8	0.1	0.0	0.1	0.0	0.0	0.0	0.0	0.0	0.2	0.1	0.1	0.0	2.5	0.3	1.5	0.1	17.3	0.9	5.2	0.4	18.9	1.2	3.3	0.2	28.7	2.1	4.7	0.4
KA014-24	19	23	109	2	0.1	0.0	0.1	0.0	0.0	0.0	0.0	0.0	0.2	0.0	0.1	0.0	2.6	0.2	1.4	0.1	13.8	0.6	3.4	0.2	10.6	0.4	1.7	0.1	13.2	0.7	2.1	0.1
KA014-25	3	31	91	2	0.0	0.0	0.1	0.0	0.0	0.0	0.0	0.0	0.2	0.1	0.1	0.0	2.3	0.2	1.1	0.1	11.3	0.4	2.8	0.1	8.9	0.3	1.4	0.1	11.5	0.3	1.7	0.1
KA014-26	2	28	118	4	0.0	0.0	0.1	0.0	0.0	0.0	0.1	0.0	0.2	0.1	0.1	0.0	3.0	0.3	1.4	0.1	14.9	0.7	3.6	0.2	12.0	0.7	1.9	0.1	14.0	0.9	2.1	0.1
KA014-27	0	23	122	5	0.1	0.0	0.1	0.0	0.0	0.0	0.0	0.0	0.2	0.1	0.2	0.0	3.2	0.2	1.7	0.1	16.2	0.7	4.1	0.2	14.0	0.8	2.3	0.1	18.0	1.1	2.8	0.1
KA014-28	2	19	254	13	0.0	0.0	0.1	0.0	0.0	0.0	0.1	0.0	0.3	0.1	0.1	0.0	3.0	0.3	1.8	0.1	25.0	1.7	7.9	0.5	28.7	1.9	4.6	0.3	35.1	2.0	5.0	0.3
KA014-30	-5	25	319	10	0.0	0.0	0.1	0.0	0.0	0.0	0.1	0.0	0.4	0.1	0.3	0.0	6.0	0.4	3.4	0.1	41.0	2.0	10.9	0.5	36.4	1.8	5.5	0.3	39.1	2.0	5.4	0.2
KA014-31	21	21	199	5	0.0	0.0	0.0	0.0	0.0	0.0	0.1	0.0	0.6	0.1	0.4	0.0	7.9	0.5	3.4	0.2	29.0	1.0	5.9	0.2	14.9	0.6	1.8	0.1	10.8	0.5	1.2	0.1
KA014-32	-7	28	454	13	0.1	0.1	0.3	0.1	0.0	0.0	0.2	0.1	0.6	0.1	0.4	0.1	8.2	0.5	4.8	0.2	55.9	2.4	14.8	0.6	44.7	1.9	5.9	0.3	36.1	1.9	4.2	0.2
KA014-33	65	28	281	7	0.0	0.0	0.1	0.0	0.0	0.0	0.4	0.1	3.2	0.2	1.6	0.1	40.4	1.8	12.6	0.5	71.1	2.7	9.8	0.4	18.1	0.7	1.8	0.1	8.9	0.3	0.9	0.0
KA014-34	54	19	144	5	0.1	0.0	0.3	0.1	0.1	0.0	0.5	0.1	3.6	0.3	2.0	0.1	33.4	1.3	9.2	0.3	42.0	2.2	4.7	0.3	7.6	0.5	0.6	0.1	2.9	0.3	0.3	0.0
KA014-35	91	24	155	4	0.2	0.1	0.4	0.1	0.1	0.0	0.5	0.1	3.6	0.3	2.3	0.1	35.5	1.3	9.6	0.3	44.9	1.6	5.4	0.2	10.0	0.4	1.0	0.1	5.0	0.3	0.5	0.0
KA014-36	72	31	500	19	0.1	0.0	0.2	0.1	0.0	0.0	0.3	0.1	3.0	0.3	1.8	0.1	31.4	1.6	14.6	0.9	116.1	5.7	20.3	1.2	42.8	2.4	4.5	0.2	24.0	1.5	2.5	0.2
KA031-1	66	25	242	5	0.0	0.0	0.0	0.0	0.0	0.0	0.0	0.0	0.7	0.2	0.4	0.1	9.6	0.7	3.5	0.2	34.0	1.0	7.7	0.3	22.2	0.8	3.0	0.1	20.4	0.8	2.8	0.1
KA031-2	157	96	338	8	0.1	0.0	0.3	0.2	0.0	0.0	0.2	0.2	0.4	0.1	0.2	0.0	5.2	0.4	3.4	0.1	43.9	1.3	11.7	0.4	33.4	1.0	4.3	0.2	25.0	1.0	3.3	0.1
KA031-3	27	20	344	6	0.0	0.0	0.0	0.0	0.0	0.0	-0.1	0.0	0.3	0.1	0.2	0.0	4.9	0.3	3.6	0.1	46.3	1.7	12.0	0.4	33.1	1.2	4.1	0.2	22.5	1.1	2.5	0.1
KA031-4	19	21	419	8	0.0	0.0	0.0	0.0	0.0	0.0	-0.1	0.0	0.3	0.1	0.2	0.0	4.8	0.3	3.6	0.1	49.5	1.7	14.8	0.4	48.2	1.5	6.8	0.2	41.3	1.3	4.7	0.2
KA031-5	32	20	636	10	0.0	0.0	0.0	0.0	0.0	0.0	-0.1	0.0	0.4	0.1	0.3	0.1	10.7	0.5	7.8	0.2	106.5	2.6	27.2	0.7	67.8	2.2	7.7	0.3	39.5	1.7	4.1	0.2
KA031-6	76	25	571	9	0.0	0.0	0.0	0.0	0.1	0.0	0.1	0.1	0.6	0.1	0.3	0.0	13.0	0.6	6.9	0.2	79.6	1.7	20.9	0.6	62.2	1.9	8.9	0.3	60.3	2.3	7.5	0.3
KA031-7	42	19	687	8	0.0	0.0	0.0	0.0	0.0	0.0	0.1	0.0	0.5	0.1	0.2	0.0	10.6	0.7	6.5	0.2	80.3	2.0	22.2	0.6	71.7	1.8	10.9	0.3	71.5	2.3	9.4	0.2
KA031-8	11	20	1261	18	0.0	0.0	0.0	0.0	0.0	0.0	0.1	0.0	0.2	0.1	0.1	0.0	4.0	0.3	4.2	0.1	91.1	2.0	49.2	0.9	282.0	4.5	65.2	1.3	613.0	13.7	102.3	2.2
KA031-10	55	21	957	15	0.0	0.0	0.0	0.0	0.0	0.0	0.1	0.0	0.2	0.1	0.2	0.0	7.5	0.5	5.5	0.2	92.6	2.3	37.4	1.0	173.9	4.5	34.0	1.0	283.6	9.7	45.7	1.4
KA031-12	264	64	1473	134	0.0	0.0	0.4	0.1	0.2	0.1	1.8	0.5	2.5	0.6	0.8	0.2	23.6	4.3	12.4	1.6	159.8	15.1	54.1	3.5	218.8	10.4	39.1	1.4	312.5	9.3	52.4	1.3
KA031-13	26	26	909	17	0.0	0.0	0.0	0.0	0.0	0.0	0.1	0.0	0.3	0.1	0.2	0.0	8.9	0.5	6.5	0.3	95.0	3.0	32.5	1.0	122.2	3.4	21.1	0.7	161.9	6.0	22.6	0.8

Table A2. Garnet trace element geochemistry

Analysis #	P	2SE	Y	2SE	La	2SE	Ce	2SE	Pr	2SE	Nd	2SE	Sm	2SE	Eu	2SE	Gd	2SE	Tb	2SE	Dy	2SE	Ho	2SE	Er	2SE	Tm	2SE	Yb	2SE	Lu	2SE
KA031-14	204	102	1221	224	0.1	0.0	0.5	0.3	0.2	0.1	2.1	1.1	3.3	1.6	1.2	0.6	24.9	10.1	13.6	4.5	158.9	39.0	46.5	8.7	157.6	21.6	24.2	2.2	162.7	11.9	22.0	1.2
KA031-15	48	24	643	9	0.0	0.0	0.0	0.0	0.0	0.0	0.1	0.0	0.4	0.1	0.2	0.0	8.0	0.5	5.5	0.2	81.7	1.6	28.3	0.6	100.3	2.6	14.3	0.5	91.6	3.7	12.2	0.5
KA031-16	82	22	412	7	0.0	0.0	0.0	0.0	0.0	0.0	0.0	0.0	0.3	0.1	0.1	0.0	4.3	0.2	3.1	0.1	48.4	1.3	15.5	0.4	53.6	1.4	8.0	0.2	51.0	1.7	6.8	0.3
KA031-17	66	20	245	5	0.0	0.0	0.0	0.0	0.0	0.0	0.0	0.0	0.4	0.1	0.3	0.0	7.3	0.5	4.0	0.2	43.5	1.5	9.8	0.3	23.8	0.7	2.7	0.2	16.6	0.6	2.8	0.1
KA031-18	129	29	225	5	0.0	0.0	0.0	0.0	0.0	0.0	0.1	0.0	0.9	0.2	0.6	0.1	9.2	0.5	3.7	0.2	34.6	1.1	8.1	0.3	22.7	0.8	3.2	0.2	23.0	0.9	3.5	0.1
KA044-2	88	26	120	3	0.0	0.0	0.1	0.0	0.1	0.0	1.0	0.2	4.1	0.4	0.6	0.1	15.1	0.7	3.6	0.1	25.0	0.9	4.8	0.2	12.7	0.5	1.7	0.1	10.3	0.6	1.3	0.1
KA044-3	68	23	94	3	0.0	0.0	0.1	0.0	0.0	0.0	1.1	0.2	4.1	0.2	0.5	0.0	14.6	0.8	3.3	0.1	20.5	0.9	3.6	0.2	8.4	0.4	1.0	0.1	6.3	0.3	0.9	0.1
KA044-4	11	24	105	1	0.0	0.0	0.1	0.0	0.0	0.0	1.0	0.1	4.1	0.4	0.6	0.1	14.6	0.6	3.4	0.1	21.6	0.8	4.0	0.1	10.3	0.4	1.4	0.1	8.5	0.5	1.1	0.1
KA044-5	48	22	118	3	0.0	0.0	0.1	0.0	0.1	0.0	1.0	0.1	3.9	0.3	0.6	0.1	13.6	0.6	3.4	0.1	23.0	0.7	4.7	0.2	13.0	0.5	1.8	0.1	11.1	0.6	1.4	0.1
KA044-6	16	19	121	2	0.0	0.0	0.0	0.0	0.0	0.0	1.1	0.2	4.2	0.3	0.6	0.1	13.5	0.6	3.2	0.1	22.7	0.7	4.7	0.2	14.1	0.5	2.0	0.1	13.0	0.7	1.8	0.1
KA044-7	30	22	141	4	0.0	0.0	0.0	0.0	0.0	0.0	0.9	0.1	4.2	0.4	0.5	0.1	14.1	0.6	3.5	0.2	25.1	1.0	5.8	0.2	18.3	0.7	2.7	0.1	18.3	0.9	2.8	0.1
KA044-8	13	23	139	3	0.0	0.0	0.0	0.0	0.0	0.0	1.0	0.1	4.1	0.4	0.5	0.1	14.2	0.8	3.6	0.1	24.9	0.8	5.5	0.2	17.0	0.6	2.4	0.1	16.1	0.7	2.2	0.1
KA044-9	25	23	159	3	0.2	0.1	0.4	0.2	0.1	0.0	0.7	0.1	3.8	0.3	0.4	0.1	14.5	0.7	3.8	0.1	28.5	0.8	6.3	0.2	19.0	0.8	2.8	0.1	19.2	0.9	2.9	0.1
KA044-10	23	18	151	3	0.1	0.0	0.3	0.0	0.1	0.0	0.9	0.1	4.0	0.3	0.3	0.0	14.4	0.7	3.8	0.1	27.3	1.1	6.0	0.2	17.7	0.6	2.6	0.1	18.3	0.7	2.6	0.1
KA044-11	30	19	140	3	0.0	0.0	0.1	0.0	0.1	0.0	0.6	0.1	3.6	0.3	0.4	0.0	13.4	0.5	3.5	0.1	24.5	0.9	5.5	0.2	16.9	0.6	2.5	0.1	17.1	0.7	2.6	0.1
KA044-12	53	29	144	3	0.0	0.0	0.0	0.0	0.0	0.0	0.8	0.1	3.4	0.2	0.4	0.1	13.1	0.4	3.2	0.1	24.0	0.7	5.8	0.2	18.8	0.7	3.1	0.1	24.2	0.7	4.0	0.2
KA044-13	14	30	156	3	0.0	0.0	0.1	0.0	0.0	0.0	0.9	0.1	3.7	0.3	0.4	0.0	12.9	0.6	3.1	0.1	24.7	0.7	6.5	0.2	25.4	0.9	4.9	0.2	42.0	1.4	8.3	0.3
KA044-14	12	22	174	4	0.0	0.0	0.1	0.0	0.0	0.0	1.0	0.1	3.7	0.3	0.5	0.1	11.8	0.6	3.1	0.1	24.1	0.8	6.9	0.3	30.1	0.9	6.2	0.2	58.3	2.1	11.1	0.4
KA044-15	30	26	197	4	0.1	0.0	0.2	0.0	0.1	0.0	1.1	0.2	3.8	0.2	0.5	0.1	11.2	0.5	2.9	0.1	24.6	0.8	8.0	0.3	37.8	1.2	7.5	0.2	69.3	2.3	13.3	0.4
KA044-16	5	23	209	4	0.0	0.0	0.1	0.0	0.1	0.0	1.0	0.2	3.8	0.3	0.6	0.0	11.0	0.5	2.8	0.1	24.8	0.8	8.6	0.2	42.4	1.4	8.9	0.3	84.6	2.9	16.3	0.5
KA044-17	52	30	200	4	0.0	0.0	0.2	0.0	0.1	0.0	1.0	0.2	3.7	0.4	0.5	0.1	11.3	0.6	2.8	0.1	25.1	1.0	7.8	0.3	35.7	1.0	7.1	0.2	62.5	1.5	11.7	0.4
KA044-18	28	29	196	4	0.0	0.0	0.1	0.0	0.1	0.0	1.0	0.1	3.5	0.2	0.5	0.1	11.7	0.5	3.0	0.1	25.1	0.8	7.8	0.2	33.2	1.1	6.3	0.2	55.9	1.6	10.0	0.3
KA044-19	30	26	173	4	0.1	0.0	0.3	0.1	0.1	0.0	1.1	0.1	3.7	0.3	0.5	0.1	11.8	0.6	3.1	0.1	24.3	0.8	6.7	0.3	24.9	1.0	4.3	0.2	34.9	1.3	5.8	0.2
KA044-20	16	22	165	3	0.2	0.1	0.6	0.2	0.1	0.0	1.2	0.2	3.7	0.3	0.5	0.1	13.0	0.7	3.3	0.1	25.4	0.9	6.3	0.2	20.7	0.8	3.2	0.1	24.0	0.8	3.8	0.1
KA044-21	26	24	174	3	0.0	0.0	0.1	0.0	0.1	0.0	1.2	0.1	3.7	0.3	0.5	0.1	13.3	0.7	3.3	0.2	26.1	1.0	6.5	0.2	21.2	0.8	3.4	0.2	23.8	0.9	3.6	0.1
KA044-22	-4	22	169	3	0.0	0.0	0.1	0.0	0.0	0.0	0.9	0.1	4.0	0.3	0.5	0.1	12.6	0.6	3.3	0.1	26.7	0.8	6.6	0.3	22.0	0.8	3.3	0.2	24.0	1.0	3.4	0.1
KA044-23	50	32	176	4	0.0	0.0	0.1	0.0	0.0	0.0	0.9	0.1	4.1	0.3	0.5	0.0	13.3	0.6	3.6	0.1	27.5	1.0	6.9	0.3	23.1	0.7	3.6	0.2	25.6	0.8	3.8	0.2
KA044-24	52	30	177	4	0.0	0.0	0.1	0.0	0.0	0.0	0.8	0.1	3.8	0.3	0.5	0.0	12.8	0.6	3.5	0.1	27.7	1.2	7.0	0.2	24.1	0.9	3.7	0.2	26.5	1.2	4.0	0.2
KA044-25	81	31	171	3	0.0	0.0	0.1	0.0	0.0	0.0	0.9	0.1	4.1	0.3	0.5	0.1	12.5	0.6	3.3	0.1	27.0	0.9	7.0	0.2	23.4	0.6	3.6	0.1	25.2	0.7	3.7	0.1
KA044-26	51	29	162	3	0.0	0.0	0.1	0.0	0.1	0.0	0.8	0.1	4.1	0.3	0.5	0.1	13.3	0.6	3.6	0.1	26.8	0.8	6.8	0.2	22.4	0.6	3.5	0.1	24.6	0.9	3.7	0.1
KA044-27	42	31	153	3	0.2	0.1	0.5	0.2	0.1	0.0	1.3	0.2	4.4	0.3	0.5	0.1	13.2	0.6	3.6	0.2	26.0	0.9	6.2	0.2	18.6	0.6	2.6	0.1	17.9	0.7	2.5	0.1
KA044-28	41	32	136	3	0.0	0.0	0.1	0.0	0.0	0.0	0.9	0.1	3.8	0.3	0.6	0.0	13.2	0.6	3.4	0.1	24.3	0.9	5.4	0.2	15.2	0.5	2.1	0.1	12.8	0.4	1.8	0.1
KA044-29	64	32	110	3	0.0	0.0	0.1	0.0	0.0	0.0	1.1	0.2	4.3	0.4	0.5	0.1	14.6	0.7	3.4	0.1	22.3	1.0	4.3	0.2	10.7	0.3	1.4	0.1	8.4	0.5	1.1	0.1
KA044-30	40	31	95	2	0.0	0.0	0.0	0.0	0.0	0.0	0.9	0.1	4.1	0.3	0.5	0.1	14.1	0.6	3.4	0.2	20.3	0.7	3.7	0.1	9.1	0.4	1.1	0.1	6.2	0.3	0.8	0.1
KA044-31	46	32	83	2	0.0	0.0	0.1	0.0	0.0	0.0	0.8	0.1	4.4	0.3	0.6	0.1	14.4	0.7	3.4	0.2	18.7	0.6	3.0	0.1	6.8	0.4	0.9	0.1	4.9	0.3	0.6	0.0
KA044-32	40	28	78	2	0.0	0.0	0.0	0.0	0.0	0.0	0.8	0.1	4.2	0.3	0.5	0.0	15.3	0.6	3.3	0.1	18.4	0.6	2.9	0.1	6.9	0.3	0.8	0.0	4.8	0.3	0.7	0.0
KA044-33	56	32	83	2	0.0	0.0	0.1	0.0	0.0	0.0	1.0	0.1	4.4	0.4	0.4	0.1	16.2	0.6	3.4	0.1	18.8	0.6	3.2	0.1	7.5	0.4	0.9	0.1	5.8	0.3	0.7	0.1
KA044-34	36	34	100	2	0.0	0.0	0.1	0.0	0.0	0.0	0.8	0.1	4.2	0.4	0.4	0.0	16.9	0.7	4.0	0.1	22.7	0.8	3.9	0.2	8.9	0.4	1.1	0.1	6.7	0.3	0.9	0.1
KA064-1	-4	33	377	6	0.0	0.0	0.0	0.0	0.0	0.0	0.1	0.0	0.5	0.1	0.1	0.0	6.2	0.4	3.6	0.2	45.8	1.2	13.2	0.4	43.8	1.4	6.6	0.2	44.7	1.3	6.0	0.2
KA064-2	57	52	366	5	0.0	0.0	0.0	0.0	0.0	0.0	0.1	0.0	0.6	0.1	0.1	0.0	6.8	0.3	4.0	0.2	47.2	1.4	13.0	0.4	42.5	1.3	6.4	0.2	43.4	1.5	6.3	0.2
KA064-3	-4	39	396	6	0.0	0.0	0.0	0.0	0.0	0.0	0.1	0.0	0.3	0.1	0.0	0.0	5.4	0.4	3.8	0.1	50.0	1.1	14.3	0.4	47.4	1.5	6.7	0.2	43.6	1.6	6.2	0.2
KA064-4	14	36	354	5	0.0	0.0	0.0	0.0	0.0	0.0	0.1	0.1	0.6	0.1	0.1	0.0	9.7	0.5	5.2	0.2	53.5	1.3	12.9	0.3	34.7	0.9	4.6	0.2	28.1	0.8	3.3	0.1
KA064-5	50	38	438	7	0.0	0.0	0.0	0.0	0.0	0.0	0.1	0.0	0.6	0.1	0.2	0.0	12.2	0.5	6.6	0.2	70.1	1.4	17.2	0.4	47.2	1.2	6.2	0.2	37.4	1.1	4.7	0.1
KA064-6	18	42	415	8	0.0	0.0	0.0	0.1	0.0	0.0	0.1	0.0	0.6	0.1	0.1	0.0	8.3	0.5	4.9	0.2	57.1	1.6	15.4	0.4	46.1	1.5	6.5	0.2	42.2	1.7	5.5	0.2
KA064-7	7	40	458	7	0.0	0.0	0.1	0.1	0.0	0.0	0.2	0.1	0.5	0.1	0.1	0.0	6.1	0.4	4.4	0.2	64.0	1.9	19.9	0.5	62.4	1.6	8.6	0.3	57.2	1.5	7.8	0.2
KA064-8	124	50	710	57	0.0	0.0	0.2	0.1	0.1	0.0	0.8	0.4	1.3	0.5	0.2	0.1	9.2	1.9	5.6	0.7	89.3	7.8	30.4	1.7	106.3	4.6	15.7	0.6	106.7	3.6	15.2	0.4
KA064-9	91	49	571	10	0.1	0.1	0.1	0.0	0.0	0.0	0.1	0.1	0.3	0.1	0.1	0.0	4.5	0.3	3.7	0.1	63.4	1.6	23.6	0.6	90.4	2.3	14.8	0.4	106.2	3.0	14.5	0.3
KA064-10	158	42	527	10	0.2	0.1	0.3	0.1	0.1	0.0	0.3	0.1	0.4	0.1	0.1	0.0	4.7	0.4	3.7	0.1	60.7	1.6	22.9	0.6	88.4	2.3	14.3	0.4	106.4	3.1	14.9	0.5
KA064-11	204	37	552	37	0.4	0.1	1.1	0.3	0.2	0.0	0.9	0.3	0.9	0.2	0.2	0.1	6.2	1.2	4.3	0.5	66.1	4.8	22.6	1.2	84.7	3.5	13.8	0.5	99.1	3.6	13.4	0.4
KA064-12	170	45	427	6	1.4	0.2	3.2	0.5	0.4	0.1	1.4	0.2	0.5	0.1	0.1	0.0	4.1	0.3	3.1	0.1	51.3	1.4	18.5	0.6	76.1	1.9	13.9	0.5	109.5	3.7	15.6	0.5
KA064-13	190	39	360	5	0.9	0.3	1.8	0.4	0.3	0.1	0.8	0.2	0.5	0.1	0.2	0.0	5.3	0.4	3.1	0.1	42.9	1.1	13.8	0.4	54.8	1.4	10.1	0.3	81.1	2.5	11.1	0.3
KA064-14	171	35	444	10	0.0	0.0	0.0	0.0	0.0	0.0	0.1	0.0	0.3	0.1	0.1	0.0	3.4	0.2	2.7	0.1	48.6	1.3	20.0	0.5	92.2	3.2	19.0	0.7	166.8	6.0	26.1	0.9
KA064-15	161	29	330	34	0.0	0.0	0.1	0.0	0.0	0.0	0.1	0.0	0.2	0.1	0.1	0.0	2.4	0.4	1.9	0.2	34.7	4.0	14.3	1.6	71.0	7.8	15.4	1.7	146.4	16.8	23.6	2.7
KA064-16	154	33	427	17	0.2	0.0	0.5	0.2	0.1	0.0	0.3	0.1	0.3	0.1	0.1	0.0	3.4	0.3	2.7	0.1	46.5	2.3	19.5	0.9	93.1	4.3	21.0	1.1	204.5	10.2	34.1	1.6
KA064-18	249	42	442	8	0.2	0.1	0.5	0.1	0.1	0.0	0.2	0.1	0.4	0.1	0.1	0.0	3.3	0.3	2.6	0.1	47.7	1.0	20.3	0.5	99.3	2.0	21.9	0.6	202.1	5.1	33.7	0.9
KA064-19	263	35	423	9	1.2	0.4	3.3	1.0	0.4	0.1	1.4	0.3	0.6	0.1	0.2	0.0	3.7	0.3	2.6	0.1	45.7	1.4	19.3	0.5	93.0	2.4	20.5	0.5	196.8	5.0	32.4	1.0
KA064-20	175	40	443	7	0.0	0.0	0.0	0.0	0.0	0.0	0.1	0.0	0.3	0.1	0.1	0.0	3.4	0.3	2.7	0.1	47.4	1.2	19.5	0.5	91.5	2.2	19.5	0.5	172.9	4.8	26.9	0.7
KA064-21	200	40	484	7	0.0	0.0	0.0	0.0	0.0	0.0	0.1	0.0	0.3	0.1	0.1	0.0	4.1	0.4	3.1	0.1	53.6	1.3	21.0	0.4	87.1	1.8	16.7	0.5	134.8	2.7	18.7	0.4
KA064-22	170	40	516	11	0.0	0.0	0.0	0.0	0.0	0.0	0.1	0.0	0.3	0.1	0.1	0.0	3.9	0.3	3.1	0.1	56.9	1.9	22.5	0.6	98.0	2.3	17.5	0.6	136.0	4.6	20.2	0.6

Table A2. Garnet trace element geochemistry

Analysis #	P	2SE	Y	2SE	La	2SE	Ce	2SE	Pr	2SE	Nd	2SE	Sm	2SE	Eu	2SE	Gd	2SE	Tb	2SE	Dy	2SE	Ho	2SE	Er	2SE	Tm	2SE	Yb	2SE	Lu	2SE
KA064-24	173	35	503	8	0.0	0.0	0.0	0.0	0.0	0.0	0.1	0.0	0.3	0.1	0.1	0.0	3.8	0.3	3.1	0.1	55.7	1.4	20.7	0.4	84.3	2.1	14.3	0.4	108.6	3.7	15.1	0.4
KA064-25	147	28	527	17	0.0	0.0	0.0	0.0	0.0	0.0	0.1	0.0	0.3	0.1	0.1	0.0	3.8	0.4	3.4	0.2	56.9	2.3	21.1	0.7	82.4	3.0	13.6	0.6	100.8	4.2	13.8	0.6
KA064-26	122	33	546	10	0.0	0.0	0.0	0.0	0.0	0.0	0.1	0.0	0.5	0.1	0.1	0.0	4.6	0.3	3.7	0.2	61.1	1.8	22.0	0.6	82.3	2.0	13.4	0.4	95.8	2.7	13.2	0.4
KA064-27	133	32	604	24	0.0	0.0	0.2	0.0	0.0	0.0	0.7	0.2	1.0	0.2	0.1	0.0	7.9	1.0	4.8	0.4	70.9	4.2	23.7	1.1	85.2	3.7	12.9	0.6	91.6	4.3	12.6	0.7
KA064-28	70	30	469	8	0.0	0.0	0.0	0.0	0.0	0.0	0.2	0.1	0.5	0.1	0.1	0.0	6.5	0.4	4.5	0.1	65.3	1.6	18.2	0.4	53.9	1.5	7.6	0.2	49.9	1.6	6.3	0.2
KA064-29	31	26	400	6	0.0	0.0	0.0	0.0	0.0	0.0	0.1	0.0	0.4	0.1	0.1	0.0	7.0	0.4	4.5	0.2	54.8	1.7	15.5	0.4	48.8	1.0	6.7	0.2	44.2	1.4	6.0	0.2
KA064-30	30	32	398	8	0.1	0.0	0.0	0.0	0.0	0.0	0.2	0.1	0.6	0.1	0.2	0.0	7.2	0.4	4.5	0.1	54.7	1.6	14.9	0.4	45.7	1.2	6.3	0.2	39.4	1.1	5.1	0.2
KA064-31	44	33	401	8	0.0	0.0	0.0	0.0	0.0	0.0	0.1	0.0	0.6	0.1	0.1	0.0	7.0	0.4	4.2	0.2	51.7	1.4	13.9	0.4	41.7	0.9	6.0	0.2	37.8	1.4	4.9	0.2
KA064-32	-5	24	299	7	0.0	0.0	0.0	0.0	0.0	0.0	0.1	0.0	0.5	0.1	0.1	0.0	6.1	0.5	3.6	0.2	41.4	1.4	10.6	0.4	30.7	0.9	4.3	0.1	27.0	0.9	3.2	0.1
KA064-33	16	29	348	5	0.0	0.0	0.0	0.0	0.0	0.0	0.1	0.0	0.5	0.1	0.0	0.0	5.5	0.3	3.5	0.1	44.0	1.2	12.1	0.3	39.3	1.1	5.7	0.2	39.2	1.1	5.2	0.2
KA064-34	40	30	317	6	0.0	0.0	0.0	0.0	0.0	0.0	0.1	0.0	0.5	0.1	0.0	0.0	5.2	0.3	3.1	0.1	38.6	1.1	10.7	0.3	35.1	1.0	5.2	0.2	35.3	0.9	4.6	0.1
KA064-35	235	84	313	9	0.1	0.0	0.3	0.1	0.0	0.0	0.2	0.1	0.5	0.1	0.1	0.0	4.8	0.3	3.0	0.1	38.4	1.5	10.8	0.4	36.8	1.4	5.5	0.3	36.7	1.7	4.7	0.2
KA064-36	1177	194	297	30	0.4	0.1	1.5	0.4	0.1	0.0	0.5	0.2	0.5	0.2	0.3	0.1	4.5	0.6	2.8	0.4	35.6	3.8	10.3	1.1	37.5	5.7	5.0	0.5	34.9	3.7	4.7	0.5
NIST610																																
run1																																
610-1	474	18	466	7	445	6	461	8	456	7	441	6	461	8	454	9	443	8	449	8	444	8	461	9	460	9	438	9	466	8	449	7
610-2	485	20	463	7	445	7	458	7	452	7	439	8	460	6	450	7	443	6	447	7	442	6	457	7	456	8	437	7	465	7	449	6
610-3	470	20	461	7	440	8	456	7	448	7	435	7	455	8	445	7	441	9	443	8	435	8	453	8	449	7	435	8	460	8	444	7
610-4	465	18	467	7	449	6	465	7	461	7	442	6	466	6	459	6	453	7	453	5	443	6	462	7	461	7	446	7	471	8	454	6
610-5	441	16	463	6	441	7	458	9	454	7	439	8	457	8	450	9	445	8	447	8	440	9	458	9	455	9	438	9	459	9	452	8
610-6	412	16	463	6	439	7	456	10	450	7	437	8	453	9	444	7	448	10	447	8	440	8	459	8	455	9	438	9	461	9	446	8
610-7	425	21	458	5	436	5	455	7	447	6	432	6	448	7	446	6	440	5	441	5	437	7	454	7	449	7	432	7	460	6	441	7
run2																																
610-1	436	13	450	6	438	6	451	6	448	6	434	6	459	7	449	8	441	7	440	8	433	7	445	7	453	6	434	6	462	7	443	7
610-2	417	15	448	6	435	6	447	6	441	6	431	7	452	6	444	7	434	6	436	6	427	6	444	7	441	6	427	7	457	7	435	8
610-3	443	25	462	8	450	8	467	8	459	7	443	8	464	8	459	7	450	7	449	7	437	9	457	8	454	9	436	9	468	9	449	8
610-4	444	18	459	9	442	9	461	10	450	9	435	10	459	9	456	9	445	9	442	8	432	9	449	8	449	9	433	9	464	9	442	8
610-5	462	26	461	7	444	6	464	7	455	10	443	7	459	7	455	8	440	9	442	9	434	6	449	6	447	6	436	8	466	8	440	7
610-6	499	26	450	7	433	6	454	8	444	7	431	7	446	7	445	7	437	8	439	7	430	9	444	7	444	8	426	8	460	9	437	9
610-7	507	23	454	7	432	7	454	10	444	7	430	9	446	9	446	10	440	7	440	7	429	6	443	8	444	7	425	9	460	11	434	8
run3																																
610-1	388	14	462	6	442	6	458	8	455	7	436	6	461	6	455	6	447	6	453	6	442	5	461	6	460	5	443	6	470	6	455	5
610-2	410	18	465	8	447	6	461	9	453	8	435	5	459	7	454	8	448	7	451	8	439	8	462	7	459	8	441	8	462	9	454	8
610-3	406	17	471	6	452	6	463	5	460	6	444	7	465	6	457	8	452	8	457	7	445	7	465	7	465	7	444	7	470	7	455	6
610-4	441	26	466	7	450	7	465	9	454	9	436	8	466	9	451	8	445	8	448	8	437	9	457	8	454	9	440	8	463	8	454	7
610-5	453	25	467	8	445	6	464	8	453	4	440	6	461	7	453	7	445	6	452	7	441	6	462	7	459	7	440	7	465	7	452	7
610-6	481	26	466	7	444	5	461	6	449	6	439	6	462	5	448	5	449	6	447	7	440	6	462	6	454	7	438	5	465	6	449	5
610-7	505	29	451	7	437	5	446	7	442	7	431	7	454	6	438	7	437	7	438	7	431	7	450	7	444	8	431	7	453	9	440	7
610-8	583	28	460	6	440	6	447	7	442	8	431	5	456	8	442	9	445	7	444	7	437	8	454	7	452	7	436	8	462	7	446	7

Table A3. Monazite and xenotime geochronology data

Specimen/Mnz	Mineral	Location	Near crack	Comment	Pb ppm	U ppm	Th ppm	Th/U	207Pb/206Pb	2 SE %	207Pb/235U	2 SE %	206Pb/238U	2 SE %	Rho	208Pb/232Th	2 SE %
007_M1	Monazite	Grt rim	N		51	202	1480	6.37	0.0603	11.94	0.384	13.81	0.0474	6.93	0.50	0.0283	7.68
007_M2	Monazite	Grt rim	N		67	437	3570	7.65	0.0574	10.81	0.156	12.59	0.0199	6.45	0.51	0.0143	6.78
~~007_M3~~	~~Monazite~~			no signal													
~~031_M1~~	~~Monazite~~			no signal													
031_M2	Monazite	Grt rim	N		26	978	11800	12.17	0.3808	3.26	0.289	5.17	0.00547	4.01	0.78	0.0016	4.62
031_M3	Monazite	Grt rim	N		26	3230	26160	8.61	0.1123	6.72	0.034	8.62	0.00225	5.40	0.63	0.0007	5.71
031_X1	Xenotime	Grt core	N		1	891	501	0.62	0.135	7.67	0.0525	8.54	0.002796	3.76	0.44	0.0021	5.54
031_X2	Xenotime	Grt core	Y		0	266	117	0.41	0.111	34.29	0.0281	34.78	0.00226	5.79	0.17	0.0018	27.02
031_X3	Xenotime	Grt core	Y		0	663	329	0.53	0.046	86.98	0.019	87.59	0.00219	10.31	0.12	0.0009	29.56
~~031_X4~~	~~Xenotime~~			no signal													
064_M2	Monazite	Grt core	N		84	230	1882	7.43	0.0593	4.51	0.633	6.61	0.0776	4.83	0.73	0.0330	4.48
064_M3	Monazite	Grt rim	N		1245	2769	39280	13.21	0.05684	2.14	0.571	3.93	0.0722	3.29	0.84	0.0230	3.78
064_M4	Monazite	Grt rim	N		465	998	17110	16.75	0.0592	2.97	0.349	5.80	0.043	4.98	0.86	0.0204	5.29
064_M5	Monazite	Grt rim	N		372	915	11250	12.24	0.0566	3.76	0.53	6.23	0.0681	4.97	0.80	0.0248	5.03
064_M6	Monazite	Grt core	N		91	159	1860	12.38	0.0579	6.53	0.651	8.80	0.081	5.90	0.67	0.0359	5.61
064_M7	Monazite	Grt rim	N		19	457	5690	13.44	0.0782	11.43	0.0666	12.44	0.00601	4.90	0.39	0.0024	4.88
064_X1	Xenotime	Grt rim	N		8	58	171	3.17	0.074	28.45	0.96	47.82	0.086	38.44	0.80	0.0382	17.02
064_X2	Xenotime	Grt core	N		1	600	237	0.41	0.0553	16.22	0.0416	17.22	0.00565	5.79	0.34	0.0024	13.78
~~064_X3~~	~~Xenotime~~			no signal													

Table A3. Monazite and xenotime geochronology data

Specimen/Mnz	Mineral	Location	Near crack	Comment	207Pb/206Pb (Ma)	2 SE	207Pb/235U (Ma)	2 SE	206Pb/238U (Ma)	2 SE	corr. 206Pb/238U (Ma)	2 SE	208Pb/232Th (Ma)	2 SE
007_M1	Monazite	Grt rim	N		558.0	336.0	330.0	39.0	298.5	20.2	295.6	20.0	563.8	42.6
007_M2	Monazite	Grt rim	N		486.0	312.0	147.2	17.3	127.0	8.1	125.6	8.0	287.0	19.3
~~007_M3~~	~~Monazite~~			no signal										
~~031_M1~~	~~Monazite~~			no signal										
031_M2	Monazite	Grt rim	N		3844.4	98.8	257.8	11.8	35.2	1.4	20.3	0.8	32.2	1.5
031_M3	Monazite	Grt rim	N		1792.7	185.2	34.0	2.9	14.5	0.8	13.3	0.7	14.5	0.8
031_X1	Xenotime	Grt core	N		2163.2	133.8	52.0	4.3	18.0	0.7	16.0	0.6	41.6	2.3
031_X2	Xenotime	Grt core	Y		1815.0	622.0	28.1	9.7	14.6	0.8	13.4	0.8	35.3	9.5
031_X3	Xenotime	Grt core	Y		0.0	2165.2	19.1	16.6	14.1	1.5	14.1	1.5	17.2	5.1
~~031_X4~~	~~Xenotime~~			no signal										
064_M2	Monazite	Grt core	N		573.1	178.2	498.0	26.0	481.8	22.4	480.3	11.4	655.9	29.0
064_M3	Monazite	Grt rim	N		505.3	112.8	458.7	14.5	449.4	14.3	448.9	14.3	458.8	17.2
064_M4	Monazite	Grt rim	N		562.1	166.6	304.0	15.2	271.4	13.2	268.9	13.1	408.2	21.4
064_M5	Monazite	Grt rim	N		469.9	176.4	431.8	22.0	424.7	20.4	424.0	20.4	494.9	24.6
064_M6	Monazite	Grt core	N		541.0	232.0	509.1	35.2	502.1	28.4	501.7	28.4	712.5	39.2
064_M7	Monazite	Grt rim	N		1206.0	264.0	65.5	7.9	38.6	1.9	37.1	1.8	48.3	2.4
064_X1	Xenotime	Grt rim	N		1041.0	574.0	683.0	238.0	531.8	196.2	521.7	192.6	757.3	126.6
064_X2	Xenotime	Grt core	N		423.0	362.0	41.4	7.0	36.3	2.1	35.9	2.1	48.0	6.6
~~064_X3~~	~~Xenotime~~			no signal										

Table A4. Quartz trace element geochemistry

KA007 Grt1

Spot an. #	Si (wt. %)	Ti (wt. %)	O (wt. %)	Total	SD Ti (wt. %)	Ti corrected (ppm)
2_1	46.38	0.0019	52.84	99.23	0.0008	39
2_2	46.49	0.0047	52.97	99.46	0.0008	66
2_3	46.29	0.0021	52.74	99.02	0.0008	40
2_4	46.38	0.0011	52.84	99.22	0.0008	30
2_5	46.31	0.0018	52.77	99.08	0.0008	37
2_6	46.31	0.0036	52.77	99.08	0.0008	55
2_7	46.22	0.0027	52.66	98.88	0.0008	46
2_8	46.19	0.0023	52.63	98.82	0.0008	42
2_9	46.13	0.0034	52.57	98.71	0.0008	52
2_10	46.53	0.0259	53.03	99.59	0.0009	277
2_11	46.17	0.0019	52.60	98.77	0.0008	37
2_12	46.24	0.0013	52.68	98.92	0.0008	31
2_14	46.35	0.0081	52.81	99.16	0.0008	99
2_15	46.23	0.0018	52.68	98.91	0.0008	36
2_18	46.22	0.0016	52.67	98.89	0.0008	33
					Wt. Mean	40 +/- 2 ppm

KA007 Grt2

Spot an. #	Si (wt. %)	Ti (wt. %)	O (wt. %)	Total	SD Ti (wt. %)	Ti corrected (ppm)
2_1	46.17	0.0265	52.62	98.81	0.0009	289
2_2	45.99	0.0004	52.40	98.40	0.0008	28
2_3	46.16	0.0043	52.60	98.76	0.0008	67
2_4	45.92	0.0009	52.32	98.24	0.0008	33
2_5	45.98	0.0007	52.39	98.36	0.0008	31
2_6	46.13	0.0014	52.56	98.68	0.0008	38
2_7	45.49	0.0047	51.83	97.33	0.0008	71
2_8	46.50	0.0025	52.99	99.49	0.0008	49
2_9	45.85	0.0015	52.24	98.09	0.0008	39
2_10	45.91	0.0002	52.31	98.22	0.0008	26
2_11	45.44	0.0012	51.77	97.21	0.0008	35
2_12	46.23	0.0006	52.68	98.91	0.0008	29
2_13	46.08	0.0026	52.50	98.58	0.0008	49
2_14	45.88	0.0008	52.27	98.15	0.0008	31
2_15	45.68	0.0018	52.05	97.74	0.0008	41
2_16	45.98	0.0008	52.39	98.37	0.0008	31
2_17	45.78	-0.0003	52.16	97.94	0.0008	20
2_18	45.61	0.0021	51.97	97.58	0.0008	44
2_19	45.48	0	51.82	97.30	0.0008	23
2_20	46.23	0.0019	52.68	98.91	0.0008	42
2_21	45.45	0	51.79	97.24	0.0008	23
					Wt. Mean	34 +/- 2 ppm

Table A4. Quartz trace element geochemistry

KA014 Grt1

Spot an. #	Si (wt. %)	Ti (wt. %)	O (wt. %)	Total	SD Ti (wt. %)	Ti corrected (ppm)
2_1	46.90	-0.0006	53.44	100.34	0.0008	7
2_2	46.96	0.03	53.53	100.52	0.0009	313
2_3	46.96	-0.0001	53.51	100.47	0.0008	12
2_4	47.17	0.0154	53.75	100.93	0.0008	167
2_5	47.11	-0.0005	53.68	100.79	0.0008	8
2_7	46.90	-0.0013	53.43	100.33	0.0008	1
2_8	46.98	-0.001	53.53	100.50	0.0008	4
2_9	46.38	0.0198	52.86	99.26	0.0008	212
2_10	46.67	0.0008	53.17	99.84	0.0008	22
2_11	46.86	-0.0015	53.39	100.26	0.0008	-1
2_12	46.80	-0.001	53.33	100.13	0.0008	4
2_14	46.98	0.0066	53.53	100.51	0.0008	81
2_15	46.81	0.0025	53.33	100.14	0.0008	40
2_17	46.81	-0.0006	53.33	100.14	0.0008	9
2_18	46.75	-0.0013	53.27	100.02	0.0008	2
2_19	46.68	-0.0001	53.18	99.86	0.0008	14
2_21	46.76	0.011	53.28	100.06	0.0008	126
2_23	46.64	-0.001	53.14	99.78	0.0008	6
4_1	46.64	0.0065	53.14	99.78	0.0008	82
4_2	46.83	-0.0003	53.36	100.19	0.0008	14
4_3	46.55	-0.0018	53.03	99.58	0.0008	-1
4_4	46.44	-0.0009	52.91	99.35	0.0008	8
4_6	46.70	-0.0014	53.21	99.91	0.0008	3
4_7	46.70	-0.0013	53.21	99.90	0.0008	5
4_8	46.59	0.002	53.08	99.67	0.0008	38
4_9	46.55	-0.0001	53.04	99.59	0.0008	17
4_10	46.64	-0.0001	53.14	99.79	0.0008	17
4_11	46.62	0.0306	53.14	99.78	0.0009	324
4_12	46.75	-0.0006	53.27	100.02	0.0008	12
4_13	46.40	-0.0016	52.87	99.27	0.0008	2
4_14	46.65	-0.0005	53.15	99.79	0.0008	14
4_15	46.52	0.0007	53.00	99.52	0.0008	26
4_16	46.58	-0.0015	53.07	99.65	0.0008	4
4_17	46.33	-0.0008	52.79	99.12	0.0008	11
4_18	46.52	-0.0013	53.00	99.51	0.0008	6
4_19	46.44	-0.0008	52.91	99.34	0.0008	11
4_21	46.31	0.0001	52.76	99.07	0.0008	21
4_23	46.42	-0.0004	52.89	99.30	0.0008	16
4_24	46.24	-0.0007	52.68	98.92	0.0008	13
4_25	46.46	-0.0016	52.94	99.39	0.0008	4
4_26	46.40	-0.0008	52.87	99.26	0.0008	12
					Wt. Mean	9 +/- 1 ppm

Table A4. Quartz trace element geochemistry

KA031 Grt1

Spot an. #	Si (wt. %)	Ti (wt. %)	O (wt. %)	Total	SD Ti (wt. %)	Ti corrected (ppm)
2_4	46.61	0.0008	53.10	99.71	0.0008	32
2_5	46.72	0.0011	53.23	99.96	0.0008	34
2_6	46.47	0.0006	52.95	99.41	0.0008	29
2_7	46.64	0.0082	53.15	99.80	0.0008	104
2_8	46.33	-0.001	52.78	99.11	0.0008	12
2_9	46.35	0.0005	52.81	99.15	0.0008	26
2_10	46.54	0.0038	53.03	99.57	0.0008	59
2_12	46.38	0.0009	52.85	99.24	0.0008	29
2_13	46.19	0.0011	52.63	98.82	0.0008	31
2_14	46.38	0.0002	52.85	99.23	0.0008	21
2_16	46.53	0.0002	53.01	99.54	0.0008	20
2_18	46.46	-0.0005	52.93	99.39	0.0008	12
2_19	46.37	-0.0006	52.84	99.21	0.0008	11
2_20	46.54	0.0034	53.03	99.57	0.0008	50
2_21	46.72	0.0004	53.24	99.96	0.0008	20
2_22	46.27	0.0007	52.72	98.98	0.0008	22
					Wt. Mean	23 +/- 2 ppm

KA031 Grt2

Spot an. #	Si (wt. %)	Ti (wt. %)	O (wt. %)	Total	SD Ti (wt. %)	Ti corrected (ppm)
1_4	46.56	0.0021	53.05	99.60	0.0008	40
1_5	46.48	0.0071	52.97	99.46	0.0008	90
1_6	45.83	0.0009	52.22	98.05	0.0008	28
1_7	45.93	-0.0003	52.34	98.27	0.0008	16
1_8	45.85	-0.002	52.24	98.08	0.0008	-1
1_9	46.35	-0.0026	52.81	99.15	0.0008	-7
1_10	45.97	-0.0002	52.38	98.36	0.0008	17
1_11	45.94	-0.0001	52.34	98.28	0.0008	18
1_12	45.86	-0.0013	52.25	98.10	0.0008	7
1_13	45.80	-0.0003	52.19	97.99	0.0008	17
1_14	46.08	-0.0009	52.50	98.58	0.0008	11
1_15	46.13	-0.0015	52.55	98.68	0.0008	5
					Wt. Mean	14 +/- 2 ppm

Table A4. Quartz trace element geochemistry

KA044 Grt1

Spot an. #	Si (wt. %)	Ti (wt. %)	O (wt. %)	Total	SD Ti (wt. %)	Ti corrected (ppm)
4_1	46.49	0.0093	52.97	99.47	0.0008	111
5_1	46.38	0.0097	52.85	99.23	0.0008	115
6_1	46.51	0.0083	53.00	99.53	0.0008	101
7_1	46.51	0.0106	52.99	99.51	0.0008	124
8_1	46.32	0.0088	52.78	99.10	0.0008	106
9_1	46.41	0.0099	52.88	99.30	0.0008	117
10_1	46.42	0.0109	52.90	99.33	0.0008	127
11_1	46.38	0.0087	52.84	99.23	0.0008	105
12_1	46.48	0.007	52.97	99.46	0.0008	88
13_1	46.59	0.0127	53.09	99.68	0.0008	145
15_1	46.45	0.0053	52.93	99.39	0.0008	71
16_1	46.32	0.0076	52.78	99.11	0.0008	94
17_1	46.42	0.0055	52.89	99.32	0.0008	73
18_1	46.18	0.0064	52.62	98.81	0.0008	82
22_1	46.04	0.0087	52.47	98.52	0.0008	105
23_1	46.26	0.0082	52.71	98.98	0.0008	100
25_1	46.31	0.0084	52.77	99.10	0.0008	102
26_1	46.49	0.0082	52.97	99.47	0.0008	100
27_1	46.15	0.0075	52.59	98.75	0.0008	93
28_1	46.12	0.0089	52.55	98.67	0.0008	107
29_1	46.26	0.0058	52.72	98.98	0.0008	76
30_1	46.33	0.0306	52.80	99.16	0.0009	324
31_1	45.90	0.0059	52.30	98.20	0.0008	77
32_1	46.30	0.0061	52.76	99.06	0.0008	79
33_1	46.44	0.0042	52.91	99.35	0.0008	60
34_1	46.19	0.0085	52.63	98.83	0.0008	103
35_1	46.03	0.006	52.45	98.48	0.0008	78
36_1	46.01	0.0089	52.42	98.44	0.0008	108
38_1	46.19	0.0052	52.63	98.82	0.0008	71
39_1	46.00	0.0088	52.42	98.43	0.0008	107
42_1	46.08	0.0086	52.51	98.60	0.0008	105
					Wt. Mean	96 +/- 1 ppm

Table A4. Quartz trace element geochemistry

KA064 Grt2

Spot an. #	Si (wt. %)	Ti (wt. %)	O (wt. %)	Total	SD Ti (wt. %)	Ti corrected (ppm)
4_1	46.35	0.0043	52.81	99.16	0.0008	64
5_1	46.46	0.0042	52.94	99.40	0.0008	63
6_1	46.39	0.0036	52.85	99.24	0.0008	57
7_1	46.68	0.0032	53.19	99.87	0.0008	53
8_1	46.32	0.003	52.77	99.09	0.0008	50
9_1	46.39	0.0031	52.86	99.25	0.0008	51
10_1	46.46	0.0044	52.93	99.40	0.0008	64
11_1	46.38	0.0137	52.85	99.24	0.0008	157
12_1	46.31	0.0039	52.76	99.07	0.0008	59
13_1	46.13	0.0037	52.57	98.70	0.0008	56
14_1	46.42	0.0035	52.89	99.32	0.0008	54
15_1	46.29	0.0042	52.74	99.03	0.0008	61
16_1	46.45	0.0022	52.93	99.38	0.0008	41
17_1	46.44	0.0039	52.92	99.36	0.0008	58
18_1	46.31	0.0043	52.77	99.08	0.0008	61
22_1	46.33	0.0036	52.78	99.11	0.0008	54
23_1	46.23	0.0034	52.67	98.91	0.0008	51
24_1	46.58	0.0063	53.08	99.66	0.0008	80
25_1	46.13	0.0035	52.56	98.70	0.0008	52
26_1	46.42	0.0038	52.90	99.33	0.0008	55
27_1	46.40	0.0034	52.86	99.26	0.0008	50
28_1	46.46	0.0048	52.94	99.41	0.0008	64
29_1	46.31	0.0029	52.76	99.08	0.0008	45
30_1	46.43	0.0031	52.90	99.33	0.0008	47
31_1	46.35	0.0093	52.81	99.17	0.0008	109
32_1	46.48	0.0057	52.96	99.45	0.0008	72
33_1	46.26	0.0035	52.71	98.97	0.0008	50
34_1	46.22	0.0029	52.67	98.89	0.0008	44
35_1	46.38	0.003	52.85	99.24	0.0008	45
					Wt. Mean	55 +/- 2 ppm

Table A5. Temperature estimates for quartz and biotite inclusions

Titanium in biotite (Henry et al. 2005)

Specimen	KA014							KA031						KA064		
Garnet #	in Grt1	in Grt1	in Grt1	in Grt1	in Grt1	in Grt1	in Grt1	in Grt1	in Grt1	in Grt2	in Grt2	in Grt2	in Grt2	in Grt2	in Grt2	in Grt2
Location	mantle	mantle	mantle	mantle	rim	rim	rim	rim	rim	rim	rim	rim	rim	rim	rim	rim
An. #	1 / 1 .	1 / 3 .	1 / 4 .	1 / 5 .	3 / 1 .	3 / 2 .	3 / 4 .	4 / 3 .	4 / 4 .	2 / 2 .	2 / 3 .	2 / 4 .	2 / 5 .	1 / 2 .	1 / 4 .	2 / 1 .
T (C)	540	515	539	534	584	582	580	685	632	700	707	704	708	727	731	686
P (kbar)	6.2				6.3										9.4	

Titanium in quartz (Thomas et al. 2010)

Specimen	KA014			KA007				KA031		KA044	KA064
Garnet #	in Grt1	in Grt1	in Grt1	in Grt1	in Grt1	in Grt2	in Grt2	in Grt 1	in Grt2	in Grt1	in Grt2
Location	core	mantle	rim	core	rim	core	rim	core	core	mantle	rim
Ti wt.mean (ppm)	9	9	9	40	40	34	34	23	14	96	55
Ti SD (ppm)	1	1	1	2	2	2	2	2	2	1	2
TiO2 activity	0.85	0.85	0.85	1	1	1	1	1	1	1	1
P (kbar)	5.7	5.0	4.0	5.1	5.4	5.0	4.3	5.7	4.8	4.7	7.6
T (C)	474	461	443	560	566	545	530	528	476	630	641
T uncertainty (C)	22	22	21	26	24	25	25	24	23	29	28

Titanium in biotite (Henry et al. 2005)	Peak T (C) *		Peak P (kbar) *	
	Min	Max	Min	Max
KA014_mantle_Grt1	516	564	5.7	6.8
KA014_rim_Grt1	560	608	5.7	6.8
KA031_rim_Grt1	661	709	n/a	n/a
KA031_rim_Grt2	684	732	n/a	n/a
KA064_rim_Grt2	707	755	8.8	10.1

Titanium in quartz (Thomas et al. 2010)	Peak T (C) *		Peak P (kbar) *	
	Min	Max	Min	Max
KA014_core_Grt1	452	496	5.1	6.3
KA014_mantle_Grt1	439	483	4.4	5.7
KA014_rim_Grt1	422	464	3.4	4.6
KA007_core_Grt1	534	586	4.3	6.0
KA007_rim_Grt1	542	590	4.5	6.5
KA007_core_Grt2	520	570	4.3	5.8
KA007_rim_Grt2	505	555	3.5	5.1
KA031_core_Grt1	504	552	5.0	6.3
KA031_core_Grt2	453	499	4.2	5.3
KA044_mantle_Grt1	601	659	3.1	6.7
KA064_rim_Grt2	613	669	6.6	8.7

* uncertainty included

Table A6. Raman spectroscopy data for quartz inclusions

Specimen	Location	Grt #	Mean hydr. Pincl (GPa)	1SE	Garnet endmember composition				Entrapment P for mixed garnet composition (kbar)																		
					Alm	Grs	Pyp	Sps	450 C	475 C	500 C	525 C	550 C	575 C	600 C	625 C	650 C	675 C	700 C	725 C	750 C	775 C	800 C	825 C	850 C	875 C	900 C
KA007	core	grt1	-0.073	0.004	0.748	0.038	0.159	0.055	3.3	3.7	4.1	4.5	4.9	5.4	5.8	6.3	6.9	7.4	8.0	8.6	9.2	9.8	10.5	11.2	11.9	12.7	13.5
KA007	rim	grt1	-0.055	0.011	0.762	0.034	0.127	0.077	3.5	3.9	4.3	4.7	5.1	5.6	6.1	6.5	7.1	7.6	8.1	8.7	9.3	10.0	10.6	11.3	12.1	12.8	13.6
KA007	core	grt2	-0.058	0.004	0.748	0.038	0.159	0.055	3.5	3.9	4.3	4.7	5.1	5.6	6.0	6.5	7.0	7.6	8.1	8.7	9.3	10.0	10.6	11.3	12.0	12.8	13.6
KA007	rim	grt2	-0.095	0.008	0.762	0.034	0.127	0.077	3.0	3.4	3.8	4.2	4.6	5.1	5.6	6.1	6.6	7.2	7.7	8.3	9.0	9.6	10.3	11.0	11.8	12.6	13.4
KA014	core	grt1	0.073	0.005	0.69	0.188	0.051	0.07	5.4	5.8	6.1	6.5	6.9	7.3	7.7	8.2	8.6	9.1	9.6	10.2	10.7	11.3	11.9	12.5	13.2	13.8	14.6
KA014	mantle	grt1	0.032	0.011	0.736	0.169	0.079	0.016	4.9	5.2	5.6	6.0	6.4	6.8	7.3	7.7	8.2	8.7	9.2	9.8	10.3	10.9	11.6	12.2	12.9	13.6	14.3
KA014	rim	grt1	-0.023	0.011	0.756	0.144	0.098	0.003	4.1	4.5	4.8	5.3	5.7	6.1	6.6	7.1	7.6	8.1	8.6	9.2	9.8	10.4	11.0	11.7	12.4	13.1	13.9
KA031	core	grt1	0.007	0.0060	0.763	0.037	0.153	0.047	4.4	4.8	5.2	5.6	6.0	6.4	6.9	7.3	7.8	8.3	8.9	9.4	10.0	10.6	11.2	11.9	12.6	13.3	14.0
KA031	core	grt2	0.007	0.004	0.763	0.037	0.153	0.047	4.4	4.8	5.2	5.6	6.0	6.4	6.9	7.3	7.8	8.3	8.9	9.4	10.0	10.6	11.2	11.9	12.6	13.3	14.0
KA044	mantle	grt1	-0.234	0.011	0.668	0.098	0.225	0.009	1.1	1.6	2.0	2.5	3.0	3.5	4.0	4.6	5.2	5.8	6.4	7.1	7.8	8.6	9.3	10.2	11.0	11.8	12.7
KA064	rim	grt2	0.001	0.005	0.761	0.035	0.158	0.047	4.3	4.7	5.1	5.5	5.9	6.3	6.8	7.3	7.7	8.3	8.8	9.4	9.9	10.5	11.2	11.8	12.5	13.3	14.0

Table A7. Lu budget calculation for garnet geochronology

		KA031	KA064
core	A1 (core)	0.93	2.52
	R1 (core)	0.54	0.89
	V1 (core)	0.68	3.00
	AvLu1 (core)	40.6	19.7
	AvLu1*V1	27.5	59.2
rim	A2 (grain)	2.50	4.95
	R2 (grain)	0.89	1.26
	V2 (grain)	2.97	8.28
	V2 (rim)	2.29	5.28
	AvLu2 (rim)	3.8	5.3
	AvLu2*V2	8.8	27.9
	Lu core	76	68
	Lu rim	24	32
	Lu-Hf age (Ma)	293.3	291.3
	Est. rim age (Ma)	15	25
	Est. core age (Ma)	382	417

APPENDIX B

Supporting materials for Chapter 4

Chapter 4 Tectonometamorphic evolution of the Himalayan metamorphic core across the Makalu-Arun region, eastern Nepal

Figure B1. μ-XRF maps of analysed thin sections

Figure B2. Yttrium X-ray maps of analysed monazite grains

Figure B3. Phase equilibria modelling results for MK256

Figure B4. Phase equilibria modelling results for MK258

Figure B5. Phase equilibria modelling results for MK262

Figure B6. Phase equilibria modelling results for MK268

Table B1. Petrochronological data for monazite grains

Table B2. Garnet geochemistry

Table B3. Biotite geochemistry

Table B4. Effective bulk rock composition used for phase equilibria modelling

MK256

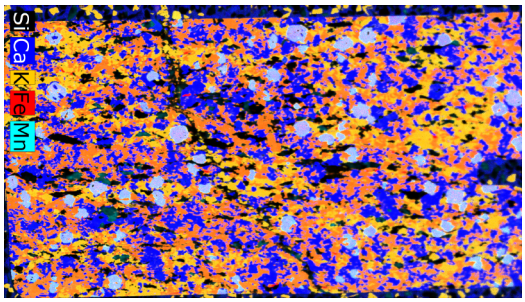

MK257

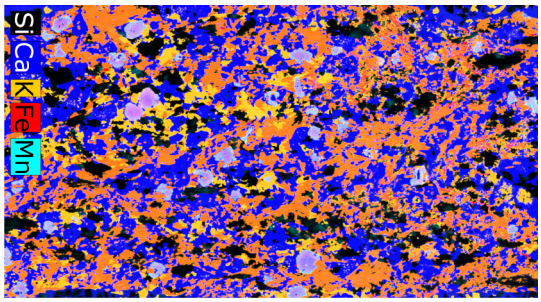

MK258

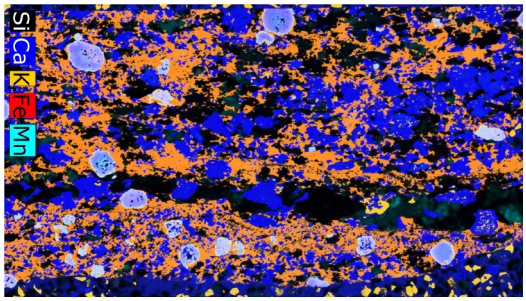

MK260

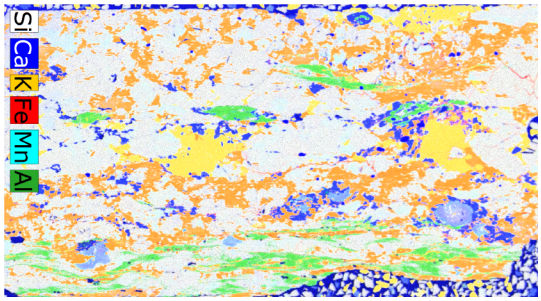

MK262

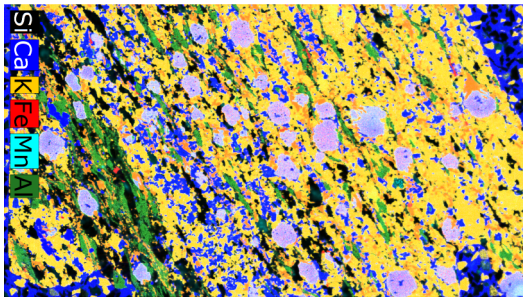

MK263

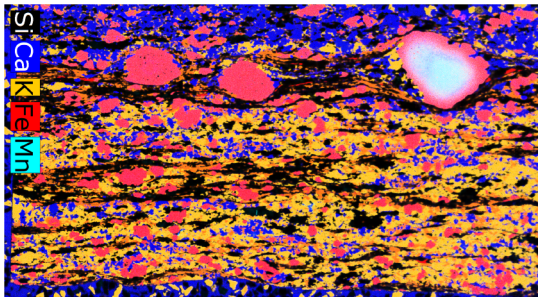

MK266

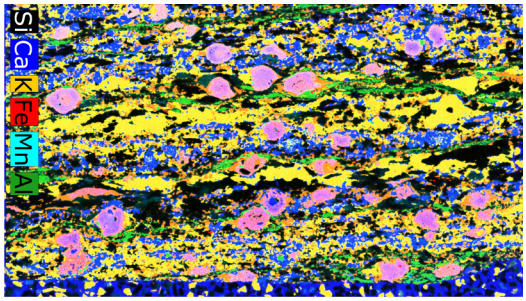

MK268

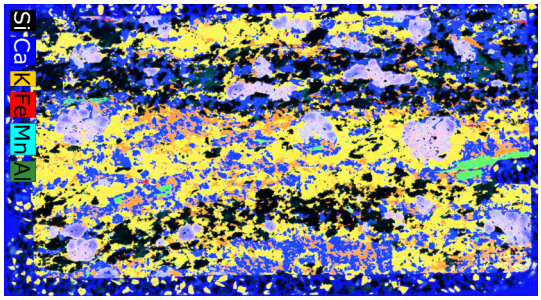

Figure B1. μ-XRF maps of analysed thin sections.

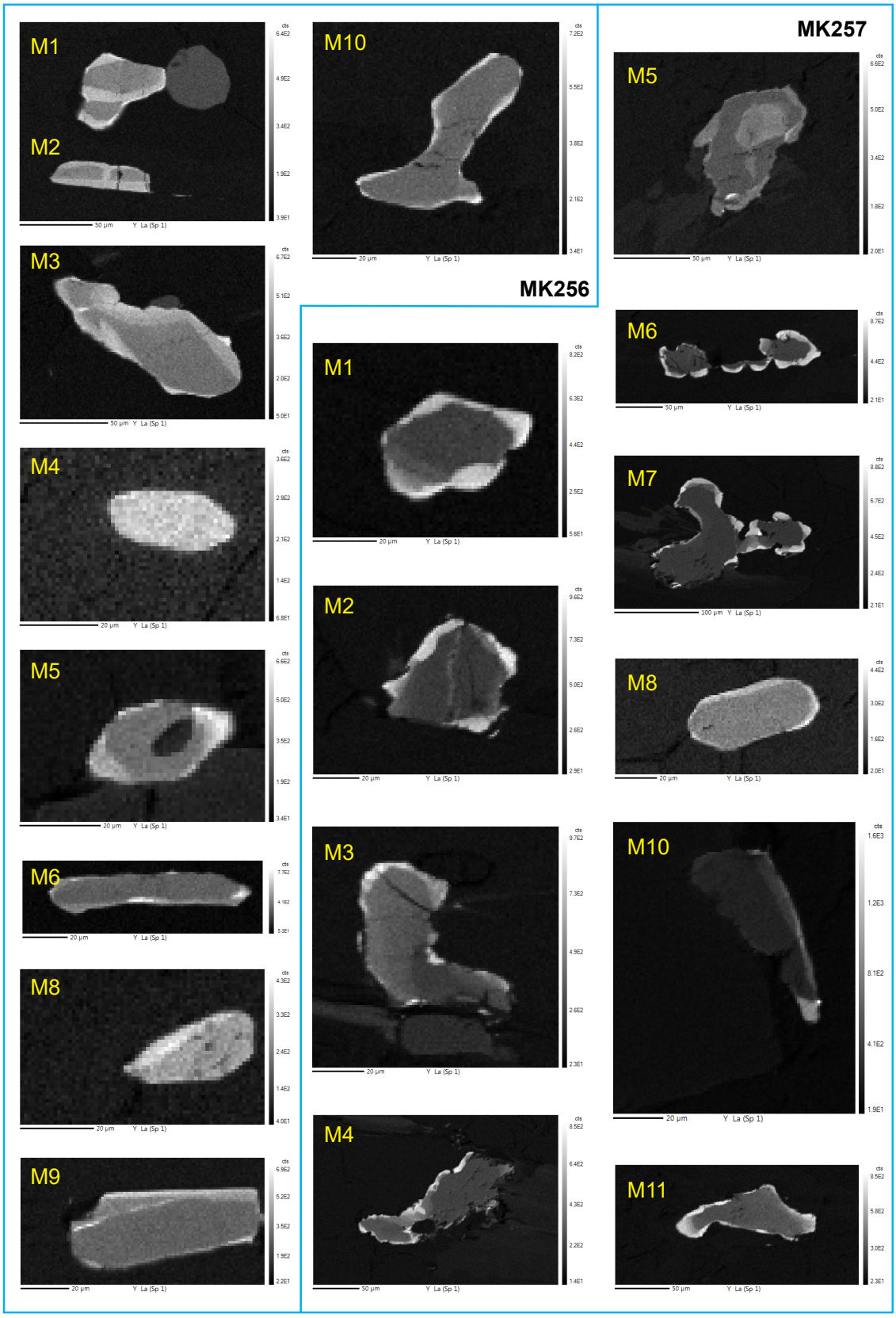

Figure B2. Yttrium X-ray maps of analysed monazite grains.

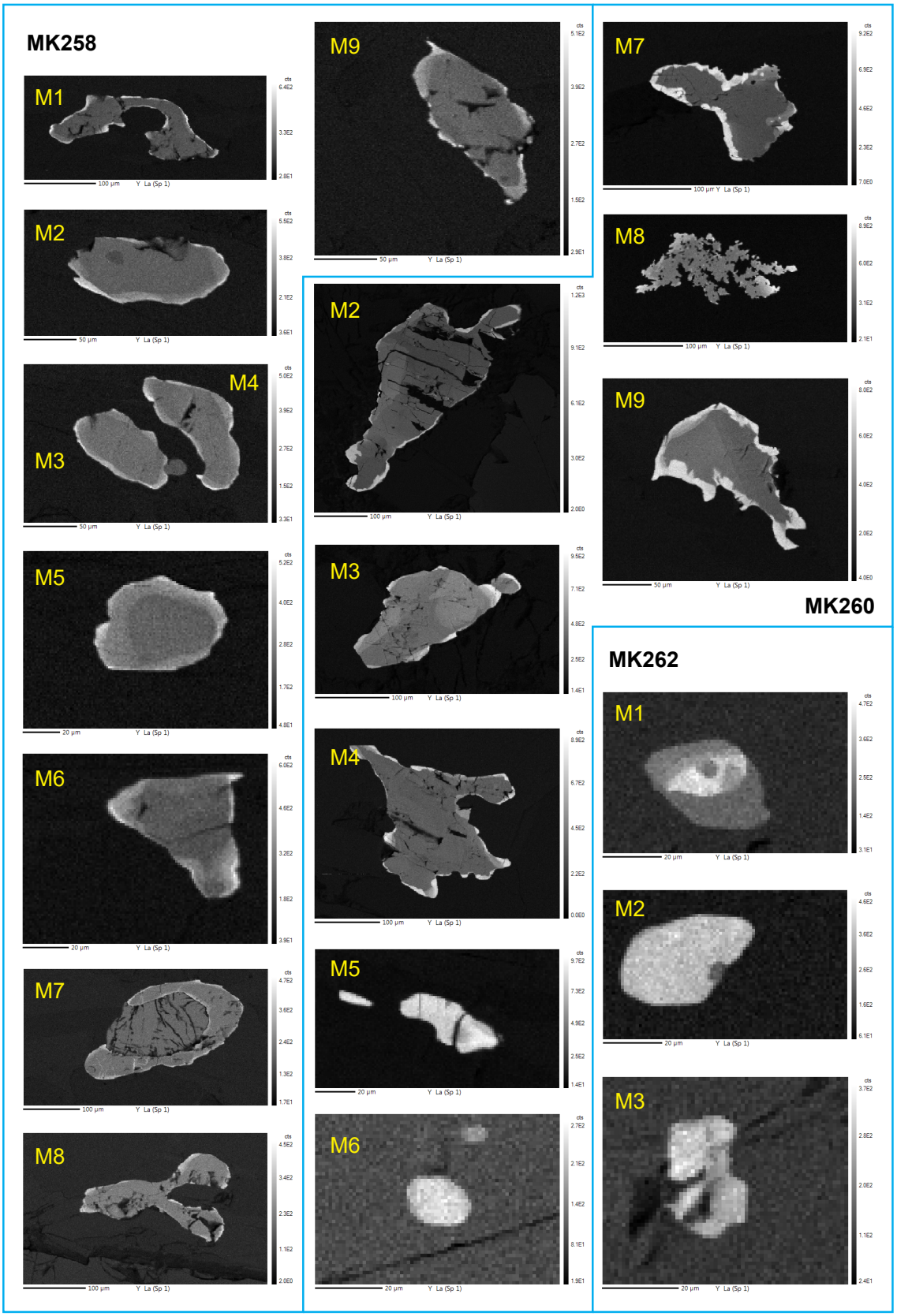

Figure B2. (Continued)

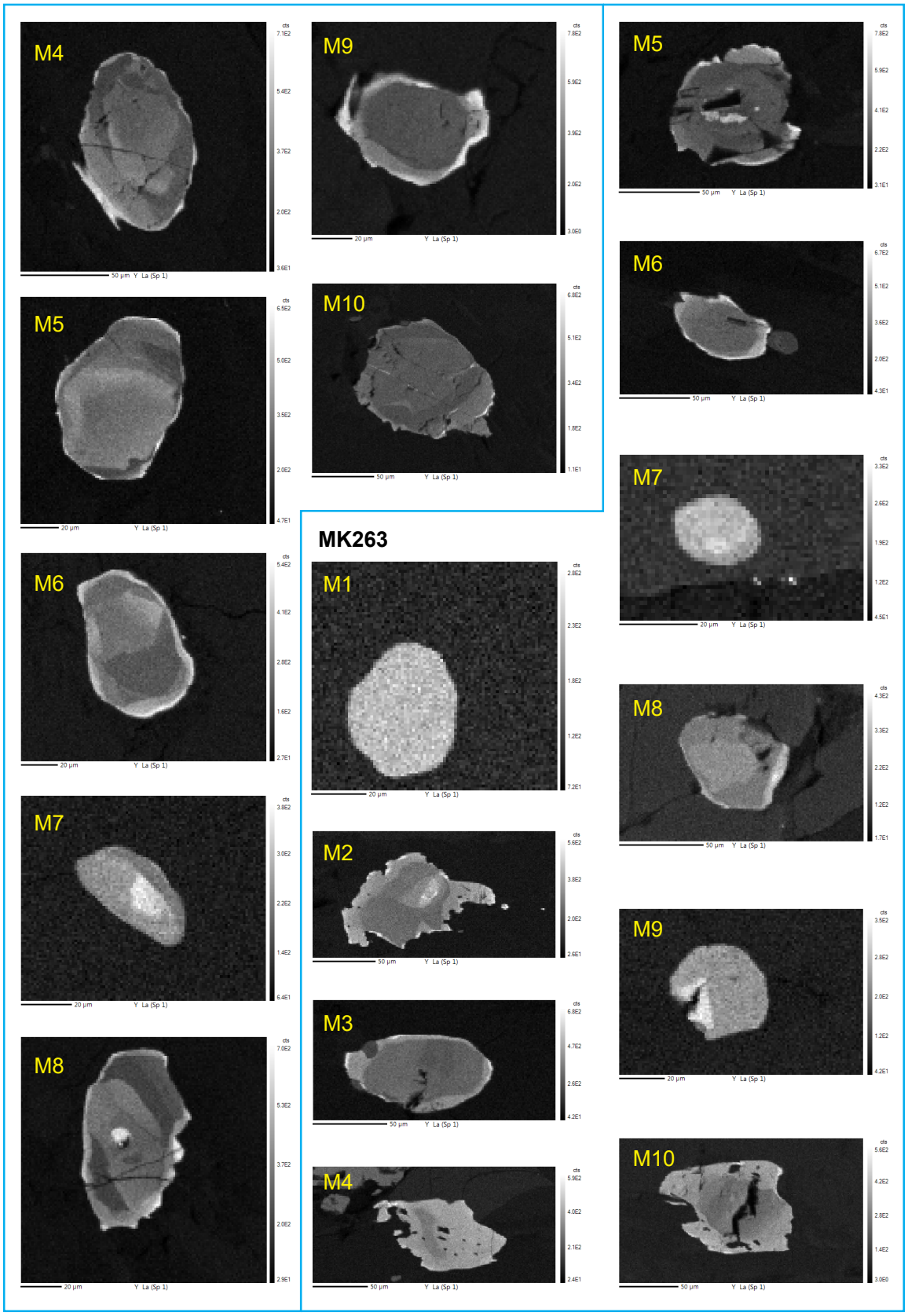

Figure B2. (Continued)

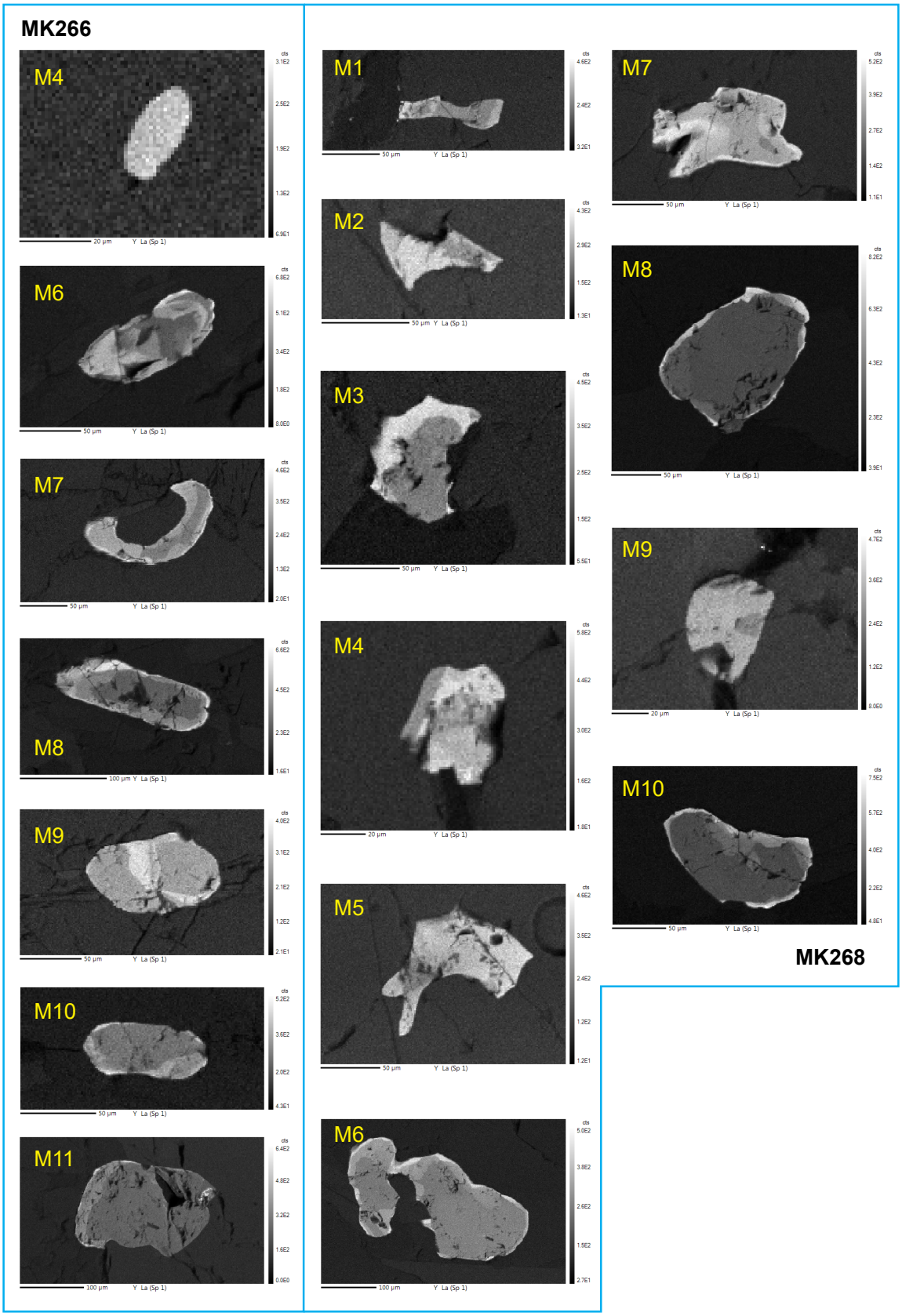

Figure B2. (Continued)

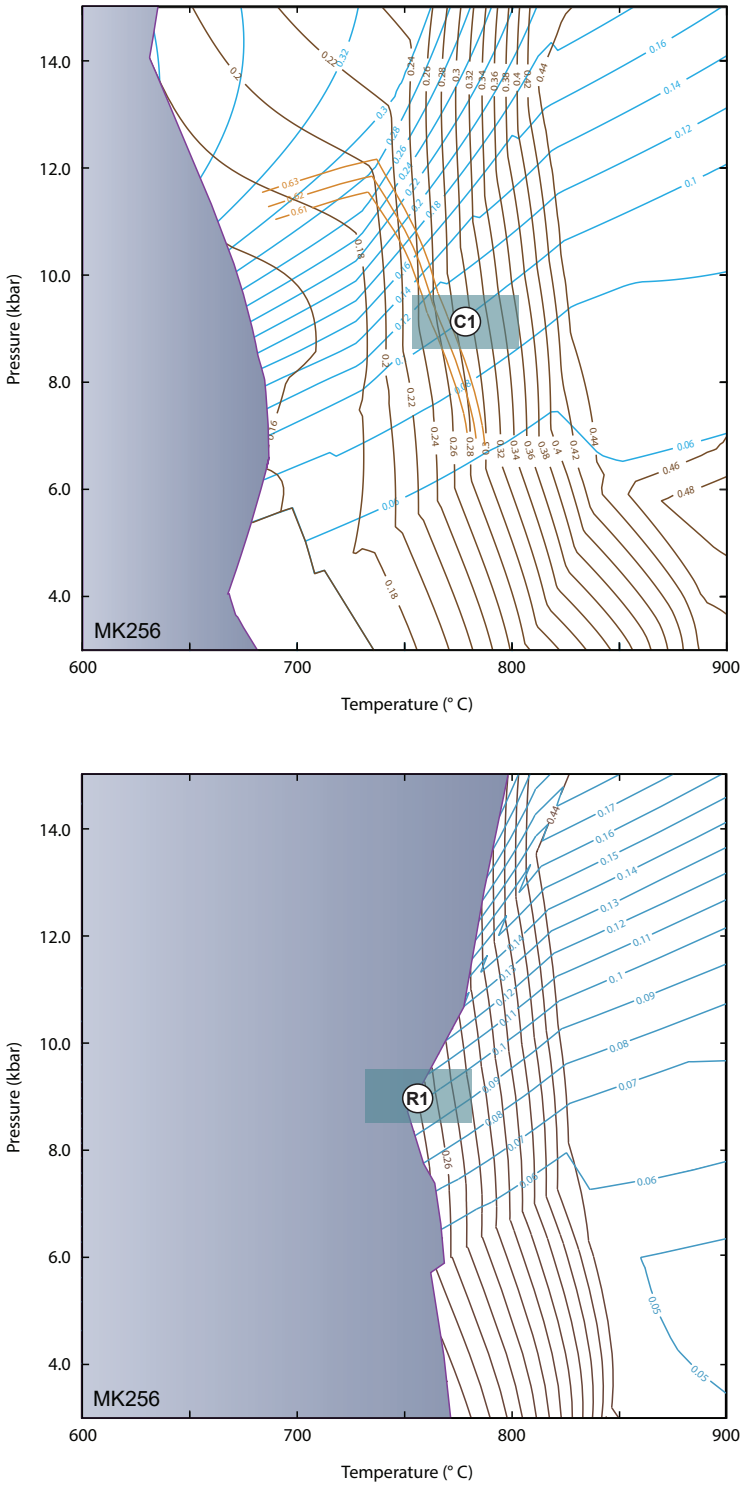

Figure B3. Phase equillibria modelling results for MK256.Calculated isopleth composition for garnet core with saturated solidus (top) and for garnet rim with calculated water (bottom). Garnet Mg# (brown), garnet grossular (blue), biotite Mg# (orange) isopleths. Subsolidus is shaded. C - core, R - rim.

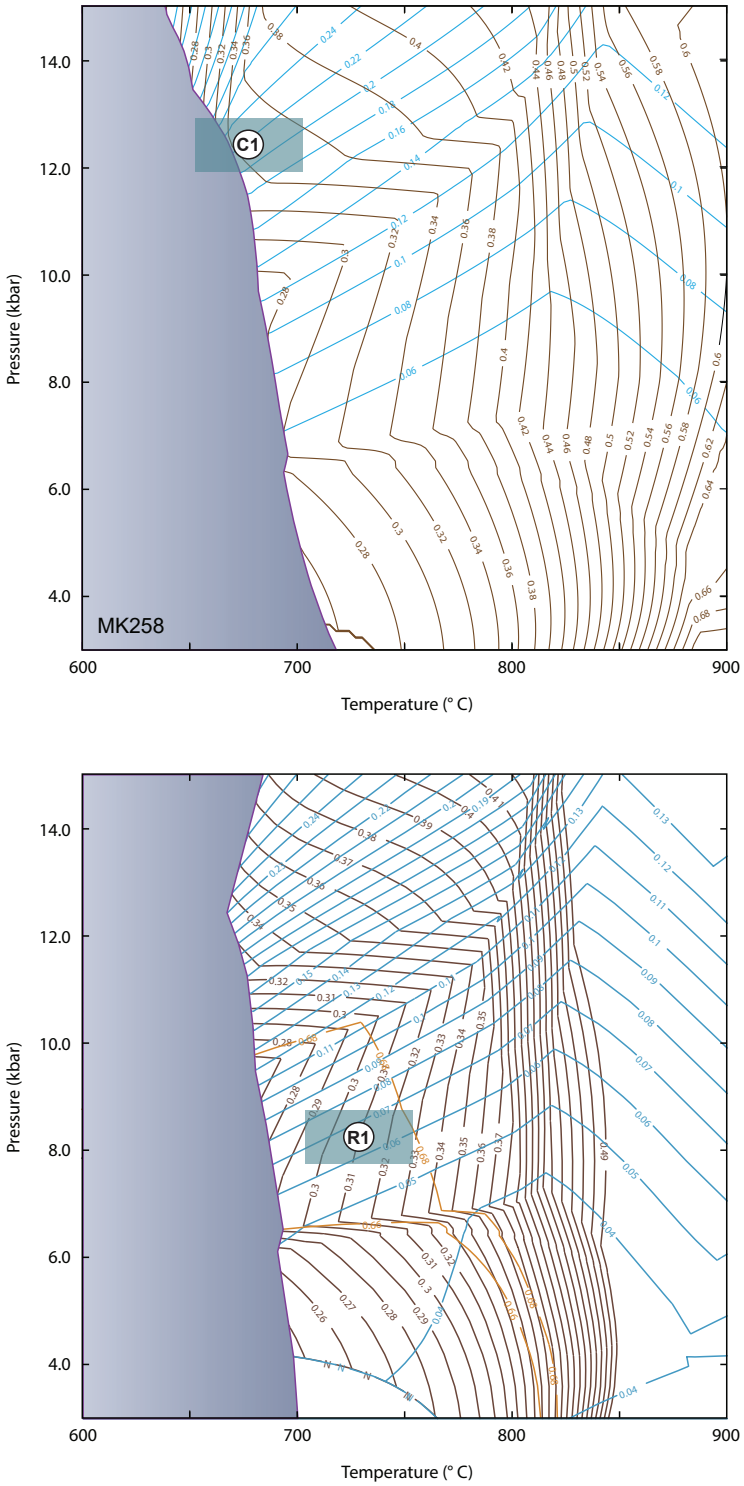

Figure B4. Phase equillibria modelling results for MK258.Calculated isopleth composition for garnet core with saturated solidus (top) and for garnet rim with calculated water (bottom). Garnet Mg# (brown), garnet grossular (blue), biotite Mg# (orange) isopleths. Subsolidus is shaded. C - core, R - rim.

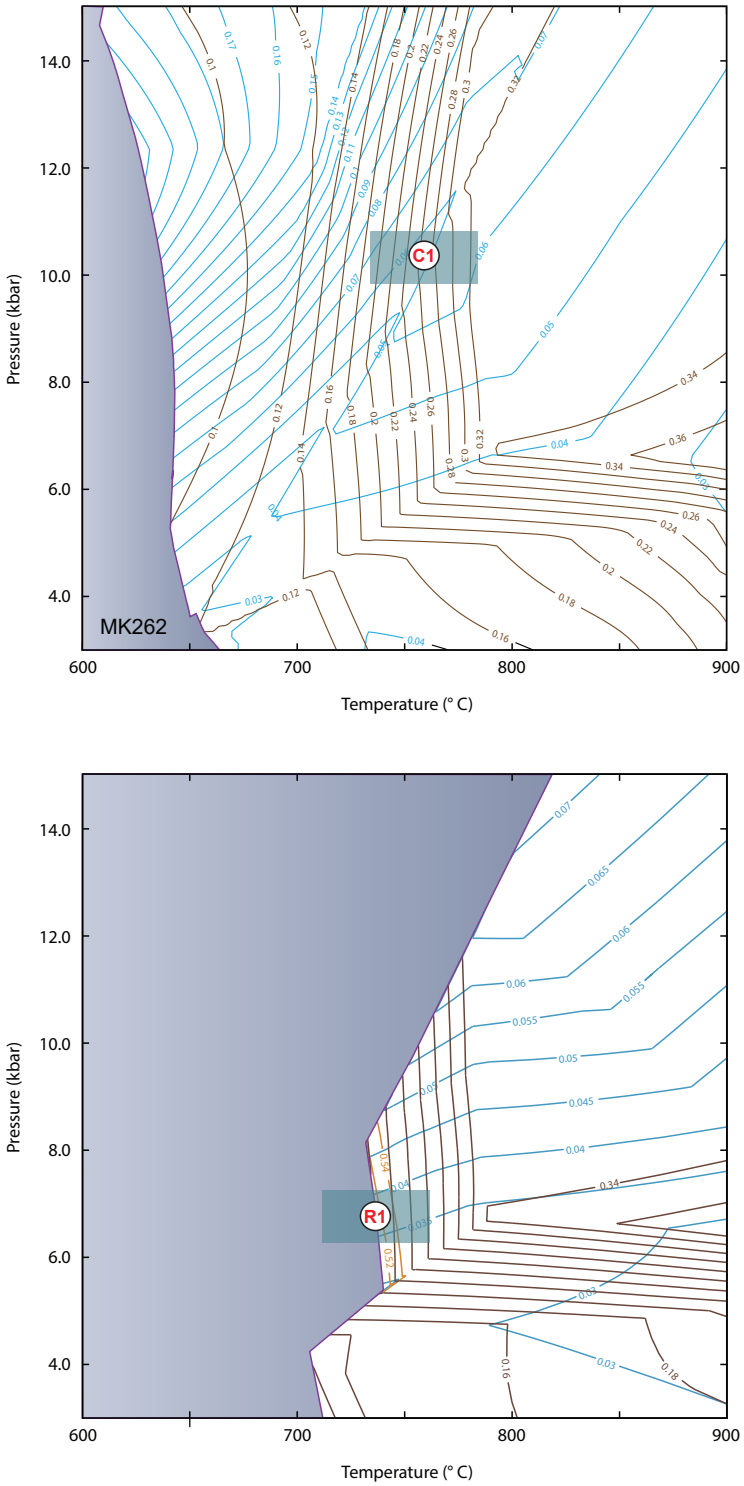

Figure B5. Phase equillibria modelling results for MK262.Calculated isopleth composition for garnet core with saturated solidus (top) and for garnet rim with calculated water (bottom). Garnet Mg# (brown), garnet grossular (blue), biotite Mg# (orange) isopleths. Subsolidus is shaded. C - core, R - rim.

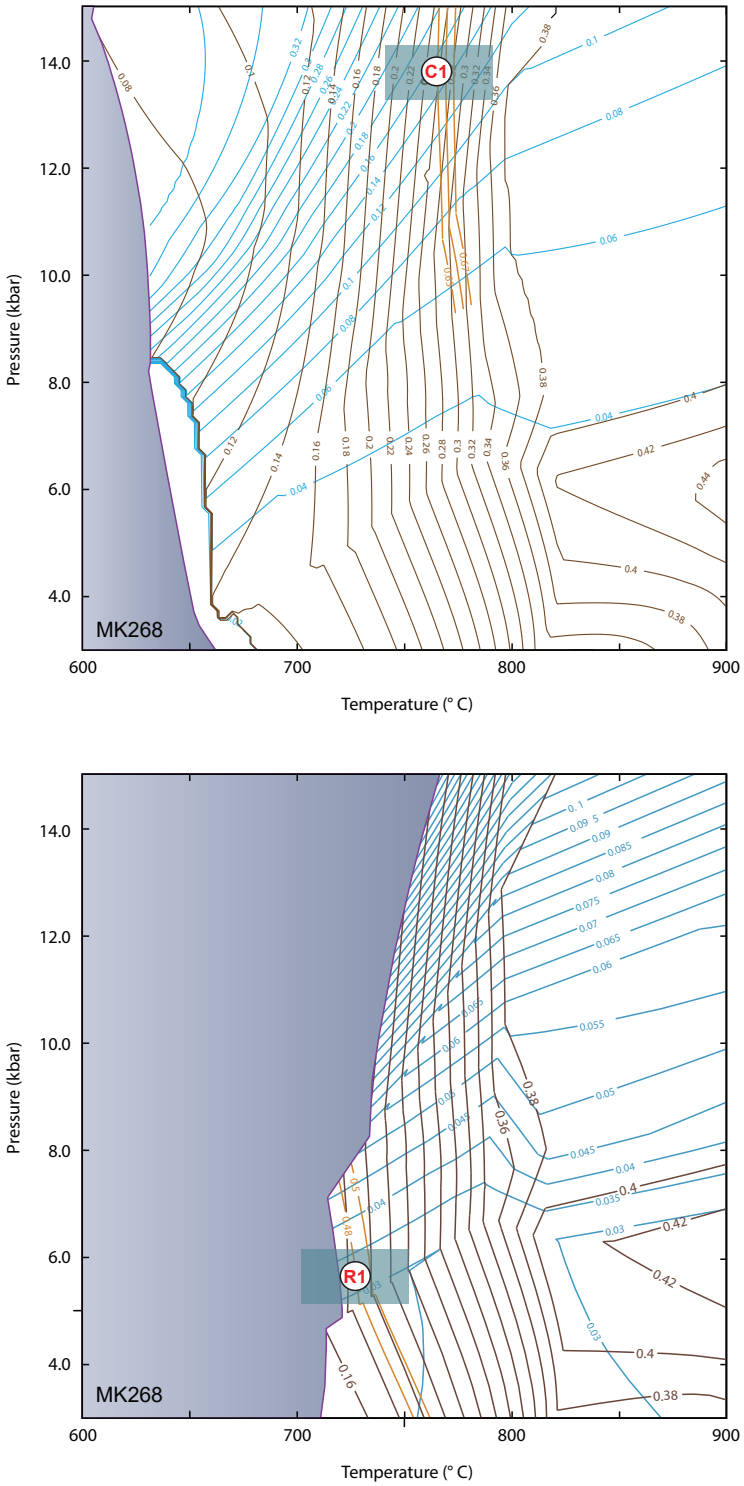

Figure B6. Phase equillibria modelling results for MK268.Calculated isopleth composition for garnet core with saturated solidus (top) and for garnet rim with calculated water (bottom). Garnet Mg# (brown), garnet grossular (blue), biotite Mg# (orange) isopleths. Subsolidus is shaded. C - core, R - rim.

Table B1. Petrochronological data for monazite grains.

Grain #	Location	207Pb/206Pb	2SE %	Pb207/U235	2SE %	206Pb/238U	2SE %	rho	208Pb/232Th	2SE %	207Pb/235U (Ma)	2SE	206Pb/238U (Ma)	2SE	corr.206Pb/238U (Ma)	2SE	208Pb/232Th (Ma)	2SE
MK256																		
MK256_m1_1	matrix	0.1060	9.88	0.0345	10.38	0.00236	3.18	0.307	0.000744	3.06	34.5	3.5	15.0	0.5	14.1	0.5	15.0	0.5
MK256_m1_2	matrix	0.0637	10.99	0.0212	11.46	0.00242	3.24	0.283	0.000786	3.92	21.3	2.4	15.6	0.5	15.0	0.5	15.9	0.6
MK256_m1_3	matrix	0.0842	9.62	0.0266	10.23	0.00229	3.49	0.341	0.000742	3.41	26.6	2.7	14.8	0.5	14.0	0.5	15.0	0.5
MK256_m1_4	matrix	0.0918	8.62	0.0307	9.49	0.00242	3.95	0.416	0.000785	3.84	30.7	2.9	15.6	0.6	14.7	0.6	15.8	0.6
MK256_m1_5	matrix	0.0623	11.49	0.0191	11.92	0.00222	3.19	0.268	0.000709	2.99	19.2	2.3	14.3	0.5	14.0	0.5	14.3	0.4
MK256_m1_6	matrix	0.0673	10.63	0.0219	11.19	0.00236	3.50	0.312	0.000764	3.33	22.0	2.4	15.2	0.5	14.8	0.5	15.4	0.5
MK256_m1_7	matrix	0.0935	10.30	0.0305	10.79	0.00237	3.24	0.300	0.000751	3.11	30.5	3.2	15.3	0.5	14.3	0.5	15.2	0.5
MK256_m1_8	matrix	0.0789	11.10	0.0251	11.59	0.00231	3.33	0.288	0.000741	3.09	25.2	2.9	14.9	0.5	14.3	0.5	15.0	0.5
~~MK256_m1_9~~	~~matrix~~	~~0.4991~~	~~9.82~~	~~0.3691~~	~~18.16~~	~~0.00537~~	~~15.27~~	~~0.841~~	~~0.001630~~	~~15.04~~	~~319.0~~	~~49.7~~	~~34.0~~	~~5.3~~	~~14.8~~	~~5.3~~	~~32.9~~	~~4.9~~
MK256_m2_1	matrix	0.0900	11.91	0.0272	12.44	0.00220	3.62	0.291	0.000735	3.30	27.3	3.4	14.1	0.5	13.4	0.5	14.8	0.5
MK256_m2_2	matrix	0.0766	11.95	0.0241	12.38	0.00228	3.22	0.260	0.000740	2.92	24.1	3.0	14.7	0.5	14.1	0.5	14.9	0.4
MK256_m2_3	matrix	0.2413	11.46	0.0839	12.11	0.00252	3.90	0.322	0.000897	3.81	82.0	9.5	16.2	0.6	12.2	0.6	18.1	0.7
MK256_m2_4	matrix	0.0796	10.82	0.0250	11.26	0.00227	3.12	0.277	0.000739	3.07	25.0	2.8	14.6	0.5	14.0	0.5	14.9	0.5
MK256_m2_5	matrix	0.0868	12.06	0.0280	12.60	0.00234	3.64	0.289	0.000745	3.76	28.0	3.5	15.1	0.5	14.3	0.5	15.1	0.6
MK256_m2_6	matrix	0.5286	7.65	0.3812	12.59	0.00523	10.00	0.794	0.001644	9.45	328.0	35.3	33.6	3.4	13.1	3.4	33.2	3.1
MK256_m3_1	matrix	0.1178	10.20	0.0362	10.71	0.00223	3.26	0.304	0.000690	3.30	36.1	3.8	14.4	0.5	13.1	0.5	13.9	0.5
MK256_m3_2	matrix	0.1023	9.44	0.0333	10.15	0.00236	3.72	0.367	0.000732	3.95	33.3	3.3	15.2	0.6	14.1	0.6	14.8	0.6
MK256_m3_3	matrix	0.1223	13.58	0.0404	14.13	0.00240	3.88	0.275	0.000726	3.78	40.2	5.6	15.4	0.6	14.0	0.6	14.7	0.6
MK256_m3_4	matrix	0.0870	10.39	0.0296	10.87	0.00246	3.20	0.295	0.000772	3.11	29.6	3.2	16.0	0.5	15.1	0.5	15.6	0.5
MK256_m3_5	matrix	0.0882	12.43	0.0290	12.73	0.00239	2.79	0.219	0.000755	3.19	29.0	3.6	15.0	0.4	14.6	0.4	15.2	0.5
MK256_m3_6	matrix	0.0912	9.82	0.0306	10.32	0.00243	3.18	0.308	0.000759	3.16	30.6	3.1	16.0	0.5	14.8	0.5	15.3	0.5
MK256_m3_7	matrix	0.0830	10.56	0.0284	11.00	0.00249	3.07	0.279	0.000788	3.06	28.5	3.1	16.0	0.5	15.3	0.5	15.9	0.5
MK256_m3_8	matrix	0.0899	7.52	0.0312	8.27	0.00252	3.45	0.417	0.000783	3.36	31.2	2.5	16.0	0.6	15.0	0.6	15.8	0.5
MK256_m3_9	matrix	0.0929	8.89	0.0307	9.37	0.00240	2.95	0.315	0.000761	3.51	30.7	2.8	15.0	0.5	15.0	0.5	15.4	0.5
MK256_m3_10	matrix	0.0963	9.02	0.0317	9.63	0.00239	3.37	0.350	0.000760	3.47	31.7	3.0	15.0	0.5	14.0	0.5	15.3	0.5
MK256_m4_1	garnet	0.1787	12.94	0.0618	13.43	0.00251	3.60	0.268	0.000835	3.37	60.9	7.9	16.0	0.6	13.0	0.6	16.9	0.6
MK256_m4_2	garnet	0.1273	10.32	0.0447	10.82	0.00255	3.25	0.301	0.000808	2.82	44.4	4.7	16.0	0.5	15.0	0.5	16.3	0.5
MK256_m4_3	garnet	0.1034	11.61	0.0361	12.03	0.00253	3.15	0.262	0.000769	3.38	36.0	4.3	16.0	0.5	15.0	0.5	15.5	0.5
MK256_m4_4	garnet	0.0850	7.60	0.0299	8.14	0.00255	2.92	0.359	0.000771	3.40	29.9	2.4	16.0	0.5	16.0	0.5	15.6	0.5
MK256_m4_5	garnet	0.0860	9.87	0.0305	10.46	0.00258	3.45	0.330	0.000794	3.27	30.5	3.1	17.0	0.6	16.0	0.6	16.0	0.5
MK256_m4_6	garnet	0.0872	7.70	0.0314	8.48	0.00261	3.55	0.418	0.000801	3.47	31.4	2.6	17.0	0.6	16.0	0.6	16.2	0.6
MK256_m5_1	matrix	0.0931	10.83	0.0329	11.23	0.00256	2.96	0.264	0.000812	3.13	32.9	3.6	17.0	0.5	16.0	0.5	16.4	0.5
MK256_m5_2	matrix	0.1096	10.40	0.0402	10.88	0.00266	3.19	0.294	0.000796	3.14	40.0	4.3	17.0	0.5	16.0	0.5	16.1	0.5
MK256_m5_3	matrix	0.4583	9.97	0.3239	14.31	0.00513	10.26	0.717	0.001187	7.30	285.0	35.5	33.0	3.4	16.0	3.4	24.0	1.7
MK256_m6_1	matrix	0.1163	10.10	0.0398	10.56	0.00249	3.10	0.293	0.000754	3.09	39.7	4.1	16.0	0.5	15.0	0.5	15.2	0.5
MK256_m6_2	matrix	0.1147	12.24	0.0397	12.63	0.00251	3.14	0.249	0.000753	3.10	39.6	4.9	16.0	0.5	15.0	0.5	15.2	0.5
MK256_m6_3	matrix	0.1223	10.39	0.0416	10.87	0.00247	3.20	0.294	0.000772	3.20	41.4	4.4	16.0	0.5	14.0	0.5	15.6	0.5
MK256_m6_4	matrix	0.1374	8.29	0.0495	9.03	0.00261	3.57	0.395	0.000776	3.36	49.0	4.3	17.0	0.6	15.0	0.6	15.7	0.5
MK256_m6_5	matrix	0.1171	9.83	0.0402	10.32	0.00249	3.14	0.305	0.000747	3.17	40.0	4.1	16.0	0.5	15.0	0.5	15.1	0.5
MK256_m6_6	matrix	0.1050	10.28	0.0355	10.85	0.00246	3.45	0.318	0.000765	3.45	35.5	3.8	16.0	0.5	15.0	0.5	15.4	0.5
MK256_m6_7	matrix	0.1961	8.70	0.0763	9.37	0.00282	3.50	0.373	0.000789	2.98	74.7	6.7	18.0	0.6	15.0	0.6	15.9	0.5
MK256_m8_1	matrix	0.0735	11.97	0.0236	12.35	0.00233	3.04	0.246	0.000734	3.34	23.7	2.9	15.0	0.5	14.5	0.5	14.8	0.5
MK256_m8_2	matrix	0.0902	12.11	0.0314	12.61	0.00252	3.51	0.278	0.000788	3.36	31.4	3.9	16.2	0.6	15.0	0.6	15.9	0.5
MK256_m9_1	matrix	0.1482	9.86	0.0444	10.48	0.00218	3.55	0.339	0.000714	3.48	44.1	4.5	14.0	0.5	12.0	0.5	14.4	0.5
MK256_m9_2	matrix	0.1198	11.17	0.0358	11.75	0.00217	3.67	0.312	0.000704	3.36	35.8	4.1	14.0	0.5	13.0	0.5	14.2	0.5
MK256_m9_3	matrix	0.1321	13.28	0.0399	13.71	0.00219	3.42	0.249	0.000728	3.82	39.7	5.3	14.0	0.5	13.0	0.5	14.7	0.6
MK256_m9_4	matrix	0.0838	9.63	0.0270	10.14	0.00233	3.18	0.313	0.000751	3.15	27.0	2.7	15.0	0.5	14.0	0.5	15.2	0.5
MK256_m9_5	matrix	0.0774	12.08	0.0253	12.49	0.00237	3.20	0.256	0.000766	2.94	25.4	3.1	15.0	0.5	15.0	0.5	15.5	0.5
MK256_m9_6	matrix	0.0693	9.20	0.0238	9.81	0.00249	3.41	0.347	0.000802	3.35	23.8	2.3	16.0	0.5	16.0	0.5	16.2	0.5
MK256_m9_7	matrix	0.0686	9.96	0.0236	10.47	0.00250	3.22	0.307	0.000808	3.22	23.7	2.5	16.0	0.5	16.0	0.5	16.3	0.5
MK256_m9_8	matrix	0.0715	9.01	0.0247	9.60	0.00251	3.32	0.346	0.000812	3.25	24.8	2.4	16.0	0.5	16.0	0.5	16.4	0.5
MK256_m9_9	matrix	0.0735	8.81	0.0254	9.61	0.00251	3.82	0.398	0.000812	3.98	25.5	2.4	16.0	0.6	16.0	0.6	16.4	0.7
MK256_m9_10	matrix	0.0654	10.06	0.0212	10.62	0.00235	3.40	0.320	0.000768	3.23	21.3	2.2	15.0	0.5	15.0	0.5	15.5	0.5
MK256_m10_1	matrix	0.1953	10.73	0.0720	11.60	0.00268	4.41	0.380	0.000855	3.76	70.6	7.9	17.0	0.8	14.0	0.8	17.3	0.6
MK256_m10_2	matrix	0.0657	8.88	0.0219	9.60	0.00242	3.65	0.380	0.000787	4.14	22.0	2.1	16.0	0.6	15.0	0.6	15.9	0.7
MK256_m10_3	matrix	0.0703	11.01	0.0236	11.71	0.00244	3.98	0.340	0.000794	3.80	23.7	2.7	15.7	0.6	15.0	0.6	16.0	0.6

Table B1. Petrochronological data for monazite grains.

Grain #	Location	207Pb/206Pb	2SE %	Pb207/U235	2SE %	206Pb/238U	2SE %	rho	208Pb/232Th	2SE %	207Pb/235U (Ma)	2SE	206Pb/238U (Ma)	2SE	corr.206Pb/238U (Ma)	2SE	208Pb/232Th (Ma)	2SE
MK256_m10_4	matrix	0.0723	9.45	0.0247	10.16	0.00248	3.74	0.368	0.000804	3.78	24.8	2.5	16.0	0.6	15.0	0.6	16.2	0.6
MK256_m10_5	matrix	0.2471	10.63	0.0965	12.64	0.00283	6.84	0.541	0.000914	6.07	94.0	11.3	18.2	1.2	14.0	1.2	18.5	1.1
MK256_m10_6	matrix	0.0682	8.77	0.0228	9.40	0.00243	3.37	0.359	0.000789	3.44	22.9	2.1	15.6	0.5	15.0	0.5	15.9	0.5
MK256_m10_7	matrix	0.0657	11.02	0.0223	11.67	0.00246	3.83	0.328	0.000794	3.69	22.4	2.6	15.8	0.6	15.5	0.6	16.0	0.6
MK256_m11_1	garnet	0.0749	12.14	0.0243	12.82	0.00235	4.10	0.320	0.000751	3.26	24.3	3.1	15.0	0.6	14.6	0.6	15.2	0.5
MK256_m11_2	garnet	0.0678	9.33	0.0230	9.98	0.00246	3.54	0.355	0.000777	3.29	23.1	2.3	15.8	0.6	15.4	0.6	15.7	0.5
MK256_m11_3	garnet	0.0681	14.10	0.0237	15.00	0.00252	5.10	0.340	0.000865	5.21	23.8	3.5	16.2	0.8	15.8	0.8	17.5	0.9
MK257																		
MK257_m1_1	matrix	0.1305	7.67	0.0506	8.17	0.00281	2.81	0.344	0.000834	2.86	50.1	4.0	18.1	0.5	16.2	0.5	16.8	0.5
MK257_m1_2	matrix	0.5505	8.65	0.5146	12.77	0.00678	9.39	0.735	0.001846	7.54	422.0	44.1	43.6	4.1	15.8	4.1	37.3	2.8
MK257_m1_3	matrix	0.2586	9.38	0.1149	10.08	0.00322	3.69	0.366	0.000887	3.50	110.0	10.5	20.7	0.8	15.2	0.8	17.9	0.6
MK257_m1_4	matrix	0.0743	11.85	0.0309	12.25	0.00302	3.09	0.252	0.000955	2.67	30.9	3.7	19.0	0.6	19.0	0.6	19.3	0.5
MK257_m1_5	matrix	0.1689	7.98	0.0822	8.51	0.00353	2.94	0.346	0.001022	3.04	80.3	6.6	22.7	0.7	19.2	0.7	20.6	0.6
MK257_m2_1	matrix	0.2101	7.96	0.1070	8.62	0.00370	3.31	0.384	0.000998	3.13	103.3	8.5	23.8	0.8	18.9	0.8	20.1	0.6
MK257_m2_2	matrix	0.0797	9.17	0.0302	9.63	0.00275	2.94	0.305	0.000882	3.00	30.2	2.9	18.0	0.5	16.9	0.5	17.8	0.5
MK257_m2_3	matrix	0.0869	11.94	0.0351	12.40	0.00293	3.36	0.271	0.000920	3.22	35.0	4.3	18.9	0.6	17.9	0.6	18.6	0.6
MK257_m2_4	matrix	0.4442	7.78	0.3843	12.03	0.00628	9.18	0.763	0.001318	5.18	330.0	33.9	40.0	3.7	20.1	3.7	26.6	1.4
MK257_m2_5	matrix	0.5073	6.43	0.4344	9.04	0.00621	6.35	0.703	0.001612	5.93	366.0	27.8	39.9	2.5	16.7	2.5	32.6	1.9
~~MK257_m2_6~~	~~matrix~~	~~0.7841~~	~~5.45~~	~~4.8744~~	~~14.36~~	~~0.04510~~	~~13.28~~	~~0.925~~	~~0.004637~~	~~10.41~~	~~1800.0~~	~~121.0~~	~~284.4~~	~~37.0~~	~~19.4~~	~~37.0~~	~~93.5~~	~~9.7~~
MK257_m2_7	matrix	0.0690	12.41	0.0299	12.82	0.00315	3.19	0.249	0.000986	3.13	29.9	3.8	20.2	0.6	19.7	0.6	19.9	0.6
MK257_m2_8	matrix	0.1875	21.46	0.0960	22.86	0.00372	7.87	0.344	0.000960	3.77	93.0	20.3	23.9	1.9	19.7	1.9	19.4	0.7
MK257_m3_1	matrix	0.4511	7.65	0.3078	10.60	0.00495	7.34	0.692	0.001070	5.07	272.0	25.3	31.8	2.3	15.5	2.3	21.6	1.1
MK257_m3_2	matrix	0.0759	11.96	0.0263	12.28	0.00252	2.77	0.226	0.000779	3.01	26.4	3.2	16.0	0.4	15.6	0.4	15.7	0.5
~~MK257_m3_3~~	~~matrix~~	~~0.7438~~	~~5.61~~	~~2.1948~~	~~13.92~~	~~0.02141~~	~~12.73~~	~~0.915~~	~~0.003415~~	~~11.41~~	~~1180.0~~	~~97.1~~	~~137.0~~	~~17.2~~	~~16.0~~	~~17.2~~	~~68.9~~	~~7.8~~
MK257_m3_4	matrix	0.1458	7.80	0.0578	8.48	0.00288	3.33	0.393	0.000848	3.48	57.0	4.7	19.0	0.6	16.0	0.6	17.1	0.6
MK257_m3_5	matrix	0.0721	10.02	0.0248	10.46	0.00249	3.01	0.288	0.000765	2.92	24.8	2.6	16.0	0.5	15.5	0.5	15.4	0.5
MK257_m3_6	matrix	0.0681	10.98	0.0240	11.54	0.00256	3.54	0.307	0.000786	3.23	24.1	2.7	16.5	0.6	16.0	0.6	15.9	0.5
MK257_m3_7	matrix	0.4194	6.60	0.2527	7.82	0.00437	4.20	0.536	0.001042	3.40	229.0	16.0	28.1	1.2	14.9	1.2	21.0	0.7
MK257_m3_8	matrix	0.1594	9.84	0.0731	10.29	0.00333	3.04	0.295	0.000966	3.20	71.6	7.1	21.4	0.6	18.4	0.6	19.5	0.6
MK257_m3_9	matrix	0.1069	8.74	0.0451	9.24	0.00306	3.01	0.326	0.000922	3.03	44.8	4.1	19.7	0.6	18.2	0.6	18.6	0.6
~~MK257_m3_10~~	~~matrix~~	~~0.6680~~	~~7.45~~	~~1.1325~~	~~19.01~~	~~0.01230~~	~~17.49~~	~~0.920~~	~~0.002178~~	~~13.08~~	~~770.0~~	~~102.5~~	~~78.8~~	~~13.7~~	~~16.9~~	~~13.7~~	~~44.0~~	~~5.7~~
MK257_m3_11	matrix	0.0696	14.67	0.0265	15.01	0.00276	3.17	0.211	0.000870	3.25	26.6	3.9	17.8	0.6	17.3	0.6	17.6	0.6
MK257_m4_1	matrix	0.3670	28.33	0.2510	36.51	0.00496	23.04	0.631	0.001118	16.75	227.0	74.4	32.0	7.3	19.0	7.3	22.6	3.8
MK257_m4_2	matrix	0.1597	34.74	0.0554	35.51	0.00251	7.37	0.208	0.000683	3.56	55.0	18.9	16.2	1.2	13.9	1.2	13.8	0.5
MK257_m4_3	matrix	0.1373	10.78	0.0524	11.28	0.00277	3.31	0.294	0.000791	2.99	51.8	5.7	17.8	0.6	15.8	0.6	16.0	0.5
MK257_m4_4	matrix	0.0637	10.45	0.0233	10.91	0.00266	3.13	0.287	0.000836	2.86	23.4	2.5	17.1	0.5	16.7	0.5	16.9	0.5
MK257_m4_5	matrix	0.4594	11.04	0.3067	15.06	0.00484	10.25	0.680	0.001112	8.03	272.0	35.9	31.1	3.2	14.9	3.2	22.5	1.8
MK257_m4_6	matrix	0.6176	7.01	0.8754	13.57	0.01029	11.62	0.856	0.001806	8.66	640.0	64.3	66.0	7.6	18.4	7.6	36.5	3.2
MK257_m4_7	matrix	0.3076	6.98	0.1469	7.89	0.00346	3.68	0.467	0.000901	3.58	139.0	10.3	22.3	0.8	14.9	0.8	18.2	0.7
MK257_m4_8	matrix	0.0759	11.25	0.0314	11.65	0.00301	3.02	0.259	0.000943	2.91	31.4	3.6	19.4	0.6	18.6	0.6	19.0	0.6
MK257_m4_9	matrix	0.0886	13.02	0.0379	13.39	0.00310	3.11	0.233	0.000978	2.93	37.8	5.0	20.0	0.6	18.9	0.6	19.8	0.6
MK257_m4_10	matrix	0.3002	9.03	0.1874	10.56	0.00453	5.47	0.518	0.001258	4.27	174.0	16.9	29.1	1.6	19.8	1.6	25.4	1.1
MK257_m5_1	matrix	0.4984	15.25	0.5309	30.15	0.00773	26.01	0.863	0.000379	3.65	430.0	106.2	50.0	12.9	21.3	12.9	7.7	0.3
MK257_m5_2	matrix	0.4854	21.85	0.8703	29.23	0.01301	19.41	0.664	0.000330	3.27	640.0	138.1	83.0	16.1	37.3	16.1	6.7	0.2
MK257_m5_3	matrix	0.0614	10.23	0.0260	10.64	0.00308	2.91	0.273	0.000972	3.01	26.1	2.7	20.0	0.6	19.0	0.6	19.6	0.6
MK257_m5_4	matrix	0.4715	18.07	0.6671	31.27	0.01027	25.53	0.816	0.001629	16.93	520.0	127.1	66.0	16.7	31.0	16.7	32.9	5.6
MK257_m5_5	matrix	0.0675	11.09	0.0284	11.73	0.00305	3.85	0.328	0.000829	3.34	28.4	3.3	20.0	0.8	19.0	0.8	16.7	0.6
MK257_m5_6	matrix	0.6658	62.34	0.1682	64.60	0.00183	16.94	0.262	0.000291	2.88	160.0	94.4	12.0	2.0	3.0	2.0	5.9	0.2
MK257_m5_7	matrix	0.5316	78.53	0.1666	80.16	0.00227	16.09	0.201	0.000282	3.39	160.0	116.2	15.0	2.4	6.0	2.4	5.7	0.2
MK257_m5_8	matrix	0.1517	16.11	0.0646	16.91	0.00309	5.13	0.304	0.000764	3.97	64.0	10.4	20.0	1.0	17.0	1.0	15.4	0.6
MK257_m5_9	matrix	0.2363	9.25	0.1259	10.00	0.00387	3.81	0.381	0.000779	3.30	120.0	11.4	25.0	0.9	19.0	0.9	15.7	0.5
MK257_m5_10	matrix	0.0996	14.70	0.0439	15.14	0.00320	3.63	0.240	0.000946	3.45	43.6	6.5	21.0	0.7	19.0	0.7	19.1	0.7
MK257_m6_1	matrix	0.5070	6.74	0.4003	8.99	0.00573	5.96	0.662	0.001233	4.18	342.0	26.1	37.0	2.2	15.0	2.2	24.9	1.0
MK257_m6_2	matrix	0.2582	8.65	0.1435	9.61	0.00403	4.17	0.434	0.001067	3.35	136.0	12.2	26.0	1.1	19.0	1.1	21.6	0.7
MK257_m6_3	matrix	0.1512	11.58	0.0663	12.15	0.00318	3.68	0.303	0.000947	3.32	65.2	7.7	20.0	0.8	18.0	0.8	19.1	0.6
MK257_m6_4	matrix	0.0708	7.36	0.0296	7.84	0.00304	2.70	0.345	0.000933	2.82	29.7	2.3	20.0	0.5	19.0	0.5	18.8	0.5

Table B1. Petrochronological data for monazite grains.

Grain #	Location	207Pb/206Pb	2SE %	Pb207/U235	2SE %	206Pb/238U	2SE %	rho	208Pb/232Th	2SE %	207Pb/235U (Ma)	2SE	206Pb/238U (Ma)	2SE	corr.206Pb/238U (Ma)	2SE	208Pb/232Th (Ma)	2SE
MK257_m6_5	matrix	0.2981	7.37	0.1241	8.03	0.00302	3.21	0.399	0.000822	3.32	119.0	9.0	19.0	0.6	13.0	0.6	16.6	0.6
MK257_m6_6	matrix	0.6310	6.69	0.6694	11.17	0.00770	8.94	0.801	0.001817	7.17	520.0	45.5	49.0	4.4	13.0	4.4	36.7	2.6
MK257_m6_7	matrix	0.0818	11.69	0.0341	12.03	0.00302	2.86	0.237	0.000948	2.79	34.1	4.0	19.0	0.6	19.0	0.6	19.1	0.5
MK257_m6_8	matrix	0.2201	6.86	0.1117	7.58	0.00368	3.22	0.425	0.001016	2.99	107.5	7.7	24.0	0.8	18.0	0.8	20.5	0.6
MK257_m6_9	matrix	0.1128	10.84	0.0438	11.45	0.00281	3.70	0.323	0.000876	3.89	43.5	4.9	18.0	0.7	17.0	0.7	17.7	0.7
MK257_m7_1	matrix	0.0840	11.72	0.0280	12.03	0.00242	2.73	0.227	0.000758	2.92	28.1	3.3	16.0	0.4	15.0	0.4	15.3	0.4
MK257_m7_2	matrix	0.3635	6.19	0.1849	6.94	0.00369	3.13	0.452	0.000981	3.13	172.0	11.0	24.0	0.7	14.0	0.7	19.8	0.6
MK257_m7_3	matrix	0.1771	11.02	0.0651	11.57	0.00267	3.54	0.306	0.000783	3.16	64.0	7.2	17.0	0.6	14.0	0.6	15.8	0.5
MK257_m7_4	matrix	0.1176	9.95	0.0403	10.53	0.00249	3.45	0.327	0.000788	3.02	40.1	4.1	16.0	0.6	15.0	0.6	15.9	0.5
MK257_m7_5	matrix	0.4882	9.96	0.3041	17.02	0.00452	13.81	0.811	0.001097	9.14	270.0	40.3	29.0	4.0	13.0	4.0	22.1	2.0
MK257_m7_6	matrix	0.0908	10.13	0.0384	10.55	0.00307	2.93	0.277	0.000939	2.98	38.2	4.0	20.0	0.6	19.0	0.6	19.0	0.6
MK257_m7_7	matrix	0.1399	8.20	0.0493	8.72	0.00256	2.97	0.340	0.000770	3.15	48.9	4.2	16.0	0.5	15.0	0.5	15.6	0.5
MK257_m7_8	matrix	0.0917	11.44	0.0311	11.80	0.00246	2.87	0.243	0.000771	2.72	31.1	3.6	16.0	0.5	15.0	0.5	15.6	0.4
MK257_m7_9	matrix	0.0896	11.49	0.0310	11.85	0.00251	2.89	0.244	0.000780	3.19	31.0	3.6	16.0	0.5	15.0	0.5	15.8	0.5
MK257_m7_10	matrix	0.0709	9.14	0.0307	9.56	0.00314	2.81	0.294	0.000988	2.87	30.7	2.9	20.0	0.6	20.0	0.6	20.0	0.6
MK257_m7_11	matrix	0.0640	8.12	0.0276	8.74	0.00312	3.23	0.369	0.000972	3.33	27.6	2.4	20.0	0.6	20.0	0.6	19.6	0.7
MK257_m7_12	matrix	0.0793	10.43	0.0336	10.89	0.00307	3.13	0.288	0.000964	3.04	33.5	3.6	20.0	0.6	19.0	0.6	19.5	0.6
MK257_m7_13	matrix	0.0808	10.62	0.0340	11.08	0.00306	3.14	0.283	0.000963	3.37	34.0	3.7	20.0	0.6	19.0	0.6	19.5	0.7
MK257_m7_14	matrix	0.1014	9.11	0.0430	9.48	0.00308	2.64	0.279	0.000922	2.70	42.8	4.0	20.0	0.5	18.0	0.5	18.6	0.5
MK257_m7_15	matrix	0.0759	10.91	0.0323	11.35	0.00309	3.14	0.277	0.000955	3.14	32.3	3.6	20.0	0.6	19.0	0.6	19.3	0.6
MK257_m8_1	matrix	0.2681	7.55	0.1262	8.10	0.00342	2.94	0.362	0.000935	3.42	121.0	9.2	22.0	0.6	16.0	0.6	18.9	0.6
MK257_m8_2	matrix	0.3033	8.70	0.1639	9.29	0.00392	3.24	0.349	0.001080	3.57	154.0	13.3	25.2	0.8	17.0	0.8	21.8	0.8
MK257_m8_3	matrix	0.1434	12.08	0.0582	12.58	0.00295	3.52	0.280	0.000885	3.40	57.5	7.0	19.0	0.7	17.0	0.7	17.9	0.6
MK257_m8_4	matrix	0.0757	9.54	0.0314	10.01	0.00301	3.01	0.301	0.000950	3.04	31.4	3.1	19.4	0.6	18.7	0.6	19.2	0.6
MK257_m8_5	matrix	0.0802	10.42	0.0320	10.90	0.00289	3.21	0.294	0.000900	3.16	31.9	3.4	18.6	0.6	17.8	0.6	18.2	0.6
MK257_m8_6	matrix	0.1103	9.22	0.0455	9.84	0.00299	3.44	0.349	0.000916	3.29	45.1	4.3	19.2	0.7	17.7	0.7	18.5	0.6
MK257_m8_7	matrix	0.1505	13.18	0.0648	13.75	0.00313	3.90	0.284	0.000914	3.47	63.8	8.5	20.0	0.8	17.5	0.8	18.5	0.6
MK257_m8_8	matrix	0.0715	12.36	0.0300	12.77	0.00305	3.21	0.252	0.000962	3.21	30.1	3.8	19.6	0.6	19.0	0.6	19.4	0.6
MK257_m8_9	matrix	0.0855	10.83	0.0352	11.25	0.00298	3.05	0.271	0.000948	3.03	35.1	3.9	19.2	0.6	18.0	0.6	19.1	0.6
MK257_m8_10	matrix	0.0767	13.33	0.0322	13.67	0.00304	3.01	0.221	0.000951	2.94	32.2	4.3	20.0	0.6	18.8	0.6	19.2	0.6
~~MK257_m10_1~~	~~matrix~~	~~0.7485~~	~~6.40~~	~~2.3262~~	~~15.72~~	~~0.02255~~	~~14.36~~	~~0.913~~	~~0.003584~~	~~15.41~~	~~1220.0~~	~~111.6~~	~~143.8~~	~~20.4~~	~~16.2~~	~~20.4~~	~~72.3~~	~~11.1~~
MK257_m10_2	matrix	0.5146	6.26	0.4312	7.50	0.00608	4.13	0.551	0.001381	3.40	364.0	22.9	39.1	1.6	16.0	1.6	27.9	0.9
MK257_m10_3	matrix	0.4775	7.23	0.3703	8.77	0.00563	4.96	0.566	0.001122	3.68	320.0	24.1	36.2	1.8	16.5	1.8	22.7	0.8
MK257_m10_4	matrix	0.0691	11.21	0.0289	11.62	0.00303	3.06	0.264	0.000977	2.93	28.9	3.3	19.5	0.6	19.0	0.6	19.7	0.6
MK257_m10_5	matrix	0.2899	7.20	0.1411	7.97	0.00353	3.41	0.428	0.000896	3.14	134.0	10.0	23.0	0.8	15.7	0.8	18.1	0.6
MK257_m10_6	matrix	0.0659	10.14	0.0282	10.63	0.00311	3.16	0.298	0.000994	3.06	28.2	3.0	20.0	0.6	19.5	0.6	20.1	0.6
MK257_m10_7	matrix	0.0687	8.95	0.0292	9.49	0.00308	3.16	0.333	0.000971	3.19	29.2	2.7	19.8	0.6	19.0	0.6	19.6	0.6
MK257_m11_1	matrix	0.2287	8.56	0.1013	9.45	0.00321	3.99	0.422	0.000912	3.61	98.0	8.8	21.0	0.8	15.9	0.8	18.4	0.7
MK257_m11_2	matrix	0.4577	5.91	0.3021	6.87	0.00479	3.50	0.510	0.001069	3.52	268.0	16.2	30.8	1.1	14.8	1.1	21.6	0.8
MK257_m11_3	matrix	0.1826	13.43	0.0863	14.12	0.00343	4.36	0.309	0.000987	3.51	84.0	11.4	22.0	1.0	18.3	1.0	19.9	0.7
MK257_m11_4	matrix	0.0645	10.52	0.0259	11.09	0.00292	3.50	0.316	0.000904	3.38	26.0	2.8	18.8	0.7	18.3	0.7	18.3	0.6
MK257_m11_5	matrix	0.0632	10.82	0.0247	11.20	0.00284	2.87	0.257	0.000854	2.83	24.8	2.7	18.3	0.5	17.9	0.5	17.3	0.5
MK257_m11_6	matrix	0.0652	9.26	0.0247	9.76	0.00275	3.07	0.315	0.000837	3.04	24.8	2.4	17.7	0.5	17.3	0.5	16.9	0.5
MK257_m11_7	matrix	0.2315	8.24	0.1002	9.06	0.00314	3.76	0.416	0.000888	3.34	96.9	8.4	20.2	0.8	15.5	0.8	17.9	0.6
MK257_m11_8	matrix	0.1312	10.36	0.0471	10.84	0.00260	3.19	0.294	0.000751	2.96	46.7	4.9	16.8	0.5	15.0	0.5	15.2	0.4
MK257_m11_9	matrix	0.1028	14.97	0.0360	15.37	0.00254	3.47	0.226	0.000749	3.25	35.9	5.4	16.0	0.6	15.2	0.6	15.1	0.5
MK257_m11_10	matrix	0.0774	11.55	0.0271	11.91	0.00254	2.93	0.246	0.000784	3.20	27.2	3.2	16.0	0.5	15.7	0.5	15.8	0.5
MK258																		
MK258_m1_1	matrix	0.0547	6.89	0.0241	7.54	0.00319	3.05	0.404	0.000989	2.77	24.1	1.8	20.5	0.6	20.3	0.6	20.0	0.6
MK258_m1_2	matrix	0.0519	7.08	0.0223	8.13	0.00311	3.99	0.491	0.000989	3.82	22.4	1.8	20.0	0.8	19.9	0.8	20.0	0.8
MK258_m1_3	matrix	0.0613	5.47	0.0267	6.23	0.00317	2.97	0.477	0.001031	3.24	26.8	1.6	20.4	0.6	20.0	0.6	20.8	0.7
MK258_m1_4	matrix	0.0598	5.79	0.0282	6.62	0.00342	3.20	0.484	0.001062	3.14	28.2	1.8	22.0	0.7	21.6	0.7	21.4	0.7
MK258_m1_5	matrix	0.0693	4.08	0.0337	5.05	0.00353	2.99	0.591	0.001122	3.09	33.7	1.7	22.7	0.7	22.1	0.7	22.7	0.7
MK258_m1_6	matrix	0.0832	4.76	0.0391	5.54	0.00341	2.83	0.512	0.001115	2.74	38.9	2.1	21.9	0.6	20.9	0.6	22.5	0.6
MK258_m1_7	matrix	0.0540	4.84	0.0243	5.87	0.00326	3.32	0.566	0.001051	3.11	24.4	1.4	21.0	0.7	20.8	0.7	21.2	0.7
MK258_m1_8	matrix	0.0621	6.45	0.0252	7.01	0.00294	2.75	0.392	0.000969	3.16	25.2	1.7	18.9	0.5	18.6	0.5	19.6	0.6

Table B1. Petrochronological data for monazite grains.

Grain #	Location	207Pb/206Pb	2SE %	Pb207/U235	2SE %	206Pb/238U	2SE %	rho	208Pb/232Th	2SE %	207Pb/235U (Ma)	2SE	206Pb/238U (Ma)	2SE	corr.206Pb/238U (Ma)	2SE	208Pb/232Th (Ma)	2SE
MK258_m1_9	matrix	0.1074	6.14	0.0468	6.71	0.00316	2.71	0.405	0.001062	3.22	46.4	3.0	20.3	0.6	18.8	0.6	21.5	0.7
MK258_m1_10	matrix	0.0496	5.79	0.0214	6.41	0.00313	2.76	0.430	0.001003	2.66	21.5	1.4	20.2	0.6	20.1	0.6	20.2	0.5
MK258_m1_11	matrix	0.0565	6.30	0.0244	7.28	0.00313	3.65	0.501	0.000993	4.06	24.5	1.8	20.2	0.7	19.9	0.7	20.1	0.8
MK258_m1_12	matrix	0.1378	4.70	0.0574	5.71	0.00302	3.25	0.568	0.000992	3.67	56.7	3.1	19.4	0.6	17.2	0.6	20.0	0.7
MK258_m1_13	matrix	0.0789	4.34	0.0386	5.07	0.00354	2.61	0.514	0.001130	2.96	38.4	1.9	22.8	0.6	21.9	0.6	22.8	0.7
MK258_m1_14	matrix	0.0654	4.92	0.0320	5.70	0.00355	2.89	0.507	0.001144	3.09	32.0	1.8	22.8	0.7	22.3	0.7	23.1	0.7
MK258_m1_15	matrix	0.0498	4.63	0.0237	5.24	0.00346	2.46	0.469	0.001101	2.43	23.8	1.2	22.3	0.5	22.2	0.5	22.2	0.5
MK258_m1_20	matrix	0.0773	5.21	0.0363	5.81	0.00341	2.57	0.443	0.001094	2.98	36.2	2.1	22.0	0.6	21.1	0.6	22.1	0.7
MK258_m2_1	matrix	0.0497	7.14	0.0214	7.66	0.00313	2.76	0.360	0.000996	3.15	21.5	1.6	20.1	0.6	20.0	0.6	20.1	0.6
MK258_m2_2	matrix	0.0503	5.45	0.0217	6.08	0.00313	2.71	0.445	0.000996	2.75	21.8	1.3	20.1	0.5	20.0	0.5	20.1	0.6
MK258_m2_3	matrix	0.0470	6.62	0.0206	7.36	0.00318	3.23	0.439	0.000983	3.35	20.7	1.5	20.5	0.7	20.5	0.7	19.9	0.7
MK258_m2_4	matrix	0.0473	5.34	0.0171	6.25	0.00262	3.25	0.519	0.000811	3.49	17.2	1.1	16.8	0.5	16.8	0.5	16.4	0.6
MK258_m2_5	matrix	0.0479	7.12	0.0192	7.56	0.00290	2.56	0.338	0.000904	2.91	19.3	1.4	18.7	0.5	19.0	0.5	18.3	0.5
MK258_m2_6	matrix	0.0673	4.92	0.0312	5.63	0.00336	2.73	0.485	0.001073	2.95	31.2	1.7	22.0	0.6	21.1	0.6	21.7	0.6
MK258_m2_7	matrix	0.0487	5.04	0.0226	6.09	0.00338	3.42	0.562	0.001082	3.45	22.7	1.4	21.7	0.7	21.7	0.7	21.9	0.8
MK258_m2_8	matrix	0.0495	5.56	0.0225	6.32	0.00330	3.02	0.477	0.001044	3.08	22.6	1.4	21.2	0.6	21.2	0.6	21.1	0.6
MK258_m2_9	matrix	0.0502	6.23	0.0228	6.87	0.00329	2.88	0.420	0.001041	3.07	22.9	1.6	21.2	0.6	21.1	0.6	21.0	0.6
MK258_m2_10	matrix	0.0496	7.45	0.0227	7.88	0.00333	2.57	0.326	0.001044	2.77	22.8	1.8	21.0	0.5	21.3	0.5	21.1	0.6
MK258_m2_11	matrix	0.0501	5.34	0.0224	6.05	0.00324	2.84	0.469	0.001024	3.11	22.5	1.3	20.9	0.6	20.8	0.6	20.7	0.6
MK258_m2_12	matrix	0.0603	8.03	0.0228	8.48	0.00275	2.75	0.324	0.000851	3.05	22.9	1.9	18.0	0.5	17.4	0.5	17.2	0.5
MK258_m2_13	matrix	0.0666	5.88	0.0251	6.78	0.00273	3.38	0.499	0.000849	3.60	25.2	1.7	17.6	0.6	17.1	0.6	17.2	0.6
MK258_m2_14	matrix	0.1283	7.10	0.0484	7.89	0.00274	3.44	0.436	0.000979	4.04	48.0	3.7	17.6	0.6	15.8	0.6	19.8	0.8
MK258_m2_15	matrix	0.0883	5.38	0.0291	6.35	0.00239	3.38	0.532	0.000852	3.78	29.1	1.8	15.4	0.5	14.6	0.5	17.2	0.6
MK258_m2_16	matrix	0.1762	5.78	0.0698	7.16	0.00288	4.23	0.590	0.001239	4.91	68.5	4.7	18.5	0.8	15.0	0.8	25.0	1.2
MK258_m2_17	matrix	0.1960	7.27	0.0775	8.38	0.00287	4.18	0.498	0.001180	5.36	75.8	6.1	18.5	0.8	15.0	0.8	23.8	1.3
MK258_m2_18	matrix	0.0491	6.69	0.0227	7.29	0.00335	2.87	0.394	0.001058	3.08	22.8	1.6	21.6	0.6	21.5	0.6	21.4	0.7
MK258_m2_19	matrix	0.0534	5.48	0.0240	6.33	0.00327	3.18	0.502	0.001032	3.47	24.1	1.5	21.0	0.7	21.0	0.7	20.8	0.7
MK258_m2_20	matrix	0.0460	5.87	0.0209	6.64	0.00329	3.11	0.468	0.001041	3.08	21.0	1.4	21.0	0.7	21.2	0.7	21.0	0.6
MK258_m3_1	matrix	0.0480	7.25	0.0193	7.79	0.00291	2.83	0.364	0.000889	2.65	19.4	1.5	18.8	0.5	18.7	0.5	18.0	0.5
MK258_m3_2	matrix	0.0483	6.73	0.0215	7.33	0.00323	2.91	0.396	0.000996	2.76	21.6	1.6	20.8	0.6	20.7	0.6	20.1	0.6
MK258_m3_3	matrix	0.1227	19.15	0.0631	19.66	0.00373	4.46	0.227	0.001189	4.75	62.0	11.8	24.0	1.1	22.0	1.1	24.0	1.1
MK258_m3_4	matrix	0.0476	6.39	0.0221	7.06	0.00337	3.02	0.427	0.001080	3.07	22.2	1.6	22.0	0.7	21.7	0.7	21.8	0.7
MK258_m3_5	matrix	0.1901	12.10	0.1061	12.96	0.00405	4.65	0.358	0.001354	4.70	102.0	12.6	26.0	1.2	21.0	1.2	27.3	1.3
MK258_m3_6	matrix	0.0680	6.04	0.0309	6.67	0.00330	2.82	0.423	0.001054	3.27	30.9	2.0	21.0	0.6	21.0	0.6	21.3	0.7
MK258_m3_7	matrix	0.1026	4.54	0.0503	5.41	0.00356	2.93	0.543	0.001087	2.75	49.8	2.6	23.0	0.7	21.0	0.7	21.9	0.6
MK258_m3_8	matrix	0.0693	4.91	0.0338	5.91	0.00353	3.28	0.556	0.001124	3.49	33.7	2.0	23.0	0.7	22.0	0.7	22.7	0.8
~~MK258_m3_9~~	~~matrix~~	~~0.3681~~	~~22.62~~	~~0.2267~~	~~29.62~~	~~0.00447~~	~~19.12~~	~~0.645~~	~~0.001945~~	~~23.15~~	~~207.0~~	~~55.6~~	~~29.0~~	~~5.5~~	~~17.0~~	~~5.5~~	~~39.3~~	~~9.1~~
MK258_m3_10	matrix	0.0647	5.80	0.0293	6.55	0.00328	3.05	0.466	0.000994	3.20	29.3	1.9	21.0	0.6	21.0	0.6	20.1	0.6
MK258_m3_11	matrix	0.0478	5.23	0.0229	6.38	0.00347	3.65	0.573	0.001085	3.59	23.0	1.4	22.0	0.8	22.0	0.8	21.9	0.8
MK258_m3_12	matrix	0.0491	7.36	0.0238	7.89	0.00351	2.87	0.363	0.001109	2.93	23.8	1.9	23.0	0.6	23.0	0.6	22.4	0.7
MK258_m4_1	matrix	0.1337	6.91	0.0642	7.67	0.00349	3.33	0.433	0.001125	4.12	63.2	4.7	22.0	0.7	20.0	0.7	22.7	0.9
MK258_m4_2	matrix	0.1574	21.21	0.0692	22.14	0.00319	6.36	0.287	0.001023	7.30	68.0	14.6	21.0	1.3	18.0	1.3	20.7	1.5
MK258_m4_3	matrix	0.1619	11.14	0.0766	11.89	0.00343	4.15	0.349	0.001062	4.13	74.9	8.6	22.0	0.9	19.0	0.9	21.4	0.9
MK258_m4_4	matrix	0.2237	4.77	0.1049	5.69	0.00340	3.10	0.544	0.001113	3.21	101.3	5.5	22.0	0.7	17.0	0.7	22.5	0.7
MK258_m4_5	matrix	0.0466	6.49	0.0215	7.21	0.00335	3.15	0.437	0.001043	3.09	21.6	1.5	22.0	0.7	22.0	0.7	21.1	0.6
MK258_m4_6	matrix	0.1315	5.01	0.0529	5.83	0.00292	2.99	0.512	0.000932	2.93	52.4	3.0	19.0	0.6	17.0	0.6	18.8	0.6
MK258_m4_7	matrix	0.0499	7.98	0.0213	8.42	0.00309	2.69	0.320	0.000941	2.75	21.4	1.8	20.0	0.5	20.0	0.5	19.0	0.5
MK258_m4_8	matrix	0.0600	4.72	0.0271	5.48	0.00328	2.78	0.508	0.001026	2.87	27.1	1.5	21.0	0.6	21.0	0.6	20.7	0.6
MK258_m4_9	matrix	0.1311	9.05	0.0694	9.85	0.00384	3.87	0.393	0.001194	3.56	68.2	6.5	25.0	1.0	22.0	1.0	24.1	0.9
MK258_m4_10	matrix	0.1272	5.54	0.0685	6.36	0.00390	3.13	0.492	0.001193	3.19	67.2	4.1	25.0	0.8	23.0	0.8	24.1	0.8
MK258_m4_11	matrix	0.0499	7.88	0.0229	8.23	0.00334	2.40	0.291	0.000984	2.46	23.0	1.9	21.0	0.5	21.0	0.5	19.9	0.5
MK258_m4_12	matrix	0.1133	6.25	0.0449	6.82	0.00288	2.73	0.400	0.000924	3.32	44.6	3.0	19.0	0.5	17.0	0.5	18.7	0.6
MK258_m4_13	matrix	0.0700	17.08	0.0302	17.34	0.00313	2.98	0.172	0.000939	3.10	30.2	5.2	20.0	0.6	20.0	0.6	19.0	0.6
MK258_m4_14	matrix	0.0527	9.78	0.0234	10.18	0.00322	2.80	0.275	0.000941	2.79	23.4	2.4	21.0	0.6	21.0	0.6	19.0	0.5
MK258_m4_15	matrix	0.1363	4.32	0.0700	5.37	0.00373	3.20	0.596	0.001161	3.16	68.7	3.6	24.0	0.8	21.0	0.8	23.5	0.7
MK258_m4_16	matrix	0.0716	6.43	0.0310	7.11	0.00314	3.02	0.425	0.000972	3.00	31.0	2.2	20.0	0.6	20.0	0.6	19.6	0.6
MK258_m5_1	matrix	0.0550	6.07	0.0196	7.05	0.00258	3.59	0.509	0.000809	3.34	19.7	1.4	17.0	0.6	16.0	0.6	16.3	0.5

Table B1. Petrochronological data for monazite grains.

Grain #	Location	207Pb/206Pb	2SE %	Pb207/U235	2SE %	206Pb/238U	2SE %	rho	208Pb/232Th	2SE %	207Pb/235U (Ma)	2SE	206Pb/238U (Ma)	2SE	corr.206Pb/238U (Ma)	2SE	208Pb/232Th (Ma)	2SE
MK258_m5_2	matrix	0.1211	16.16	0.0474	16.78	0.00284	4.49	0.268	0.000909	5.29	47.0	7.7	18.0	0.8	17.0	0.8	18.4	1.0
MK258_m5_3	matrix	0.1400	6.38	0.0625	7.13	0.00324	3.18	0.446	0.000994	3.33	61.6	4.3	21.0	0.7	18.0	0.7	20.1	0.7
MK258_m5_4	matrix	0.0495	6.18	0.0231	6.95	0.00338	3.16	0.455	0.001061	3.19	23.2	1.6	22.0	0.7	22.0	0.7	21.4	0.7
MK258_m5_5	matrix	0.0503	5.21	0.0235	5.93	0.00339	2.84	0.479	0.001056	3.12	23.6	1.4	22.0	0.6	20.0	0.6	21.3	0.7
MK258_m5_6	matrix	0.0486	6.57	0.0232	7.13	0.00346	2.77	0.389	0.001071	3.28	23.3	1.6	20.0	0.6	22.0	0.6	21.6	0.7
MK258_m5_7	matrix	0.0468	6.44	0.0222	7.19	0.00344	3.21	0.446	0.001045	3.28	22.3	1.6	22.0	0.7	22.0	0.7	21.1	0.7
MK258_m5_8	matrix	0.0463	7.34	0.0218	7.71	0.00342	2.36	0.306	0.001039	2.78	21.9	1.7	22.0	0.5	22.0	0.5	21.0	0.6
MK258_m5_9	matrix	0.0486	5.82	0.0229	6.32	0.00342	2.46	0.389	0.001037	2.37	23.0	1.4	22.0	0.5	22.0	0.5	21.0	0.5
~~MK258_m5_10~~	~~matrix~~	~~0.4454~~	~~6.26~~	~~0.2577~~	~~10.22~~	~~0.00420~~	~~8.08~~	~~0.791~~	~~0.002284~~	~~11.07~~	~~233.0~~	~~21.3~~	~~27.0~~	~~2.2~~	~~13.0~~	~~2.2~~	~~46.1~~	~~5.1~~
MK258_m5_11	matrix	0.2412	5.52	0.0943	6.40	0.00284	3.24	0.506	0.001116	3.46	91.5	5.6	18.0	0.6	14.0	0.6	22.5	0.8
MK258_m5_12	matrix	0.1588	5.72	0.0550	6.29	0.00251	2.61	0.415	0.000891	2.96	54.4	3.3	16.0	0.4	14.0	0.4	18.0	0.5
MK258_m5_13	matrix	0.0430	6.62	0.0157	7.14	0.00265	2.68	0.375	0.000826	2.65	15.8	1.1	17.0	0.5	17.0	0.5	16.7	0.4
MK258_m5_14	matrix	0.0454	8.65	0.0181	9.19	0.00290	3.11	0.338	0.000909	3.08	18.3	1.7	19.0	0.6	19.0	0.6	18.4	0.6
MK258_m6_1	matrix	0.0818	8.58	0.0269	9.78	0.00238	4.70	0.481	0.000847	4.78	26.9	2.6	15.0	0.7	15.0	0.7	17.1	0.8
MK258_m6_2	matrix	0.0676	5.75	0.0288	6.82	0.00309	3.66	0.536	0.000986	3.06	28.8	1.9	20.0	0.7	19.0	0.7	19.9	0.6
MK258_m6_3	matrix	0.0622	4.62	0.0303	5.53	0.00353	3.03	0.549	0.001126	2.84	30.3	1.7	23.0	0.7	22.0	0.7	22.7	0.6
MK258_m6_4	matrix	0.0481	8.23	0.0213	8.99	0.00321	3.61	0.402	0.000968	3.56	21.4	1.9	21.0	0.7	21.0	0.7	19.6	0.7
MK258_m6_5	matrix	0.2051	7.45	0.0896	8.88	0.00317	4.83	0.544	0.001143	7.09	87.2	7.4	20.0	1.0	16.0	1.0	23.1	1.6
MK258_m6_6	matrix	0.2101	9.06	0.0987	10.41	0.00341	5.12	0.492	0.001184	5.04	96.0	9.5	22.0	1.1	17.0	1.1	23.9	1.2
MK258_m6_7	matrix	0.0751	7.77	0.0262	8.56	0.00253	3.59	0.419	0.000809	3.80	26.2	2.2	16.0	0.6	16.0	0.6	16.3	0.6
MK258_m6_8	matrix	0.0895	4.69	0.0321	5.36	0.00260	2.61	0.486	0.000843	2.72	32.0	1.7	17.0	0.4	16.0	0.4	17.0	0.5
MK258_m6_9	matrix	0.1113	6.19	0.0436	7.13	0.00284	3.54	0.497	0.000911	3.69	43.3	3.0	18.0	0.6	17.0	0.6	18.4	0.7
MK258_m6_10	matrix	0.1133	7.51	0.0567	8.07	0.00363	2.94	0.364	0.001065	3.32	56.0	4.4	23.0	0.7	21.0	0.7	21.5	0.7
MK258_m6_11	matrix	0.1380	15.30	0.0743	15.85	0.00391	4.13	0.261	0.001292	4.58	73.0	11.1	25.0	1.0	22.0	1.0	26.1	1.2
MK258_m6_12	matrix	0.1468	4.81	0.0830	6.26	0.00410	4.01	0.640	0.001369	4.14	81.0	4.9	26.0	1.1	23.0	1.1	27.6	1.1
MK258_m6_13	matrix	0.1884	19.69	0.1011	20.77	0.00389	6.61	0.318	0.001251	6.81	98.0	19.4	25.0	1.7	21.0	1.7	25.3	1.7
MK258_m6_14	matrix	0.1442	8.68	0.0599	9.79	0.00301	4.53	0.463	0.001028	5.39	59.0	5.6	19.0	0.9	17.0	0.9	20.8	1.1
MK258_m6_15	matrix	0.1346	6.67	0.0674	7.53	0.00363	3.50	0.465	0.001160	3.99	66.2	4.8	23.0	0.8	21.0	0.8	23.4	0.9
MK258_m7_1	matrix	0.0782	4.75	0.0365	5.67	0.00339	3.11	0.548	0.001115	3.27	36.4	2.0	22.0	0.7	21.0	0.7	22.5	0.7
MK258_m7_2	matrix	0.1253	4.11	0.0629	4.91	0.00364	2.68	0.547	0.001209	2.73	61.9	2.9	23.0	0.6	21.0	0.6	24.4	0.7
MK258_m7_3	matrix	0.0604	5.46	0.0280	6.30	0.00337	3.15	0.499	0.001091	3.44	28.1	1.7	22.0	0.7	21.0	0.7	22.0	0.8
MK258_m7_4	matrix	0.2109	14.57	0.1274	15.66	0.00438	5.73	0.366	0.001485	6.04	122.0	18.0	28.0	1.6	22.0	1.6	30.0	1.8
MK258_m7_5	matrix	0.0473	4.42	0.0220	5.34	0.00338	2.99	0.560	0.001094	2.96	22.1	1.2	22.0	0.6	22.0	0.6	22.1	0.7
MK258_m7_6	matrix	0.1421	6.38	0.0636	7.10	0.00325	3.11	0.438	0.001075	3.56	62.6	4.3	21.0	0.6	20.0	0.6	21.7	0.8
MK258_m7_7	matrix	0.0475	6.04	0.0221	6.83	0.00337	3.19	0.467	0.001059	3.21	22.2	1.5	20.0	0.7	21.7	0.7	21.4	0.7
MK258_m7_8	matrix	0.0732	4.80	0.0339	5.62	0.00336	2.91	0.519	0.001096	3.02	33.8	1.9	21.6	0.6	21.0	0.6	22.1	0.7
MK258_m7_9	matrix	0.0660	4.71	0.0294	5.68	0.00323	3.18	0.560	0.001030	3.07	29.4	1.6	21.0	0.7	20.3	0.7	20.8	0.6
MK258_m7_10	matrix	0.1709	5.82	0.0947	6.61	0.00402	3.15	0.476	0.001334	3.19	91.8	5.8	25.9	0.8	21.8	0.8	26.9	0.9
MK258_m7_11	matrix	0.0455	5.09	0.0209	5.97	0.00333	3.12	0.523	0.001065	3.07	21.0	1.2	21.4	0.7	21.5	0.7	21.5	0.7
MK258_m7_12	matrix	0.0685	4.65	0.0297	5.96	0.00315	3.72	0.625	0.000986	3.74	29.7	1.7	20.3	0.8	20.0	0.8	19.9	0.7
~~MK258_m7_13~~	~~matrix~~	~~0.3105~~	~~16.66~~	~~0.1792~~	~~20.45~~	~~0.00419~~	~~11.87~~	~~0.580~~	~~0.002127~~	~~13.70~~	~~167.0~~	~~31.6~~	~~27.0~~	~~3.2~~	~~18.0~~	~~3.2~~	~~42.9~~	~~5.9~~
MK258_m7_14	matrix	0.1449	5.84	0.0762	6.49	0.00381	2.82	0.434	0.001275	2.87	74.5	4.7	24.5	0.7	21.5	0.7	25.8	0.7
MK258_m7_15	matrix	0.1335	6.49	0.0502	7.59	0.00273	3.94	0.518	0.000956	3.94	49.7	3.7	17.6	0.7	15.6	0.7	19.3	0.8
MK258_m7_16	matrix	0.0463	5.21	0.0209	5.93	0.00328	2.84	0.479	0.001064	2.98	21.0	1.2	21.1	0.6	21.1	0.6	21.5	0.6
MK258_m7_17	matrix	0.0869	9.94	0.0294	10.31	0.00245	2.73	0.265	0.000869	3.42	29.4	3.0	15.8	0.4	15.0	0.4	17.6	0.6
MK258_m7_18	matrix	0.0758	8.12	0.0297	8.50	0.00285	2.54	0.298	0.000924	3.40	29.7	2.5	18.3	0.5	17.6	0.5	18.7	0.6
MK258_m7_19	matrix	0.1749	7.64	0.0822	8.56	0.00341	3.88	0.453	0.001120	4.05	80.2	6.6	21.9	0.8	18.4	0.8	22.6	0.9
MK258_m7_20	matrix	0.0623	8.80	0.0272	9.72	0.00317	4.13	0.425	0.001006	4.35	27.2	2.6	20.4	0.8	20.0	0.8	20.3	0.9
~~MK258_m8_1~~	~~matrix~~	~~0.4506~~	~~9.29~~	~~0.3442~~	~~17.36~~	~~0.00554~~	~~14.67~~	~~0.845~~	~~0.002025~~	~~13.78~~	~~300.0~~	~~45.1~~	~~35.6~~	~~5.2~~	~~17.4~~	~~5.2~~	~~40.9~~	~~5.6~~
MK258_m8_2	matrix	0.2950	8.90	0.1793	12.05	0.00441	8.12	0.674	0.001664	9.55	167.0	18.6	28.4	2.3	19.5	2.3	33.6	3.2
MK258_m8_3	matrix	0.0809	7.11	0.0398	8.21	0.00357	4.11	0.501	0.001095	3.78	39.6	3.2	23.0	0.9	22.0	0.9	22.1	0.8
MK258_m8_4	matrix	0.3489	3.86	0.2303	6.50	0.00479	5.23	0.805	0.001540	5.64	210.0	12.4	30.8	1.6	19.0	1.6	31.1	1.8
MK258_m8_5	matrix	0.4009	6.25	0.3489	10.42	0.00631	8.33	0.800	0.001725	7.72	304.0	27.4	40.6	3.4	22.4	3.4	34.8	2.7
MK258_m8_6	matrix	0.3202	4.77	0.2433	7.42	0.00551	5.67	0.765	0.001751	7.61	221.0	14.7	35.4	2.0	23.2	2.0	35.3	2.7
MK258_m8_7	matrix	0.0462	6.53	0.0218	7.21	0.00343	3.04	0.422	0.001082	3.10	21.9	1.6	22.1	0.7	22.1	0.7	21.9	0.7
MK258_m8_8	matrix	0.0438	8.77	0.0171	9.37	0.00284	3.30	0.352	0.000896	3.97	17.2	1.6	18.3	0.6	18.3	0.6	18.1	0.7
MK258_m8_9	matrix	0.1350	17.51	0.0466	18.45	0.00250	5.81	0.315	0.000881	6.97	46.2	8.3	16.1	0.9	14.3	0.9	17.8	1.2

Table B1. Petrochronological data for monazite grains.

Grain #	Location	207Pb/206Pb	2SE %	Pb207/U235	2SE %	206Pb/238U	2SE %	rho	208Pb/232Th	2SE %	207Pb/235U (Ma)	2SE	206Pb/238U (Ma)	2SE	corr.206Pb/238U (Ma)	2SE	208Pb/232Th (Ma)	2SE
MK258_m8_10	matrix	0.2574	6.26	0.1055	7.48	0.00298	4.09	0.546	0.001080	5.56	101.9	7.2	19.2	0.8	14.0	0.8	21.8	1.2
MK258_m8_11	matrix	0.1688	7.88	0.0876	10.08	0.00376	6.29	0.624	0.001261	6.44	85.2	8.2	24.2	1.5	20.5	1.5	25.5	1.6
~~MK258_m8_12~~	~~matrix~~	~~0.2303~~	~~21.72~~	~~0.1640~~	~~24.99~~	~~0.00517~~	~~12.36~~	~~0.495~~	~~0.001992~~	~~12.87~~	~~154.0~~	~~35.8~~	~~33.2~~	~~4.1~~	~~25.5~~	~~4.1~~	~~40.2~~	~~5.2~~
MK258_m8_13	matrix	0.2676	9.37	0.1531	11.46	0.00415	6.59	0.576	0.001392	7.01	145.0	15.4	26.7	1.8	19.3	1.8	28.1	2.0
MK258_m8_14	matrix	0.0440	6.93	0.0208	7.64	0.00344	3.20	0.419	0.001097	2.98	20.9	1.6	22.1	0.7	22.2	0.7	22.1	0.7
MK258_m8_15	matrix	0.0484	8.29	0.0217	8.72	0.00326	2.70	0.309	0.000999	2.65	21.8	1.9	21.0	0.6	20.9	0.6	20.2	0.5
MK258_m8_16	matrix	0.0463	7.55	0.0223	8.18	0.00350	3.16	0.386	0.001123	3.28	22.4	1.8	22.5	0.7	22.5	0.7	22.7	0.7
MK258_m8_17	matrix	0.0835	6.04	0.0440	6.97	0.00382	3.48	0.499	0.001204	3.51	43.7	3.0	24.6	0.9	23.4	0.9	24.3	0.9
MK258_m8_18	matrix	0.0576	6.66	0.0282	7.57	0.00355	3.59	0.475	0.001133	3.53	28.2	2.1	22.8	0.8	22.5	0.8	22.9	0.8
MK258_m8_19	matrix	0.0467	7.61	0.0223	8.07	0.00346	2.70	0.334	0.001092	2.81	22.3	1.8	22.2	0.6	22.2	0.6	22.1	0.6
MK258_m8_20	matrix	0.1009	22.52	0.0525	23.09	0.00378	5.08	0.220	0.001189	4.94	52.0	11.7	24.3	1.2	22.6	1.2	24.0	1.2
MK258_m9_1	matrix	0.2172	8.27	0.0841	11.23	0.00281	7.60	0.676	0.001399	9.80	82.0	8.8	18.1	1.4	14.0	1.4	28.2	2.8
MK258_m9_2	matrix	0.0639	14.20	0.0219	14.53	0.00249	3.10	0.214	0.000799	3.58	22.0	3.2	16.0	0.5	15.6	0.5	16.1	0.6
MK258_m9_3	matrix	0.0451	6.75	0.0154	7.59	0.00247	3.47	0.457	0.000793	3.51	15.5	1.2	16.0	0.6	15.9	0.6	16.0	0.6
MK258_m9_4	matrix	0.0488	6.47	0.0230	7.09	0.00342	2.90	0.409	0.001101	2.93	23.1	1.6	22.0	0.6	21.9	0.6	22.2	0.7
MK258_m9_5	matrix	0.0528	5.22	0.0251	5.89	0.00345	2.73	0.463	0.001108	2.79	25.2	1.5	22.2	0.6	22.0	0.6	22.4	0.6
MK258_m9_6	matrix	0.0446	8.05	0.0213	8.63	0.00346	3.10	0.360	0.001034	3.15	21.4	1.8	22.3	0.7	22.3	0.7	20.9	0.7
MK258_m9_7	matrix	0.0456	6.54	0.0213	7.24	0.00339	3.10	0.428	0.001032	3.01	21.4	1.5	22.0	0.7	21.8	0.7	20.8	0.6
MK258_m9_8	matrix	0.0463	5.65	0.0224	6.48	0.00351	3.17	0.490	0.001071	2.92	22.5	1.4	22.6	0.7	22.6	0.7	21.6	0.6
MK258_m9_9	matrix	0.0473	4.93	0.0224	5.46	0.00343	2.36	0.431	0.001083	2.63	22.4	1.2	22.0	0.5	22.0	0.5	21.9	0.6
MK258_m9_10	matrix	0.0477	7.85	0.0229	8.97	0.00348	4.34	0.484	0.001046	3.68	23.0	2.0	22.4	1.0	22.4	1.0	21.1	0.8
MK258_m9_11	matrix	0.0433	6.35	0.0207	7.39	0.00347	3.76	0.510	0.001049	3.74	20.8	1.5	22.3	0.8	22.4	0.8	21.2	0.8
MK258_m9_12	matrix	0.0473	8.12	0.0206	8.86	0.00315	3.55	0.401	0.000963	3.49	20.7	1.8	20.3	0.7	20.0	0.7	19.4	0.7
MK258_m9_13	matrix	0.0494	5.58	0.0234	6.21	0.00344	2.73	0.439	0.001094	2.71	23.5	1.4	22.2	0.6	22.1	0.6	22.1	0.6
MK258_m9_14	matrix	0.0515	5.68	0.0191	7.13	0.00269	4.32	0.606	0.000849	4.46	19.2	1.4	17.3	0.7	17.2	0.7	17.2	0.8
MK258_m9_15	matrix	0.0504	5.03	0.0239	6.32	0.00345	3.82	0.604	0.001081	3.57	24.0	1.5	22.2	0.8	22.0	0.8	21.8	0.8
MK258_m9_16	matrix	0.0655	5.54	0.0305	6.16	0.00338	2.70	0.438	0.001040	2.60	30.5	1.9	21.8	0.6	21.2	0.6	21.0	0.5
MK260																		
~~MK260_m1_1~~	~~garnet~~	~~0.0567~~	~~3.81~~	~~0.1471~~	~~19.88~~	~~0.01880~~	~~19.51~~	~~0.981~~	~~0.004199~~	~~18.10~~	~~139.0~~	~~25.9~~	~~120.0~~	~~23.2~~	~~118.8~~	~~23.2~~	~~84.7~~	~~15.3~~
MK260_m2_1	matrix	0.0669	10.48	0.0230	10.84	0.00250	2.76	0.254	0.000786	2.29	23.1	2.5	16.1	0.4	15.7	0.4	15.9	0.4
MK260_m2_2	matrix	0.0960	7.02	0.0352	7.75	0.00266	3.28	0.423	0.000836	3.16	35.1	2.7	17.1	0.6	16.0	0.6	16.9	0.5
MK260_m2_3	matrix	0.0697	10.23	0.0290	10.69	0.00302	3.10	0.290	0.000948	2.82	29.0	3.1	19.4	0.6	18.8	0.6	19.1	0.5
MK260_m2_4	matrix	0.0598	12.03	0.0245	12.49	0.00297	3.33	0.267	0.000926	3.32	24.5	3.0	19.0	0.6	19.0	0.6	18.7	0.6
MK260_m2_5	matrix	0.0626	10.94	0.0254	11.40	0.00294	3.19	0.280	0.000913	3.18	25.5	2.9	18.9	0.6	19.0	0.6	18.4	0.6
MK260_m2_6	matrix	0.0731	8.71	0.0297	9.30	0.00295	3.26	0.351	0.000892	3.51	29.8	2.7	19.0	0.6	18.0	0.6	18.0	0.6
MK260_m2_7	matrix	0.0979	8.36	0.0398	8.77	0.00295	2.65	0.302	0.000899	2.74	39.6	3.4	19.0	0.5	18.0	0.5	18.2	0.5
MK260_m2_8	matrix	0.1319	10.63	0.0556	11.24	0.00306	3.63	0.323	0.000879	3.29	54.9	6.0	20.0	0.7	18.0	0.7	17.8	0.6
MK260_m2_9	matrix	0.0546	7.69	0.0218	8.26	0.00290	3.03	0.367	0.000908	3.22	21.9	1.8	19.0	0.6	18.0	0.6	18.3	0.6
MK260_m2_10	matrix	0.0523	12.86	0.0206	13.28	0.00286	3.31	0.249	0.000890	3.53	20.7	2.7	18.0	0.6	18.0	0.6	18.0	0.6
MK260_m2_11	matrix	0.0476	17.64	0.0191	17.94	0.00291	3.29	0.183	0.000911	3.27	19.2	3.4	19.0	0.6	19.0	0.6	18.4	0.6
MK260_m2_12	matrix	0.0512	10.43	0.0204	11.03	0.00289	3.58	0.325	0.000901	3.33	20.5	2.2	19.0	0.7	19.0	0.7	18.2	0.6
MK260_m2_13	matrix	0.0471	8.90	0.0188	9.43	0.00290	3.11	0.330	0.000918	3.38	18.9	1.8	19.0	0.6	19.0	0.6	18.5	0.6
MK260_m2_14	matrix	0.0803	10.31	0.0361	10.68	0.00326	2.77	0.259	0.000993	2.84	36.0	3.8	21.0	0.6	20.0	0.6	20.1	0.6
MK260_m2_15	matrix	0.0712	8.45	0.0295	9.00	0.00301	3.09	0.343	0.000931	3.19	29.5	2.6	19.0	0.6	19.0	0.6	18.8	0.6
MK260_m2_16	matrix	0.0539	11.79	0.0229	12.25	0.00309	3.32	0.271	0.000933	3.18	23.0	2.8	20.0	0.7	20.0	0.7	18.8	0.6
MK260_m2_17	matrix	0.0536	12.53	0.0222	12.89	0.00300	3.05	0.236	0.000936	3.35	22.3	2.8	19.0	0.6	19.0	0.6	18.9	0.6
MK260_m2_18	matrix	0.0515	11.67	0.0205	12.02	0.00289	2.89	0.240	0.000913	3.00	20.6	2.5	19.0	0.5	18.0	0.5	18.4	0.6
MK260_m2_19	matrix	0.0822	15.77	0.0325	16.10	0.00287	3.24	0.201	0.000869	2.78	32.5	5.1	18.0	0.6	18.0	0.6	17.6	0.5
MK260_m2_20	matrix	0.1196	9.72	0.0508	10.44	0.00308	3.82	0.366	0.000904	2.83	50.3	5.1	20.0	0.8	18.0	0.8	18.3	0.5
MK260_m2_21	matrix	0.0473	15.64	0.0187	15.94	0.00286	3.07	0.193	0.000910	3.61	18.8	3.0	18.0	0.6	18.0	0.6	18.4	0.7
MK260_m2_22	matrix	0.0476	16.21	0.0194	16.51	0.00296	3.15	0.191	0.000935	3.43	19.5	3.2	19.0	0.6	19.0	0.6	18.9	0.6
MK260_m2_23	matrix	0.0387	20.42	0.0147	20.65	0.00276	3.09	0.150	0.000864	3.13	14.8	3.0	18.0	0.5	18.0	0.5	17.5	0.5
MK260_m2_24	matrix	0.0526	10.16	0.0207	10.60	0.00285	3.00	0.283	0.000910	3.08	20.8	2.2	18.0	0.5	18.0	0.5	18.4	0.6
MK260_m2_25	matrix	0.0488	15.51	0.0197	15.77	0.00294	2.85	0.181	0.000919	2.80	19.8	3.1	19.0	0.5	19.0	0.5	18.6	0.5
MK260_m2_26	matrix	0.0536	14.15	0.0222	14.59	0.00301	3.55	0.244	0.000927	2.79	22.3	3.2	19.0	0.7	19.0	0.7	18.7	0.5
MK260_m2_27	matrix	0.0491	11.56	0.0210	11.84	0.00310	2.55	0.215	0.000958	2.48	21.1	2.5	20.0	0.5	20.0	0.5	19.3	0.5

Table B1. Petrochronological data for monazite grains.

Grain #	Location	207Pb/206Pb	2SE %	Pb207/U235	2SE %	206Pb/238U	2SE %	rho	208Pb/232Th	2SE %	207Pb/235U (Ma)	2SE	206Pb/238U (Ma)	2SE	corr.206Pb/238U (Ma)	2SE	208Pb/232Th (Ma)	2SE
MK260_m2_28	matrix	0.0518	16.98	0.0209	17.25	0.00292	3.03	0.176	0.000898	3.15	21.0	3.6	19.0	0.6	19.0	0.6	18.1	0.6
MK260_m2_29	matrix	0.0500	12.15	0.0206	12.60	0.00299	3.36	0.266	0.000941	3.27	20.7	2.6	19.0	0.6	19.0	0.6	19.0	0.6
MK260_m2_30	matrix	0.0491	12.01	0.0194	12.34	0.00288	2.83	0.229	0.000904	3.50	19.6	2.4	19.0	0.5	18.0	0.5	18.3	0.6
MK260_m2_31	matrix	0.2144	15.64	0.0895	17.41	0.00303	7.64	0.439	0.000793	5.77	87.0	14.5	19.0	1.5	15.0	1.5	16.0	0.9
MK260_m2_32	matrix	0.0972	10.29	0.0535	10.85	0.00399	3.45	0.318	0.000958	3.35	52.9	5.6	26.0	0.9	20.0	0.9	19.3	0.6
MK260_m2_33	matrix	0.0557	8.02	0.0220	8.57	0.00287	3.04	0.354	0.000907	3.26	22.1	1.9	18.0	0.6	18.0	0.6	18.3	0.6
MK260_m2_34	matrix	0.0547	10.35	0.0218	10.82	0.00289	3.18	0.294	0.000915	3.32	21.9	2.3	20.0	0.6	18.0	0.6	18.5	0.6
MK260_m2_35	matrix	0.0667	9.18	0.0269	9.59	0.00293	2.80	0.292	0.000912	2.99	27.0	2.6	19.0	0.5	18.0	0.5	18.4	0.6
MK260_m2_36	matrix	0.2173	16.55	0.0991	20.31	0.00331	11.77	0.580	0.000880	6.97	96.0	18.6	21.0	2.5	17.0	2.5	17.8	1.2
MK260_m2_37	matrix	0.0712	14.39	0.0269	14.66	0.00274	2.82	0.193	0.000891	2.79	27.0	3.9	18.0	0.5	17.0	0.5	18.0	0.5
MK260_m2_38	matrix	0.0625	15.06	0.0267	15.54	0.00311	3.86	0.248	0.000945	4.00	26.8	4.1	20.0	0.8	20.0	0.8	19.1	0.8
MK260_m2_39	matrix	0.0457	13.19	0.0185	13.47	0.00294	2.73	0.203	0.000925	2.60	18.7	2.5	19.0	0.5	19.0	0.5	18.7	0.5
MK260_m2_40	matrix	0.0619	9.36	0.0256	9.87	0.00300	3.13	0.317	0.000947	3.09	25.7	2.5	19.0	0.6	19.0	0.6	19.1	0.6
MK260_m3_1	matrix	0.0532	13.03	0.0202	13.28	0.00275	2.60	0.196	0.000858	2.80	20.3	2.7	18.0	0.5	18.0	0.5	17.3	0.5
MK260_m3_2	matrix	0.0484	11.33	0.0197	11.80	0.00295	3.29	0.279	0.000933	3.21	19.8	2.3	19.0	0.6	19.0	0.6	18.8	0.6
MK260_m3_3	matrix	0.0827	8.93	0.0352	9.33	0.00308	2.69	0.289	0.000971	2.94	35.1	3.2	20.0	0.5	19.0	0.5	19.6	0.6
MK260_m3_4	matrix	0.0510	10.91	0.0205	11.38	0.00291	3.25	0.285	0.000925	3.20	20.6	2.3	19.0	0.6	19.0	0.6	18.7	0.6
MK260_m3_5	matrix	0.0532	8.36	0.0218	8.90	0.00297	3.04	0.342	0.000941	3.26	21.9	1.9	19.0	0.6	19.0	0.6	19.0	0.6
MK260_m3_6	matrix	0.0744	6.55	0.0310	6.96	0.00302	2.36	0.339	0.000935	2.54	31.0	2.1	19.0	0.5	19.0	0.5	18.9	0.5
MK260_m3_7	matrix	0.0512	11.00	0.0206	11.35	0.00292	2.79	0.246	0.000917	3.10	20.7	2.3	19.0	0.5	19.0	0.5	18.5	0.6
MK260_m3_8	matrix	0.0515	18.18	0.0181	18.45	0.00254	3.16	0.171	0.000804	2.94	18.2	3.3	16.0	0.5	16.0	0.5	16.2	0.5
MK260_m3_9	matrix	0.0530	11.99	0.0213	12.25	0.00291	2.53	0.206	0.000912	2.80	21.4	2.6	19.0	0.5	19.0	0.5	18.4	0.5
MK260_m3_10	matrix	0.0852	8.29	0.0358	8.72	0.00305	2.71	0.311	0.000921	2.94	35.7	3.1	20.0	0.5	19.0	0.5	18.6	0.5
MK260_m3_11	matrix	0.0525	11.23	0.0213	11.68	0.00295	3.22	0.275	0.000938	3.31	21.4	2.5	19.0	0.6	19.0	0.6	18.9	0.6
MK260_m3_12	matrix	0.0507	11.47	0.0203	11.83	0.00290	2.90	0.245	0.000915	2.83	20.4	2.4	19.0	0.5	19.0	0.5	18.5	0.5
MK260_m3_13	matrix	0.0525	9.89	0.0210	10.40	0.00290	3.24	0.311	0.000918	3.17	21.1	2.2	19.0	0.6	19.0	0.6	18.5	0.6
MK260_m3_14	matrix	0.0656	11.67	0.0271	11.95	0.00300	2.56	0.214	0.000946	2.93	27.2	3.2	19.0	0.5	19.0	0.5	19.1	0.6
MK260_m3_15	matrix	0.0610	9.45	0.0240	9.75	0.00286	2.36	0.242	0.000912	2.67	24.1	2.3	18.0	0.4	18.0	0.4	18.4	0.5
MK260_m3_16	matrix	0.0555	13.89	0.0220	14.11	0.00287	2.52	0.179	0.000911	2.55	22.1	3.1	18.0	0.5	18.0	0.5	18.4	0.5
MK260_m3_17	matrix	0.1107	9.73	0.0410	10.26	0.00269	3.27	0.319	0.000804	3.02	40.8	4.1	17.0	0.6	16.0	0.6	16.2	0.5
MK260_m3_18	matrix	0.0891	8.93	0.0307	9.65	0.00250	3.67	0.380	0.000772	3.48	30.7	2.9	16.0	0.6	15.0	0.6	15.6	0.5
MK260_m3_19	matrix	0.0625	11.65	0.0254	12.11	0.00295	3.31	0.273	0.000925	2.94	25.5	3.0	19.0	0.6	19.0	0.6	18.7	0.5
MK260_m3_20	matrix	0.2455	16.62	0.1254	19.44	0.00371	10.09	0.519	0.000868	5.84	120.0	22.0	24.0	2.4	18.0	2.4	17.5	1.0
MK260_m4_1	matrix	0.0687	12.73	0.0280	13.31	0.00296	3.90	0.293	0.000928	4.04	28.1	3.7	19.0	0.7	19.0	0.7	18.8	0.8
MK260_m4_2	matrix	0.0592	18.43	0.0197	18.73	0.00242	3.38	0.181	0.000743	3.51	19.8	3.7	16.0	0.5	20.0	0.5	15.0	0.5
~~MK260_m4_3~~	~~matrix~~	~~0.5967~~	~~7.13~~	~~1.2708~~	~~22.82~~	~~0.01545~~	~~21.68~~	~~0.950~~	~~0.003042~~	~~19.89~~	~~830.0~~	~~129.7~~	~~99.0~~	~~21.3~~	~~30.3~~	~~21.3~~	~~61.4~~	~~12.2~~
MK260_m4_4	matrix	0.0766	9.28	0.0303	9.92	0.00287	3.52	0.354	0.000886	3.92	30.3	3.0	20.0	0.6	18.0	0.6	17.9	0.7
MK260_m4_5	matrix	0.0852	9.32	0.0367	9.77	0.00313	2.93	0.300	0.000944	2.80	36.6	3.5	20.1	0.6	19.1	0.6	19.1	0.5
MK260_m4_6	matrix	0.0554	14.96	0.0228	15.20	0.00299	2.69	0.177	0.000934	2.58	22.9	3.4	19.0	0.5	19.0	0.5	18.9	0.5
MK260_m4_7	matrix	0.1516	29.23	0.0751	29.88	0.00359	6.17	0.206	0.001205	6.86	74.0	21.2	23.1	1.4	20.0	1.4	24.3	1.7
MK260_m4_8	matrix	0.0531	9.36	0.0222	9.92	0.00304	3.29	0.332	0.000959	3.10	22.3	2.2	19.5	0.6	19.0	0.6	19.4	0.6
MK260_m4_9	matrix	0.0481	11.09	0.0199	11.49	0.00301	3.01	0.262	0.000945	2.99	20.0	2.3	19.3	0.6	19.3	0.6	19.1	0.6
MK260_m4_10	matrix	0.0749	16.13	0.0236	16.79	0.00229	4.67	0.278	0.000695	4.85	23.7	3.9	15.0	0.7	14.2	0.7	14.0	0.7
MK260_m4_12	matrix	0.0549	19.65	0.0227	20.01	0.00300	3.77	0.188	0.000947	3.79	22.8	4.5	19.3	0.7	19.1	0.7	19.1	0.7
MK260_m4_13	matrix	0.0761	10.06	0.0329	10.70	0.00314	3.64	0.340	0.000965	3.31	32.8	3.5	20.2	0.7	19.4	0.7	19.5	0.6
MK260_m4_14	matrix	0.0470	14.59	0.0190	14.85	0.00294	2.74	0.184	0.000927	2.71	19.1	2.8	18.9	0.5	18.9	0.5	18.7	0.5
MK260_m4_15	matrix	0.0484	13.61	0.0196	13.91	0.00294	2.92	0.210	0.000929	3.15	19.7	2.7	18.9	0.6	18.9	0.6	18.8	0.6
MK260_m4_16	matrix	0.0476	17.36	0.0195	17.62	0.00297	3.01	0.171	0.000931	3.22	19.6	3.4	19.1	0.6	19.1	0.6	18.8	0.6
MK260_m4_17	matrix	0.0453	16.11	0.0188	16.42	0.00302	3.21	0.195	0.000946	3.24	19.0	3.1	19.4	0.6	19.4	0.6	19.1	0.6
MK260_m4_18	matrix	0.0472	18.69	0.0198	19.07	0.00304	3.79	0.199	0.000955	3.09	19.9	3.8	19.6	0.7	19.5	0.7	19.3	0.6
MK260_m4_19	matrix	0.0490	15.48	0.0201	15.77	0.00298	3.01	0.191	0.000937	2.99	20.2	3.2	19.2	0.6	19.1	0.6	18.9	0.6
MK260_m4_20	matrix	0.1037	7.92	0.0402	8.52	0.00281	3.15	0.369	0.000875	3.27	40.0	3.3	18.1	0.6	16.8	0.6	17.7	0.6
MK260_m4_21	matrix	0.0746	11.22	0.0314	11.59	0.00305	2.89	0.250	0.000949	2.91	31.4	3.6	19.7	0.6	19.0	0.6	19.2	0.6
MK260_m4_22	matrix	0.1007	9.57	0.0433	9.92	0.00312	2.61	0.263	0.000944	2.80	43.0	4.2	20.1	0.5	18.7	0.5	19.1	0.5
MK260_m4_23	matrix	0.0790	12.86	0.0254	13.18	0.00233	2.92	0.222	0.000756	3.03	25.5	3.3	15.0	0.4	14.4	0.4	15.3	0.5
MK260_m4_24	matrix	0.1701	8.25	0.0572	9.22	0.00244	4.12	0.446	0.000709	3.35	56.5	5.1	15.7	0.6	13.2	0.6	14.3	0.5
MK260_m4_25	matrix	0.0438	19.12	0.0156	19.32	0.00258	2.77	0.143	0.000810	2.75	15.7	3.0	16.6	0.5	16.7	0.5	16.4	0.4

Table B1. Petrochronological data for monazite grains.

Grain #	Location	207Pb/206Pb	2SE %	Pb207/U235	2SE %	206Pb/238U	2SE %	rho	208Pb/232Th	2SE %	207Pb/235U (Ma)	2SE	206Pb/238U (Ma)	2SE	corr.206Pb/238U (Ma)	2SE	208Pb/232Th (Ma)	2SE
MK260_m4_26	matrix	0.0555	22.93	0.0230	23.12	0.00300	2.97	0.129	0.000929	2.97	23.1	5.3	19.3	0.6	19.1	0.6	18.8	0.6
MK260_m4_27	matrix	0.0467	13.89	0.0193	14.23	0.00299	3.09	0.217	0.000945	2.84	19.4	2.7	19.3	0.6	19.3	0.6	19.1	0.5
MK260_m4_28	matrix	0.0456	17.07	0.0186	17.29	0.00296	2.71	0.157	0.000937	2.86	18.7	3.2	19.1	0.5	19.1	0.5	18.9	0.5
MK260_m4_29	matrix	0.1331	9.14	0.0615	9.72	0.00335	3.33	0.342	0.000984	3.08	60.6	5.7	21.6	0.7	19.2	0.7	19.9	0.6
MK260_m4_30	matrix	0.0481	14.55	0.0200	14.86	0.00302	3.02	0.203	0.000951	2.74	20.1	3.0	19.5	0.6	19.4	0.6	19.2	0.5
~~MK260_m5_1~~	~~matrix~~	~~0.6364~~	~~5.39~~	~~1.5642~~	~~25.94~~	~~0.01783~~	~~25.37~~	~~0.978~~	~~0.003492~~	~~20.65~~	~~960.0~~	~~160.6~~	~~114.0~~	~~28.7~~	~~29.2~~	~~28.7~~	~~70.4~~	~~14.5~~
MK260_m5_2	matrix	0.0803	25.76	0.0257	26.23	0.00232	4.92	0.187	0.000689	4.24	25.8	6.7	15.0	0.7	14.3	0.7	13.9	0.6
MK260_m5_3	matrix	0.0493	12.95	0.0161	13.42	0.00237	3.50	0.261	0.000724	2.75	16.2	2.2	15.2	0.5	15.2	0.5	14.6	0.4
MK260_m5_4	matrix	0.0820	13.03	0.0285	13.34	0.00253	2.89	0.217	0.000760	3.03	28.6	3.8	16.3	0.5	15.5	0.5	15.3	0.5
MK260_m5_5	matrix	0.0804	18.02	0.0256	18.39	0.00231	3.66	0.199	0.000726	3.88	25.7	4.7	14.9	0.5	14.2	0.5	14.7	0.6
MK260_m5_10	matrix	0.4859	5.77	0.3711	10.15	0.00554	8.36	0.823	0.001261	6.95	320.0	27.9	35.6	3.0	15.8	3.0	25.5	1.8
MK260_m6_1	garnet	0.0546	7.60	0.0412	8.35	0.00548	3.47	0.415	0.001720	3.67	41.0	3.4	35.2	1.2	34.9	1.2	34.7	1.3
MK260_m6_2	garnet	0.0557	7.28	0.0429	8.04	0.00559	3.41	0.425	0.001682	2.82	42.7	3.4	36.0	1.2	36.0	1.2	34.0	1.0
~~MK260_m6_3~~	~~garnet~~	~~0.0113~~	~~672.86~~	~~0.0103~~	~~673.07~~	~~0.00662~~	~~16.50~~	~~0.025~~	~~0.003154~~	~~24.51~~	~~10.0~~	~~69.7~~	~~42.5~~	~~7.0~~	~~44.4~~	~~7.0~~	~~63.6~~	~~15.6~~
MK260_m7_1	matrix	0.0554	21.05	0.0225	21.29	0.00295	3.15	0.148	0.000903	3.07	22.6	4.8	19.0	0.6	18.8	0.6	18.2	0.6
MK260_m7_2	matrix	0.0684	15.24	0.0273	15.49	0.00290	2.81	0.182	0.000912	2.54	27.4	4.2	19.0	0.5	18.1	0.5	18.4	0.5
MK260_m7_3	matrix	0.0713	14.88	0.0267	15.45	0.00272	4.17	0.270	0.000849	4.92	26.8	4.1	17.5	0.7	17.0	0.7	17.2	0.8
MK260_m7_4	matrix	0.0929	14.81	0.0316	15.48	0.00247	4.51	0.291	0.000739	4.44	31.6	4.8	15.9	0.7	14.9	0.7	14.9	0.7
MK260_m7_5	matrix	0.0570	12.42	0.0230	12.76	0.00292	2.94	0.231	0.000915	2.48	23.1	2.9	18.8	0.6	18.5	0.6	18.5	0.5
MK260_m7_6	matrix	0.0758	15.90	0.0256	16.66	0.00245	4.96	0.298	0.000817	5.39	25.7	4.2	16.0	0.8	15.2	0.8	16.5	0.9
MK260_m7_7	matrix	0.0759	11.87	0.0270	12.19	0.00258	2.79	0.229	0.000801	3.32	27.0	3.3	16.6	0.5	16.0	0.5	16.2	0.5
MK260_m7_8	matrix	0.0778	11.76	0.0295	12.63	0.00276	4.62	0.366	0.000810	4.43	29.6	3.7	18.0	0.8	17.0	0.8	16.4	0.7
~~MK260_m7_10~~	~~matrix~~	~~0.8411~~	~~44.84~~	~~0.6349~~	~~49.24~~	~~0.00548~~	~~20.36~~	~~0.413~~	~~0.001466~~	~~20.52~~	~~500.0~~	~~194.2~~	~~35.2~~	~~7.1~~	~~0.2~~	~~7.1~~	~~29.6~~	~~6.1~~
MK260_m7_11	matrix	0.0526	10.55	0.0217	11.22	0.00299	3.82	0.340	0.000928	3.65	21.8	2.4	19.2	0.7	19.0	0.7	18.7	0.7
MK260_m7_12	matrix	0.0525	13.74	0.0216	14.08	0.00298	3.10	0.220	0.000912	3.10	21.7	3.0	19.2	0.6	19.0	0.6	18.4	0.6
MK260_m7_13	matrix	0.0695	16.70	0.0285	17.20	0.00297	4.11	0.239	0.000925	3.33	28.5	4.8	19.1	0.8	18.6	0.8	18.7	0.6
MK260_m7_14	matrix	0.0540	14.40	0.0217	14.87	0.00291	3.72	0.250	0.000902	3.34	21.8	3.2	18.7	0.7	19.0	0.7	18.2	0.6
MK260_m7_15	matrix	0.0526	19.34	0.0214	19.69	0.00295	3.72	0.189	0.000917	3.16	21.5	4.2	19.0	0.7	18.8	0.7	18.5	0.6
MK260_m7_16	matrix	0.0672	11.70	0.0282	11.95	0.00304	2.42	0.203	0.000908	2.90	28.2	3.3	19.6	0.5	19.0	0.5	18.3	0.5
MK260_m7_17	matrix	0.1705	10.92	0.0703	12.43	0.00299	5.94	0.478	0.000874	6.27	68.9	8.3	19.0	1.1	16.2	1.1	17.6	1.1
MK260_m7_18	matrix	0.1905	13.78	0.0866	14.65	0.00330	4.98	0.340	0.000922	4.78	84.0	11.9	21.2	1.1	17.0	1.1	18.6	0.9
MK260_m7_19	matrix	0.0965	12.62	0.0404	13.02	0.00304	3.18	0.244	0.000906	3.45	40.2	5.1	19.5	0.6	18.3	0.6	18.3	0.6
MK260_m7_20	matrix	0.0746	15.60	0.0307	15.92	0.00299	3.19	0.201	0.000921	3.40	30.7	4.8	19.2	0.6	19.0	0.6	18.6	0.6
MK260_m8_1	matrix	0.0624	15.84	0.0242	16.29	0.00282	3.79	0.233	0.000890	4.11	24.3	3.9	18.0	0.7	18.0	0.7	18.0	0.7
MK260_m8_2	matrix	0.0866	13.68	0.0345	13.97	0.00289	2.87	0.205	0.000848	2.59	34.5	4.7	18.6	0.5	18.0	0.5	17.1	0.4
MK260_m8_3	matrix	0.0822	9.23	0.0307	9.84	0.00271	3.41	0.346	0.000793	3.30	30.7	3.0	17.0	0.6	17.0	0.6	16.0	0.5
MK260_m8_4	matrix	0.1002	15.96	0.0410	16.30	0.00297	3.29	0.202	0.000858	3.24	40.8	6.5	19.0	0.6	18.0	0.6	17.3	0.6
MK260_m8_5	matrix	0.0731	13.52	0.0300	13.91	0.00298	3.25	0.234	0.000868	3.52	30.0	4.1	19.0	0.6	19.0	0.6	17.5	0.6
MK260_m8_6	matrix	0.0606	10.81	0.0225	11.24	0.00270	3.10	0.276	0.000776	3.25	22.6	2.5	17.0	0.5	17.0	0.5	15.7	0.5
MK260_m8_7	matrix	0.0617	14.99	0.0246	15.36	0.00290	3.38	0.220	0.000816	3.50	24.7	3.7	19.0	0.6	18.0	0.6	16.5	0.6
MK260_m8_8	matrix	0.0725	16.07	0.0254	16.42	0.00254	3.35	0.204	0.000807	3.40	25.5	4.1	16.0	0.5	16.0	0.5	16.3	0.6
MK260_m8_10	matrix	0.0911	12.51	0.0378	13.03	0.00301	3.67	0.282	0.000887	3.81	37.6	4.8	19.0	0.7	18.0	0.7	17.9	0.7
MK260_m8_11	matrix	0.0590	11.33	0.0240	11.86	0.00296	3.52	0.297	0.000838	3.10	24.1	2.8	19.0	0.7	19.0	0.7	16.9	0.5
~~MK260_m9_1~~	~~matrix~~	~~0.1646~~	~~57.48~~	~~0.0903~~	~~62.85~~	~~0.00398~~	~~25.42~~	~~0.404~~	~~0.001633~~	~~28.15~~	~~88.0~~	~~52.9~~	~~26.0~~	~~6.5~~	~~22.0~~	~~6.5~~	~~33.0~~	~~9.3~~
MK260_m9_2	matrix	0.0528	11.48	0.0186	11.77	0.00255	2.59	0.220	0.000810	2.53	18.7	2.2	16.0	0.4	16.0	0.4	16.4	0.4
MK260_m9_3	matrix	0.0626	13.23	0.0198	13.76	0.00230	3.76	0.273	0.000732	3.78	19.9	2.7	15.0	0.6	15.0	0.6	14.8	0.6
MK260_m9_4	matrix	0.0680	13.25	0.0221	13.58	0.00236	2.95	0.218	0.000741	2.73	22.2	3.0	15.0	0.4	15.0	0.4	15.0	0.4
MK260_m9_5	matrix	0.0647	11.82	0.0226	12.28	0.00254	3.34	0.272	0.000778	3.04	22.7	2.8	16.0	0.5	16.0	0.5	15.7	0.5
MK260_m9_6	matrix	0.0658	16.20	0.0211	17.03	0.00232	5.26	0.309	0.000701	5.54	21.2	3.6	15.0	0.8	15.0	0.8	14.2	0.8
MK260_m9_7	matrix	0.0641	15.33	0.0203	15.74	0.00230	3.59	0.228	0.000696	3.59	20.4	3.2	15.0	0.5	14.0	0.5	14.1	0.5
MK260_m9_8	matrix	0.0540	10.54	0.0205	11.40	0.00276	4.33	0.380	0.000855	3.56	20.6	2.3	18.0	0.8	18.0	0.8	17.3	0.6
MK260_m9_9	matrix	0.0554	13.63	0.0183	13.93	0.00240	2.87	0.206	0.000748	2.78	18.5	2.5	15.0	0.4	15.0	0.4	15.1	0.4
MK260_m9_10	matrix	0.1462	19.19	0.0460	20.23	0.00228	6.41	0.317	0.000691	6.36	45.6	9.0	15.0	0.9	13.0	0.9	14.0	0.9
MK260_m9_11	matrix	0.1035	17.19	0.0392	17.76	0.00274	4.45	0.251	0.000829	4.66	39.0	6.8	18.0	0.8	16.0	0.8	16.8	0.8
MK260_m9_12	matrix	0.0687	11.90	0.0281	12.14	0.00296	2.42	0.199	0.000933	2.90	28.1	3.4	19.0	0.5	19.0	0.5	18.8	0.5
MK260_m9_13	matrix	0.0645	15.85	0.0268	16.09	0.00301	2.78	0.173	0.000937	2.98	26.8	4.3	19.0	0.5	19.0	0.5	18.9	0.6
MK260_m9_14	matrix	0.0851	9.64	0.0360	10.26	0.00307	3.51	0.342	0.000932	3.43	35.9	3.6	20.0	0.7	19.0	0.7	18.8	0.6

Table B1. Petrochronological data for monazite grains.

Grain #	Location	207Pb/206Pb	2SE %	Pb207/U235	2SE %	206Pb/238U	2SE %	rho	208Pb/232Th	2SE %	207Pb/235U (Ma)	2SE	206Pb/238U (Ma)	2SE	corr.206Pb/238U (Ma)	2SE	208Pb/232Th (Ma)	2SE
MK260_m9_15	matrix	0.1709	9.74	0.0628	10.54	0.00267	4.04	0.383	0.000792	3.33	61.8	6.3	17.0	0.7	14.0	0.7	16.0	0.5
MK260_m9_16	matrix	0.1733	12.17	0.0610	14.20	0.00255	7.33	0.516	0.000847	8.70	60.1	8.3	16.0	1.2	14.0	1.2	17.1	1.5
MK260_m9_17	matrix	0.1162	17.77	0.0406	18.82	0.00253	6.18	0.329	0.000833	5.73	40.4	7.4	16.0	1.0	10.0	1.0	16.8	1.0
MK260_m9_18	matrix	0.0818	9.39	0.0291	10.16	0.00258	3.88	0.382	0.000824	4.54	29.1	2.9	17.0	0.6	16.0	0.6	16.6	0.8
MK260_m9_19	matrix	0.0564	11.70	0.0196	12.07	0.00252	2.94	0.244	0.000785	2.96	19.7	2.4	16.0	0.5	16.0	0.5	15.8	0.5
MK260_m9_20	matrix	0.0534	12.80	0.0216	13.13	0.00294	2.91	0.222	0.000934	2.90	21.7	2.8	20.0	0.5	19.0	0.5	18.9	0.5
MK260_m9_21	matrix	0.1232	17.93	0.0468	18.38	0.00275	4.04	0.220	0.000873	3.19	46.4	8.3	18.0	0.7	16.0	0.7	17.6	0.6
MK260_m9_22	matrix	0.0648	11.82	0.0261	12.30	0.00292	3.38	0.274	0.000937	3.23	26.2	3.2	19.0	0.6	18.0	0.6	18.9	0.6
MK260_m9_23	matrix	0.0534	7.32	0.0214	7.96	0.00291	3.13	0.393	0.000940	3.40	21.5	1.7	19.0	0.6	19.0	0.6	19.0	0.6
MK260_m9_24	matrix	0.0634	16.09	0.0259	16.50	0.00297	3.66	0.222	0.000915	3.95	26.0	4.2	19.0	0.7	19.0	0.7	18.5	0.7
MK260_m9_25	matrix	0.0983	11.10	0.0422	11.90	0.00312	4.27	0.359	0.000950	4.24	42.0	4.9	20.0	0.9	19.0	0.9	19.2	0.8
MK262																		
~~MK262_m1_1~~	~~garnet~~	~~0.2446~~	~~71.58~~	~~0.1593~~	~~73.58~~	~~0.00473~~	~~17.04~~	~~0.232~~	~~0.001624~~	~~16.20~~	~~150.0~~	~~102.7~~	~~30.4~~	~~5.2~~	~~22.8~~	~~5.2~~	~~32.8~~	~~5.3~~
MK262_m1_3	garnet	0.1063	4.26	0.0611	4.67	0.00417	1.92	0.412	0.001302	2.07	60.3	2.7	26.8	0.5	24.8	0.5	26.3	0.5
MK262_m1_4	garnet	0.1248	4.08	0.0743	4.37	0.00432	1.57	0.358	0.001329	1.86	72.8	3.1	27.8	0.4	25.0	0.4	26.8	0.5
MK262_m1_5	garnet	0.0949	3.22	0.0548	3.62	0.00419	1.65	0.456	0.001381	1.83	54.2	1.9	27.0	0.4	25.0	0.4	27.9	0.5
MK262_m1_6	garnet	0.0982	3.90	0.0546	4.29	0.00403	1.80	0.420	0.001267	1.84	53.9	2.3	25.9	0.5	24.0	0.5	25.6	0.5
MK262_m1_7	garnet	0.0950	6.31	0.0503	6.57	0.00385	1.83	0.279	0.001158	1.89	49.9	3.2	24.7	0.5	23.2	0.5	23.4	0.4
MK262_m2_1	garnet	0.1245	5.82	0.0785	6.03	0.00457	1.59	0.263	0.001436	1.69	76.7	4.5	29.4	0.5	26.5	0.5	29.0	0.5
MK262_m2_2	garnet	0.1256	3.79	0.0777	4.41	0.00449	2.25	0.511	0.001381	2.25	76.0	3.2	28.9	0.6	26.0	0.6	27.9	0.6
MK262_m2_3	garnet	0.1040	3.74	0.0828	5.80	0.00578	4.44	0.765	0.001650	3.68	80.8	4.5	37.1	1.6	34.5	1.6	33.3	1.2
MK262_m2_4	garnet	0.1667	21.35	0.1079	23.07	0.00470	8.76	0.379	0.001726	9.63	104.0	22.8	30.2	2.6	25.6	2.6	34.8	3.4
MK262_m2_5	garnet	0.1166	4.16	0.0721	4.51	0.00449	1.76	0.390	0.001408	2.06	70.7	3.1	28.9	0.5	26.3	0.5	28.4	0.6
MK262_m2_6	garnet	0.1102	4.90	0.0680	5.24	0.00447	1.84	0.351	0.001390	2.18	66.8	3.4	28.8	0.5	26.5	0.5	28.1	0.6
MK262_m2_7	garnet	0.1197	4.38	0.0745	4.85	0.00452	2.09	0.431	0.001378	2.41	73.0	3.4	29.0	0.6	26.4	0.6	27.8	0.7
~~MK262_m3_1~~	~~garnet (crack)~~	~~0.2995~~	~~49.61~~	~~0.3949~~	~~52.75~~	~~0.00957~~	~~17.94~~	~~0.340~~	~~0.007166~~	~~33.19~~	~~340.0~~	~~151.6~~	~~61.4~~	~~11.0~~	~~41.9~~	~~11.0~~	~~144.2~~	~~47.7~~
~~MK262_m3_2~~	~~garnet (crack)~~	~~0.1022~~	~~339.64~~	~~0.0582~~	~~340.37~~	~~0.00413~~	~~22.25~~	~~0.065~~	~~0.001903~~	~~25.97~~	~~60.0~~	~~190.0~~	~~26.6~~	~~5.9~~	~~24.7~~	~~5.9~~	~~38.4~~	~~10.0~~
MK262_m3_4	garnet (crack)	0.1478	5.69	0.0855	6.23	0.00420	2.52	0.406	0.001253	2.69	83.3	5.0	27.0	0.7	23.5	0.7	25.3	0.7
MK262_m3_5	garnet (crack)	0.1159	3.76	0.0689	4.21	0.00431	1.91	0.452	0.001298	2.06	67.6	2.8	27.7	0.5	25.3	0.5	26.2	0.5
MK262_m4_1	matrix	0.1048	11.16	0.0382	11.37	0.00264	2.19	0.193	0.000845	2.09	38.1	4.2	17.0	0.4	15.8	0.4	17.1	0.4
MK262_m4_2	matrix	0.0579	20.14	0.0202	20.26	0.00253	2.23	0.110	0.000788	2.08	20.3	4.1	16.3	0.4	16.1	0.4	15.9	0.3
MK262_m4_3	matrix	0.0585	16.39	0.0196	16.56	0.00243	2.39	0.144	0.000757	2.08	19.7	3.2	15.7	0.4	15.4	0.4	15.3	0.3
MK262_m4_4	matrix	0.0572	15.19	0.0203	15.32	0.00258	1.99	0.130	0.000788	1.93	20.4	3.1	16.6	0.3	16.4	0.3	15.9	0.3
MK262_m4_5	matrix	0.0693	16.94	0.0286	17.13	0.00300	2.57	0.150	0.000911	2.57	28.7	4.8	19.3	0.5	18.7	0.5	18.4	0.5
MK262_m4_6	matrix	0.0871	14.18	0.0330	14.40	0.00275	2.55	0.177	0.000870	2.63	32.9	4.7	17.7	0.5	16.8	0.5	17.6	0.5
MK262_m4_7	matrix	0.0930	21.04	0.0403	21.18	0.00314	2.45	0.116	0.000945	2.44	40.1	8.3	20.2	0.5	19.0	0.5	19.1	0.5
MK262_m4_8	matrix	0.1083	3.76	0.0671	4.16	0.00450	1.79	0.430	0.001365	1.90	66.0	2.7	28.9	0.5	26.7	0.5	27.6	0.5
MK262_m4_9	matrix	0.1194	5.36	0.0731	6.22	0.00444	3.15	0.506	0.001282	4.21	71.7	4.3	28.6	0.9	26.0	0.9	25.9	1.1
MK262_m4_10	matrix	0.0805	10.95	0.0365	11.72	0.00329	4.18	0.357	0.000972	2.84	36.4	4.2	21.2	0.9	20.3	0.9	19.6	0.6
MK262_m4_11	matrix	0.1169	4.09	0.0711	4.85	0.00441	2.62	0.540	0.001355	3.02	69.8	3.3	28.4	0.7	25.9	0.7	27.4	0.8
MK262_m4_12	matrix	0.1344	5.96	0.0839	6.40	0.00453	2.31	0.361	0.001326	2.70	81.8	5.0	29.1	0.7	25.9	0.7	26.8	0.7
MK262_m4_13	matrix	0.1266	3.55	0.0834	4.15	0.00478	2.15	0.518	0.001504	2.22	81.3	3.2	30.7	0.7	27.6	0.7	30.4	0.7
MK262_m4_14	matrix	0.1157	3.53	0.0742	4.01	0.00466	1.90	0.474	0.001425	2.05	72.7	2.8	29.9	0.6	27.3	0.6	28.8	0.6
MK262_m4_15	matrix	0.1847	13.60	0.0661	14.14	0.00260	3.87	0.273	0.000931	7.85	65.0	8.9	16.7	0.6	13.8	0.6	18.8	1.5
MK262_m4_16	matrix	0.1211	10.20	0.0698	11.38	0.00418	5.03	0.443	0.001039	1.49	68.5	7.5	26.9	1.4	24.4	1.4	21.0	0.3
MK262_m4_17	matrix	0.1090	2.99	0.0682	3.68	0.00454	2.14	0.582	0.001408	2.25	67.0	2.4	29.2	0.6	26.9	0.6	28.4	0.6
MK262_m4_18	matrix	0.1226	2.83	0.0789	3.53	0.00467	2.11	0.596	0.001411	2.39	77.2	2.6	30.0	0.6	27.2	0.6	28.5	0.7
MK262_m4_19	matrix	0.0972	6.47	0.0553	7.04	0.00413	2.78	0.395	0.001148	1.57	54.7	3.7	26.5	0.7	25.0	0.7	23.2	0.4
MK262_m4_20	matrix	0.1011	4.05	0.0583	4.74	0.00419	2.45	0.518	0.001249	2.59	57.5	2.7	27.0	0.7	25.1	0.7	25.2	0.7
MK262_m4_21	matrix	0.0845	6.91	0.0449	7.16	0.00386	1.88	0.262	0.001155	2.37	44.6	3.1	24.8	0.5	24.0	0.5	23.3	0.6
MK262_m4_22	matrix	0.1066	7.99	0.0509	8.50	0.00346	2.91	0.342	0.001051	3.14	50.4	4.2	22.3	0.6	20.6	0.6	21.2	0.7
MK262_m4_23	matrix	0.1806	10.86	0.0752	11.30	0.00302	3.14	0.278	0.000995	3.26	73.6	8.0	19.5	0.6	16.2	0.6	20.1	0.7
MK262_m4_24	matrix	0.1066	16.79	0.0456	16.97	0.00310	2.42	0.143	0.000929	2.75	45.2	7.5	20.0	0.5	18.4	0.5	18.8	0.5
MK262_m4_25	matrix	0.1308	8.24	0.0650	9.14	0.00360	3.97	0.434	0.001012	2.96	63.9	5.7	23.2	0.9	20.7	0.9	20.4	0.6
MK262_m4_26	matrix	0.1343	8.62	0.0704	9.70	0.00380	4.44	0.458	0.001013	2.39	69.0	6.5	24.5	1.1	21.7	1.1	20.5	0.5
MK262_m4_27	matrix	0.1118	4.39	0.0699	4.61	0.00454	1.41	0.305	0.001393	1.65	68.6	3.1	29.0	0.4	26.8	0.4	28.1	0.5

Table B1. Petrochronological data for monazite grains.

Grain #	Location	207Pb/206Pb	2SE %	Pb207/U235	2SE %	206Pb/238U	2SE %	rho	208Pb/232Th	2SE %	207Pb/235U (Ma)	2SE	206Pb/238U (Ma)	2SE	corr.206Pb/238U (Ma)	2SE	208Pb/232Th (Ma)	2SE
MK262_m4_28	matrix	0.1120	2.31	0.0696	2.72	0.00451	1.43	0.526	0.001386	1.75	68.3	1.8	29.0	0.4	27.0	0.4	28.0	0.5
MK262_m4_29	matrix	0.1195	3.36	0.0749	3.86	0.00455	1.89	0.490	0.001391	2.28	73.4	2.7	29.0	0.6	26.6	0.6	28.1	0.6
MK262_m4_30	matrix	0.1344	3.66	0.0868	4.11	0.00469	1.86	0.454	0.001433	2.13	84.5	3.3	30.1	0.6	27.0	0.6	28.9	0.6
MK262_m4_31	matrix	0.1138	3.18	0.0694	4.01	0.00443	2.43	0.607	0.001345	2.54	68.2	2.6	28.0	0.7	26.1	0.7	27.2	0.7
MK262_m5_1	matrix	0.3810	13.58	0.2095	15.36	0.00399	7.18	0.467	0.000896	5.83	193.0	27.0	26.0	1.8	15.0	1.8	18.1	1.1
MK262_m5_2	matrix	0.1085	12.67	0.0379	12.95	0.00253	2.69	0.208	0.000740	2.25	37.7	4.8	16.0	0.4	15.0	0.4	14.9	0.3
MK262_m5_3	matrix	0.2189	10.77	0.0877	11.26	0.00291	3.29	0.292	0.000792	2.56	85.4	9.2	19.0	0.6	15.0	0.6	16.0	0.4
MK262_m5_4	matrix	0.0734	13.84	0.0290	14.06	0.00287	2.49	0.177	0.000868	2.75	29.0	4.0	18.0	0.5	18.0	0.5	17.5	0.5
MK262_m5_5	matrix	0.0903	6.97	0.0460	7.11	0.00370	1.42	0.199	0.001092	1.94	45.7	3.2	24.0	0.3	22.0	0.3	22.1	0.4
MK262_m5_6	matrix	0.0842	7.76	0.0392	8.20	0.00338	2.63	0.320	0.000997	2.11	39.1	3.1	22.0	0.6	21.0	0.6	20.1	0.4
MK262_m5_7	matrix	0.1226	4.81	0.0769	5.04	0.00455	1.50	0.297	0.001381	1.73	75.3	3.7	29.0	0.4	26.0	0.4	27.9	0.5
MK262_m5_8	matrix	0.1156	5.79	0.0737	6.19	0.00463	2.20	0.356	0.001414	2.38	72.2	4.3	30.0	0.7	27.0	0.7	28.6	0.7
MK262_m5_9	matrix	0.0993	8.24	0.0477	8.74	0.00349	2.90	0.332	0.000994	3.05	47.3	4.0	22.0	0.6	21.0	0.6	20.1	0.6
MK262_m5_10	matrix	0.1107	3.76	0.0615	4.72	0.00403	2.86	0.605	0.001181	2.85	60.6	2.8	26.0	0.7	24.0	0.7	23.9	0.7
MK262_m5_11	matrix	0.1157	3.38	0.0719	4.08	0.00451	2.28	0.559	0.001392	2.33	70.5	2.8	29.0	0.7	26.0	0.7	28.1	0.7
MK262_m5_12	matrix	0.1192	2.93	0.0757	3.63	0.00461	2.14	0.590	0.001416	2.22	74.1	2.6	29.6	0.6	27.0	0.6	28.6	0.6
MK262_m5_13	matrix	0.1246	4.52	0.0794	5.23	0.00463	2.63	0.503	0.001426	3.15	77.6	3.9	29.8	0.8	26.8	0.8	28.8	0.9
MK262_m5_14	matrix	0.1227	5.83	0.0775	6.34	0.00458	2.49	0.393	0.001428	2.53	75.8	4.6	29.5	0.7	26.6	0.7	28.8	0.7
MK262_m5_15	matrix	0.1041	8.49	0.0489	9.06	0.00341	3.16	0.349	0.000945	2.95	48.5	4.3	21.9	0.7	20.4	0.7	19.1	0.6
MK262_m5_16	matrix	0.1323	3.13	0.0754	3.79	0.00414	2.14	0.565	0.001183	1.65	73.8	2.7	26.6	0.6	23.7	0.6	23.9	0.4
MK262_m5_17	matrix	0.1228	4.05	0.0773	4.56	0.00457	2.09	0.458	0.001415	2.42	75.6	3.3	29.4	0.6	26.6	0.6	28.6	0.7
MK262_m5_18	matrix	0.1323	2.75	0.0842	3.62	0.00461	2.36	0.652	0.001406	2.49	82.0	2.9	29.7	0.7	26.5	0.7	28.4	0.7
MK262_m5_19	matrix	0.1183	2.96	0.0750	3.50	0.00460	1.86	0.533	0.001424	1.59	73.4	2.5	29.6	0.6	26.9	0.6	28.7	0.5
MK262_m5_20	matrix	0.1155	4.29	0.0721	4.61	0.00453	1.68	0.364	0.001396	1.54	70.6	3.1	29.1	0.5	26.6	0.5	28.2	0.4
MK262_m5_21	matrix	0.1146	2.80	0.0712	3.74	0.00451	2.48	0.663	0.001383	2.44	69.8	2.5	29.0	0.7	26.5	0.7	27.9	0.7
MK262_m5_22	matrix	0.1210	3.44	0.0761	4.00	0.00456	2.05	0.512	0.001407	2.17	74.5	2.9	29.3	0.6	26.6	0.6	28.4	0.6
MK262_m5_23	matrix	0.1206	4.81	0.0779	5.31	0.00469	2.26	0.426	0.001467	2.26	76.1	3.9	30.1	0.7	27.3	0.7	29.6	0.7
MK262_m5_24	matrix	0.1361	3.55	0.0883	3.88	0.00471	1.56	0.401	0.001430	2.01	85.9	3.2	30.3	0.5	26.8	0.5	28.9	0.6
MK262_m5_25	matrix	0.1335	3.38	0.0869	4.08	0.00472	2.29	0.561	0.001412	2.20	84.6	3.3	30.4	0.7	27.0	0.7	28.5	0.6
MK262_m5_26	matrix	0.1137	3.87	0.0708	4.50	0.00452	2.31	0.512	0.001388	2.71	69.5	3.0	29.0	0.7	26.6	0.7	28.0	0.8
MK262_m5_27	matrix	0.1413	3.43	0.0906	4.27	0.00465	2.56	0.598	0.001388	2.68	88.0	3.6	29.9	0.8	26.0	0.8	28.0	0.8
MK262_m5_28	matrix	0.1279	3.41	0.0823	4.21	0.00467	2.47	0.586	0.001417	2.45	80.3	3.3	30.0	0.7	27.0	0.7	28.6	0.7
MK262_m5_29	matrix	0.1319	3.10	0.0835	3.70	0.00459	2.02	0.546	0.001377	2.46	81.4	2.9	29.5	0.6	26.4	0.6	27.8	0.7
MK262_m6_1	matrix	0.0588	10.44	0.0240	10.84	0.00296	2.89	0.267	0.000915	2.37	24.1	2.6	19.1	0.6	18.8	0.6	18.5	0.4
MK262_m6_2	matrix	0.0724	10.55	0.0297	10.71	0.00298	1.81	0.169	0.000924	2.02	29.7	3.1	19.2	0.3	18.5	0.3	18.7	0.4
MK262_m6_3	matrix	0.1529	12.31	0.0774	12.82	0.00367	3.58	0.279	0.001013	2.53	76.0	9.3	23.6	0.8	20.5	0.8	20.5	0.5
MK262_m6_4	matrix	0.2218	15.22	0.1011	16.13	0.00331	5.33	0.331	0.000836	3.18	98.0	15.0	21.3	1.1	16.6	1.1	16.9	0.5
MK262_m6_5	matrix	0.0943	18.00	0.0335	18.33	0.00257	3.44	0.188	0.000779	2.07	33.4	6.0	16.6	0.6	15.6	0.6	15.7	0.3
MK262_m6_6	matrix	0.0622	11.36	0.0238	11.50	0.00278	1.82	0.158	0.000861	1.70	23.9	2.7	17.9	0.3	17.5	0.3	17.4	0.3
MK262_m6_7	matrix	0.0750	15.57	0.0344	15.82	0.00333	2.82	0.178	0.001010	2.46	34.4	5.3	21.4	0.6	20.7	0.6	20.4	0.5
MK262_m6_8	matrix	0.0860	6.91	0.0458	7.18	0.00386	1.97	0.275	0.001182	2.01	45.4	3.2	24.8	0.5	23.6	0.5	23.9	0.5
MK262_m6_9	matrix	0.0901	7.16	0.0468	7.56	0.00377	2.41	0.319	0.001121	2.13	46.5	3.4	24.3	0.6	22.9	0.6	22.6	0.5
MK262_m6_10	matrix	0.1093	10.54	0.0544	10.76	0.00361	2.18	0.202	0.001038	2.13	53.8	5.6	23.2	0.5	21.4	0.5	21.0	0.4
MK262_m6_11	matrix	0.0847	12.55	0.0325	12.93	0.00278	3.11	0.240	0.000850	2.66	32.5	4.1	17.9	0.6	17.1	0.6	17.2	0.5
MK262_m6_12	matrix	0.0912	5.83	0.0480	6.43	0.00381	2.71	0.422	0.001164	2.28	47.6	3.0	24.5	0.7	23.2	0.7	23.5	0.5
MK262_m6_13	matrix	0.1084	6.90	0.0615	7.31	0.00412	2.41	0.330	0.001229	2.82	60.6	4.3	26.5	0.6	24.4	0.6	24.8	0.7
MK262_m6_14	matrix	0.1188	3.46	0.0760	4.46	0.00464	2.82	0.632	0.001441	2.40	74.3	3.2	29.8	0.8	27.1	0.8	29.1	0.7
MK262_m6_15	matrix	0.0784	6.51	0.0420	6.95	0.00389	2.41	0.347	0.001186	2.36	41.8	2.8	25.0	0.6	24.0	0.6	24.0	0.6
MK262_m6_16	matrix	0.1213	2.62	0.0789	3.48	0.00472	2.29	0.659	0.001448	2.35	77.1	2.6	30.3	0.7	27.5	0.7	29.2	0.7
MK262_m6_17	matrix	0.1282	4.69	0.0836	5.23	0.00473	2.30	0.441	0.001465	2.23	81.5	4.1	30.4	0.7	27.3	0.7	29.6	0.7
MK262_m6_18	matrix	0.0833	6.79	0.0447	7.11	0.00390	2.11	0.296	0.001189	2.15	44.4	3.1	25.1	0.5	23.9	0.5	24.0	0.5
MK262_m6_19	matrix	0.1077	4.16	0.0654	5.06	0.00441	2.88	0.568	0.001354	3.02	64.3	3.2	28.3	0.8	26.2	0.8	27.3	0.8
MK262_m6_20	matrix	0.0850	8.61	0.0420	8.84	0.00359	1.99	0.226	0.001032	1.89	41.8	3.6	23.1	0.5	22.0	0.5	20.9	0.4
MK262_m6_21	matrix	0.1444	2.11	0.0966	3.11	0.00486	2.29	0.736	0.001440	2.16	93.7	2.8	31.2	0.7	27.4	0.7	29.1	0.6
MK262_m7_1	garnet (crack)	0.1722	3.35	0.1127	4.66	0.00475	3.24	0.695	0.001350	3.14	108.4	4.8	30.5	1.0	25.7	1.0	27.3	0.9
MK262_m7_2	garnet (crack)	0.1155	4.72	0.0676	5.29	0.00425	2.40	0.454	0.001279	2.77	66.5	3.4	27.3	0.7	24.9	0.7	25.8	0.7
MK262_m7_3	garnet (crack)	0.1022	6.37	0.0571	6.92	0.00406	2.69	0.388	0.001208	2.99	56.4	3.8	26.1	0.7	24.3	0.7	24.4	0.7

Table B1. Petrochronological data for monazite grains.

Grain #	Location	207Pb/206Pb	2SE %	Pb207/U235	2SE %	206Pb/238U	2SE %	rho	208Pb/232Th	2SE %	207Pb/235U (Ma)	2SE	206Pb/238U (Ma)	2SE	corr.206Pb/238U (Ma)	2SE	208Pb/232Th (Ma)	2SE
MK262_m7_4	garnet (crack)	0.1023	6.84	0.0571	7.35	0.00405	2.70	0.367	0.001260	2.88	56.4	4.0	26.1	0.7	24.2	0.7	25.4	0.7
MK262_m7_5	garnet (crack)	0.1184	14.31	0.0709	17.07	0.00434	9.31	0.545	0.001517	10.29	70.0	11.5	27.9	2.6	25.4	2.6	30.6	3.1
MK262_m7_6	garnet (crack)	0.1755	3.61	0.1118	4.67	0.00462	2.95	0.633	0.001332	2.91	107.6	4.8	29.7	0.9	24.9	0.9	26.9	0.8
MK262_m7_7	garnet (crack)	0.1526	3.81	0.0977	4.42	0.00465	2.24	0.507	0.001388	2.62	94.7	4.0	30.0	0.7	25.9	0.7	28.0	0.7
MK262_m7_8	garnet (crack)	0.1399	4.19	0.0912	4.41	0.00473	1.38	0.313	0.001418	1.77	88.6	3.7	30.4	0.4	26.8	0.4	28.6	0.5
MK262_m7_9	garnet (crack)	0.1305	3.15	0.0807	4.25	0.00449	2.85	0.671	0.001327	2.61	78.8	3.2	29.0	0.8	26.0	0.8	26.8	0.7
MK262_m7_10	garnet (crack)	0.1482	4.05	0.0916	4.76	0.00448	2.49	0.524	0.001336	2.59	89.0	4.1	28.8	0.7	25.1	0.7	27.0	0.7
MK262_m8_1	matrix	0.1630	6.99	0.0753	7.51	0.00335	2.74	0.365	0.000951	2.74	73.7	5.3	21.6	0.6	18.0	0.6	19.2	0.5
MK262_m8_2	matrix	0.0940	7.45	0.0467	7.89	0.00360	2.58	0.328	0.001093	2.56	46.3	3.6	23.2	0.6	21.8	0.6	22.1	0.6
MK262_m8_3	matrix	0.0965	11.31	0.0369	11.58	0.00278	2.52	0.217	0.000842	2.55	36.8	4.2	17.9	0.4	16.7	0.4	17.0	0.4
MK262_m8_4	matrix	0.1233	10.10	0.0546	10.39	0.00321	2.45	0.236	0.000946	1.98	54.0	5.5	20.7	0.5	18.7	0.5	19.1	0.4
MK262_m8_5	matrix	0.1501	7.55	0.0704	7.75	0.00340	1.73	0.224	0.000964	2.13	69.1	5.2	21.9	0.4	19.0	0.4	19.5	0.4
MK262_m8_6	matrix	0.1002	3.54	0.0564	4.49	0.00409	2.77	0.617	0.001224	2.71	55.7	2.4	26.0	0.7	24.5	0.7	24.7	0.7
MK262_m8_7	matrix	0.1187	3.33	0.0738	3.60	0.00451	1.37	0.382	0.001398	1.85	72.3	2.5	29.0	0.4	26.4	0.4	28.2	0.5
MK262_m8_8	matrix	0.1409	2.69	0.0917	3.20	0.00472	1.74	0.544	0.001476	1.70	89.1	2.7	30.0	0.5	27.0	0.5	29.8	0.5
MK262_m8_9	matrix	0.1261	3.33	0.0802	3.82	0.00462	1.87	0.490	0.001441	1.58	78.3	2.9	29.7	0.6	26.7	0.6	29.1	0.5
MK262_m8_10	matrix	0.1193	3.35	0.0718	4.06	0.00437	2.31	0.568	0.001347	2.54	70.4	2.8	28.0	0.6	26.0	0.6	27.2	0.7
MK262_m8_11	matrix	0.1294	8.23	0.0565	9.11	0.00317	3.92	0.430	0.000951	3.44	55.8	5.0	20.0	0.8	18.3	0.8	19.2	0.7
MK262_m8_12	matrix	0.1105	5.31	0.0617	6.09	0.00405	2.98	0.490	0.001175	2.52	60.8	3.6	26.0	0.8	24.0	0.8	23.7	0.6
MK262_m8_13	matrix	0.1403	3.17	0.0900	4.51	0.00465	3.20	0.710	0.001442	2.81	87.5	3.8	30.0	1.0	26.0	1.0	29.1	0.8
MK262_m8_14	matrix	0.1149	3.94	0.0664	4.32	0.00419	1.78	0.410	0.001279	1.69	65.3	2.7	27.0	0.5	25.0	0.5	25.8	0.4
MK262_m8_15	matrix	0.1185	2.79	0.0731	3.73	0.00448	2.49	0.666	0.001410	2.66	71.7	2.6	29.0	0.7	26.0	0.7	28.5	0.8
MK262_m8_16	matrix	0.1683	6.90	0.0963	7.61	0.00415	3.20	0.421	0.001221	3.03	93.4	6.8	27.0	0.9	23.0	0.9	24.6	0.7
MK262_m8_17	matrix	0.0768	9.93	0.0342	10.16	0.00323	2.12	0.209	0.000972	2.55	34.2	3.4	21.0	0.4	20.0	0.4	19.6	0.5
MK262_m8_18	matrix	0.1089	8.26	0.0374	8.87	0.00249	3.24	0.365	0.000750	3.12	37.3	3.3	16.0	0.5	15.0	0.5	15.2	0.5
MK262_m8_19	matrix	0.1237	11.98	0.0471	12.19	0.00276	2.24	0.184	0.000789	1.98	46.8	5.6	18.0	0.4	16.0	0.4	15.9	0.3
MK262_m8_20	matrix	0.1338	10.19	0.0515	10.79	0.00279	3.55	0.329	0.000805	3.54	51.0	5.4	18.0	0.6	16.0	0.6	16.3	0.6
MK262_m8_21	matrix	0.1444	3.48	0.0861	4.87	0.00433	3.40	0.699	0.001254	3.22	83.9	3.9	28.0	0.9	24.0	0.9	25.3	0.8
MK262_m8_22	matrix	0.1759	4.04	0.1207	4.83	0.00498	2.65	0.548	0.001551	2.70	115.7	5.3	32.0	0.8	27.0	0.8	31.3	0.8
MK262_m8_23	matrix	0.1225	3.72	0.0731	4.27	0.00433	2.09	0.490	0.001342	1.69	71.7	3.0	27.9	0.6	25.0	0.6	27.1	0.5
MK262_m8_24	matrix	0.0914	6.12	0.0491	6.52	0.00390	2.25	0.345	0.001183	2.52	48.6	3.1	25.1	0.6	23.7	0.6	23.9	0.6
MK262_m9_1	matrix	0.1183	4.26	0.0654	4.83	0.00401	2.27	0.470	0.001184	2.85	64.3	3.0	25.8	0.6	23.5	0.6	23.9	0.7
MK262_m9_2	matrix	0.1236	4.42	0.0705	4.80	0.00414	1.87	0.389	0.001222	2.16	69.1	3.2	26.6	0.5	24.0	0.5	24.7	0.5
MK262_m9_3	matrix	0.1335	3.56	0.0835	3.79	0.00454	1.29	0.340	0.001354	1.51	81.4	3.0	29.0	0.4	26.0	0.4	27.3	0.4
MK262_m9_4	matrix	0.1326	3.97	0.0797	4.08	0.00436	0.94	0.229	0.001315	1.56	77.9	3.1	28.1	0.3	25.0	0.3	26.5	0.4
MK262_m9_5	matrix	0.1209	8.02	0.0434	8.20	0.00261	1.73	0.211	0.000768	1.38	43.2	3.5	17.0	0.3	15.2	0.3	15.5	0.2
MK262_m9_6	matrix	0.0631	14.65	0.0211	14.77	0.00243	1.82	0.123	0.000775	1.05	21.2	3.1	15.6	0.3	15.3	0.3	15.7	0.2
MK262_m9_7	matrix	0.0502	14.90	0.0175	15.02	0.00253	1.88	0.125	0.000816	1.73	17.6	2.6	16.3	0.3	16.2	0.3	16.5	0.3
MK262_m9_8	matrix	0.0646	15.86	0.0231	16.02	0.00259	2.26	0.141	0.000823	1.96	23.2	3.7	16.7	0.4	16.3	0.4	16.6	0.3
MK262_m9_9	matrix	0.1219	7.49	0.0536	7.81	0.00319	2.21	0.283	0.000928	1.78	53.0	4.0	21.0	0.5	18.6	0.5	18.7	0.3
MK262_m9_10	matrix	0.1299	3.43	0.0794	3.79	0.00443	1.62	0.427	0.001358	1.74	77.6	2.8	28.5	0.5	25.5	0.5	27.4	0.5
MK262_m9_11	matrix	0.1286	3.54	0.0791	3.90	0.00447	1.64	0.420	0.001328	1.57	77.3	2.9	28.7	0.5	26.0	0.5	26.8	0.4
MK262_m9_12	matrix	0.1336	3.10	0.0813	3.71	0.00441	2.03	0.548	0.001344	1.94	79.3	2.8	28.4	0.6	25.3	0.6	27.1	0.5
MK262_m9_13	matrix	0.1349	4.36	0.0833	4.62	0.00448	1.51	0.327	0.001371	1.76	81.2	3.6	28.8	0.4	26.0	0.4	27.7	0.5
MK262_m9_14	matrix	0.1298	3.44	0.0771	3.70	0.00431	1.37	0.370	0.001322	1.37	75.5	2.7	27.7	0.4	24.8	0.4	26.7	0.4
MK262_m9_15	matrix	0.1383	3.66	0.0827	4.01	0.00434	1.62	0.406	0.001315	1.72	80.6	3.1	27.9	0.5	24.7	0.5	26.6	0.5
MK262_m9_16	matrix	0.1363	2.92	0.0844	3.63	0.00449	2.16	0.595	0.001371	2.11	82.3	2.9	28.9	0.6	25.6	0.6	27.7	0.6
MK262_m9_17	matrix	0.1312	3.45	0.0801	3.66	0.00443	1.23	0.336	0.001360	1.32	78.2	2.8	28.5	0.3	25.0	0.3	27.5	0.4
MK262_m9_18	matrix	0.1389	4.07	0.0832	4.38	0.00435	1.60	0.367	0.001330	1.44	81.2	3.4	28.0	0.4	24.7	0.4	26.9	0.4
MK262_m10_1	matrix	0.4186	3.97	0.2585	4.99	0.00448	3.02	0.605	0.001545	3.80	233.0	10.4	28.8	0.9	15.3	0.9	31.2	1.2
MK262_m10_2	matrix	0.1334	35.69	0.0691	38.12	0.00376	13.37	0.351	0.001063	9.67	68.0	25.0	24.0	3.2	21.5	3.2	21.5	2.1
MK262_m10_3	matrix	0.1508	6.14	0.0865	6.31	0.00416	1.44	0.229	0.001288	1.51	84.3	5.1	26.8	0.4	23.3	0.4	26.0	0.4
MK262_m10_4	matrix	0.0678	5.30	0.0345	5.55	0.00369	1.62	0.292	0.001142	1.79	34.4	1.9	24.0	0.4	23.1	0.4	23.1	0.4
MK262_m10_5	matrix	0.0686	6.04	0.0353	6.37	0.00373	2.02	0.318	0.001119	2.17	35.2	2.2	24.0	0.5	23.4	0.5	22.6	0.5
MK262_m10_6	matrix	0.0716	5.79	0.0372	5.98	0.00378	1.51	0.253	0.001144	1.80	37.1	2.2	24.0	0.4	23.5	0.4	23.1	0.4
MK262_m10_7	matrix	0.0642	5.02	0.0324	5.18	0.00367	1.29	0.249	0.001190	1.50	32.4	1.7	24.0	0.3	23.1	0.3	24.0	0.4
MK262_m10_8	matrix	0.0751	4.76	0.0390	4.89	0.00376	1.10	0.226	0.001229	1.12	38.8	1.9	24.2	0.3	23.4	0.3	24.8	0.3

Table B1. Petrochronological data for monazite grains.

Grain #	Location	207Pb/206Pb	2SE %	Pb207/U235	2SE %	206Pb/238U	2SE %	rho	208Pb/232Th	2SE %	207Pb/235U (Ma)	2SE	206Pb/238U (Ma)	2SE	corr.206Pb/238U (Ma)	2SE	208Pb/232Th (Ma)	2SE
MK262_m10_9	matrix	0.0984	4.60	0.0534	4.85	0.00394	1.54	0.317	0.001282	1.04	52.8	2.5	25.3	0.4	23.7	0.4	25.9	0.3
MK262_m10_10	matrix	0.0751	5.04	0.0387	5.28	0.00374	1.56	0.296	0.001216	1.66	38.5	2.0	24.0	0.4	23.2	0.4	24.6	0.4
MK262_m10_11	matrix	0.0685	5.82	0.0355	6.10	0.00376	1.83	0.299	0.001203	1.83	35.4	2.1	24.0	0.4	23.0	0.4	24.3	0.4
MK262_m10_12	matrix	0.0904	4.74	0.0483	4.97	0.00388	1.47	0.295	0.001285	1.55	47.9	2.3	24.9	0.4	23.6	0.4	26.0	0.4
MK262_m10_13	matrix	0.0833	3.84	0.0431	4.15	0.00376	1.59	0.383	0.001236	1.86	42.9	1.7	24.2	0.4	23.0	0.4	25.0	0.5
MK262_m10_14	matrix	0.0916	6.00	0.0488	6.23	0.00387	1.68	0.269	0.001272	2.01	48.4	2.9	24.9	0.4	23.5	0.4	25.7	0.5
MK262_m10_15	matrix	0.0798	4.41	0.0419	4.82	0.00382	1.94	0.403	0.001237	2.11	41.7	2.0	24.5	0.5	24.0	0.5	25.0	0.5
MK262_m10_16	matrix	0.0624	4.98	0.0318	5.20	0.00369	1.49	0.286	0.001193	1.40	31.8	1.6	23.8	0.4	23.0	0.4	24.1	0.3
MK262_m10_17	matrix	0.0686	4.70	0.0350	4.81	0.00370	1.02	0.211	0.001110	1.56	34.9	1.6	23.8	0.2	23.1	0.2	22.4	0.3
MK262_m10_18	matrix	0.0688	5.56	0.0363	5.97	0.00383	2.19	0.367	0.001092	1.79	36.2	2.1	25.0	0.5	24.0	0.5	22.0	0.4
MK262_m10_19	matrix	0.0681	19.56	0.0312	19.65	0.00333	1.83	0.093	0.001081	2.92	31.2	6.0	21.4	0.4	21.0	0.4	21.8	0.6
MK262_m10_20	matrix	0.0687	7.03	0.0335	7.34	0.00354	2.13	0.290	0.001108	2.84	33.4	2.4	23.0	0.5	22.0	0.5	22.4	0.6
MK262_m10_21	matrix	0.0619	15.80	0.0304	16.62	0.00356	5.15	0.310	0.001322	6.80	30.4	5.0	23.0	1.2	22.5	1.2	26.7	1.8
MK262_m10_22	matrix	0.0628	3.81	0.0318	4.29	0.00368	1.97	0.459	0.001183	1.21	31.8	1.3	24.0	0.5	23.2	0.5	23.9	0.3
MK262_m10_23	matrix	0.1290	18.79	0.0482	19.04	0.00271	3.09	0.162	0.000871	4.27	47.8	8.9	17.5	0.5	15.6	0.5	17.6	0.8
MK262_m10_24	matrix	0.1047	8.74	0.0539	9.13	0.00373	2.64	0.290	0.001066	2.04	53.3	4.7	24.0	0.6	22.3	0.6	21.5	0.4
MK263																		
MK263_m1_1	garnet	0.1309	19.04	0.0655	19.21	0.00363	2.59	0.135	0.001077	2.56	64.0	12.0	23.0	0.6	20.9	0.6	21.7	0.6
MK263_m1_2	garnet	0.1284	9.10	0.0648	9.35	0.00366	2.18	0.233	0.001032	2.06	63.7	5.8	23.6	0.5	21.1	0.5	20.8	0.4
MK263_m1_3	garnet	0.1384	8.96	0.0689	9.11	0.00361	1.64	0.181	0.001031	2.00	67.6	6.0	23.0	0.4	21.0	0.4	20.8	0.4
MK263_m1_4	garnet	0.1274	4.68	0.0652	4.98	0.00371	1.69	0.340	0.001119	2.03	64.2	3.1	23.9	0.4	21.5	0.4	22.6	0.5
MK263_m1_5	garnet	0.1138	4.61	0.0580	4.98	0.00370	1.89	0.379	0.001141	1.79	57.3	2.8	24.0	0.4	22.0	0.4	23.0	0.4
MK263_m1_6	garnet	0.1222	4.31	0.0637	4.50	0.00378	1.28	0.286	0.001164	1.64	62.7	2.7	24.0	0.3	22.0	0.3	23.5	0.4
MK263_m1_7	garnet	0.1197	7.64	0.0620	7.79	0.00376	1.54	0.198	0.001114	1.50	61.1	4.6	24.0	0.4	22.0	0.4	22.5	0.3
MK263_m1_8	garnet	0.1244	4.39	0.0659	4.85	0.00385	2.06	0.425	0.001176	1.78	64.8	3.0	25.0	0.5	22.3	0.5	23.7	0.4
MK263_m1_9	garnet	0.1157	5.38	0.0589	5.59	0.00369	1.52	0.271	0.001105	1.94	58.1	3.2	23.8	0.4	22.0	0.4	22.3	0.4
MK263_m1_10	garnet	0.1234	4.58	0.0638	4.94	0.00375	1.85	0.374	0.001131	2.26	62.8	3.0	24.1	0.4	22.0	0.4	22.8	0.5
MK263_m1_11	garnet	0.1259	5.03	0.0656	5.26	0.00378	1.53	0.290	0.001144	1.64	64.5	3.3	24.3	0.4	21.9	0.4	23.1	0.4
MK263_m1_12	garnet	0.1443	9.54	0.0758	9.71	0.00381	1.80	0.186	0.001079	1.55	74.2	6.9	24.5	0.4	22.0	0.4	21.8	0.3
MK263_m1_13	garnet	0.1335	5.24	0.0696	5.48	0.00378	1.61	0.294	0.001127	1.37	68.3	3.6	24.3	0.4	21.7	0.4	22.8	0.3
MK263_m1_14	garnet	0.1165	4.82	0.0609	5.16	0.00379	1.86	0.360	0.001172	2.03	60.0	3.0	24.4	0.5	22.0	0.5	23.7	0.5
MK263_m1_15	garnet	0.1167	4.88	0.0616	5.21	0.00383	1.84	0.354	0.001185	1.81	60.7	3.1	24.6	0.5	22.0	0.5	23.9	0.4
MK263_m1_16	garnet	0.1208	5.63	0.0628	5.79	0.00377	1.38	0.238	0.001153	1.49	61.8	3.5	24.3	0.3	22.0	0.3	23.3	0.3
MK263_m2_1	matrix	0.0843	8.78	0.0295	8.97	0.00254	1.82	0.203	0.000792	1.85	29.5	2.6	16.3	0.3	16.0	0.3	16.0	0.3
MK263_m2_2	matrix	0.0538	14.53	0.0196	14.65	0.00264	1.89	0.129	0.000820	2.10	19.7	2.9	17.0	0.3	16.8	0.3	16.6	0.3
MK263_m2_3	matrix	0.0638	20.52	0.0223	20.68	0.00253	2.55	0.123	0.000769	1.83	22.4	4.6	16.3	0.4	15.9	0.4	15.5	0.3
MK263_m2_4	matrix	0.0868	13.69	0.0393	13.86	0.00328	2.18	0.157	0.000957	1.87	39.1	5.3	21.0	0.5	20.1	0.5	19.3	0.4
MK263_m2_5	matrix	0.0937	12.47	0.0435	12.59	0.00337	1.79	0.142	0.000978	1.41	43.2	5.3	21.7	0.4	20.4	0.4	19.7	0.3
MK263_m2_6	matrix	0.1079	11.37	0.0525	11.58	0.00353	2.18	0.188	0.001004	1.75	51.9	5.9	23.0	0.5	21.0	0.5	20.3	0.4
MK263_m2_7	matrix	0.1054	12.21	0.0507	12.29	0.00349	1.45	0.118	0.000997	1.88	50.3	6.0	22.5	0.3	20.8	0.3	20.1	0.4
MK263_m2_8	matrix	0.1600	4.77	0.0908	5.18	0.00412	2.03	0.391	0.001105	1.78	88.2	4.4	26.5	0.5	22.7	0.5	22.3	0.4
MK263_m2_9	matrix	0.1943	4.69	0.1141	5.02	0.00426	1.77	0.353	0.001127	1.84	109.7	5.2	27.4	0.5	22.3	0.5	22.8	0.4
MK263_m2_10	matrix	0.0551	21.31	0.0213	21.40	0.00280	1.95	0.091	0.000847	2.06	21.4	4.5	18.0	0.4	17.8	0.4	17.1	0.4
MK263_m2_13	matrix	0.0988	17.52	0.0357	17.61	0.00262	1.77	0.101	0.000794	2.30	35.6	6.2	16.9	0.3	15.7	0.3	16.0	0.4
MK263_m2_14	matrix	0.1885	4.05	0.1003	4.63	0.00386	2.25	0.486	0.001026	1.88	97.1	4.3	24.8	0.6	20.4	0.6	20.7	0.4
MK263_m2_15	matrix	0.1841	3.04	0.1109	3.50	0.00437	1.73	0.495	0.001338	1.94	106.8	3.6	28.1	0.5	23.2	0.5	27.0	0.5
MK263_m2_16	matrix	0.2378	2.83	0.1510	3.32	0.00461	1.75	0.526	0.001268	2.41	142.8	4.4	29.6	0.5	22.5	0.5	25.6	0.6
MK263_m2_17	matrix	0.2009	3.40	0.1221	3.99	0.00441	2.10	0.527	0.001138	1.94	116.9	4.4	28.4	0.6	22.8	0.6	23.0	0.4
MK263_m2_18	matrix	0.0487	21.60	0.0167	21.81	0.00249	2.99	0.137	0.000776	2.89	16.8	3.6	16.0	0.5	16.0	0.5	15.7	0.5
MK263_m2_19	matrix	0.0520	21.23	0.0169	21.37	0.00235	2.47	0.116	0.000751	1.62	17.0	3.6	15.1	0.4	15.0	0.4	15.2	0.2
MK263_m2_20	matrix	0.1153	9.37	0.0531	10.10	0.00334	3.76	0.372	0.000964	2.52	52.6	5.2	21.5	0.8	19.6	0.8	19.5	0.5
MK263_m2_21	matrix	0.1858	3.96	0.1095	4.48	0.00427	2.08	0.464	0.001131	1.94	105.5	4.5	27.5	0.6	22.7	0.6	22.8	0.4
MK263_m2_22	matrix	0.1377	6.02	0.0736	6.49	0.00388	2.41	0.371	0.001056	2.44	72.1	4.5	24.9	0.6	22.1	0.6	21.3	0.5
MK263_m2_23	matrix	0.1047	11.34	0.0509	11.63	0.00352	2.57	0.221	0.001014	1.55	50.4	5.7	23.0	0.6	21.0	0.6	20.5	0.3
MK263_m2_24	matrix	0.0823	15.00	0.0389	15.14	0.00343	2.06	0.136	0.000981	1.99	38.8	5.8	22.1	0.5	21.1	0.5	19.8	0.4
MK263_m2_25	matrix	0.0839	14.94	0.0392	15.07	0.00339	1.97	0.130	0.000976	1.84	39.0	5.8	22.0	0.4	21.0	0.4	19.7	0.4

Table B1. Petrochronological data for monazite grains.

Grain #	Location	207Pb/206Pb	2SE %	Pb207/U235	2SE %	206Pb/238U	2SE %	rho	208Pb/232Th	2SE %	207Pb/235U (Ma)	2SE	206Pb/238U (Ma)	2SE	corr.206Pb/238U (Ma)	2SE	208Pb/232Th (Ma)	2SE
MK263_m2_26	matrix	0.0735	19.47	0.0297	19.59	0.00293	2.17	0.111	0.000875	2.25	29.7	5.7	18.9	0.4	18.2	0.4	17.7	0.4
MK263_m2_27	matrix	0.0468	16.49	0.0162	16.64	0.00250	2.21	0.133	0.000757	1.99	16.3	2.7	16.0	0.4	16.1	0.4	15.3	0.3
MK263_m2_28	matrix	0.0948	13.19	0.0358	13.37	0.00274	2.18	0.163	0.000815	2.11	35.8	4.7	18.0	0.4	16.6	0.4	16.5	0.3
MK263_m3_1	matrix	0.0428	36.19	0.0142	36.26	0.00242	2.11	0.058	0.000747	1.74	14.4	5.2	15.6	0.3	16.0	0.3	15.1	0.3
MK263_m3_2	matrix	0.0329	66.98	0.0126	67.05	0.00278	3.01	0.045	0.000905	2.26	12.7	8.5	17.9	0.5	18.2	0.5	18.3	0.4
MK263_m3_3	matrix	0.0641	54.62	0.0279	54.70	0.00316	2.97	0.054	0.000939	2.64	28.0	15.1	20.0	0.6	19.9	0.6	19.0	0.5
MK263_m3_4	matrix	0.0600	59.88	0.0248	59.94	0.00300	2.66	0.044	0.000914	1.52	25.0	14.7	19.0	0.5	19.0	0.5	18.5	0.3
MK263_m3_5	matrix	0.0266	86.88	0.0111	86.95	0.00303	3.59	0.041	0.000943	1.93	11.2	9.7	19.5	0.7	20.0	0.7	19.0	0.4
MK263_m3_6	matrix	0.0871	30.18	0.0368	30.32	0.00307	2.94	0.097	0.000955	2.48	37.0	10.9	19.7	0.6	18.7	0.6	19.3	0.5
MK263_m3_7	matrix	0.1483	5.12	0.0785	5.72	0.00384	2.56	0.447	0.001089	2.74	76.7	4.2	24.7	0.6	21.5	0.6	22.0	0.6
MK263_m3_8	matrix	0.1648	15.76	0.0796	16.19	0.00351	3.70	0.228	0.000963	2.32	78.0	12.1	22.6	0.8	19.2	0.8	19.5	0.5
MK263_m3_9	matrix	0.1029	40.75	0.0446	40.88	0.00314	3.26	0.080	0.000951	1.42	44.0	17.7	20.2	0.7	18.8	0.7	19.2	0.3
MK263_m3_10	matrix	0.0785	25.72	0.0265	25.89	0.00245	2.94	0.114	0.000764	2.70	26.6	6.8	15.8	0.5	15.1	0.5	15.4	0.4
MK263_m3_11	matrix	0.0663	25.84	0.0218	25.98	0.00239	2.70	0.104	0.000760	2.65	21.9	5.6	15.0	0.4	15.0	0.4	15.4	0.4
MK263_m3_12	matrix	0.0774	40.54	0.0336	40.73	0.00315	3.86	0.095	0.000952	2.52	34.0	13.4	20.3	0.8	19.5	0.8	19.2	0.5
MK263_m3_13	matrix	0.0728	28.17	0.0259	28.42	0.00259	3.76	0.132	0.000815	2.76	26.0	7.3	17.0	0.6	16.0	0.6	16.5	0.5
MK263_m3_14	matrix	0.0495	74.51	0.0220	74.62	0.00322	4.04	0.054	0.000962	2.64	22.0	16.3	21.0	0.8	20.6	0.8	19.4	0.5
MK263_m3_15	matrix	0.0571	29.70	0.0199	29.77	0.00253	2.06	0.069	0.000836	1.67	20.0	5.9	16.0	0.3	16.0	0.3	16.9	0.3
MK263_m3_16	matrix	0.0843	22.68	0.0306	22.75	0.00263	1.86	0.082	0.000869	1.90	30.6	6.9	17.0	0.3	16.1	0.3	17.6	0.3
MK263_m3_17	matrix	0.1284	18.92	0.0505	19.13	0.00285	2.85	0.149	0.000880	2.02	50.0	9.3	18.0	0.5	16.0	0.5	17.8	0.4
MK263_m3_18	matrix	0.1589	13.58	0.0708	13.87	0.00323	2.86	0.206	0.000922	2.69	69.5	9.3	21.0	0.6	18.0	0.6	18.6	0.5
MK263_m3_19	matrix	0.1200	29.07	0.0524	29.34	0.00317	3.97	0.135	0.000941	2.37	52.0	14.8	20.4	0.8	18.5	0.8	19.0	0.4
MK263_m3_20	matrix	0.1213	40.88	0.0558	41.03	0.00334	3.54	0.086	0.000971	2.29	55.0	22.0	21.0	0.8	19.4	0.8	19.6	0.4
MK263_m4_1	matrix	0.1038	13.14	0.0293	13.54	0.00205	3.29	0.243	0.000620	3.33	29.3	3.9	13.2	0.4	12.0	0.4	12.5	0.4
MK263_m4_2	matrix	0.0893	18.07	0.0264	18.23	0.00214	2.35	0.129	0.000649	2.50	26.4	4.8	14.0	0.3	13.0	0.3	13.1	0.3
MK263_m4_3	matrix	0.1262	10.41	0.0420	10.55	0.00241	1.74	0.165	0.000718	1.68	41.8	4.3	16.0	0.3	14.0	0.3	14.5	0.2
MK263_m4_4	matrix	0.0793	16.73	0.0320	17.01	0.00293	3.09	0.182	0.000871	3.09	32.0	5.4	19.0	0.6	18.1	0.6	17.6	0.5
MK263_m4_5	matrix	0.0853	16.31	0.0345	16.52	0.00293	2.59	0.157	0.000874	2.46	34.4	5.6	19.0	0.5	18.0	0.5	17.6	0.4
MK263_m4_6	matrix	0.1207	9.99	0.0507	10.16	0.00304	1.85	0.182	0.000890	2.32	50.2	5.0	19.6	0.4	17.8	0.4	18.0	0.4
MK263_m4_7	matrix	0.0884	14.92	0.0305	15.12	0.00250	2.46	0.163	0.000755	2.30	30.5	4.5	16.1	0.4	15.3	0.4	15.3	0.4
MK263_m4_8	matrix	0.1121	11.00	0.0371	11.32	0.00240	2.64	0.233	0.000717	2.14	37.0	4.1	15.4	0.4	14.2	0.4	14.5	0.3
MK263_m4_9	matrix	0.1566	9.62	0.0506	9.84	0.00235	2.08	0.211	0.000700	1.73	50.2	4.8	15.1	0.3	13.0	0.3	14.1	0.2
MK263_m4_10	matrix	0.1094	16.56	0.0362	16.90	0.00240	3.34	0.198	0.000731	3.06	36.1	6.0	15.5	0.5	14.2	0.5	14.8	0.5
MK263_m4_11	matrix	0.0909	13.22	0.0279	13.49	0.00222	2.67	0.198	0.000675	2.12	27.9	3.7	14.3	0.4	14.0	0.4	13.6	0.3
MK263_m4_12	matrix	0.0932	13.57	0.0352	13.87	0.00274	2.88	0.207	0.000816	2.65	35.1	4.8	17.6	0.5	17.0	0.5	16.5	0.4
MK263_m4_13	matrix	0.1611	7.90	0.0602	8.19	0.00271	2.18	0.266	0.000804	1.88	59.4	4.7	17.5	0.4	15.0	0.4	16.2	0.3
MK263_m4_14	matrix	0.1043	11.21	0.0364	11.47	0.00254	2.42	0.211	0.000775	2.29	36.3	4.1	16.3	0.4	15.1	0.4	15.6	0.4
MK263_m5_1	matrix	0.2253	12.22	0.0832	12.57	0.00268	2.97	0.236	0.000774	2.57	81.0	9.8	17.2	0.5	13.0	0.5	15.6	0.4
MK263_m5_2	matrix	0.2193	9.83	0.0908	10.10	0.00300	2.32	0.230	0.000771	1.86	88.2	8.5	19.3	0.4	15.0	0.4	15.6	0.3
MK263_m5_3	matrix	0.1457	12.58	0.0500	12.77	0.00249	2.17	0.170	0.000723	2.21	49.5	6.2	16.0	0.3	14.0	0.3	14.6	0.3
MK263_m5_4	matrix	0.1441	4.81	0.0785	5.23	0.00395	2.05	0.393	0.001137	1.66	76.8	3.9	25.4	0.5	22.0	0.5	23.0	0.4
MK263_m5_5	matrix	0.1351	4.73	0.0741	4.92	0.00398	1.34	0.272	0.001162	1.43	72.6	3.4	26.0	0.3	22.7	0.3	23.5	0.3
MK263_m5_6	matrix	0.1426	5.31	0.0762	5.83	0.00388	2.41	0.413	0.001117	2.00	74.6	4.2	25.0	0.6	22.0	0.6	22.6	0.5
MK263_m5_7	matrix	0.1472	5.95	0.0777	6.27	0.00383	1.96	0.312	0.001073	1.83	75.9	4.6	24.6	0.5	22.0	0.5	21.7	0.4
MK263_m5_8	matrix	0.0950	14.36	0.0373	14.56	0.00285	2.40	0.165	0.000866	2.28	37.2	5.3	18.3	0.4	17.0	0.4	17.5	0.4
MK263_m5_9	matrix	0.1178	15.37	0.0479	15.70	0.00295	3.21	0.204	0.000847	2.62	47.5	7.3	19.0	0.6	17.0	0.6	17.1	0.4
MK263_m5_10	matrix	0.1366	5.63	0.0741	6.05	0.00394	2.22	0.367	0.001131	2.08	72.6	4.2	25.3	0.6	22.4	0.6	22.8	0.5
~~MK263_m5_11~~	~~matrix~~	~~0.0641~~	~~2.71~~	~~0.3029~~	~~7.87~~	~~0.03429~~	~~7.39~~	~~0.939~~	~~0.010804~~	~~6.67~~	~~269.0~~	~~18.6~~	~~217.3~~	~~15.8~~	~~213.7~~	~~15.8~~	~~217.1~~	~~14.4~~
~~MK263_m5_12~~	~~matrix~~	~~0.0781~~	~~4.08~~	~~0.1200~~	~~8.73~~	~~0.01115~~	~~7.72~~	~~0.884~~	~~0.003301~~	~~7.66~~	~~115.0~~	~~9.5~~	~~71.5~~	~~5.5~~	~~68.7~~	~~5.5~~	~~66.6~~	~~5.1~~
~~MK263_m5_13~~	~~matrix~~	~~0.1268~~	~~14.09~~	~~0.2034~~	~~25.16~~	~~0.01164~~	~~20.84~~	~~0.828~~	~~0.002048~~	~~16.53~~	~~188.0~~	~~43.2~~	~~74.6~~	~~15.5~~	~~67.2~~	~~15.5~~	~~41.3~~	~~6.8~~
MK263_m6_1	matrix	0.1892	18.54	0.0745	18.90	0.00286	3.64	0.193	0.000821	3.17	73.0	13.3	18.4	0.7	15.1	0.7	16.6	0.5
MK263_m6_2	matrix	0.0844	15.86	0.0327	16.05	0.00281	2.47	0.154	0.000848	2.25	32.7	5.2	18.1	0.4	17.2	0.4	17.1	0.4
MK263_m6_3	matrix	0.1059	22.76	0.0505	23.31	0.00346	5.03	0.216	0.000945	2.40	50.0	11.4	22.3	1.1	20.6	1.1	19.1	0.5
MK263_m6_4	matrix	0.1191	7.54	0.0627	7.87	0.00382	2.24	0.284	0.001071	2.69	61.7	4.7	24.6	0.5	22.3	0.5	21.6	0.6
MK263_m6_5	matrix	0.1134	6.99	0.0583	7.65	0.00373	3.10	0.405	0.001005	3.30	57.6	4.3	24.0	0.7	22.0	0.7	20.3	0.7
MK263_m6_6	matrix	0.1374	10.92	0.0636	12.58	0.00336	6.25	0.497	0.000894	4.05	62.6	7.6	21.6	1.3	19.1	1.3	18.1	0.7
MK263_m6_7	matrix	0.1241	8.52	0.0567	9.50	0.00332	4.22	0.444	0.000868	3.63	56.0	5.2	21.0	0.9	19.2	0.9	17.5	0.6

Table B1. Petrochronological data for monazite grains.

Grain #	Location	207Pb/206Pb	2SE %	Pb207/U235	2SE %	206Pb/238U	2SE %	rho	208Pb/232Th	2SE %	207Pb/235U (Ma)	2SE	206Pb/238U (Ma)	2SE	corr.206Pb/238U (Ma)	2SE	208Pb/232Th (Ma)	2SE
MK263_m6_8	matrix	0.1299	11.74	0.0633	12.58	0.00354	4.52	0.359	0.000970	3.51	62.3	7.6	22.8	1.0	20.4	1.0	19.6	0.7
MK263_m6_9	matrix	0.1264	9.30	0.0671	9.68	0.00385	2.67	0.276	0.001018	3.14	65.9	6.2	25.0	0.7	22.3	0.7	20.6	0.6
MK263_m6_10	matrix	0.1241	5.07	0.0679	5.54	0.00397	2.24	0.405	0.001121	2.39	66.7	3.6	25.5	0.6	23.0	0.6	22.6	0.5
MK263_m6_11	matrix	0.1345	3.62	0.0742	4.16	0.00400	2.05	0.492	0.001242	1.80	72.6	2.9	26.0	0.5	22.9	0.5	25.1	0.5
MK263_m7_1	garnet	0.1632	2.90	0.0955	4.28	0.00425	3.15	0.735	0.001277	3.28	92.6	3.8	27.0	0.9	23.3	0.9	25.8	0.8
MK263_m7_2	garnet	0.1483	8.41	0.0790	8.92	0.00387	2.95	0.330	0.001179	2.82	77.2	6.6	24.9	0.7	21.7	0.7	23.8	0.7
MK263_m7_3	garnet	0.1660	6.11	0.0920	6.42	0.00402	1.96	0.306	0.001216	1.88	89.4	5.5	25.9	0.5	22.0	0.5	24.5	0.5
MK263_m7_4	garnet	0.1674	7.61	0.0925	8.06	0.00401	2.67	0.331	0.001287	2.48	89.8	6.9	26.0	0.7	21.8	0.7	26.0	0.6
~~MK263_m8_1~~	~~garnet (crack)~~	~~0.5734~~	~~20.95~~	~~1.0362~~	~~29.92~~	~~0.01311~~	~~21.37~~	~~0.714~~	~~0.003533~~	~~19.42~~	~~720.0~~	~~154.6~~	~~84.0~~	~~17.8~~	~~28.0~~	~~17.8~~	~~71.3~~	~~13.8~~
MK263_m8_2	garnet (crack)	0.1294	6.36	0.0651	6.82	0.00365	2.49	0.364	0.001077	2.47	64.0	4.2	23.5	0.6	21.0	0.6	21.8	0.5
MK263_m8_3	garnet (crack)	0.1140	5.41	0.0581	5.79	0.00370	2.05	0.354	0.001123	2.40	57.3	3.2	23.8	0.5	22.0	0.5	22.7	0.5
MK263_m8_4	garnet (crack)	0.1538	3.24	0.0816	3.66	0.00385	1.70	0.463	0.001218	2.32	79.6	2.8	24.8	0.4	21.4	0.4	24.6	0.6
MK263_m8_5	garnet (crack)	0.1528	4.41	0.0771	4.72	0.00366	1.68	0.357	0.001138	1.99	75.4	3.4	23.6	0.4	20.4	0.4	23.0	0.5
MK263_m8_6	garnet (crack)	0.1578	3.32	0.0788	3.97	0.00362	2.17	0.546	0.001105	2.07	77.0	2.9	23.3	0.5	20.0	0.5	22.3	0.5
MK263_m8_7	garnet (crack)	0.1214	5.92	0.0595	6.51	0.00356	2.71	0.417	0.001067	2.59	58.7	3.7	22.9	0.6	21.0	0.6	21.6	0.6
MK263_m8_8	garnet (crack)	0.1160	6.08	0.0592	6.61	0.00370	2.59	0.392	0.001124	2.54	58.4	3.7	24.0	0.6	21.7	0.6	22.7	0.6
MK263_m8_9	garnet (crack)	0.1910	10.37	0.0763	11.17	0.00290	4.13	0.370	0.000840	2.61	74.6	8.0	18.6	0.8	15.2	0.8	17.0	0.4
MK263_m8_10	garnet (crack)	0.1004	11.24	0.0400	11.71	0.00289	3.31	0.282	0.000824	2.96	39.8	4.6	19.0	0.6	17.3	0.6	16.7	0.5
MK263_m8_11	garnet (crack)	0.1520	3.87	0.0824	4.82	0.00393	2.88	0.597	0.001171	2.50	80.4	3.7	25.0	0.7	21.9	0.7	23.6	0.6
MK263_m8_12	garnet (crack)	0.1627	4.29	0.0936	4.76	0.00417	2.06	0.434	0.001242	1.94	90.8	4.1	27.0	0.6	22.9	0.6	25.1	0.5
MK263_m8_13	garnet (crack)	0.1659	3.58	0.0890	4.16	0.00389	2.13	0.511	0.001204	1.89	86.6	3.5	25.0	0.5	21.3	0.5	24.3	0.5
MK263_m8_14	garnet (crack)	0.1189	4.59	0.0612	4.97	0.00373	1.92	0.386	0.001133	2.27	60.3	2.9	24.0	0.5	21.8	0.5	22.9	0.5
MK263_m8_15	garnet (crack)	0.1568	13.58	0.0889	15.94	0.00411	8.35	0.524	0.001325	8.02	86.0	13.2	26.0	2.2	22.8	2.2	26.8	2.1
MK263_m9_1	matrix	0.1255	5.10	0.0656	5.45	0.00379	1.92	0.352	0.001172	2.07	64.5	3.4	24.4	0.5	22.0	0.5	23.7	0.5
MK263_m9_2	matrix	0.1230	4.49	0.0628	5.14	0.00371	2.48	0.484	0.001137	2.23	61.9	3.1	24.0	0.6	21.6	0.6	23.0	0.5
MK263_m9_3	matrix	0.1209	4.84	0.0624	5.34	0.00375	2.25	0.421	0.001145	2.06	61.5	3.2	24.1	0.5	21.8	0.5	23.1	0.5
MK263_m9_4	matrix	0.1240	4.52	0.0622	5.14	0.00364	2.44	0.475	0.001098	2.41	61.3	3.1	23.0	0.6	21.0	0.6	22.2	0.5
MK263_m9_5	matrix	0.1925	10.39	0.1068	11.04	0.00402	3.71	0.336	0.001107	3.65	103.0	10.8	26.0	1.0	21.1	1.0	22.4	0.8
MK263_m9_8	matrix	0.1331	3.82	0.0678	4.26	0.00369	1.88	0.443	0.001146	2.16	66.6	2.7	24.0	0.4	21.0	0.4	23.1	0.5
MK263_m9_9	matrix	0.1303	4.02	0.0682	4.22	0.00380	1.28	0.303	0.001158	1.56	67.0	2.7	24.0	0.3	21.8	0.3	23.4	0.4
MK263_m9_10	matrix	0.1224	6.31	0.0627	6.88	0.00372	2.73	0.398	0.001114	2.75	61.8	4.1	23.9	0.7	22.0	0.7	22.5	0.6
MK263_m9_11	matrix	0.1447	6.54	0.0754	7.17	0.00378	2.93	0.409	0.001034	2.68	73.8	5.1	24.3	0.7	21.0	0.7	20.9	0.6
MK263_m10_1	matrix	0.0550	12.57	0.0191	12.79	0.00253	2.32	0.182	0.000791	2.48	19.2	2.4	16.3	0.4	16.1	0.4	16.0	0.4
MK263_m10_2	matrix	0.0977	10.24	0.0349	10.53	0.00259	2.45	0.232	0.000797	2.27	34.8	3.6	16.7	0.4	15.6	0.4	16.1	0.4
MK263_m10_3	matrix	0.0459	17.01	0.0167	17.20	0.00263	2.54	0.148	0.000810	2.02	16.8	2.9	16.9	0.4	17.0	0.4	16.4	0.3
MK263_m10_4	matrix	0.0635	11.34	0.0247	11.51	0.00282	1.96	0.170	0.000899	2.57	24.7	2.8	18.2	0.4	18.0	0.4	18.2	0.5
MK263_m10_5	matrix	0.1411	29.75	0.0528	30.43	0.00272	6.41	0.211	0.001180	11.98	52.0	15.5	17.5	1.1	15.4	1.1	23.8	2.9
MK263_m10_6	matrix	0.0676	16.46	0.0248	16.73	0.00267	2.99	0.179	0.000883	2.37	24.9	4.1	17.2	0.5	16.7	0.5	17.8	0.4
MK263_m10_7	matrix	0.1036	11.17	0.0518	11.58	0.00363	3.03	0.262	0.001035	2.45	51.3	5.8	23.4	0.7	21.7	0.7	20.9	0.5
MK263_m10_8	matrix	0.1210	8.55	0.0615	9.19	0.00369	3.37	0.367	0.001029	2.52	60.6	5.4	23.7	0.8	21.5	0.8	20.8	0.5
MK263_m10_9	matrix	0.0670	21.40	0.0273	21.66	0.00296	3.38	0.156	0.000907	3.44	27.4	5.8	19.0	0.6	18.5	0.6	18.3	0.6
MK263_m10_10	matrix	0.0663	15.67	0.0235	15.97	0.00257	3.07	0.192	0.000810	2.85	23.6	3.7	17.0	0.5	16.1	0.5	16.4	0.5
MK263_m10_11	matrix	0.1086	12.88	0.0488	13.11	0.00326	2.44	0.187	0.000955	2.25	48.4	6.2	21.0	0.5	19.0	0.5	19.3	0.4
MK263_m10_12	matrix	0.0731	15.85	0.0250	16.06	0.00249	2.58	0.161	0.000770	2.55	25.1	4.0	16.0	0.4	15.5	0.4	15.6	0.4
MK263_m10_13	matrix	0.0564	14.19	0.0198	14.43	0.00254	2.60	0.180	0.000777	2.49	19.9	2.8	16.4	0.4	16.0	0.4	15.7	0.4
MK263_m10_14	matrix	0.0605	13.29	0.0219	13.58	0.00262	2.78	0.205	0.000813	2.34	22.0	3.0	16.9	0.5	17.0	0.5	16.4	0.4
MK263_m10_15	matrix	0.0713	15.67	0.0314	15.85	0.00320	2.37	0.150	0.000958	2.36	31.4	4.9	20.6	0.5	20.0	0.5	19.4	0.5
MK263_m10_16	matrix	0.0855	14.04	0.0402	14.32	0.00341	2.80	0.196	0.000990	2.89	40.0	5.6	22.0	0.6	20.8	0.6	20.0	0.6
MK263_m10_17	matrix	0.0910	10.11	0.0438	10.37	0.00349	2.33	0.224	0.001021	2.29	43.5	4.4	22.4	0.5	21.0	0.5	20.6	0.5
MK263_m10_18	matrix	0.0866	14.30	0.0397	14.53	0.00332	2.54	0.175	0.000983	2.52	39.5	5.6	21.4	0.5	20.0	0.5	19.8	0.5
MK263_m10_19	matrix	0.0566	12.94	0.0218	13.15	0.00280	2.39	0.182	0.000877	3.01	21.9	2.8	18.0	0.4	17.8	0.4	17.7	0.5
MK263_m10_20	matrix	0.0470	20.66	0.0178	20.80	0.00274	2.43	0.117	0.000838	2.54	17.9	3.7	17.7	0.4	18.0	0.4	16.9	0.4
MK263_m10_21	matrix	0.0513	18.05	0.0193	18.24	0.00273	2.64	0.145	0.000817	2.64	19.4	3.5	17.6	0.5	17.5	0.5	16.5	0.4
MK263_m10_22	matrix	0.0724	22.05	0.0310	22.19	0.00310	2.45	0.110	0.000939	2.37	31.0	6.8	20.0	0.5	19.0	0.5	19.0	0.4
MK266																		
~~MK266_m1_1~~	~~garnet~~	~~0.0617~~	~~2.28~~	~~0.4951~~	~~3.05~~	~~0.05824~~	~~2.03~~	~~0.665~~	~~0.019754~~	~~2.47~~	~~408.0~~	~~10.3~~	~~364.9~~	~~7.2~~	~~361.5~~	~~7.2~~	~~395.2~~	~~9.7~~

Table B1. Petrochronological data for monazite grains.

Grain #	Location	207Pb/206Pb	2SE %	Pb207/U235	2SE %	206Pb/238U	2SE %	rho	208Pb/232Th	2SE %	207Pb/235U (Ma)	2SE	206Pb/238U (Ma)	2SE	corr.206Pb/238U (Ma)	2SE	208Pb/232Th (Ma)	2SE
~~MK266_m1_2~~	~~garnet~~	~~0.0599~~	~~2.17~~	~~0.6486~~	~~2.72~~	~~0.07861~~	~~1.65~~	~~0.606~~	~~0.024585~~	~~1.29~~	~~508.0~~	~~10.9~~	~~487.8~~	~~7.8~~	~~486.1~~	~~7.8~~	~~490.7~~	~~6.2~~
~~MK266_m1_3~~	~~garnet~~	~~0.0607~~	~~2.17~~	~~0.6483~~	~~2.63~~	~~0.07748~~	~~1.49~~	~~0.565~~	~~0.023970~~	~~1.72~~	~~507.0~~	~~10.5~~	~~481.1~~	~~6.9~~	~~478.8~~	~~6.9~~	~~478.5~~	~~8.1~~
~~MK266_m1_4~~	~~garnet~~	~~0.0620~~	~~2.25~~	~~0.5604~~	~~3.86~~	~~0.06553~~	~~3.13~~	~~0.812~~	~~0.020886~~	~~2.33~~	~~452.0~~	~~14.1~~	~~409.0~~	~~12.4~~	~~406.0~~	~~12.4~~	~~417.6~~	~~9.6~~
~~MK266_m3_1~~	~~garnet~~	~~0.0599~~	~~2.25~~	~~0.6312~~	~~2.95~~	~~0.07643~~	~~1.91~~	~~0.648~~	~~0.023561~~	~~1.91~~	~~497.0~~	~~11.6~~	~~474.8~~	~~8.8~~	~~472.9~~	~~8.8~~	~~470.5~~	~~8.9~~
MK266_m4_1	garnet	0.0902	24.06	0.0377	24.24	0.00303	3.00	0.124	0.001053	3.38	37.6	8.9	19.5	0.6	18.4	0.6	21.3	0.7
MK266_m4_2	garnet	0.1030	8.13	0.0434	8.35	0.00306	1.93	0.232	0.000982	2.60	43.1	3.5	19.7	0.4	18.3	0.4	19.8	0.5
MK266_m6_1	matrix	0.0849	10.28	0.0356	10.46	0.00304	1.92	0.183	0.000937	1.72	35.5	3.6	19.6	0.4	18.6	0.4	18.9	0.3
MK266_m6_2	matrix	0.0931	8.77	0.0395	8.88	0.00308	1.36	0.153	0.000941	1.39	39.3	3.4	19.8	0.3	18.6	0.3	19.0	0.3
MK266_m6_3	matrix	0.2935	4.86	0.1521	5.10	0.00376	1.56	0.305	0.001012	1.42	143.8	6.8	24.2	0.4	16.6	0.4	20.4	0.3
MK266_m6_4	matrix	0.0879	9.11	0.0367	9.33	0.00303	2.00	0.214	0.000939	1.73	36.6	3.4	19.5	0.4	18.5	0.4	19.0	0.3
MK266_m6_5	matrix	0.1846	3.88	0.0976	4.15	0.00384	1.48	0.357	0.001090	1.48	94.6	3.7	24.7	0.4	20.4	0.4	22.0	0.3
MK266_m6_6	matrix	0.1410	4.06	0.0696	4.56	0.00358	2.06	0.452	0.001052	1.85	68.4	3.0	23.1	0.5	20.3	0.5	21.3	0.4
MK266_m6_7	matrix	0.1565	5.51	0.0789	5.74	0.00366	1.61	0.281	0.001032	1.68	77.1	4.3	23.5	0.4	20.3	0.4	20.8	0.4
MK266_m6_8	matrix	0.1143	7.17	0.0462	7.33	0.00293	1.49	0.204	0.000910	1.56	45.9	3.3	18.9	0.3	17.3	0.3	18.4	0.3
MK266_m6_9	matrix	0.0862	14.72	0.0362	14.81	0.00305	1.68	0.114	0.000923	1.51	36.1	5.3	19.6	0.3	18.6	0.3	18.6	0.3
MK266_m6_10	matrix	0.1567	6.88	0.0715	6.96	0.00331	1.10	0.157	0.000968	1.17	70.1	4.7	21.3	0.2	18.3	0.2	19.6	0.2
MK266_m6_11	matrix	0.1529	27.42	0.0612	27.94	0.00290	5.35	0.191	0.000867	2.92	60.0	16.4	18.7	1.0	16.2	1.0	17.5	0.5
MK266_m6_12	matrix	0.2246	5.01	0.1178	5.27	0.00381	1.64	0.311	0.000993	1.40	113.1	5.6	24.5	0.4	19.0	0.4	20.1	0.3
MK266_m6_13	matrix	0.1566	5.74	0.0777	6.09	0.00360	2.04	0.335	0.001030	1.88	76.0	4.5	23.2	0.5	19.9	0.5	20.8	0.4
MK266_m7_1	matrix	0.1431	8.53	0.0558	8.85	0.00283	2.33	0.263	0.000801	1.74	55.1	4.7	18.2	0.4	16.0	0.4	16.2	0.3
MK266_m7_2	matrix	0.0505	6.52	0.0192	6.71	0.00275	1.61	0.239	0.000874	1.66	19.3	1.3	17.7	0.3	17.6	0.3	17.7	0.3
MK266_m7_3	matrix	0.0563	12.18	0.0212	12.27	0.00273	1.49	0.121	0.000854	1.74	21.3	2.6	18.0	0.3	17.3	0.3	17.2	0.3
MK266_m7_4	matrix	0.1065	4.93	0.0405	5.19	0.00276	1.62	0.312	0.000863	1.57	40.3	2.1	17.8	0.3	16.4	0.3	17.4	0.3
MK266_m7_5	matrix	0.2218	5.71	0.1189	6.09	0.00389	2.13	0.350	0.001101	1.93	114.1	6.6	25.0	0.5	19.0	0.5	22.2	0.4
MK266_m7_6	matrix	0.1642	3.96	0.0851	4.25	0.00376	1.55	0.364	0.001100	1.35	82.9	3.4	24.2	0.4	20.6	0.4	22.2	0.3
MK266_m7_7	matrix	0.1450	3.15	0.0714	3.37	0.00357	1.21	0.358	0.001071	1.30	70.0	2.3	23.0	0.3	20.0	0.3	21.6	0.3
MK266_m7_8	matrix	0.0699	15.06	0.0244	15.18	0.00253	1.83	0.121	0.000754	1.79	24.5	3.7	16.3	0.3	15.8	0.3	15.2	0.3
MK266_m7_9	matrix	0.1220	3.54	0.0587	3.66	0.00349	0.93	0.254	0.001058	1.08	57.9	2.1	22.5	0.2	20.0	0.2	21.4	0.2
MK266_m7_10	matrix	0.1175	7.39	0.0479	7.60	0.00296	1.77	0.232	0.000851	1.62	47.5	3.5	19.0	0.3	17.3	0.3	17.2	0.3
MK266_m7_11	matrix	0.0566	12.04	0.0195	12.24	0.00250	2.22	0.182	0.000780	1.81	19.6	2.4	16.1	0.4	15.9	0.4	15.8	0.3
MK266_m7_12	matrix	0.1097	3.89	0.0519	4.10	0.00344	1.30	0.316	0.001039	1.50	51.4	2.1	22.1	0.3	20.0	0.3	21.0	0.3
MK266_m7_13	matrix	0.0825	6.90	0.0359	7.11	0.00315	1.73	0.244	0.000975	1.42	35.8	2.5	20.3	0.4	19.4	0.4	19.7	0.3
MK266_m7_14	matrix	0.0993	5.08	0.0404	5.27	0.00295	1.40	0.266	0.000886	1.18	40.2	2.1	19.0	0.3	17.7	0.3	17.9	0.2
MK266_m7_15	matrix	0.2236	5.53	0.0920	5.82	0.00299	1.84	0.316	0.000814	1.36	89.4	5.0	19.0	0.4	14.9	0.4	16.4	0.2
MK266_m8_1	matrix	0.0711	13.22	0.0261	13.29	0.00266	1.29	0.097	0.000835	1.20	26.2	3.4	17.1	0.2	16.6	0.2	16.9	0.2
MK266_m8_2	matrix	0.0806	7.20	0.0327	7.50	0.00295	2.09	0.278	0.000916	2.04	32.7	2.4	19.0	0.4	18.0	0.4	18.5	0.4
MK266_m8_3	matrix	0.0942	5.07	0.0401	5.29	0.00309	1.49	0.282	0.000940	1.28	40.0	2.1	19.9	0.3	18.7	0.3	19.0	0.2
MK266_m8_4	matrix	0.0996	5.71	0.0394	5.83	0.00287	1.18	0.203	0.000884	1.44	39.2	2.2	18.5	0.2	17.2	0.2	17.9	0.3
MK266_m8_5	matrix	0.0871	5.10	0.0388	5.37	0.00323	1.68	0.313	0.001011	1.86	38.6	2.0	21.0	0.3	19.7	0.3	20.4	0.4
MK266_m8_6	matrix	0.0793	4.71	0.0348	4.96	0.00318	1.55	0.313	0.000993	1.33	34.7	1.7	20.5	0.3	19.6	0.3	20.1	0.3
MK266_m8_7	matrix	0.0752	11.37	0.0264	11.68	0.00255	2.70	0.231	0.000812	2.17	26.4	3.0	16.4	0.4	16.0	0.4	16.4	0.4
MK266_m8_8	matrix	0.0770	6.26	0.0326	6.44	0.00307	1.53	0.237	0.000954	1.59	32.5	2.1	19.8	0.3	19.0	0.3	19.3	0.3
MK266_m8_9	matrix	0.0749	6.00	0.0317	6.12	0.00306	1.20	0.197	0.000956	1.42	31.6	1.9	19.7	0.2	19.0	0.2	19.3	0.3
MK266_m8_10	matrix	0.0777	6.80	0.0336	6.95	0.00314	1.43	0.206	0.000967	1.85	33.5	2.3	20.2	0.3	19.4	0.3	19.5	0.4
MK266_m8_11	matrix	0.0870	5.11	0.0391	5.27	0.00326	1.27	0.242	0.001023	1.57	39.0	2.0	21.0	0.3	19.9	0.3	20.7	0.3
MK266_m8_12	matrix	0.1423	7.04	0.0540	7.41	0.00275	2.31	0.312	0.000851	2.21	53.4	3.9	18.0	0.4	15.6	0.4	17.2	0.4
MK266_m8_13	matrix	0.0788	7.88	0.0268	7.95	0.00247	1.03	0.130	0.000769	1.86	26.9	2.1	16.0	0.2	15.0	0.2	15.5	0.3
MK266_m8_14	matrix	0.0694	6.43	0.0290	6.76	0.00303	2.10	0.310	0.000955	2.73	29.0	1.9	19.0	0.4	19.0	0.4	19.3	0.5
MK266_m8_15	matrix	0.0899	4.86	0.0399	5.12	0.00322	1.60	0.312	0.001009	1.62	39.7	2.0	21.0	0.3	20.0	0.3	20.4	0.3
MK266_m8_16	matrix	0.1178	5.38	0.0547	5.65	0.00337	1.70	0.301	0.001046	1.87	54.1	3.0	21.7	0.4	20.0	0.4	21.1	0.4
MK266_m8_17	matrix	0.1606	4.24	0.0801	4.65	0.00362	1.91	0.411	0.001132	2.14	78.2	3.5	23.3	0.4	20.0	0.4	22.9	0.5
MK266_m8_18	matrix	0.0657	9.81	0.0250	10.05	0.00276	2.19	0.218	0.000857	2.07	25.1	2.5	17.8	0.4	17.3	0.4	17.3	0.4
MK266_m8_19	matrix	0.0829	5.97	0.0359	6.27	0.00314	1.90	0.303	0.000968	2.07	35.8	2.2	20.2	0.4	19.3	0.4	19.6	0.4
MK266_m9_1	matrix	0.1153	5.35	0.0557	5.57	0.00350	1.55	0.279	0.001039	1.23	55.0	3.0	22.5	0.3	20.6	0.3	21.0	0.3
MK266_m9_2	matrix	0.1275	4.52	0.0613	4.95	0.00349	2.02	0.409	0.001042	2.16	60.4	2.9	22.4	0.5	20.1	0.5	21.1	0.5
MK266_m9_3	matrix	0.1168	4.51	0.0556	4.75	0.00346	1.50	0.315	0.001033	1.32	55.0	2.5	22.2	0.3	20.3	0.3	20.9	0.3
MK266_m9_4	matrix	0.1087	5.57	0.0495	5.87	0.00331	1.85	0.316	0.000995	2.04	49.1	2.8	21.3	0.4	19.6	0.4	20.1	0.4

Table B1. Petrochronological data for monazite grains.

Grain #	Location	207Pb/206Pb	2SE %	Pb207/U235	2SE %	206Pb/238U	2SE %	rho	208Pb/232Th	2SE %	207Pb/235U (Ma)	2SE	206Pb/238U (Ma)	2SE	corr.206Pb/238U (Ma)	2SE	208Pb/232Th (Ma)	2SE
MK266_m9_5	matrix	0.0824	11.42	0.0341	11.55	0.00301	1.75	0.152	0.000913	1.88	34.1	3.9	19.3	0.3	18.5	0.3	18.4	0.3
MK266_m9_6	matrix	0.0757	13.29	0.0302	13.37	0.00290	1.50	0.112	0.000889	1.24	30.2	4.0	18.6	0.3	18.0	0.3	18.0	0.2
MK266_m9_7	matrix	0.1083	11.57	0.0470	11.71	0.00315	1.82	0.155	0.000939	2.06	46.6	5.3	20.3	0.4	18.7	0.4	19.0	0.4
MK266_m9_8	matrix	0.1339	4.31	0.0651	4.62	0.00353	1.66	0.359	0.001055	1.92	64.0	2.9	22.7	0.4	20.2	0.4	21.3	0.4
MK266_m9_9	matrix	0.1273	4.86	0.0616	5.22	0.00351	1.92	0.367	0.001052	1.62	60.7	3.1	22.6	0.4	20.3	0.4	21.2	0.3
MK266_m9_10	matrix	0.1344	3.59	0.0665	3.76	0.00359	1.11	0.296	0.001048	1.18	65.4	2.4	23.1	0.3	20.5	0.3	21.2	0.3
MK266_m9_11	matrix	0.1382	14.67	0.0631	15.13	0.00331	3.71	0.245	0.000883	1.51	62.1	9.1	21.3	0.8	18.8	0.8	17.8	0.3
MK266_m9_12	matrix	0.1138	4.19	0.0529	4.63	0.00338	1.97	0.425	0.000995	2.23	52.4	2.4	22.0	0.4	19.9	0.4	20.1	0.4
MK266_m9_13	matrix	0.1194	4.34	0.0573	4.75	0.00348	1.93	0.406	0.001053	1.96	56.5	2.6	22.4	0.4	20.3	0.4	21.3	0.4
MK266_m9_14	matrix	0.1247	5.37	0.0602	5.70	0.00351	1.89	0.332	0.001073	1.87	59.4	3.3	22.6	0.4	20.0	0.4	21.7	0.4
MK266_m9_15	matrix	0.1178	3.52	0.0558	3.87	0.00344	1.61	0.416	0.001057	1.66	55.1	2.1	22.1	0.4	20.1	0.4	21.3	0.4
MK266_m9_16	matrix	0.1122	4.42	0.0529	4.67	0.00342	1.52	0.325	0.001051	1.80	52.3	2.4	22.0	0.3	20.2	0.3	21.2	0.4
MK266_m9_17	matrix	0.1141	4.44	0.0537	4.81	0.00341	1.86	0.386	0.001042	2.05	53.1	2.5	22.0	0.4	20.1	0.4	21.1	0.4
MK266_m10_1	matrix	0.1986	6.42	0.1020	6.98	0.00373	2.73	0.391	0.001057	2.11	98.6	6.6	24.0	0.7	19.4	0.7	21.4	0.5
MK266_m10_2	matrix	0.1192	4.36	0.0570	4.71	0.00347	1.79	0.381	0.001064	1.69	56.3	2.6	22.3	0.4	20.3	0.4	21.5	0.4
MK266_m10_3	matrix	0.1069	5.18	0.0488	5.44	0.00331	1.67	0.307	0.001018	2.18	48.4	2.6	21.3	0.4	19.7	0.4	20.6	0.4
MK266_m10_4	matrix	0.1108	4.31	0.0526	4.64	0.00344	1.71	0.368	0.001058	1.93	52.0	2.4	22.2	0.4	20.4	0.4	21.4	0.4
MK266_m10_5	matrix	0.1147	3.91	0.0549	4.22	0.00347	1.58	0.375	0.001064	2.06	54.2	2.2	22.3	0.4	20.4	0.4	21.5	0.4
MK266_m10_6	matrix	0.1111	4.82	0.0509	5.38	0.00332	2.38	0.443	0.000992	1.82	50.4	2.6	21.4	0.5	19.6	0.5	20.0	0.4
MK266_m10_7	matrix	0.1175	4.38	0.0548	4.88	0.00339	2.14	0.440	0.001033	1.92	54.2	2.6	21.8	0.5	19.8	0.5	20.9	0.4
MK266_m10_8	matrix	0.1909	8.20	0.0868	8.71	0.00330	2.94	0.338	0.000855	1.87	84.5	7.1	21.2	0.6	17.3	0.6	17.3	0.3
MK266_m10_9	matrix	0.1740	8.74	0.0854	9.36	0.00356	3.37	0.359	0.000998	1.99	83.2	7.5	22.9	0.8	19.2	0.8	20.2	0.4
MK266_m10_10	matrix	0.1414	3.50	0.0697	3.98	0.00357	1.90	0.477	0.001080	1.77	68.4	2.6	23.0	0.4	20.2	0.4	21.8	0.4
MK266_m11_1	matrix	0.0832	5.37	0.0366	5.76	0.00319	2.11	0.365	0.001000	1.81	36.5	2.1	20.6	0.4	19.6	0.4	20.2	0.4
MK266_m11_2	matrix	0.0811	5.28	0.0356	5.72	0.00318	2.20	0.384	0.001009	2.73	35.5	2.0	20.5	0.4	19.6	0.4	20.4	0.6
MK266_m11_3	matrix	0.0682	8.03	0.0279	8.26	0.00297	1.93	0.234	0.000920	1.94	28.0	2.3	19.1	0.4	18.6	0.4	18.6	0.4
MK266_m11_4	matrix	0.0622	9.19	0.0239	9.60	0.00279	2.78	0.290	0.000883	2.92	24.0	2.3	18.0	0.5	17.6	0.5	17.8	0.5
MK266_m11_5	matrix	0.0681	8.84	0.0262	9.11	0.00279	2.21	0.243	0.000886	2.06	26.3	2.4	18.0	0.4	17.5	0.4	17.9	0.4
MK266_m11_6	matrix	0.0782	7.16	0.0329	7.32	0.00305	1.53	0.209	0.000959	2.03	32.8	2.4	20.0	0.3	18.8	0.3	19.4	0.4
MK266_m11_7	matrix	0.1082	4.76	0.0513	4.95	0.00344	1.37	0.276	0.001033	1.37	50.8	2.5	22.1	0.3	20.4	0.3	20.9	0.3
MK266_m11_8	matrix	0.0826	5.62	0.0360	5.84	0.00316	1.60	0.273	0.000998	1.80	35.9	2.1	20.0	0.3	19.0	0.3	20.1	0.4
MK266_m11_9	matrix	0.0929	7.22	0.0411	7.62	0.00321	2.44	0.320	0.000994	2.00	40.9	3.1	20.7	0.5	19.4	0.5	20.1	0.4
MK266_m11_10	matrix	0.1029	4.67	0.0474	5.04	0.00334	1.89	0.376	0.001039	2.00	47.1	2.3	21.5	0.4	20.0	0.4	21.0	0.4
MK266_m11_11	matrix	0.1313	4.00	0.0673	4.73	0.00372	2.53	0.536	0.001110	2.57	66.1	3.0	24.0	0.6	21.4	0.6	22.4	0.6
MK266_m11_12	matrix	0.1232	3.92	0.0625	4.35	0.00368	1.89	0.434	0.001152	2.17	61.6	2.6	23.7	0.4	21.0	0.4	23.3	0.5
MK266_m11_13	matrix	0.1167	3.74	0.0596	4.52	0.00371	2.55	0.564	0.001167	2.83	58.8	2.6	23.9	0.6	21.7	0.6	23.6	0.7
MK266_m11_14	matrix	0.1222	3.86	0.0621	4.40	0.00369	2.12	0.483	0.001168	2.38	61.2	2.6	23.7	0.5	21.4	0.5	23.6	0.6
MK266_m11_15	matrix	0.1126	3.55	0.0567	4.14	0.00365	2.12	0.513	0.001142	2.10	56.0	2.3	23.5	0.5	22.0	0.5	23.1	0.5
MK266_m11_16	matrix	0.1136	3.54	0.0569	4.13	0.00363	2.13	0.515	0.001146	2.17	56.2	2.3	23.0	0.5	21.4	0.5	23.1	0.5
MK266_m11_17	matrix	0.1148	3.11	0.0584	3.49	0.00369	1.59	0.455	0.001156	1.22	57.7	2.0	23.8	0.4	21.7	0.4	23.3	0.3
MK266_m11_18	matrix	0.1197	3.18	0.0613	3.87	0.00372	2.22	0.572	0.001151	2.43	60.5	2.3	23.9	0.5	21.7	0.5	23.2	0.6
MK266_m11_19	matrix	0.1178	3.60	0.0596	3.93	0.00368	1.56	0.398	0.001142	2.04	58.8	2.2	23.6	0.4	21.5	0.4	23.1	0.5
MK266_m11_20	matrix	0.1130	4.46	0.0564	4.71	0.00362	1.51	0.321	0.001127	1.72	55.7	2.6	23.3	0.4	21.0	0.4	22.8	0.4
MK266_m11_21	matrix	0.1158	3.05	0.0585	3.50	0.00367	1.72	0.492	0.001146	1.97	57.7	2.0	24.0	0.4	21.5	0.4	23.1	0.5
MK266_m11_22	matrix	0.1144	4.00	0.0592	4.42	0.00375	1.89	0.427	0.001185	2.00	58.4	2.5	24.2	0.5	22.1	0.5	23.9	0.5
MK266_m11_23	matrix	0.1133	3.70	0.0577	4.22	0.00370	2.03	0.481	0.001168	2.65	57.0	2.3	23.8	0.5	21.8	0.5	23.6	0.6
MK266_m11_24	matrix	0.1093	3.54	0.0559	3.78	0.00371	1.32	0.348	0.001184	1.90	55.3	2.0	23.9	0.3	22.0	0.3	23.9	0.5
MK266_m11_25	matrix	0.1085	3.54	0.0557	4.41	0.00373	2.63	0.597	0.001179	2.50	55.1	2.4	24.0	0.6	22.0	0.6	23.8	0.6
MK266_m11_26	matrix	0.1284	3.03	0.0697	4.13	0.00394	2.82	0.681	0.001241	2.69	68.4	2.7	25.3	0.7	22.7	0.7	25.1	0.7
MK266_m11_27	matrix	0.1067	3.71	0.0540	4.18	0.00367	1.92	0.461	0.001167	2.11	53.4	2.2	24.0	0.5	21.8	0.5	23.6	0.5
MK266_m11_28	matrix	0.1065	3.86	0.0536	4.33	0.00365	1.97	0.455	0.001151	1.90	53.0	2.2	24.0	0.5	21.7	0.5	23.2	0.4
MK266_m11_29	matrix	0.1019	3.40	0.0521	3.71	0.00371	1.48	0.399	0.001184	1.82	51.6	1.9	24.0	0.4	22.2	0.4	23.9	0.4
MK266_m11_30	matrix	0.1015	3.98	0.0523	4.64	0.00374	2.39	0.514	0.001176	2.20	51.8	2.3	24.0	0.6	22.4	0.6	23.8	0.5
MK266_m11_31	matrix	0.1014	3.69	0.0523	4.25	0.00374	2.12	0.497	0.001173	2.26	51.7	2.1	24.0	0.5	22.0	0.5	23.7	0.5
MK266_m11_32	matrix	0.1027	4.33	0.0526	4.79	0.00372	2.06	0.429	0.001180	2.26	52.0	2.4	23.9	0.5	22.0	0.5	23.8	0.5
MK266_m11_33	matrix	0.0991	3.65	0.0512	4.27	0.00375	2.21	0.518	0.001186	1.97	50.7	2.1	24.1	0.5	23.0	0.5	24.0	0.5
MK266_m11_34	matrix	0.1014	3.60	0.0515	4.04	0.00369	1.84	0.456	0.001160	2.00	51.0	2.0	23.7	0.4	22.0	0.4	23.4	0.5

Table B1. Petrochronological data for monazite grains.

Grain #	Location	207Pb/206Pb	2SE %	Pb207/U235	2SE %	206Pb/238U	2SE %	rho	208Pb/232Th	2SE %	207Pb/235U (Ma)	2SE	206Pb/238U (Ma)	2SE	corr.206Pb/238U (Ma)	2SE	208Pb/232Th (Ma)	2SE
MK266_m11_35	matrix	0.1063	4.87	0.0543	5.45	0.00370	2.43	0.447	0.001161	2.30	53.7	2.8	23.8	0.6	22.0	0.6	23.5	0.5
MK268																		
MK268_m1_1	matrix	0.0477	67.49	0.0215	67.55	0.00328	3.02	0.045	0.001098	2.62	22.0	14.4	21.1	0.6	21.1	0.6	22.2	0.6
MK268_m1_3	matrix	0.2249	17.25	0.1327	20.19	0.00428	10.48	0.519	0.001164	5.32	127.0	24.0	27.5	2.9	21.3	2.9	23.5	1.2
MK268_m1_4	matrix	0.1117	10.52	0.0525	10.97	0.00341	3.13	0.285	0.001009	3.06	52.0	5.6	21.9	0.7	20.1	0.7	20.4	0.6
MK268_m1_5	matrix	0.0836	13.50	0.0370	13.69	0.00321	2.28	0.167	0.000948	2.61	36.8	5.0	20.6	0.5	19.7	0.5	19.2	0.5
MK268_m1_7	matrix	0.4455	6.18	0.3411	8.33	0.00555	5.58	0.670	0.001195	4.51	298.0	21.5	35.7	2.0	17.7	2.0	24.1	1.1
MK268_m1_8	matrix	0.3106	7.13	0.2016	7.63	0.00471	2.69	0.353	0.001134	3.04	186.0	13.0	30.3	0.8	20.2	0.8	22.9	0.7
MK268_m1_9	matrix	0.3018	7.24	0.1511	8.36	0.00363	4.18	0.500	0.001013	4.20	143.0	11.1	23.4	1.0	15.8	1.0	20.5	0.9
MK268_m2_1	garnet (crack)	0.3450	18.37	0.2413	24.18	0.00507	15.72	0.650	0.001345	11.45	219.0	47.7	32.6	5.1	20.3	5.1	27.2	3.1
MK268_m2_2	garnet (crack)	0.0617	20.25	0.0235	20.40	0.00276	2.45	0.120	0.000825	2.16	23.5	4.7	17.7	0.4	17.4	0.4	16.7	0.4
MK268_m2_3	garnet (crack)	0.3133	21.82	0.1943	25.86	0.00450	13.88	0.537	0.001192	9.90	180.0	42.7	29.0	4.0	19.2	4.0	24.1	2.4
MK268_m2_4	garnet (crack)	0.1069	10.52	0.0397	10.84	0.00269	2.64	0.243	0.000772	1.91	39.5	4.2	17.3	0.5	16.0	0.5	15.6	0.3
~~MK268_m2_6~~	~~garnet (crack)~~	~~0.5597~~	~~7.22~~	~~0.8175~~	~~15.49~~	~~0.01060~~	~~13.71~~	~~0.885~~	~~0.002147~~	~~10.73~~	~~610.0~~	~~70.8~~	~~68.0~~	~~9.3~~	~~23.9~~	~~9.3~~	~~43.3~~	~~4.6~~
MK268_m3_1	matrix	0.0840	6.01	0.0375	6.31	0.00324	1.94	0.307	0.001002	1.68	37.4	2.3	20.9	0.4	19.9	0.4	20.2	0.3
MK268_m3_2	matrix	0.0767	6.32	0.0346	6.68	0.00327	2.16	0.323	0.001021	2.22	34.6	2.3	21.1	0.5	20.3	0.5	20.6	0.5
MK268_m3_3	matrix	0.0916	6.02	0.0411	6.16	0.00326	1.27	0.206	0.001007	1.87	40.9	2.5	21.0	0.3	19.8	0.3	20.3	0.4
MK268_m3_4	matrix	0.0851	6.06	0.0390	6.46	0.00332	2.23	0.345	0.001027	2.43	38.8	2.5	21.4	0.5	20.0	0.5	20.7	0.5
MK268_m3_5	matrix	0.0916	6.55	0.0413	6.86	0.00327	2.04	0.298	0.001004	2.17	41.1	2.8	21.1	0.4	19.9	0.4	20.3	0.4
MK268_m3_6	matrix	0.0858	6.01	0.0399	6.26	0.00337	1.74	0.278	0.001043	1.99	39.7	2.4	21.7	0.4	20.6	0.4	21.1	0.4
MK268_m3_7	matrix	0.0942	7.10	0.0433	7.34	0.00333	1.86	0.254	0.001012	1.88	43.0	3.1	21.5	0.4	20.2	0.4	20.4	0.4
MK268_m3_8	matrix	0.1351	5.45	0.0538	5.86	0.00289	2.16	0.368	0.000822	1.79	53.2	3.0	18.6	0.4	16.5	0.4	16.6	0.3
MK268_m3_9	matrix	0.0909	8.04	0.0337	8.27	0.00269	1.91	0.231	0.000786	1.90	33.6	2.7	17.3	0.3	16.3	0.3	15.9	0.3
MK268_m3_10	matrix	0.0651	11.28	0.0259	11.46	0.00288	2.04	0.178	0.000845	1.77	25.9	2.9	18.6	0.4	18.1	0.4	17.1	0.3
MK268_m3_11	matrix	0.0826	5.72	0.0370	6.10	0.00325	2.14	0.351	0.001020	1.80	36.9	2.2	20.9	0.4	20.0	0.4	20.6	0.4
MK268_m3_12	matrix	0.0763	5.70	0.0335	5.97	0.00318	1.76	0.295	0.001009	2.28	33.4	2.0	20.5	0.4	19.7	0.4	20.4	0.5
MK268_m3_13	matrix	0.1123	9.62	0.0446	9.99	0.00288	2.72	0.272	0.000827	2.60	44.3	4.3	18.5	0.5	17.0	0.5	16.7	0.4
MK268_m4_1	garnet (crack)	0.0534	11.34	0.0207	11.61	0.00281	2.49	0.214	0.000897	2.42	20.8	2.4	18.1	0.4	17.9	0.4	18.1	0.4
MK268_m4_2	garnet (crack)	0.0507	12.37	0.0199	12.48	0.00285	1.65	0.132	0.000915	1.70	20.1	2.5	18.4	0.3	18.3	0.3	18.5	0.3
MK268_m4_3	garnet (crack)	0.0706	12.59	0.0297	12.89	0.00305	2.75	0.214	0.000951	2.22	29.7	3.8	19.6	0.5	19.0	0.5	19.2	0.4
MK268_m4_4	garnet (crack)	0.0513	12.03	0.0201	12.24	0.00284	2.28	0.187	0.000902	1.74	20.2	2.4	18.3	0.4	18.2	0.4	18.2	0.3
MK268_m4_5	garnet (crack)	0.0526	14.05	0.0205	14.17	0.00282	1.78	0.126	0.000917	1.91	20.6	2.9	18.2	0.3	18.0	0.3	18.5	0.4
MK268_m4_6	garnet (crack)	0.0537	10.53	0.0215	10.67	0.00290	1.75	0.164	0.000926	2.22	21.6	2.3	19.0	0.3	18.5	0.3	18.7	0.4
MK268_m5_1	garnet (crack)	0.1580	4.49	0.0697	5.32	0.00320	2.86	0.537	0.000899	2.52	68.4	3.5	20.6	0.6	17.7	0.6	18.2	0.5
MK268_m5_2	garnet (crack)	0.2633	4.29	0.1328	4.80	0.00366	2.16	0.450	0.000952	2.09	126.6	5.7	24.0	0.5	17.1	0.5	19.2	0.4
MK268_m5_3	garnet (crack)	0.2096	4.54	0.1057	5.06	0.00366	2.25	0.444	0.000958	2.31	102.0	4.9	23.5	0.5	18.7	0.5	19.3	0.4
MK268_m5_4	garnet (crack)	0.2225	3.33	0.1200	3.74	0.00391	1.71	0.458	0.001092	1.92	115.1	4.1	25.0	0.4	19.6	0.4	22.1	0.4
MK268_m5_5	garnet (crack)	0.3563	7.62	0.2464	9.72	0.00502	6.03	0.620	0.001236	4.96	224.0	19.5	32.3	1.9	19.6	1.9	25.0	1.2
MK268_m5_6	garnet (crack)	0.2545	5.44	0.1341	5.97	0.00382	2.45	0.411	0.000975	2.33	127.8	7.2	24.6	0.6	18.0	0.6	19.7	0.5
MK268_m5_7	garnet (crack)	0.0642	9.63	0.0249	9.81	0.00282	1.82	0.186	0.000862	2.05	25.0	2.4	18.0	0.3	17.7	0.3	17.4	0.4
MK268_m5_8	garnet (crack)	0.1014	10.19	0.0415	10.45	0.00297	2.28	0.218	0.000893	1.99	41.3	4.2	19.1	0.4	18.0	0.4	18.0	0.4
MK268_m5_9	garnet (crack)	0.1578	7.19	0.0691	7.73	0.00318	2.83	0.367	0.000905	2.59	67.9	5.1	20.4	0.6	17.6	0.6	18.3	0.5
MK268_m5_10	garnet (crack)	0.0644	14.85	0.0251	15.05	0.00283	2.49	0.165	0.000842	2.74	25.2	3.7	18.2	0.5	18.0	0.5	17.0	0.5
MK268_m5_11	garnet (crack)	0.0951	9.94	0.0380	10.14	0.00290	1.99	0.196	0.000839	1.98	37.9	3.8	18.7	0.4	17.5	0.4	16.9	0.3
MK268_m5_12	garnet (crack)	0.0822	12.27	0.0327	12.48	0.00288	2.32	0.186	0.000871	2.07	32.6	4.0	19.0	0.4	17.7	0.4	17.6	0.4
MK268_m5_13	garnet (crack)	0.1029	12.79	0.0416	13.02	0.00293	2.47	0.190	0.000849	2.19	41.4	5.3	18.9	0.5	18.0	0.5	17.2	0.4
MK268_m5_14	garnet (crack)	0.2686	9.28	0.1490	11.05	0.00403	6.00	0.543	0.001050	4.92	141.0	14.6	25.9	1.6	18.6	1.6	21.2	1.0
MK268_m5_15	garnet (crack)	0.0549	11.39	0.0204	11.57	0.00270	2.05	0.177	0.000798	1.89	20.5	2.4	17.4	0.4	17.2	0.4	16.1	0.3
MK268_m6_1	matrix	0.0884	8.84	0.0395	9.16	0.00324	2.40	0.262	0.001001	2.53	39.3	3.5	20.9	0.5	19.7	0.5	20.2	0.5
MK268_m6_2	matrix	0.0809	9.59	0.0368	9.99	0.00330	2.80	0.280	0.001011	2.59	36.7	3.6	21.0	0.6	20.3	0.6	20.4	0.5
MK268_m6_3	matrix	0.0993	7.47	0.0459	7.71	0.00336	1.90	0.247	0.001035	2.07	45.6	3.4	21.6	0.4	20.0	0.4	20.9	0.4
MK268_m6_4	matrix	0.1926	6.08	0.0911	6.28	0.00343	1.56	0.248	0.000924	1.61	88.6	5.3	22.1	0.3	18.0	0.3	18.7	0.3
MK268_m6_5	matrix	0.0873	17.12	0.0357	17.23	0.00297	1.98	0.115	0.000936	1.97	35.6	6.0	19.1	0.4	18.1	0.4	18.9	0.4
MK268_m6_6	matrix	0.0887	11.73	0.0395	11.92	0.00323	2.14	0.179	0.001006	2.56	39.4	4.6	20.8	0.4	19.7	0.4	20.3	0.5
MK268_m6_7	matrix	0.0824	7.94	0.0373	8.13	0.00328	1.71	0.211	0.001020	1.97	37.2	3.0	21.1	0.4	20.2	0.4	20.6	0.4
MK268_m6_8	matrix	0.0784	9.83	0.0336	10.01	0.00311	1.89	0.189	0.000928	1.92	33.6	3.3	20.0	0.4	19.0	0.4	18.7	0.4

Table B1. Petrochronological data for monazite grains.

Grain #	Location	207Pb/206Pb	2SE %	Pb207/U235	2SE %	206Pb/238U	2SE %	rho	208Pb/232Th	2SE %	207Pb/235U (Ma)	2SE	206Pb/238U (Ma)	2SE	corr.206Pb/238U (Ma)	2SE	208Pb/232Th (Ma)	2SE
MK268_m6_9	matrix	0.0849	9.10	0.0393	9.35	0.00336	2.16	0.231	0.001033	2.14	39.2	3.6	22.0	0.5	20.6	0.5	20.9	0.4
MK268_m6_10	matrix	0.0973	10.14	0.0443	10.42	0.00330	2.40	0.230	0.001018	2.30	44.0	4.5	21.0	0.5	19.9	0.5	20.6	0.5
MK268_m6_11	matrix	0.0795	10.20	0.0351	10.40	0.00321	2.04	0.196	0.000974	1.98	35.1	3.6	21.0	0.4	19.8	0.4	19.7	0.4
MK268_m6_12	matrix	0.0985	23.46	0.0426	23.59	0.00314	2.50	0.106	0.000941	1.78	42.0	9.8	20.0	0.5	18.9	0.5	19.0	0.3
MK268_m6_13	matrix	0.0769	15.59	0.0292	15.75	0.00275	2.21	0.141	0.000853	2.36	29.2	4.5	17.7	0.4	17.0	0.4	17.2	0.4
MK268_m6_14	matrix	0.1158	18.45	0.0515	18.58	0.00323	2.19	0.118	0.000959	2.14	51.0	9.2	20.8	0.5	19.0	0.5	19.4	0.4
MK268_m6_15	matrix	0.0794	11.23	0.0351	11.43	0.00321	2.11	0.184	0.000991	1.95	35.1	3.9	20.7	0.4	20.0	0.4	20.0	0.4
MK268_m6_16	matrix	0.1326	18.44	0.0590	18.60	0.00323	2.41	0.130	0.000941	2.06	58.0	10.5	20.8	0.5	19.0	0.5	19.0	0.4
MK268_m6_17	matrix	0.1343	14.73	0.0622	14.95	0.00336	2.53	0.169	0.000969	2.86	61.2	8.9	21.6	0.5	19.0	0.5	19.6	0.6
MK268_m6_18	matrix	0.3892	5.48	0.2748	6.43	0.00512	3.37	0.524	0.001056	2.86	247.0	14.1	32.9	1.1	19.0	1.1	21.3	0.6
MK268_m6_19	matrix	0.0759	11.46	0.0278	11.76	0.00265	2.65	0.225	0.000805	2.33	27.8	3.2	17.1	0.5	16.4	0.5	16.3	0.4
MK268_m6_20	matrix	0.2307	6.21	0.1066	6.71	0.00335	2.55	0.380	0.000879	2.32	102.8	6.6	21.6	0.5	16.6	0.5	17.8	0.4
MK268_m6_21	matrix	0.0748	18.03	0.0251	18.23	0.00243	2.71	0.149	0.000736	2.41	25.1	4.5	15.7	0.4	15.1	0.4	14.9	0.4
MK268_m6_22	matrix	0.1393	14.04	0.0623	14.28	0.00325	2.61	0.183	0.000940	2.13	61.4	8.5	20.9	0.5	18.4	0.5	19.0	0.4
MK268_m6_23	matrix	0.0984	20.86	0.0453	21.02	0.00334	2.62	0.125	0.000952	1.92	45.0	9.3	21.5	0.6	20.1	0.6	19.2	0.4
MK268_m6_24	matrix	0.0675	19.68	0.0292	19.84	0.00314	2.52	0.127	0.000946	2.14	29.2	5.7	20.2	0.5	19.6	0.5	19.1	0.4
MK268_m6_25	matrix	0.0904	7.19	0.0413	7.52	0.00331	2.21	0.294	0.001021	2.32	41.1	3.0	21.3	0.5	20.1	0.5	20.6	0.5
MK268_m6_26	matrix	0.1046	16.26	0.0498	16.54	0.00346	3.07	0.185	0.000978	2.35	49.4	8.0	22.2	0.7	20.6	0.7	19.8	0.5
MK268_m6_27	matrix	0.2503	10.22	0.1139	10.67	0.00330	3.05	0.286	0.000861	2.36	110.0	11.1	21.3	0.6	15.8	0.6	17.4	0.4
MK268_m6_28	matrix	0.0952	11.74	0.0413	11.93	0.00315	2.09	0.175	0.000954	2.10	41.1	4.8	20.0	0.4	19.0	0.4	19.3	0.4
MK268_m6_29	matrix	0.1366	15.95	0.0619	16.05	0.00329	1.79	0.111	0.000936	1.97	61.0	9.5	21.2	0.4	18.8	0.4	18.9	0.4
MK268_m6_30	matrix	0.3433	4.92	0.2371	5.47	0.00501	2.40	0.439	0.001052	1.40	216.0	10.6	32.2	0.8	20.1	0.8	21.2	0.3
MK268_m6_31	matrix	0.2269	8.09	0.0956	8.59	0.00306	2.89	0.336	0.000810	2.92	92.7	7.6	19.7	0.6	15.2	0.6	16.4	0.5
MK268_m6_32	matrix	0.1833	9.38	0.0735	9.71	0.00291	2.48	0.255	0.000767	2.20	72.0	6.7	18.7	0.5	15.5	0.5	15.5	0.3
MK268_m6_33	matrix	0.1433	9.82	0.0627	10.56	0.00318	3.88	0.367	0.000884	3.33	61.8	6.3	20.5	0.8	17.9	0.8	17.8	0.6
MK268_m6_34	matrix	0.0876	9.12	0.0381	9.64	0.00315	3.12	0.324	0.000944	2.64	37.9	3.6	20.3	0.6	19.0	0.6	19.1	0.5
MK268_m6_35	matrix	0.0910	6.30	0.0401	6.94	0.00319	2.92	0.420	0.000986	2.77	39.9	2.7	20.5	0.6	19.4	0.6	19.9	0.6
MK268_m6_36	matrix	0.0876	5.86	0.0393	6.11	0.00325	1.72	0.282	0.001017	1.35	39.1	2.3	20.9	0.4	19.8	0.4	20.5	0.3
MK268_m6_37	matrix	0.0884	6.05	0.0401	6.46	0.00329	2.25	0.348	0.001028	2.06	39.9	2.5	21.2	0.5	20.1	0.5	20.8	0.4
MK268_m6_38	matrix	0.0792	7.18	0.0358	7.61	0.00328	2.54	0.334	0.001014	2.75	35.7	2.7	21.1	0.5	20.2	0.5	20.5	0.6
MK268_m6_39	matrix	0.0813	6.62	0.0369	6.87	0.00330	1.85	0.269	0.001018	1.85	36.8	2.5	21.2	0.4	20.3	0.4	20.6	0.4
MK268_m6_40	matrix	0.0810	5.38	0.0358	6.04	0.00321	2.74	0.455	0.000996	2.89	35.7	2.1	20.7	0.6	19.7	0.6	20.1	0.6
MK268_m6_41	matrix	0.0854	6.90	0.0388	7.10	0.00330	1.67	0.235	0.001023	1.69	38.6	2.7	21.2	0.4	20.2	0.4	20.7	0.3
MK268_m6_42	matrix	0.1216	22.75	0.0543	22.97	0.00324	3.18	0.138	0.000949	2.16	54.0	12.0	20.8	0.7	18.9	0.7	19.2	0.4
MK268_m6_43	matrix	0.0881	10.81	0.0390	10.94	0.00321	1.67	0.153	0.000966	1.11	38.8	4.2	20.7	0.3	19.6	0.3	19.5	0.2
MK268_m6_44	matrix	0.0861	8.31	0.0387	8.71	0.00326	2.62	0.300	0.001010	2.54	38.6	3.3	21.0	0.5	19.9	0.5	20.4	0.5
MK268_m6_45	matrix	0.0823	7.92	0.0374	8.28	0.00330	2.42	0.292	0.001022	2.20	37.3	3.0	21.2	0.5	20.2	0.5	20.6	0.5
MK268_m6_46	matrix	0.0868	7.25	0.0395	7.53	0.00330	2.05	0.272	0.001024	2.32	39.3	2.9	21.2	0.4	20.1	0.4	20.7	0.5
MK268_m6_47	matrix	0.1282	6.04	0.0620	6.34	0.00351	1.92	0.304	0.001056	1.77	61.1	3.8	23.0	0.4	20.3	0.4	21.3	0.4
MK268_m6_48	matrix	0.0808	8.80	0.0367	9.07	0.00329	2.18	0.240	0.001024	2.77	36.6	3.3	21.2	0.5	20.3	0.5	20.7	0.6
MK268_m6_49	matrix	0.0892	9.37	0.0409	9.65	0.00332	2.31	0.239	0.001028	2.42	40.7	3.8	21.0	0.5	20.2	0.5	20.8	0.5
MK268_m6_50	matrix	0.0850	8.04	0.0387	8.34	0.00330	2.22	0.267	0.001011	2.21	38.5	3.2	21.3	0.5	20.2	0.5	20.4	0.4
MK268_m6_51	matrix	0.0912	8.45	0.0412	8.80	0.00328	2.46	0.280	0.001013	2.36	41.0	3.5	21.0	0.5	19.9	0.5	20.5	0.5
MK268_m6_52	matrix	0.0841	6.05	0.0379	6.83	0.00327	3.16	0.463	0.001004	3.01	37.8	2.5	21.1	0.7	20.1	0.7	20.3	0.6
MK268_m6_53	matrix	0.0815	5.11	0.0363	5.70	0.00323	2.52	0.442	0.001016	2.46	36.2	2.0	20.8	0.5	19.9	0.5	20.5	0.5
MK268_m6_54	matrix	0.0802	5.25	0.0364	5.69	0.00329	2.18	0.384	0.001015	1.86	36.3	2.0	21.0	0.5	20.3	0.5	20.5	0.4
MK268_m6_55	matrix	0.1184	6.52	0.0564	7.01	0.00345	2.57	0.367	0.001061	2.38	55.7	3.8	22.2	0.6	20.0	0.6	21.4	0.5
MK268_m6_56	matrix	0.0759	6.24	0.0341	6.75	0.00326	2.57	0.382	0.001014	2.46	34.0	2.3	21.0	0.5	20.2	0.5	20.5	0.5
MK268_m7_1	matrix	0.1165	12.02	0.0436	12.14	0.00271	1.75	0.144	0.000816	1.51	43.3	5.1	17.5	0.3	15.9	0.3	16.5	0.2
MK268_m7_2	matrix	0.4119	5.29	0.2696	6.58	0.00475	3.91	0.595	0.000992	1.83	242.0	14.2	30.5	1.2	16.4	1.2	20.0	0.4
MK268_m7_3	matrix	0.1858	10.33	0.0731	10.51	0.00285	1.93	0.184	0.000807	1.29	71.6	7.3	18.4	0.4	15.1	0.4	16.3	0.2
MK268_m7_4	matrix	0.0984	15.19	0.0361	15.30	0.00266	1.80	0.118	0.000792	1.87	36.0	5.4	17.1	0.3	16.0	0.3	16.0	0.3
MK268_m7_5	matrix	0.1957	8.74	0.0815	9.19	0.00302	2.85	0.310	0.000836	2.42	79.6	7.0	19.5	0.6	15.8	0.6	16.9	0.4
MK268_m7_6	matrix	0.0657	27.33	0.0228	27.39	0.00252	1.76	0.064	0.000773	1.67	22.9	6.2	16.2	0.3	15.8	0.3	15.6	0.3
MK268_m7_7	matrix	0.0835	20.53	0.0341	20.61	0.00297	1.82	0.088	0.000920	1.28	34.1	6.9	19.1	0.3	18.2	0.3	18.6	0.2
MK268_m7_8	matrix	0.0874	22.66	0.0362	22.72	0.00301	1.60	0.071	0.000920	1.18	36.1	8.1	19.4	0.3	18.3	0.3	18.6	0.2
MK268_m7_9	matrix	0.0773	19.04	0.0325	19.12	0.00305	1.76	0.092	0.000910	1.76	32.4	6.1	19.6	0.3	18.8	0.3	18.4	0.3

Table B1. Petrochronological data for monazite grains.

Grain #	Location	207Pb/206Pb	2SE %	Pb207/U235	2SE %	206Pb/238U	2SE %	rho	208Pb/232Th	2SE %	207Pb/235U (Ma)	2SE	206Pb/238U (Ma)	2SE	corr.206Pb/238U (Ma)	2SE	208Pb/232Th (Ma)	2SE
MK268_m7_10	matrix	0.0957	20.27	0.0406	20.36	0.00308	1.82	0.090	0.000928	1.86	40.4	8.1	19.8	0.4	18.6	0.4	18.7	0.3
MK268_m7_11	matrix	0.1504	16.52	0.0614	16.65	0.00296	2.09	0.125	0.000861	1.26	61.0	9.8	19.1	0.4	16.6	0.4	17.4	0.2
MK268_m7_12	matrix	0.2754	12.85	0.1344	13.52	0.00354	4.19	0.310	0.000898	2.35	128.0	16.3	23.0	1.0	16.2	1.0	18.1	0.4
MK268_m7_13	matrix	0.2145	7.16	0.0994	7.37	0.00336	1.75	0.238	0.000887	1.77	96.2	6.8	21.6	0.4	17.0	0.4	17.9	0.3
MK268_m7_14	matrix	0.1937	10.97	0.0968	11.39	0.00363	3.04	0.267	0.000981	1.75	94.0	10.2	23.3	0.7	19.0	0.7	19.8	0.3
MK268_m8_1	matrix	0.0924	10.78	0.0424	10.87	0.00333	1.42	0.130	0.001014	1.48	42.2	4.5	21.4	0.3	20.0	0.3	20.5	0.3
MK268_m8_2	matrix	0.1467	16.96	0.0594	17.06	0.00294	1.82	0.107	0.000840	1.42	59.0	9.7	18.9	0.3	16.5	0.3	17.0	0.2
MK268_m8_3	matrix	0.0954	17.87	0.0381	17.94	0.00289	1.56	0.087	0.000859	1.84	37.9	6.7	18.6	0.3	17.5	0.3	17.3	0.3
MK268_m8_4	matrix	0.0777	9.84	0.0349	9.90	0.00326	1.09	0.110	0.000997	1.22	34.8	3.4	21.0	0.2	20.1	0.2	20.1	0.2
MK268_m8_5	matrix	0.0803	14.15	0.0332	14.27	0.00300	1.86	0.131	0.000895	1.91	33.2	4.7	19.3	0.4	18.5	0.4	18.1	0.3
MK268_m8_6	matrix	0.0863	8.91	0.0395	9.00	0.00332	1.23	0.137	0.001015	1.28	39.3	3.5	21.4	0.3	20.3	0.3	20.5	0.3
MK268_m8_7	matrix	0.0986	11.51	0.0451	11.61	0.00332	1.46	0.126	0.001015	1.41	44.8	5.1	21.3	0.3	19.9	0.3	20.5	0.3
MK268_m8_8	matrix	0.0982	16.09	0.0400	16.13	0.00295	1.23	0.076	0.000850	2.01	39.8	6.3	19.0	0.2	17.8	0.2	17.2	0.3
MK268_m8_9	matrix	0.2705	4.87	0.1224	5.26	0.00328	2.00	0.380	0.000827	1.94	117.3	5.8	21.1	0.4	15.1	0.4	16.7	0.3
MK268_m8_10	matrix	0.1419	11.57	0.0521	11.67	0.00266	1.51	0.130	0.000752	1.54	51.6	5.9	17.2	0.3	15.1	0.3	15.2	0.2
MK268_m8_11	matrix	0.1713	7.30	0.0805	7.87	0.00341	2.93	0.372	0.000958	2.13	78.6	6.0	21.9	0.6	18.5	0.6	19.3	0.4
MK268_m8_12	matrix	0.1023	6.08	0.0463	6.21	0.00328	1.23	0.198	0.001002	1.64	45.9	2.8	21.1	0.3	19.6	0.3	20.2	0.3
MK268_m8_13	matrix	0.1808	7.33	0.0989	7.64	0.00397	2.14	0.280	0.001130	1.43	95.8	7.0	25.5	0.5	21.2	0.5	22.8	0.3
MK268_m8_14	matrix	0.1556	4.52	0.0796	4.73	0.00371	1.38	0.291	0.001091	1.40	77.8	3.5	23.9	0.3	20.6	0.3	22.0	0.3
MK268_m8_15	matrix	0.0880	6.82	0.0410	6.98	0.00338	1.45	0.208	0.001035	1.49	40.8	2.8	21.7	0.3	20.6	0.3	20.9	0.3
MK268_m8_16	matrix	0.0732	8.53	0.0329	8.66	0.00326	1.53	0.177	0.001034	1.47	32.9	2.8	21.0	0.3	20.3	0.3	20.9	0.3
MK268_m8_17	matrix	0.0731	8.26	0.0331	8.40	0.00329	1.51	0.179	0.001035	1.39	33.1	2.7	21.2	0.3	20.5	0.3	20.9	0.3
MK268_m8_18	matrix	0.0733	9.08	0.0330	9.18	0.00327	1.40	0.152	0.001003	1.24	33.0	3.0	21.0	0.3	20.3	0.3	20.3	0.3
MK268_m8_19	matrix	0.0804	9.60	0.0365	9.76	0.00330	1.76	0.181	0.000992	1.71	36.4	3.5	21.2	0.4	20.3	0.4	20.0	0.3
MK268_m8_20	matrix	0.0752	8.14	0.0344	8.30	0.00332	1.60	0.193	0.001017	1.70	34.4	2.8	21.4	0.3	20.6	0.3	20.5	0.3
MK268_m8_21	matrix	0.0692	7.85	0.0316	7.88	0.00331	0.78	0.099	0.001015	1.30	31.6	2.5	21.3	0.2	20.7	0.2	20.5	0.3
MK268_m8_22	matrix	0.0768	8.25	0.0351	8.46	0.00332	1.83	0.217	0.001027	1.75	35.1	2.9	21.3	0.4	20.5	0.4	20.7	0.4
MK268_m8_23	matrix	0.0771	6.59	0.0352	6.80	0.00332	1.65	0.243	0.001016	1.64	35.1	2.3	21.3	0.4	20.5	0.4	20.5	0.3
MK268_m8_24	matrix	0.0772	6.91	0.0362	7.15	0.00340	1.86	0.261	0.001038	1.80	36.1	2.5	21.9	0.4	21.0	0.4	21.0	0.4
MK268_m9_1	garnet (crack)	0.0964	12.44	0.0410	12.63	0.00308	2.18	0.173	0.000918	1.87	40.8	5.0	19.9	0.4	18.6	0.4	18.5	0.3
MK268_m9_2	garnet (crack)	0.2877	5.46	0.1717	5.76	0.00433	1.85	0.321	0.001012	1.26	160.9	8.6	27.8	0.5	19.4	0.5	20.4	0.3
MK268_m9_3	garnet (crack)	0.1198	16.50	0.0542	16.71	0.00328	2.65	0.158	0.000956	1.94	53.6	8.7	21.1	0.6	19.2	0.6	19.3	0.4
MK268_m9_4	garnet (crack)	0.1025	12.92	0.0469	13.20	0.00332	2.70	0.204	0.000964	1.84	46.5	6.0	21.4	0.6	19.8	0.6	19.5	0.4
MK268_m9_5	garnet (crack)	0.0863	12.20	0.0401	12.35	0.00337	1.92	0.156	0.000987	1.35	39.9	4.8	22.0	0.4	20.6	0.4	19.9	0.3
MK268_m9_6	garnet (crack)	0.1241	12.58	0.0586	12.76	0.00343	2.14	0.168	0.000970	1.58	57.8	7.2	22.1	0.5	19.9	0.5	19.6	0.3
MK268_m9_7	garnet (crack)	0.0639	33.95	0.0282	34.01	0.00320	2.08	0.061	0.000931	1.27	28.3	9.5	21.0	0.4	20.2	0.4	18.8	0.2
MK268_m9_8	garnet (crack)	0.0649	21.87	0.0272	21.93	0.00304	1.63	0.074	0.000912	1.68	27.3	5.9	19.6	0.3	19.0	0.3	18.4	0.3
MK268_m9_9	garnet (crack)	0.0841	16.09	0.0357	16.20	0.00308	1.83	0.113	0.000933	1.42	35.6	5.7	19.8	0.4	18.9	0.4	18.9	0.3
MK268_m10_1	matrix	0.0776	12.82	0.0305	12.97	0.00285	1.96	0.151	0.000843	1.68	30.5	3.9	18.4	0.4	18.0	0.4	17.0	0.3
MK268_m10_2	matrix	0.3042	10.14	0.1533	12.06	0.00366	6.52	0.541	0.000938	4.08	145.0	16.3	23.5	1.5	15.9	1.5	18.9	0.8
MK268_m10_3	matrix	0.0972	6.82	0.0454	6.95	0.00339	1.31	0.188	0.001029	1.13	45.1	3.1	21.8	0.3	20.4	0.3	20.8	0.2
MK268_m10_4	matrix	0.1056	13.56	0.0501	13.70	0.00344	1.91	0.139	0.001006	1.98	49.6	6.6	22.1	0.4	20.5	0.4	20.3	0.4
MK268_m10_5	matrix	0.0831	15.45	0.0317	15.57	0.00277	1.98	0.127	0.000850	1.94	31.7	4.9	18.0	0.4	17.0	0.4	17.2	0.3
MK268_m10_6	matrix	0.0818	17.01	0.0327	17.15	0.00290	2.24	0.131	0.000895	1.85	32.6	5.5	18.6	0.4	17.8	0.4	18.1	0.3
MK268_m10_7	matrix	0.3244	12.97	0.1729	16.68	0.00387	10.49	0.629	0.000892	4.59	162.0	25.0	25.0	2.6	16.1	2.6	18.0	0.8
MK268_m10_8	matrix	0.4178	5.37	0.3031	8.36	0.00526	6.40	0.766	0.001089	3.40	269.0	19.7	33.8	2.2	18.0	2.2	22.0	0.7
MK268_m10_9	matrix	0.2112	8.48	0.1042	8.80	0.00358	2.33	0.264	0.000967	2.04	100.7	8.4	23.0	0.5	18.2	0.5	19.5	0.4
MK268_m10_10	matrix	0.2738	18.24	0.1331	22.07	0.00353	12.42	0.563	0.000873	4.45	127.0	26.3	23.0	2.8	16.0	2.8	17.6	0.8
MK268_m10_11	matrix	0.1062	6.06	0.0495	6.26	0.00338	1.58	0.253	0.001031	1.85	49.0	3.0	22.0	0.3	20.1	0.3	20.8	0.4
MK268_m10_12	matrix	0.1077	8.02	0.0511	8.22	0.00344	1.78	0.216	0.001030	1.60	50.6	4.1	22.0	0.4	20.0	0.4	20.8	0.3
MK268_m10_13	matrix	0.1043	6.41	0.0472	6.59	0.00329	1.52	0.231	0.000995	1.75	46.8	3.0	21.0	0.3	20.0	0.3	20.1	0.4
MK268_m10_14	matrix	0.2534	6.47	0.1172	6.98	0.00336	2.63	0.376	0.000843	1.37	112.5	7.4	22.0	0.6	16.0	0.6	17.0	0.2
MK268_m10_15	matrix	0.0935	7.74	0.0441	7.93	0.00342	1.74	0.220	0.001037	1.87	43.8	3.4	22.0	0.4	21.0	0.4	20.9	0.4
MK268_m10_16	matrix	0.1115	6.66	0.0530	6.87	0.00345	1.67	0.243	0.001039	1.50	52.5	3.5	22.0	0.4	20.0	0.4	21.0	0.3
MK268_m10_17	matrix	0.2314	6.71	0.1226	7.11	0.00384	2.35	0.331	0.001023	1.90	117.4	7.9	25.0	0.6	19.0	0.6	20.7	0.4
MK268_m10_18	matrix	0.0967	15.37	0.0409	15.43	0.00307	1.31	0.085	0.000912	1.27	40.7	6.2	20.0	0.3	19.0	0.3	18.4	0.2
MK268_m10_19	matrix	0.2589	10.31	0.1274	11.57	0.00357	5.25	0.454	0.000901	2.60	122.0	13.3	23.0	1.2	17.0	1.2	18.2	0.5

Table B1. Petrochronological data for monazite grains.

Grain #	Location	207Pb/206Pb	2SE %	Pb207/U235	2SE %	206Pb/238U	2SE %	rho	208Pb/232Th	2SE %	207Pb/235U (Ma)	2SE	206Pb/238U (Ma)	2SE	corr.206Pb/238U (Ma)	2SE	208Pb/232Th (Ma)	2SE
MK268_m10_20	matrix	0.1201	15.30	0.0437	15.40	0.00264	1.72	0.111	0.000798	1.78	43.5	6.6	17.0	0.3	15.0	0.3	16.1	0.3
MK268_m10_21	matrix	0.1562	8.69	0.0644	8.92	0.00299	2.04	0.229	0.000833	1.75	63.4	5.5	19.3	0.4	17.0	0.4	16.8	0.3
MK268_m10_22	matrix	0.1137	10.30	0.0490	10.43	0.00313	1.62	0.156	0.000904	1.30	48.6	4.9	20.1	0.3	18.0	0.3	18.2	0.2
MK268_m10_23	matrix	0.0998	11.58	0.0440	11.70	0.00320	1.69	0.144	0.000945	1.75	43.7	5.0	20.6	0.3	19.0	0.3	19.1	0.3
MK268_m10_24	matrix	0.0755	11.75	0.0344	11.84	0.00331	1.44	0.122	0.001011	1.39	34.4	4.0	21.3	0.3	20.5	0.3	20.4	0.3
MK268_m10_25	matrix	0.0886	10.02	0.0408	10.14	0.00334	1.58	0.156	0.001008	1.93	40.6	4.0	21.5	0.3	20.3	0.3	20.4	0.4
MK268_m10_26	matrix	0.0877	11.40	0.0400	11.51	0.00331	1.61	0.139	0.001028	1.46	39.9	4.5	21.3	0.3	20.2	0.3	20.8	0.3
MK268_m10_27	matrix	0.0852	10.03	0.0390	10.22	0.00332	1.96	0.192	0.001015	1.83	38.8	3.9	21.4	0.4	20.3	0.4	20.5	0.4
MK268_m10_28	matrix	0.0777	7.63	0.0355	7.80	0.00331	1.58	0.203	0.001004	1.49	35.4	2.7	21.3	0.3	20.5	0.3	20.3	0.3
MK268_m10_29	matrix	0.1054	7.47	0.0494	7.66	0.00340	1.69	0.220	0.001028	1.81	49.0	3.7	21.9	0.4	20.3	0.4	20.8	0.4
MK268_m10_30	matrix	0.2041	5.35	0.1118	5.81	0.00397	2.26	0.390	0.001119	1.98	107.6	5.9	25.6	0.6	20.5	0.6	22.6	0.4
MK268_m10_31	matrix	0.0913	8.58	0.0426	8.73	0.00339	1.61	0.184	0.001040	1.93	42.4	3.6	21.8	0.4	20.6	0.4	21.0	0.4
MK268_m10_32	matrix	0.0911	9.57	0.0423	9.78	0.00337	2.04	0.208	0.001029	1.96	42.1	4.0	21.7	0.4	20.5	0.4	20.8	0.4
MK268_m10_33	matrix	0.1453	9.23	0.0719	9.42	0.00359	1.90	0.201	0.001078	1.99	70.5	6.4	23.1	0.4	20.2	0.4	21.8	0.4
MK268_m10_34	matrix	0.0932	6.71	0.0437	6.99	0.00340	1.98	0.283	0.001032	1.54	43.4	3.0	21.9	0.4	20.6	0.4	20.8	0.3
MK268_m10_35	matrix	0.2917	8.52	0.1847	9.92	0.00460	5.08	0.512	0.001149	2.48	172.0	15.7	30.0	1.5	20.4	1.5	23.2	0.6
MK268_m10_36	matrix	0.1086	7.76	0.0508	7.97	0.00339	1.83	0.230	0.001014	1.48	50.3	3.9	21.8	0.4	20.1	0.4	20.5	0.3
MK268_m10_37	matrix	0.1180	8.89	0.0560	9.09	0.00344	1.90	0.209	0.001034	1.79	55.3	4.9	22.2	0.4	20.2	0.4	20.9	0.4

Table B1. Petrochronological data for monazite grains.

Grain #	Y (ppm)	2SE	La (ppm)	2SE	Ce (ppm)	2SE	Pr (ppm)	2SE	Nd (ppm)	2SE	Sm (ppm)	2SE	Eu (ppm)	2SE	Gd (ppm)	2SE	Tb (ppm)	2SE	Dy (ppm)	2SE	Ho (ppm)	2SE	Er (ppm)	2SE	Tm (ppm)	2SE	Yb (ppm)	2SE	Lu (ppm)	2SE	Gd/Yb(N)
MK256																															
MK256_m1_1	6552	682	81124	5666	196807	16554	17862	1756	73295	4253	14127	1056	1281	84	10749	1181	840	85	2361	159	249	21	307	25	30	4	64	8	7	1	135
MK256_m1_2	5074	445	100974	8226	221907	18446	24031	2635	85612	4823	17770	1468	1337	142	13005	1096	840	89	2065	184	193	18	236	18	14	2	45	7	4	1	235
MK256_m1_3	8317	741	98869	8428	219941	19661	22018	2447	83196	7177	17408	1449	1554	138	12524	955	1015	87	3049	285	305	25	379	29	43	4	89	9	10	1	114
MK256_m1_4	4710	438	96648	12632	223396	21931	24316	2905	84817	5733	18373	1649	1438	145	12429	1016	825	62	2200	150	188	18	272	26	16	2	36	4	4	1	276
MK256_m1_5	7772	593	99153	10811	217909	15120	20904	2093	84606	7504	15867	1200	1700	170	12622	1362	1041	114	2696	250	323	23	377	37	36	4	100	11	10	2	102
MK256_m1_6	5797	474	99830	10221	224891	21779	21461	2191	84780	6207	16589	1232	1413	161	12579	1164	849	98	2335	231	233	24	298	25	21	2	57	7	5	1	177
MK256_m1_7	7123	681	88991	8155	219190	26404	22126	2704	77539	4345	15473	1141	1381	124	11129	757	876	83	2611	273	287	29	311	37	31	3	79	11	8	1	114
MK256_m1_8	5694	622	105457	7572	218260	19630	23743	3253	84483	7170	18295	1663	1482	122	11927	1114	853	82	2393	217	223	17	292	30	23	3	52	8	7	1	187
~~MK256_m1_9~~	~~3260~~	~~370~~	~~23674~~	~~3404~~	~~61372~~	~~6529~~	~~5945~~	~~595~~	~~25339~~	~~2692~~	~~5001~~	~~551~~	~~541~~	~~60~~	~~3064~~	~~272~~	~~337~~	~~42~~	~~1103~~	~~132~~	~~127~~	~~19~~	~~140~~	~~17~~	~~18~~	~~2~~	~~41~~	~~6~~	~~5~~	~~1~~	~~60~~
MK256_m2_1	5243	418	74215	9247	151533	15970	15397	1261	59463	5006	11495	1040	1101	103	8923	655	774	76	1979	136	221	22	273	27	27	3	71	7	8	1	102
MK256_m2_2	5368	403	104664	9445	230462	22731	21961	2510	81231	6469	15716	770	1425	103	12505	972	917	88	2115	193	229	19	289	33	21	3	56	7	6	1	181
MK256_m2_3	2327	227	18838	1547	57226	6726	5273	501	19376	1552	3858	335	413	45	3027	312	254	28	712	73	85	9	101	13	9	2	23	4	3	1	105
MK256_m2_4	6951	745	91114	8683	207713	16464	23468	3105	76640	5512	15103	1297	1506	129	12294	1038	925	73	2402	219	286	29	336	33	31	3	81	9	9	1	123
MK256_m2_5	6799	937	107048	13273	207234	20991	23031	2353	85539	7076	15684	1351	1487	140	13572	1078	863	78	2358	209	265	29	326	36	28	3	77	10	9	1	142
MK256_m2_6	3071	254	22617	2518	64700	7643	6397	491	25450	2176	5004	470	533	57	3854	401	311	29	1009	113	120	11	142	14	16	2	44	5	5	1	71
MK256_m3_1	10348	727	94766	8074	217085	19078	24724	2788	83905	6208	17625	1574	1771	134	14135	1505	1153	105	3288	243	443	43	484	32	44	3	123	13	14	2	93
MK256_m3_2	7691	869	111766	9744	265180	25314	24873	2359	99675	10312	17081	1478	1700	135	12638	1117	1120	112	3016	346	296	34	411	38	30	5	89	14	10	1	114
MK256_m3_3	4800	427	90701	11517	181822	18161	16119	1127	70268	6729	13588	1588	1245	103	10329	1156	733	60	1775	136	183	14	238	23	16	2	46	6	6	1	180
MK256_m3_4	4547	386	112249	10079	232737	16965	26813	2705	103387	13304	17974	1533	1525	154	13730	1063	856	78	2055	186	177	15	242	21	15	2	38	5	4	1	291
MK256_m3_5	6692	554	113338	9731	231169	18434	27414	3102	94984	10779	17546	1551	1646	151	12817	1267	1058	66	2498	227	243	19	303	30	23	3	64	8	8	1	162
MK256_m3_6	5488	508	108804	8055	234492	19083	28816	2525	101036	8761	16123	1750	1586	124	13381	1222	978	60	2205	190	242	23	324	30	23	3	63	8	7	1	172
MK256_m3_7	4807	394	121636	10870	243873	17989	26057	2811	95217	6681	17389	1389	1491	119	13529	1214	880	86	2177	248	203	21	286	29	15	3	45	6	4	1	245
MK256_m3_8	4832	514	111713	9743	224593	17296	26370	3351	91787	6720	17697	1827	1464	112	14226	1253	895	74	2108	158	187	13	252	24	15	2	44	6	4	1	259
MK256_m3_9	5987	467	112521	11513	238979	18215	25699	2408	94778	10706	17528	1367	1695	184	12379	789	1017	88	2372	284	247	23	338	22	21	3	61	8	6	2	165
MK256_m3_10	5955	583	108341	9762	243960	19833	23981	2756	90621	7198	16760	1276	1696	147	13562	1266	994	102	2418	241	258	19	304	24	21	3	60	8	6	1	183
MK256_m4_1	1880	179	39740	4866	86540	7995	9497	942	32715	2413	6004	496	584	62	4689	531	321	32	751	57	73	8	103	11	7	1	27	4	4	1	142
MK256_m4_2	2303	181	58696	4616	127924	8318	13160	938	51146	4749	9519	775	905	106	7594	540	491	42	1027	91	92	8	137	13	7	1	24	4	3	1	253
MK256_m4_3	3145	355	106559	10234	207628	13505	22746	2226	78952	6090	15123	969	1474	149	11467	761	791	79	1581	106	130	11	197	22	9	2	29	4	3	1	316
MK256_m4_4	3400	299	100741	6100	198590	17875	20190	1859	82098	6961	13647	1161	1323	135	11612	987	793	79	1645	142	139	14	200	18	9	1	27	4	2	1	342
MK256_m4_5	3491	228	104721	9878	214505	17552	23186	2433	80155	4995	15653	1599	1360	107	11712	1010	777	62	1632	191	142	12	225	21	10	1	30	3	3	1	311
MK256_m4_6	3769	290	103758	9159	169618	12857	21077	2449	77030	4906	14857	1019	1236	105	10209	895	789	62	1552	107	139	12	203	20	10	1	29	4	3	1	282
MK256_m5_1	4060	415	105429	8728	199508	15298	23714	2129	81992	5895	16312	1413	1392	108	12019	775	887	85	1847	137	162	18	223	21	12	2	34	5	3	1	284
MK256_m5_2	3567	279	93570	7810	179530	15204	16534	1168	66558	5380	13185	1214	1120	83	9385	885	639	70	1456	152	135	13	198	16	9	1	33	4	3	1	231
MK256_m5_3	2702	243	67444	5834	132642	13403	14608	818	54270	3996	11299	1103	843	69	8010	751	531	42	1227	113	106	10	152	13	10	1	44	5	6	2	147
MK256_m6_1	4630	420	106011	8327	200002	17008	22800	2372	77095	4882	14755	1317	1362	107	12159	1360	852	84	1958	162	200	16	242	22	14	2	38	5	4	1	258
MK256_m6_2	5383	488	99650	10965	217079	15000	19648	1734	77687	6322	14747	895	1432	124	12281	937	943	82	2088	216	207	20	262	23	16	2	47	7	5	1	210
MK256_m6_3	4440	289	99386	7053	211666	18724	23005	2534	78190	5678	14477	1012	1368	127	11315	957	833	54	2000	175	179	16	228	20	12	2	35	5	4	1	262
MK256_m6_4	4416	334	107041	8046	205889	21567	22129	2371	74768	6468	14037	1067	1335	94	10815	1069	866	70	2092	142	188	16	251	25	13	2	38	6	4	1	229
MK256_m6_5	4579	348	107034	7996	202443	18295	24859	2395	72456	6118	14888	1256	1345	87	11751	953	811	69	2053	127	178	19	235	25	13	2	39	6	4	1	246
MK256_m6_6	4564	347	103261	8335	195811	17117	20493	2675	77538	5072	16563	1021	1459	111	13162	987	889	76	2020	165	201	19	253	17	14	2	42	3	4	1	256
MK256_m6_7	4505	366	94045	9817	195688	20170	19403	2328	66400	6067	13469	1361	1377	142	10309	732	874	59	2002	183	180	11	244	26	12	2	40	5	4	1	207
MK256_m8_1	4439	253	124189	10052	216798	19651	27068	2827	92365	6323	16389	1261	1414	119	12490	1221	910	87	2194	164	202	21	251	22	15	2	33	5	5	1	308
MK256_m8_2	3830	329	120408	9542	209272	18140	24944	2706	86111	5222	16526	1343	1231	94	12556	1122	807	70	1762	158	161	16	228	27	8	1	31	4	3	1	325
MK256_m9_1	7740	998	65778	9399	134363	18613	12959	1272	55134	7431	11230	1711	1233	149	8140	1087	824	93	2781	369	309	39	341	43	30	4	72	11	9	2	91
MK256_m9_2	7736	859	69945	9292	158853	20318	15579	2593	62314	7696	11875	1282	1230	125	7828	1068	861	92	3022	331	341	36	382	44	28	4	63	11	8	1	101
MK256_m9_3	7577	683	81401	11185	144592	20721	15625	1945	67775	7991	11772	1559	1294	139	9897	1248	966	129	2959	399	357	47	365	40	32	5	74	11	9	1	109
MK256_m9_4	5428	437	113155	7728	216021	18324	25357	3136	89661	5027	17564	1590	1383	102	12299	1036	902	58	2503	186	229	21	287	28	18	2	50	7	5	1	200
MK256_m9_5	4198	471	126145	9917	215572	13090	27447	3175	90217	6280	16827	1463	1457	163	12435	1096	874	78	2006	171	174	15	257	22	12	1	34	5	4	1	295
MK256_m9_6	3696	271	124459	11048	233690	21177	26119	2654	94169	5180	16449	1564	1315	112	11899	1009	853	70	1781	147	153	12	234	20	10	2	28	4	4	1	342
MK256_m9_7	3616	272	114224	8108	202743	14627	25669	2848	94665	10141	15105	832	1326	111	12178	985	811	81	1647	135	144	10	218	24	12	2	30	4	4	1	329
MK256_m9_8	3166	307	117929	11942	219411	18179	24673	2537	86533	7603	15849	919	1258	100	11983	1273	762	67	1633	127	146	13	222	19	11	2	23	4	4	1	415
MK256_m9_9	3434	284	119746	11293	230126	23788	22822	1950	83911	5719	17821	1548	1363	114	12478	756	747	66	1631	167	147	13	229	19	11	1	27	4	3	1	374
MK256_m9_10	4570	382	121844	12598	220130	21573	25936	2851	90498	6406	16680	1638	1463	148	12558	1068	975	71	2238	150	209	17	268	26	16	3	38	5	6	1	266
MK256_m10_1	3371	310	85211	5514	154412	11547	17050	1138	71418	4723	12582	1021	1057	119	9468	834	682	60	1710	167	149	12	191	17	14	2	36	6	4	1	213
MK256_m10_2	3969	326	126202	13363	263280	29459	26557	3394	96271	7338	17075	1549	1492	114	12841	1063	890	71	1992	194	171	18	242	19	14	2	37	6	3	1	282
MK256_m10_3	4147	291	132821	15073	244937	23575	28077	2669	88253	6013	17065	1607	1311	110	13622	1065	870	79	1952	170	188	22	268	29	15	2	41	4	5	1	271
MK256_m10_4	4126	346	124334	11123	230722	18874	29175	2622	94250	8793	17764	1772	1441	143	12065	976	827	69	2165	190	179	14	260	25	15	3	42	5	5	1	235
MK256_m10_5	3188	444	52931	9459	101258	14536	10708	1499	43313	6601	6978	1102	735	114	5402	890	482	100	1155	155	141	27	182	30	16	3	36	8	5	1	121
MK256_m10_6	4354	351	120045	10815	234976	15939	25156	3184	99004	6344	16357	1492	1400	122	12677	1080	861	67	2093	163	199	17	287	27	14	2	40	5	5	1	259
MK256_m10_7	4309	353	126404	9251	234676	22651	27702	2418	93239	7263	15937	1336	1420	128	12798	932	836	67	1924	175	179	16	271	27	16	2	39	6	3	1	263
MK256_m11_1	3833	233	93821	7720	185776	15139	18386	1625	75482	6303	14101	1484	1075	83	9987	676	705	53	1696	157	163	17	198	18	14	2	36	5	4	1	227
MK256_m11_2	3806	262	110343	6590	203976	18109	22279	2645	83592	7421	14391	1295	1173	94	11263	919	758	66	1760	163	143	16	219	19	13	2	33	5	3	1	277
MK256_m11_3	1955	199	52446	6117	96416	9859	10007	1030	41279	4338	7100	993	578	65	5297	539	353	41	834	81	87	9	113	15	8	2	22	4	5	1	196
MK257																															
MK257_m1_1	6214	759	93164	7448	215767	14558	24034	2596	101528	13067	17883	1922	1140	94	12469	1403	999	78	2727	245	238	24	218	20	16	3	37	5	3	1	269
MK257_m1_2	1883	231	8299	865	20379	2930	2247	285	9666	1310	1951	266	181	20	1682	244	192	24	617	87	83	11	67	9	8	1	21	3	2	1	64
MK257_m1_3	13030	1144	86729	8120	172352	16236	17092	1309	79805	7215	16668	1334	1316	133	12194	1003	1439	109	4943	386	609	55	590	53	65	8	159	16	17	2	62

Table B1. Petrochronological data for monazite grains.

Grain #	Y (ppm)	2SE	La (ppm)	2SE	Ce (ppm)	2SE	Pr (ppm)	2SE	Nd (ppm)	2SE	Sm (ppm)	2SE	Eu (ppm)	2SE	Gd (ppm)	2SE	Tb (ppm)	2SE	Dy (ppm)	2SE	Ho (ppm)	2SE	Er (ppm)	2SE	Tm (ppm)	2SE	Yb (ppm)	2SE	Lu (ppm)	2SE	Gd/Yb(N)
MK257_m1_4	2704	284	103704	10702	205350	15329	24043	2850	85552	7359	15771	1665	1171	130	12709	1392	779	77	1226	106	108	13	186	20	5	1	24	5	2	1	430
MK257_m1_5	1330	126	106110	12911	231294	24721	24560	2702	91733	9987	14443	1117	1138	126	12548	1185	639	64	868	93	55	7	124	14	2	1	12	2	1	0	860
MK257_m2_1	2422	256	92489	7593	202299	18038	20018	1934	84158	7069	14832	1247	1081	88	12096	1017	692	54	1339	103	95	11	149	15	3	1	15	3	2	0	657
MK257_m2_2	5023	539	104183	9502	225419	24413	25594	2773	91763	5972	18257	1960	1268	81	13818	1509	990	97	2669	226	200	20	219	26	11	2	31	5	3	1	366
MK257_m2_3	3990	480	100695	8237	243321	26918	24458	2567	95254	10303	16656	1541	1305	121	14240	1276	904	99	2043	211	171	25	225	29	10	2	27	4	3	1	434
MK257_m2_4	2981	381	111710	11516	245102	28119	26211	2748	96012	8193	16337	1068	1445	133	13405	1196	725	44	1483	134	112	11	188	17	8	2	27	5	3	1	397
MK257_m2_5	1437	259	23148	5432	53224	8832	6450	1007	25081	3542	4356	805	388	66	3465	644	269	46	711	156	54	9	65	15	4	1	12	5	1	0	228
~~MK257_m2_6~~	~~4299~~	~~621~~	~~20757~~	~~3963~~	~~52833~~	~~10272~~	~~5126~~	~~679~~	~~23262~~	~~3658~~	~~4881~~	~~1010~~	~~614~~	~~178~~	~~3845~~	~~623~~	~~432~~	~~55~~	~~1424~~	~~181~~	~~185~~	~~26~~	~~172~~	~~29~~	~~18~~	~~3~~	~~43~~	~~7~~	~~5~~	~~1~~	~~73~~
MK257_m2_7	1334	85	131909	12697	225531	22739	25906	2863	87857	5896	17455	1546	1263	113	12378	1355	674	55	1002	91	56	4	147	19	2	1	10	3	1	0	1017
MK257_m2_8	2021	155	110978	9743	232047	15119	27387	2170	90468	7496	16492	1794	1820	176	13043	1389	709	57	1265	140	85	10	165	16	4	1	17	3	2	1	604
MK257_m3_1	9433	882	67999	5385	158305	17712	13985	774	61891	5957	12292	1098	1209	101	10163	947	1016	105	3375	486	389	30	345	28	39	4	97	11	12	2	85
MK257_m3_2	7009	655	107906	12160	216949	21477	24000	2573	87645	5587	17534	1220	1251	90	15021	1377	1215	144	3413	323	331	21	298	29	20	3	43	5	5	1	284
~~MK257_m3_3~~	~~6093~~	~~522~~	~~63308~~	~~7244~~	~~142355~~	~~17194~~	~~13491~~	~~1199~~	~~61837~~	~~6192~~	~~12174~~	~~1439~~	~~812~~	~~95~~	~~9963~~	~~936~~	~~917~~	~~94~~	~~2721~~	~~235~~	~~254~~	~~20~~	~~245~~	~~25~~	~~21~~	~~3~~	~~51~~	~~5~~	~~6~~	~~1~~	~~159~~
MK257_m3_4	6529	537	102738	8366	201324	18800	23533	2590	95873	8048	17241	1722	1303	99	14555	899	1208	87	3127	297	259	25	275	24	13	2	38	6	3	1	307
MK257_m3_5	5811	468	102800	7887	251460	23920	24812	2986	90935	6105	18774	1361	1364	116	15423	1247	1251	124	3383	245	278	25	259	28	15	2	35	5	3	1	354
MK257_m3_6	5952	390	107743	9547	228024	19080	23993	2572	83552	7007	17565	1666	1211	117	13595	1249	1278	117	3219	237	291	26	262	25	14	2	35	6	4	1	315
MK257_m3_7	6678	662	108804	11690	221745	17457	24856	2191	85318	5630	16806	1443	1296	151	13940	1397	1237	128	3305	288	262	20	286	29	16	3	40	7	5	1	281
MK257_m3_8	1868	141	108048	10737	218252	27178	21855	2146	86421	6573	16820	1931	1255	98	11765	1093	658	63	1197	133	77	8	161	15	3	1	15	3	1	0	618
MK257_m3_9	2089	210	98905	9140	212755	21818	25674	3899	89374	9312	16324	1618	1269	105	12889	1223	743	57	1379	135	87	10	149	13	4	1	11	2	1	0	923
~~MK257_m3_10~~	~~6798~~	~~590~~	~~85627~~	~~9853~~	~~167011~~	~~17902~~	~~17878~~	~~2134~~	~~70493~~	~~8135~~	~~13512~~	~~1258~~	~~1129~~	~~113~~	~~11864~~	~~1401~~	~~967~~	~~89~~	~~2898~~	~~304~~	~~267~~	~~28~~	~~286~~	~~26~~	~~22~~	~~2~~	~~57~~	~~7~~	~~6~~	~~1~~	~~167~~
MK257_m3_11	3299	266	116822	13990	233164	22562	24125	2660	84749	4856	17024	1568	1235	101	13501	1349	886	91	1946	183	152	16	191	21	6	1	24	3	2	1	464
MK257_m4_1	14323	1441	111426	10443	221975	18936	23562	2894	91179	6050	20475	1324	1561	179	16122	1350	1798	136	5650	483	639	65	574	55	58	7	129	12	15	2	101
MK257_m4_2	15399	1127	100776	9562	214349	26373	24654	2300	91575	8292	21096	1954	1680	128	17299	1325	1773	191	5788	544	700	80	599	60	59	8	157	18	22	3	89
MK257_m4_3	6180	521	111037	11030	238006	17499	24884	2950	84426	5590	18560	1765	1519	132	15137	1581	1158	111	2847	210	259	23	295	25	22	3	49	7	5	1	248
MK257_m4_4	3666	286	110936	7955	238619	23441	24840	2888	91938	6486	17187	1137	1301	123	14428	1283	986	91	2007	176	147	16	201	19	8	1	24	4	2	0	494
MK257_m4_5	8654	880	56432	7446	117859	18073	11452	1276	53201	6239	11545	1563	822	100	9156	1244	930	99	3187	424	353	49	328	39	32	4	91	9	12	2	81
MK257_m4_6	9901	1074	77714	8470	161109	18876	15622	1210	67390	7558	13846	1479	1045	83	11129	1210	1087	108	3499	410	413	40	371	45	40	4	96	15	13	2	93
MK257_m4_7	16677	1385	104019	6811	203199	23641	21970	2301	88762	9046	18671	1896	1498	126	16202	1252	1641	147	6021	397	725	85	727	66	92	8	207	18	27	3	63
MK257_m4_8	1855	171	106430	8717	232727	22671	27520	2582	94324	9481	18225	1729	1377	118	13461	806	726	58	1332	123	83	9	161	14	3	1	14	3	1	1	760
MK257_m4_9	1503	170	126151	14809	231257	25644	25783	2067	94299	6034	17272	1476	1276	133	12033	1285	790	47	1181	113	64	7	144	14	2	0	13	2	1	0	757
MK257_m4_10	1597	143	123120	10339	226190	17258	27597	2292	91929	7897	16539	1457	1209	99	13214	1308	769	73	1167	86	63	6	147	15	2	1	14	2	2	1	741
MK257_m5_1	4715	354	126385	11182	227644	21936	26352	2912	107338	10587	18409	1868	2445	214	15488	1437	1011	109	2579	200	228	16	273	26	18	3	42	5	5	1	296
MK257_m5_2	4534	369	122386	11913	244873	20051	26286	2399	106992	12506	18154	1710	2827	295	13250	1127	999	94	2394	184	191	16	276	23	16	2	44	5	5	1	242
MK257_m5_3	1360	114	112819	8495	245385	23024	25571	2394	92045	6477	14520	1217	1205	117	12210	1028	663	42	1001	84	55	6	137	13	2	0	12	2	1	0	848
MK257_m5_4	1706	236	107224	7470	203365	14081	19536	1929	82116	5934	15173	1830	1091	105	11958	925	655	53	1174	154	69	10	146	15	4	1	16	3	2	1	594
MK257_m5_5	2077	137	112661	9371	229189	17055	24807	2422	95722	6094	16623	1516	1504	131	13908	1039	826	59	1508	95	103	9	180	15	5	1	21	4	2	1	534
MK257_m5_6	5097	437	113843	9097	252326	29428	28440	3508	109058	12376	17920	1226	2817	251	15312	1345	1106	115	2788	241	227	19	251	17	19	2	48	6	5	1	259
MK257_m5_7	4725	442	109601	7625	228728	16230	28020	2883	94325	5745	18238	1274	2651	233	14941	1361	1098	73	2788	273	211	18	238	26	12	2	40	7	4	1	306
MK257_m5_8	5152	467	113391	10889	230818	21310	25540	2603	91188	5352	17241	1379	1156	116	13416	1087	1014	85	2586	208	217	24	268	30	15	2	43	7	5	1	253
MK257_m5_9	3429	327	100680	5486	208345	15030	22281	2969	82509	5315	14793	903	1456	80	13059	983	793	56	2027	165	148	14	190	19	9	1	27	4	3	1	390
MK257_m5_10	1528	148	118860	12380	231236	18165	26078	2878	94147	11070	17309	1389	1225	84	12546	1200	699	56	1091	101	61	6	147	12	3	1	15	3	1	0	663
MK257_m6_1	1441	159	30928	5533	68039	7756	6929	794	29334	4111	4884	664	455	52	3736	502	248	31	653	81	56	7	78	11	6	1	21	4	3	1	143
MK257_m6_2	876	80	62574	5462	128705	14303	11828	1230	57903	4710	8639	821	665	59	7166	802	389	32	601	46	34	3	77	10	1	0	8	3	1	0	722
MK257_m6_3	3744	386	104955	10063	231302	14448	22425	2640	86989	5489	14575	1155	1174	86	12371	1021	800	75	2111	237	160	30	200	17	11	2	35	5	3	1	283
MK257_m6_4	1668	139	104961	11027	213807	19480	22110	1888	91217	6970	17165	1336	1212	113	12174	956	727	62	1132	115	61	6	148	14	3	1	15	3	1	0	640
MK257_m6_5	17690	1076	75683	5503	154570	12072	17935	1990	75195	5487	16149	1733	1834	130	12927	848	1576	129	5793	552	713	63	706	74	96	9	260	22	32	3	40
MK257_m6_6	4565	458	22050	3301	52548	6151	5150	472	22466	1995	4476	449	589	62	3669	379	448	41	1636	220	185	21	174	20	19	3	46	7	7	1	65
MK257_m6_7	1589	92	115094	10279	233381	20409	26506	2151	98219	10559	17037	1102	1291	133	14407	982	751	53	1303	151	77	7	157	15	2	1	11	2	1	0	1069
MK257_m6_8	2486	239	95279	7574	195702	17889	22319	1994	84018	8355	15383	1175	1214	97	12274	1218	683	48	1452	119	107	11	186	16	6	1	26	4	3	1	389
MK257_m6_9	12068	1380	97836	7679	211107	20699	25501	2837	100334	8863	17720	2156	1387	142	14168	939	1407	121	4921	491	421	45	503	54	44	7	125	17	12	2	92
MK257_m7_1	13463	1130	115475	14165	201798	16457	22823	2217	89249	6021	18556	1507	1342	85	16003	1310	1600	158	5576	396	537	48	513	40	56	6	124	18	13	2	104
MK257_m7_2	9990	1079	54108	5010	114068	11778	11226	1021	52372	4165	10435	781	874	82	8455	777	1054	106	3546	343	420	45	331	28	38	4	83	10	9	2	83
MK257_m7_3	16749	1449	98694	11041	175192	17109	18485	1798	81194	6170	18010	1107	1379	130	13965	919	1716	180	6002	495	701	49	682	61	73	7	179	19	19	2	63
MK257_m7_4	16262	1309	98625	7831	204580	22686	20337	2560	89425	5309	20975	1881	1443	134	16194	1430	1684	138	5883	581	714	52	678	57	69	6	162	13	17	2	81
MK257_m7_5	6268	796	25609	3577	60445	8178	5731	835	25654	3142	5539	696	650	76	4863	540	560	58	1969	232	269	33	237	21	30	4	79	11	9	1	50
MK257_m7_6	3031	415	112232	9216	226734	25093	23340	2356	99592	10839	14843	812	1076	86	13202	747	776	68	1669	159	107	11	182	16	9	1	26	4	2	1	416
MK257_m7_7	19630	1794	98026	8372	204104	16436	21145	2227	87077	6528	18834	1607	1652	171	15844	1249	1708	101	6949	701	746	62	742	72	92	10	255	26	23	3	50
MK257_m7_8	12191	1171	101765	7858	202544	17428	22655	2372	95151	9507	18904	1450	1338	88	15751	1128	1676	128	5135	403	520	49	500	36	43	4	103	10	11	2	124
MK257_m7_9	9519	1051	106994	7711	212856	16053	22885	2047	84838	5929	17508	1435	1364	132	14376	1094	1328	110	4176	376	385	32	354	42	31	4	85	15	8	2	137
MK257_m7_10	1156	86	106271	10146	204648	18360	20816	2242	81628	6299	15360	1179	968	85	12139	1036	606	35	993	83	49	4	137	13	1	0	13	4	1	0	743
MK257_m7_11	1238	104	110503	8377	206882	14632	23367	3066	80298	4890	14714	1379	1067	105	11671	1006	664	51	948	85	47	5	138	12	2	1	11	2	1	0	833
MK257_m7_12	1138	91	119978	10751	216500	19230	25399	2932	83164	4937	15139	1220	992	76	11115	818	580	50	864	74	50	5	128	12	1	1	9	3	0	0	1006
MK257_m7_13	1300	127	108811	9497	219821	20969	25459	2925	81638	4877	15010	1246	1025	55	11398	849	622	55	991	78	49	5	133	12	2	1	10	3	1	0	881
MK257_m7_14	2061	174	115369	9093	224556	17320	25453	2759	85626	5437	15173	1103	1209	110	12676	832	752	67	1298	99	85	6	156	17	4	1	18	3	2	0	573
MK257_m7_15	1197	98	109828	7814	212956	14788	23216	1730	81071	5053	14058	1006	1054	86	11742	1016	629	59	973	72	47	4	135	14	2	1	12	2	1	0	819
MK257_m8_1	3485	380	65479	6031	137273	9390	13323	931	54052	3453	9967	847	849	92	8198	605	689	52	1681	129	123	12	132	10	9	2	18	3	2	1	365
MK257_m8_2	1289	114	44417	2770	100787	10327	8792	894	34839	2945	5848	725	485	39	5052	412	314	40	660	51	53	6	72	8	3	1	10	2	1	0	422
MK257_m8_3	3220	320	88092	7697	175278	12931	18883	1654	78295	5272	14593	1178	974	84	11841	976	835	62	1706	144	129	11	177	16	7	1	22	3	2	0	441
MK257_m8_4	1374	96	101354	8400	211918	18021	22012	2498	82117	6649	13716	1161	1001	76	11958	986	647	43	999	87	58	6	122	12	2	1	12	3	1	1	794

Table B1. Petrochronological data for monazite grains.

Grain #	Y (ppm)	2SE	La (ppm)	2SE	Ce (ppm)	2SE	Pr (ppm)	2SE	Nd (ppm)	2SE	Sm (ppm)	2SE	Eu (ppm)	2SE	Gd (ppm)	2SE	Tb (ppm)	2SE	Dy (ppm)	2SE	Ho (ppm)	2SE	Er (ppm)	2SE	Tm (ppm)	2SE	Yb (ppm)	2SE	Lu (ppm)	2SE	Gd/Yb(N)
MK257_m8_5	1425	134	99558	9564	211586	17686	24799	2858	81704	10977	14644	1139	1034	87	11417	900	581	57	1094	79	60	6	134	13	2	1	10	2	1	0	913
MK257_m8_6	1428	130	101655	6968	214345	18184	19159	2172	80028	5776	13843	880	994	88	11045	1124	577	54	1086	95	59	5	128	10	2	1	11	2	1	1	849
MK257_m8_7	3768	293	103391	11756	199623	15867	17338	1552	79072	5092	13898	1275	1062	95	13068	1029	842	66	2083	165	152	14	196	18	10	2	24	2	2	1	442
MK257_m8_8	1331	99	100300	11080	208206	14844	22836	2560	87587	5800	14581	1014	1042	90	10966	739	645	48	938	80	49	4	131	15	2	0	11	2	1	0	806
MK257_m8_9	1689	166	108494	7901	200344	12451	24032	2838	83339	4517	13582	1130	1162	95	11335	901	630	47	1174	114	61	6	134	10	3	1	12	2	1	0	750
MK257_m8_10	1262	87	101262	6924	221433	17328	20802	2413	87977	7661	13174	1054	1078	93	11557	973	618	66	928	88	50	5	123	15	2	0	9	2	1	0	1097
~~MK257_m10_1~~	~~2837~~	~~550~~	~~6735~~	~~1334~~	~~14107~~	~~2321~~	~~1502~~	~~285~~	~~6851~~	~~1340~~	~~1199~~	~~287~~	~~158~~	~~31~~	~~1148~~	~~238~~	~~150~~	~~28~~	~~848~~	~~201~~	~~118~~	~~25~~	~~117~~	~~22~~	~~16~~	~~4~~	~~64~~	~~12~~	~~11~~	~~2~~	~~15~~
MK257_m10_2	3724	284	30235	4735	67590	5657	6873	454	29745	2485	5247	576	398	42	4854	479	469	39	1709	159	153	14	150	11	12	2	32	4	2	1	122
MK257_m10_3	7544	519	53850	5378	109463	9144	11160	901	49549	3214	8829	904	723	59	7151	507	777	61	2747	237	320	29	327	34	28	3	69	8	7	1	84
MK257_m10_4	1502	138	123388	10101	259281	20589	27647	2238	93180	6107	16300	1693	1145	103	12517	835	692	57	1121	89	59	5	154	12	2	1	16	3	1	0	619
MK257_m10_5	6870	617	83926	7326	173767	14146	16646	1437	75928	5378	13269	940	877	77	10788	982	998	97	2982	275	257	18	259	22	19	2	47	7	6	1	185
MK257_m10_6	1241	118	110579	6875	242016	21598	22631	2308	105788	12171	14808	1288	1141	82	12536	1140	669	59	1079	108	57	7	130	12	2	1	10	2	1	0	998
MK257_m10_7	1765	184	114108	10453	235252	19061	24106	2295	99801	9107	15660	1170	1265	143	12321	1129	698	56	1224	89	67	7	152	13	3	0	13	2	1	0	792
MK257_m11_1	8234	656	110667	11389	222408	23898	25058	2761	101851	7193	17830	1634	1308	104	15691	1049	1304	108	3946	319	367	34	348	35	24	3	65	8	6	1	195
MK257_m11_2	14696	1294	88462	9185	194667	19061	22199	2579	93249	7518	17138	1363	1626	157	13945	1192	1602	133	6110	406	703	69	673	56	77	8	182	19	23	3	62
MK257_m11_3	3767	507	110661	10732	233141	20339	23659	2097	93882	7863	17542	1600	1287	129	13772	885	867	76	2201	164	148	17	185	15	9	2	28	6	2	1	393
MK257_m11_4	3348	275	107683	10697	246577	21581	23450	2159	96744	11994	17192	1380	1307	113	13382	1299	882	65	2093	207	140	13	190	17	7	1	22	3	2	1	502
MK257_m11_5	3395	321	107408	11428	247831	20552	25336	2300	115732	11992	18076	1547	1292	139	14108	1353	949	84	2015	128	155	18	203	21	6	1	24	4	2	1	477
MK257_m11_6	4144	340	105137	7141	237079	16515	24329	2719	102013	7422	17194	1698	1291	110	12982	1148	1067	75	2311	158	173	13	188	22	7	1	22	5	2	1	485
MK257_m11_7	9998	694	106356	8487	219873	19682	23993	2679	88187	6412	18301	1528	1271	113	15074	1618	1323	101	4369	336	432	42	419	33	32	3	80	9	9	1	153
MK257_m11_8	12910	1107	106719	10699	221813	19570	23263	2183	93646	6239	19697	1951	1384	130	16060	1393	1508	160	5370	490	498	40	484	33	43	5	113	14	13	2	115
MK257_m11_9	14032	1249	97899	9070	231410	23242	23158	2358	93906	6995	19848	1530	1361	123	15947	1395	1803	148	6162	496	547	48	504	54	44	6	114	10	11	2	113
MK257_m11_10	6311	643	108081	10793	220933	17834	25104	3174	100426	9817	18412	1238	1255	100	14257	1378	1135	83	3355	436	245	23	267	24	13	2	40	6	4	1	286
MK258																															
MK258_m1_1	758	75	101625	12808	207587	16392	22811	1875	88744	9050	16295	1432	611	70	11748	971	591	43	692	72	34	4	140	20	1	0	10	2	1	0	911
MK258_m1_2	1166	131	104907	12800	220535	18271	20083	1847	87894	6264	14818	1638	632	74	10758	959	606	57	900	78	42	4	151	16	3	1	13	2	1	0	696
MK258_m1_3	2200	272	108222	12250	211166	19404	22518	2866	82038	5758	13616	1418	668	69	11381	979	637	62	1143	139	81	10	160	22	8	2	23	4	3	1	397
MK258_m1_4	974	88	111087	8140	212856	21708	21650	2530	85634	6427	13087	874	611	63	10940	896	599	58	740	57	41	5	134	13	2	1	12	2	1	0	765
MK258_m1_5	1123	77	117202	11876	209081	20693	25739	2632	82471	8425	14340	1099	675	67	12354	1067	630	61	908	108	50	5	133	12	2	1	11	3	1	1	869
MK258_m1_6	777	92	106133	12220	217850	24624	22980	2805	90466	5636	14057	1356	593	56	11056	996	537	42	678	59	28	3	138	16	2	0	10	3	1	0	865
MK258_m1_7	950	92	114178	11377	230461	21481	23045	2219	86103	6911	14023	1000	595	52	11529	976	584	42	826	61	41	4	139	15	1	0	10	2	1	0	969
MK258_m1_8	4025	391	100513	10159	213489	18804	22761	1938	83155	6064	15568	1499	767	75	12136	1157	847	88	1782	165	158	22	223	19	15	2	43	6	5	1	228
MK258_m1_9	2712	246	81246	7275	177879	19796	17602	1778	68877	6236	13197	776	585	40	10452	1009	630	54	1169	113	125	13	187	24	12	2	32	4	3	1	261
MK258_m1_10	996	111	105025	11888	210783	20499	25201	2547	90141	8325	15891	1383	571	50	12074	948	649	66	844	80	42	5	133	11	2	1	13	2	1	0	775
MK258_m1_11	1375	158	72358	6658	165395	14881	16775	1356	65997	6122	11914	1023	511	40	8732	854	529	46	808	69	53	7	117	10	5	1	15	3	2	1	473
MK258_m1_12	2674	259	106638	11550	212686	22344	23504	2420	82749	6958	16361	1259	796	50	12986	1075	750	49	1450	102	111	13	179	12	7	1	26	4	3	1	399
MK258_m1_13	1264	155	108619	13141	216301	26122	22595	2534	79976	10068	14629	1638	668	77	11749	1065	680	71	871	88	51	6	136	15	2	0	12	3	1	0	787
MK258_m1_14	1234	98	105351	10313	211830	19198	22252	2450	87846	5460	14544	1322	701	81	11828	998	631	62	838	77	48	5	140	15	2	1	10	2	1	1	984
MK258_m1_15	1282	123	125671	11731	220052	17864	22455	2312	88949	8281	13350	1010	655	63	12441	1040	627	59	933	52	52	4	141	16	2	0	14	3	1	0	732
MK258_m1_20	1860	175	104837	9836	188125	19297	23912	2523	77554	6528	13220	1171	591	53	10646	887	654	63	1103	108	72	8	142	15	5	1	17	4	1	0	508
MK258_m2_1	1537	162	109464	8354	231537	20819	26467	2506	88246	6065	17207	1484	644	51	11939	1141	692	64	966	106	62	8	152	15	5	1	20	4	1	0	483
MK258_m2_2	1415	151	113226	10850	227302	21290	24015	2487	97761	10397	15952	1307	727	79	12634	1005	637	60	873	80	50	3	142	17	4	1	17	2	1	1	609
MK258_m2_3	1058	81	111536	13045	234009	23173	25095	2418	90319	6409	15469	1019	629	50	12027	952	572	45	758	67	41	5	152	17	2	1	13	3	1	0	749
MK258_m2_4	3755	328	103991	8395	233447	22457	27324	1971	98221	7055	18990	1393	716	66	14319	1182	900	77	1909	162	141	10	215	20	12	1	34	4	3	1	338
MK258_m2_5	2188	156	111423	10976	236609	21319	26122	2264	106243	10483	18689	1466	675	66	13259	1063	798	62	1334	109	81	6	159	16	7	1	22	3	2	1	495
MK258_m2_6	955	89	114612	12009	239773	25213	26467	2420	90395	6184	15920	1273	618	53	12424	917	627	47	803	74	43	6	123	10	2	0	13	2	1	0	760
MK258_m2_7	1003	104	109141	10232	225382	17685	25998	2673	90950	4824	16092	1056	748	57	12176	880	641	59	832	88	38	5	136	14	2	0	12	3	1	0	794
MK258_m2_8	886	75	120002	9659	222768	23549	25909	2561	90316	8997	16520	1198	696	49	13365	785	577	45	701	67	37	4	135	14	1	0	10	2	1	0	1030
MK258_m2_9	812	67	114385	10262	246443	25592	26300	2934	91522	4639	16006	1349	740	67	12588	1198	563	58	790	81	36	3	137	13	2	1	13	2	1	0	793
MK258_m2_10	902	53	118501	12187	234176	25261	27089	2641	92416	7471	16036	1507	809	90	11203	973	570	46	791	84	32	3	152	18	2	1	12	2	1	0	755
MK258_m2_11	1109	78	119118	7737	237701	17936	29553	2259	100194	7134	17641	1454	726	71	12947	943	655	42	905	78	43	4	145	17	2	1	18	3	1	0	582
MK258_m2_12	3598	395	108124	9568	239074	25180	28965	2282	99746	9467	19885	1962	730	64	12988	935	823	85	1728	143	124	14	217	22	11	2	43	7	4	1	246
MK258_m2_13	3161	262	103982	9490	221280	24406	25454	2240	91569	7015	18542	1892	698	64	13118	1021	832	76	1682	150	116	9	201	18	11	2	29	5	3	1	368
MK258_m2_14	3357	322	74559	5850	165255	13317	18158	1530	72256	5593	14297	1239	568	47	9783	723	662	47	1532	108	120	8	180	12	13	1	32	3	4	1	244
MK258_m2_15	4324	360	68965	9205	129868	9273	15009	986	69371	6949	13247	1301	547	57	9921	806	794	82	1725	132	157	10	209	16	13	2	46	4	6	1	175
MK258_m2_16	1593	184	25851	3216	60091	6762	6119	569	24983	1836	4601	434	242	22	3787	393	280	26	641	74	57	7	77	8	6	1	16	2	2	0	186
MK258_m2_17	2158	192	41305	5720	87966	10514	10379	1102	40478	5513	7854	826	377	47	6424	593	395	50	937	87	76	6	101	10	9	1	24	3	3	1	212
MK258_m2_18	932	67	114151	10596	258768	22973	27121	2527	100268	8370	17319	1444	742	76	11248	927	640	52	765	75	37	3	141	14	1	0	11	2	1	0	850
MK258_m2_19	1215	103	118446	10487	227030	20380	23855	2307	92782	5811	16650	1184	721	65	12222	945	616	43	939	87	47	6	130	15	3	1	15	3	2	1	649
MK258_m2_20	925	50	124699	11363	239264	17768	28571	2701	99311	7921	16789	1680	784	68	12801	1043	625	55	814	66	34	3	133	16	1	0	13	3	1	0	801
MK258_m3_1	2170	190	111882	10180	224513	14631	23639	2335	89823	6445	16607	1394	658	59	11828	885	664	55	1074	82	74	6	165	18	5	1	20	4	1	0	470
MK258_m3_2	1614	194	112466	14507	220578	22743	23538	2166	91180	10741	16129	1574	643	52	12135	961	641	53	933	67	69	8	136	12	4	1	13	2	1	0	761
MK258_m3_3	1542	101	111199	7792	227231	21261	23829	2572	98960	8965	16215	957	738	60	11476	683	616	54	1108	78	61	6	163	18	4	1	15	3	1	0	616
MK258_m3_4	1850	210	113658	9257	221806	19684	25659	2118	88256	6227	15584	1344	728	54	11838	1030	697	62	1015	87	60	6	159	21	3	1	15	3	1	0	648
MK258_m3_5	1892	161	92120	8802	157638	16094	17837	1736	73670	4196	10565	781	666	90	8922	609	537	49	986	72	79	10	130	15	7	1	20	4	2	1	364
MK258_m3_6	2816	373	100559	8395	208006	16185	23253	2286	91971	5653	15137	1321	721	59	12889	1130	685	80	1354	124	99	11	171	18	8	1	27	5	2	0	391
MK258_m3_7	1370	126	117117	15197	228596	20733	26310	3090	92797	5830	15011	1039	713	73	11705	1032	544	48	747	79	43	5	144	15	2	1	13	3	1	0	742
MK258_m3_8	1324	123	113222	8000	218459	15345	24460	2008	89086	6187	15139	1425	706	65	12562	774	595	43	920	89	49	4	134	15	2	0	12	3	1	0	832

Table B1. Petrochronological data for monazite grains.

Grain #	Y (ppm)	2SE	La (ppm)	2SE	Ce (ppm)	2SE	Pr (ppm)	2SE	Nd (ppm)	2SE	Sm (ppm)	2SE	Eu (ppm)	2SE	Gd (ppm)	2SE	Tb (ppm)	2SE	Dy (ppm)	2SE	Ho (ppm)	2SE	Er (ppm)	2SE	Tm (ppm)	2SE	Yb (ppm)	2SE	Lu (ppm)	2SE	Gd/Yb(N)
~~MK258_m3_9~~	~~83~~	~~28~~	~~1672~~	~~412~~	~~4340~~	~~1323~~	~~501~~	~~188~~	~~2171~~	~~792~~	~~428~~	~~130~~	~~22~~	~~7~~	~~256~~	~~91~~	~~21~~	~~7~~	~~32~~	~~11~~	~~3~~	~~1~~	~~5~~	~~2~~	~~0~~	~~0~~	~~1~~	~~1~~	~~0~~	~~0~~	~~176~~
MK258_m3_10	1643	147	114918	12416	225898	20050	24253	2319	88712	7442	16031	1268	727	56	11872	940	607	47	938	52	58	6	142	15	3	1	15	3	1	0	638
MK258_m3_11	1386	161	116966	10238	209576	15518	25428	2983	88910	7330	15899	1535	717	68	10975	991	595	47	891	86	53	6	136	11	2	0	12	3	1	0	732
MK258_m3_12	1272	108	110995	7479	220603	18612	27161	2111	90452	6520	16141	1602	696	81	11294	924	568	48	818	69	44	4	127	17	2	1	12	2	1	0	758
MK258_m4_1	1976	171	110201	11400	213129	18558	23008	2457	90466	6690	15097	1357	685	47	11211	905	700	73	1110	91	73	5	148	14	4	1	18	3	1	0	505
MK258_m4_2	2934	262	98519	8932	194920	15327	22990	1976	82307	7576	15451	1358	713	67	12149	1193	818	65	1406	121	119	9	183	20	9	1	30	4	3	1	323
MK258_m4_3	1941	148	105496	9148	220213	19187	24695	2198	97357	5146	16231	1535	762	74	11135	931	693	49	1027	85	77	7	177	18	6	1	21	4	2	1	431
MK258_m4_4	3006	256	105845	8936	201694	17506	23131	2236	98413	12152	15184	837	831	79	13211	996	835	73	1516	131	123	12	200	16	10	2	32	4	3	0	333
MK258_m4_5	1310	167	106310	11298	230570	22572	24159	1988	87190	5085	16329	1150	681	48	10690	867	607	35	843	67	53	5	135	14	2	1	12	2	1	0	743
MK258_m4_6	2858	242	98996	7592	197397	12611	24386	2634	95734	10309	17214	1167	800	63	13074	1303	828	74	1657	159	122	11	214	20	8	1	28	4	3	1	382
MK258_m4_7	1337	113	107990	6746	234190	20935	25161	2337	88184	5799	15055	822	644	55	11400	1045	572	56	851	51	53	5	137	15	3	1	14	4	1	0	658
MK258_m4_8	1854	220	104015	9401	228880	17694	22460	2345	92407	8168	15164	1060	686	60	12002	737	606	61	1069	95	71	6	146	16	4	1	15	3	1	0	643
MK258_m4_9	1460	131	113880	9144	214952	15223	24724	2127	92727	5643	15760	1163	773	74	11670	1014	600	41	936	85	55	5	142	17	2	1	13	2	2	0	721
MK258_m4_10	1097	92	109083	5293	203488	19025	26063	2402	87547	7979	14536	971	775	63	11837	1257	586	37	799	68	43	4	139	13	2	0	13	2	1	1	751
MK258_m4_11	762	60	103839	10048	225004	22707	24306	2403	87333	6672	14386	1372	653	55	10349	992	448	41	611	74	27	2	125	9	2	0	11	2	0	0	736
MK258_m4_12	2729	227	102760	8993	214869	16938	20628	1636	91878	9251	15666	1398	676	39	12327	877	797	74	1509	126	96	11	200	19	8	1	27	4	3	1	372
MK258_m4_13	1253	119	115445	15618	222002	16091	25724	2814	89325	7422	14910	1673	695	55	11062	1094	543	49	841	69	49	5	153	14	2	0	13	3	1	0	694
MK258_m4_14	844	65	126527	15813	222305	19319	24293	2564	87289	6606	14575	1113	662	64	9837	863	503	40	625	55	34	3	137	12	2	1	11	2	1	0	712
MK258_m4_15	1359	127	120527	12493	197687	12746	24880	3069	87096	7338	14843	1278	636	46	11471	989	567	53	814	82	52	4	126	11	3	1	12	3	1	0	755
MK258_m4_16	1772	148	112600	14728	208640	21482	21788	2228	85537	7883	16233	1457	667	51	11287	1126	627	58	920	94	69	7	147	13	5	1	19	3	1	0	471
MK258_m5_1	3245	295	106761	13378	216939	19016	24295	3038	98382	8431	19436	1359	673	58	12891	886	832	86	1697	158	137	11	209	22	9	1	29	3	3	1	357
MK258_m5_2	2970	289	91009	10756	201326	17804	26509	2890	88279	7114	15866	1940	655	60	11966	1348	722	80	1479	113	108	11	168	13	9	2	26	4	2	0	378
MK258_m5_3	2515	240	118017	10754	230405	20679	26304	2432	108122	10359	17382	1126	828	75	13735	1234	780	61	1359	99	98	8	191	22	7	1	24	4	2	1	463
MK258_m5_4	1274	115	115831	8411	227376	24729	25363	2289	100767	7786	15462	1237	763	43	12046	1102	641	59	922	69	55	5	153	11	3	1	14	3	1	0	680
MK258_m5_5	1224	100	100140	7527	234903	17805	24561	1906	86158	8020	15322	1367	683	58	11148	799	573	36	886	86	47	6	133	14	2	0	13	3	1	0	684
MK258_m5_6	1202	136	117766	12265	220773	18731	25064	2642	91239	9334	15134	899	765	61	10509	916	606	55	857	66	41	3	150	18	2	0	11	3	1	0	806
MK258_m5_7	1098	91	100981	8025	208092	18348	23631	2522	85862	6069	15080	1191	689	62	10697	954	540	42	723	71	41	5	127	13	1	0	11	2	1	0	760
MK258_m5_8	817	57	111541	9365	195616	17026	25263	2832	90322	5238	15850	1458	663	54	9971	848	482	49	615	47	34	4	123	15	2	1	9	2	1	0	861
MK258_m5_9	1042	121	110732	10008	210912	15047	23905	2468	92959	7969	15250	1126	708	69	10380	597	536	39	728	67	40	3	120	11	1	0	10	2	1	0	867
~~MK258_m5_10~~	~~1107~~	~~194~~	~~11428~~	~~1906~~	~~26652~~	~~5706~~	~~3485~~	~~525~~	~~13673~~	~~2738~~	~~2651~~	~~419~~	~~178~~	~~29~~	~~1768~~	~~337~~	~~158~~	~~30~~	~~391~~	~~65~~	~~34~~	~~7~~	~~46~~	~~9~~	~~4~~	~~1~~	~~12~~	~~3~~	~~1~~	~~0~~	~~115~~
MK258_m5_11	2355	161	40755	4620	83552	9286	8944	880	41263	5521	6831	668	378	40	5108	559	435	40	1122	167	94	10	115	18	9	1	26	5	3	1	156
MK258_m5_12	6191	457	90345	12012	170053	14770	19691	1739	85915	9961	16815	1377	836	61	12855	1387	1182	106	2894	212	273	18	330	39	26	4	74	8	7	1	141
MK258_m5_13	3570	324	110676	9123	208476	13376	25063	1997	97585	11757	18736	1488	706	61	13362	883	832	63	1684	169	135	13	213	17	11	2	35	4	3	1	311
MK258_m5_14	2407	207	101598	9145	215030	16911	22936	2525	91306	7750	17492	1542	691	53	12086	1337	724	52	1215	135	90	7	172	17	7	1	23	3	2	1	433
MK258_m6_1	3184	350	54550	6990	121374	13766	11693	860	56970	3472	10439	972	398	39	8150	764	567	64	1320	109	117	12	159	18	12	2	34	6	3	1	197
MK258_m6_2	2537	308	112193	10345	211748	19406	24012	1909	95654	9918	15097	1230	713	55	11488	1104	676	78	1493	178	100	14	189	15	7	2	26	5	2	1	364
MK258_m6_3	1367	99	108601	7276	240278	23055	23047	2721	94375	7288	15617	1052	699	61	11955	916	598	51	843	80	59	6	144	16	2	1	11	3	1	0	843
MK258_m6_4	1127	133	106751	9644	230281	21067	24605	2193	95125	6713	15701	918	639	44	11537	819	531	44	733	64	38	4	130	13	2	1	10	3	1	0	889
MK258_m6_5	2038	211	51836	3857	127593	13937	13809	1497	56867	4485	9727	989	490	42	7002	470	445	35	966	80	80	7	118	12	6	1	23	4	3	1	252
MK258_m6_6	1445	150	50857	6021	113454	16298	11840	1449	52001	4915	8076	835	510	68	7322	837	408	52	730	66	60	8	95	12	4	1	17	4	2	1	351
MK258_m6_7	4567	400	99035	7311	195586	19035	24668	2384	102749	11704	18562	1731	754	70	12603	1163	939	92	2174	224	178	18	256	36	13	2	42	6	4	1	246
MK258_m6_8	4934	500	96544	10157	193474	18094	24888	2470	92713	6616	17797	1246	742	61	13770	1231	967	84	2209	200	177	14	255	24	15	2	46	6	5	1	241
MK258_m6_9	3170	214	97944	8044	218499	17976	23747	2784	93753	5454	16445	1522	737	56	13445	1078	840	71	1747	192	135	15	186	14	12	1	37	6	3	1	294
MK258_m6_10	775	90	107718	13860	208990	16985	23677	2488	82772	7665	13169	1097	611	71	10347	849	441	51	536	49	31	3	117	13	1	1	9	2	1	0	953
MK258_m6_11	1629	134	114594	11819	216806	25026	24046	2378	86866	5475	16435	1444	813	96	11230	977	580	45	984	90	61	6	148	14	4	1	19	3	2	1	481
MK258_m6_12	1477	135	104428	7887	208542	19566	23544	2337	89271	6775	14885	1227	905	86	11222	938	543	51	943	84	54	5	143	14	4	1	17	3	2	0	547
MK258_m6_13	2088	205	93647	5833	207204	14707	23362	2074	74378	7762	13271	907	653	60	10362	710	630	49	1097	90	89	7	148	17	8	1	27	3	2	1	308
MK258_m6_14	2609	192	66869	5332	142561	11981	14848	1127	62106	6273	11365	965	527	43	8543	849	533	48	1137	90	84	9	140	15	8	1	25	4	2	1	278
MK258_m6_15	1711	143	107623	10017	204622	22718	25167	1960	98912	9608	14982	1458	755	58	12113	1134	626	52	1016	85	65	7	147	12	4	1	16	3	1	1	610
MK258_m7_1	1014	87	124279	12059	228088	17931	27060	2139	100486	9126	15829	1316	780	89	11790	972	651	56	837	79	40	5	130	18	1	1	11	2	1	0	848
MK258_m7_2	1146	96	112712	11023	239677	22559	28034	2526	100151	10476	17569	1252	865	70	13171	1276	671	70	894	102	45	4	130	11	3	1	18	3	2	1	588
MK258_m7_3	918	81	112342	9201	232795	19052	26819	2848	91445	6563	16451	1509	677	58	11671	746	640	54	899	78	37	4	130	14	1	0	12	2	1	0	812
MK258_m7_4	1184	139	102445	8695	222881	21407	23017	1974	86136	6875	14604	980	890	131	10859	1098	585	52	891	93	47	7	140	19	4	1	25	6	3	1	356
MK258_m7_5	973	91	97984	6659	223714	15247	25949	2622	89970	6717	16510	1014	735	67	13113	1386	634	51	794	95	40	4	127	14	1	0	10	2	1	0	1072
MK258_m7_6	2179	310	91027	10719	197717	23477	20692	2561	79254	6605	14112	1241	726	76	10783	1319	650	55	1249	121	92	7	163	15	8	1	25	4	3	1	349
MK258_m7_7	860	67	119918	11234	260617	29012	26617	2248	100738	9830	16866	1679	709	40	11493	1006	570	47	818	81	35	4	130	13	1	0	12	3	1	0	745
MK258_m7_8	959	83	115360	13320	206637	18002	26306	2410	101904	9440	15319	1171	662	59	11721	796	624	69	765	48	34	4	123	12	1	0	10	3	1	0	907
MK258_m7_9	1110	114	108486	12290	249798	22409	26569	2908	96083	7350	16502	1484	634	41	13595	1444	590	60	968	100	45	5	136	15	2	0	13	2	1	1	867
MK258_m7_10	1171	128	98628	8112	206135	15669	25064	2711	90181	5591	17760	1349	922	86	11596	900	582	68	958	95	50	6	130	14	3	1	18	3	3	1	515
MK258_m7_11	845	80	107818	12671	219653	21207	27979	2894	90108	6137	15712	1584	712	68	12609	945	627	72	796	103	37	3	129	12	1	0	12	2	1	0	869
MK258_m7_12	1544	152	94840	7046	225926	17104	24387	2598	98664	9620	17348	1336	681	83	12468	1034	611	52	983	78	60	7	139	14	4	1	19	3	1	0	532
~~MK258_m7_13~~	~~842~~	~~63~~	~~28201~~	~~4052~~	~~62838~~	~~5550~~	~~6991~~	~~499~~	~~29113~~	~~3625~~	~~4935~~	~~442~~	~~317~~	~~35~~	~~3609~~	~~385~~	~~212~~	~~21~~	~~465~~	~~46~~	~~31~~	~~4~~	~~63~~	~~8~~	~~4~~	~~1~~	~~15~~	~~3~~	~~2~~	~~1~~	~~197~~
MK258_m7_14	1131	139	111293	8509	226530	19769	27029	2603	91253	5112	17552	1521	916	97	12894	1067	645	72	926	92	49	5	136	12	2	1	19	3	2	1	560
MK258_m7_15	3262	301	86211	8438	169290	17088	20129	2496	70823	6808	14739	1461	728	92	11499	1157	789	94	1721	149	126	15	189	17	11	2	35	5	4	1	264
MK258_m7_16	919	79	106209	7771	238951	32197	26172	2729	91696	6770	18152	1490	714	72	13174	1213	599	35	873	78	39	4	142	11	1	1	10	2	1	0	1113
MK258_m7_17	4588	482	98574	9832	191426	17622	25129	3496	94015	5898	19848	1871	916	87	12912	1095	964	76	2253	206	175	15	249	27	17	2	53	8	5	1	197
MK258_m7_18	2606	255	100136	11131	228924	26998	25397	2756	90165	9126	18456	1360	792	71	12713	940	747	69	1519	130	111	13	170	15	8	1	26	3	3	1	403
MK258_m7_19	2224	195	96135	7447	221352	20413	23817	2721	90102	5276	15208	1080	690	56	11022	831	673	74	1328	139	86	7	170	16	6	1	20	3	1	0	457
MK258_m7_20	1075	122	111134	11864	256177	24971	26476	2192	106162	10219	17405	1721	747	54	13873	1363	651	48	837	83	45	5	145	15	2	1	14	2	1	0	792

Table B1. Petrochronological data for monazite grains.

Grain #	Y (ppm)	2SE	La (ppm)	2SE	Ce (ppm)	2SE	Pr (ppm)	2SE	Nd (ppm)	2SE	Sm (ppm)	2SE	Eu (ppm)	2SE	Gd (ppm)	2SE	Tb (ppm)	2SE	Dy (ppm)	2SE	Ho (ppm)	2SE	Er (ppm)	2SE	Tm (ppm)	2SE	Yb (ppm)	2SE	Lu (ppm)	2SE	Gd/Yb(N)
~~MK258_m8_1~~	~~1501~~	~~198~~	~~24183~~	~~3625~~	~~55245~~	~~7894~~	~~6102~~	~~806~~	~~25830~~	~~2949~~	~~4942~~	~~657~~	~~288~~	~~29~~	~~3345~~	~~337~~	~~270~~	~~30~~	~~622~~	~~98~~	~~58~~	~~7~~	~~72~~	~~10~~	~~5~~	~~1~~	~~16~~	~~4~~	~~2~~	~~0~~	~~174~~
MK258_m8_2	1098	111	19814	2034	53750	6382	5967	569	24461	3284	4277	398	194	19	3411	406	211	24	488	51	42	5	64	11	3	1	13	2	1	0	210
MK258_m8_3	996	85	91027	6475	220491	17716	24475	2736	76459	6398	14609	1325	679	61	10567	885	532	52	700	64	39	4	134	14	1	0	11	3	1	0	804
MK258_m8_4	1285	193	42642	5445	95480	9304	9826	608	39740	4673	6701	726	350	36	5177	586	289	36	643	84	53	7	87	11	5	1	16	4	1	1	265
MK258_m8_5	232	29	14789	1924	35442	5051	3769	469	15453	2086	2522	482	150	17	1888	269	80	11	123	15	9	2	24	4	1	0	4	1	0	0	404
MK258_m8_6	256	42	17678	1877	44155	6461	4498	696	19348	2731	3046	300	180	24	2409	299	102	17	168	29	9	2	32	5	1	0	3	1	1	0	741
MK258_m8_7	1065	115	102795	9296	197357	13907	20793	2265	78670	6547	13053	969	592	54	10438	770	516	46	712	74	49	6	127	10	2	1	10	2	0	0	825
MK258_m8_8	2092	169	88342	8061	196943	13947	20132	2425	83850	5839	14927	1603	609	53	12118	1179	653	64	1160	90	87	8	141	13	5	1	21	3	2	1	463
MK258_m8_9	3183	320	57089	6494	116237	16041	12009	1082	49623	4171	9857	829	443	44	6428	586	567	54	1377	141	133	11	166	17	12	2	32	5	3	1	165
MK258_m8_10	2615	299	36459	5467	80658	9042	8771	733	36273	4135	7335	695	354	35	5728	583	385	50	1140	123	109	14	139	14	11	2	28	3	2	1	167
MK258_m8_11	800	90	24262	3958	54188	7044	5198	496	25635	3642	4297	456	251	37	3198	384	170	24	363	55	33	5	54	8	3	1	8	2	1	0	313
~~MK258_m8_12~~	~~71~~	~~19~~	~~3680~~	~~1059~~	~~5945~~	~~1237~~	~~916~~	~~232~~	~~2658~~	~~714~~	~~596~~	~~147~~	~~34~~	~~10~~	~~291~~	~~81~~	~~25~~	~~9~~	~~33~~	~~9~~	~~2~~	~~0~~	~~6~~	~~2~~	~~0~~	~~0~~	~~1~~	~~1~~	~~0~~	~~0~~	~~253~~
MK258_m8_13	408	81	11704	1396	27271	4808	2825	310	13709	2317	2032	312	115	19	1768	294	94	13	192	28	14	3	27	6	2	1	5	2	1	0	305
MK258_m8_14	1114	74	95369	10284	189591	16521	21779	2499	81757	4749	13135	1178	622	51	10760	798	566	55	749	69	46	4	133	16	2	1	11	2	1	0	823
MK258_m8_15	1323	153	88167	9161	186682	15599	22045	2728	78857	6891	14144	1359	662	39	9661	951	515	40	825	61	46	5	134	13	2	1	12	3	1	0	669
MK258_m8_16	1360	148	98483	8011	201501	18719	22268	2477	78117	5359	12491	945	651	51	10036	865	509	42	831	54	46	3	142	13	2	1	12	2	1	0	703
MK258_m8_17	1292	178	90781	6958	177872	17215	19743	2200	71434	5808	10989	795	566	46	8916	725	455	48	774	69	49	3	121	12	3	1	13	3	1	0	569
MK258_m8_18	1111	106	109499	11792	198925	19083	18908	1348	75388	6401	14279	1269	601	66	9486	897	491	47	814	90	45	4	137	17	2	0	12	3	1	0	647
MK258_m8_19	1184	103	95578	9437	212920	21862	20865	2427	77895	7512	13663	1250	622	49	9853	808	523	55	763	75	43	4	124	15	2	0	12	2	1	0	661
MK258_m8_20	1230	114	95669	7748	198597	17174	20495	1815	76005	6171	12971	1420	640	50	9538	838	489	46	764	71	47	5	117	11	2	1	11	3	1	0	698
MK258_m9_1	1846	235	15474	2390	43080	5595	4301	551	17511	1861	3884	407	216	20	2754	420	276	35	822	101	74	8	79	13	7	1	23	4	2	1	99
MK258_m9_2	4799	538	96950	7489	200602	16904	24278	2606	83817	7760	17637	1818	658	63	12416	997	977	72	2124	203	189	20	244	24	18	2	42	4	5	1	237
MK258_m9_3	4191	311	94505	9186	204563	18054	25565	2508	85579	6447	19197	1503	716	62	12244	1282	980	66	2069	192	183	16	242	28	13	2	40	5	4	1	247
MK258_m9_4	1403	169	113185	8327	210646	22897	23384	2208	94496	11276	13723	1192	635	68	10581	809	591	49	1002	77	55	6	150	17	3	1	13	3	1	0	646
MK258_m9_5	1346	116	93509	8391	210577	14821	22220	2225	82612	6937	14720	1217	764	76	10754	1129	565	38	908	76	57	6	123	11	3	1	14	3	1	0	624
MK258_m9_6	856	87	101829	10823	225548	21043	22927	2390	85932	7245	15721	1050	633	49	10300	1142	483	44	660	49	36	5	131	14	2	0	9	2	1	0	930
MK258_m9_7	966	117	106416	10777	230027	19454	22643	2055	82159	6092	14723	1332	630	54	11115	963	467	37	651	67	36	4	114	13	1	0	8	2	1	0	1100
MK258_m9_8	976	89	102366	10327	225943	19807	23347	2717	83274	7567	15904	1212	649	73	9800	759	527	48	726	39	40	4	141	15	2	0	9	2	1	0	887
MK258_m9_9	1455	107	98706	8739	212296	17328	23724	1667	86273	8909	14519	1143	708	55	11255	906	575	54	967	94	56	5	133	13	2	1	16	4	1	0	585
MK258_m9_10	972	78	99178	10907	223080	15107	24274	2456	83460	6507	15125	1507	634	59	9329	601	518	50	679	61	40	4	130	10	2	0	9	2	1	0	859
MK258_m9_11	813	81	111229	9303	206088	16272	21905	2116	83647	7657	14549	1199	705	61	10701	679	505	36	633	59	37	4	131	11	1	0	8	2	0	0	1099
MK258_m9_12	1324	117	107920	10412	221551	21756	22077	2083	82158	6002	15107	1470	619	46	10807	1046	541	45	848	82	53	7	140	14	3	1	13	2	1	0	649
MK258_m9_13	1436	131	99434	8194	205804	17054	20786	1972	81457	5763	14267	1212	651	60	9770	702	601	43	968	78	54	5	120	9	2	1	13	2	1	0	605
MK258_m9_14	3623	276	92604	9198	210843	15336	23679	2635	90015	10716	17993	1302	705	46	12338	1084	883	66	1908	152	166	16	203	18	10	2	29	4	3	1	340
MK258_m9_15	1337	129	96425	9486	198054	14521	21969	2186	90662	9089	14183	1066	655	68	10811	928	558	52	966	81	58	5	132	15	2	1	14	3	1	0	617
MK258_m9_16	1478	133	104054	11725	212879	22112	21755	2625	83366	7378	14366	1210	670	59	11465	1090	589	48	959	100	56	5	149	15	4	1	15	3	1	0	633
MK260																															
~~MK260_m1_1~~	~~2835~~	~~406~~	~~80123~~	~~6589~~	~~157644~~	~~14450~~	~~15771~~	~~1285~~	~~62291~~	~~6254~~	~~11982~~	~~855~~	~~2163~~	~~179~~	~~9496~~	~~817~~	~~680~~	~~66~~	~~1421~~	~~204~~	~~120~~	~~22~~	~~179~~	~~25~~	~~13~~	~~3~~	~~37~~	~~9~~	~~4~~	~~1~~	~~205~~
MK260_m2_1	19018	1507	90619	7592	217025	22305	21467	2340	81923	4901	16526	1142	565	41	13624	1011	1582	147	6531	617	981	78	1187	117	179	15	481	47	63	6	23
MK260_m2_2	20379	2407	104322	9595	207370	16763	22113	1845	88039	8298	15965	1297	565	36	13898	1210	1419	92	6154	518	880	66	975	76	154	14	401	30	56	5	28
MK260_m2_3	7548	591	107004	9864	229495	20385	25538	2295	85101	4925	17149	1753	591	52	13514	965	1042	85	3154	151	330	25	362	38	34	4	80	8	10	1	137
MK260_m2_4	6469	529	122073	10312	229445	19352	23428	2172	80193	5974	14963	1118	521	51	12673	1003	982	51	2661	197	265	23	321	35	28	3	67	9	7	1	154
MK260_m2_5	6601	460	122649	7296	204803	17166	19258	1617	82743	5605	14835	1426	535	56	12238	708	978	73	2759	175	259	19	323	31	25	3	64	8	7	1	154
MK260_m2_6	6145	466	115413	9000	202868	15239	21991	1550	80555	5339	15422	1183	520	42	12757	958	1065	111	2807	175	290	27	343	26	27	2	63	7	8	2	164
MK260_m2_7	9970	915	116433	13427	234338	17063	26392	2512	88105	6270	16987	1358	653	59	14964	1197	1204	126	3964	412	433	33	476	39	49	5	118	9	14	2	102
MK260_m2_8	9728	911	118737	6990	217394	17898	24020	2333	88754	5856	17663	1608	703	72	14110	1369	1284	106	4031	370	450	38	501	49	47	4	134	11	14	2	85
MK260_m2_9	12645	734	118752	8846	239626	15168	24689	2344	93042	6433	17434	1389	658	45	14976	1167	1359	100	4445	386	594	49	684	47	65	6	190	23	20	2	64
MK260_m2_10	10065	886	115076	10682	234538	19128	26668	2497	85482	5324	15858	1527	598	54	15434	1401	1229	121	4025	274	451	46	476	50	56	6	117	11	14	2	107
MK260_m2_11	7454	533	107307	10735	207595	18466	23620	2407	87996	8350	17114	1553	646	63	14160	1158	1154	115	3095	148	372	35	410	30	35	3	86	8	10	2	133
MK260_m2_12	7248	576	109574	10628	226383	20630	23253	2213	80203	5935	17773	1758	638	61	13094	1090	1074	90	3235	247	337	33	396	37	29	3	83	7	10	2	128
MK260_m2_13	7616	799	100426	9661	229390	20814	23333	2463	87704	7141	17793	1699	564	50	12484	766	1189	99	3107	234	372	31	363	25	32	3	76	9	9	1	134
MK260_m2_14	6932	443	86662	7020	189196	15371	19499	1969	72220	5580	14853	1044	518	59	12340	1049	954	77	2758	245	281	23	322	33	28	3	69	7	8	1	145
MK260_m2_15	7178	592	102424	8700	202361	18255	20610	1846	85788	5862	15721	1182	592	58	14191	1206	1067	83	3135	243	327	23	362	39	34	4	80	9	9	2	143
MK260_m2_16	7557	519	105648	11985	220896	18625	21789	1828	93120	5773	16854	1139	603	53	12858	1085	1094	113	3204	321	365	33	391	35	37	4	83	8	11	2	125
MK260_m2_17	6746	649	98005	9938	176367	16782	18956	2117	75659	6936	13861	1112	545	60	12064	1154	905	82	2899	314	311	31	355	38	30	4	72	9	9	1	135
MK260_m2_18	8158	553	106021	8369	210960	21480	19976	1563	89052	5736	16631	1810	617	56	13184	949	1102	88	3488	324	369	43	412	30	35	4	74	9	9	1	144
MK260_m2_19	11166	860	105568	9636	229896	19070	22776	2096	84176	6069	17100	1353	547	33	14251	1451	1235	90	4100	404	508	38	521	50	64	6	154	20	17	2	75
MK260_m2_20	11066	939	109021	10066	200784	17495	24108	2386	91171	7986	17238	1416	552	48	14520	1170	1225	112	3986	364	495	58	538	49	63	7	135	12	17	2	87
MK260_m2_21	9132	553	120525	10901	231300	15526	25451	2466	83592	6591	17256	1702	552	49	14112	1100	1194	102	3590	311	393	34	426	40	40	3	113	13	13	2	101
MK260_m2_22	6333	703	116431	10164	222561	24582	27294	2804	85248	5684	16456	1315	613	58	13916	1077	977	97	2809	190	284	28	366	34	27	3	69	7	8	1	163
MK260_m2_23	10263	744	108898	7938	222705	22690	24562	2235	88048	6686	16469	1153	561	53	14785	1440	1205	106	3942	321	486	39	536	56	56	7	142	16	16	3	84
MK260_m2_24	10747	848	101495	7035	215931	14815	22129	2046	84130	6842	16460	1360	608	55	13081	998	1206	125	4165	300	501	41	571	64	58	5	142	13	17	2	75
MK260_m2_25	7711	706	115927	10246	241054	21907	23115	1992	83937	6015	16364	1360	589	66	14422	1716	1132	113	3173	203	338	35	356	41	31	3	68	9	7	1	171
MK260_m2_26	7812	703	106182	10678	191321	15100	24690	2157	80747	6336	15265	1534	575	61	13701	839	1050	85	3080	295	323	32	353	34	29	3	71	8	9	1	156
MK260_m2_27	5860	484	114199	12164	206356	19503	20092	2141	71612	4939	15026	1285	464	39	12342	1070	943	81	2672	189	272	23	310	35	24	3	67	7	7	1	149
MK260_m2_28	6494	687	106764	9556	196298	15823	18229	1672	74137	5959	13377	1396	544	44	12352	1038	954	104	2658	157	286	21	306	19	27	2	69	8	7	1	146
MK260_m2_29	8804	411	108304	12245	211586	19322	24711	2628	84065	4895	17673	1867	580	49	14293	745	1138	105	3307	229	374	39	379	31	34	4	90	8	9	1	129
MK260_m2_30	12752	1157	113209	11504	211590	19268	26917	2475	82143	5282	18757	1448	617	57	16759	1694	1344	145	4812	360	541	30	610	52	73	7	162	17	23	2	83

Table B1. Petrochronological data for monazite grains.

Grain #	Y (ppm)	2SE	La (ppm)	2SE	Ce (ppm)	2SE	Pr (ppm)	2SE	Nd (ppm)	2SE	Sm (ppm)	2SE	Eu (ppm)	2SE	Gd (ppm)	2SE	Tb (ppm)	2SE	Dy (ppm)	2SE	Ho (ppm)	2SE	Er (ppm)	2SE	Tm (ppm)	2SE	Yb (ppm)	2SE	Lu (ppm)	2SE	Gd/Yb(N)
MK260_m2_31	17397	2680	62013	7057	151218	20318	14389	1694	60812	8979	11602	1776	470	55	10073	1543	1123	162	5804	878	778	108	1008	127	153	24	478	74	59	10	17
MK260_m2_32	4605	450	50162	3645	101867	10519	11851	1125	48601	3799	9382	853	322	27	7170	588	625	51	1977	116	223	24	229	16	25	2	54	6	6	1	108
MK260_m2_33	8937	751	105659	10720	201287	20925	22019	2152	83797	6523	17232	1343	591	52	15172	1642	1176	96	3668	313	397	35	438	44	44	5	115	14	16	2	107
MK260_m2_34	8962	854	103452	8746	210180	19167	21821	1959	79056	6356	16482	1287	558	53	13256	900	1163	90	3600	292	349	31	414	31	39	3	101	9	11	2	106
MK260_m2_35	9412	693	108670	7280	229399	18633	24425	2397	86079	6125	14926	1000	629	56	13583	1125	1158	92	3506	293	389	27	437	45	45	5	107	12	11	2	103
MK260_m2_36	20786	2342	76288	7079	148133	16998	15410	1261	63914	6599	12581	1361	481	43	10480	983	1233	118	6196	574	867	92	1160	117	185	16	538	52	80	8	16
MK260_m2_37	15957	1239	108514	11089	231065	21612	22690	1792	85544	5507	17757	1490	655	67	13398	1101	1289	101	5775	445	768	84	872	93	129	18	352	46	42	4	31
MK260_m2_38	10266	957	90947	8436	202307	23854	19432	2290	72331	5216	14272	1003	504	41	12276	1106	1078	87	4223	408	463	37	503	46	63	6	160	17	16	2	62
MK260_m2_39	8466	640	116592	7998	230029	17779	24081	2442	90909	8378	17493	2108	588	61	13799	1127	1236	104	3279	254	342	24	443	38	39	3	91	9	11	2	122
MK260_m2_40	7286	473	98306	6594	201804	15172	24481	2321	87119	6890	16505	1336	644	56	13680	1290	1130	95	3398	270	325	25	408	40	31	3	76	8	9	1	146
MK260_m3_1	13024	925	109305	8618	228623	21050	22142	1619	88799	7278	17143	1274	563	56	14242	1184	1413	111	5119	334	618	37	670	61	77	8	205	17	21	3	56
MK260_m3_2	8873	528	116405	12606	214037	21097	25544	2730	86372	5151	16058	885	592	45	13471	1205	1189	104	3516	286	401	37	434	34	43	4	104	9	11	1	105
MK260_m3_3	8573	742	96096	7039	204936	18224	22729	1942	83076	6262	15908	1089	581	52	11935	1040	1097	81	3428	307	409	37	415	32	41	4	116	12	12	2	83
MK260_m3_4	8331	648	113722	12175	214117	19396	23159	2386	78401	6936	14892	1356	575	58	12817	1258	995	104	3332	291	392	38	398	38	41	4	109	11	11	2	95
MK260_m3_5	8297	709	116138	9755	206649	18667	23214	2140	81722	6888	17739	1293	591	56	12858	1311	1207	86	3699	265	411	38	409	27	42	5	104	10	11	2	100
MK260_m3_6	9310	1032	104019	10063	219804	17694	22806	2272	92118	9255	17916	1225	668	62	14888	1060	1270	85	3837	467	498	35	487	53	46	5	114	12	14	1	106
MK260_m3_7	9838	862	100886	8737	219660	20070	19652	1586	81452	5964	17132	1527	620	69	13802	1135	1176	124	3715	293	411	36	457	33	42	5	120	13	13	2	93
MK260_m3_8	18597	1345	109398	9311	241827	25030	23624	2370	89660	8157	17501	1411	618	33	14775	1263	1426	142	6146	502	838	81	1031	98	171	16	456	40	66	8	26
MK260_m3_9	9398	714	115239	12578	231254	19826	24538	3019	99777	10912	17252	1445	655	63	13985	1305	1162	76	4037	407	517	48	556	65	55	6	138	15	16	2	82
MK260_m3_10	11250	731	109339	11011	208711	16035	23569	2444	87366	8012	17331	1632	679	54	13841	1154	1268	108	4247	283	589	51	545	55	56	5	148	13	19	3	76
MK260_m3_11	9485	827	115516	10748	226482	18233	24031	2409	94105	9375	15997	1419	646	71	13692	1026	1162	131	3731	318	397	28	462	39	41	4	110	12	12	1	101
MK260_m3_12	9247	860	119083	11252	229213	17573	26026	2130	85401	9124	17582	1290	678	68	12929	1251	1314	96	3873	311	435	51	474	35	48	5	118	10	13	2	89
MK260_m3_13	10117	871	113066	10158	226713	21764	26214	2440	85653	6897	17999	1426	589	37	13804	1254	1197	101	4017	281	441	38	472	43	49	4	129	16	14	2	86
MK260_m3_14	10346	978	99741	8103	220252	15837	23059	2652	86545	6690	15940	1427	586	57	12292	886	1130	93	3629	276	457	42	545	41	59	6	154	16	16	2	65
MK260_m3_15	12077	976	107138	10147	223526	17738	27954	3263	88238	4828	18387	1821	690	61	14669	961	1363	117	4362	369	583	51	582	39	65	6	163	12	20	2	73
MK260_m3_16	12287	1095	99548	9277	235797	17493	25117	2373	92162	9109	18523	1780	696	56	13087	1036	1307	122	4585	414	539	57	664	55	74	7	174	17	23	3	61
MK260_m3_17	21420	2644	91655	7819	190155	14472	20440	2030	79310	5333	15676	1207	567	45	12607	981	1439	87	6495	500	940	74	1053	98	161	11	462	48	69	6	22
MK260_m3_18	24198	2256	101184	7263	204663	17000	23084	2338	82331	7809	16148	1427	616	65	13496	1054	1597	172	7402	630	1186	105	1246	101	239	22	679	73	87	11	16
MK260_m3_19	12279	1040	112759	10470	227514	20098	25136	2399	88417	7614	17251	1219	629	51	14452	1296	1347	93	4713	417	598	58	637	59	67	7	182	17	20	2	64
MK260_m3_20	13629	1452	77955	9080	141350	12519	14058	1042	61108	5838	11758	1168	470	53	9628	1085	1099	110	4752	420	644	57	760	61	126	15	361	42	41	4	22
MK260_m4_1	7412	709	93094	9322	185743	13728	19656	2335	76286	3679	13381	1091	477	42	11599	922	959	95	2775	216	346	38	372	35	41	4	102	10	12	2	92
MK260_m4_2	17867	1384	95079	8635	205981	15366	20521	1816	78364	5554	14368	1142	614	57	12334	1214	1343	108	5482	463	801	60	900	69	138	13	433	44	56	5	23
~~MK260_m4_3~~	~~5091~~	~~609~~	~~22480~~	~~3306~~	~~56206~~	~~7183~~	~~5038~~	~~607~~	~~20316~~	~~2476~~	~~3668~~	~~422~~	~~163~~	~~21~~	~~3281~~	~~428~~	~~335~~	~~41~~	~~1547~~	~~204~~	~~223~~	~~28~~	~~269~~	~~30~~	~~42~~	~~6~~	~~147~~	~~18~~	~~19~~	~~2~~	~~18~~
MK260_m4_4	10004	834	94811	9666	211324	17766	18845	1442	76143	6950	14511	1323	504	44	11013	789	992	72	3103	232	429	47	552	53	62	7	190	25	27	4	47
MK260_m4_5	5492	494	105934	7404	203591	18636	22196	2197	88845	7101	15029	1452	453	38	10859	876	908	95	2568	196	247	24	272	23	18	2	54	5	6	1	162
MK260_m4_6	5312	551	104555	12043	197775	15552	20888	2097	79775	4063	14197	1201	437	29	12024	821	821	59	2316	198	223	19	236	21	17	2	46	7	5	1	211
MK260_m4_7	647	90	10352	984	18789	1460	2138	178	9828	1266	1509	185	50	6	1260	153	95	13	289	33	29	4	37	6	3	1	9	2	1	0	113
MK260_m4_8	6899	705	103192	7107	204099	18423	21704	2527	81139	6215	15152	1208	492	43	12085	871	914	95	2713	201	255	21	306	26	21	3	55	8	6	1	178
MK260_m4_9	5634	379	93397	6777	217843	16740	22493	2107	84145	5841	16522	1463	497	40	13066	1387	1029	75	2862	219	268	22	316	28	27	2	60	7	7	1	177
MK260_m4_10	11373	1053	53345	6033	109170	13104	10874	871	45043	4672	8335	710	351	35	7283	723	794	51	3680	296	517	33	660	78	102	9	315	38	45	4	19
MK260_m4_12	5708	405	113178	12261	229858	19700	21192	1866	77552	4837	15321	1470	481	58	12132	837	902	77	2617	222	233	19	279	21	20	2	56	6	5	1	176
MK260_m4_13	6316	436	101799	10287	203787	14215	19810	1932	83598	6312	16810	1402	499	48	11936	830	952	55	2615	213	248	27	286	25	20	3	56	6	6	1	172
MK260_m4_14	6150	507	97263	7682	204631	19146	21263	2312	79516	6216	14469	1115	464	41	12638	949	993	90	2666	219	259	24	298	25	20	3	55	5	6	1	187
MK260_m4_15	5718	417	103942	10596	208167	19685	23067	2611	81099	6051	15512	1095	493	41	12643	1036	912	96	2476	238	261	27	279	30	20	2	56	7	6	1	182
MK260_m4_16	5547	485	106128	10306	206969	16100	22173	1611	84802	6675	15617	1008	468	47	12481	1089	900	73	2292	184	231	18	271	30	16	2	48	7	5	1	210
MK260_m4_17	4903	312	114472	11415	220071	15028	24896	2341	80132	7345	15760	1515	447	51	12881	1101	931	82	2214	198	232	24	278	26	16	2	45	6	4	1	231
MK260_m4_18	4873	386	109035	10063	224336	18748	23912	2324	84393	5393	14585	923	441	45	11918	966	890	90	2186	241	206	14	248	21	14	2	43	5	4	1	227
MK260_m4_19	5347	562	108822	10560	191509	14280	22565	2655	85596	5408	14879	1428	499	44	12770	1244	898	79	2317	144	215	18	278	25	18	2	50	5	6	1	206
MK260_m4_20	12902	971	106143	7696	211858	18032	23218	2654	79044	5924	15908	1098	560	62	12076	1110	1213	91	4727	423	565	58	721	61	90	10	282	24	35	5	35
MK260_m4_21	5571	465	114167	11790	214434	19286	21344	2193	84154	6787	15228	1102	553	52	12675	1061	982	107	2718	299	238	23	309	31	23	2	56	8	7	1	182
MK260_m4_22	8502	908	92627	9484	190383	14567	22074	2485	76151	8036	12866	889	465	53	11872	848	1060	109	2759	267	351	31	406	58	45	5	126	18	15	2	76
MK260_m4_23	13124	1002	59470	5223	120787	9322	11863	1216	49389	3389	8943	775	383	32	8600	676	942	75	3746	324	616	55	689	51	120	11	394	38	57	6	18
MK260_m4_24	9713	737	47578	4542	107847	6742	10263	800	42194	3258	7655	851	475	50	6614	653	741	53	3550	362	472	46	561	57	90	11	305	38	39	5	18
MK260_m4_25	15034	1176	102594	11404	217204	20417	23743	2212	84496	10707	14089	1178	539	47	13351	991	1179	113	4620	438	620	58	845	74	91	9	289	25	37	4	37
MK260_m4_26	5393	367	100058	8517	209147	15390	21542	2409	82921	6070	14790	1438	452	43	12414	1304	882	88	2499	241	217	16	285	28	19	3	55	6	6	1	184
MK260_m4_27	5203	406	101171	9696	224197	24069	23185	2403	80521	5353	14923	1276	443	37	12766	1143	858	51	2358	209	218	18	279	24	16	2	46	5	5	1	225
MK260_m4_28	5658	415	109891	8149	228926	22331	23945	2826	80854	5823	14867	1281	551	65	14037	1189	939	69	2419	199	263	26	343	29	24	2	60	8	6	1	190
MK260_m4_29	7301	602	107042	8693	209259	14820	23975	2119	91123	12124	14734	1319	607	60	12453	1120	940	89	2964	252	288	17	360	25	25	3	73	7	9	1	139
MK260_m4_30	4934	292	118054	9480	219268	17487	24101	2315	85220	4674	14894	1009	430	33	12266	980	885	67	2370	161	238	14	277	22	16	2	47	6	4	1	212
~~MK260_m5_1~~	~~13328~~	~~1400~~	~~51548~~	~~5157~~	~~101333~~	~~9894~~	~~10413~~	~~860~~	~~42193~~	~~3832~~	~~7910~~	~~769~~	~~428~~	~~42~~	~~7334~~	~~774~~	~~936~~	~~100~~	~~4270~~	~~325~~	~~631~~	~~62~~	~~794~~	~~51~~	~~122~~	~~13~~	~~387~~	~~36~~	~~50~~	~~6~~	~~15~~
MK260_m5_2	10614	881	54820	5551	104373	11363	11044	985	41265	3364	8364	714	494	34	6634	526	803	80	3795	348	510	51	636	69	103	8	349	33	41	6	15
MK260_m5_3	20362	1174	78594	8420	164759	16524	16754	2061	64539	5780	13731	1344	530	44	11605	830	1298	95	6578	685	986	77	1226	89	181	20	599	50	77	8	16
MK260_m5_4	17364	1107	68534	6766	136652	11880	13317	667	59069	4358	10323	787	454	50	8894	769	1101	109	5328	436	743	71	972	99	163	12	444	30	66	7	16
MK260_m5_5	13682	1072	54266	5310	117609	14642	11680	982	45150	3201	9460	950	406	38	7281	645	1031	109	4525	456	692	74	852	67	143	12	432	42	53	7	14
MK260_m5_10	16339	1450	58539	5730	122982	9534	12663	973	53764	4415	9910	767	452	34	9121	896	1077	98	5271	363	796	82	978	85	142	14	467	50	60	5	16
MK260_m6_1	2134	208	100574	8497	222422	24854	20292	2314	82738	5522	18115	1349	3077	232	13020	1439	1016	85	1749	222	99	12	174	17	4	1	18	3	2	0	575
MK260_m6_2	2343	190	96782	8580	196600	22089	20554	2057	86438	7282	17480	1315	2769	217	13151	1065	1070	82	2097	211	117	12	193	19	5	1	18	3	2	1	586
~~MK260_m6_3~~	~~152~~	~~24~~	~~2987~~	~~935~~	~~6837~~	~~2069~~	~~701~~	~~240~~	~~2774~~	~~854~~	~~472~~	~~162~~	~~101~~	~~36~~	~~375~~	~~146~~	~~24~~	~~8~~	~~60~~	~~15~~	~~5~~	~~1~~	~~12~~	~~3~~	~~2~~	~~0~~	~~10~~	~~2~~	~~2~~	~~0~~	~~31~~
MK260_m7_1	5549	578	90093	9766	187657	17406	20409	2660	68857	5222	14305	1567	467	32	11271	1253	820	71	2486	255	230	26	295	36	27	4	73	10	8	1	125

Table B1. Petrochronological data for monazite grains.

Grain #	Y (ppm)	2SE	La (ppm)	2SE	Ce (ppm)	2SE	Pr (ppm)	2SE	Nd (ppm)	2SE	Sm (ppm)	2SE	Eu (ppm)	2SE	Gd (ppm)	2SE	Tb (ppm)	2SE	Dy (ppm)	2SE	Ho (ppm)	2SE	Er (ppm)	2SE	Tm (ppm)	2SE	Yb (ppm)	2SE	Lu (ppm)	2SE	Gd/Yb(N)
MK260_m7_2	6726	701	92088	9477	186970	12469	18657	2115	72965	4949	13478	1271	425	42	10481	851	893	51	2600	231	274	20	333	27	32	4	76	10	11	2	111
MK260_m7_3	8554	792	88063	8075	171892	13236	16050	1409	68955	4339	11545	968	474	49	10358	819	931	67	2850	181	371	45	429	41	50	6	143	17	20	3	58
MK260_m7_4	12170	1052	52469	3875	99879	9097	11854	1020	48776	5057	8085	828	409	42	7604	932	1057	106	3925	398	657	50	725	61	108	12	340	32	45	3	18
MK260_m7_5	4560	407	99431	8025	189646	15120	20893	2449	77570	5360	13637	1231	454	37	11245	820	848	85	2238	200	198	20	274	25	17	2	48	7	5	1	189
MK260_m7_6	10220	1010	37962	3299	79404	6477	8054	669	33641	2703	6152	617	264	22	5921	627	598	56	3143	317	432	39	503	36	83	9	259	25	32	4	18
MK260_m7_7	18886	1689	83543	7503	181108	25455	18621	1838	72300	7075	14852	1719	553	44	12291	914	1376	124	5822	492	906	89	991	95	150	15	466	47	58	6	21
MK260_m7_8	9924	846	67518	5665	125654	9646	13386	1136	54745	4413	9773	958	391	39	8937	981	874	84	3418	371	437	41	497	50	65	5	198	20	27	4	36
~~MK260_m7_10~~	~~296~~	~~75~~	~~1195~~	~~331~~	~~3175~~	~~720~~	~~368~~	~~91~~	~~1625~~	~~492~~	~~222~~	~~62~~	~~32~~	~~9~~	~~210~~	~~57~~	~~25~~	~~9~~	~~130~~	~~42~~	~~16~~	~~5~~	~~18~~	~~6~~	~~3~~	~~1~~	~~11~~	~~4~~	~~2~~	~~1~~	~~16~~
MK260_m7_11	3603	330	98426	8118	187164	20415	16346	1700	75582	5937	12798	1092	402	48	10690	916	736	68	1866	164	181	16	214	13	11	1	32	5	3	1	267
MK260_m7_12	4143	307	95714	7514	172044	16121	18208	2102	74037	5247	13354	905	364	30	11297	946	731	46	1902	136	169	15	233	28	13	2	35	5	3	1	260
MK260_m7_13	5142	468	91116	12091	196165	15457	17289	1941	78514	7337	13667	941	437	32	12109	1009	835	72	2033	201	217	17	275	24	19	3	44	4	6	1	221
MK260_m7_14	6982	590	99822	9728	205897	17468	18158	1739	77856	6043	13614	1295	502	52	11945	896	930	75	2930	273	317	27	366	33	37	5	94	11	11	1	103
MK260_m7_15	5064	645	92212	9196	190415	19580	18792	2139	80651	7142	13895	1197	456	56	11801	1104	876	101	2115	188	211	20	252	20	17	2	45	6	5	1	211
MK260_m7_16	4272	332	98630	8729	179586	18794	19067	2346	72138	6287	13586	1254	418	42	10464	934	742	85	1977	201	192	18	242	17	13	1	44	5	4	1	194
MK260_m7_17	5551	497	53953	7308	95730	10399	10553	825	42837	4465	7178	647	331	32	6543	615	540	54	1830	198	244	25	293	27	38	4	96	10	13	2	55
MK260_m7_18	4882	471	55821	4960	114540	11669	11110	1185	45364	4091	7205	743	329	30	6620	698	537	55	1957	219	213	19	252	20	29	3	75	10	12	2	72
MK260_m7_19	3819	375	80281	7902	156486	14824	14679	1210	66972	8283	10741	687	363	29	9307	855	653	55	1781	233	150	17	204	22	16	2	40	4	5	1	187
MK260_m7_20	4224	532	96747	10231	197366	17849	17934	1853	76756	7370	13500	1122	406	26	10882	1026	785	71	2120	179	186	18	209	22	17	2	38	5	4	1	232
MK260_m8_1	6514	612	54307	4636	110870	10015	11328	1094	43892	3869	7757	667	321	35	7280	685	606	57	2143	197	259	20	328	30	40	5	107	14	14	2	55
MK260_m8_2	9098	815	109662	9572	190694	16550	18862	1421	71616	5541	13334	1269	537	52	12062	1113	977	73	3046	195	372	31	495	51	57	6	130	14	19	2	75
MK260_m8_3	13105	1151	83377	8223	189181	16234	20352	2110	78220	7034	14229	1520	535	38	12894	1164	1143	81	4259	273	625	64	698	61	89	10	250	25	30	4	42
MK260_m8_4	8820	823	103795	12141	221030	18789	19788	1193	74314	5171	13575	1246	555	50	11914	871	982	79	3118	338	365	26	445	39	51	5	150	17	19	3	64
MK260_m8_5	7777	594	93259	10943	195023	19334	16952	2007	70919	6372	12871	1156	481	41	10981	868	803	68	2789	296	350	24	420	33	51	6	128	15	18	2	69
MK260_m8_6	14759	866	93039	9527	187200	17295	19228	1664	78080	6170	14072	1196	559	60	12546	1269	1241	109	4986	466	625	41	705	49	107	10	270	26	37	4	38
MK260_m8_7	10084	875	91648	9457	189826	16363	19322	2179	75018	5389	12844	1060	545	63	11299	653	991	88	3677	346	454	39	527	63	68	6	166	15	25	2	55
MK260_m8_8	8863	874	49210	3905	107826	9377	10587	804	45724	4146	7598	682	292	25	7101	620	703	66	2571	239	365	42	443	55	54	6	168	23	23	3	34
MK260_m8_10	8263	871	90414	6885	172631	14364	19242	1882	74780	5543	12209	1123	472	41	10597	1019	865	54	2739	265	360	36	372	27	50	4	131	13	18	2	66
MK260_m8_11	8607	713	103339	8656	193640	13910	21550	2535	71726	5639	13408	1248	557	63	10892	869	984	79	3133	281	367	33	459	37	53	5	154	16	19	3	57
~~MK260_m9_1~~	~~1549~~	~~411~~	~~6647~~	~~1717~~	~~10783~~	~~2441~~	~~1485~~	~~384~~	~~6343~~	~~1551~~	~~1060~~	~~239~~	~~40~~	~~10~~	~~823~~	~~215~~	~~96~~	~~28~~	~~400~~	~~113~~	~~65~~	~~20~~	~~64~~	~~16~~	~~11~~	~~3~~	~~40~~	~~13~~	~~4~~	~~1~~	~~16~~
MK260_m9_2	16714	1390	99353	8833	209795	18207	24142	2911	87860	6946	16911	1203	608	59	14509	905	1521	130	5078	409	708	58	893	74	118	10	337	29	46	5	35
MK260_m9_3	25553	2644	105712	8318	213558	22721	21564	2037	90624	7145	16493	1150	684	69	14742	1171	1694	126	8064	626	1056	103	1230	71	229	16	674	44	90	7	18
MK260_m9_4	21904	1870	91536	5963	201404	13187	23063	2332	86958	5795	15962	1175	611	42	14778	1185	1618	164	6448	425	1015	79	1178	89	192	17	527	50	68	6	23
MK260_m9_5	16197	1324	93592	7124	199151	16146	20927	2122	86205	6518	16365	1371	668	58	11899	1002	1353	120	5455	307	733	68	890	63	142	13	360	36	54	8	27
MK260_m9_6	13972	1531	60943	5722	117066	14844	12795	1500	59013	6253	10731	1164	401	48	9329	1326	1002	104	4429	488	641	64	736	76	131	18	327	27	50	6	23
MK260_m9_7	18201	1830	86039	10173	179727	16057	18126	1920	75680	7973	14784	1125	620	67	12507	981	1378	126	6300	633	933	85	987	85	171	20	419	36	59	6	24
MK260_m9_8	13575	1556	111635	10049	206285	14539	22328	2292	92532	5882	17485	1296	586	84	14242	1212	1355	107	4697	527	612	79	771	87	94	11	269	43	34	6	43
MK260_m9_9	23317	2892	104703	10603	199543	16757	23402	2436	92511	6000	16363	1399	631	49	14176	1460	1697	100	7394	624	966	66	1197	132	175	17	470	34	64	6	24
MK260_m9_10	8876	2062	34506	6812	75506	17387	7932	1710	34485	7314	5915	1248	286	61	5068	1228	570	117	2422	553	364	85	472	104	73	18	203	42	32	7	20
MK260_m9_11	7011	597	65086	8001	141541	12923	13438	1144	58272	4399	10629	876	424	43	8747	909	816	94	2364	253	317	24	376	41	56	6	156	19	23	3	46
MK260_m9_12	6069	633	117243	10692	230854	20655	24076	2582	92059	6705	15574	1445	459	40	11666	980	843	82	2499	209	247	21	376	32	29	4	69	6	9	1	137
MK260_m9_13	5505	356	114976	12137	221205	15145	23162	2065	87028	6517	15452	1507	457	38	11653	760	926	61	2445	217	253	28	326	36	30	3	72	11	9	1	131
MK260_m9_14	6171	534	112032	15460	226693	19979	25927	3081	88879	6332	16395	1484	492	41	13260	1209	1025	81	2677	173	264	23	328	28	31	3	77	8	9	2	139
MK260_m9_15	17442	1321	60678	6495	141277	12026	14543	1238	64330	5349	13881	1160	573	48	10770	1139	1193	139	4921	395	790	88	910	83	153	16	485	43	61	7	18
MK260_m9_16	7748	1223	26050	4755	60618	11272	6929	1414	26810	3657	5025	945	233	38	4008	675	471	86	2078	410	311	60	412	91	67	14	176	37	28	5	18
MK260_m9_17	7426	871	31444	5289	77509	10840	7538	1240	30012	4319	5617	920	234	32	5091	866	534	94	1869	275	311	52	357	48	63	9	161	25	24	4	26
MK260_m9_18	16709	1107	99704	7237	200567	19493	21179	2440	89172	6418	16709	1784	624	62	13835	1107	1547	113	5496	509	868	68	922	81	146	14	397	44	58	7	28
MK260_m9_19	15999	1272	110281	11619	208316	16420	23318	2253	91316	7317	16302	1135	605	47	14279	953	1470	120	5489	649	795	67	853	87	124	6	352	34	46	5	33
MK260_m9_20	8770	814	110730	9411	218181	17468	27932	2303	89159	6250	16500	1142	627	48	13651	982	1229	111	3434	220	392	36	469	32	52	6	125	12	16	2	88
MK260_m9_21	10816	1094	101296	7945	178227	18383	19852	1931	84640	6910	13599	1065	554	53	12311	1198	1139	101	4085	426	526	65	614	71	96	11	237	31	34	4	42
MK260_m9_22	8303	642	98218	6482	209777	19270	25144	2790	98369	5612	16889	1295	594	51	14624	1383	1197	105	3221	291	352	30	437	42	49	5	120	14	15	2	98
MK260_m9_23	7714	744	105170	7490	239492	18829	21949	1914	102643	11293	16634	1267	552	39	13440	1254	1070	85	3213	278	357	28	441	39	46	5	112	10	15	2	97
MK260_m9_24	6765	513	110724	8050	204906	23395	24099	2425	94480	9913	15879	1635	485	53	13122	1235	950	80	2745	257	299	23	348	34	36	4	91	9	8	2	117
MK260_m9_25	8367	692	110104	12473	221529	17030	26762	2581	98957	9045	16536	1247	599	46	14530	1545	1152	84	3453	322	371	35	438	40	44	4	130	14	13	1	91
MK262																															
~~MK262_m1_1~~	~~102~~	~~17~~	~~3918~~	~~1214~~	~~9535~~	~~2561~~	~~971~~	~~300~~	~~3467~~	~~1056~~	~~608~~	~~196~~	~~47~~	~~20~~	~~339~~	~~94~~	~~18~~	~~6~~	~~35~~	~~10~~	~~3~~	~~1~~	~~9~~	~~3~~	~~1~~	~~0~~	~~5~~	~~2~~	~~1~~	~~0~~	~~55~~
MK262_m1_3	4450	319	127427	8973	241755	16664	29702	3065	100355	10094	19037	1229	2158	238	11514	1056	929	100	2314	237	188	27	199	28	9	2	23	4	2	1	408
MK262_m1_4	3826	380	125805	10544	274376	26816	28395	2948	103191	7426	18039	1473	2204	205	11754	1379	899	103	1957	201	135	13	124	15	7	1	15	4	2	1	614
MK262_m1_5	8594	704	127741	10303	224589	22983	27360	3392	98069	5295	19723	2028	2264	195	14164	1084	1385	99	4108	332	410	38	355	40	21	3	48	7	5	1	241
MK262_m1_6	4477	512	135303	17129	270374	18504	29657	3566	101952	9319	18307	1457	2024	192	10512	1009	764	60	2347	295	212	25	221	28	11	2	32	5	3	1	269
MK262_m1_7	400	44	131107	12780	293552	28791	27139	2804	93767	6916	17061	1418	1781	168	7335	714	296	27	317	38	15	2	30	4	1	1	3	1	0	0	1808
MK262_m2_1	7718	825	133588	11624	251054	22413	29286	2796	97688	5108	20871	1781	3832	320	14764	840	1342	133	4093	364	353	34	250	26	11	2	27	6	2	1	442
MK262_m2_2	7557	662	117606	10626	276277	22687	31078	2749	97959	8322	21370	1594	3440	287	15162	1463	1437	115	4430	335	321	31	272	27	13	2	24	5	2	1	506
MK262_m2_3	6700	540	124428	11926	261343	24629	27767	2676	95839	7391	21130	1771	3680	343	14440	1371	1472	141	3601	279	294	25	232	19	9	1	29	6	3	1	404
MK262_m2_4	779	122	10041	2471	23368	5379	2533	428	9538	1921	1788	406	268	56	1483	300	139	31	396	85	30	7	34	8	2	1	6	2	1	1	199
MK262_m2_5	6958	636	111395	12764	273594	26532	29951	3634	93761	7911	22450	1661	3334	333	14823	1290	1405	151	3784	267	301	36	265	32	11	2	23	4	1	0	516
MK262_m2_6	8058	615	123212	11944	259762	27438	27719	2676	102729	8890	20990	1484	3597	266	15022	1365	1435	152	4348	327	319	26	246	36	11	2	22	4	1	0	555
MK262_m2_7	6917	460	110820	11729	239633	19665	27026	3016	98268	7944	21161	2081	3443	280	13960	1195	1430	123	4071	366	293	23	241	24	10	2	26	4	2	1	428
~~MK262_m3_1~~	~~91~~	~~14~~	~~899~~	~~369~~	~~2217~~	~~856~~	~~295~~	~~107~~	~~899~~	~~332~~	~~143~~	~~59~~	~~17~~	~~7~~	~~81~~	~~35~~	~~7~~	~~2~~	~~20~~	~~5~~	~~3~~	~~1~~	~~6~~	~~2~~	~~1~~	~~0~~	~~5~~	~~2~~	~~1~~	~~0~~	~~12~~

Table B1. Petrochronological data for monazite grains.

Grain #	Y (ppm)	2SE	La (ppm)	2SE	Ce (ppm)	2SE	Pr (ppm)	2SE	Nd (ppm)	2SE	Sm (ppm)	2SE	Eu (ppm)	2SE	Gd (ppm)	2SE	Tb (ppm)	2SE	Dy (ppm)	2SE	Ho (ppm)	2SE	Er (ppm)	2SE	Tm (ppm)	2SE	Yb (ppm)	2SE	Lu (ppm)	2SE	Gd/Yb(N)
~~MK262_m3_2~~	~~217~~	~~68~~	~~3259~~	~~1281~~	~~7095~~	~~2470~~	~~943~~	~~343~~	~~3298~~	~~1272~~	~~818~~	~~317~~	~~17~~	~~7~~	~~660~~	~~294~~	~~42~~	~~19~~	~~57~~	~~20~~	~~8~~	~~3~~	~~9~~	~~2~~	~~1~~	~~1~~	~~8~~	~~2~~	~~1~~	~~1~~	~~70~~
MK262_m3_4	1997	200	71661	7138	151658	14251	15930	1547	62928	6079	10880	699	1467	139	7174	531	485	53	983	127	69	9	61	10	4	1	12	4	1	0	492
MK262_m3_5	3807	308	106350	11782	248409	26678	24610	2362	93263	5993	16405	1325	2432	139	11257	934	1014	85	2307	177	152	14	96	12	3	1	9	3	1	0	965
MK262_m4_1	4340	355	87323	8205	205395	17243	22670	1702	91684	7510	18395	1155	372	37	14107	1078	1129	74	2433	225	184	21	186	17	12	2	31	6	3	1	369
MK262_m4_2	5342	432	96887	9581	217368	17717	25535	2638	95099	8493	20487	1605	425	35	15768	1211	1178	111	2937	361	228	21	226	25	15	2	45	8	5	1	281
MK262_m4_3	6842	575	98210	12071	211001	17401	26871	2915	97972	4864	22620	2471	430	32	16263	1718	1489	111	3489	363	282	29	280	34	15	3	49	6	4	1	266
MK262_m4_4	5401	509	97764	9494	240846	31885	24409	2208	99086	6656	22296	2005	409	35	13525	1018	1301	122	2647	280	244	25	217	26	13	2	33	6	3	1	334
MK262_m4_5	2916	285	100564	8932	236067	21196	23430	2099	110777	11233	20511	1762	393	37	13412	1373	859	93	1752	140	121	14	122	16	6	1	20	3	2	1	556
MK262_m4_6	3661	328	80088	9138	179114	15575	21919	2407	81798	7475	14649	1483	365	33	9621	858	721	82	1810	162	153	16	163	23	7	1	26	4	3	1	302
MK262_m4_7	2517	250	109697	11197	226647	16534	21519	2166	89962	7426	17221	1659	406	40	11639	1208	676	48	1315	157	104	12	101	9	6	1	23	5	2	1	411
MK262_m4_8	5659	637	104847	9497	219985	21997	24459	2548	96042	7471	19091	1752	2879	232	12996	1024	1202	111	3162	287	249	21	201	20	8	2	23	4	2	1	456
MK262_m4_9	5660	536	110151	10332	249480	21490	23447	1592	90891	6718	18339	1402	2373	316	12051	820	1048	86	2896	355	255	25	198	18	10	2	21	4	2	1	474
MK262_m4_10	2919	329	100109	10136	228023	24763	25773	2458	98059	9307	18387	1537	751	119	13341	1593	833	69	1680	135	124	14	104	12	4	1	13	3	1	1	800
MK262_m4_11	6563	472	119622	11972	223157	23848	27242	2929	94256	8199	18655	1602	2812	260	13067	1261	1202	114	3377	314	267	23	209	22	9	1	20	4	2	1	524
MK262_m4_12	5257	472	109178	13046	226979	18822	24580	2025	96896	8157	17619	1635	2434	158	11824	1050	995	99	2738	227	185	18	167	14	8	1	21	4	2	1	445
MK262_m4_13	3376	400	100307	8546	201751	17029	21462	1662	91069	7758	15576	914	2708	257	12155	823	1022	74	2438	291	155	14	126	13	5	1	12	3	2	1	835
MK262_m4_14	4132	458	110251	11269	199023	17699	20969	2006	92005	6279	18343	1542	2572	287	12995	1186	1166	96	2812	264	216	25	139	17	5	2	12	3	2	1	873
MK262_m4_15	3589	490	35508	5404	69241	8633	8954	1191	39473	6273	7085	1022	205	24	6361	804	532	44	1575	173	145	16	171	21	11	2	28	4	3	1	186
MK262_m4_16	2682	209	108487	10190	214229	20366	24375	2165	104073	6334	17102	1196	759	83	10469	874	707	67	1482	133	115	11	129	19	6	1	15	3	2	1	553
MK262_m4_17	3943	324	111324	8335	214262	18249	24173	2140	92465	5264	19769	1604	2882	214	15165	1449	1226	102	2678	236	181	20	130	13	4	1	14	2	1	1	850
MK262_m4_18	2658	227	102484	7231	202717	19621	22184	2103	83719	7247	18584	1029	2666	268	14004	1020	996	49	2104	232	127	11	101	10	4	1	11	3	1	1	1031
MK262_m4_19	1938	198	111850	11571	212410	21736	26301	2670	100692	7282	18028	1791	1569	192	10957	640	657	73	1331	141	85	11	69	9	3	1	9	2	1	0	996
MK262_m4_20	1564	169	118418	11479	220910	23467	25211	2863	93328	6982	17152	1688	1826	138	9845	1043	653	86	1137	127	70	10	64	9	2	1	6	2	1	0	1268
MK262_m4_21	763	82	107771	8627	197412	21462	24939	2664	83722	8331	16864	1357	1486	148	9082	1079	436	54	612	57	29	4	37	6	1	1	6	2	1	0	1195
MK262_m4_22	3223	303	92767	10145	187634	18508	22418	1275	83047	5849	16078	1356	1058	94	9971	1141	715	61	1398	146	127	13	133	16	7	1	24	5	3	1	337
MK262_m4_23	2442	235	54243	6658	100489	9965	13320	914	53947	4672	9859	955	230	26	6519	561	528	43	1195	106	101	13	110	13	7	1	22	5	3	1	237
MK262_m4_24	2080	156	92301	10763	208799	26364	20607	1479	96421	8524	17186	1327	344	28	9728	781	663	68	1286	113	82	7	97	10	5	1	14	3	2	1	573
MK262_m4_25	2717	267	83286	9766	166869	20692	19291	1903	74365	6602	13474	1159	694	87	8740	559	711	80	1750	241	118	12	117	14	7	1	21	6	2	1	336
MK262_m4_26	2664	388	84587	8789	178938	17014	20325	1382	83229	7632	15873	1476	550	93	9345	1102	692	89	1481	186	111	14	108	18	6	1	14	4	2	1	531
MK262_m4_27	3524	283	120470	9101	197947	18234	25254	2899	94488	6807	19234	1237	2818	234	13761	1104	1179	134	2777	289	161	16	126	14	6	1	13	3	2	1	887
MK262_m4_28	3184	260	108100	9843	213750	13413	25694	2765	96894	8780	19181	1915	2701	313	13396	1176	1135	76	2372	243	137	12	107	12	3	1	11	3	1	1	987
MK262_m4_29	3421	342	107022	8983	187918	17961	23299	2445	96839	8171	18738	1707	2509	269	13494	1499	975	89	2554	298	125	15	96	10	3	1	11	3	1	1	994
MK262_m4_30	2812	235	94253	8384	202556	19861	20904	1915	88264	4809	15991	1117	2143	198	12611	1293	850	81	2030	252	107	15	101	13	4	1	12	3	1	1	867
MK262_m4_31	3199	291	107732	7940	200535	16074	21578	1768	93691	6865	18863	1836	2428	212	13498	1251	967	88	2424	197	132	17	100	10	4	1	13	4	2	1	819
MK262_m5_1	2636	343	21626	2921	48833	6718	4997	731	23286	3422	4224	616	94	15	3521	523	359	42	1206	128	110	17	111	12	7	1	18	5	3	1	159
MK262_m5_2	8249	495	112575	10927	224279	20385	25685	2606	98681	6849	19955	2133	320	33	14297	1559	1294	119	3963	308	370	39	378	41	20	2	58	10	7	1	201
MK262_m5_3	5864	534	62531	6689	131536	13474	14549	1288	54965	5216	10763	1360	193	25	8282	715	788	66	2777	354	262	27	282	30	17	3	44	7	5	1	153
MK262_m5_4	3405	295	99201	10577	245998	19071	28501	3210	112100	7871	19701	1807	285	28	14001	1598	956	85	1947	172	134	17	126	15	5	1	14	3	2	1	796
MK262_m5_5	1939	152	121800	10961	270790	22004	30388	3227	101590	7806	18881	1415	1549	170	11183	731	814	72	1400	100	82	9	82	8	3	1	11	2	1	1	812
MK262_m5_6	1909	206	109593	9432	263574	31592	26262	2353	105034	7671	18502	1697	968	107	10453	1005	686	40	1139	77	75	8	82	9	3	1	8	2	1	0	1079
MK262_m5_7	5371	567	125279	11554	256153	26907	30033	3009	103432	9968	18624	1879	3114	212	13457	1075	1315	97	3445	339	234	24	182	23	7	1	14	4	1	1	794
MK262_m5_8	6695	651	119614	8810	258412	23025	30962	2558	106774	7532	19225	1536	3606	316	14253	1534	1438	136	4113	304	269	21	208	23	8	2	15	3	2	1	755
MK262_m5_9	2747	242	119553	11807	277340	31017	27463	3325	98457	7011	17814	1592	1147	170	10558	951	700	63	1738	199	132	22	129	18	7	1	17	4	2	1	507
MK262_m5_10	2458	270	116699	11136	253265	26282	24464	2653	99403	7266	16935	1505	1791	159	9831	948	692	48	1431	141	94	10	91	11	4	1	13	3	2	1	597
MK262_m5_11	5229	351	123584	10217	274674	29880	27982	2664	105835	8300	20412	1652	3266	260	14114	1484	1227	120	3622	338	251	27	166	23	6	1	11	3	2	1	1039
MK262_m5_12	5988	678	128731	11711	268902	30492	27602	2888	98579	6799	21484	1757	3536	332	14344	984	1383	128	3946	405	249	27	181	20	6	1	16	4	2	1	747
MK262_m5_13	6941	535	118934	11465	265011	27061	26722	2360	102085	9997	19466	1714	3411	371	14389	1117	1533	100	4021	413	250	21	212	23	7	1	17	4	2	1	681
MK262_m5_14	7218	525	118469	9292	255728	22782	30006	2474	101945	7954	20890	2210	3425	299	14764	1455	1480	114	4456	411	312	30	217	22	9	1	20	5	2	1	598
MK262_m5_15	3652	286	116596	15040	240967	16639	26879	2717	104884	7609	19781	1913	884	164	12117	996	925	69	2428	177	155	13	158	17	6	1	20	4	2	1	494
MK262_m5_16	3430	335	116228	7739	252309	22371	27111	2584	98814	7954	19819	1564	1994	224	11929	1003	925	69	1878	149	124	9	118	11	6	1	15	3	2	1	661
MK262_m5_17	7359	615	114650	10107	249620	21304	28842	3069	97731	6751	22415	2818	3681	337	13966	1331	1556	135	4186	352	314	23	249	25	10	2	20	5	3	1	552
MK262_m5_18	4559	508	111305	8459	255187	21397	26569	2744	93613	6969	19468	1543	3084	279	14599	1539	1230	101	2905	254	203	22	127	16	5	1	13	4	1	1	943
MK262_m5_19	4963	453	131280	15184	252632	24840	28164	3326	99509	8587	21154	2339	3102	332	14515	1534	1338	118	3090	306	179	15	151	14	5	1	12	3	1	1	948
MK262_m5_20	6105	458	117340	9409	252880	19869	26748	2747	107051	10248	18831	1932	3321	305	13259	1212	1299	126	3935	313	269	21	185	23	7	1	16	4	2	1	653
MK262_m5_21	5116	461	103939	9195	237653	20605	25538	2084	101766	8553	20368	1538	3236	244	12867	1202	1298	127	3760	368	220	22	160	14	5	1	17	4	2	1	610
MK262_m5_22	5089	510	115337	14167	222480	22610	26836	3207	102566	8110	20011	1930	3011	266	14390	1502	1297	142	3433	304	195	16	174	22	5	1	11	3	2	1	1063
MK262_m5_23	5914	451	126387	12222	252826	19177	30410	2970	105243	7976	20527	1720	3191	215	15405	1249	1334	117	3624	275	277	28	210	24	8	1	20	5	2	1	633
MK262_m5_24	4522	342	123681	12360	242532	29914	24124	2468	97727	8825	19977	2370	3055	315	12837	1056	1171	110	2889	327	180	15	149	15	6	1	13	4	2	1	774
MK262_m5_25	3766	353	122515	12531	230589	17894	26425	2592	106110	6437	21237	1904	3150	317	14570	1028	1119	102	2886	251	161	17	137	19	4	1	15	4	1	1	808
MK262_m5_26	5665	504	113704	11819	237513	20286	25529	2305	103675	6619	22640	2415	3338	397	13651	1004	1262	84	3713	300	205	17	162	20	6	1	14	3	2	1	800
MK262_m5_27	5933	533	118182	11392	258377	22019	27732	3367	102079	6788	17476	1654	2882	231	13507	1287	1220	112	2906	232	193	18	186	14	9	2	23	5	2	1	466
MK262_m5_28	4380	426	122705	13867	228255	16483	25269	2436	92224	6443	19571	976	3346	336	13542	1515	1268	98	2946	215	187	15	145	13	4	1	11	3	1	1	1026
MK262_m5_29	5318	532	124614	12610	233009	23926	25944	2758	105971	7532	19339	1969	3384	317	14323	1614	1187	109	2877	220	162	13	169	16	7	2	26	6	2	1	447
MK262_m6_1	2558	202	126822	13183	262874	25115	31865	2569	115642	7374	19796	1226	386	38	12896	1466	879	80	1619	222	111	13	124	18	4	1	15	2	2	1	697
MK262_m6_2	2821	257	127826	9643	241178	21558	30954	3357	110079	8123	20699	1955	385	37	11988	960	825	85	1658	157	115	15	111	12	6	1	18	5	2	1	552
MK262_m6_3	4123	392	110984	9699	219973	18236	25954	2600	97945	7911	17928	1225	1077	76	11123	940	921	73	2172	157	166	19	191	24	13	3	33	6	4	1	276
MK262_m6_4	5909	500	99658	11249	204621	19337	22739	1674	96523	8202	17992	1425	461	51	12868	1256	1092	87	2563	261	220	20	255	28	18	3	57	8	6	1	183
MK262_m6_5	8715	743	122718	14529	236849	23199	31614	3141	120922	12074	23688	1963	435	36	17545	1752	1532	132	3978	293	362	29	396	34	21	3	59	10	6	1	242
MK262_m6_6	3102	306	118185	8793	256443	24102	35771	2832	123482	12819	24806	2413	312	31	15249	1403	933	80	2046	275	113	13	134	16	6	1	14	3	2	1	894

Table B1. Petrochronological data for monazite grains.

Grain #	Y (ppm)	2SE	La (ppm)	2SE	Ce (ppm)	2SE	Pr (ppm)	2SE	Nd (ppm)	2SE	Sm (ppm)	2SE	Eu (ppm)	2SE	Gd (ppm)	2SE	Tb (ppm)	2SE	Dy (ppm)	2SE	Ho (ppm)	2SE	Er (ppm)	2SE	Tm (ppm)	2SE	Yb (ppm)	2SE	Lu (ppm)	2SE	Gd/Yb(N)
MK262_m6_7	1647	179	134505	11263	259138	25804	32639	3815	119904	10841	23486	2525	596	71	10725	775	587	45	1156	91	65	8	76	7	2	0	10	3	1	0	844
MK262_m6_8	429	44	145181	13910	280327	23899	29971	2721	101340	8772	18296	1583	1786	122	7833	823	355	34	378	54	16	2	33	5	1	0	4	2	0	0	1804
MK262_m6_9	501	63	136139	12252	287554	30640	30761	3486	108096	8670	18394	1478	1618	166	7675	548	353	35	417	36	18	2	36	4	1	0	4	1	1	0	1646
MK262_m6_10	985	119	131768	14379	280990	30724	33609	3138	109710	10743	20559	1992	1031	100	9418	899	476	43	729	60	34	5	59	6	2	1	8	2	1	1	945
MK262_m6_11	4589	397	123687	12123	266847	23816	31350	4006	127392	14898	24277	1968	452	45	14715	1799	1102	97	2398	297	170	18	179	18	9	2	24	4	2	1	500
MK262_m6_12	452	34	132512	8555	261641	22781	33807	2702	110832	6827	19526	1961	1640	103	8235	868	393	48	427	37	16	2	32	5	1	0	4	2	0	0	1707
MK262_m6_13	860	78	137592	13614	266046	23012	30892	2891	104072	10012	19424	1775	2049	155	9769	1179	502	37	742	76	31	5	44	7	2	1	6	3	0	0	1321
MK262_m6_14	6840	686	132887	15499	251867	20499	28141	2762	121357	13534	21107	2249	3722	317	13739	1467	1462	102	3727	305	284	25	227	22	7	1	16	4	2	1	689
MK262_m6_15	371	40	146413	13777	261981	19909	33189	2380	113245	10386	17978	1485	1744	181	7782	724	370	30	412	36	14	2	35	6	0	0	4	2	0	0	1562
MK262_m6_16	2803	241	129683	10660	219757	25198	28415	2972	102040	6525	20606	1926	3112	282	12800	788	974	83	1998	186	121	12	91	9	4	1	14	3	1	1	751
MK262_m6_17	3115	297	131950	11078	257112	21917	27427	2048	112436	9609	24077	2061	3322	294	14713	1502	1040	75	2040	156	129	11	97	9	4	1	13	3	2	1	944
MK262_m6_18	464	46	139075	12646	279192	33818	27633	2441	112643	8351	19579	2053	1822	158	7957	679	383	35	437	53	16	2	31	4	0	0	3	1	0	0	2506
MK262_m6_19	1465	184	123520	10657	254785	20755	32134	3473	115648	11306	20617	1191	2633	218	11087	1244	650	52	1077	119	56	7	56	8	1	0	6	3	1	0	1408
MK262_m6_20	2326	249	133379	17630	266936	23154	31909	2970	130289	15416	21665	1441	1255	127	12735	1044	797	80	1373	142	85	11	83	7	4	1	11	3	1	0	979
MK262_m6_21	2294	254	139786	9280	249477	24354	26038	2328	113322	10253	22235	1830	2861	258	12553	968	925	95	1586	192	80	8	78	10	3	1	9	3	1	1	1107
MK262_m7_1	2344	147	134278	14365	271117	22142	29516	3086	108983	11099	20999	2331	2985	319	11543	1115	860	88	1544	135	83	8	88	9	4	1	14	4	1	1	653
MK262_m7_2	1202	94	135090	12977	271750	19125	27838	2610	108191	12944	19020	1661	2404	226	9182	677	551	49	797	84	42	4	47	6	1	0	7	2	0	0	1059
MK262_m7_3	974	94	118045	12329	221090	19352	28921	3406	97720	7981	18145	1535	2152	247	8861	840	473	42	728	87	34	4	42	6	1	1	8	2	1	0	952
MK262_m7_4	612	54	108855	11703	212408	19091	24144	2191	87290	6445	14954	1144	1597	142	6824	714	358	30	443	38	20	3	34	6	1	0	6	2	0	0	974
MK262_m7_5	251	29	25241	5242	46055	7203	5882	848	21010	2996	3656	614	378	50	1479	208	80	13	124	18	7	1	12	2	1	0	3	1	1	0	422
MK262_m7_6	2408	231	127224	13494	260443	20559	29197	1894	98738	9253	19147	1747	2749	227	10917	869	772	81	1248	131	71	7	76	8	4	1	13	3	1	1	694
MK262_m7_7	3311	326	139204	16051	250635	21536	30235	2895	105722	5070	20450	1242	3285	276	11508	999	979	89	1820	157	126	14	103	11	6	1	14	3	2	1	646
MK262_m7_8	5428	458	130305	12106	254132	21070	32067	3293	108630	6881	21639	2007	3470	370	12754	1112	1220	107	3054	241	205	22	164	14	6	1	19	3	1	0	554
MK262_m7_9	4650	486	111431	12417	225955	28266	26360	2354	109017	11430	21319	1676	3513	405	13207	1532	1138	121	2745	176	195	17	136	11	5	1	13	3	1	1	815
MK262_m7_10	3820	307	135849	10169	245887	22762	27833	2943	100200	5889	22912	1880	3338	251	11464	1003	994	81	2004	223	130	15	116	14	5	1	12	2	2	1	760
MK262_m8_1	5600	541	109435	13563	220836	21334	22875	1996	87265	7331	15209	1305	789	72	11022	888	933	89	2473	261	205	20	241	27	15	2	40	6	4	1	221
MK262_m8_2	850	82	132668	14244	277882	27546	28149	2966	113570	13939	17445	1541	1303	104	7708	964	449	40	589	75	31	4	52	6	1	0	7	2	0	0	924
MK262_m8_3	5551	500	122094	11259	254378	22923	25222	2845	95327	6848	20722	2157	399	38	12609	1054	1155	116	2750	327	201	15	257	27	15	2	41	6	4	1	251
MK262_m8_4	2329	216	101298	12674	200613	21275	20855	1842	81281	4641	16891	1732	295	37	8816	514	662	52	1291	88	77	8	81	10	4	1	13	3	1	1	555
MK262_m8_5	2546	251	111456	9139	231070	26128	25135	2534	96582	6822	19470	1773	356	31	9385	822	766	59	1346	126	74	7	100	11	5	1	12	2	2	1	616
MK262_m8_6	1583	186	130563	11309	255010	26117	27668	2822	105264	12074	17355	1341	2134	165	9406	881	500	51	1102	112	63	7	57	6	2	0	8	2	0	0	978
MK262_m8_7	6164	634	115527	7791	257454	22922	28870	3081	103211	6715	21919	1833	3462	324	12810	1042	1250	111	3570	354	228	17	172	21	7	1	15	3	2	1	695
MK262_m8_8	5552	475	130812	12459	250865	23089	26477	3061	94491	7169	20205	1695	3353	350	11730	972	1112	88	3055	224	206	20	152	18	7	1	19	5	1	0	505
MK262_m8_9	5798	406	115280	12555	246808	20415	23433	2299	97611	6879	19044	1760	3326	234	13004	1140	1371	140	3289	187	225	20	159	17	6	1	18	4	1	1	588
MK262_m8_10	4088	391	111621	11267	246170	22799	28205	2610	103448	12568	21423	2270	2811	298	11115	878	1118	121	2651	265	165	14	126	13	5	1	10	3	1	0	866
MK262_m8_11	6611	638	112182	9732	221638	23696	21328	1600	83885	7786	18314	1801	894	108	10489	917	967	86	2738	279	257	29	290	37	20	3	55	8	5	1	154
MK262_m8_12	2859	340	138924	13150	238922	22168	27169	2618	100384	7625	21887	1686	1903	194	11355	1149	977	112	1965	208	103	13	92	13	3	1	12	4	1	0	738
MK262_m8_13	4464	453	111153	9618	246561	23129	29374	3036	102785	8420	19905	2371	3252	322	12116	1075	1122	81	2685	274	153	14	119	12	6	1	15	3	1	0	636
MK262_m8_14	2855	339	130802	12821	249518	24450	25423	2713	99974	8473	18460	1740	2398	216	10310	808	791	84	1598	160	111	12	79	9	3	1	10	3	1	0	836
MK262_m8_15	5857	498	131162	11368	261322	24376	25985	3173	91267	8012	19264	1202	3395	266	12228	1189	1260	92	3243	257	221	20	153	20	6	1	13	3	1	0	787
MK262_m8_16	594	72	105708	10617	199711	16813	19272	2102	78003	6439	13484	1357	1375	97	5593	438	270	25	398	50	19	2	26	5	1	0	6	2	1	0	698
MK262_m8_17	2678	274	117430	12946	262306	26940	25230	2942	106449	11155	20327	2209	905	98	10252	949	857	86	1668	149	122	15	136	16	8	2	19	4	2	1	441
MK262_m8_18	6381	619	88452	8616	182201	20483	19112	1812	80365	6547	17160	1890	310	40	10585	1178	1130	133	2759	294	266	32	234	25	16	3	40	5	5	1	214
MK262_m8_19	8062	581	112974	10307	230922	16380	23629	2372	93564	7241	21507	1944	682	93	14590	1233	1324	138	3810	348	308	26	335	26	21	3	58	8	4	1	203
MK262_m8_20	11729	922	119979	11527	230071	21404	23671	2840	93770	8775	20558	1790	737	85	13056	1143	1566	132	4942	429	438	50	478	42	36	4	84	11	8	1	125
MK262_m8_21	4803	424	111965	11629	222702	19820	22547	2051	92586	8153	19093	2777	2377	221	12597	1190	1070	79	2623	256	181	18	152	20	7	2	21	4	2	1	489
MK262_m8_22	4042	251	96303	7770	190953	18878	20327	1638	80532	6720	16027	1218	2731	217	9465	946	955	87	2593	251	161	13	126	16	5	1	10	2	1	0	731
MK262_m8_23	4524	471	120380	9696	261560	25613	26293	2772	93150	5599	20984	1636	3530	372	11599	1236	1113	112	2987	341	198	25	157	18	6	1	13	3	1	0	725
MK262_m8_24	591	63	143258	15693	273732	26386	27848	2879	100210	6323	15994	1140	1748	134	7701	715	398	36	498	58	22	3	35	6	1	0	4	2	0	0	1718
MK262_m9_1	3975	508	97388	7190	187574	16151	23786	2217	94404	6042	17276	1366	1793	188	12097	987	1020	102	2266	295	167	31	172	28	10	2	24	5	2	1	400
MK262_m9_2	3560	470	100061	6928	202596	23286	23556	2667	95008	6777	18476	1662	1845	178	12016	877	937	106	1929	189	131	15	134	15	7	2	17	4	1	0	562
MK262_m9_3	1749	181	104185	9937	200872	17171	22966	2133	89905	5416	16767	1279	2252	235	10255	870	691	67	1101	90	61	6	56	7	2	1	7	2	0	0	1115
MK262_m9_4	1872	146	111578	10406	221195	20129	24639	2891	92818	6085	16985	1185	2242	199	10728	845	716	65	1396	183	71	7	72	8	2	1	8	2	1	0	1128
MK262_m9_5	7240	673	89532	11905	185461	24115	20168	1563	88305	8362	20917	1808	383	33	14954	1083	1203	67	2971	215	259	27	289	27	18	3	50	7	5	1	242
MK262_m9_6	7287	655	105408	11527	196929	17442	22155	1977	96814	7879	19757	1807	385	37	13566	1245	1305	127	3069	262	260	24	305	20	18	3	48	7	4	1	229
MK262_m9_7	6117	585	99048	8581	209095	18616	24903	2967	97456	7329	19510	1922	364	31	13172	1169	1174	104	2742	272	234	26	278	34	16	2	43	8	4	1	245
MK262_m9_8	5128	642	103304	9123	193725	17454	24791	2420	95833	8373	19781	1775	361	39	12168	896	1139	91	2392	217	187	19	210	22	13	2	33	8	3	1	297
MK262_m9_9	7203	752	99284	8030	217880	16836	25874	3196	96556	6912	19974	1789	853	70	11308	1192	1285	113	2945	271	287	38	306	40	24	4	54	11	5	1	169
MK262_m9_10	2826	253	100196	8210	215980	13502	24576	2656	93520	5722	19293	1739	2333	188	11913	1156	896	69	1714	157	106	12	83	8	2	1	8	2	1	0	1280
MK262_m9_11	2007	144	113148	12603	208046	15949	22269	2573	89956	8082	16305	1495	2345	180	10895	1046	768	58	1584	133	88	8	65	8	3	1	6	2	1	0	1395
MK262_m9_12	2007	192	108026	9376	226942	22583	23107	1974	94938	7255	17123	1511	2500	191	10842	891	813	70	1661	133	91	8	70	7	2	1	9	3	0	0	991
MK262_m9_13	2032	218	108656	8767	223058	18814	26068	2151	91612	6839	16559	978	2704	281	10639	895	788	79	1399	108	79	7	70	9	2	1	6	2	1	0	1394
MK262_m9_14	2584	338	103382	9755	216729	20223	27828	2684	95826	8237	16756	2069	2409	239	11338	1172	768	64	1606	204	96	11	92	15	3	1	11	3	1	1	852
MK262_m9_15	2767	402	102115	10518	218575	21548	24846	2778	90636	7836	15601	1567	2272	201	11130	947	886	77	1756	210	113	15	106	24	5	2	9	3	1	1	967
MK262_m9_16	2341	197	107760	9822	232307	24747	24189	2959	96670	6819	17284	1562	2526	161	12139	1212	811	69	1660	134	91	8	81	7	3	1	8	2	1	0	1269
MK262_m9_17	2854	200	110228	11213	210368	17746	28625	2636	98854	7207	18772	1724	2803	242	11767	959	1030	82	1944	167	115	11	85	9	3	1	7	2	1	0	1334
MK262_m9_18	2631	192	109190	11358	214897	17101	24032	2691	97154	7913	16454	1227	2309	228	11363	946	843	79	1643	154	105	11	82	10	2	1	8	3	1	0	1084
MK262_m10_1	6550	614	114765	10380	223880	24526	28032	2426	112375	10663	21710	1736	962	101	13090	1355	1042	97	2686	261	308	32	404	51	42	6	180	21	24	3	59
MK262_m10_2	2683	311	115443	9364	223886	18378	29705	3107	101489	7937	18955	1487	827	92	9644	821	691	69	1221	134	95	8	123	15	6	1	20	5	2	1	383

Table B1. Petrochronological data for monazite grains.

Grain #	Y (ppm)	2SE	La (ppm)	2SE	Ce (ppm)	2SE	Pr (ppm)	2SE	Nd (ppm)	2SE	Sm (ppm)	2SE	Eu (ppm)	2SE	Gd (ppm)	2SE	Tb (ppm)	2SE	Dy (ppm)	2SE	Ho (ppm)	2SE	Er (ppm)	2SE	Tm (ppm)	2SE	Yb (ppm)	2SE	Lu (ppm)	2SE	Gd/Yb(N)
MK262_m10_3	1135	96	121638	14107	225012	24271	23862	2130	93556	7124	15137	1109	1496	122	7701	602	401	39	692	80	51	4	86	10	6	1	30	5	4	1	211
MK262_m10_4	1438	104	129438	7717	251192	21772	25308	2972	94143	7002	16460	1125	1714	178	8959	984	501	43	787	77	47	6	64	9	3	1	9	3	1	0	848
MK262_m10_5	1038	116	122271	10619	250254	20400	30416	2877	100900	7825	17177	1586	1642	164	7540	630	428	40	573	60	38	6	50	6	2	1	5	2	0	0	1239
MK262_m10_6	911	74	119462	13033	264799	34748	27618	3296	95021	8813	16101	1376	1576	126	7220	748	406	40	595	66	35	4	51	8	2	1	7	2	1	0	791
MK262_m10_7	1819	136	129080	12641	258355	18818	27532	3189	112466	12584	18116	2013	1731	203	9619	654	579	55	1086	90	73	7	94	10	5	1	17	4	2	1	451
MK262_m10_8	1773	138	123602	10048	248702	26851	28565	2756	98144	6722	18977	1765	1714	192	10244	707	661	71	1080	108	70	6	82	9	4	1	14	3	1	0	593
MK262_m10_9	2153	193	126694	14894	225238	17035	27335	2966	88363	6689	19832	1885	1806	170	9892	915	659	90	1067	90	69	7	80	10	6	1	18	4	2	1	445
MK262_m10_10	1786	185	136427	13819	259905	28397	28767	3113	94985	7914	17995	1661	1936	137	10980	1143	701	84	1110	103	62	7	89	11	4	1	10	3	1	0	910
MK262_m10_11	1763	116	118661	14785	253818	25647	28663	3238	94127	7624	19124	1619	2078	218	10413	1063	677	60	1077	98	67	8	87	9	4	1	16	3	1	1	543
MK262_m10_12	2028	199	114696	10808	223562	19788	30070	3138	95561	7818	20734	2112	1967	197	10930	1191	686	69	1199	114	74	8	103	15	6	1	31	6	3	1	289
MK262_m10_13	1962	176	121357	15773	253685	28990	26527	2950	100155	6853	21389	2417	1891	198	11512	671	679	63	1208	106	76	7	92	8	6	1	26	5	3	1	357
MK262_m10_14	1680	155	118982	10105	236350	23472	26103	2505	91629	6736	19927	1699	1767	202	10803	896	737	75	1048	134	66	8	78	10	5	1	21	4	2	1	425
MK262_m10_15	1817	153	117084	10529	242744	21192	26247	3210	100746	6047	18596	1835	1625	144	9513	777	675	56	1094	111	61	6	87	13	5	1	19	4	3	1	416
MK262_m10_16	1732	175	117705	10956	268029	22717	26689	2768	101904	8237	20118	1537	1729	156	10588	1024	693	53	1049	92	68	7	88	12	4	1	12	4	1	1	703
MK262_m10_17	900	63	127072	12057	247648	23275	25901	3615	97979	9025	16570	1290	1559	152	6559	616	350	34	575	54	34	4	48	6	2	1	7	2	1	1	770
MK262_m10_18	1239	122	112211	10717	223346	21888	21974	2229	81972	6948	14314	1537	1183	139	6854	696	365	37	635	71	41	6	57	8	3	1	16	4	2	1	339
MK262_m10_19	938	100	51295	5837	110556	9220	12126	1010	45537	4881	8036	993	449	48	3328	380	238	30	417	41	36	4	46	5	3	1	11	3	1	0	251
MK262_m10_20	1949	170	86154	9128	196240	24533	21067	2270	79975	4368	17160	1603	1337	123	9288	830	550	60	988	85	72	6	85	10	5	1	17	4	2	1	430
MK262_m10_21	570	79	18337	2577	52899	7113	4888	732	19334	2564	4183	668	300	43	2128	372	135	20	289	44	20	4	25	6	1	1	4	2	1	0	389
MK262_m10_22	2261	230	131562	13398	253150	25285	29367	3509	101338	6793	22379	1871	1961	229	11595	975	733	78	1223	114	71	7	88	9	5	1	15	4	1	1	611
MK262_m10_23	4376	482	99819	9800	226731	19425	23813	2184	102106	7199	19728	1138	501	52	11171	1141	871	91	1959	180	159	15	196	29	12	2	47	7	5	1	190
MK262_m10_24	1770	209	110721	10109	235127	19400	27203	2876	99609	6759	19225	1805	848	58	9125	834	540	55	1012	98	63	8	90	13	4	1	18	5	2	1	414
MK263																															
MK263_m1_1	395	50	83536	7891	144181	11403	15846	1367	56437	5341	9770	982	877	102	3727	339	158	19	230	22	13	2	25	4	1	0	4	2	1	1	727
MK263_m1_2	566	38	123844	8813	228326	19554	23011	2069	90309	6811	15228	1418	1309	114	5695	582	265	28	341	34	22	2	37	4	1	0	5	1	0	0	911
MK263_m1_3	603	52	109724	9867	232525	22112	25997	2714	91043	8129	16012	1470	1578	140	5635	565	264	31	421	56	21	2	37	6	1	0	5	2	1	0	965
MK263_m1_4	732	65	125436	11994	233339	20689	26403	2660	89420	6015	16057	1184	2342	211	6898	694	311	26	474	51	28	4	43	6	2	1	6	3	1	0	906
MK263_m1_5	771	80	119048	11414	250418	20423	25890	2529	90880	8972	17262	1685	2158	153	6903	669	323	29	539	56	35	3	48	5	2	1	7	2	0	0	780
MK263_m1_6	773	74	119977	11067	236127	15938	23664	2412	91328	6940	16377	1046	2348	232	7702	771	359	48	536	47	29	4	50	7	1	1	9	2	0	0	665
MK263_m1_7	720	65	107198	9064	220469	19222	19188	1749	80697	7512	15024	1360	2003	206	7205	576	364	34	496	48	26	3	42	4	2	1	8	2	1	0	741
MK263_m1_8	658	58	112486	8868	253907	23933	23110	1986	91143	7319	17341	1125	2206	161	8015	712	363	33	506	50	25	2	42	6	2	1	6	2	0	0	1039
MK263_m1_9	723	90	114103	11736	210272	16688	23918	2507	93014	6156	16237	1561	2343	240	7635	654	306	25	471	35	30	3	41	4	1	0	8	2	1	0	759
MK263_m1_10	772	70	124884	13777	229938	20768	22992	2312	95702	8124	17066	1227	2189	193	7580	734	317	23	495	58	31	4	49	6	2	1	8	2	0	0	782
MK263_m1_11	860	57	119317	12589	228860	25601	25248	2330	96464	7409	17543	1456	2300	221	6718	592	328	33	536	46	28	2	51	8	2	1	5	1	1	0	1067
MK263_m1_12	603	69	121730	10856	238445	26650	21372	2126	86842	6795	15240	1582	1643	138	6097	572	244	14	360	28	22	2	35	6	1	0	5	2	1	0	1058
MK263_m1_13	662	63	127892	10361	219275	14307	25481	2312	86142	6344	15356	1455	1982	153	7109	561	287	22	514	59	30	4	47	6	1	0	7	2	1	0	784
MK263_m1_14	701	66	116514	9976	236928	24331	24704	2570	97720	7635	15461	1370	2160	216	7031	617	310	33	413	39	27	3	41	5	2	1	7	2	1	0	777
MK263_m1_15	697	71	125798	14766	227244	23580	25850	2919	87063	7518	16460	1400	2141	203	8283	889	343	29	443	39	25	2	41	6	1	1	5	2	1	0	1433
MK263_m1_16	660	50	119396	11026	227336	19398	22367	2194	89775	8827	15455	1059	2304	207	7312	569	350	29	445	44	20	3	39	5	1	0	7	2	0	0	795
MK263_m2_1	5303	385	106660	8968	219992	25529	23249	2088	95084	6473	19307	1627	472	53	12422	1389	999	81	2754	247	226	23	270	28	19	3	52	7	6	2	192
MK263_m2_2	5201	446	123449	10851	239275	25824	24502	2699	95195	7535	19474	2570	379	36	12108	1198	952	103	2409	205	186	16	270	26	16	2	50	8	5	1	197
MK263_m2_3	4386	398	87865	8095	167592	16731	16928	1460	73955	5195	15187	1243	310	33	9492	823	815	83	2060	154	172	16	216	23	13	2	41	6	4	1	188
MK263_m2_4	1965	221	118644	13434	229344	24112	25245	2644	90647	8029	14617	1244	411	32	7780	545	493	39	1013	82	77	8	93	12	5	1	17	3	2	1	364
MK263_m2_5	1710	146	125578	11909	212600	27232	24352	2087	89215	6557	13534	1181	693	81	6985	793	383	38	817	68	60	8	80	13	4	1	12	3	1	1	483
MK263_m2_6	1362	121	124518	11348	234277	20373	26636	2791	92376	8208	13091	1413	730	71	6997	541	371	32	737	56	54	5	66	8	3	1	9	3	1	1	607
MK263_m2_7	1245	131	109830	10385	242031	28691	26545	2289	88298	6683	14210	1342	850	71	6232	446	306	23	604	57	45	7	55	7	2	1	7	3	1	1	740
MK263_m2_8	1681	166	138409	13738	220417	22728	21599	2028	82982	7268	11196	821	1989	168	6035	487	405	40	841	101	60	7	68	9	3	1	10	3	1	0	495
MK263_m2_9	1860	144	132064	12494	229405	19765	20396	1802	83435	4750	11671	876	2693	189	6702	593	460	45	982	108	72	9	85	14	5	1	13	4	1	1	403
MK263_m2_10	3583	301	103086	6921	211238	15449	24062	2267	90037	4901	15624	1453	369	40	9470	872	727	81	1677	157	142	10	179	21	11	2	41	7	4	1	189
MK263_m2_13	3175	317	73604	9868	130716	14633	15333	1526	59313	7081	11145	1138	315	41	8151	1033	629	68	1606	165	143	17	179	24	12	2	33	6	4	1	198
MK263_m2_14	2244	209	109071	12386	195009	19523	18587	1295	77714	7374	12641	1050	1393	175	6989	533	464	44	1052	90	95	11	110	12	7	1	28	6	2	1	202
MK263_m2_15	4918	359	119072	11824	221199	19966	25833	2653	93287	5837	16375	1364	3201	332	10771	839	1051	95	2588	344	201	15	180	19	10	2	32	7	3	1	274
MK263_m2_16	3102	326	129252	14381	213050	18739	18275	1227	82596	7751	13313	1551	2998	296	8799	940	714	65	1617	129	126	12	133	13	7	2	21	5	2	1	342
MK263_m2_17	1719	218	120144	9613	220601	23755	20350	1936	77505	5809	12638	1226	2500	236	6442	617	436	50	888	81	65	7	88	9	5	1	15	4	2	0	345
MK263_m2_18	5057	433	107032	10763	196528	17031	19293	1387	92703	6936	16365	1735	458	41	11760	720	967	85	2582	291	209	13	270	31	18	2	62	8	8	1	154
MK263_m2_19	4661	562	85837	7624	166642	18248	18008	1611	68608	6701	15807	1651	353	34	9246	689	822	77	1963	197	172	17	228	25	17	3	43	7	5	1	175
MK263_m2_20	3096	319	118035	12659	213066	21868	24207	2717	91225	8061	17753	2189	910	149	9201	940	739	80	1380	114	131	15	145	12	10	2	35	6	4	1	212
MK263_m2_21	1412	148	140247	11615	228681	19242	19036	1874	80019	7125	11864	914	2491	252	6896	689	404	33	738	53	62	6	80	14	4	1	13	3	1	1	423
MK263_m2_22	1185	128	144352	15936	230302	16692	26994	2893	85091	6207	14098	1429	1517	137	6735	620	335	20	651	73	47	6	58	6	2	1	7	3	0	0	768
MK263_m2_23	1038	97	136258	10160	235422	21564	29782	2906	92788	8658	15137	978	1033	77	6670	718	352	41	617	58	45	4	52	7	2	1	6	2	1	0	849
MK263_m2_24	1402	108	127813	8984	267381	27195	26104	2662	93477	5671	15354	1117	887	70	8029	707	429	37	797	78	53	6	67	7	3	1	11	3	1	0	585
MK263_m2_25	1535	141	117180	10080	232299	24993	24204	2626	98218	7689	16594	1637	755	71	7622	542	432	42	822	78	63	6	79	8	4	1	13	4	1	1	476
MK263_m2_26	2962	246	119553	11433	245779	21009	24978	2242	108181	10096	18695	1846	338	25	10540	850	778	63	1596	161	130	11	159	18	9	1	29	7	3	1	294
MK263_m2_27	5488	357	114132	8169	227465	20050	25228	2328	106273	8961	21802	1628	409	33	12698	1297	1042	70	2483	222	219	18	255	24	18	2	55	9	6	1	187
MK263_m2_28	3703	277	96521	9204	205555	24363	19637	1353	88914	6461	18338	1771	352	35	9215	813	801	68	1712	184	158	17	185	22	12	2	36	6	3	1	206
MK263_m3_1	5885	652	110002	11902	194975	14298	22471	2658	91233	6383	17307	1435	305	33	13030	1466	1152	95	2846	237	246	26	272	27	18	2	51	8	6	2	205
MK263_m3_2	3781	408	118738	12501	221928	17291	23341	2195	94216	6752	17169	1760	308	31	9986	901	746	86	1758	194	155	19	173	27	12	2	30	6	3	1	270
MK263_m3_3	2497	243	114832	10759	207912	22505	22350	2015	86781	9654	14595	902	311	39	8343	661	551	41	1175	127	104	11	126	17	8	2	18	4	2	1	374

Table B1. Petrochronological data for monazite grains.

Grain #	Y (ppm)	2SE	La (ppm)	2SE	Ce (ppm)	2SE	Pr (ppm)	2SE	Nd (ppm)	2SE	Sm (ppm)	2SE	Eu (ppm)	2SE	Gd (ppm)	2SE	Tb (ppm)	2SE	Dy (ppm)	2SE	Ho (ppm)	2SE	Er (ppm)	2SE	Tm (ppm)	2SE	Yb (ppm)	2SE	Lu (ppm)	2SE	Gd/Yb(N)
MK263_m3_4	2383	230	103375	10026	219216	25309	22315	2711	94077	6513	13822	999	299	32	9177	711	595	54	1361	117	114	13	134	11	8	2	23	5	4	1	327
MK263_m3_5	2312	152	115676	11291	211489	23103	26235	3223	91604	7675	16728	1261	304	23	9132	896	623	65	1319	103	107	9	109	15	7	1	22	4	2	1	334
MK263_m3_6	2492	250	106121	11905	227404	23038	23653	2725	98168	7223	15905	1680	304	27	9566	922	618	65	1368	116	102	10	117	15	6	1	21	4	2	1	371
MK263_m3_7	1123	107	111911	11954	210202	19857	21658	2446	85445	7337	12846	1551	1766	169	6697	600	384	44	657	72	45	4	52	9	3	1	8	3	1	0	644
MK263_m3_8	1349	115	104550	9790	203215	19552	22296	1844	90612	7732	15946	1065	514	50	8140	832	508	50	876	83	52	7	74	8	3	1	14	4	2	1	488
MK263_m3_9	2418	194	107051	9259	223554	20251	21588	1664	91253	6924	15400	1289	332	19	8212	1000	625	50	1382	101	110	9	128	15	7	1	23	5	2	1	295
MK263_m3_10	5448	566	81837	10050	177728	14754	20110	2442	76590	5134	15099	1364	400	37	10989	1029	980	85	2659	276	245	18	262	31	19	2	50	7	5	1	176
MK263_m3_11	4811	379	97554	8543	199155	16294	20351	1517	94866	7848	16721	1381	324	30	11775	1066	1047	78	2777	277	211	18	261	31	16	2	46	7	5	1	206
MK263_m3_12	2254	171	104025	9948	203931	21048	22039	2513	88644	6242	15332	1187	332	37	8137	817	590	45	1450	174	96	11	119	14	7	1	20	4	2	0	335
MK263_m3_13	3797	302	84668	9156	172948	22149	17169	1104	79612	6294	15642	1461	295	31	8910	843	872	68	2263	173	181	18	184	24	12	2	31	6	4	1	236
MK263_m3_14	2347	198	97992	8786	196900	15130	21017	1641	88510	6680	16093	1532	352	39	9016	939	632	64	1241	116	106	12	124	14	7	1	28	4	2	1	264
MK263_m3_15	4700	394	115108	11281	217008	22440	21676	1904	93877	9009	17326	1740	379	37	10896	974	903	96	2463	244	190	24	201	24	13	2	37	7	3	1	237
MK263_m3_16	3552	385	108928	13886	218820	15115	25828	2880	93756	8819	16041	1537	398	39	11033	1034	858	78	1951	167	154	15	185	27	11	2	28	6	3	1	316
MK263_m3_17	3299	268	103227	10206	220704	21485	24523	2690	97223	8979	16619	1526	359	38	9436	910	839	80	1964	196	140	13	157	14	10	2	30	6	3	1	255
MK263_m3_18	2865	270	101646	8268	222422	15057	20260	1732	89719	9031	16103	1256	325	34	8366	766	614	50	1487	118	115	10	141	10	8	2	21	5	2	1	321
MK263_m3_19	3058	281	100680	7874	229011	18137	22500	3119	92159	8291	16212	1762	317	30	8764	687	630	61	1574	169	137	13	148	15	9	2	28	5	3	1	257
MK263_m3_20	2924	215	107119	10471	233552	23188	24712	2798	97965	6518	14609	1279	315	29	9303	936	669	58	1581	181	127	14	144	13	8	1	25	5	3	1	299
MK263_m4_1	5684	495	83331	10083	191443	14479	22490	2087	93892	6097	18652	1956	411	39	13371	1036	1141	86	2763	264	256	22	272	28	19	3	65	7	6	1	166
MK263_m4_2	4995	470	96222	7101	233652	19782	22275	2349	96606	7775	20186	1591	354	41	12075	1252	1005	83	2597	235	215	15	231	20	17	2	57	8	6	1	171
MK263_m4_3	4851	437	98002	11949	231872	24920	24096	2613	95199	8925	18407	1948	359	31	11591	951	938	105	2394	206	205	23	237	23	18	3	59	10	6	1	159
MK263_m4_4	2520	236	97790	7136	210671	16622	25925	3652	91969	6696	15611	1369	282	31	8560	805	615	41	1500	137	106	11	123	14	8	1	24	4	3	1	283
MK263_m4_5	2799	303	105084	13685	216285	19795	20413	2173	86769	6209	14819	1479	288	26	8433	813	605	59	1404	139	109	10	135	17	7	1	21	4	2	1	320
MK263_m4_6	2443	204	97145	10664	212016	16628	22383	2542	84848	7145	15460	1575	288	28	8062	540	618	56	1420	125	119	11	129	13	8	1	22	5	3	1	300
MK263_m4_7	4786	482	105365	11907	226582	18679	24783	3048	95432	7672	15775	1428	336	34	10403	918	922	82	2252	182	201	16	217	24	16	2	46	7	5	1	181
MK263_m4_8	5523	482	91444	8673	210399	16752	23054	2633	90281	8513	18048	1483	366	41	12701	903	1030	125	2458	218	210	22	244	26	16	2	48	7	5	1	213
MK263_m4_9	4637	383	86297	6517	187453	20270	20440	1984	81669	7710	16043	1386	392	42	11222	780	882	58	2311	152	198	16	221	20	16	2	53	8	6	1	171
MK263_m4_10	4219	429	105536	10310	193144	15836	22083	2276	91786	8321	16759	1031	392	39	11031	918	960	82	2349	213	218	22	253	25	13	2	50	6	5	1	179
MK263_m4_11	5310	555	99067	10878	209426	20014	22680	2630	89653	7081	16611	1296	398	47	13464	1490	1056	81	2698	319	229	21	254	34	18	2	59	10	5	1	186
MK263_m4_12	4465	405	102735	14177	204668	23207	24629	2676	85489	7030	16696	1417	368	42	11458	1201	882	74	2221	199	182	15	209	25	14	2	43	5	4	1	214
MK263_m4_13	4008	314	95800	11807	206649	12842	23907	2829	90242	8159	15877	1456	398	37	10045	759	815	87	2076	199	162	17	195	26	14	2	40	8	7	2	203
MK263_m4_14	4126	395	93306	4728	202521	18340	21620	2239	87916	7842	16460	1820	342	43	11388	919	769	79	1971	174	183	19	200	20	14	2	39	7	5	1	234
MK263_m5_1	5755	580	72368	5312	142475	12165	15784	1151	65614	8013	10728	993	495	62	9294	746	900	90	2724	252	222	24	264	28	19	4	63	11	7	2	119
MK263_m5_2	5151	513	98463	8972	178077	16738	20999	1964	84247	6570	15037	1183	351	31	11672	1289	1081	98	2837	276	227	21	249	25	19	3	57	7	7	1	165
MK263_m5_3	6529	460	84400	8515	187685	15698	18504	2292	73947	6869	13467	1270	317	31	12430	1380	1190	126	3140	278	278	17	282	25	19	3	55	7	5	1	182
MK263_m5_4	1358	166	104464	11507	211789	23983	19903	1023	79284	6401	12871	1399	1804	166	7330	642	461	57	926	108	57	5	68	8	3	1	10	4	1	1	573
MK263_m5_5	2106	181	100338	8603	215220	26446	22586	2064	92514	8008	15409	1181	2092	193	8570	580	609	50	1236	135	92	8	102	11	5	1	17	4	2	1	418
MK263_m5_6	1351	123	101142	9430	217191	23098	20108	2217	77557	5257	12833	1237	2169	206	7839	701	463	46	834	70	56	5	71	10	3	1	10	2	1	0	650
MK263_m5_7	1380	131	109221	9491	230257	19171	21304	1889	78422	6500	13220	963	1969	174	7630	745	454	35	774	83	55	7	70	9	3	1	13	3	1	0	480
MK263_m5_8	3721	307	99572	10043	218327	18938	23101	2789	95936	6652	15580	1787	278	28	12065	809	962	115	1958	196	160	15	143	17	10	2	25	5	3	1	394
MK263_m5_9	2800	228	93902	10233	180464	14720	19218	2297	79527	7062	13127	1255	218	21	8787	621	787	76	1711	185	137	11	142	13	8	1	17	3	3	1	419
MK263_m5_10	1224	116	108442	8118	218329	20392	21523	2338	82811	6423	12303	991	2044	206	6723	627	461	39	766	65	51	5	57	7	3	1	8	3	1	1	679
~~MK263_m5_11~~	~~5602~~	~~572~~	~~99212~~	~~9836~~	~~190931~~	~~17072~~	~~20470~~	~~2251~~	~~79659~~	~~6016~~	~~13429~~	~~1265~~	~~2078~~	~~181~~	~~10197~~	~~938~~	~~778~~	~~76~~	~~2459~~	~~280~~	~~238~~	~~26~~	~~330~~	~~36~~	~~31~~	~~4~~	~~115~~	~~15~~	~~14~~	~~2~~	~~72~~
~~MK263_m5_12~~	~~2800~~	~~288~~	~~119242~~	~~10587~~	~~217073~~	~~19304~~	~~22431~~	~~2517~~	~~83381~~	~~7386~~	~~14352~~	~~919~~	~~1813~~	~~160~~	~~9594~~	~~805~~	~~683~~	~~71~~	~~1552~~	~~133~~	~~114~~	~~9~~	~~161~~	~~17~~	~~9~~	~~2~~	~~42~~	~~6~~	~~5~~	~~2~~	~~184~~
~~MK263_m5_13~~	~~1642~~	~~152~~	~~92116~~	~~9828~~	~~181826~~	~~19738~~	~~17827~~	~~1002~~	~~72870~~	~~7727~~	~~11435~~	~~1155~~	~~1064~~	~~120~~	~~5763~~	~~766~~	~~359~~	~~39~~	~~802~~	~~77~~	~~65~~	~~8~~	~~84~~	~~12~~	~~5~~	~~2~~	~~23~~	~~5~~	~~3~~	~~1~~	~~206~~
MK263_m6_1	3416	242	60449	5905	126877	12116	14190	1254	58087	5383	10096	1093	181	16	7946	582	704	61	1730	122	143	12	154	16	8	2	28	5	3	1	232
MK263_m6_2	4000	354	97762	8952	207775	19122	22776	2007	83508	6748	16186	1431	249	20	12527	1007	933	80	2109	206	157	14	173	20	10	1	29	6	4	1	348
MK263_m6_3	2255	216	109664	6731	213241	15831	22014	1989	83341	6432	14460	1344	367	31	9329	1119	572	42	1363	148	100	9	111	12	7	1	17	3	2	1	449
MK263_m6_4	2629	222	99912	10003	205598	16518	19618	1778	89509	7517	16013	1266	1272	175	11013	1011	766	59	1648	106	125	12	116	12	6	1	16	4	2	1	564
MK263_m6_5	3036	311	103293	10023	211519	21907	23690	2293	80870	7113	15760	1027	1083	178	10921	1316	818	83	1970	199	120	16	133	22	8	1	18	5	2	1	496
MK263_m6_6	4098	434	93134	9029	206115	23197	18500	1614	70950	4425	14188	1287	660	134	9649	1218	927	93	2125	254	172	16	186	20	13	2	39	6	4	1	201
MK263_m6_7	5189	656	104096	8102	205738	17520	19871	2140	79138	6561	15178	956	836	139	10972	1252	938	82	2541	214	217	28	230	33	14	3	42	8	4	1	210
MK263_m6_8	2575	250	112775	10507	221617	19578	20436	1815	84653	8561	14779	1340	669	173	8820	860	612	53	1335	152	107	17	113	17	6	1	22	5	2	1	331
MK263_m6_9	2785	211	107324	12492	213470	15889	22622	2766	82621	6134	15690	1175	973	160	9050	712	661	45	1641	191	112	11	118	13	6	1	20	4	2	1	358
MK263_m6_10	2671	257	107529	10751	219864	21656	21291	1801	84668	8208	15564	1315	1645	126	9710	851	758	63	1606	181	90	7	111	12	6	1	18	4	1	1	427
MK263_m6_11	2331	222	96199	7657	200286	17478	18293	1260	71209	5447	14476	1255	2027	191	9585	794	747	77	1419	120	85	6	95	11	4	1	17	5	1	1	467
MK263_m7_1	2013	216	104837	9372	216681	23453	22033	2863	78389	5306	15811	1336	2746	245	8757	616	685	76	1188	104	68	4	78	8	4	1	14	3	1	0	499
MK263_m7_2	569	92	50926	5328	99667	7576	10099	830	37163	2608	6859	674	974	137	3964	447	220	26	381	69	19	3	21	6	1	1	7	2	1	0	459
MK263_m7_3	1113	140	72210	8387	142936	16467	14791	1304	50589	4133	10542	1175	1580	162	5974	523	428	53	710	115	40	6	39	7	1	1	6	2	1	1	749
MK263_m7_4	646	64	36746	4469	82773	9474	7822	644	27615	2005	5435	482	864	80	3212	254	220	17	404	46	24	3	28	5	2	1	5	2	1	0	499
~~MK263_m8_1~~	~~114~~	~~27~~	~~2427~~	~~601~~	~~6242~~	~~1450~~	~~579~~	~~159~~	~~2365~~	~~560~~	~~440~~	~~121~~	~~12~~	~~3~~	~~258~~	~~50~~	~~22~~	~~5~~	~~54~~	~~16~~	~~5~~	~~1~~	~~6~~	~~2~~	~~1~~	~~0~~	~~4~~	~~1~~	~~1~~	~~0~~	~~59~~
MK263_m8_2	804	80	108867	11073	217126	18873	19017	2205	71381	6457	14285	1300	1368	142	5998	459	308	29	516	58	35	6	43	9	2	1	5	2	1	0	1048
MK263_m8_3	518	46	115480	12880	235301	26843	25619	3320	80305	5542	15425	1102	1802	151	7025	652	317	26	380	35	18	3	32	5	1	1	7	2	0	0	849
MK263_m8_4	1831	168	114428	11715	235332	19580	22140	2072	83093	5981	14700	1195	2878	339	8199	754	634	41	1118	115	62	6	64	8	3	1	14	3	1	0	484
MK263_m8_5	1881	157	124863	13655	208918	15776	24212	2901	86856	6518	16057	1617	2887	285	9304	857	672	46	1248	118	62	6	72	9	3	1	14	3	1	1	548
MK263_m8_6	1907	143	112638	10575	223791	20841	21937	2179	80718	5962	14465	1083	2764	247	9627	975	664	47	1352	118	73	7	71	7	3	1	12	3	1	0	666
MK263_m8_7	569	53	116530	12150	224238	20720	23874	2742	86325	6320	14991	1300	1730	166	6568	511	283	33	410	52	22	3	36	6	1	1	6	2	0	0	877
MK263_m8_8	476	64	115666	10018	247166	22682	24527	2289	83265	6061	14585	1210	1353	132	6058	482	257	27	323	40	19	2	32	6	2	1	4	2	1	0	1109
MK263_m8_9	2420	237	70216	6968	146611	17087	15145	981	53233	5168	12300	892	250	28	8636	596	690	58	1410	102	100	8	109	12	6	1	14	4	2	1	501
MK263_m8_10	2664	320	114378	12312	209840	17155	23628	1876	86874	5848	17287	1356	626	62	10365	1195	767	71	1617	207	97	10	101	12	5	1	14	3	1	1	578

Table B1. Petrochronological data for monazite grains.

Grain #	Y (ppm)	2SE	La (ppm)	2SE	Ce (ppm)	2SE	Pr (ppm)	2SE	Nd (ppm)	2SE	Sm (ppm)	2SE	Eu (ppm)	2SE	Gd (ppm)	2SE	Tb (ppm)	2SE	Dy (ppm)	2SE	Ho (ppm)	2SE	Er (ppm)	2SE	Tm (ppm)	2SE	Yb (ppm)	2SE	Lu (ppm)	2SE	Gd/Yb(N)
MK263_m8_11	1076	133	113565	11723	214939	17800	22633	2269	78176	5081	14366	1478	2082	182	7508	642	483	44	758	64	42	5	54	5	2	1	8	2	1	0	786
MK263_m8_12	1528	118	91639	6630	190857	14229	16673	1420	70006	6406	12695	1213	2158	202	7398	631	587	52	1028	83	56	5	52	6	3	1	11	3	1	0	536
MK263_m8_13	1770	189	107436	9593	228467	20562	22198	1944	74622	5658	15107	1581	2803	208	9598	803	657	61	1143	113	65	4	66	6	4	1	11	4	2	1	680
MK263_m8_14	409	36	113674	11612	227954	21723	25305	2943	78461	7765	14767	1335	1830	176	6408	653	285	30	292	24	15	2	30	4	0	0	5	2	0	0	1110
MK263_m8_15	528	174	38059	8562	83115	16158	7409	1284	30549	6278	5184	1132	342	49	2802	630	164	47	290	84	25	8	24	8	1	0	4	2	1	0	568
MK263_m9_1	1249	127	111434	11642	212404	21552	22330	2293	77618	7989	13423	1187	2487	245	7593	722	453	36	847	77	57	6	60	7	3	1	10	4	1	0	590
MK263_m9_2	955	111	110692	9082	213188	20853	18871	1656	79554	8566	13991	1177	2279	229	6829	615	384	35	608	65	41	4	60	7	2	0	8	3	1	1	652
MK263_m9_3	1067	98	110694	11305	225520	23068	22951	2300	79051	5552	13806	1070	2158	213	6933	336	425	42	713	59	46	5	52	6	2	1	8	3	0	0	670
MK263_m9_4	975	82	104510	10053	208924	19033	23963	2607	89333	10266	13646	1538	1814	177	6748	631	372	40	657	63	34	4	47	6	2	1	7	2	1	0	786
MK263_m9_5	645	70	78030	8142	167078	16082	14963	1088	58076	5843	9663	737	1126	117	4864	420	219	17	395	37	28	4	36	6	2	0	9	3	1	0	432
MK263_m9_8	921	87	115198	12673	215600	17762	21930	2179	75721	5764	14430	1253	1972	157	6657	629	387	30	598	49	38	4	50	8	2	1	11	3	1	0	503
MK263_m9_9	936	89	104430	6210	228443	20629	23760	2743	73137	4751	13365	1136	2291	235	6709	870	372	39	610	67	42	5	50	6	2	1	9	3	2	1	598
MK263_m9_10	1055	87	111259	8300	225504	23051	21482	2338	75072	6032	13817	1287	1702	155	7433	501	426	44	749	73	51	7	50	8	3	1	12	3	1	0	510
MK263_m9_11	1113	110	97990	7819	186978	19916	17147	1529	69847	6120	12345	1130	1278	129	6157	541	346	33	653	57	43	5	55	8	3	1	8	2	1	0	602
MK263_m10_1	6008	608	107441	8941	237652	23431	26975	2578	100560	6542	20204	2067	380	33	15026	1330	1083	106	2584	226	245	21	253	23	16	3	45	6	5	1	270
MK263_m10_2	5036	360	96364	7530	189612	24038	24165	2390	79289	6574	16709	1436	369	32	12513	1103	1086	90	2410	237	221	21	247	26	14	2	46	8	6	1	222
MK263_m10_3	4988	342	111194	11917	245592	24957	24334	2747	97813	7121	18259	1125	372	37	12931	850	973	83	2307	191	229	23	203	21	14	2	36	5	5	1	287
MK263_m10_4	4044	347	105655	10268	232862	23938	26213	2412	100135	10490	17363	1570	328	31	12774	1317	836	75	1860	174	181	18	182	22	11	2	24	5	4	1	424
MK263_m10_5	1181	315	19119	4802	44974	11230	5033	1211	18867	4293	3610	994	84	19	2629	729	189	49	494	133	43	12	43	13	3	1	8	3	1	1	268
MK263_m10_6	3824	374	82974	10927	184097	19035	18387	1944	67022	5630	14069	1389	368	36	8894	773	708	69	1731	199	157	14	156	19	12	2	30	7	3	1	244
MK263_m10_7	796	65	120581	12418	248591	21937	23449	1992	82894	5976	12567	1495	901	74	5515	389	279	25	415	20	28	3	40	7	1	0	3	2	1	0	1298
MK263_m10_8	1253	149	116211	9911	242180	17728	28675	3676	95956	6477	13549	1137	752	77	6448	630	313	32	584	56	48	6	65	8	3	1	6	2	1	0	901
MK263_m10_9	3096	285	111162	12509	247984	23220	28839	2862	95335	7456	18913	1438	297	28	9685	948	793	97	1688	131	130	14	149	13	8	1	25	5	3	1	315
MK263_m10_10	5852	628	104216	8051	250975	28433	25525	2174	102234	9488	18727	1959	386	23	13578	977	1066	93	2534	230	235	28	235	27	14	3	46	7	5	1	241
MK263_m10_11	2829	263	113143	12660	232659	21738	24850	2307	88538	6124	16164	1660	394	22	9153	1053	648	72	1310	120	104	12	132	15	6	1	19	4	4	1	393
MK263_m10_12	5301	477	83260	9423	209488	18798	21269	2839	85734	7446	16926	1471	395	43	11653	1034	970	78	2398	178	226	20	265	23	18	2	44	7	6	1	214
MK263_m10_13	5511	575	99651	10104	208195	16514	26186	2610	91413	8182	18437	1999	376	28	13412	1270	1109	165	2503	220	197	20	238	21	15	2	40	6	5	1	270
MK263_m10_14	5544	311	101166	9584	233705	28624	25617	3148	98334	10917	20079	1489	419	50	12666	1083	1140	124	2362	199	214	22	212	14	15	2	37	6	5	1	280
MK263_m10_15	2230	270	112363	8771	252111	21393	25362	2424	101671	7632	15202	1472	588	76	7906	713	550	45	1071	109	83	12	106	11	6	1	16	4	1	1	396
MK263_m10_16	1625	212	115451	10640	236070	18910	26585	2439	98247	9804	15521	1434	718	90	7262	502	422	33	802	91	59	6	77	10	3	1	10	3	1	1	586
MK263_m10_17	1288	139	120137	11666	256445	21834	26674	2984	93844	7594	14456	1419	770	109	6615	606	394	23	714	61	52	5	62	8	3	1	8	2	0	0	652
MK263_m10_18	2212	170	113534	11582	209902	12047	26263	2202	87599	7392	17412	1473	419	47	7919	746	566	54	1038	109	78	6	100	12	6	1	16	4	2	1	410
MK263_m10_19	4153	495	114174	8054	251639	23569	23509	2475	94077	8694	18722	1552	378	33	12559	764	910	76	1980	177	170	17	181	21	10	2	32	5	3	1	317
MK263_m10_20	4167	552	108339	10639	230784	25798	25618	2827	98247	8935	17281	1577	352	43	12216	923	969	81	2067	171	171	19	204	18	12	2	34	5	4	1	294
MK263_m10_21	4198	401	103297	7992	236700	18078	26202	2942	93869	9379	18026	1829	375	50	11861	1216	1027	78	2121	189	174	15	209	25	13	2	36	5	4	1	270
MK263_m10_22	2546	187	101376	8721	237305	22332	26470	2636	91400	4881	17019	1471	333	22	9540	742	740	69	1441	155	107	10	123	14	7	1	22	4	1	1	356
MK266																															
~~MK266_m1_1~~	~~7163~~	~~985~~	~~82887~~	~~11155~~	~~167813~~	~~20009~~	~~20179~~	~~2493~~	~~73791~~	~~8072~~	~~12110~~	~~1325~~	~~1878~~	~~208~~	~~8487~~	~~995~~	~~887~~	~~101~~	~~2591~~	~~325~~	~~319~~	~~44~~	~~476~~	~~60~~	~~36~~	~~6~~	~~98~~	~~12~~	~~8~~	~~1~~	~~70~~
~~MK266_m1_2~~	~~10021~~	~~727~~	~~109898~~	~~10553~~	~~243068~~	~~21055~~	~~27371~~	~~2280~~	~~97779~~	~~9509~~	~~17969~~	~~1987~~	~~1957~~	~~128~~	~~11663~~	~~914~~	~~1312~~	~~97~~	~~3781~~	~~274~~	~~463~~	~~36~~	~~663~~	~~44~~	~~60~~	~~6~~	~~185~~	~~21~~	~~19~~	~~3~~	~~51~~
~~MK266_m1_3~~	~~9659~~	~~591~~	~~127942~~	~~10643~~	~~223663~~	~~14081~~	~~25319~~	~~1937~~	~~92625~~	~~7462~~	~~17813~~	~~1806~~	~~2028~~	~~226~~	~~12095~~	~~1082~~	~~1192~~	~~107~~	~~3856~~	~~302~~	~~467~~	~~49~~	~~683~~	~~61~~	~~57~~	~~5~~	~~165~~	~~17~~	~~15~~	~~2~~	~~59~~
~~MK266_m1_4~~	~~8724~~	~~864~~	~~99171~~	~~9602~~	~~234951~~	~~25915~~	~~26398~~	~~3274~~	~~81693~~	~~6974~~	~~16839~~	~~1803~~	~~2518~~	~~229~~	~~10897~~	~~1191~~	~~1207~~	~~131~~	~~3546~~	~~347~~	~~443~~	~~47~~	~~584~~	~~61~~	~~55~~	~~8~~	~~142~~	~~11~~	~~14~~	~~3~~	~~62~~
~~MK266_m3_1~~	~~8477~~	~~811~~	~~103120~~	~~8342~~	~~235829~~	~~24060~~	~~24407~~	~~2330~~	~~81104~~	~~6868~~	~~15360~~	~~1450~~	~~2143~~	~~196~~	~~10873~~	~~832~~	~~1167~~	~~97~~	~~3497~~	~~304~~	~~390~~	~~29~~	~~564~~	~~40~~	~~43~~	~~4~~	~~110~~	~~13~~	~~10~~	~~2~~	~~80~~
MK266_m4_1	251	36	36750	4462	84512	10399	9835	1085	29720	3571	4682	575	403	51	2057	236	93	10	145	18	9	1	17	4	1	0	3	1	1	0	650
MK266_m4_2	445	47	60552	4847	117629	12878	15008	1487	46058	4429	6845	731	707	61	3267	342	150	17	271	30	17	3	26	5	1	1	4	1	0	0	705
MK266_m6_1	7349	652	120764	11620	235401	24150	26573	2407	94506	6872	18202	1466	633	47	12190	1272	1177	96	3171	193	316	26	498	49	38	5	127	15	16	2	78
MK266_m6_2	7793	694	106039	10978	236775	17976	27994	2124	93704	6897	18411	1675	638	52	11355	1106	1133	82	3166	233	333	21	471	37	40	4	115	13	15	2	80
MK266_m6_3	4527	398	96912	8951	217677	16231	26182	1910	92688	8248	17260	1511	465	43	9771	703	887	78	2189	206	173	19	241	24	16	2	59	7	8	1	133
MK266_m6_4	4344	432	111142	9643	263236	19995	29407	3030	101115	6115	19492	1441	751	56	10882	895	840	79	1997	163	178	17	237	24	17	2	45	6	7	1	196
MK266_m6_5	202	14	118017	8518	256648	19759	27713	1821	97536	6195	15319	1239	1656	137	5023	435	175	13	162	15	8	1	34	5	1	0	3	1	0	0	1404
MK266_m6_6	224	21	116555	8611	249675	20138	29269	2092	92615	5799	15582	1403	1699	139	5456	341	188	14	177	16	9	1	31	4	1	0	3	1	0	0	1473
MK266_m6_7	443	54	118342	9485	251620	17297	28535	2037	93994	7374	16237	1298	1591	116	5940	462	248	18	300	25	18	2	42	6	2	0	7	2	1	0	675
MK266_m6_8	6645	325	109268	9322	241144	16534	26545	2079	97097	6507	18898	1550	622	48	12823	987	1198	92	2956	300	259	21	380	31	28	3	80	8	12	2	130
MK266_m6_9	5613	423	101066	7061	233846	14458	28884	2068	98970	6459	18898	1252	658	49	11414	853	911	91	2502	225	233	17	365	36	24	2	80	8	11	1	116
MK266_m6_10	4136	384	106389	10257	236336	23779	29204	2615	95351	9078	19418	1672	629	56	10726	905	837	71	1719	131	155	19	200	23	13	2	48	8	6	1	180
MK266_m6_11	4300	506	105890	9438	233183	16931	28883	2051	93008	5026	19926	1544	473	41	12608	1069	917	84	2161	162	162	14	203	21	14	2	40	6	5	1	254
MK266_m6_12	6021	519	111592	9726	236980	17794	28869	1841	95956	7736	17356	1226	750	72	11178	920	1037	85	2620	216	231	18	350	30	29	4	85	12	11	2	107
MK266_m6_13	2568	229	120836	11697	241950	20091	29146	2349	103445	7862	17778	1501	1084	98	8666	879	564	58	1260	124	102	12	158	20	9	1	32	5	3	1	222
MK266_m7_1	2750	207	93531	7078	229292	18473	28716	2640	101958	6464	20539	1546	178	13	11726	953	797	51	1720	122	99	8	121	14	6	1	18	4	2	1	515
MK266_m7_2	2744	215	104003	6548	222010	18707	28864	2896	99546	6764	22217	1868	399	23	12479	969	1055	86	1668	113	106	8	120	11	5	1	13	3	2	1	759
MK266_m7_3	2836	262	99334	9662	230168	24729	25032	2060	97974	8590	20809	1624	359	28	12338	1077	993	83	1688	149	110	10	113	11	5	1	16	3	2	1	612
MK266_m7_4	2845	271	100022	8717	222508	16556	27031	1930	91532	5996	20009	1542	414	41	11931	1071	839	76	1715	191	103	6	110	10	5	1	15	3	2	1	624
MK266_m7_5	2258	257	107555	6480	223996	19029	25504	2597	86902	4829	15119	1193	1223	90	7300	561	510	39	1115	124	88	10	131	15	8	2	24	4	2	1	243
MK266_m7_6	527	45	113200	10491	254778	18616	24157	1873	88922	6121	14348	998	1907	172	6020	515	269	24	368	36	24	3	44	6	2	0	7	2	1	0	730
MK266_m7_7	560	68	117758	7729	222094	20847	26338	1678	82880	6360	13000	1160	1802	186	5689	416	283	24	402	39	23	3	44	5	1	0	4	1	0	0	1201
MK266_m7_8	2253	194	97064	8644	213412	16857	25723	2097	94788	5924	18596	1272	225	19	11906	1062	749	65	1404	101	84	8	99	11	5	1	14	3	2	0	687
MK266_m7_9	337	35	125918	9891	251742	26735	26415	1708	90147	7706	13938	926	1836	166	5798	420	230	22	278	22	17	2	32	4	1	0	5	2	0	0	971
MK266_m7_10	1827	168	102598	9629	234124	20798	25693	2360	95617	7261	17566	1430	605	84	10075	862	656	50	1194	96	76	8	86	8	3	1	11	3	1	0	763
MK266_m7_11	2147	222	105149	8037	232208	19179	27468	2349	98609	5590	18506	1192	227	23	11351	925	831	68	1314	86	89	8	98	11	4	1	12	3	2	0	760

Table B1. Petrochronological data for monazite grains.

Grain #	Y (ppm)	2SE	La (ppm)	2SE	Ce (ppm)	2SE	Pr (ppm)	2SE	Nd (ppm)	2SE	Sm (ppm)	2SE	Eu (ppm)	2SE	Gd (ppm)	2SE	Tb (ppm)	2SE	Dy (ppm)	2SE	Ho (ppm)	2SE	Er (ppm)	2SE	Tm (ppm)	2SE	Yb (ppm)	2SE	Lu (ppm)	2SE	Gd/Yb(N)
MK266_m7_12	362	25	119341	9917	243177	20824	26954	2106	94190	9267	14723	984	1756	114	6230	498	251	20	277	15	15	2	32	5	1	1	3	1	0	0	1452
MK266_m7_13	564	46	111663	10126	224812	21818	29259	1864	91049	6506	16398	1122	1200	87	6605	558	284	26	397	28	23	3	43	5	2	1	4	2	1	0	1397
MK266_m7_14	1725	145	112066	9243	224863	19866	26867	2027	89218	6355	17057	1186	669	68	9776	838	635	46	1003	105	59	6	78	8	3	1	10	2	1	1	779
MK266_m7_15	2572	256	93886	7554	215013	20871	27569	1738	91072	6603	21188	1799	178	14	12205	1078	866	88	1441	133	104	10	113	16	5	1	20	4	3	1	501
MK266_m8_1	3831	319	101883	11073	197047	16638	23835	1797	88810	7770	17959	1423	375	39	11965	1138	961	80	2112	234	150	14	175	15	12	2	36	6	3	1	268
MK266_m8_2	2851	425	99937	9163	220532	15598	25276	2164	85892	6775	17271	1400	519	88	10583	978	755	111	1423	175	112	15	123	13	6	1	18	4	2	1	477
MK266_m8_3	2196	239	96216	10853	210268	18274	22247	1909	80402	5188	16146	1400	495	50	9577	751	608	46	1161	139	89	9	112	15	6	1	15	3	2	1	517
MK266_m8_4	3036	290	97332	5704	213271	19722	24546	2003	82632	5845	18204	1843	310	25	11918	799	918	76	1717	154	118	12	138	12	6	1	15	3	2	1	651
MK266_m8_5	357	23	103404	8510	224175	21167	24345	2071	80317	6694	14045	872	1188	81	5968	543	227	16	288	31	16	2	34	6	1	0	4	1	1	0	1377
MK266_m8_6	574	61	100915	7328	224069	15605	24004	2552	81292	6052	14238	1237	1170	101	6465	481	274	17	408	37	25	3	44	5	1	0	5	2	0	0	1154
MK266_m8_7	5253	789	107559	8590	208969	19825	24653	1981	84485	5338	17836	1146	698	71	11035	1105	895	107	2383	282	209	33	278	45	22	5	54	11	6	1	165
MK266_m8_8	1322	264	100370	8029	212116	18518	22703	1622	81896	5897	14423	1276	1013	98	6576	451	426	58	727	132	51	11	76	13	3	1	9	2	1	1	566
MK266_m8_9	1607	192	106003	8664	210487	17218	24888	2153	85425	6912	14102	1107	834	93	8765	881	532	65	909	94	60	6	75	9	3	1	9	2	1	0	771
MK266_m8_10	1272	137	98688	9366	199059	17814	24896	1985	81803	6358	14158	1265	952	100	7695	753	428	49	606	77	46	6	55	7	3	1	6	2	1	1	1079
MK266_m8_11	344	33	92407	7102	223441	18481	23351	1917	81798	7571	14074	1309	1167	102	5487	440	238	20	259	28	15	2	34	5	1	0	4	2	1	0	1068
MK266_m8_12	4231	362	78083	8167	172043	14183	21365	1631	72930	5671	15779	1416	290	28	11443	1262	844	86	1965	180	151	12	181	18	11	1	35	4	4	1	263
MK266_m8_13	4620	477	83436	8398	197891	14725	23427	2243	81323	5478	17314	1528	342	28	11290	907	956	62	2197	177	178	15	207	20	13	2	39	6	4	1	233
MK266_m8_14	2054	170	101866	9138	206619	19216	24750	1869	81604	4266	15077	1149	699	77	8569	689	623	49	1116	99	73	7	98	11	4	1	12	3	1	0	575
MK266_m8_15	331	29	108554	7674	219927	19479	24170	1798	84275	6088	13189	942	1253	130	5661	514	241	20	262	21	13	2	28	4	1	0	3	1	0	0	1451
MK266_m8_16	335	37	103621	6814	209107	18189	23416	1898	82677	5316	12409	949	1122	75	5818	445	213	17	264	22	15	2	32	3	1	0	3	1	0	0	1539
MK266_m8_17	353	29	99627	9840	209477	19323	21476	1730	72722	4389	13078	1076	1104	91	4860	340	211	24	274	20	15	2	30	5	1	0	3	1	0	0	1204
MK266_m8_18	2863	274	92641	8268	183777	15130	23700	2165	80290	7723	16142	1095	331	31	10563	990	793	69	1582	152	114	12	137	15	7	1	19	4	2	1	452
MK266_m8_19	1482	177	92076	5381	200461	19133	24203	2320	81595	5914	14420	1417	740	74	7831	765	436	57	831	87	61	10	78	10	4	1	9	3	1	0	704
MK266_m9_1	453	39	105311	9250	237640	18288	26279	1811	88899	6291	14895	1424	1464	122	7006	543	265	28	337	32	20	3	39	5	1	0	4	1	0	0	1575
MK266_m9_2	448	38	113360	10210	211398	16736	27060	2592	90106	6276	15099	1173	1496	98	6943	690	235	18	341	36	20	2	42	5	1	0	3	1	0	0	1706
MK266_m9_3	580	45	115571	6619	227562	21858	25590	1758	89631	6173	16268	1548	1527	120	7852	576	329	27	437	35	27	3	41	6	2	1	4	2	0	0	1434
MK266_m9_4	1262	92	106599	9325	219218	17993	27757	2907	85772	6767	14661	1392	1336	142	8098	685	459	39	883	101	56	6	78	11	3	1	10	3	1	0	635
MK266_m9_5	3104	282	103783	10122	212472	15396	26184	2064	89742	7055	16337	1274	455	47	10539	874	789	58	1746	123	129	12	163	13	9	1	22	4	3	1	384
MK266_m9_6	2535	275	95645	8718	199976	18657	24692	2251	83679	6496	15865	1158	372	44	10091	758	717	69	1389	110	100	9	125	14	6	1	18	3	2	1	460
MK266_m9_7	1977	185	107139	9372	231685	21728	26796	2095	90351	8621	14645	986	677	65	9809	710	581	57	1165	100	74	7	104	14	5	1	16	3	2	1	501
MK266_m9_8	511	36	118436	12507	229591	23241	26027	2936	87896	6100	15556	1214	1599	124	6973	606	308	24	398	38	24	2	44	6	1	0	4	2	1	0	1342
MK266_m9_9	417	31	116346	10528	234558	20004	25825	2272	91097	4355	14606	1422	1588	184	6695	524	245	22	365	36	19	1	41	6	1	0	4	1	1	0	1492
MK266_m9_10	509	43	120495	13882	234695	21230	25868	2340	87265	6128	14697	1333	1412	122	6087	520	253	23	358	33	20	2	42	4	1	0	4	2	1	0	1317
MK266_m9_11	1769	138	94132	7829	214551	16586	23178	1936	89424	7873	15699	1171	358	36	9637	655	578	38	1055	67	62	7	86	8	3	1	13	3	1	0	612
MK266_m9_12	932	115	112005	11666	219947	17222	26880	2333	89007	7317	16172	1523	1438	120	7525	686	385	32	628	59	37	5	54	7	2	1	9	3	1	1	685
MK266_m9_13	531	50	104264	6424	215402	22449	24648	1954	90284	5819	14466	986	1517	133	7249	473	310	34	408	37	24	2	37	6	1	0	6	2	0	0	904
MK266_m9_14	557	49	114905	9236	241706	26138	25857	2339	91874	7848	13780	1129	1549	90	6363	586	295	20	389	36	24	4	44	5	1	0	4	1	1	0	1350
MK266_m9_15	585	51	116640	11179	231331	21453	25953	1988	86759	6332	16846	1515	1606	152	7073	511	340	34	497	40	28	3	41	5	1	0	5	2	0	0	1152
MK266_m9_16	697	60	106211	10352	223467	18463	26918	2599	88796	6237	16008	1421	1630	136	7408	760	362	36	504	34	28	3	42	5	1	0	5	2	1	0	1165
MK266_m9_17	651	60	110743	6407	222955	17268	28068	2261	86830	5387	17297	1185	1750	145	7380	731	327	29	466	39	25	3	46	6	1	0	5	2	0	0	1262
MK266_m10_1	1470	151	124711	10570	255954	25764	27906	2682	98925	7140	16883	1735	1484	141	7668	648	373	38	688	66	55	8	88	11	4	1	14	3	1	0	457
MK266_m10_2	448	34	115570	9745	239640	22802	28624	2502	102512	7954	15453	1389	1609	158	6472	637	224	24	363	26	20	3	36	5	1	0	5	1	0	0	994
MK266_m10_3	809	69	125922	13740	258967	22876	30467	2303	101964	7319	17982	1489	1302	118	7524	671	328	32	616	78	32	3	55	8	3	1	7	2	1	0	875
MK266_m10_4	443	34	125326	9234	240453	18394	30201	2801	96323	7071	15765	1255	1569	178	6087	507	224	19	309	37	20	2	40	4	1	0	4	2	0	0	1372
MK266_m10_5	370	30	123248	11353	263070	22996	29150	1656	96671	5900	15764	1499	1671	139	6112	528	199	21	292	24	16	2	35	5	1	0	4	2	1	0	1170
MK266_m10_6	1778	181	122446	12266	225449	18407	29042	2494	100765	10690	16340	1154	1022	99	7906	689	471	47	911	105	63	7	83	9	3	1	15	4	1	0	431
MK266_m10_7	899	170	130030	14063	245798	16295	25017	1635	89613	6550	14373	1069	1431	139	6405	596	267	23	453	57	29	4	55	9	3	1	7	2	1	1	735
MK266_m10_8	1894	199	110135	8126	241184	18621	28428	2299	99056	6560	18688	1310	254	19	10978	958	673	54	1083	105	71	6	84	9	4	1	9	2	1	0	995
MK266_m10_9	1716	211	110032	8745	232495	22100	27734	2671	95253	7704	17292	1147	802	71	9848	860	530	40	927	89	58	7	77	10	4	1	8	2	1	1	938
MK266_m10_10	555	36	121133	12623	257234	21545	27714	2631	107025	8022	15325	1455	1497	104	6871	550	225	21	345	36	23	3	44	6	1	0	5	2	1	0	1138
MK266_m11_1	746	71	124641	12155	246135	22604	29008	3080	96641	8279	17319	952	1455	161	8400	701	360	35	469	46	26	3	45	5	2	0	6	2	1	0	1202
MK266_m11_2	700	64	110699	10069	234136	19794	25654	2438	107322	10102	16698	1346	1351	125	7911	618	346	35	475	47	25	2	45	7	1	0	5	2	1	0	1221
MK266_m11_3	3568	287	122748	10537	248422	20644	29498	3374	103429	7300	17903	1815	579	67	11285	898	827	73	1788	169	132	13	165	15	9	1	27	4	3	1	336
MK266_m11_4	3083	264	101921	9373	238961	18418	28276	2819	106168	9419	21658	2397	431	40	11951	1081	1012	82	1757	163	115	11	105	12	5	1	18	5	2	1	541
MK266_m11_5	3080	296	121619	11032	254386	21727	27997	2259	114083	11107	21717	1763	456	37	13961	1007	931	98	1804	171	123	12	126	14	6	1	17	4	1	1	655
MK266_m11_6	1460	193	113335	9887	257566	22263	28321	2815	107790	9444	20968	2348	1018	102	9760	853	563	55	887	113	54	4	72	10	3	1	10	3	1	0	784
MK266_m11_7	312	35	126934	10594	259084	26505	30014	2540	99748	8192	15750	1253	1660	161	6527	631	242	19	250	25	12	1	34	5	0	0	2	1	0	0	2151
MK266_m11_8	594	66	119352	11052	231543	18135	27022	3022	98572	6879	17401	1459	1364	124	8083	702	343	34	468	44	25	4	43	4	1	0	6	2	0	0	1171
MK266_m11_9	426	49	125637	13906	237390	22155	27779	2270	104575	8223	18596	1357	1550	168	7787	503	283	27	326	27	17	3	40	5	1	1	4	2	1	0	1628
MK266_m11_10	344	33	118553	10223	267094	29295	28262	2883	101527	9314	17473	1836	1643	152	6689	593	268	24	277	32	14	2	41	6	1	0	4	1	0	0	1492
MK266_m11_11	256	25	132204	16814	248299	25482	26162	2009	98317	6854	16316	1157	2064	226	6771	669	214	21	242	20	11	1	31	4	1	0	3	1	0	0	1641
MK266_m11_12	369	39	123471	12274	274284	30742	29357	2378	97239	5098	17609	1645	2716	246	6884	571	300	29	327	31	16	2	30	4	1	0	4	2	1	0	1476
MK266_m11_13	309	24	129646	12954	267699	27438	29690	2981	100803	8883	15778	1565	2543	264	7263	590	265	23	334	36	14	2	30	5	1	0	4	1	0	0	1454
MK266_m11_14	302	35	129049	13476	252496	21506	27177	2904	93448	7205	16614	1859	2455	158	6523	515	234	21	288	33	13	2	29	4	1	0	3	1	0	0	1510
MK266_m11_15	504	49	124742	11265	274852	26342	28480	1983	106311	8459	18695	1984	2870	262	7792	491	371	36	443	38	22	2	35	4	1	0	4	1	1	0	1580
MK266_m11_16	467	46	115669	10366	246950	15833	29631	2760	106285	12400	17762	1642	2647	196	8558	766	374	43	455	52	25	4	41	6	1	0	5	2	0	0	1482
MK266_m11_17	460	43	122797	10308	262775	19409	30802	2580	99379	5699	16332	1149	2545	221	7848	728	339	27	422	49	19	2	42	5	1	0	4	1	0	0	1497
MK266_m11_18	453	45	127038	12228	241834	15814	28977	2079	94264	6165	16201	1265	2564	221	6889	511	316	32	379	39	18	2	38	5	1	0	4	1	1	0	1368
MK266_m11_19	444	44	120345	8396	278199	26262	30493	2127	94982	7452	17296	1443	2630	236	7572	786	305	24	365	30	18	1	34	6	1	0	3	1	0	0	2163

Table B1. Petrochronological data for monazite grains.

Grain #	Y (ppm)	2SE	La (ppm)	2SE	Ce (ppm)	2SE	Pr (ppm)	2SE	Nd (ppm)	2SE	Sm (ppm)	2SE	Eu (ppm)	2SE	Gd (ppm)	2SE	Tb (ppm)	2SE	Dy (ppm)	2SE	Ho (ppm)	2SE	Er (ppm)	2SE	Tm (ppm)	2SE	Yb (ppm)	2SE	Lu (ppm)	2SE	Gd/Yb(N)
MK266_m11_20	527	57	129885	12828	259443	32117	29072	2706	101230	9411	16686	1424	2683	227	7660	695	306	26	396	52	21	3	33	4	1	0	6	2	1	0	1034
MK266_m11_21	512	46	120358	12663	224360	18271	29380	2711	98125	7288	17545	1645	2358	161	7914	703	354	31	458	40	23	3	35	7	1	0	4	2	1	0	1630
MK266_m11_22	659	58	123103	11315	260623	25935	29723	2785	102921	9609	18883	2021	2565	214	8698	846	398	42	530	53	29	3	38	4	1	0	5	2	0	0	1371
MK266_m11_23	676	58	114990	10699	255917	20194	31671	2647	108542	11652	20213	1998	2693	240	8341	574	382	36	533	50	29	3	41	6	1	0	5	2	0	0	1313
MK266_m11_24	561	59	131622	13027	241892	19497	29672	2400	98129	10454	16581	1300	2580	206	7788	568	371	37	459	42	24	3	42	6	1	0	4	2	1	0	1440
MK266_m11_25	631	55	113288	10148	253357	26451	29502	2685	99423	6728	19600	1887	2632	232	8303	595	411	29	546	52	30	4	40	6	1	0	6	2	0	0	1180
MK266_m11_26	684	74	116236	11165	265792	29866	29455	2998	100040	4930	18216	1559	2550	228	8729	756	392	39	556	59	27	3	40	6	1	0	5	1	1	0	1568
MK266_m11_27	477	33	119551	10178	232865	18811	28319	2688	96479	9270	16791	1189	2325	194	7289	703	306	27	395	36	17	2	32	4	1	0	5	2	1	0	1246
MK266_m11_28	455	29	137855	13737	259271	21363	29141	1808	93688	8755	17664	1190	2320	197	7491	549	329	29	415	37	17	2	33	5	1	0	3	1	0	0	2118
MK266_m11_29	531	44	128489	6876	257968	22936	28018	2298	104698	10225	17459	1876	2332	181	7031	671	345	32	402	40	19	2	38	5	1	0	4	1	0	0	1342
MK266_m11_30	429	45	125946	10118	244803	27472	30517	2710	101914	8390	17712	1474	2439	190	6897	678	312	33	381	32	17	2	35	5	0	0	4	1	0	0	1514
MK266_m11_31	403	30	120904	8828	241889	19777	28373	2847	108887	11547	16987	1811	2464	253	7857	720	322	31	357	31	20	3	31	5	1	0	4	1	1	0	1646
MK266_m11_32	403	35	123332	10387	224899	24064	28395	2791	102712	8535	18974	1767	2315	162	7888	675	316	32	386	39	18	3	33	4	0	0	4	2	1	0	1562
MK266_m11_33	496	40	119766	9745	248030	23402	26180	2356	105926	8125	17932	1385	2317	223	7516	735	329	31	454	37	20	2	35	4	1	0	4	2	0	0	1461
MK266_m11_34	467	35	134451	10918	260652	20354	31425	3258	99550	7794	18087	1488	2354	220	7952	657	339	38	446	39	18	3	36	6	1	1	4	2	0	0	1530
MK266_m11_35	561	43	118579	7322	248257	17849	29134	2250	102896	6153	17538	1301	2623	190	8170	626	378	29	495	45	23	2	40	4	1	0	6	2	0	0	1047
MK268																															
MK268_m1_1	640	64	36843	5041	87535	7314	9098	898	35618	3473	4756	471	149	18	2779	266	189	15	386	37	30	3	36	5	2	1	11	2	2	1	196
MK268_m1_3	819	143	54098	8065	106373	14755	11928	1729	42860	6233	7188	1170	199	28	3399	445	226	29	476	75	35	6	47	9	2	1	9	3	1	0	305
MK268_m1_4	1587	134	115213	9505	255313	25928	25804	1872	99830	9284	14170	1168	689	78	7794	632	474	40	894	106	67	6	86	11	4	1	12	3	1	0	539
MK268_m1_5	1480	123	108709	10802	244057	24575	26626	2001	93521	8115	14907	1314	461	49	7935	701	498	58	996	82	75	6	74	8	5	1	11	2	1	1	607
MK268_m1_7	2566	236	71265	6751	158995	14439	16716	1127	64069	5198	13663	920	330	26	9177	626	763	60	1515	104	117	11	113	10	8	2	24	4	2	1	305
MK268_m1_8	2554	232	103116	9668	204973	13084	23549	2024	95693	6151	16729	1470	426	44	10035	1104	735	63	1441	142	108	14	116	12	7	1	21	4	2	1	391
MK268_m1_9	4878	369	97586	10259	212032	17258	24956	2057	94565	7255	21307	2155	406	44	15382	1728	1201	94	2588	206	192	22	202	20	13	2	41	5	4	1	306
MK268_m2_1	544	89	14384	2011	37011	5699	4524	627	15664	2481	3430	545	73	12	2228	399	167	28	334	54	23	4	22	5	2	0	6	2	1	0	292
MK268_m2_2	3490	325	93294	6858	206058	19992	26622	2546	96281	7152	19757	1527	431	41	13503	1336	1149	106	2134	162	151	15	156	13	10	1	31	5	3	1	349
MK268_m2_3	718	95	20165	2752	47693	7112	5714	865	21996	3052	4548	580	92	13	2758	339	214	34	412	68	32	4	31	6	3	1	7	2	1	1	301
MK268_m2_4	3903	388	73576	6346	171195	16066	20791	1876	76282	5556	17650	1413	277	23	12191	928	995	78	2037	154	163	13	161	16	10	1	34	5	2	1	286
~~MK268_m2_6~~	~~358~~	~~84~~	~~9119~~	~~1893~~	~~22572~~	~~4252~~	~~2972~~	~~697~~	~~11233~~	~~2419~~	~~2012~~	~~377~~	~~56~~	~~13~~	~~1353~~	~~219~~	~~100~~	~~24~~	~~207~~	~~42~~	~~16~~	~~4~~	~~17~~	~~4~~	~~1~~	~~0~~	~~5~~	~~2~~	~~0~~	~~0~~	~~216~~
MK268_m3_1	1093	84	121782	13350	246044	18486	26373	2315	105382	10987	17014	1018	1223	119	8301	780	474	38	739	73	45	4	68	8	3	1	15	4	1	0	451
MK268_m3_2	1149	96	118593	10583	254194	24819	26830	2963	103163	7390	19006	1760	1349	109	8873	1016	466	37	703	57	49	4	57	6	4	1	8	2	1	1	849
MK268_m3_3	988	75	121780	8993	273278	26937	26151	2319	101228	8996	17061	1156	1280	88	8870	765	434	41	646	53	39	3	55	9	2	1	10	3	1	1	699
MK268_m3_4	779	71	121248	9002	256818	30690	29995	2457	103541	9066	17620	1282	1370	123	7856	633	367	37	528	48	31	3	55	5	2	1	10	2	1	0	647
MK268_m3_5	719	56	119704	9714	247834	19212	27147	2393	109746	10702	16874	1508	1235	114	7732	769	339	38	513	46	29	3	49	6	3	1	7	2	1	0	879
MK268_m3_6	585	47	135599	11484	257600	22372	27942	1953	96765	5957	16332	1471	1322	102	7003	599	278	21	397	43	23	3	42	5	2	0	5	1	1	0	1090
MK268_m3_7	1291	143	115425	10829	202836	16266	25489	2396	93052	6975	15777	1220	1042	120	8451	797	463	26	816	102	53	6	66	7	3	1	13	3	1	0	512
MK268_m3_8	5290	538	98087	7931	236638	24807	29909	2118	105671	6608	23859	1725	441	44	18667	990	1537	151	3007	247	215	21	240	21	15	2	47	6	4	1	321
MK268_m3_9	5419	437	103330	10141	226628	23377	29390	2169	108655	8981	22606	2333	436	44	17982	1276	1419	140	3091	289	227	25	214	26	13	1	47	8	4	1	311
MK268_m3_10	4705	417	111405	11615	224903	21334	29481	2323	101014	6938	21873	1882	664	64	17872	1511	1281	84	2643	172	194	21	212	16	14	2	41	6	4	1	356
MK268_m3_11	1380	137	126005	13114	255255	21834	30077	2868	107311	8216	18445	1520	1440	108	8921	625	497	51	764	55	55	6	66	6	3	1	15	3	1	0	481
MK268_m3_12	1305	129	117446	7849	276865	24527	31814	2763	97054	6420	18370	1749	1292	124	10215	966	537	47	846	86	55	5	74	8	3	1	14	2	1	1	577
MK268_m3_13	5230	475	105298	10150	240079	23302	28004	2915	102863	7182	24510	1592	457	27	18232	1265	1437	92	2612	202	201	17	230	21	14	2	45	7	5	1	329
MK268_m4_1	9023	537	124035	10837	244896	16218	29289	2136	100052	5215	20071	1764	1530	113	14219	1017	1154	80	3802	392	387	28	439	40	30	3	77	9	7	1	150
MK268_m4_2	7148	630	111246	8360	234285	20906	27713	1958	98643	7386	17813	1283	1634	124	11621	697	1039	78	3003	255	335	32	381	30	28	3	66	8	5	2	143
MK268_m4_3	6046	557	126859	10303	234071	20770	29199	3345	99011	8649	17549	1339	1513	133	11053	985	896	82	2367	190	261	15	282	28	18	2	47	6	4	1	192
MK268_m4_4	6510	505	105158	10915	223885	20970	26798	2166	92415	5733	18951	1464	1624	116	12202	962	1068	98	2750	227	289	22	335	30	19	2	53	9	6	1	185
MK268_m4_5	7054	553	119644	11993	242258	25525	25889	2491	92102	7212	19699	1697	1579	141	11820	1110	1056	121	3338	289	322	31	376	37	25	2	65	6	7	1	147
MK268_m4_6	7094	749	118966	10234	245654	17490	24510	2700	93564	7524	18504	1272	1555	135	11721	982	1114	75	3314	253	339	23	381	26	23	2	65	8	7	1	146
MK268_m5_1	5625	418	112678	12338	226472	18240	28372	2993	117756	8692	23369	1970	479	34	16886	983	1335	139	2862	205	224	23	242	22	16	2	53	6	4	1	256
MK268_m5_2	4892	351	97894	9612	222850	16703	26011	1982	103065	7407	22211	1473	481	54	16699	1289	1189	99	2433	172	203	19	210	16	12	2	44	7	4	1	306
MK268_m5_3	4264	312	116506	13024	252568	25465	28614	2577	115992	13117	23399	1669	575	58	15745	1072	1128	86	2120	177	165	16	196	17	9	1	34	5	4	1	380
MK268_m5_4	1683	178	124097	10518	237288	20628	27850	2343	97398	8499	18854	1331	1189	131	9833	995	568	53	987	111	62	7	73	7	4	1	11	3	2	1	732
MK268_m5_5	1516	178	71420	6432	159142	17123	17236	1421	64154	5638	12970	968	614	67	6628	520	450	34	852	66	63	5	72	6	4	1	16	2	2	1	330
MK268_m5_6	4171	310	115561	12221	225575	16628	29786	2042	112048	7471	23297	1674	602	57	16454	1401	1153	91	2249	188	177	20	194	18	11	2	44	6	4	1	303
MK268_m5_7	4724	311	107938	10751	267777	19074	30513	3159	111680	13618	23990	2458	497	38	16415	1419	1203	77	2905	237	186	16	208	20	14	2	40	5	5	1	329
MK268_m5_8	4560	253	109735	10548	251801	24537	28813	3054	110204	8019	23205	2151	461	31	16276	1569	1227	105	2540	251	204	20	218	22	15	2	46	6	5	1	283
MK268_m5_9	5387	506	115537	13043	243175	27601	30546	3137	110436	11553	24280	1838	502	45	17604	1741	1346	117	2802	297	228	29	228	23	15	2	45	6	5	1	313
MK268_m5_10	5374	541	106658	10617	246217	23160	26793	2579	105699	7453	23689	1919	514	54	17565	1544	1338	97	2677	218	206	16	235	18	16	2	48	7	6	1	295
MK268_m5_11	6147	633	106380	8726	262780	22718	28683	2278	114420	12636	24562	1799	484	45	19395	1950	1494	147	3083	265	236	16	267	19	15	2	57	7	6	2	277
MK268_m5_12	5249	437	105930	10281	225545	22429	30224	2667	102396	6583	23264	2031	480	38	17551	1432	1216	109	2585	162	194	16	222	19	13	2	39	6	4	1	369
MK268_m5_13	6244	426	113039	7000	238758	22578	33098	3217	108300	12625	25824	1653	463	53	18348	1521	1454	130	3244	281	242	22	273	26	18	2	56	9	6	1	266
MK268_m5_14	4911	524	85793	8697	205558	18245	24053	2210	92977	9862	20523	1846	383	38	14242	1098	1236	111	2486	247	202	19	231	16	17	2	47	8	5	1	248
MK268_m5_15	6386	586	113036	10037	225077	20403	29092	2640	107050	8008	25470	2408	470	45	20598	2530	1545	130	3063	199	281	33	274	25	17	2	57	9	6	1	291
MK268_m6_1	1315	100	128532	15285	263756	29432	29643	2683	109211	10914	19220	1755	1151	114	8898	745	545	58	789	75	53	5	70	10	3	1	10	3	1	0	694
MK268_m6_2	1346	103	120764	8205	256607	27703	30965	2101	102300	6399	18014	1467	1218	120	9023	601	526	56	947	96	57	3	63	9	3	1	12	3	1	0	630
MK268_m6_3	1019	79	127128	10328	249347	17623	30576	2380	106994	11002	18020	1532	1276	123	7146	594	431	46	739	86	55	6	67	7	2	1	7	2	1	0	821
MK268_m6_4	3195	284	118690	9509	226732	19931	29873	2868	107080	8016	21084	2112	532	51	13589	1087	925	67	1939	170	136	11	151	15	9	1	29	5	3	1	384
MK268_m6_5	2975	278	116973	12083	248244	22661	28455	2510	103123	9645	21691	1511	533	42	12105	862	874	75	1671	132	138	12	145	16	9	2	26	4	3	1	381

Table B1. Petrochronological data for monazite grains.

Grain #	Y (ppm)	2SE	La (ppm)	2SE	Ce (ppm)	2SE	Pr (ppm)	2SE	Nd (ppm)	2SE	Sm (ppm)	2SE	Eu (ppm)	2SE	Gd (ppm)	2SE	Tb (ppm)	2SE	Dy (ppm)	2SE	Ho (ppm)	2SE	Er (ppm)	2SE	Tm (ppm)	2SE	Yb (ppm)	2SE	Lu (ppm)	2SE	Gd/Yb(N)
MK268_m6_6	1381	125	124632	7948	245095	17986	29291	2304	103998	7560	17723	1617	1041	104	9358	956	521	50	909	89	62	6	81	8	2	1	13	3	1	0	597
MK268_m6_7	895	91	116996	8052	229367	14169	27145	2675	100674	7151	16585	1955	1247	95	7923	671	417	35	690	71	47	5	58	7	2	1	8	2	0	0	822
MK268_m6_8	2039	209	132773	12071	239633	20587	28456	3331	103048	8103	19215	1263	859	76	10101	865	686	57	1176	90	91	10	101	12	5	1	13	3	2	1	615
MK268_m6_9	1002	79	122802	12329	251644	18313	31484	3607	102012	7666	18280	1386	1108	106	8376	824	437	41	705	64	48	5	64	7	2	1	9	3	1	0	786
MK268_m6_10	991	88	123985	8164	254204	20559	27432	2456	105007	8691	18661	1620	1243	91	8353	708	422	28	761	74	48	5	65	8	2	1	9	2	1	0	794
MK268_m6_11	940	88	111948	10614	259636	23302	27901	3228	119264	15258	18459	1515	1066	107	9614	911	504	48	784	100	41	5	52	7	1	0	6	2	1	0	1256
MK268_m6_12	2737	232	113158	9600	229739	16730	29590	2103	110870	10195	21312	2046	549	45	11718	834	860	76	1573	127	138	13	159	15	8	2	25	4	2	1	380
MK268_m6_13	3611	376	111273	10599	252697	17723	28860	2801	103753	8284	20025	1668	441	44	13794	1153	963	86	1902	159	169	22	193	22	11	2	34	6	4	1	328
MK268_m6_14	2745	242	119359	9114	242889	16917	29059	2661	101983	6796	19873	1725	656	60	10704	909	680	55	1424	129	114	12	144	13	9	2	24	3	4	1	366
MK268_m6_15	990	87	119994	10702	254140	17989	29774	3109	102208	7647	20118	1740	1067	87	9293	893	518	56	721	71	38	4	50	8	2	1	8	3	1	0	903
MK268_m6_16	3092	410	109002	8047	236952	25834	29334	2394	101857	8797	21784	1833	612	53	11432	962	758	67	1637	147	127	10	181	17	11	2	41	7	3	1	227
MK268_m6_17	2444	257	104760	8395	244166	30586	29777	2709	110578	7869	21222	1686	661	57	11286	1052	788	87	1463	102	100	9	132	15	8	1	21	4	3	1	444
MK268_m6_18	2121	218	115267	7041	250436	21901	28288	2534	99419	6893	21234	1645	666	58	10493	1088	724	69	1408	115	99	11	117	10	8	2	22	5	3	1	384
MK268_m6_19	3357	322	112079	9253	240518	22316	27181	2126	107517	5899	20014	1740	317	31	13106	1017	1060	94	2020	192	143	11	158	14	8	1	23	3	3	1	460
MK268_m6_20	3275	274	104289	6813	241105	19353	27875	2576	106391	8116	20995	1660	313	24	13469	985	1043	78	2218	212	156	13	145	14	9	2	26	5	2	1	423
MK268_m6_21	6225	580	105052	9905	240837	20604	25844	1792	98690	9804	19393	1606	267	29	14234	1341	1296	139	2944	239	251	25	340	38	20	2	57	9	7	1	201
MK268_m6_22	3038	293	120504	10971	245713	26647	29964	2357	110272	10317	22104	1933	612	43	11988	928	742	75	1401	109	125	11	183	16	10	1	35	5	4	1	275
MK268_m6_23	3127	250	113299	11986	271812	23045	27859	2427	104182	6994	23313	2525	667	67	11570	1251	746	57	1675	135	133	13	185	22	12	2	37	6	4	1	254
MK268_m6_24	2945	272	109093	11075	238979	20337	29806	2652	108872	5968	20483	1825	479	42	12761	1513	794	56	1591	129	128	13	142	13	9	2	19	3	3	1	553
MK268_m6_25	898	66	117885	11463	262353	30269	28589	2586	102971	6663	16563	1237	1063	101	7002	721	371	28	624	57	43	5	52	5	2	1	5	2	1	0	1044
MK268_m6_26	2344	166	124122	12886	256951	18981	27702	2743	107200	10850	22446	1883	767	62	11558	1117	660	59	1322	112	98	10	123	12	8	1	28	3	3	1	331
MK268_m6_27	5431	452	119090	10131	233122	20525	28961	3660	108410	11722	20384	1419	492	51	11370	994	1010	108	2469	221	214	19	274	34	17	2	56	7	6	1	166
MK268_m6_28	1975	286	116590	9505	235265	22344	27225	2719	108680	8314	21014	1271	813	81	10592	1108	668	61	1176	88	82	10	108	10	5	1	17	4	2	1	513
MK268_m6_29	3101	248	116921	12190	241463	20527	29972	3016	112956	9705	21939	2155	677	66	11304	926	794	81	1502	122	122	11	155	22	10	2	30	5	4	1	303
MK268_m6_30	2186	187	111926	10333	239791	22701	31186	3118	108494	8854	21474	2398	755	74	10896	988	691	56	1326	108	89	7	110	12	7	1	22	4	2	1	402
MK268_m6_31	5511	540	109432	10522	237225	23070	29439	2355	113125	11362	19937	2224	283	22	14069	1291	1060	100	2733	270	196	20	258	21	17	3	46	7	5	1	246
MK268_m6_32	5339	425	94355	11064	211866	16967	24414	2352	95874	8276	17061	1309	377	37	11823	816	959	96	2515	290	216	19	253	19	17	2	55	6	6	1	175
MK268_m6_33	2869	283	103990	10171	237152	20930	25866	2855	101412	9911	18448	1430	470	49	12162	1171	877	77	1613	169	106	11	135	13	6	1	16	4	2	1	608
MK268_m6_34	2031	226	107076	10256	224326	23432	28048	2409	100341	6399	17814	1561	958	83	10352	1040	614	62	1171	88	88	10	103	16	3	1	12	3	1	0	711
MK268_m6_35	1635	155	121708	9509	258322	27342	29869	2683	110828	6853	18801	2042	1186	103	8895	631	546	51	940	113	73	7	82	8	3	1	8	2	1	0	877
MK268_m6_36	1270	153	120929	9800	236023	18678	27034	2220	107975	7563	17281	1417	1296	131	8052	726	456	37	797	75	57	5	77	8	3	1	6	2	1	0	1053
MK268_m6_37	1308	138	127195	10573	232387	12705	30241	3429	97676	8208	18415	2191	1393	152	8945	761	473	43	822	66	57	6	75	8	2	1	8	2	0	0	950
MK268_m6_38	1217	116	118220	10297	252866	21021	28500	2545	108148	9448	17185	1615	1375	115	8422	640	411	32	764	70	53	4	69	9	2	1	7	2	0	0	954
MK268_m6_39	1262	81	123691	9765	248177	19054	28598	3444	99751	7147	18070	1533	1295	133	8543	748	422	35	803	69	57	5	73	8	3	1	6	2	1	0	1161
MK268_m6_40	1217	128	123954	13764	254127	20441	29444	3262	103271	7919	18226	1574	1345	107	8106	635	407	39	774	67	52	6	70	7	3	1	10	3	1	1	662
MK268_m6_41	1224	145	129872	11801	238020	20006	27207	2100	109004	11957	16845	1344	1320	91	8090	865	445	31	802	75	56	5	65	8	3	1	7	2	1	0	945
MK268_m6_42	2202	256	118826	9349	232643	19917	28798	2198	112997	10533	20281	2036	820	62	11989	906	630	47	1164	97	83	7	104	8	6	1	21	3	2	1	458
MK268_m6_43	1167	80	114859	12741	238277	19833	30619	2601	112070	6958	20433	1665	1169	93	10405	1050	503	44	809	79	45	4	62	8	3	1	8	2	1	0	1035
MK268_m6_44	1159	120	126422	10177	233103	16665	28730	3275	105260	8210	17604	1917	1435	136	7810	562	459	28	849	76	58	6	69	10	3	1	6	2	1	0	1016
MK268_m6_45	1152	118	124961	12014	257668	16624	27537	2590	105241	7820	17645	1538	1552	132	8447	756	449	36	849	67	58	5	75	8	3	1	10	3	1	0	661
MK268_m6_46	987	91	122465	10396	251535	20496	28769	2341	107870	10138	17628	1562	1322	106	8542	704	451	44	729	68	46	4	58	8	2	1	6	2	1	0	1110
MK268_m6_47	1010	92	117160	11584	248989	22574	29304	2013	98634	6551	18072	1138	1275	103	7812	703	391	40	789	97	49	5	68	6	1	0	5	2	1	0	1238
MK268_m6_48	1178	128	130465	10408	257844	28548	26337	2321	108833	7175	18834	1829	1470	88	8160	590	433	33	808	62	57	4	78	9	2	1	8	2	1	0	787
MK268_m6_49	992	91	131811	12615	242913	18531	27578	2507	100111	6121	17166	1319	1230	109	7622	559	447	47	764	77	47	5	69	8	3	1	6	2	1	0	972
MK268_m6_50	1268	101	118878	7874	245832	18479	30567	3712	104846	9924	17348	1513	1508	158	7672	682	479	39	801	63	55	4	75	9	3	1	7	2	1	0	941
MK268_m6_51	1174	94	115675	7236	247333	21137	28298	3508	107482	8135	18158	1368	1360	120	7976	686	464	50	767	71	54	5	78	8	2	1	11	3	1	0	596
MK268_m6_52	1162	128	121830	11561	234997	28519	26766	2401	98748	7726	17698	1778	1357	132	8004	696	404	30	883	84	48	4	72	8	2	1	7	2	1	0	868
MK268_m6_53	1087	132	135929	11468	249712	22510	29958	3250	101534	8916	17230	1187	1312	77	8378	554	405	29	749	69	53	4	66	7	3	1	6	2	0	0	1043
MK268_m6_54	1050	95	133715	12905	259153	23438	28884	3313	104957	8432	17508	1265	1355	108	8091	649	441	50	680	45	49	5	65	8	2	1	6	2	0	0	1066
MK268_m6_55	963	85	118901	10289	246262	21457	28061	3433	102739	6591	17264	1162	1318	144	7656	515	382	33	697	69	42	5	70	11	2	1	7	2	1	0	879
MK268_m6_56	1104	109	143407	10777	259543	19179	28680	3097	101987	6964	16285	1518	1386	144	8197	551	444	41	809	64	53	4	65	7	2	1	9	3	1	0	774
MK268_m7_1	4761	549	125835	9777	350295	27480	30001	2694	131182	9453	26982	2470	362	34	14948	962	1198	94	2735	195	232	25	214	28	13	2	32	6	3	1	377
MK268_m7_2	3968	355	109554	11104	322294	26808	29163	2335	127576	15094	23227	2158	366	31	13379	1203	1041	85	2256	173	182	21	166	17	11	2	37	9	3	1	294
MK268_m7_3	4642	532	114064	9829	284189	25556	32124	2669	118330	7468	23449	2617	337	32	12767	1120	1058	89	2588	289	224	25	212	19	13	2	38	7	3	1	271
MK268_m7_4	3897	337	122602	8454	279481	25142	27900	2706	124674	8885	22556	2267	333	28	13955	906	1092	96	2587	237	208	18	199	18	12	2	33	5	4	1	341
MK268_m7_5	4179	420	110161	12892	302592	25971	26817	2854	110974	8180	20728	1518	354	33	12749	997	1054	113	2537	316	223	33	243	38	17	4	47	10	5	2	222
MK268_m7_6	4921	516	110122	10458	295712	26825	27591	2151	119275	7258	22009	2078	328	35	13621	1030	1160	117	2720	262	224	24	208	18	14	2	42	8	3	1	263
MK268_m7_7	3121	315	124091	11399	297691	29206	29896	3462	120848	8224	24724	1658	584	53	12555	1081	917	88	1791	152	156	16	146	12	9	2	25	6	2	1	408
MK268_m7_8	3023	288	131980	13009	319133	28386	31213	3394	117639	7776	25091	2498	657	65	13225	1429	1018	68	1828	150	161	12	156	14	9	2	29	4	2	1	369
MK268_m7_9	2960	285	109711	11176	287092	32026	27120	2476	115382	7924	24918	2948	605	62	12124	997	870	51	1811	145	151	11	147	13	8	1	30	4	2	1	325
MK268_m7_10	3084	311	107313	9807	283511	21729	26748	2729	111236	7650	23632	2060	575	44	13596	1381	877	91	1974	239	153	13	153	13	9	2	28	4	2	1	393
MK268_m7_11	4048	286	98041	11195	226877	19109	21754	2432	90974	7642	17877	1566	340	38	11309	1274	919	99	2283	170	214	20	217	24	16	2	45	6	4	1	203
MK268_m7_12	2867	298	54376	6583	149670	16047	14036	1353	56660	6244	10786	1140	208	25	6311	750	531	48	1501	176	132	14	169	21	9	2	27	5	3	1	186
MK268_m7_13	3460	330	128870	13248	279718	27723	30221	2831	129962	12315	22770	1821	648	67	12000	1262	906	81	1990	224	148	16	150	16	7	1	25	6	2	1	386
MK268_m7_14	2615	262	118591	11961	304624	33077	28563	3483	116555	9842	23913	2671	728	66	12534	1239	885	86	1695	211	132	20	133	22	6	1	23	4	2	1	445
MK268_m8_1	987	65	133279	12071	323851	26331	31720	3372	125521	12251	17738	972	1247	95	7686	573	400	32	693	60	43	5	64	5	2	1	8	3	1	0	824
MK268_m8_2	7423	1012	118651	11602	265689	29521	28412	2831	113853	7052	23575	2116	466	34	15376	1404	1317	94	3508	366	325	32	341	38	25	3	88	13	8	2	142
MK268_m8_3	3477	464	123053	13570	279146	20719	31111	3159	112490	11323	24508	1617	455	40	14648	1526	1137	103	2270	265	156	13	160	16	8	1	29	6	3	1	407
MK268_m8_4	1078	92	139313	13427	316038	34984	31149	2838	125098	13910	21635	2530	1445	134	10004	865	506	44	822	88	52	5	65	8	2	1	8	2	1	0	1029

Table B1. Petrochronological data for monazite grains.

Grain #	Y (ppm)	2SE	La (ppm)	2SE	Ce (ppm)	2SE	Pr (ppm)	2SE	Nd (ppm)	2SE	Sm (ppm)	2SE	Eu (ppm)	2SE	Gd (ppm)	2SE	Tb (ppm)	2SE	Dy (ppm)	2SE	Ho (ppm)	2SE	Er (ppm)	2SE	Tm (ppm)	2SE	Yb (ppm)	2SE	Lu (ppm)	2SE	Gd/Yb(N)
MK268_m8_5	5552	715	121767	11152	289869	24804	29260	3358	117235	10464	22335	1779	854	104	12892	1314	1027	88	2613	329	233	33	261	41	23	5	60	10	7	1	175
MK268_m8_6	1360	130	114999	8401	266175	22948	27266	2710	112115	9603	22802	2312	1430	119	9621	843	567	57	915	76	59	7	66	10	3	1	9	3	1	0	828
MK268_m8_7	2549	352	133474	11429	281962	29359	29805	2657	111724	6721	18418	1434	1278	132	9168	802	627	59	1458	168	132	23	154	24	9	2	32	6	3	1	230
MK268_m8_8	8388	778	116287	10993	258192	18495	28133	2771	98052	6405	19659	1879	736	64	13751	1302	1291	128	3799	403	431	49	549	72	45	5	135	18	15	3	83
MK268_m8_9	7831	736	92895	10402	177250	14959	19659	1719	82835	6255	18011	2011	351	35	12516	1061	1244	124	3782	310	360	33	406	35	30	3	95	9	10	2	107
MK268_m8_10	14794	1548	109704	10562	266845	30125	27799	2744	114139	8779	23504	1609	545	61	16819	1270	1845	163	6233	501	674	65	866	92	75	9	199	22	22	3	68
MK268_m8_11	3419	374	104841	8423	248693	18036	26821	2749	111833	7826	20565	1987	663	93	11516	1017	927	104	1977	302	153	20	153	19	8	2	36	6	3	1	261
MK268_m8_12	1660	212	133194	15522	268754	22535	29999	3123	110556	13325	18054	1547	1337	123	8606	856	523	48	969	116	75	9	88	11	3	1	11	2	1	1	649
MK268_m8_13	1114	90	130609	14642	292010	19783	28489	2584	108909	11331	17966	1478	1314	77	7890	588	429	35	750	80	44	4	65	9	2	1	8	2	1	0	766
MK268_m8_14	1272	104	141508	14489	287303	24261	30100	2989	116226	7542	19670	1759	1537	151	8263	617	434	44	885	70	54	6	68	9	3	1	10	2	1	0	666
MK268_m8_15	1033	69	141638	14206	288885	21506	31290	3339	119000	7298	19474	1698	1410	103	8185	748	446	45	731	70	49	5	63	7	3	1	8	2	1	0	821
MK268_m8_16	1422	136	145124	14077	291127	24965	32845	3127	116631	7585	19629	1693	1641	135	9622	719	516	45	958	81	63	5	68	6	4	1	9	3	0	0	879
MK268_m8_17	1457	147	141090	9776	285997	34559	30432	2451	122740	10380	21960	1960	1745	126	9219	872	524	55	983	77	65	6	75	11	3	1	9	2	1	0	830
MK268_m8_18	1103	109	129951	12181	273545	25482	30243	2655	116007	8965	21725	2260	1516	124	9304	657	553	49	836	86	45	5	59	7	2	1	8	3	1	0	934
MK268_m8_19	1839	252	130137	10778	274279	20489	31823	2578	123004	9387	23030	1820	1288	88	11472	1011	657	58	1143	104	65	7	89	8	5	1	17	5	2	1	549
MK268_m8_20	1107	92	128703	13329	261977	17159	28722	3182	107631	9344	21864	1959	1525	135	9723	690	572	48	879	78	51	6	66	8	2	1	6	2	1	0	1212
MK268_m8_21	1267	102	136391	13651	282632	22185	30121	3033	117810	8813	23177	2323	1448	140	9552	848	527	50	894	68	52	4	55	7	2	0	6	2	1	0	1271
MK268_m8_22	1424	161	138384	11407	277248	20347	30780	3187	114647	11606	23011	2161	1587	112	9356	778	532	50	958	94	59	6	66	7	3	1	7	3	1	1	1146
MK268_m8_23	1245	96	139089	13148	294460	28500	30642	2770	107476	7641	18980	1582	1517	154	9418	964	530	52	805	63	63	7	71	7	3	0	7	3	1	0	1153
MK268_m8_24	1109	86	143150	13934	288273	27811	29756	2770	94876	5280	17652	1982	1228	116	8056	643	394	30	677	73	48	5	67	9	2	1	6	2	1	1	1007
MK268_m9_1	3305	279	104840	10567	228089	19900	24461	2381	105694	7531	19717	1565	492	40	13599	958	934	103	1871	186	122	9	131	15	8	1	22	5	2	1	508
MK268_m9_2	2812	273	107707	9239	234693	20301	26947	2855	100206	7226	19565	1785	572	51	12769	896	864	60	1580	165	129	12	139	14	8	2	29	5	2	1	352
MK268_m9_3	3597	305	105907	7833	245287	24429	23692	1633	101112	7238	20010	1959	573	45	10888	822	829	74	1741	107	144	13	170	16	10	2	29	5	3	1	305
MK268_m9_4	2976	326	111989	9799	221907	23949	27516	2602	96313	7533	19057	1836	663	67	11569	765	711	71	1505	117	114	10	152	18	7	2	25	4	3	1	379
MK268_m9_5	2265	387	126989	12748	232543	17219	28138	2336	102196	8290	20144	1343	1028	126	10350	912	637	60	1247	153	99	16	112	18	8	2	21	6	2	1	401
MK268_m9_6	3289	250	113476	11362	221433	19713	27234	2561	103451	6025	19584	2060	613	52	9598	893	688	66	1355	128	113	10	155	15	9	2	27	5	2	1	286
MK268_m9_7	3401	294	118658	11820	252120	21221	26554	2446	101865	7139	20067	1449	547	38	12259	1025	800	49	1606	140	134	11	154	17	8	1	30	4	4	1	334
MK268_m9_8	3351	353	105881	9292	232120	16623	23578	2110	90543	7382	21509	2094	530	51	11648	1405	865	81	1579	106	146	16	169	19	11	2	27	5	3	1	347
MK268_m9_9	3051	258	108435	11218	242875	22552	25558	2559	105160	8702	19812	1877	546	50	12079	941	852	81	1818	147	127	12	152	15	8	1	31	6	2	1	319
MK268_m10_1	5308	382	119646	10790	262547	26719	30963	3125	105926	8294	23283	1478	628	66	14703	1072	1136	119	2749	193	226	21	283	32	18	2	51	8	5	1	235
MK268_m10_2	6567	936	71432	7148	155759	15990	16009	1758	64101	6963	12176	1431	439	49	10066	1006	993	103	2885	288	265	36	346	38	24	3	83	10	8	2	98
MK268_m10_3	1123	83	147515	13739	282883	23887	33252	2382	123048	11174	19207	2126	1394	119	8672	850	400	31	703	75	53	5	63	7	2	1	7	2	1	0	1061
MK268_m10_4	1102	88	129043	12326	260250	20501	28541	2449	111815	7431	18680	1448	1199	154	9111	878	496	45	784	72	45	4	64	8	2	1	9	2	1	0	860
MK268_m10_5	4418	416	120794	12295	234369	21484	30988	3138	127357	12931	25365	2437	499	56	15003	1490	1115	109	2618	259	182	13	219	21	12	2	41	7	3	1	296
MK268_m10_6	3591	331	126952	9391	259217	21212	29488	2479	114000	7368	23116	1666	582	51	14451	773	1076	90	2184	225	148	14	165	15	8	2	23	4	2	1	504
MK268_m10_7	8184	643	93884	11675	216304	22614	22900	2450	86103	6672	19915	2076	441	45	14617	1087	1298	145	3721	394	352	36	505	44	35	4	90	10	12	2	132
MK268_m10_8	3010	275	102672	7491	204718	15208	21818	1676	90708	6538	20100	1796	481	43	12326	1057	878	60	1730	185	118	8	128	14	6	1	25	5	2	1	407
MK268_m10_9	3073	256	121590	11190	248996	22743	29479	2551	106079	10032	21725	1964	790	75	12991	818	908	73	1843	189	119	11	149	18	6	1	19	4	2	1	547
MK268_m10_10	8009	768	113546	9646	244741	30231	26506	2765	110331	11033	24069	2688	425	41	17769	1491	1333	111	3540	213	298	24	475	53	29	3	87	10	10	2	165
MK268_m10_11	825	80	136765	12549	282260	17306	28076	2083	102062	6494	16381	1810	1205	96	7932	744	335	35	586	58	44	5	53	5	2	1	7	2	1	0	974
MK268_m10_12	869	68	140161	10680	299062	22430	33287	3293	116329	7235	19279	1477	1381	99	8047	478	369	37	578	55	39	3	65	7	2	1	6	2	1	0	1123
MK268_m10_13	1754	289	149213	16837	300984	26022	33908	2856	112980	10159	18986	1793	1283	122	9378	918	537	43	1046	140	78	8	103	14	5	1	14	4	2	1	559
MK268_m10_14	7928	811	115977	9450	240018	18367	27453	2459	116485	10378	23094	1571	494	38	18292	1041	1512	119	3849	367	327	21	424	32	27	3	83	11	10	2	178
MK268_m10_15	933	71	148897	12556	296614	24927	27881	2121	114838	8979	19266	1464	1413	109	8145	733	376	39	720	77	43	3	62	6	2	1	6	2	0	0	1088
MK268_m10_16	797	65	156100	15501	306949	25554	30886	3135	109771	6787	17080	1649	1261	120	7436	1046	326	32	572	47	36	4	61	9	2	1	8	3	1	0	714
MK268_m10_17	2525	223	143089	12418	301211	32951	32061	2608	115356	10958	22184	1901	858	76	13407	1224	778	60	1516	159	116	11	117	15	6	1	18	3	2	1	610
MK268_m10_18	3773	405	128473	11328	282516	23986	30674	2752	117027	10728	23141	1304	713	58	14369	953	1073	93	2188	162	151	12	175	15	10	2	30	6	3	1	392
MK268_m10_19	6954	533	129574	13697	281151	24727	28967	2734	115491	11011	23198	2015	443	51	18004	1187	1595	160	3291	301	324	35	380	31	29	4	84	13	7	1	173
MK268_m10_20	7235	641	115304	11594	272690	25733	30476	2791	104310	9139	22852	1928	401	44	17915	1184	1480	156	3921	347	329	30	404	36	26	4	77	12	11	2	188
MK268_m10_21	7393	769	125548	12690	237844	20222	27813	2298	117236	12405	22361	1442	760	64	15259	1627	1339	136	3479	301	309	22	384	31	29	4	93	13	9	2	133
MK268_m10_22	4776	462	122987	12624	281476	26106	28601	2468	109428	9802	21842	1433	906	78	13749	929	1113	117	2360	206	194	25	271	31	16	2	41	6	4	1	273
MK268_m10_23	2278	194	123855	9701	299853	21381	31188	3459	120280	9853	21566	1801	1092	95	13589	1036	805	60	1347	151	97	11	124	18	5	1	18	4	1	0	618
MK268_m10_24	1062	78	139109	11882	274332	20253	31952	3190	108274	6872	20934	1554	1355	124	9813	912	529	56	753	54	46	4	68	9	2	1	7	2	0	0	1160
MK268_m10_25	1117	143	126216	10733	297406	31642	29517	2598	107807	8576	19824	1614	1491	124	9998	651	510	37	863	88	49	5	68	10	2	1	10	3	1	0	798
MK268_m10_26	1070	85	143982	12615	276461	28866	30112	3028	104248	6453	20720	1548	1352	105	9678	738	473	44	808	78	48	5	61	10	2	1	10	3	1	1	794
MK268_m10_27	1050	102	148576	12645	286542	18721	32911	2875	115965	9224	19404	1539	1286	114	10028	966	487	48	859	75	46	4	57	8	2	1	10	4	1	0	845
MK268_m10_28	1142	89	134087	11785	267904	26079	31633	2960	98950	7288	19051	1259	1403	119	9484	712	485	38	788	77	46	5	57	7	2	1	6	3	1	0	1326
MK268_m10_29	1036	104	133288	11608	276194	25055	30905	2862	110358	6317	19514	1729	1363	124	10288	945	471	48	781	66	47	6	61	9	2	1	6	2	0	0	1346
MK268_m10_30	1054	85	131435	10250	270510	17094	31959	2648	103672	6773	19513	1843	1359	115	9814	721	470	38	763	68	43	4	52	7	2	1	8	2	0	0	1006
MK268_m10_31	971	105	135809	9195	268590	23559	28897	2584	104119	9872	18865	2019	1334	102	9517	745	429	40	700	56	42	5	58	7	2	1	6	2	1	0	1362
MK268_m10_32	928	97	127299	11471	281703	24662	30550	2972	106851	6298	18280	1552	1307	112	8635	727	468	45	771	75	46	5	55	8	2	1	6	2	1	0	1207
MK268_m10_33	1025	102	117526	10034	269033	32110	29045	3001	102456	10224	19096	1623	1194	84	9334	1136	443	29	748	62	46	4	54	8	2	0	5	2	0	0	1473
MK268_m10_34	1087	84	132885	13066	278218	19715	33778	3114	109907	9401	18386	1491	1372	128	9938	1006	501	42	781	54	48	5	57	9	2	1	8	3	0	0	971
MK268_m10_35	1065	95	148876	18083	269232	25575	26381	2655	103199	7414	17837	1451	1256	132	7777	845	336	25	707	70	48	6	54	6	3	1	9	3	1	1	665
MK268_m10_36	946	102	129754	10825	294665	20326	29029	2491	104126	8132	16632	1183	1107	69	7622	661	359	35	668	54	52	5	57	7	3	1	8	2	1	1	809
MK268_m10_37	1042	84	129553	9196	294122	29390	32227	2344	99479	5980	20819	1695	1259	77	9916	546	478	50	783	73	50	5	62	6	2	1	7	2	0	0	1130

* Crossed data are excluded from the interpretation.

Table B2. Garnet geochemistry.

Specimen	MK256			MK258			MK262				MK268	
Location	rim - R1	core - C1	core - C1	rim - R1	core - C1	core - C1	rim - R1	core - C1	core - C1	rim - R1	core - C1	rim - R1
SiO2	35.89	35.86	35.80	36.31	36.92	36.44	35.61	35.92	35.82	36.29	36.13	35.71
TiO2	0.02	0.04	0.01	0.05	0.04	0.04	0.04	0.02	0.01	0.03	0.04	0.03
Al2O3	21.56	22.13	22.18	22.50	22.86	22.60	22.27	22.45	22.48	22.60	22.18	21.90
FeO	32.77	30.27	30.19	29.96	24.03	23.99	34.88	33.07	33.06	35.24	29.35	35.49
MnO	1.71	0.85	0.80	1.58	1.19	1.26	1.20	0.72	0.75	1.13	0.87	1.33
MgO	3.15	3.62	3.81	7.44	6.96	6.99	5.05	6.24	6.40	4.88	5.38	4.46
CaO	0.00	0.01	0.01	2.43	8.13	8.47	1.36	2.05	2.05	1.35	5.84	1.14
Na2O	4.27	6.79	6.86	0.02	0.02	0.02	0.02	0.00	0.00	0.00	0.00	0.03
K2O	0.01	0.00	0.00	0.00	0.00	0.00	0.00	0.00	0.00	0.01	0.00	0.00
P2O5	0.01	0.00	0.01	0.03	0.01	0.00	0.01	0.02	0.00	0.02	0.01	0.02
Total	99.39	99.57	99.66	100.32	100.17	99.81	100.43	100.49	100.57	101.57	99.79	100.11
Si	2.89	2.84	2.83	2.85	2.86	2.84	2.85	2.84	2.83	2.87	2.86	2.87
Al iv	0.11	0.16	0.17	0.15	0.14	0.16	0.15	0.16	0.17	0.13	0.14	0.13
Al vi	1.95	1.92	1.91	1.94	1.96	1.92	1.95	1.94	1.93	1.97	1.94	1.95
Ti	0.00	0.00	0.00	0.00	0.00	0.00	0.00	0.00	0.00	0.00	0.00	0.00
Fe3+	0.05	0.07	0.08	0.06	0.04	0.07	0.04	0.05	0.06	0.02	0.05	0.04
Fe2+	2.16	1.93	1.92	1.91	1.52	1.50	2.29	2.14	2.12	2.31	1.89	2.35
Mn	0.12	0.06	0.05	0.10	0.08	0.08	0.08	0.05	0.05	0.08	0.06	0.09
Mg	0.51	0.80	0.81	0.87	0.80	0.81	0.60	0.74	0.75	0.58	0.64	0.54
Ca	0.27	0.31	0.32	0.20	0.68	0.71	0.12	0.17	0.17	0.11	0.50	0.10
Alm	0.71	0.62	0.62	0.62	0.49	0.48	0.74	0.69	0.68	0.75	0.61	0.76
Grs	0.09	0.10	0.10	0.07	0.22	0.23	0.04	0.06	0.06	0.04	0.16	0.03
Prp	0.17	0.26	0.26	0.28	0.26	0.26	0.20	0.24	0.24	0.19	0.21	0.17
Sps	0.04	0.02	0.02	0.03	0.03	0.03	0.03	0.02	0.02	0.02	0.02	0.03
Mg#	0.19	0.29	0.30	0.31	0.35	0.35	0.21	0.26	0.26	0.20	0.25	0.19
Oxygen	12.00	12.00	12.00	12.00	12.00	12.00	12.00	12.00	12.00	12.00	12.00	12.00

Table B3. Biotite geochemistry.

MK256																
Location	In grt	In grt	In grt	In grt	In grt	In grt	In grt	Matrix	Matrix	Matrix	Matrix	Matrix	Matrix	Matrix	Matrix	Matrix
SiO2	35.17	35.24	35.94	35.36	36.12	35.60	35.93	35.26	35.34	34.99	35.18	35.06	34.80	34.81	34.97	34.62
TiO2	1.91	1.94	3.70	3.69	3.87	3.32	3.56	2.98	2.90	3.07	3.22	2.82	2.95	2.98	2.98	2.93
Al2O3	19.43	19.51	18.86	18.73	18.49	18.89	18.72	18.74	18.96	18.54	19.26	18.72	18.57	18.45	18.73	18.37
FeO	16.71	17.04	14.90	14.58	14.64	15.33	14.64	18.37	18.51	18.67	18.14	18.46	18.13	18.29	18.11	19.06
MnO	0.02	0.01	0.05	0.03	0.00	0.05	0.00	0.07	0.09	0.07	0.02	0.06	0.06	0.03	0.02	0.09
MgO	10.93	10.98	12.90	12.73	13.45	13.39	13.56	10.43	10.49	10.15	10.20	10.47	10.02	10.04	10.02	10.42
CaO	0.02	0.00	0.00	0.00	0.00	0.02	0.00	0.00	0.00	0.00	0.00	0.00	0.00	0.00	0.00	0.00
Na2O	0.16	0.17	0.16	0.17	0.24	0.20	0.22	0.11	0.12	0.10	0.09	0.14	0.12	0.14	0.11	0.12
K2O	9.98	10.02	10.46	10.20	10.10	9.33	10.00	10.38	10.26	10.42	10.62	10.30	10.10	10.12	10.22	10.41
Cl	0.60	0.69	0.59	0.64	0.77	0.75	0.73	0.51	0.63	0.60	0.50	0.71	0.54	0.65	0.44	0.51
F	0.01	0.02	0.00	0.00	0.01	0.00	0.00	0.00	0.01	0.00	0.00	0.02	0.01	0.01	0.00	0.00
H2O	3.65	3.62	3.79	3.71	3.71	3.69	3.73	3.73	3.69	3.67	3.76	3.62	3.65	3.60	3.72	3.70
Total	98.60	99.23	101.34	99.84	101.41	100.58	101.09	100.59	100.99	100.27	101.00	100.37	98.96	99.11	99.32	100.22
Si	5.36	5.34	5.30	5.28	5.31	5.27	5.29	5.32	5.31	5.31	5.28	5.31	5.33	5.33	5.33	5.27
Al iv	2.64	2.66	2.70	2.72	2.69	2.73	2.71	2.68	2.69	2.69	2.72	2.69	2.67	2.67	2.67	2.73
Al vi	0.85	0.83	0.57	0.58	0.51	0.57	0.54	0.65	0.67	0.63	0.69	0.65	0.69	0.66	0.70	0.57
Ti	0.22	0.22	0.41	0.41	0.43	0.37	0.39	0.34	0.33	0.35	0.36	0.32	0.34	0.34	0.34	0.34
Fe	2.13	2.16	1.84	1.82	1.80	1.90	1.80	2.32	2.33	2.37	2.28	2.34	2.32	2.34	2.31	2.43
Mn	0.00	0.00	0.01	0.00	0.00	0.01	0.00	0.01	0.01	0.01	0.00	0.01	0.01	0.00	0.00	0.01
Mg	2.48	2.48	2.83	2.84	2.95	2.96	2.98	2.35	2.35	2.30	2.28	2.36	2.29	2.29	2.28	2.37
Ca	0.00	0.00	0.00	0.00	0.00	0.00	0.00	0.00	0.00	0.00	0.00	0.00	0.00	0.00	0.00	0.00
Na	0.05	0.05	0.04	0.05	0.07	0.06	0.06	0.03	0.03	0.03	0.03	0.04	0.04	0.04	0.03	0.04
K	1.94	1.94	1.97	1.94	1.89	1.76	1.88	2.00	1.97	2.02	2.03	1.99	1.97	1.98	1.99	2.02
OH	3.71	3.67	3.72	3.70	3.64	3.65	3.66	3.76	3.70	3.71	3.76	3.66	3.74	3.68	3.79	3.76
F	0.29	0.33	0.28	0.30	0.36	0.35	0.34	0.24	0.30	0.29	0.24	0.34	0.26	0.32	0.21	0.24
Cl	0.00	0.00	0.00	0.00	0.00	0.00	0.00	0.00	0.00	0.00	0.00	0.00	0.00	0.00	0.00	0.00
XMg	0.54	0.53	0.61	0.61	0.62	0.61	0.62	0.50	0.50	0.49	0.50	0.50	0.50	0.49	0.50	0.49
Oxygen	22	22	22	22	22	22	22	22	22	22	22	22	22	22	22	22

Table B3. Biotite geochemistry.

MK256

Location	Matrix	Matrix	Matrix	Matrix	Matrix	Matrix	Matrix	Matrix	Matrix	Matrix	Matrix	Matrix	Matrix	Matrix	Matrix	Matrix
SiO2	35.00	34.74	35.02	35.25	35.10	34.80	34.97	34.60	34.45	35.30	34.68	35.54	35.91	35.72	35.55	35.01
TiO2	3.25	3.24	3.02	3.26	2.87	2.80	2.84	2.88	3.01	3.07	3.19	3.08	3.09	3.02	3.04	3.36
Al2O3	18.25	18.29	18.48	19.02	18.67	18.73	18.70	18.54	19.07	19.13	18.52	19.29	19.16	19.39	19.31	18.37
FeO	18.83	18.91	19.15	18.45	19.15	18.74	18.77	18.71	18.15	18.26	18.22	17.93	18.69	17.56	17.66	18.57
MnO	0.05	0.05	0.07	0.02	0.03	0.08	0.07	0.04	0.03	0.06	0.06	0.03	0.06	0.08	0.04	0.06
MgO	10.53	10.31	10.46	10.30	10.53	10.09	10.31	10.22	10.33	10.18	9.81	9.50	9.63	10.30	9.78	10.52
CaO	0.00	0.00	0.00	0.00	0.00	0.06	0.00	0.02	0.00	0.00	0.00	0.00	0.00	0.00	0.01	0.00
Na2O	0.12	0.10	0.10	0.12	0.12	0.15	0.13	0.16	0.11	0.10	0.12	0.13	0.10	0.13	0.12	0.08
K2O	10.49	10.48	10.44	10.37	10.40	10.12	10.47	10.19	10.35	10.46	10.10	9.89	9.75	10.25	9.95	10.44
Cl	0.55	0.46	0.60	0.49	0.61	0.57	0.44	0.51	0.67	0.63	0.61	0.58	0.50	0.45	0.56	0.64
F	0.01	0.00	0.00	0.00	0.00	0.03	0.01	0.02	0.00	0.01	0.00	0.00	0.01	0.01	0.00	0.00
H2O	3.70	3.73	3.69	3.76	3.69	3.66	3.75	3.68	3.62	3.69	3.62	3.69	3.76	3.79	3.70	3.66
Total	100.77	100.31	101.05	101.04	101.17	99.81	100.46	99.57	99.78	100.89	98.93	99.66	100.66	100.71	99.71	100.72
Si	5.29	5.28	5.29	5.29	5.29	5.30	5.30	5.29	5.25	5.31	5.32	5.38	5.39	5.34	5.37	5.29
Al iv	2.71	2.72	2.71	2.71	2.71	2.70	2.70	2.71	2.75	2.69	2.68	2.62	2.61	2.66	2.63	2.71
Al vi	0.55	0.56	0.58	0.66	0.60	0.67	0.64	0.63	0.67	0.70	0.67	0.82	0.77	0.76	0.81	0.56
Ti	0.37	0.37	0.34	0.37	0.33	0.32	0.32	0.33	0.35	0.35	0.37	0.35	0.35	0.34	0.34	0.38
Fe	2.38	2.40	2.42	2.32	2.41	2.39	2.38	2.39	2.31	2.30	2.34	2.27	2.34	2.20	2.23	2.35
Mn	0.01	0.01	0.01	0.00	0.00	0.01	0.01	0.00	0.00	0.01	0.01	0.00	0.01	0.01	0.01	0.01
Mg	2.37	2.34	2.36	2.30	2.37	2.29	2.33	2.33	2.34	2.28	2.24	2.14	2.15	2.30	2.20	2.37
Ca	0.00	0.00	0.00	0.00	0.00	0.01	0.00	0.00	0.00	0.00	0.00	0.00	0.00	0.00	0.00	0.00
Na	0.03	0.03	0.03	0.04	0.03	0.04	0.04	0.05	0.03	0.03	0.04	0.04	0.03	0.04	0.04	0.02
K	2.02	2.03	2.01	1.99	2.00	1.97	2.02	1.99	2.01	2.01	1.98	1.91	1.87	1.96	1.92	2.01
OH	3.74	3.78	3.71	3.77	3.71	3.72	3.79	3.75	3.68	3.70	3.71	3.72	3.76	3.79	3.73	3.69
F	0.26	0.22	0.29	0.23	0.29	0.27	0.21	0.25	0.32	0.30	0.29	0.28	0.24	0.21	0.27	0.31
Cl	0.00	0.00	0.00	0.00	0.00	0.01	0.00	0.00	0.00	0.00	0.00	0.00	0.00	0.00	0.00	0.00
XMg	0.50	0.49	0.49	0.50	0.49	0.49	0.49	0.49	0.50	0.50	0.49	0.49	0.48	0.51	0.50	0.50
Oxygen	22	22	22	22	22	22	22	22	22	22	22	22	22	22	22	22

Table B3. Biotite geochemistry.

MK258																								
Location	In grt	In grt	In grt	In grt	In grt	In grt	Matrix	Matrix	Matrix	Matrix	Matrix	Matrix	Matrix	Matrix	Matrix	Matrix	Matrix	Matrix	Matrix	Matrix	Matrix	Matrix	Matrix	Matrix
SiO2	36.61	36.84	36.72	36.66	36.72	36.70	36.22	36.45	36.95	36.08	36.46	36.14	36.46	36.18	36.14	36.38	36.48	36.50	36.42	36.56	36.27	36.27	36.02	36.42
TiO2	2.48	2.51	2.52	2.49	2.54	2.50	2.73	2.73	2.58	2.26	2.77	2.73	2.55	2.42	2.57	2.91	2.54	2.40	2.69	2.87	3.03	2.77	2.81	2.96
Al2O3	19.72	20.03	19.61	18.98	19.14	19.08	19.01	19.22	20.38	18.79	19.18	19.25	19.19	18.80	19.30	19.14	19.78	19.18	19.44	18.69	18.83	18.53	18.26	18.90
FeO	11.19	11.08	11.30	12.23	12.21	12.11	12.38	12.79	12.57	13.57	12.84	12.43	12.56	13.22	12.84	12.90	12.29	13.05	12.57	12.97	12.68	12.99	13.65	12.66
MnO	0.01	0.00	0.03	0.03	0.03	0.01	0.02	0.07	0.00	0.05	0.03	0.01	0.07	0.04	0.03	0.02	0.05	0.05	0.05	0.03	0.04	0.05	0.06	0.02
MgO	15.88	16.08	16.42	15.93	16.07	15.97	14.96	15.18	14.07	15.37	15.15	14.84	15.19	15.07	15.30	14.90	15.15	15.14	15.07	15.01	15.05	14.97	15.15	14.99
CaO	0.01	0.00	0.00	0.00	0.00	0.00	0.00	0.00	0.00	0.00	0.00	0.09	0.00	0.00	0.00	0.00	0.00	0.01	0.00	0.01	0.00	0.00	0.00	0.00
Na2O	0.19	0.13	0.13	0.19	0.15	0.14	0.09	0.13	0.09	0.11	0.11	0.10	0.12	0.09	0.10	0.09	0.10	0.13	0.11	0.11	0.09	0.09	0.10	0.10
K2O	10.08	10.18	10.30	9.97	10.27	10.33	10.35	10.38	9.92	10.19	10.31	10.10	10.34	10.25	10.43	10.50	10.37	10.27	10.53	10.26	10.46	10.41	10.22	10.28
Cl	0.77	0.88	0.88	0.81	0.91	0.82	0.56	0.66	0.78	0.80	0.83	0.85	0.76	0.91	0.80	0.84	0.83	0.72	0.61	0.84	0.88	0.81	0.78	0.86
F	0.01	0.00	0.00	0.01	0.01	0.00	0.00	0.01	0.00	0.01	0.01	0.02	0.00	0.01	0.01	0.00	0.01	0.00	0.00	0.01	0.00	0.00	0.00	0.01
H2O	3.76	3.75	3.74	3.73	3.71	3.74	3.81	3.80	3.76	3.70	3.72	3.67	3.74	3.64	3.72	3.71	3.73	3.76	3.83	3.70	3.68	3.69	3.70	3.69
Total	100.71	101.47	101.64	101.04	101.77	101.39	100.13	101.42	101.12	100.94	101.40	100.23	100.98	100.63	101.23	101.39	101.33	101.22	101.31	101.06	101.00	100.57	100.76	100.89
Si	5.32	5.31	5.30	5.33	5.32	5.33	5.33	5.31	5.36	5.30	5.31	5.32	5.33	5.33	5.28	5.31	5.30	5.33	5.30	5.35	5.31	5.34	5.31	5.33
Al iv	2.68	2.69	2.70	2.67	2.68	2.67	2.67	2.69	2.64	2.70	2.69	2.68	2.67	2.67	2.72	2.69	2.70	2.67	2.70	2.65	2.69	2.66	2.69	2.67
Al vi	0.69	0.71	0.63	0.59	0.58	0.59	0.63	0.60	0.84	0.56	0.60	0.65	0.63	0.59	0.60	0.60	0.69	0.63	0.64	0.57	0.56	0.56	0.48	0.59
Ti	0.27	0.27	0.27	0.27	0.28	0.27	0.30	0.30	0.28	0.25	0.30	0.30	0.28	0.27	0.28	0.32	0.28	0.26	0.29	0.32	0.33	0.31	0.31	0.33
Fe	1.36	1.33	1.36	1.49	1.48	1.47	1.52	1.56	1.52	1.67	1.56	1.53	1.53	1.63	1.57	1.57	1.49	1.59	1.53	1.59	1.55	1.60	1.68	1.55
Mn	0.00	0.00	0.00	0.00	0.00	0.00	0.00	0.01	0.00	0.01	0.00	0.00	0.01	0.01	0.00	0.00	0.01	0.01	0.01	0.00	0.00	0.01	0.01	0.00
Mg	3.44	3.45	3.53	3.46	3.47	3.46	3.28	3.30	3.04	3.37	3.29	3.25	3.31	3.31	3.33	3.24	3.28	3.29	3.27	3.27	3.29	3.29	3.33	3.27
Ca	0.00	0.00	0.00	0.00	0.00	0.00	0.00	0.00	0.00	0.00	0.00	0.01	0.00	0.00	0.00	0.00	0.00	0.00	0.00	0.00	0.00	0.00	0.00	0.00
Na	0.05	0.04	0.04	0.05	0.04	0.04	0.03	0.04	0.03	0.03	0.03	0.03	0.03	0.03	0.03	0.03	0.03	0.04	0.03	0.03	0.03	0.03	0.03	0.03
K	1.87	1.87	1.89	1.85	1.90	1.91	1.94	1.93	1.83	1.91	1.92	1.89	1.93	1.93	1.94	1.95	1.92	1.91	1.96	1.92	1.95	1.95	1.92	1.92
OH	3.64	3.60	3.60	3.62	3.58	3.62	3.74	3.69	3.64	3.63	3.62	3.60	3.65	3.57	3.63	3.61	3.62	3.67	3.72	3.61	3.59	3.62	3.64	3.60
F	0.35	0.40	0.40	0.37	0.42	0.38	0.26	0.30	0.36	0.37	0.38	0.40	0.35	0.43	0.37	0.39	0.38	0.33	0.28	0.39	0.41	0.38	0.36	0.40
Cl	0.00	0.00	0.00	0.00	0.00	0.00	0.00	0.00	0.00	0.00	0.00	0.00	0.00	0.00	0.00	0.00	0.00	0.00	0.00	0.00	0.00	0.00	0.00	0.00
XMg	0.72	0.72	0.72	0.70	0.70	0.70	0.68	0.68	0.67	0.67	0.68	0.68	0.68	0.67	0.68	0.67	0.69	0.67	0.68	0.67	0.68	0.67	0.66	0.68
Oxygen	22	22	22	22	22	22	22	22	22	22	22	22	22	22	22	22	22	22	22	22	22	22	22	22

Table B3. Biotite geochemistry.

MK262																					
Location	In grt	In grt	In grt	Matrix	Matrix	Matrix	Matrix	Matrix	Matrix	Matrix	Matrix	Matrix	Matrix	Matrix	Matrix	Matrix	Matrix	Matrix	Matrix	Matrix	Matrix
SiO2	34.44	35.10	35.09	35.10	34.91	34.56	35.23	34.30	35.02	35.26	34.47	34.70	34.74	34.49	35.20	34.95	34.76	34.78	34.95	34.92	34.94
TiO2	4.02	4.02	3.98	4.91	4.83	4.41	4.77	4.59	4.21	2.74	5.00	4.73	5.01	4.88	5.18	5.04	5.00	4.90	4.25	3.98	3.83
Al2O3	17.94	17.95	18.00	17.79	17.62	17.46	17.50	17.49	17.89	18.57	17.37	17.88	17.60	17.92	17.61	17.76	18.00	17.62	17.61	17.63	17.56
FeO	18.14	18.46	18.24	17.87	18.34	17.77	18.12	18.21	17.73	17.02	18.42	17.92	18.60	17.73	18.10	17.94	17.89	18.08	18.52	18.63	18.51
MnO	0.04	0.00	0.05	0.04	0.03	0.02	0.05	0.06	0.01	0.02	0.03	0.03	0.03	0.04	0.06	0.04	0.01	0.00	0.03	0.00	0.04
MgO	10.60	10.85	10.67	10.21	10.11	10.82	10.74	10.34	10.83	11.58	10.41	10.61	10.19	10.14	9.90	10.38	10.17	10.43	10.60	10.77	11.11
CaO	0.00	0.00	0.00	0.00	0.00	0.00	0.00	0.00	0.00	0.00	0.00	0.00	0.00	0.00	0.00	0.00	0.00	0.00	0.00	0.00	0.00
Na2O	0.16	0.12	0.14	0.13	0.12	0.15	0.15	0.16	0.19	0.13	0.12	0.14	0.15	0.15	0.17	0.14	0.14	0.12	0.11	0.14	0.15
K2O	10.16	10.15	10.07	10.27	10.26	10.19	10.29	10.05	10.38	9.75	10.18	10.30	10.17	10.11	10.26	10.28	10.29	10.37	10.23	10.25	10.25
Cl	1.14	1.14	1.30	1.11	1.00	1.02	1.17	0.96	0.99	1.20	1.04	0.99	0.97	0.91	0.99	1.07	0.90	0.99	1.02	1.12	1.26
F	0.00	0.00	0.00	0.00	0.00	0.00	0.00	0.04	0.00	0.00	0.00	0.00	0.00	0.00	0.00	0.00	0.00	0.00	0.00	0.01	0.00
H2O	3.39	3.44	3.36	3.45	3.49	3.45	3.44	3.45	3.50	3.39	3.45	3.50	3.51	3.51	3.51	3.47	3.54	3.50	3.48	3.43	3.37
Total	100.03	101.23	100.90	100.88	100.71	99.85	101.46	99.65	100.75	99.66	100.49	100.80	100.97	99.88	100.98	101.07	100.70	100.79	100.80	100.88	101.02
Si	5.25	5.28	5.30	5.29	5.28	5.27	5.29	5.25	5.28	5.34	5.24	5.24	5.25	5.25	5.30	5.26	5.25	5.26	5.29	5.29	5.28
Al iv	2.75	2.72	2.70	2.71	2.72	2.73	2.71	2.75	2.72	2.66	2.76	2.76	2.75	2.75	2.70	2.74	2.75	2.74	2.71	2.71	2.72
Al vi	0.48	0.47	0.50	0.45	0.43	0.41	0.39	0.41	0.47	0.65	0.35	0.42	0.39	0.46	0.43	0.42	0.45	0.40	0.43	0.43	0.42
Ti	0.46	0.45	0.45	0.56	0.55	0.51	0.54	0.53	0.48	0.31	0.57	0.54	0.57	0.56	0.59	0.57	0.57	0.56	0.48	0.45	0.44
Fe	2.31	2.32	2.30	2.25	2.32	2.27	2.28	2.33	2.24	2.15	2.34	2.26	2.35	2.26	2.28	2.26	2.26	2.29	2.34	2.36	2.34
Mn	0.01	0.00	0.01	0.01	0.00	0.00	0.01	0.01	0.00	0.00	0.00	0.00	0.00	0.01	0.01	0.01	0.00	0.00	0.00	0.00	0.01
Mg	2.41	2.43	2.40	2.29	2.28	2.46	2.40	2.36	2.44	2.61	2.36	2.39	2.30	2.30	2.22	2.33	2.29	2.35	2.39	2.43	2.51
Ca	0.00	0.00	0.00	0.00	0.00	0.00	0.00	0.00	0.00	0.00	0.00	0.00	0.00	0.00	0.00	0.00	0.00	0.00	0.00	0.00	0.00
Na	0.05	0.04	0.04	0.04	0.04	0.04	0.04	0.05	0.06	0.04	0.04	0.04	0.04	0.04	0.05	0.04	0.04	0.04	0.03	0.04	0.04
K	1.98	1.95	1.94	1.98	1.98	1.98	1.97	1.96	2.00	1.88	1.97	1.98	1.96	1.96	1.97	1.97	1.98	2.00	1.97	1.98	1.98
OH	3.45	3.46	3.38	3.47	3.52	3.51	3.44	3.52	3.53	3.43	3.50	3.53	3.54	3.56	3.53	3.49	3.57	3.53	3.51	3.46	3.40
F	0.55	0.54	0.62	0.53	0.48	0.49	0.56	0.46	0.47	0.57	0.50	0.47	0.46	0.44	0.47	0.51	0.43	0.47	0.49	0.54	0.60
Cl	0.00	0.00	0.00	0.00	0.00	0.00	0.00	0.01	0.00	0.00	0.00	0.00	0.00	0.00	0.00	0.00	0.00	0.00	0.00	0.00	0.00
XMg	0.51	0.51	0.51	0.50	0.50	0.52	0.51	0.50	0.52	0.55	0.50	0.51	0.49	0.50	0.49	0.51	0.50	0.51	0.50	0.51	0.52
Oxygen	22	22	22	22	22	22	22	22	22	22	22	22	22	22	22	22	22	22	22	22	22

Table B3. Biotite geochemistry.

MK268																										
Location	In Grt	In Grt	In Grt	In Grt	Matrix	Matrix	Matrix	Matrix	Matrix	Matrix	Matrix	Matrix	Matrix	Matrix	Matrix	Matrix	Matrix	Matrix	Matrix	Matrix	Matrix	Matrix	Matrix	Matrix	Matrix	Matrix
SiO2	36.46	36.00	35.32	35.37	34.40	34.79	34.76	34.55	34.61	34.81	34.55	34.53	34.83	34.77	35.01	34.85	34.66	34.50	34.78	34.87	34.74	34.27	34.79	34.91	34.54	34.48
TiO2	4.87	4.84	3.48	3.41	5.71	5.61	5.27	5.78	5.28	4.96	4.92	5.35	5.17	4.76	5.19	5.56	5.34	5.37	5.51	5.48	5.49	5.40	5.30	4.90	5.44	5.48
Al2O3	16.44	16.46	17.93	18.21	16.62	17.53	17.89	16.99	16.92	17.11	17.29	17.24	17.03	17.42	17.41	17.19	17.47	17.02	17.30	17.40	17.30	17.16	17.23	17.41	17.24	17.27
FeO	13.36	13.33	12.87	12.97	17.88	17.55	17.16	18.23	18.07	17.70	17.18	17.74	17.93	17.48	17.83	17.87	17.26	17.57	17.41	17.05	17.48	17.50	17.81	17.51	17.18	17.34
MnO	0.00	0.01	0.02	0.00	0.06	0.03	0.02	0.01	0.03	0.05	0.04	0.04	0.03	0.05	0.04	0.03	0.04	0.03	0.04	0.02	0.00	0.03	0.04	0.04	0.05	0.06
MgO	15.13	15.04	14.33	14.37	10.80	10.50	10.49	10.17	10.86	11.39	11.13	10.96	11.06	11.30	10.88	10.49	10.73	10.33	10.83	10.68	10.66	10.43	10.55	11.08	10.40	10.67
CaO	0.00	0.00	0.00	0.00	0.00	0.00	0.00	0.00	0.00	0.00	0.00	0.00	0.00	0.00	0.00	0.00	0.00	0.06	0.00	0.00	0.00	0.00	0.00	0.00	0.00	0.00
Na2O	0.18	0.16	0.07	0.06	0.09	0.09	0.09	0.09	0.08	0.11	0.11	0.09	0.07	0.07	0.11	0.14	0.13	0.13	0.13	0.09	0.09	0.17	0.14	0.12	0.11	0.10
K2O	9.60	9.94	10.54	10.48	10.37	10.24	10.40	10.35	10.28	10.39	10.42	10.37	10.43	10.40	10.24	10.45	10.29	10.06	10.34	10.17	10.29	10.22	10.34	10.12	10.24	10.27
Cl	1.49	1.47	1.32	1.43	1.05	0.89	0.95	0.84	1.01	1.03	1.08	1.05	0.96	1.18	1.11	0.89	0.95	0.84	1.18	1.06	1.05	0.94	1.06	1.08	0.96	1.04
F	0.00	0.01	0.01	0.00	0.00	0.00	0.00	0.00	0.00	0.00	0.00	0.00	0.00	0.00	0.00	0.00	0.00	0.01	0.00	0.00	0.00	0.01	0.00	0.00	0.00	0.00
H2O	3.36	3.35	3.36	3.33	3.44	3.56	3.52	3.55	3.47	3.49	3.44	3.47	3.52	3.41	3.46	3.55	3.51	3.52	3.42	3.46	3.47	3.47	3.46	3.46	3.48	3.45
Total	100.89	100.61	99.25	99.63	100.42	100.79	100.55	100.56	100.61	101.04	100.16	100.84	101.03	100.84	101.28	101.02	100.38	99.44	100.94	100.28	100.57	99.60	100.72	100.63	99.64	100.16
Si	5.37	5.34	5.30	5.29	5.23	5.24	5.24	5.24	5.25	5.25	5.25	5.22	5.26	5.25	5.26	5.26	5.24	5.27	5.24	5.27	5.25	5.24	5.26	5.27	5.27	5.24
Al iv	2.63	2.66	2.70	2.71	2.77	2.76	2.76	2.76	2.75	2.75	2.75	2.78	2.74	2.75	2.74	2.74	2.76	2.73	2.76	2.73	2.75	2.76	2.74	2.73	2.73	2.76
Al vi	0.23	0.21	0.48	0.50	0.22	0.36	0.43	0.28	0.27	0.29	0.34	0.29	0.29	0.35	0.34	0.31	0.36	0.34	0.32	0.37	0.34	0.33	0.34	0.37	0.36	0.33
Ti	0.54	0.54	0.39	0.38	0.65	0.64	0.60	0.66	0.60	0.56	0.56	0.61	0.59	0.54	0.59	0.63	0.61	0.62	0.62	0.62	0.62	0.62	0.60	0.56	0.62	0.63
Fe	1.65	1.65	1.62	1.62	2.28	2.21	2.17	2.31	2.29	2.23	2.18	2.24	2.26	2.21	2.24	2.25	2.18	2.25	2.20	2.16	2.21	2.24	2.25	2.21	2.19	2.20
Mn	0.00	0.00	0.00	0.00	0.01	0.00	0.00	0.00	0.00	0.01	0.01	0.01	0.00	0.01	0.01	0.00	0.01	0.00	0.01	0.00	0.00	0.00	0.01	0.01	0.01	0.01
Mg	3.32	3.32	3.21	3.20	2.45	2.36	2.36	2.30	2.46	2.56	2.52	2.47	2.49	2.54	2.44	2.36	2.42	2.35	2.43	2.41	2.40	2.38	2.38	2.49	2.36	2.42
Ca	0.00	0.00	0.00	0.00	0.00	0.00	0.00	0.00	0.00	0.00	0.00	0.00	0.00	0.00	0.00	0.00	0.00	0.01	0.00	0.00	0.00	0.00	0.00	0.00	0.00	0.00
Na	0.05	0.05	0.02	0.02	0.03	0.03	0.03	0.03	0.02	0.03	0.03	0.03	0.02	0.02	0.03	0.04	0.04	0.04	0.04	0.03	0.03	0.05	0.04	0.04	0.03	0.03
K	1.80	1.88	2.02	2.00	2.01	1.97	2.00	2.00	1.99	2.00	2.02	2.00	2.01	2.00	1.96	2.01	1.99	1.96	1.99	1.96	1.98	1.99	2.00	1.95	1.99	1.99
OH	3.31	3.31	3.37	3.32	3.49	3.58	3.55	3.60	3.52	3.51	3.48	3.50	3.54	3.44	3.47	3.58	3.55	3.59	3.44	3.49	3.50	3.54	3.49	3.48	3.54	3.50
F	0.69	0.69	0.63	0.68	0.51	0.42	0.45	0.40	0.48	0.49	0.52	0.50	0.46	0.56	0.53	0.42	0.45	0.41	0.56	0.51	0.50	0.45	0.51	0.52	0.46	0.50
Cl	0.00	0.00	0.00	0.00	0.00	0.00	0.00	0.00	0.00	0.00	0.00	0.00	0.00	0.00	0.00	0.00	0.00	0.00	0.00	0.00	0.00	0.00	0.00	0.00	0.00	0.00
XMg	0.67	0.67	0.66	0.66	0.52	0.52	0.52	0.50	0.52	0.53	0.54	0.52	0.52	0.54	0.52	0.51	0.53	0.51	0.53	0.53	0.52	0.52	0.51	0.53	0.52	0.52
Oxygen	22	22	22	22	22	22	22	22	22	22	22	22	22	22	22	22	22	22	22	22	22	22	22	22	22	22

Table B4. Effective bulk rock composition used for phase equilibria modelling

	MK256		MK258		MK262		MK268	
	Oxide Wt %	Mole % Cations	Oxide Wt %	Mole % Cations	Oxide Wt %	Mole % Cations	Oxide Wt %	Mole % Cations
MnO	0.08	0.0744	0.08	0.0695	0.13	0.1047	0.11	0.0904
Na2O	1.44	3.0652	1.96	3.8987	2.00	3.6884	3.00	5.6433
CaO	2.82	3.2320	2.07	2.1958	0.71	0.6431	1.50	1.4840
K2O	3.96	5.5463	2.26	2.9579	5.36	6.5041	3.53	4.3691
FeO		6.1424		3.5540		4.7194		4.1054
MgO	3.01	4.9264	3.43	5.2459	1.65	2.3397	1.74	2.5166
Al2O3	16.74	21.6602	12.59	15.2228	18.48	20.7167	14.82	16.9459
SiO2	49.73	54.5972	64.71	66.3873	63.77	60.6567	66.17	64.1980
TiO2	0.84	0.6938	0.56	0.4322	0.81	0.5796	0.83	0.6058
H2O		0.0000		0.0000		0.0000		0.0000
Fe2O3	7.51	0.0620	4.65	0.0359	6.66	0.0477	5.68	0.0415
P2O5	0.11	0.0000	0.11	0.0000	0.12	0.0000	0.11	0.0000
S		0.0000		0.0000		0.0000		0.0000
∑	86.24	100.00	92.42	100.00	99.69	100.00	97.49	100.00
H2O SS		12.2700		9.2665		14.0410		9.0459
H2O CW		5.7807		6.5455		2.6815		4.1896

For all specimens:
Fe 3+ set at 1 %
50% P2O5 (apatite correction)

SS - saturated solidus
CW - calculated water

APPENDIX C

Supporting materials for Chapter 5

Chapter 5 Contact metamorphism of the Tethyan Sedimentary Sequence, Upper Mustang region, west-central Nepal

Appendix C1. Heat diffusion parameters

Figure C1. Monazite X-ray maps and BSE images for metamorphic specimens

Figure C2. BSE images of accessory minerals in metamorphic specimens

Table C1. Compositional mineral analyses for garnet, biotite, muscovite and feldspar

Table C2. Trace element composition of garnet

Table C3. Monazite U-Th-Pb geochronology data and trace elements

Table C4. Modal proportions of minerals

Table C5. Temperature and pressure estimates for metamorphic specimens

Table C6. Whole-rock XRF analysis (wt. %)

Table C7. Thermal diffusion model of a sheet-like intrusion

APPENDIX

C1. Heat diffusion parameters

Thermal diffusivity: 31.5 m2/year

Initial temp. of magma: 750 °C (Montel, 1993; Godin et al. 2006)

Radius/half-thickness of a pluton: 10 000 m

Distance from the pluton: 22 m (UM09), 361 m (UM07), 445 m (UM05), 1 500 m

Time: 0 (0.1 in error function), 10 000, 100 000, 500 000, 1 000 000, 2 000 000 years

Initial temp. of rocks: 0 °C, 450 °C* (geothermal gradient 25 °C/km at 18 km depth)

* initial temperature used in calculation as in Jaeger, 1964; 1968

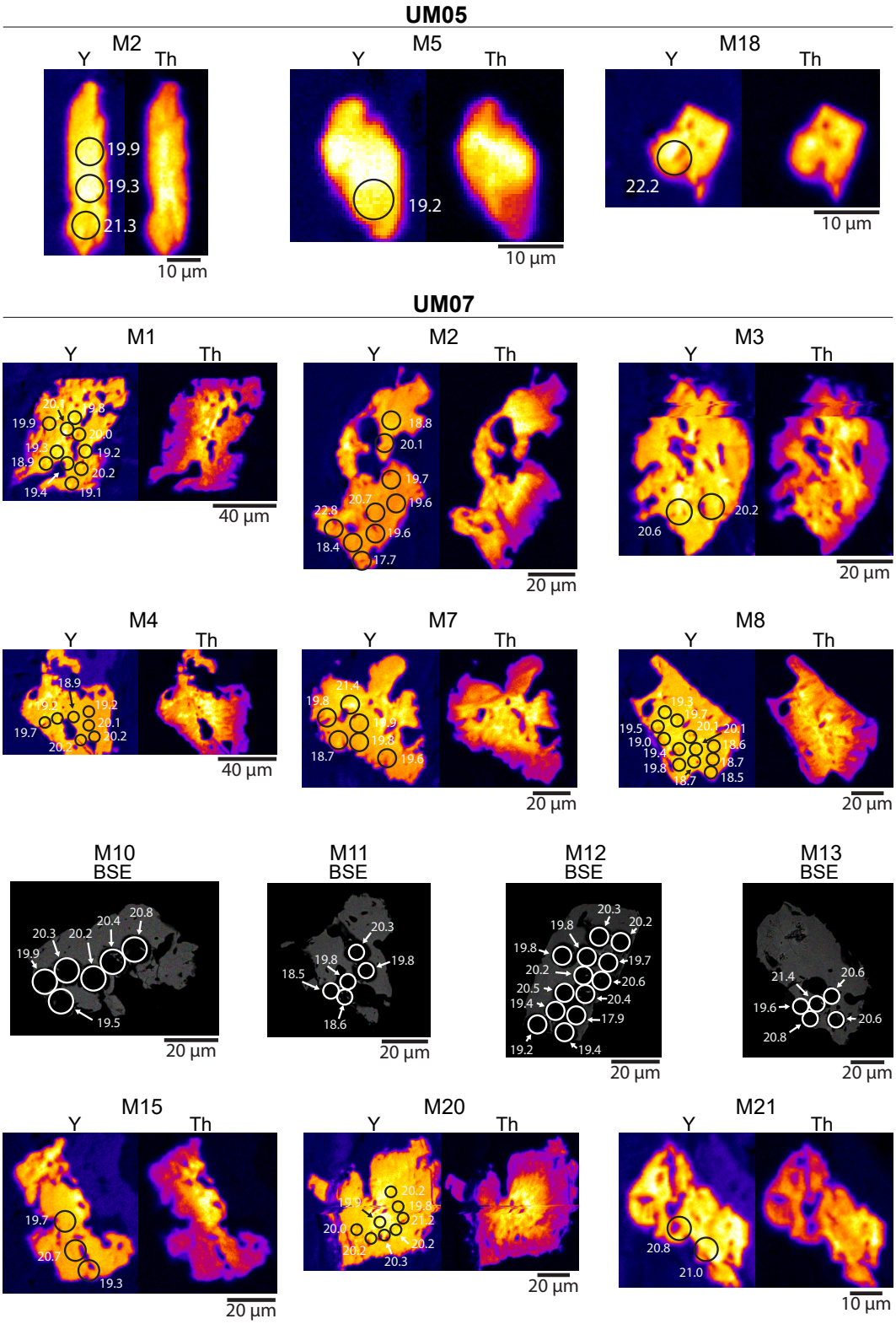

Figure C1. Monazite X-ray maps and BSE images for metamorphic specimens. Black/dark purple colour represents the lowest concentration, while yellow/white represents the highest concentration of each element.

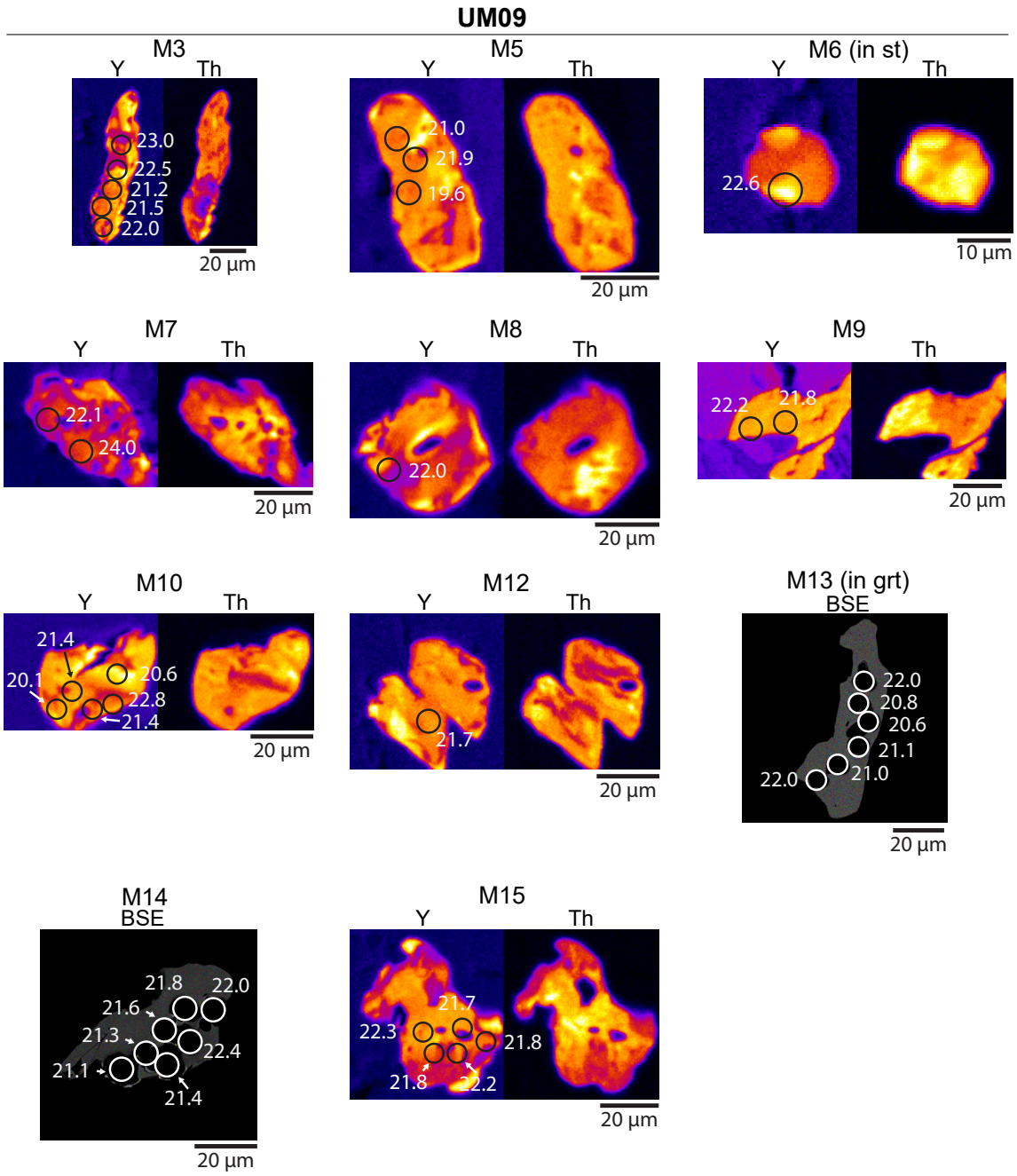

Figure C1. Continued

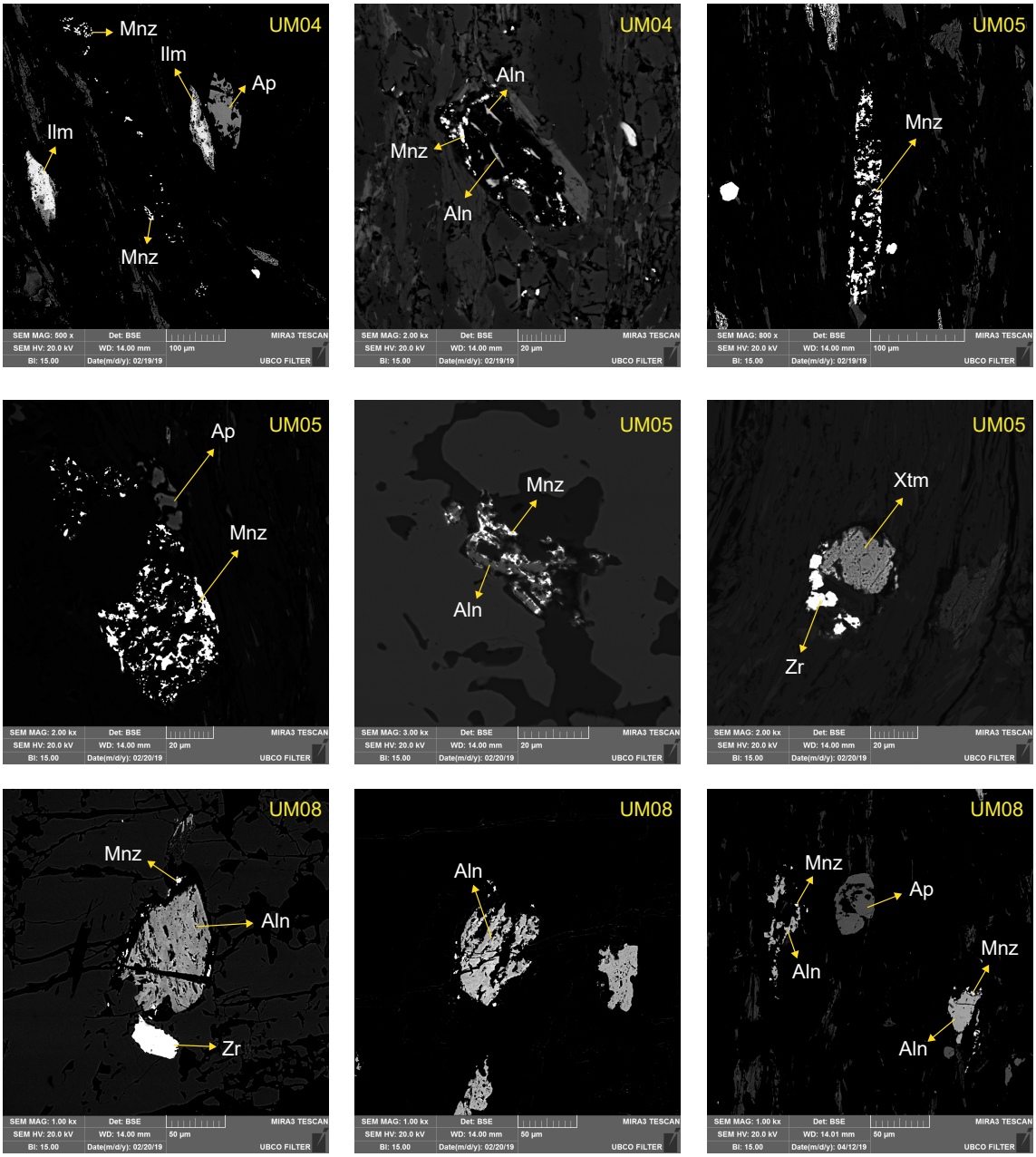

Figure C2. BSE images of accessory minerals in metamorphic specimens. Apatite and allanite occur as common phases in specimens with monazite scarcity. Allanite is partially replaced by monazite.

Table C1. Compositional mineral analysis for garnet, biotite, muscovite and feldspa

UM04 Garnet

Analysis #	1/2.	1/3.	1/4.	1/5.	1/6.	1/7.	1/8.	1/9.	1/10.	1/11.	1/12.	1/13.	1/14.	1/15.	1/16.	1/17.	1/18.	1/19.	1/20.	1/21.	1/22.	1/23.	1/24.	1/25.	1/26.	1/27.	1/28.	1/29.	1/30.
SiO2	37.16	37.12	37.03	37.11	36.82	36.75	37.07	36.76	36.80	36.58	36.88	36.78	36.75	36.83	36.67	36.52	36.63	36.63	36.70	36.74	36.71	36.70	36.74	36.75	36.81	36.83	36.59	36.61	36.45
TiO2	0.09	0.10	0.10	0.09	0.11	0.11	0.12	0.10	0.10	0.12	0.11	0.11	0.11	0.12	0.11	0.10	0.09	0.11	0.11	0.11	0.12	0.09	0.13	0.11	0.10	0.11	0.09	0.10	0.08
Al2O3	21.27	21.23	21.07	21.12	21.11	20.98	21.17	20.94	21.05	21.12	21.01	21.03	20.84	21.18	21.05	21.02	21.09	20.91	21.02	20.99	21.16	21.04	21.10	21.03	20.99	20.93	21.15	21.00	20.86
FeO	35.03	34.98	34.52	34.50	34.55	33.97	33.60	33.45	33.29	33.00	32.74	32.59	32.39	32.02	32.03	32.34	32.44	32.43	32.52	33.08	33.01	33.35	33.40	33.67	34.21	34.45	35.21	35.22	35.11
MnO	2.58	2.97	3.26	3.54	3.96	4.23	4.41	4.72	4.77	4.80	5.00	5.32	5.58	5.54	5.45	5.61	5.52	5.39	5.18	5.12	4.79	4.67	4.34	4.06	3.69	3.38	3.18	2.71	2.42
MgO	2.52	2.36	2.23	2.14	2.01	1.96	1.92	1.91	1.84	1.84	1.77	1.76	1.77	1.74	1.72	1.72	1.73	1.74	1.79	1.81	1.81	1.86	1.88	1.95	2.06	2.15	2.28	2.45	2.56
CaO	2.32	2.42	2.48	2.44	2.46	2.62	2.78	2.65	2.77	2.89	2.90	2.84	2.75	3.02	2.92	2.96	3.03	3.02	3.09	2.83	2.97	2.79	3.11	2.82	2.58	2.58	2.44	2.46	2.24
Na2O	0.01	0.00	0.00	0.00	0.02	0.00	0.02	0.00	0.00	0.00	0.01	0.02	0.00	0.01	0.01	0.01	0.01	0.01	0.01	0.00	0.01	0.00	0.02	0.02	0.01	0.01	0.01	0.01	0.00
K2O	0.01	0.02	0.03	0.03	0.03	0.02	0.02	0.02	0.02	0.03	0.02	0.02	0.02	0.03	0.02	0.02	0.03	0.02	0.02	0.03	0.02	0.02	0.02	0.02	0.03	0.02	0.03	0.02	0.03
P2O5	0.06	0.03	0.05	0.06	0.05	0.07	0.04	0.07	0.05	0.06	0.04	0.05	0.04	0.05	0.05	0.05	0.06	0.04	0.05	0.05	0.05	0.06	0.05	0.05	0.06	0.07	0.05	0.06	0.06
Total	101.05	101.23	100.77	101.03	101.12	100.71	101.15	100.62	100.69	100.44	100.48	100.52	100.25	100.54	100.03	100.35	100.63	100.30	100.49	100.76	100.65	100.58	100.79	100.48	100.54	100.53	101.03	100.64	99.81
Si	2.98	2.97	2.98	2.98	2.96	2.97	2.98	2.97	2.97	2.96	2.98	2.97	2.98	2.97	2.98	2.96	2.96	2.97	2.97	2.97	2.96	2.97	2.96	2.97	2.97	2.97	2.95	2.95	2.96
Al iv	0.02	0.03	0.02	0.02	0.04	0.03	0.02	0.03	0.03	0.04	0.02	0.03	0.02	0.03	0.02	0.04	0.04	0.03	0.03	0.03	0.04	0.03	0.04	0.03	0.03	0.03	0.05	0.05	0.04
Al vi	1.98	1.98	1.98	1.98	1.97	1.97	1.98	1.97	1.97	1.98	1.98	1.98	1.97	1.99	1.99	1.97	1.97	1.97	1.97	1.97	1.98	1.97	1.97	1.97	1.97	1.97	1.95	1.95	1.96
Ti	0.01	0.01	0.01	0.01	0.01	0.01	0.01	0.01	0.01	0.01	0.01	0.01	0.01	0.01	0.01	0.01	0.01	0.01	0.01	0.01	0.01	0.01	0.01	0.01	0.01	0.01	0.01	0.01	0.00
Fe3+	0.01	0.02	0.01	0.01	0.02	0.02	0.01	0.02	0.02	0.01	0.01	0.01	0.02	0.00	0.00	0.02	0.02	0.02	0.02	0.02	0.01	0.02	0.02	0.02	0.02	0.02	0.04	0.04	0.03
Fe2+	2.34	2.33	2.31	2.30	2.30	2.27	2.24	2.24	2.23	2.22	2.20	2.19	2.18	2.16	2.17	2.17	2.17	2.18	2.18	2.21	2.22	2.23	2.23	2.26	2.29	2.30	2.33	2.34	2.36
Mn	0.18	0.20	0.22	0.24	0.27	0.29	0.30	0.32	0.33	0.33	0.34	0.36	0.38	0.38	0.37	0.39	0.38	0.37	0.35	0.35	0.33	0.32	0.30	0.28	0.25	0.23	0.22	0.19	0.17
Mg	0.30	0.28	0.27	0.26	0.24	0.24	0.23	0.23	0.22	0.22	0.21	0.21	0.21	0.21	0.21	0.21	0.21	0.21	0.22	0.22	0.22	0.22	0.23	0.23	0.25	0.26	0.27	0.29	0.31
Ca	0.20	0.21	0.21	0.21	0.21	0.23	0.24	0.23	0.24	0.25	0.25	0.25	0.24	0.26	0.25	0.26	0.26	0.26	0.27	0.24	0.26	0.24	0.27	0.24	0.22	0.22	0.21	0.21	0.19
Alm	0.78	0.77	0.77	0.77	0.76	0.75	0.74	0.74	0.74	0.73	0.73	0.73	0.72	0.72	0.72	0.72	0.72	0.72	0.72	0.73	0.73	0.74	0.74	0.75	0.76	0.76	0.77	0.77	0.78
Grs	0.07	0.07	0.07	0.07	0.07	0.08	0.08	0.08	0.08	0.08	0.08	0.08	0.08	0.09	0.08	0.09	0.09	0.09	0.09	0.08	0.09	0.08	0.09	0.08	0.07	0.07	0.07	0.07	0.06
Prp	0.10	0.09	0.09	0.09	0.08	0.08	0.08	0.08	0.07	0.07	0.07	0.07	0.07	0.07	0.07	0.07	0.07	0.07	0.07	0.07	0.07	0.07	0.07	0.08	0.08	0.09	0.09	0.10	0.10
Sps	0.06	0.07	0.07	0.08	0.09	0.10	0.10	0.11	0.11	0.11	0.11	0.12	0.13	0.13	0.12	0.13	0.13	0.12	0.12	0.12	0.11	0.11	0.10	0.09	0.08	0.08	0.07	0.06	0.06
Oxygen	12	12	12	12	12	12	12	12	12	12	12	12	12	12	12	12	12	12	12	12	12	12	12	12	12	12	12	12	12

UM05 Garnet

Analysis #	6/2.	6/3.	6/4.	6/5.	6/6.	6/7.	6/8.	6/9.	6/10.	6/13.	6/14.	6/23.	6/30.	6/34.	6/36.	6/38.	6/41.	6/46.	6/49.	6/50.	6/52.	6/53.	6/54.	6/56.	6/59.	6/60.	6/61.	6/62.	6/63.	6/64.	6/65.	6/66.	6/67.	6/68.	6/69.
SiO2	36.47	36.63	36.55	36.78	36.72	36.59	36.72	36.83	36.84	36.82	36.45	36.59	36.71	36.59	36.57	36.87	36.64	36.63	36.60	36.50	36.63	36.58	36.56	36.35	36.58	36.56	36.61	36.53	36.65	36.99	36.54	36.68	36.61	36.78	37.00
TiO2	0.12	0.12	0.12	0.12	0.15	0.15	0.14	0.13	0.16	0.15	0.16	0.17	0.18	0.19	0.18	0.18	0.16	0.18	0.18	0.17	0.16	0.17	0.16	0.14	0.15	0.14	0.13	0.13	0.11	0.12	0.13	0.13	0.11	0.10	0.11
Al2O3	19.74	19.86	19.75	19.59	19.63	19.72	19.43	19.74	19.47	19.64	19.66	19.67	19.69	19.68	19.66	19.63	19.64	19.45	19.68	19.62	19.46	19.77	19.59	20.05	19.70	19.61	19.62	19.57	19.63	20.01	19.64	19.78	19.70	19.74	19.98
FeO	34.79	33.89	33.23	32.74	32.36	31.82	31.47	31.05	30.46	30.06	29.92	28.58	28.23	28.03	28.09	27.73	28.38	28.65	29.01	28.92	29.37	29.35	29.71	30.16	30.61	30.93	31.48	32.23	32.93	32.64	33.16	33.67	34.38	34.86	35.45
MnO	2.03	2.64	3.33	3.72	4.26	4.68	5.07	5.55	5.90	6.58	6.58	7.61	7.85	8.07	8.21	8.08	8.08	7.61	7.38	7.25	6.93	6.82	6.42	6.11	5.78	5.51	4.99	4.60	3.98	3.48	3.19	2.74	2.34	1.88	1.66
MgO	2.24	1.97	1.82	1.61	1.56	1.50	1.43	1.38	1.33	1.29	1.31	1.23	1.22	1.14	1.15	1.14	1.19	1.21	1.21	1.20	1.24	1.25	1.29	1.33	1.36	1.39	1.47	1.54	1.67	1.65	1.80	1.97	2.15	2.33	2.41
CaO	3.34	3.87	4.02	4.30	4.16	4.18	4.37	4.53	4.39	4.26	4.56	4.73	4.76	4.86	4.69	4.80	4.41	4.73	4.76	4.79	4.76	4.76	4.77	4.29	4.71	4.35	4.40	4.12	3.83	4.09	4.00	3.80	3.35	3.22	2.61
Na2O	0.01	0.02	0.02	0.01	0.01	0.02	0.01	0.01	0.00	0.01	0.01	0.01	0.00	0.01	0.00	0.01	0.01	0.01	0.00	0.01	0.00	0.00	0.02	0.02	0.01	0.01	0.01	0.02	0.01	0.02	0.02	0.01	0.01	0.01	0.01
K2O	0.04	0.03	0.03	0.03	0.03	0.02	0.03	0.03	0.03	0.02	0.03	0.02	0.03	0.03	0.03	0.02	0.03	0.03	0.03	0.03	0.02	0.03	0.03	0.04	0.02	0.03	0.04	0.03	0.03	0.04	0.03	0.02	0.03	0.03	0.05
P2O5	0.02	0.03	0.03	0.03	0.05	0.03	0.02	0.05	0.02	0.03	0.03	0.04	0.05	0.05	0.04	0.03	0.03	0.06	0.05	0.04	0.04	0.05	0.05	0.04	0.03	0.03	0.02	0.05	0.04	0.04	0.04	0.03	0.02	0.04	0.03
Total	98.80	99.06	98.90	98.93	98.93	98.71	98.69	99.30	98.60	98.86	98.71	98.65	98.72	98.65	98.62	98.49	98.57	98.56	98.90	98.53	98.61	98.78	98.60	98.53	98.95	98.56	98.77	98.82	98.88	99.08	98.55	98.83	98.70	98.99	99.31
Si	2.99	3.00	3.00	3.02	3.01	3.01	3.02	3.01	3.03	3.02	3.00	3.01	3.02	3.01	3.01	3.03	3.02	3.02	3.01	3.01	3.02	3.01	3.01	3.00	3.00	3.01	3.01	3.01	3.01	3.02	3.01	3.01	3.01	3.01	3.02
Al iv	0.01	0.00	0.00	0.00	0.00	0.00	0.00	0.00	0.00	0.00	0.00	0.00	0.00	0.00	0.00	0.00	0.00	0.00	0.00	0.00	0.00	0.00	0.00	0.00	0.00	0.00	0.00	0.00	0.00	0.00	0.00	0.00	0.00	0.00	0.00
Al vi	1.91	1.92	1.91	1.90	1.90	1.92	1.89	1.91	1.89	1.91	1.91	1.91	1.91	1.91	1.91	1.91	1.91	1.89	1.91	1.91	1.89	1.92	1.91	1.95	1.91	1.91	1.91	1.90	1.91	1.93	1.91	1.92	1.91	1.91	1.92
Ti	0.01	0.01	0.01	0.01	0.01	0.01	0.01	0.01	0.01	0.01	0.01	0.01	0.01	0.01	0.01	0.01	0.01	0.01	0.01	0.01	0.01	0.01	0.01	0.01	0.01	0.01	0.01	0.01	0.01	0.01	0.01	0.01	0.01	0.01	0.01
Fe3+	0.07	0.07	0.07	0.07	0.06	0.06	0.07	0.06	0.06	0.05	0.07	0.06	0.05	0.06	0.06	0.04	0.05	0.07	0.06	0.06	0.07	0.06	0.06	0.04	0.07	0.06	0.07	0.07	0.07	0.04	0.07	0.06	0.07	0.07	0.05
Fe2+	2.31	2.25	2.21	2.18	2.16	2.13	2.09	2.06	2.04	2.01	1.99	1.91	1.89	1.87	1.88	1.87	1.90	1.91	1.93	1.93	1.95	1.96	1.98	2.04	2.03	2.07	2.10	2.14	2.19	2.20	2.22	2.25	2.29	2.32	2.37
Mn	0.14	0.18	0.23	0.26	0.30	0.33	0.35	0.38	0.41	0.46	0.46	0.53	0.55	0.56	0.57	0.56	0.56	0.53	0.51	0.51	0.48	0.47	0.45	0.43	0.40	0.38	0.35	0.32	0.28	0.24	0.22	0.19	0.16	0.13	0.11
Mg	0.27	0.24	0.22	0.20	0.19	0.18	0.18	0.17	0.16	0.16	0.16	0.15	0.15	0.14	0.14	0.14	0.15	0.15	0.15	0.15	0.15	0.15	0.16	0.16	0.17	0.17	0.18	0.19	0.20	0.20	0.22	0.24	0.26	0.28	0.29
Ca	0.29	0.34	0.35	0.38	0.37	0.37	0.39	0.40	0.39	0.37	0.40	0.42	0.42	0.43	0.41	0.42	0.39	0.42	0.42	0.42	0.42	0.42	0.42	0.38	0.41	0.38	0.39	0.36	0.34	0.36	0.35	0.33	0.29	0.28	0.23
Alm	0.77	0.75	0.73	0.72	0.72	0.71	0.70	0.68	0.68	0.67	0.66	0.63	0.63	0.62	0.62	0.62	0.63	0.63	0.64	0.64	0.65	0.65	0.66	0.68	0.67	0.69	0.70	0.71	0.73	0.73	0.74	0.75	0.76	0.77	0.79
Grs	0.10	0.11	0.12	0.13	0.12	0.12	0.13	0.13	0.13	0.12	0.13	0.14	0.14	0.14	0.14	0.14	0.13	0.14	0.14	0.14	0.14	0.14	0.14	0.13	0.14	0.13	0.13	0.12	0.11	0.12	0.12	0.11	0.10	0.09	0.08
Prp	0.09	0.08	0.07	0.07	0.06	0.06	0.06	0.06	0.05	0.05	0.05	0.05	0.05	0.05	0.05	0.05	0.05	0.05	0.05	0.05	0.05	0.05	0.05	0.05	0.06	0.06	0.06	0.06	0.07	0.07	0.07	0.08	0.09	0.09	0.10
Sps	0.05	0.06	0.08	0.09	0.10	0.11	0.12	0.13	0.14	0.15	0.15	0.18	0.18	0.19	0.19	0.19	0.19	0.18	0.17	0.17	0.16	0.16	0.15	0.14	0.13	0.13	0.12	0.11	0.09	0.08	0.07	0.06	0.05	0.04	0.04
Oxygen	12	12	12	12	12	12	12	12	12	12	12	12	12	12	12	12	12	12	12	12	12	12	12	12	12	12	12	12	12	12	12	12	12	12	12

UM07 Garnet

Analysis #	1/2.	1/3.	1/4.	1/5.	1/6.	1/7.	1/8.	1/9.	1/10.	1/11.	1/12.	1/13.	1/14.	1/15.	1/16.	1/17.	1/20.	1/22.	1/23.	1/24.	1/25.	1/26.	1/27.	1/28.	1/29.	1/30.	1/31.	1/32.	1/33.	1/34.	1/35.	1/36.
SiO2	36.79	36.93	36.64	36.67	36.68	36.60	36.60	36.43	36.58	36.62	36.69	36.61	36.49	36.62	36.60	36.60	36.44	36.63	36.57	36.50	36.69	36.60	36.67	36.72	36.53	36.71	36.64	36.71	36.70	36.68	36.65	36.97
TiO2	0.10	0.11	0.15	0.13	0.13	0.12	0.12	0.14	0.13	0.13	0.13	0.15	0.13	0.14	0.13	0.14	0.11	0.12	0.12	0.11	0.14	0.16	0.14	0.14	0.14	0.14	0.14	0.14	0.15	0.11	0.14	0.12
Al2O3	19.69	19.57	19.48	19.53	19.56	19.50	19.56	19.39	19.51	19.67	19.70	19.55	19.36	19.44	19.58	19.53	19.45	19.44	19.50	19.48	19.42	19.49	19.50	19.53	19.51	19.46	19.57	19.46	19.51	19.53	19.70	19.66
FeO	36.19	36.23	36.25	35.75	35.75	36.00	35.00	35.18	35.01	34.82	34.83	34.36	33.92	33.85	33.55	33.19	33.06	32.93	33.06	33.49	33.62	33.38	33.53	34.06	34.19	34.53	34.98	35.44	35.57	35.88	36.18	36.12
MnO	1.79	1.81	2.10	2.31	2.50	2.64	2.85	3.31	3.51	3.74	3.89	4.13	4.37	4.54	4.72	4.64	4.85	4.90	4.76	4.72	4.62	4.59	4.27	4.18	3.92	3.72	3.39	2.98	2.72	2.41	2.10	1.80
MgO	2.38	2.41	2.23	2.08	1.99	1.97	1.86	1.72	1.71	1.65	1.63	1.57	1.53	1.52	1.51	1.48	1.44	1.45	1.46	1.46	1.50	1.51	1.52	1.58	1.60	1.63	1.70	1.82	1.92	2.02	2.18	2.39
CaO	2.38	2.50	2.35	2.45	2.61	2.47	2.72	2.77	2.79	2.74	2.87	2.81	2.99	3.15	3.06	3.05	3.05	3.13	3.05	3.10	3.10	3.14	3.20	3.12	2.97	2.97	2.79	2.81	2.70	2.66	2.49	2.33
Na2O	0.02	0.03	0.02	0.01	0.01	0.01	0.02	0.02	0.02	0.01	0.02	0.01	0.01	0.03	0.02	0.03	0.05	0.06	0.05	0.03	0.03	0.02	0.02	0.02	0.02	0.03	0.02	0.02	0.01	0.02	0.02	0.01
K2O	0.03	0.03	0.03	0.03	0.02	0.03	0.03	0.03	0.03	0.02	0.03	0.03	0.02	0.02	0.03	0.02	0.02	0.02	0.02	0.03	0.02	0.03	0.03	0.03	0.03	0.03	0.02	0.02	0.03	0.02	0.03	0.04
P2O5	0.04	0.05	0.04	0.05	0.05	0.05	0.04	0.05	0.05	0.04	0.03	0.07	0.03	0.04	0.05	0.03	0.04	0.04	0.05	0.03	0.01	0.06	0.05	0.05	0.05	0.03	0.06	0.05	0.06	0.05	0.06	0.06
Total	99.41	99.67	99.29	99.01	99.30	99.39	98.80	99.04	99.34	99.44	99.82	99.29	98.85	99.35	99.25	98.71	98.51	98.72	98.64	98.95	99.15	98.98	98.93	99.43	98.96	99.25	99.31	99.45	99.37	99.38	99.55	99.50
Si	3.01	3.01	3.00	3.01	3.01	3.00	3.01	3.00	3.00	3.00	3.00	3.01	3.01	3.01	3.01	3.02	3.02	3.02	3.02	3.01	3.02	3.01	3.02	3.01	3.01	3.01	3.01	3.01	3.01	3.00	3.00	3.02
Al iv	0.00	0.00	0.00	0.00	0.00	0.00	0.00	0.00	0.00	0.00	0.00	0.00	0.00	0.00	0.00	0.00	0.00	0.00	0.00	0.00	0.00	0.00	0.00	0.00	0.00	0.00	0.00	0.00	0.00	0.00	0.00	0.00
Al vi	1.90	1.89	1.89	1.90	1.90	1.89	1.90	1.89	1.89	1.91	1.90	1.90	1.89	1.89	1.90	1.90	1.90	1.90	1.90	1.90	1.89	1.90	1.90	1.89	1.90	1.89	1.90	1.89	1.89	1.89	1.90	1.90
Ti	0.01	0.01	0.01	0.01	0.01	0.01	0.01	0.01	0.01	0.01	0.01	0.01	0.01	0.01	0.01	0.01	0.01	0.01	0.01	0.01	0.01	0.01	0.01	0.01	0.01	0.01	0.01	0.01	0.01	0.01	0.01	0.01
Fe3+	0.08	0.09	0.09	0.07	0.08	0.09	0.07	0.09	0.08	0.07	0.08	0.07	0.08	0.08	0.07	0.06	0.07	0.07	0.06	0.08	0.08	0.07	0.07	0.08	0.07	0.08	0.07	0.09	0.08	0.08	0.08	0.07
Fe2+	2.40	2.38	2.40	2.38	2.37	2.38	2.34	2.34	2.32	2.32	2.30	2.29	2.26	2.24	2.23	2.23	2.22	2.21	2.22	2.23	2.23	2.23	2.24	2.26	2.28	2.29	2.33	2.34	2.36	2.37	2.39	2.39
Mn	0.12	0.12	0.15	0.16	0.17	0.18	0.20	0.23	0.24	0.26	0.27	0.29	0.31	0.32	0.33	0.32	0.34	0.34	0.33	0.33	0.32	0.32	0.30	0.29	0.27	0.26	0.24	0.21	0.19	0.17	0.15	0.12
Mg	0.29	0.29	0.27	0.25	0.24	0.24	0.23	0.21	0.21	0.20	0.20	0.19	0.19	0.19	0.18	0.18	0.18	0.18	0.18	0.18	0.18	0.19	0.19	0.19	0.20	0.20	0.21	0.22	0.23	0.25	0.27	0.29
Ca	0.21	0.22	0.21	0.22	0.23	0.22	0.24	0.24	0.25	0.24	0.25	0.25	0.26	0.28	0.27	0.27	0.27	0.28	0.27	0.27	0.27	0.28	0.28	0.27	0.26	0.26	0.25	0.25	0.24	0.23	0.22	0.20
Alm	0.79	0.79	0.79	0.79	0.79	0.79	0.78	0.77	0.77	0.77	0.76	0.76	0.75	0.74	0.74	0.74	0.74	0.73	0.74	0.74	0.74	0.74	0.75	0.75	0.76	0.76	0.77	0.78	0.78	0.79	0.79	0.79
Grs	0.07	0.07	0.07	0.07	0.08	0.07	0.08	0.08	0.08	0.08	0.08	0.08	0.09	0.09	0.09	0.09	0.09	0.09	0.09	0.09	0.09	0.09	0.09	0.09	0.09	0.09	0.08	0.08	0.08	0.08	0.07	0.07
Prp	0.10	0.10	0.09	0.08	0.08	0.08	0.08	0.07	0.07	0.07	0.07	0.06	0.06	0.06	0.06	0.06	0.06	0.06	0.06	0.06	0.06	0.06	0.06	0.06	0.07	0.07	0.07	0.07	0.08	0.08	0.09	0.10
Sps	0.04	0.04	0.05	0.05	0.06	0.06	0.07	0.08	0.08	0.09	0.09	0.10	0.10	0.10	0.11	0.11	0.11	0.11	0.11	0.11	0.11	0.11	0.10	0.10	0.09	0.09	0.08	0.07	0.06	0.06	0.05	0.04
Oxygen	12	12	12	12	12	12	12	12	12	12	12	12	12	12	12	12	12	12	12	12	12	12	12	12	12	12	12	12	12	12	12	12

Table C1. Compositional mineral analysis for garnet, biotite, muscovite and feldspar

UM08 Garnet

Analysis #	1/1.	1/2.	1/3.	1/4.	1/5.	1/6.	1/7.	1/8.	1/9.	1/10.	1/11.	1/12.	1/13.	1/15.	1/16.	1/17.	1/18.	1/19.	1/20.	1/21.	1/22.	1/23.	1/24.	1/25.	1/26.	1/27.	1/28.	1/29.	1/30.
SiO2	37.65	37.22	37.23	37.23	37.10	37.06	37.12	37.09	36.68	37.44	36.97	37.11	36.67	37.02	37.08	36.91	37.08	37.08	37.18	36.97	37.27	37.17	37.33	37.23	37.21	37.35	37.40	37.10	37.56
TiO2	0.04	0.01	0.02	0.09	0.10	0.10	0.13	0.14	0.16	0.13	0.13	0.36	0.35	0.10	0.11	0.15	0.14	0.13	0.15	0.11	0.13	0.11	0.09	0.11	0.10	0.09	0.05	0.04	0.03
Al2O3	21.15	21.28	21.16	21.08	20.84	20.99	21.02	21.08	20.92	20.97	20.86	21.10	20.80	20.85	20.93	20.78	21.00	20.99	20.85	20.93	20.87	21.03	21.03	20.92	20.99	21.06	20.84	21.04	21.47
FeO	31.93	31.52	30.57	28.73	28.31	27.58	27.09	26.81	26.79	25.95	25.35	25.32	24.98	24.80	24.76	24.54	24.79	25.27	25.39	25.53	26.02	26.55	26.71	27.14	27.71	28.40	29.27	31.06	31.76
MnO	5.51	6.33	7.21	7.99	8.53	9.13	9.32	9.51	9.74	10.04	10.62	10.88	11.14	11.50	11.48	11.45	11.59	10.98	10.73	10.58	10.13	10.07	9.60	9.35	8.70	8.18	7.39	6.45	5.92
MgO	1.61	1.56	1.45	1.32	1.24	1.19	1.13	1.17	1.18	0.61	1.07	1.06	1.04	1.01	1.04	1.04	1.01	1.09	1.08	1.08	1.11	1.18	1.15	1.18	1.26	1.26	1.39	1.55	1.63
CaO	2.85	2.79	2.96	4.29	4.38	4.48	4.84	4.61	4.54	4.77	5.01	4.90	4.71	4.83	4.86	5.09	4.86	5.07	4.97	4.88	4.85	4.53	4.67	4.73	4.45	4.43	4.02	3.41	3.07
Na2O	0.02	0.03	0.02	0.02	0.02	0.04	0.02	0.01	0.04	0.00	0.05	0.05	0.07	0.04	0.03	0.04	0.03	0.03	0.02	0.02	0.03	0.02	0.02	0.03	0.02	0.03	0.02	0.03	0.05
K2O	0.00	0.00	0.00	0.01	0.00	0.00	0.00	0.00	0.01	0.01	0.02	0.01	0.02	0.01	0.01	0.01	0.00	0.00	0.00	0.00	0.01	0.00	0.00	0.00	0.01	0.00	0.00	0.01	0.00
P2O5	0.00	0.00	0.00	0.00	0.00	0.00	0.00	0.00	0.01	0.00	0.00	0.00	0.00	0.00	0.00	0.00	0.00	0.01	0.00	0.01	0.01	0.00	0.00	0.00	0.00	0.00	0.00	0.00	0.00
Total	100.76	100.74	100.62	100.76	100.52	100.57	100.67	100.42	100.07	99.92	100.08	100.79	99.78	100.16	100.30	100.01	100.50	100.65	100.37	100.11	100.43	100.66	100.60	100.69	100.45	100.80	100.38	100.69	101.49
Si	3.01	2.99	3.00	2.99	2.99	2.99	2.99	2.99	2.98	3.02	2.99	2.98	2.98	3.00	3.00	2.99	2.99	2.99	3.00	2.99	3.00	2.99	3.00	3.00	3.00	3.00	3.02	2.99	2.99
Al iv	0.00	0.01	0.00	0.01	0.01	0.01	0.01	0.01	0.02	0.00	0.01	0.02	0.02	0.00	0.00	0.01	0.01	0.01	0.00	0.01	0.00	0.01	0.00	0.00	0.00	0.00	0.00	0.01	0.01
Al vi	2.00	2.01	2.01	1.99	1.98	1.98	1.98	1.99	1.98	2.00	1.98	1.98	1.98	1.99	1.99	1.98	1.99	1.98	1.98	1.99	1.98	1.99	1.99	1.98	1.99	1.99	1.98	1.99	2.01
Ti	0.00	0.00	0.00	0.01	0.01	0.01	0.01	0.01	0.01	0.01	0.01	0.02	0.02	0.01	0.01	0.01	0.01	0.01	0.01	0.01	0.01	0.01	0.01	0.01	0.01	0.01	0.00	0.00	0.00
Fe3+	0.00	0.00	0.00	0.00	0.02	0.01	0.01	0.00	0.01	0.00	0.01	0.00	0.00	0.01	0.00	0.01	0.00	0.01	0.01	0.00	0.00	0.00	0.00	0.01	0.00	0.00	0.00	0.01	0.00
Fe2+	2.16	2.13	2.07	1.93	1.89	1.85	1.82	1.81	1.80	1.78	1.71	1.71	1.70	1.67	1.67	1.65	1.67	1.69	1.71	1.72	1.75	1.78	1.80	1.82	1.87	1.91	1.97	2.09	2.13
Mn	0.37	0.43	0.49	0.54	0.58	0.62	0.64	0.65	0.67	0.69	0.73	0.74	0.77	0.79	0.79	0.79	0.79	0.75	0.73	0.73	0.69	0.69	0.65	0.64	0.59	0.56	0.50	0.44	0.40
Mg	0.19	0.19	0.17	0.16	0.15	0.14	0.14	0.14	0.14	0.07	0.13	0.13	0.13	0.12	0.13	0.13	0.12	0.13	0.13	0.13	0.13	0.14	0.14	0.14	0.15	0.15	0.17	0.19	0.19
Ca	0.24	0.24	0.26	0.37	0.38	0.39	0.42	0.40	0.39	0.41	0.43	0.42	0.41	0.42	0.42	0.44	0.42	0.44	0.43	0.42	0.42	0.39	0.40	0.41	0.38	0.38	0.35	0.29	0.26
Alm	0.73	0.71	0.69	0.64	0.63	0.62	0.60	0.60	0.60	0.60	0.57	0.57	0.57	0.56	0.56	0.55	0.56	0.56	0.57	0.57	0.58	0.59	0.60	0.60	0.62	0.64	0.66	0.69	0.71
Grs	0.08	0.08	0.09	0.12	0.13	0.13	0.14	0.13	0.13	0.14	0.14	0.14	0.14	0.14	0.14	0.15	0.14	0.15	0.14	0.14	0.14	0.13	0.13	0.14	0.13	0.13	0.12	0.10	0.09
Prp	0.06	0.06	0.06	0.05	0.05	0.05	0.05	0.05	0.05	0.02	0.04	0.04	0.04	0.04	0.04	0.04	0.04	0.04	0.04	0.04	0.04	0.05	0.05	0.05	0.05	0.05	0.06	0.06	0.06
Sps	0.13	0.14	0.16	0.18	0.19	0.21	0.21	0.22	0.22	0.23	0.24	0.25	0.26	0.26	0.26	0.26	0.26	0.25	0.24	0.24	0.23	0.23	0.22	0.21	0.20	0.19	0.17	0.15	0.13
Oxygen	12	12	12	12	12	12	12	12	12	12	12	12	12	12	12	12	12	12	12	12	12	12	12	12	12	12	12	12	12

UM09 Garnet

Analysis #	9/3.	9/5.	9/7.	9/9.	9/10.	9/11.	9/13.	9/14.	9/16.	9/17.	9/18.	9/19.	9/20.	9/21.	9/22.	9/23.	9/25.	9/26.	9/27.	9/29.	9/30.	9/32.	9/33.	9/34.	9/35.	9/36.
SiO2	37.69	37.49	37.56	37.59	37.53	37.70	36.69	36.43	37.31	36.75	36.85	37.15	37.22	36.70	37.08	37.21	37.69	37.51	37.67	37.50	37.34	36.92	37.31	37.28	38.01	37.21
TiO2	0.05	0.09	0.11	0.09	0.11	0.12	0.11	0.11	0.13	0.09	0.10	0.10	0.09	0.08	0.08	0.09	0.07	0.08	0.06	0.07	0.07	0.08	0.07	0.07	0.07	0.06
Al2O3	20.62	20.57	20.54	20.55	20.68	20.85	21.60	22.17	21.01	22.48	22.11	21.37	21.34	21.90	21.61	21.23	20.70	20.80	20.63	20.78	20.97	21.77	21.28	21.40	21.00	20.96
FeO	38.00	37.85	37.42	37.02	36.78	36.27	36.13	35.20	35.64	34.91	34.83	35.21	35.03	34.58	34.76	34.57	34.86	34.76	34.74	34.60	34.42	33.96	33.92	33.73	34.27	34.24
MnO	1.02	1.46	1.89	2.20	2.33	2.44	2.68	2.76	3.02	2.98	3.17	3.18	3.23	3.23	3.29	3.30	3.42	3.36	3.33	3.38	3.41	3.36	3.40	3.40	3.36	3.33
MgO	2.50	2.29	2.15	2.07	2.06	2.02	1.95	1.90	1.95	1.89	1.86	1.90	1.86	1.87	1.88	1.90	1.89	1.88	1.89	1.93	1.89	1.90	1.88	1.90	1.87	1.92
CaO	1.44	1.59	1.74	1.78	1.84	1.95	2.01	2.08	2.18	2.12	2.23	2.35	2.38	2.50	2.53	2.49	2.57	2.60	2.61	2.60	2.60	2.65	2.67	2.59	2.63	2.65
Na2O	0.01	0.03	0.03	0.03	0.02	0.03	0.03	0.02	0.03	0.02	0.02	0.02	0.03	0.01	0.04	0.03	0.02	0.04	0.04	0.03	0.04	0.05	0.04	0.05	0.05	0.05
K2O	0.00	0.00	0.00	0.00	0.00	0.00	0.00	0.00	0.00	0.00	0.00	0.00	0.00	0.00	0.00	0.00	0.00	0.00	0.00	0.00	0.00	0.00	0.00	0.00	0.00	0.00
P2O5	0.05	0.03	0.04	0.05	0.05	0.05	0.07	0.03	0.05	0.05	0.05	0.04	0.04	0.04	0.04	0.02	0.03	0.03	0.03	0.02	0.05	0.02	0.00	0.03	0.01	0.04
Total	101.38	101.40	101.48	101.38	101.40	101.43	101.27	100.70	101.32	101.29	101.22	101.32	101.22	100.91	101.31	100.84	101.25	101.06	101.00	100.91	100.79	100.71	100.57	100.45	101.27	100.46
Si	3.01	3.00	3.01	3.01	3.01	3.02	2.95	2.92	2.99	2.92	2.94	2.98	2.98	2.94	2.97	2.99	3.02	3.01	3.02	3.01	3.00	2.96	2.99	2.99	3.03	3.00
Al iv	0.00	0.00	0.00	0.00	0.00	0.00	0.05	0.08	0.01	0.08	0.06	0.02	0.02	0.06	0.03	0.01	0.00	0.00	0.00	0.00	0.00	0.04	0.01	0.01	0.00	0.00
Al vi	1.95	1.95	1.94	1.94	1.96	1.97	2.00	2.03	1.98	2.04	2.03	2.00	2.00	2.02	2.01	2.00	1.96	1.97	1.95	1.97	1.99	2.02	2.01	2.02	1.98	1.99
Ti	0.00	0.01	0.01	0.01	0.01	0.01	0.01	0.01	0.01	0.01	0.01	0.01	0.01	0.00	0.00	0.01	0.00	0.00	0.00	0.00	0.00	0.00	0.00	0.00	0.00	0.00
Fe3+	0.03	0.04	0.04	0.03	0.03	0.01	0.00	0.00	0.01	0.00	0.00	0.00	0.00	0.00	0.00	0.00	0.02	0.01	0.02	0.01	0.00	0.00	0.00	0.00	0.00	0.00
Fe2+	2.51	2.50	2.47	2.45	2.44	2.42	2.43	2.40	2.38	2.38	2.37	2.36	2.35	2.35	2.34	2.33	2.32	2.32	2.31	2.31	2.31	2.31	2.30	2.29	2.30	2.31
Mn	0.07	0.10	0.13	0.15	0.16	0.17	0.18	0.19	0.21	0.20	0.21	0.22	0.22	0.22	0.22	0.22	0.23	0.23	0.23	0.23	0.23	0.23	0.23	0.23	0.23	0.23
Mg	0.30	0.27	0.26	0.25	0.25	0.24	0.23	0.23	0.23	0.22	0.22	0.23	0.22	0.22	0.22	0.23	0.23	0.22	0.23	0.23	0.23	0.23	0.22	0.23	0.22	0.23
Ca	0.12	0.14	0.15	0.15	0.16	0.17	0.17	0.18	0.19	0.18	0.19	0.20	0.20	0.21	0.22	0.21	0.22	0.22	0.22	0.22	0.22	0.23	0.23	0.22	0.22	0.23
Alm	0.84	0.83	0.82	0.82	0.81	0.81	0.80	0.80	0.79	0.80	0.79	0.79	0.78	0.78	0.78	0.78	0.77	0.77	0.77	0.77	0.77	0.77	0.77	0.77	0.77	0.77
Grs	0.04	0.05	0.05	0.05	0.05	0.06	0.06	0.06	0.06	0.06	0.06	0.07	0.07	0.07	0.07	0.07	0.07	0.07	0.08	0.07	0.07	0.08	0.08	0.07	0.08	0.08
Prp	0.10	0.09	0.09	0.08	0.08	0.08	0.08	0.08	0.08	0.08	0.07	0.08	0.07	0.07	0.07	0.08	0.08	0.08	0.08	0.08	0.08	0.08	0.08	0.08	0.07	0.08
Sps	0.02	0.03	0.04	0.05	0.05	0.06	0.06	0.06	0.07	0.07	0.07	0.07	0.07	0.07	0.07	0.07	0.08	0.08	0.08	0.08	0.08	0.08	0.08	0.08	0.08	0.08
Oxygen	12	12	12	12	12	12	12	12	12	12	12	12	12	12	12	12	12	12	12	12	12	12	12	12	12	12

UM09 Garnet

Analysis #	9/37.	9/38.	9/39.	9/40.	9/41.	9/42.	9/43.	9/44.	9/45.	9/46.	9/47.	9/48.	9/49.	9/50.	9/51.	9/52.	9/54.	9/55.	9/56.	9/57.	9/60.	9/61.	9/62.	9/63.	9/65.	9/68.
SiO2	37.08	36.97	37.11	37.58	38.25	36.36	37.39	37.62	37.37	37.50	37.49	37.53	37.60	37.50	37.65	37.30	37.39	37.23	36.82	37.33	37.31	37.55	36.71	37.20	36.85	37.25
TiO2	0.08	0.09	0.09	0.08	0.04	0.07	0.06	0.08	0.10	0.09	0.11	0.09	0.10	0.11	0.10	0.11	0.12	0.10	0.06	0.09	0.10	0.10	0.10	0.08	0.08	0.07
Al2O3	21.18	22.03	21.54	20.68	21.04	22.66	20.79	20.69	20.63	20.65	20.63	20.61	20.54	20.81	20.88	21.39	21.16	21.10	22.17	21.22	21.03	20.61	22.04	21.28	21.97	21.71
FeO	33.98	33.97	33.79	34.44	34.04	33.65	34.53	34.20	34.45	34.69	35.04	34.71	35.06	35.10	34.83	35.07	35.15	35.32	35.25	35.79	36.47	36.85	36.26	37.02	36.95	37.34
MnO	3.30	3.25	3.36	3.46	3.32	3.31	3.38	3.34	3.43	3.42	3.41	3.46	3.36	3.33	3.34	3.24	3.13	3.03	2.89	2.85	2.51	2.34	2.22	2.00	1.67	1.03
MgO	1.87	1.88	1.88	1.91	1.73	1.86	1.88	1.87	1.89	1.90	1.89	1.88	1.94	1.91	1.89	1.89	1.93	1.94	1.90	1.94	1.99	2.02	2.02	2.09	2.17	2.42
CaO	2.67	2.74	2.72	2.62	2.56	2.55	2.76	2.69	2.67	2.60	2.52	2.55	2.54	2.48	2.44	2.36	2.23	2.17	2.05	2.04	1.90	1.79	1.77	1.78	1.68	1.54
Na2O	0.05	0.04	0.06	0.04	0.05	0.05	0.05	0.05	0.03	0.03	0.02	0.03	0.02	0.03	0.02	0.02	0.04	0.01	0.03	0.02	0.02	0.02	0.03	0.02	0.03	0.02
K2O	0.00	0.00	0.00	0.00	0.00	0.00	0.00	0.00	0.00	0.00	0.00	0.00	0.00	0.00	0.00	0.00	0.00	0.00	0.00	0.00	0.00	0.00	0.00	0.00	0.00	0.00
P2O5	0.01	0.03	0.03	0.03	0.03	0.03	0.02	0.03	0.01	0.03	0.03	0.03	0.03	0.03	0.03	0.03	0.05	0.04	0.01	0.03	0.07	0.05	0.04	0.03	0.04	0.05
Total	100.22	101.00	100.58	100.84	101.06	100.54	100.86	100.57	100.58	100.91	101.14	100.89	101.19	101.30	101.18	101.41	101.20	100.94	101.18	101.31	101.40	101.33	101.19	101.50	101.44	101.43
Si	2.99	2.95	2.98	3.02	3.04	2.90	3.01	3.03	3.01	3.01	3.01	3.02	3.02	3.00	3.02	2.98	3.00	2.99	2.94	2.99	2.99	3.01	2.94	2.98	2.94	2.97
Al iv	0.01	0.05	0.02	0.00	0.00	0.10	0.00	0.00	0.00	0.00	0.00	0.00	0.00	0.00	0.00	0.02	0.00	0.01	0.06	0.01	0.01	0.00	0.06	0.02	0.06	0.03
Al vi	2.01	2.03	2.02	1.96	1.98	2.05	1.97	1.96	1.96	1.96	1.95	1.95	1.94	1.97	1.97	2.00	2.00	1.99	2.03	2.00	1.98	1.95	2.02	1.99	2.01	2.01
Ti	0.00	0.01	0.01	0.00	0.00	0.00	0.00	0.00	0.01	0.01	0.01	0.01	0.01	0.01	0.01	0.01	0.01	0.01	0.00	0.01	0.01	0.01	0.01	0.00	0.00	0.00
Fe3+	0.00	0.00	0.00	0.01	0.00	0.00	0.02	0.00	0.02	0.02	0.03	0.02	0.03	0.02	0.01	0.00	0.00	0.00	0.00	0.00	0.01	0.03	0.00	0.01	0.00	0.00
Fe2+	2.31	2.31	2.30	2.30	2.30	2.32	2.31	2.30	2.30	2.31	2.33	2.31	2.32	2.33	2.33	2.35	2.36	2.37	2.40	2.40	2.43	2.44	2.46	2.47	2.49	2.51
Mn	0.23	0.22	0.23	0.24	0.22	0.22	0.23	0.23	0.23	0.23	0.23	0.24	0.23	0.23	0.23	0.22	0.21	0.21	0.20	0.19	0.17	0.16	0.15	0.14	0.11	0.07
Mg	0.22	0.22	0.22	0.23	0.21	0.22	0.23	0.22	0.23	0.23	0.23	0.23	0.23	0.23	0.23	0.23	0.23	0.23	0.23	0.23	0.24	0.24	0.24	0.25	0.26	0.29
Ca	0.23	0.23	0.23	0.23	0.22	0.22	0.24	0.23	0.23	0.22	0.22	0.22	0.22	0.21	0.21	0.20	0.19	0.19	0.18	0.18	0.16	0.15	0.15	0.15	0.14	0.13
Alm	0.77	0.77	0.77	0.77	0.78	0.78	0.77	0.77	0.77	0.77	0.78	0.77	0.77	0.78	0.78	0.78	0.79	0.79	0.80	0.80	0.81	0.82	0.82	0.82	0.83	0.84
Grs	0.08	0.08	0.08	0.08	0.07	0.07	0.08	0.08	0.08	0.07	0.07	0.07	0.07	0.07	0.07	0.07	0.06	0.06	0.06	0.06	0.05	0.05	0.05	0.05	0.05	0.04
Prp	0.08	0.07	0.08	0.08	0.07	0.07	0.08	0.08	0.08	0.08	0.08	0.08	0.08	0.08	0.08	0.08	0.08	0.08	0.08	0.08	0.08	0.08	0.08	0.08	0.09	0.10
Sps	0.08	0.07	0.08	0.08	0.08	0.08	0.08	0.08	0.08	0.08	0.08	0.08	0.08	0.08	0.08	0.07	0.07	0.07	0.07	0.06	0.06	0.05	0.05	0.05	0.04	0.02
Oxygen	12	12	12	12	12	12	12	12	12	12	12	12	12	12	12	12	12	12	12	12	12	12	12	12	12	12

Table C1. Compositional mineral analysis for garnet, biotite, muscovite and feldspar

UM04 Biotite

Analysis #	3/1.	3/2.	3/3.	3/4.	3/5.	3/6.	3/7.	3/9.	3/10.	3/12.	3/13.	3/16.	3/17.	3/19.	5/1.	5/2.	5/3.	5/4.	5/5.	5/6.	5/7.	5/8.	5/10.	5/11.	5/12.	5/16.	5/18.
Location	Matrix	Matrix	Matrix	Matrix	Matrix	Matrix	Matrix	Matrix	Matrix	Matrix	Matrix	Matrix	Matrix	Matrix	Near Grt	Near Grt	Near Grt	Near Grt	Near Grt	Near Grt	Near Grt	Near Grt	Near Grt	Near Grt	Near Grt	Near Grt	Near Grt
SiO2	36.01	36.58	37.25	36.79	36.04	35.71	35.67	36.14	35.05	34.93	36.45	37.01	36.80	36.61	35.94	36.09	36.71	36.23	36.60	36.52	36.99	36.75	36.58	36.70	36.59	35.95	35.16
TiO2	1.80	1.67	1.51	1.68	1.80	1.83	1.55	1.73	1.73	1.91	1.87	1.07	1.70	1.80	2.06	2.01	1.76	1.78	1.69	1.80	1.73	1.66	1.70	1.91	1.17	1.46	1.34
Al2O3	19.41	19.29	19.78	19.27	19.49	18.97	19.50	19.95	19.42	19.50	19.09	20.40	20.27	19.70	19.70	19.52	19.64	19.53	19.73	19.85	19.57	19.94	19.78	19.69	20.24	19.58	19.73
FeO	19.40	19.49	19.15	19.18	20.51	20.28	19.85	19.05	19.93	19.91	19.45	18.96	18.68	19.37	19.64	19.45	19.58	19.81	19.75	19.68	19.45	19.38	19.32	19.66	19.36	19.65	20.38
MnO	0.03	0.05	0.04	0.06	0.04	0.06	0.04	0.05	0.07	0.07	0.04	0.04	0.06	0.04	0.06	0.06	0.03	0.04	0.07	0.02	0.04	0.05	0.05	0.06	0.07	0.05	0.07
MgO	10.33	10.03	9.82	9.91	10.30	9.94	9.73	9.19	10.60	9.91	9.75	9.45	9.22	9.78	8.95	8.77	9.21	9.65	9.34	9.47	9.63	10.05	9.99	9.86	10.03	10.09	9.67
CaO	0.00	0.00	0.02	0.03	0.03	0.06	0.10	0.04	0.05	0.04	0.01	0.02	0.02	0.03	0.05	0.04	0.05	0.05	0.03	0.07	0.03	0.01	0.01	0.00	0.02	0.06	0.04
Na2O	0.11	0.10	0.10	0.18	0.10	0.18	0.14	0.11	0.13	0.12	0.11	0.16	0.24	0.13	0.13	0.14	0.12	0.09	0.11	0.14	0.16	0.12	0.13	0.13	0.12	0.17	0.15
K2O	9.97	9.63	9.43	9.76	8.86	8.95	8.46	9.07	8.79	8.52	9.61	9.83	9.51	9.42	9.20	9.33	9.48	9.01	9.20	8.94	9.54	9.42	9.21	9.37	9.67	9.08	8.38
P2O5	0.02	0.03	0.02	0.01	0.08	0.13	0.24	0.11	0.02	0.01	0.03	0.02	0.02	0.01	0.03	0.01	0.02	0.02	0.02	0.02	0.01	0.04	0.02	0.02	0.01	0.01	0.03
Cl	0.02	0.04	0.02	0.03	0.03	0.06	0.04	0.03	0.03	0.04	0.03	0.04	0.05	0.03	0.06	0.05	0.02	0.03	0.02	0.04	0.03	0.02	0.03	0.02	0.02	0.03	0.05
F	0.59	0.57	0.62	0.46	0.54	0.38	0.43	0.45	0.48	0.35	0.42	0.56	0.40	0.44	0.32	0.46	0.50	0.44	0.33	0.39	0.45	0.47	0.53	0.52	0.58	0.44	0.33
H2O	3.73	3.73	3.75	3.79	3.76	3.77	3.74	3.75	3.73	3.76	3.79	3.76	3.82	3.81	3.80	3.73	3.77	3.78	3.85	3.82	3.82	3.82	3.77	3.79	3.76	3.77	3.76
Total	101.42	101.21	101.51	101.15	101.58	100.32	99.49	99.67	100.03	99.07	100.65	101.32	100.79	101.17	99.94	99.66	100.89	100.46	100.74	100.76	101.45	101.73	101.12	101.73	101.64	100.34	99.09
Si	5.38	5.46	5.52	5.49	5.37	5.40	5.41	5.45	5.31	5.33	5.47	5.50	5.48	5.45	5.43	5.47	5.49	5.44	5.47	5.45	5.49	5.44	5.45	5.44	5.43	5.41	5.36
Al iv	2.62	2.54	2.48	2.51	2.63	2.60	2.59	2.55	2.69	2.67	2.53	2.50	2.52	2.55	2.57	2.53	2.51	2.56	2.53	2.55	2.51	2.56	2.55	2.56	2.57	2.59	2.64
Al vi	0.80	0.86	0.97	0.88	0.80	0.78	0.90	1.00	0.77	0.83	0.85	1.07	1.04	0.91	0.93	0.95	0.95	0.90	0.95	0.95	0.92	0.92	0.92	0.88	0.97	0.88	0.91
Ti	0.20	0.19	0.17	0.19	0.20	0.21	0.18	0.20	0.20	0.22	0.21	0.12	0.19	0.20	0.23	0.23	0.20	0.20	0.19	0.20	0.19	0.18	0.19	0.21	0.13	0.17	0.15
Fe	2.43	2.43	2.37	2.39	2.56	2.56	2.52	2.40	2.52	2.54	2.44	2.36	2.33	2.41	2.48	2.46	2.45	2.49	2.47	2.46	2.42	2.40	2.41	2.44	2.40	2.47	2.60
Mn	0.00	0.01	0.01	0.01	0.01	0.01	0.01	0.01	0.01	0.01	0.01	0.01	0.01	0.01	0.01	0.01	0.00	0.01	0.01	0.00	0.01	0.01	0.01	0.01	0.01	0.01	0.01
Mg	2.30	2.23	2.17	2.20	2.29	2.24	2.20	2.07	2.39	2.25	2.18	2.09	2.05	2.17	2.01	1.98	2.05	2.16	2.08	2.11	2.13	2.22	2.22	2.18	2.22	2.26	2.20
Ca	0.00	0.00	0.00	0.00	0.00	0.01	0.02	0.01	0.01	0.01	0.00	0.00	0.00	0.00	0.01	0.01	0.01	0.01	0.00	0.01	0.00	0.00	0.00	0.00	0.00	0.01	0.01
Na	0.03	0.03	0.03	0.05	0.03	0.05	0.04	0.03	0.04	0.04	0.03	0.05	0.07	0.04	0.04	0.04	0.03	0.03	0.03	0.04	0.05	0.03	0.04	0.04	0.03	0.05	0.04
K	1.90	1.83	1.78	1.86	1.68	1.73	1.64	1.75	1.70	1.66	1.84	1.86	1.81	1.79	1.77	1.80	1.81	1.73	1.75	1.70	1.81	1.78	1.75	1.77	1.83	1.74	1.63
OH	3.72	3.72	3.70	3.78	3.74	3.80	3.78	3.78	3.76	3.82	3.79	3.73	3.80	3.79	3.83	3.77	3.76	3.78	3.84	3.81	3.78	3.77	3.74	3.75	3.72	3.78	3.83
F	0.28	0.27	0.29	0.22	0.25	0.18	0.21	0.21	0.23	0.17	0.20	0.26	0.19	0.21	0.15	0.22	0.24	0.21	0.16	0.18	0.21	0.22	0.25	0.24	0.27	0.21	0.16
Cl	0.01	0.01	0.01	0.01	0.01	0.02	0.01	0.01	0.01	0.01	0.01	0.01	0.01	0.01	0.02	0.01	0.01	0.01	0.01	0.01	0.01	0.01	0.01	0.01	0.01	0.01	0.01
XMg	0.49	0.48	0.48	0.48	0.47	0.47	0.47	0.46	0.49	0.47	0.47	0.47	0.47	0.47	0.45	0.45	0.46	0.46	0.46	0.46	0.47	0.48	0.48	0.47	0.48	0.48	0.46
Oxygen	22	22	22	22	22	22	22	22	22	22	22	22	22	22	22	22	22	22	22	22	22	22	22	22	22	22	22

UM05 Biotite

Analysis #	1/1.	1/2.	1/6.	1/10.	6/6.	6/7.	6/8.	10/1.	10/2.	10/4.	10/5.	10/7.	12/2.	12/6.	12/9.	12/12.
Location	Matrix	Matrix	Matrix	Matrix	Near Grt	Near Grt	Near Grt	Near Grt	Near Grt	Near Grt	Near Grt	Near Grt	Matrix	Matrix	Matrix	Matrix
SiO2	35.53	35.43	35.45	35.67	34.76	35.28	35.73	35.45	35.83	35.22	35.97	35.24	35.35	35.69	35.40	38.04
TiO2	1.62	1.76	1.57	1.47	1.16	1.10	1.04	1.65	1.53	1.54	1.50	1.65	1.58	1.53	1.71	1.38
Al2O3	18.65	18.48	18.49	19.12	18.92	18.83	19.08	18.15	19.19	18.35	19.14	18.73	18.50	18.43	18.39	19.41
FeO	20.53	20.63	20.53	19.92	20.26	20.74	20.55	20.86	20.13	20.70	20.08	20.10	20.47	20.63	20.22	19.62
MnO	0.01	0.03	0.00	0.00	0.03	0.02	0.00	0.01	0.02	0.01	0.04	0.00	0.03	0.04	0.03	0.01
MgO	9.37	9.26	9.47	9.38	9.63	9.76	9.87	9.51	9.23	10.12	9.62	9.35	9.40	9.67	9.44	9.19
CaO	0.00	0.01	0.03	0.00	0.02	0.00	0.00	0.06	0.03	0.08	0.00	0.00	0.07	0.00	0.00	0.06
Na2O	0.17	0.16	0.18	0.15	0.18	0.18	0.18	0.17	0.19	0.23	0.20	0.17	0.19	0.18	0.16	0.20
K2O	9.62	9.42	9.26	8.87	9.55	9.51	9.57	8.73	8.86	8.63	9.48	9.58	9.21	9.68	9.77	8.52
P2O5	0.02	0.01	0.00	0.00	0.01	0.01	0.01	0.02	0.02	0.03	0.00	0.01	0.02	0.00	0.02	0.02
Cl	0.01	0.02	0.02	0.02	0.02	0.01	0.00	0.05	0.00	0.03	0.00	0.01	0.01	0.01	0.01	0.04
F	0.41	0.34	0.34	0.58	0.54	0.62	0.44	0.50	0.53	0.67	0.52	0.56	0.50	0.37	0.45	0.60
H2O	3.73	3.74	3.74	3.64	3.62	3.62	3.74	3.65	3.68	3.58	3.72	3.63	3.66	3.75	3.69	3.75
Total	99.67	99.29	99.08	98.82	98.70	99.68	100.21	98.81	99.24	99.19	100.27	99.03	98.99	99.98	99.29	100.84
Si	5.43	5.43	5.44	5.46	5.37	5.40	5.42	5.46	5.46	5.40	5.44	5.42	5.44	5.44	5.44	5.64
Al iv	2.57	2.57	2.56	2.54	2.63	2.60	2.58	2.54	2.54	2.60	2.56	2.58	2.56	2.56	2.56	2.36
Al vi	0.79	0.78	0.79	0.91	0.82	0.80	0.84	0.75	0.91	0.72	0.85	0.81	0.79	0.75	0.76	1.04
Ti	0.19	0.20	0.18	0.17	0.13	0.13	0.12	0.19	0.18	0.18	0.17	0.19	0.18	0.18	0.20	0.15
Fe	2.62	2.65	2.64	2.55	2.62	2.66	2.61	2.69	2.57	2.66	2.54	2.58	2.63	2.63	2.60	2.43
Mn	0.00	0.00	0.00	0.00	0.00	0.00	0.00	0.00	0.00	0.00	0.01	0.00	0.00	0.01	0.00	0.00
Mg	2.14	2.12	2.17	2.14	2.22	2.23	2.23	2.18	2.10	2.31	2.17	2.14	2.15	2.20	2.16	2.03
Ca	0.00	0.00	0.00	0.00	0.00	0.00	0.00	0.01	0.00	0.01	0.00	0.00	0.01		0.00	0.01
Na	0.05	0.05	0.05	0.04	0.05	0.05	0.05	0.05	0.06	0.07	0.06	0.05	0.06	0.05	0.05	0.06
K	1.88	1.84	1.81	1.73	1.88	1.86	1.85	1.71	1.72	1.69	1.83	1.88	1.81	1.88	1.91	1.61
OH	3.80	3.83	3.83	3.71	3.73	3.70	3.79	3.74	3.74	3.67	3.75	3.73	3.75	3.82	3.78	3.71
F	0.20	0.16	0.17	0.28	0.26	0.30	0.21	0.24	0.26	0.33	0.25	0.27	0.24	0.18	0.22	0.28
Cl	0.00	0.01	0.01	0.01	0.01	0.00	0.00	0.01	0.00	0.01	0.00	0.00	0.00	0.00	0.00	0.01
XMg	0.45	0.44	0.45	0.46	0.46	0.46	0.46	0.45	0.45	0.47	0.46	0.45	0.45	0.46	0.45	0.46
Oxygen	22	22	22	22	22	22	22	22	22	22	22	22	22	22	22	22

Table C1. Compositional mineral analysis for garnet, biotite, muscovite and feldspar

UM07 Biotite

Analysis #	1/1.	1/2.	1/3.	1/4.	1/5.	1/6.	1/7.	1/9.	1/10.	1/11.	1/12.	1/13.	3/3.	5/6.	5/8.	5/10.	7/2.	7/3.	7/4.	7/6.	7/9.	9/15.	9/17.
Location	Matrix	Matrix	Matrix	Matrix	Matrix	Matrix	Matrix	Matrix	Matrix	Matrix	Matrix	Matrix	Matrix	Matrix	Matrix	Matrix	Near Grt	Near Grt	Near Grt	Near Grt	Near Grt	Near Grt	Near Grt
SiO2	35.98	35.70	35.67	35.34	35.24	35.74	35.41	35.43	35.32	34.80	35.23	35.49	35.33	35.76	36.06	35.41	35.29	36.09	35.68	38.34	37.38	35.41	37.15
TiO2	1.50	1.35	1.48	1.49	1.35	1.50	1.44	1.37	1.77	1.84	1.72	1.82	1.51	1.61	1.41	1.42	1.79	1.89	1.83	1.20	1.42	1.38	1.58
Al2O3	19.04	19.25	18.93	18.47	18.91	18.79	18.75	18.76	18.55	18.20	18.33	18.57	18.00	18.67	20.14	18.87	18.30	18.87	18.36	19.15	18.26	18.76	18.91
FeO	21.14	20.90	21.06	21.47	20.64	20.39	20.70	20.13	21.47	21.65	21.21	21.51	21.60	20.71	19.97	20.51	21.44	20.86	21.06	19.20	19.60	20.85	19.28
MnO	0.02	0.01	0.02	0.00	0.02	0.00	0.00	0.02	0.01	0.01	0.02	0.01	0.06	0.01	0.00	0.00	0.03	0.02	0.01	0.01	0.00	0.00	0.00
MgO	9.18	9.24	9.49	9.36	9.55	9.32	9.55	9.63	9.53	9.15	9.19	9.31	9.27	9.59	8.44	9.37	8.71	8.56	8.96	8.73	9.33	9.74	8.94
CaO	0.01	0.00	0.00	0.01	0.00	0.00	0.00	0.00	0.00	0.03	0.00	0.00	0.00	0.00	0.02	0.00	0.00	0.00	0.00	0.03	0.01	0.00	0.00
Na2O	0.25	0.25	0.26	0.23	0.24	0.23	0.22	0.22	0.23	0.27	0.25	0.24	0.21	0.23	0.19	0.25	0.21	0.25	0.25	0.24	0.22	0.28	0.27
K2O	9.17	9.20	9.10	8.95	8.99	9.13	9.12	9.14	9.10	8.67	8.85	9.16	9.17	9.21	8.68	9.39	8.89	8.80	8.94	8.40	8.69	9.17	9.03
P2O5	0.04	0.00	0.01	0.00	0.00	0.00	0.00	0.00	0.00	0.02	0.01	0.01	0.00	0.01	0.00	0.00	0.02	0.03	0.01	0.09	0.03	0.00	0.01
Cl	0.01	0.01	0.01	0.02	0.03	0.02	0.03	0.02	0.01	0.04	0.03	0.01	0.01	0.01	0.06	0.01	0.02	0.01	0.01	0.03	0.00	0.06	0.03
F	n/a	n/a	n/a	n/a	n/a	n/a	n/a	n/a	n/a	n/a	n/a	n/a	n/a	n/a	n/a	n/a	n/a	n/a	n/a	n/a	n/a	n/a	n/a
H2O	3.96	3.95	3.95	3.90	3.90	3.92	3.91	3.90	3.93	3.86	3.88	3.94	3.89	3.94	3.93	3.91	3.88	3.93	3.91	4.00	3.96	3.91	3.96
Total	100.30	99.86	99.98	99.24	98.87	99.04	99.13	98.62	99.92	98.54	98.72	100.07	99.05	99.75	98.90	99.14	98.58	99.31	99.02	99.42	98.90	99.56	99.16
Si	5.45	5.42	5.42	5.42	5.41	5.46	5.42	5.44	5.39	5.39	5.43	5.40	5.45	5.44	5.48	5.42	5.45	5.50	5.47	5.74	5.66	5.41	5.61
Al iv	2.55	2.58	2.58	2.58	2.59	2.54	2.58	2.56	2.61	2.61	2.57	2.60	2.55	2.56	2.52	2.58	2.55	2.50	2.53	2.26	2.34	2.59	2.39
Al vi	0.84	0.87	0.81	0.76	0.83	0.85	0.80	0.83	0.72	0.71	0.76	0.74	0.72	0.79	1.08	0.83	0.78	0.88	0.79	1.11	0.92	0.78	0.98
Ti	0.17	0.15	0.17	0.17	0.16	0.17	0.17	0.16	0.20	0.21	0.20	0.21	0.18	0.18	0.16	0.16	0.21	0.22	0.21	0.14	0.16	0.16	0.18
Fe	2.68	2.66	2.67	2.75	2.65	2.61	2.65	2.58	2.74	2.80	2.73	2.74	2.78	2.63	2.54	2.63	2.77	2.66	2.70	2.40	2.48	2.66	2.44
Mn	0.00	0.00	0.00	0.00	0.00	0.00	0.00	0.00	0.00	0.00	0.00	0.00	0.01	0.00	0.00	0.00	0.00	0.00	0.00	0.00	0.00	0.00	0.00
Mg	2.07	2.09	2.15	2.14	2.18	2.12	2.18	2.20	2.17	2.11	2.11	2.11	2.13	2.17	1.91	2.14	2.01	1.94	2.05	1.95	2.11	2.22	2.01
Ca	0.00	0.00	0.00	0.00	0.00	0.00	0.00	0.00	0.00	0.00	0.00	0.00	0.00	0.00	0.00	0.00	0.00	0.00	0.00	0.00	0.00	0.00	0.00
Na	0.07	0.07	0.08	0.07	0.07	0.07	0.07	0.07	0.07	0.08	0.07	0.07	0.06	0.07	0.06	0.07	0.06	0.07	0.07	0.07	0.06	0.08	0.08
K	1.77	1.78	1.76	1.75	1.76	1.78	1.78	1.79	1.77	1.71	1.74	1.78	1.80	1.79	1.68	1.83	1.75	1.71	1.75	1.60	1.68	1.79	1.74
OH	4.00	4.00	4.00	3.99	3.99	3.99	3.99	3.99	4.00	3.99	3.99	4.00	4.00	4.00	3.98	4.00	3.99	4.00	4.00	3.99	4.00	3.98	3.99
F	0.00	0.00	0.00	0.00	0.00	0.00	0.00	0.00	0.00	0.00	0.00	0.00	0.00	0.00	0.00	0.00	0.00	0.00	0.00	0.00	0.00	0.00	0.00
Cl	0.00	0.00	0.00	0.01	0.01	0.01	0.01	0.01	0.00	0.01	0.01	0.00	0.00	0.00	0.02	0.00	0.01	0.00	0.00	0.01	0.00	0.02	0.01
XMg	0.44	0.44	0.45	0.44	0.45	0.45	0.45	0.46	0.44	0.43	0.44	0.44	0.43	0.45	0.43	0.45	0.42	0.42	0.43	0.45	0.46	0.45	0.45
Oxygen	22	22	22	22	22	22	22	22	22	22	22	22	22	22	22	22	22	22	22	22	22	22	22

UM08 Biotite

Analysis #	1/1.	1/3.	1/4.	1/6.	3/1.	3/2.	3/3.	3/6.	3/8.	3/9.	3/11.	6/2.	6/3.	6/7.	6/10.	6/11.	6/12.	6/13.	6/15.	10/2.
Location	Matrix	Matrix	Matrix	Matrix	Matrix	Matrix	Matrix	Matrix	Matrix	Matrix	Matrix	Near Grt	Near Grt	Matrix	Matrix	Matrix	Matrix	Matrix	Matrix	Matrix
SiO2	37.25	36.91	36.89	36.33	37.25	37.07	36.70	36.63	36.74	36.86	36.83	37.43	36.67	37.03	36.85	37.17	36.55	37.48	37.41	37.20
TiO2	1.74	1.71	1.72	2.34	1.72	1.86	1.98	1.76	1.73	1.48	1.37	1.60	1.75	1.59	1.58	1.91	1.80	1.77	1.64	1.67
Al2O3	19.88	19.26	19.43	18.32	19.09	19.19	18.79	19.04	19.47	19.39	19.46	20.16	19.39	18.96	19.52	19.59	19.03	19.77	20.09	20.58
FeO	20.11	21.02	20.70	21.33	20.55	20.89	21.72	21.84	20.68	21.47	20.56	20.09	20.61	20.49	19.73	20.39	21.16	19.89	19.25	19.08
MnO	0.09	0.13	0.08	0.08	0.08	0.09	0.10	0.07	0.09	0.11	0.09	0.14	0.17	0.13	0.12	0.13	0.17	0.08	0.07	0.06
MgO	8.32	8.58	8.71	8.03	8.53	8.63	8.64	8.67	8.34	8.57	8.71	8.33	8.55	8.48	8.22	8.23	8.81	7.96	8.14	7.96
CaO	0.04	0.07	0.09	0.11	0.07	0.08	0.03	0.06	0.10	0.10	0.02	0.01	0.04	0.04	0.11	0.02	0.04	0.06	0.10	0.07
Na2O	0.14	0.15	0.13	0.11	0.13	0.11	0.11	0.15	0.15	0.13	0.12	0.09	0.11	0.11	0.11	0.10	0.12	0.09	0.14	0.12
K2O	9.45	9.26	9.10	8.73	8.97	9.25	9.05	8.99	8.85	9.04	9.43	8.85	9.12	8.85	8.86	9.51	9.36	8.72	8.27	8.26
P2O5	0.00	0.00	0.00	0.00	0.01	0.00	0.00	0.00	0.00	0.00	0.01	0.00	0.01	0.00	0.00	0.00	0.01	0.02	0.00	0.00
Cl	0.00	0.01	0.00	0.01	0.00	0.00	0.00	0.00	0.02	0.00	0.00	0.00	0.00	0.02	0.03	0.00	0.00	0.01	0.00	0.00
F	0.37	0.39	0.45	0.46	0.59	0.53	0.57	0.48	0.48	0.60	0.54	0.52	0.69	0.54	0.55	0.54	0.61	0.60	0.43	0.45
H2O	3.85	3.82	3.80	3.71	3.72	3.77	3.73	3.78	3.75	3.72	3.74	3.79	3.66	3.71	3.69	3.76	3.71	3.72	3.79	3.78
Total	101.24	101.31	101.10	99.56	100.71	101.47	101.42	101.47	100.40	101.47	100.88	101.01	100.77	99.95	99.37	101.35	101.37	100.17	99.33	99.23
Si	5.55	5.52	5.52	5.54	5.59	5.53	5.51	5.49	5.53	5.51	5.53	5.56	5.51	5.59	5.58	5.55	5.49	5.61	5.61	5.58
Al iv	2.45	2.48	2.48	2.46	2.41	2.47	2.49	2.51	2.47	2.49	2.47	2.44	2.49	2.41	2.42	2.45	2.51	2.39	2.39	2.42
Al vi	1.03	0.92	0.94	0.83	0.96	0.91	0.83	0.86	0.98	0.93	0.97	1.10	0.95	0.97	1.06	0.99	0.85	1.11	1.17	1.22
Ti	0.19	0.19	0.19	0.27	0.19	0.21	0.22	0.20	0.20	0.17	0.15	0.18	0.20	0.18	0.18	0.21	0.20	0.20	0.19	0.19
Fe	2.50	2.63	2.59	2.72	2.58	2.61	2.73	2.74	2.60	2.69	2.58	2.50	2.59	2.59	2.50	2.54	2.66	2.49	2.42	2.39
Mn	0.01	0.02	0.01	0.01	0.01	0.01	0.01	0.01	0.01	0.01	0.01	0.02	0.02	0.02	0.02	0.02	0.02	0.01	0.01	0.01
Mg	1.85	1.91	1.94	1.83	1.91	1.92	1.93	1.94	1.87	1.91	1.95	1.85	1.92	1.91	1.86	1.83	1.97	1.78	1.82	1.78
Ca	0.01	0.01	0.01	0.02	0.01	0.01	0.00	0.01	0.02	0.02	0.00	0.00	0.01	0.01	0.02	0.00	0.01	0.01	0.02	0.01
Na	0.04	0.04	0.04	0.03	0.04	0.03	0.03	0.04	0.04	0.04	0.03	0.03	0.03	0.03	0.03	0.03	0.03	0.03	0.04	0.03
K	1.79	1.77	1.74	1.70	1.72	1.76	1.73	1.72	1.70	1.73	1.81	1.68	1.75	1.71	1.71	1.81	1.79	1.67	1.58	1.58
OH	3.83	3.81	3.79	3.78	3.72	3.75	3.73	3.77	3.77	3.72	3.74	3.76	3.67	3.74	3.73	3.75	3.71	3.71	3.80	3.79
F	0.17	0.18	0.21	0.22	0.28	0.25	0.27	0.23	0.23	0.28	0.26	0.24	0.33	0.26	0.26	0.25	0.29	0.28	0.20	0.21
Cl	0.00	0.00	0.00	0.00	0.00	0.00	0.00	0.00	0.01	0.00	0.00	0.00	0.00	0.01	0.01	0.00	0.00	0.00	0.00	0.00
XMg	0.42	0.42	0.43	0.40	0.43	0.42	0.41	0.41	0.42	0.42	0.43	0.42	0.43	0.42	0.43	0.42	0.43	0.42	0.43	0.43
Oxygen	22	22	22	22	22	22	22	22	22	22	22	22	22	22	22	22	22	22	22	22

Table C1. Compositional mineral analysis for garnet, biotite, muscovite and feldspar

UM09 Biotite

Analysis #	1/1.	1/2.	1/4.	1/5.	1/6.	1/7.	1/9.	1/10.	1/11.	1/13.	1/14.	1/15.	2/2.	2/5.	2/6.	2/7.	2/8.	2/10.	4/2.	4/3.
Location	Near Grt	Near Grt	Near Grt	Near Grt	Near Grt	Near Grt	Near Grt	Near Grt	Near Grt	Near Grt	Near Grt	Near Grt	Near Grt	Near Grt	Near Grt	Near Grt	Near Grt	Near Grt	Matrix	Matrix
SiO2	34.76	35.07	34.93	35.02	35.09	34.46	34.75	34.60	34.46	34.15	34.74	33.73	34.51	33.95	34.23	34.03	34.17	34.73	34.62	33.95
TiO2	2.45	2.46	2.50	2.53	2.49	2.51	2.39	1.61	1.78	1.67	1.88	1.71	2.06	2.00	2.00	2.27	2.25	2.30	2.31	2.21
Al2O3	18.28	18.44	18.29	18.53	18.61	18.16	18.03	18.96	19.20	18.42	18.72	19.66	18.73	18.34	18.38	18.07	18.18	19.13	18.26	18.69
FeO	22.84	22.96	22.91	22.33	22.80	22.72	22.75	23.43	23.23	23.94	22.58	22.67	23.67	24.38	24.23	23.90	23.60	22.44	23.46	23.08
MnO	0.02	0.01	0.04	0.01	0.02	0.00	0.00	0.02	0.02	0.02	0.00	0.01	0.04	0.02	0.00	0.03	0.01	0.02	0.00	0.01
MgO	7.40	7.45	7.45	7.29	7.38	7.44	7.62	7.40	7.36	7.52	7.61	7.43	7.06	7.06	7.34	7.19	7.65	6.90	7.51	7.56
CaO	0.00	0.00	0.00	0.00	0.00	0.00	0.00	0.00	0.00	0.00	0.00	0.01	0.00	0.00	0.00	0.00	0.00	0.00	0.00	0.00
Na2O	0.37	0.34	0.38	0.39	0.41	0.36	0.38	0.39	0.37	0.32	0.40	0.40	0.29	0.31	0.28	0.30	0.31	0.28	0.34	0.35
K2O	9.10	9.21	9.23	9.10	9.16	9.18	9.12	9.11	9.24	9.07	9.24	9.18	9.21	9.13	9.10	9.28	9.21	9.46	9.09	9.01
P2O5	0.00	0.01	0.00	0.01	0.00	0.00	0.00	0.00	0.01	0.00	0.00	0.00	0.00	0.00	0.00	0.00	0.00	0.00	0.01	0.00
Cl	0.01	0.01	0.02	0.02	0.02	0.01	0.02	0.03	0.02	0.03	0.03	0.05	0.01	0.01	0.01	0.01	0.01	0.01	0.01	0.01
F	0.27	0.27	0.31	0.22	0.41	0.33	0.23	0.25	0.22	0.28	0.36	0.27	0.19	0.20	0.37	0.33	0.31	0.41	0.39	0.33
H2O	3.73	3.77	3.73	3.77	3.70	3.69	3.74	3.74	3.77	3.69	3.69	3.70	3.77	3.73	3.67	3.67	3.70	3.68	3.68	3.68
Total	99.23	100.00	99.79	99.22	100.09	98.86	99.03	99.54	99.68	99.11	99.25	98.82	99.54	99.13	99.61	99.08	99.40	99.36	99.68	98.88
Si	5.39	5.40	5.39	5.41	5.39	5.37	5.40	5.36	5.33	5.34	5.39	5.26	5.36	5.32	5.33	5.33	5.32	5.38	5.37	5.30
Al iv	2.61	2.60	2.61	2.59	2.61	2.63	2.60	2.64	2.67	2.66	2.61	2.74	2.64	2.68	2.67	2.67	2.68	2.62	2.63	2.70
Al vi	0.73	0.74	0.72	0.79	0.76	0.71	0.70	0.83	0.83	0.73	0.81	0.87	0.78	0.71	0.71	0.67	0.66	0.87	0.70	0.74
Ti	0.29	0.28	0.29	0.29	0.29	0.29	0.28	0.19	0.21	0.20	0.22	0.20	0.24	0.24	0.23	0.27	0.26	0.27	0.27	0.26
Fe	2.96	2.96	2.96	2.89	2.93	2.96	2.96	3.04	3.01	3.13	2.93	2.96	3.07	3.20	3.16	3.13	3.08	2.91	3.04	3.01
Mn	0.00	0.00	0.01	0.00	0.00	0.00	0.00	0.00	0.00	0.00	0.00	0.00	0.01	0.00	0.00	0.00	0.00	0.00	0.00	0.00
Mg	1.71	1.71	1.71	1.68	1.69	1.73	1.77	1.71	1.70	1.75	1.76	1.73	1.63	1.65	1.70	1.68	1.78	1.59	1.74	1.76
Ca	0.00	0.00	0.00	0.00	0.00	0.00	0.00	0.00	0.00	0.00	0.00	0.00	0.00	0.00	0.00	0.00	0.00	0.00	0.00	0.00
Na	0.11	0.10	0.11	0.12	0.12	0.11	0.11	0.12	0.11	0.10	0.12	0.12	0.09	0.09	0.08	0.09	0.09	0.08	0.10	0.11
K	1.80	1.81	1.82	1.79	1.80	1.83	1.81	1.80	1.82	1.81	1.83	1.83	1.82	1.83	1.81	1.86	1.83	1.87	1.80	1.79
OH	3.86	3.87	3.84	3.89	3.80	3.83	3.88	3.87	3.89	3.85	3.82	3.85	3.90	3.90	3.82	3.83	3.84	3.80	3.81	3.83
F	0.13	0.13	0.15	0.11	0.20	0.16	0.11	0.12	0.11	0.14	0.18	0.13	0.09	0.10	0.18	0.16	0.15	0.20	0.19	0.16
Cl	0.00	0.00	0.01	0.01	0.01	0.00	0.01	0.01	0.01	0.01	0.01	0.01	0.00	0.00	0.00	0.00	0.00	0.00	0.00	0.00
XMg	0.37	0.37	0.37	0.37	0.37	0.37	0.37	0.36	0.36	0.36	0.38	0.37	0.35	0.34	0.35	0.35	0.37	0.35	0.36	0.37
Oxygen	22	22	22	22	22	22	22	22	22	22	22	22	22	22	22	22	22	22	22	22

UM09 Biotite

Analysis #	4/4.	4/5.	4/6.	4/7.	4/8.	4/9.	4/10.	7/1.	7/2.	7/4.	7/5.	7/6.	7/7.	7/8.	7/9.	7/10.	7/11.	9/4.	9/12.	9/13.
Location	Matrix	Matrix	Matrix	Matrix	Matrix	Matrix	Matrix	Matrix	Matrix	Matrix	Matrix	Matrix	Matrix	Matrix	Matrix	Matrix	Matrix	Near Grt	Near Grt	Near Grt
SiO2	34.38	34.75	34.81	34.50	34.25	34.73	35.03	34.64	34.78	34.42	34.20	34.50	34.30	34.48	34.53	34.35	34.36	34.82	34.47	34.57
TiO2	2.09	2.67	2.50	2.39	2.36	2.42	2.45	2.63	2.60	2.36	2.52	2.53	2.66	2.71	2.64	2.63	2.71	2.37	2.34	2.56
Al2O3	18.52	18.45	18.56	18.34	18.21	18.58	18.85	18.31	18.38	18.09	18.43	18.49	18.63	18.45	18.15	18.89	18.56	18.75	18.89	18.23
FeO	23.37	22.62	23.31	22.62	23.35	22.41	21.86	22.58	22.64	23.25	22.92	22.95	23.00	22.91	23.22	22.40	22.72	21.76	22.56	22.76
MnO	0.01	0.01	0.01	0.01	0.02	0.02	0.02	0.02	0.01	0.03	0.03	0.02	0.01	0.03	0.00	0.00	0.02	0.01	0.01	0.02
MgO	7.49	7.12	7.50	7.54	7.78	7.39	7.23	7.37	7.36	7.64	7.47	7.44	7.37	7.35	7.37	7.21	7.32	7.46	7.37	7.23
CaO	0.00	0.00	0.00	0.00	0.00	0.00	0.00	0.00	0.00	0.05	0.00	0.00	0.00	0.03	0.03	0.07	0.02	0.03	0.00	0.00
Na2O	0.34	0.35	0.32	0.34	0.34	0.35	0.38	0.33	0.35	0.33	0.37	0.36	0.37	0.38	0.36	0.38	0.36	0.33	0.34	0.28
K2O	9.15	9.26	9.12	9.08	8.79	9.19	9.26	9.25	9.34	9.26	9.18	9.16	9.39	9.24	9.20	9.11	9.25	9.17	9.21	9.34
P2O5	0.00	0.00	0.00	0.00	0.00	0.00	0.00	0.00	0.00	0.00	0.01	0.00	0.00	0.00	0.00	0.00	0.00	0.00	0.00	0.00
Cl	0.01	0.01	0.01	0.01	0.01	0.01	0.01	0.00	0.01	0.01	0.00	0.01	0.00	0.00	0.01	0.01	0.00	0.02	0.01	0.00
F	0.31	0.22	0.35	0.31	0.29	0.23	0.41	0.35	0.39	0.23	0.39	0.34	0.31	0.32	0.40	0.26	0.28	0.27	0.33	0.33
H2O	3.71	3.76	3.73	3.70	3.71	3.76	3.68	3.70	3.69	3.75	3.67	3.71	3.73	3.72	3.67	3.74	3.73	3.73	3.71	3.69
Total	99.38	99.22	100.22	98.84	99.11	99.09	99.18	99.18	99.55	99.42	99.19	99.51	99.77	99.62	99.58	99.05	99.33	98.72	99.24	99.01
Si	5.34	5.39	5.36	5.37	5.33	5.38	5.41	5.38	5.38	5.35	5.32	5.35	5.31	5.34	5.36	5.33	5.33	5.40	5.34	5.38
Al iv	2.66	2.61	2.64	2.63	2.67	2.62	2.59	2.62	2.62	2.65	2.68	2.65	2.69	2.66	2.64	2.67	2.67	2.60	2.66	2.62
Al vi	0.74	0.76	0.72	0.74	0.67	0.78	0.84	0.73	0.73	0.67	0.71	0.72	0.71	0.71	0.68	0.78	0.72	0.83	0.80	0.73
Ti	0.24	0.31	0.29	0.28	0.28	0.28	0.28	0.31	0.30	0.28	0.30	0.29	0.31	0.32	0.31	0.31	0.32	0.28	0.27	0.30
Fe	3.04	2.93	3.00	2.95	3.04	2.91	2.82	2.93	2.93	3.02	2.98	2.97	2.98	2.97	3.01	2.91	2.95	2.82	2.92	2.96
Mn	0.00	0.00	0.00	0.00	0.00	0.00	0.00	0.00	0.00	0.00	0.00	0.00	0.00	0.00	0.00	0.00	0.00	0.00	0.00	0.00
Mg	1.74	1.65	1.72	1.75	1.81	1.71	1.66	1.71	1.70	1.77	1.73	1.72	1.70	1.70	1.70	1.67	1.69	1.72	1.70	1.68
Ca	0.00	0.00	0.00	0.00	0.00	0.00	0.00	0.00	0.00	0.01	0.00	0.00	0.00	0.00	0.00	0.01	0.00	0.00	0.00	0.00
Na	0.10	0.11	0.10	0.10	0.10	0.11	0.11	0.10	0.11	0.10	0.11	0.11	0.11	0.11	0.11	0.11	0.11	0.10	0.10	0.08
K	1.81	1.83	1.79	1.80	1.75	1.82	1.82	1.83	1.84	1.84	1.82	1.81	1.85	1.82	1.82	1.80	1.83	1.81	1.82	1.86
OH	3.84	3.89	3.83	3.84	3.85	3.88	3.80	3.83	3.81	3.88	3.81	3.83	3.85	3.84	3.80	3.87	3.86	3.86	3.84	3.84
F	0.15	0.11	0.17	0.15	0.14	0.11	0.20	0.17	0.19	0.11	0.19	0.17	0.15	0.16	0.20	0.13	0.14	0.13	0.16	0.16
Cl	0.00	0.00	0.00	0.00	0.00	0.00	0.00	0.00	0.00	0.00	0.00	0.00	0.00	0.00	0.00	0.00	0.00	0.01	0.00	0.00
XMg	0.36	0.36	0.36	0.37	0.37	0.37	0.37	0.37	0.37	0.37	0.37	0.37	0.36	0.36	0.36	0.36	0.36	0.38	0.37	0.36
Oxygen	22	22	22	22	22	22	22	22	22	22	22	22	22	22	22	22	22	22	22	22

Table C1. Compositional mineral analysis for garnet, biotite, muscovite and feldspar

UM04 Muscovite

Analysis #	4/1.	4/5.	4/6.	4/7.	4/8.	4/10.	4/13.	4/14.	4/15.
SiO2	47.61	47.67	47.64	47.55	47.68	48.56	47.33	47.96	47.66
TiO2	0.31	0.37	0.45	0.32	0.27	0.25	0.40	0.32	0.37
Al2O3	35.10	35.31	35.50	34.99	35.20	34.81	34.73	35.34	35.80
FeO	1.07	1.08	0.97	0.82	0.90	0.95	1.78	1.00	0.89
MnO	0.00	0.00	0.00	0.00	0.00	0.00	0.00	0.00	0.00
MgO	0.65	0.59	0.56	0.56	0.56	0.76	0.97	0.63	0.47
CaO	0.00	0.00	0.00	0.00	0.00	0.00	0.00	0.00	0.00
Na2O	0.67	0.89	0.86	0.82	0.83	0.80	0.87	0.77	0.99
K2O	10.65	10.32	10.66	10.32	10.44	10.61	10.37	10.68	10.46
P2O5	0.01	0.01	0.01	0.01	0.00	0.03	0.02	0.01	0.00
Cl	0.01	0.02	0.01	0.03	0.01	0.01	0.01	0.01	0.01
F	0.04	0.00	0.08	0.14	0.17	0.16	0.13	0.15	0.20
H2O	4.53	4.56	4.54	4.46	4.47	4.51	4.49	4.51	4.49
Total	100.65	100.82	101.28	100.02	100.53	101.45	101.10	101.38	101.34
Si	6.27	6.26	6.24	6.29	6.28	6.34	6.23	6.27	6.23
Al iv	1.73	1.74	1.76	1.71	1.72	1.66	1.77	1.73	1.77
Al vi	3.72	3.73	3.72	3.75	3.75	3.70	3.63	3.72	3.75
Ti	0.03	0.04	0.04	0.03	0.03	0.02	0.04	0.03	0.04
Fe	0.12	0.12	0.11	0.09	0.10	0.10	0.20	0.11	0.10
Mn	0.00	0.00	0.00	0.00	0.00	0.00	0.00	0.00	0.00
Mg	0.13	0.12	0.11	0.11	0.11	0.15	0.19	0.12	0.09
Ca	0.00	0.00	0.00	0.00	0.00	0.00	0.00	0.00	0.00
Na	0.17	0.23	0.22	0.21	0.21	0.20	0.22	0.20	0.25
K	1.79	1.73	1.78	1.74	1.75	1.77	1.74	1.78	1.74
OH	3.98	4.00	3.96	3.93	3.93	3.93	3.94	3.94	3.92
F	0.02	0.00	0.03	0.06	0.07	0.07	0.05	0.06	0.08
Cl	0.00	0.00	0.00	0.01	0.00	0.00	0.00	0.00	0.00
XMg	0.52	0.49	0.51	0.55	0.53	0.59	0.49	0.53	0.48
Oxygen	22	22	22	22	22	22	22	22	22

UM05 Muscovite

Analysis #	2/10.	3/4.	3/6.	4/8.
SiO2	46.33	46.21	46.12	45.69
TiO2	0.28	0.24	0.57	0.31
Al2O3	37.82	38.02	37.51	38.40
FeO	0.86	0.76	0.85	0.79
MnO	0.00	0.00	0.01	0.00
MgO	0.55	0.54	0.56	0.45
CaO	0.00	0.00	0.00	0.00
Na2O	0.84	0.89	0.82	0.96
K2O	9.73	9.65	9.73	9.85
P2O5	n/a	n/a	n/a	n/a
Cl	n/a	n/a	n/a	n/a
F	n/a	n/a	n/a	n/a
H2O	4.59	4.59	4.58	4.59
Total	101.00	100.90	100.75	101.04
Si	6.05	6.03	6.04	5.97
Al iv	1.95	1.97	1.96	2.03
Al vi	3.87	3.89	3.83	3.89
Ti	0.03	0.02	0.06	0.03
Fe	0.09	0.08	0.09	0.09
Mn	0.00	0.00	0.00	0.00
Mg	0.11	0.11	0.11	0.09
Ca	0.00	0.00	0.00	0.00
Na	0.21	0.23	0.21	0.24
K	1.62	1.61	1.63	1.64
OH	4.00	4.00	4.00	4.00
F	n/a	n/a	n/a	n/a
Cl	n/a	n/a	n/a	n/a
XMg	0.53	0.56	0.54	0.50
Oxygen	22	22	22	22

UM07 Muscovite

Analysis #	6/3.	6/4.	6/5.	6/6.	6/8.	6/10.
SiO2	46.51	46.87	47.38	47.14	47.73	47.29
TiO2	0.32	0.32	0.35	0.23	0.30	0.26
Al2O3	35.91	35.67	35.04	35.71	35.35	35.79
FeO	0.95	1.08	0.88	0.89	0.94	0.85
MnO	0.00	0.02	0.01	0.00	0.01	0.01
MgO	0.44	0.48	0.68	0.51	0.66	0.56
CaO	0.02	0.02	0.01	0.03	0.02	0.03
Na2O	1.19	1.14	0.95	1.15	1.16	1.11
K2O	10.29	10.17	10.54	10.20	10.33	10.07
P2O5	0.02	0.03	0.02	0.02	0.03	0.02
Cl	0.02	0.01	0.01	0.02	0.01	0.02
F	0.29	0.20	0.13	0.21	0.16	0.18
H2O	4.39	4.44	4.48	4.44	4.50	4.47
Total	100.35	100.45	100.48	100.55	101.20	100.66
Si	6.16	6.19	6.25	6.21	6.25	6.22
Al iv	1.84	1.81	1.75	1.79	1.75	1.78
Al vi	3.76	3.75	3.71	3.76	3.71	3.76
Ti	0.03	0.03	0.03	0.02	0.03	0.03
Fe	0.11	0.12	0.10	0.10	0.10	0.09
Mn	0.00	0.00	0.00	0.00	0.00	0.00
Mg	0.09	0.09	0.13	0.10	0.13	0.11
Ca	0.00	0.00	0.00	0.00	0.00	0.00
Na	0.31	0.29	0.24	0.29	0.29	0.28
K	1.74	1.71	1.77	1.71	1.73	1.69
OH	3.87	3.91	3.94	3.91	3.93	3.92
F	0.12	0.08	0.05	0.09	0.07	0.07
Cl	0.00	0.00	0.00	0.00	0.00	0.00
XMg	0.45	0.44	0.58	0.51	0.56	0.54
Oxygen	22	22	22	22	22	22

UM08 Muscovite

Analysis #	2/4.	2/7.	4/3.	5/1.	5/2.	9/4.	9/6.	11/11.
SiO2	49.43	48.26	48.32	48.37	48.52	48.10	47.32	47.73
TiO2	0.45	0.21	0.63	0.34	0.38	0.14	0.21	0.22
Al2O3	33.30	35.92	34.97	34.96	34.83	35.41	35.00	35.10
FeO	1.32	0.63	0.91	1.01	0.92	0.87	0.85	0.80
MnO	0.00	0.00	0.00	0.00	0.00	0.00	0.00	0.00
MgO	1.08	0.35	0.63	0.68	0.65	0.56	0.60	0.58
CaO	0.00	0.00	0.00	0.00	0.00	0.00	0.00	0.00
Na2O	0.79	1.12	1.13	0.89	0.80	0.73	0.56	0.71
K2O	10.45	9.39	10.22	10.55	10.64	10.75	11.08	10.69
P2O5	0.00	0.00	0.00	0.00	0.00	0.00	0.00	0.00
Cl	0.01	0.00	0.00	0.00	0.00	0.00	0.00	0.00
F	0.00	0.00	0.00	0.00	0.00	0.00	0.12	0.00
H2O	4.61	4.64	4.65	4.65	4.59	4.66	4.47	4.60
Total	101.44	100.52	101.46	101.45	101.33	101.22	100.21	100.43
Si	6.45	6.30	6.30	6.32	6.34	6.30	6.27	6.29
Al iv	1.55	1.70	1.70	1.68	1.66	1.70	1.73	1.71
Al vi	3.58	3.83	3.68	3.70	3.70	3.76	3.74	3.75
Ti	0.04	0.02	0.06	0.03	0.04	0.01	0.02	0.02
Fe	0.14	0.07	0.10	0.11	0.10	0.10	0.09	0.09
Mn	0.00	0.00	0.00	0.00	0.00	0.00	0.00	0.00
Mg	0.21	0.07	0.12	0.13	0.13	0.11	0.12	0.11
Ca	0.00	0.00	0.00	0.00	0.00	0.00	0.00	0.00
Na	0.20	0.28	0.29	0.23	0.20	0.19	0.14	0.18
K	1.74	1.56	1.70	1.76	1.77	1.79	1.87	1.80
OH	4.02	4.04	4.04	4.05	4.00	4.07	3.95	4.04
F	0.00	0.00	0.00	0.00	0.00	0.00	0.05	0.00
Cl	0.00	0.00	0.00	0.00	0.00	0.00	0.00	0.00
XMg	0.59	0.50	0.55	0.55	0.56	0.53	0.56	0.56
Oxygen	22	22	22	22	22	22	22	22

UM09 Muscovite

Analysis #	3/1.	3/9.	4/2.	4/4.	4/6.
SiO2	45.48	45.19	45.51	45.25	45.21
TiO2	0.80	0.76	0.45	0.50	0.57
Al2O3	38.47	37.83	38.61	38.34	38.05
FeO	0.86	1.02	0.96	1.13	1.16
MnO	0.00	0.00	0.00	0.00	0.00
MgO	0.33	0.38	0.33	0.35	0.39
CaO	0.00	0.01	0.02	0.01	0.00
Na2O	1.08	1.05	1.14	1.06	1.13
K2O	9.65	9.67	9.62	9.86	9.80
P2O5	n/a	n/a	n/a	n/a	n/a
Cl	n/a	n/a	n/a	n/a	n/a
F	n/a	n/a	n/a	n/a	n/a
H2O	4.60	4.55	4.59	4.57	4.56
Total	101.27	100.46	101.23	101.07	100.87
Si	5.93	5.95	5.94	5.93	5.94
Al iv	2.07	2.05	2.06	2.07	2.06
Al vi	3.85	3.83	3.88	3.86	3.83
Ti	0.08	0.08	0.04	0.05	0.06
Fe	0.09	0.11	0.10	0.12	0.13
Mn	0.00	0.00	0.00	0.00	0.00
Mg	0.06	0.07	0.06	0.07	0.08
Ca	0.00	0.00	0.00	0.00	0.00
Na	0.27	0.27	0.29	0.27	0.29
K	1.61	1.62	1.60	1.65	1.64
OH	4.00	4.00	4.00	4.00	4.00
F	n/a	n/a	n/a	n/a	n/a
Cl	n/a	n/a	n/a	n/a	n/a
XMg	0.41	0.40	0.38	0.36	0.37
Oxygen	22	22	22	22	22

Table C1. Compositional mineral analysis for garnet, biotite, muscovite and feldspar

UM04 Feldspar

Analysis #	1/14.	1/17.	2/4.	2/8.	2/9.
SiO2	58.75	58.40	58.43	58.57	57.86
TiO2	0.03	0.01	0.02	0.02	0.02
Al2O3	25.26	27.12	26.69	25.82	26.58
FeO	0.37	0.17	0.13	0.20	0.31
MnO	0.02	0.00	0.00	0.00	0.00
MgO	0.23	0.02	0.04	0.00	0.02
CaO	5.22	7.81	7.65	6.05	7.09
Na2O	7.04	7.20	7.01	7.71	7.01
K2O	1.78	0.24	0.47	0.58	0.44
P2O5	0.01	0.03	0.02	0.03	0.04
Total	98.71	101.00	100.46	98.98	99.37
Si	2.66	2.59	2.60	2.64	2.60
Al	1.35	1.42	1.40	1.37	1.41
Ti	0.00	0.00	0.00	0.00	0.00
Fe	0.01	0.01	0.00	0.01	0.01
Mn	0.00	0.00	0.00	0.00	0.00
Mg	0.02	0.00	0.00	0.00	0.00
Ca	0.25	0.37	0.37	0.29	0.34
Na	0.62	0.62	0.61	0.67	0.61
K	0.10	0.01	0.03	0.03	0.03
An	0.26	0.37	0.37	0.29	0.35
Ab	0.63	0.62	0.61	0.67	0.62
Or	0.11	0.01	0.03	0.03	0.03
Oxygen	8	8	8	8	8

UM05 Feldspar

Analysis #	1/3.	2/3.	2/4.	2/5.	5/9.
SiO2	60.40	60.35	60.84	60.63	61.88
TiO2	0.01	0.10	0.00	0.04	0.01
Al2O3	24.76	24.63	24.06	24.40	23.67
FeO	0.04	0.23	0.12	0.25	0.11
MnO	0.00	0.00	0.00	0.00	0.00
MgO	0.02	0.05	0.01	0.03	0.03
CaO	7.29	4.95	6.88	5.91	6.32
Na2O	7.44	7.78	8.15	7.79	7.54
K2O	0.20	0.47	0.10	0.37	0.32
P2O5	0.02	0.04	0.20	0.02	0.04
Total	100.18	98.60	100.36	99.44	99.92
Si	2.69	2.72	2.71	2.71	2.75
Al	1.30	1.31	1.26	1.29	1.24
Ti	0.00	0.00	0.00	0.00	0.00
Fe	0.00	0.01	0.00	0.01	0.00
Mn	0.00	0.00	0.00	0.00	0.00
Mg	0.00	0.00	0.00	0.00	0.00
Ca	0.35	0.24	0.33	0.28	0.30
Na	0.64	0.68	0.70	0.68	0.65
K	0.01	0.03	0.01	0.02	0.02
An	0.35	0.25	0.32	0.29	0.31
Ab	0.64	0.72	0.68	0.69	0.67
Or	0.01	0.03	0.01	0.02	0.02
Oxygen	8	8	8	8	8

UM07 Feldspar

Analysis #	1/1.	1/2.	2/3.	2/6.	2/7.	2/14.
SiO2	60.33	59.93	60.41	60.31	61.02	60.73
TiO2	0.01	0.01	0.02	0.03	0.02	0.01
Al2O3	23.78	23.76	23.58	24.04	23.60	23.39
FeO	0.11	0.34	0.16	0.10	0.09	0.12
MnO	0.01	0.00	0.01	0.00	0.03	0.03
MgO	0.00	0.00	0.04	0.00	0.00	0.01
CaO	6.79	6.43	6.21	6.85	6.39	6.37
Na2O	8.00	8.08	8.23	8.18	8.50	8.37
K2O	0.09	0.12	0.42	0.06	0.07	0.27
P2O5	0.02	0.02	0.03	0.04	0.03	0.04
Total	99.14	98.69	99.11	99.61	99.75	99.34
Si	2.71	2.71	2.72	2.70	2.73	2.73
Al	1.26	1.27	1.25	1.27	1.24	1.24
Ti	0.00	0.00	0.00	0.00	0.00	0.00
Fe	0.00	0.01	0.01	0.00	0.00	0.00
Mn	0.00	0.00	0.00	0.00	0.00	0.00
Mg	0.00	0.00	0.00	0.00	0.00	0.00
Ca	0.33	0.31	0.30	0.33	0.31	0.31
Na	0.70	0.71	0.72	0.71	0.74	0.73
K	0.01	0.01	0.02	0.00	0.00	0.02
An	0.32	0.30	0.29	0.32	0.29	0.29
Ab	0.68	0.69	0.69	0.68	0.70	0.69
Or	0.01	0.01	0.02	0.00	0.00	0.01
Oxygen	8	8	8	8	8	8

UM08 Feldspar

Analysis #	1/1.	1/4.	1/8.	1/9.
SiO2	59.93	59.31	59.52	58.87
TiO2	0.01	0.01	0.00	0.00
Al2O3	25.64	25.37	25.84	25.53
FeO	0.16	0.31	0.13	0.20
MnO	0.03	0.00	0.00	0.01
MgO	0.01	0.02	0.00	0.00
CaO	6.40	6.59	6.88	7.03
Na2O	7.91	7.81	7.84	7.70
K2O	0.39	0.16	0.11	0.13
P2O5	0.03	0.02	0.01	0.01
Total	100.51	99.60	100.33	99.48
Si	2.66	2.66	2.65	2.64
Al	1.34	1.34	1.35	1.35
Ti	0.00	0.00	0.00	0.00
Fe	0.01	0.01	0.00	0.01
Mn	0.00	0.00	0.00	0.00
Mg	0.00	0.00	0.00	0.00
Ca	0.30	0.32	0.33	0.34
Na	0.68	0.68	0.68	0.67
K	0.02	0.01	0.01	0.01
An	0.30	0.32	0.32	0.33
Ab	0.68	0.68	0.67	0.66
Or	0.02	0.01	0.01	0.01
Oxygen	8	8	8	8

UM09 Feldspar

Analysis #	2/4.	2/5.	2/6.	4/4.	4/5.	5/2.	5/3.	5/5.	6/9.	7/8.	7/9.	7/11.	7/15.	7/16.	7/17.	7/18.	8/1.	8/3.	8/7.	8/9.	8/11.	8/13.	10/2.	10/5.	10/8.	10/10.	10/11.	11/1.	11/3.	11/5.
SiO2	63.54	64.99	62.05	63.06	62.36	63.64	62.26	63.03	63.50	62.26	61.72	62.65	63.62	63.65	63.73	63.72	63.59	63.47	63.90	64.50	62.68	62.46	64.51	63.07	62.99	62.58	62.14	61.86	62.91	62.64
TiO2	0.00	0.00	0.00	0.00	0.00	0.00	0.00	0.00	0.00	0.00	0.00	0.00	0.00	0.00	0.00	0.00	0.00	0.00	0.00	0.00	0.00	0.00	0.00	0.00	0.00	0.00	0.00	0.00	0.00	0.11
Al2O3	23.07	22.53	24.22	23.23	23.70	23.25	23.26	23.30	23.69	23.85	24.09	23.16	23.43	23.33	23.42	23.42	23.64	23.59	23.30	22.82	24.05	23.48	21.96	23.17	23.67	23.92	23.90	24.93	24.14	22.95
FeO	0.12	0.02	0.10	0.20	0.13	0.00	0.00	0.00	0.00	0.16	0.01	0.00	0.00	0.00	0.00	0.00	0.00	0.00	0.00	0.00	0.00	0.00	0.00	0.14	0.00	0.00	0.00	0.00	0.00	0.38
MnO	0.00	0.00	0.00	0.00	0.00	0.00	0.00	0.00	0.00	0.00	0.00	0.00	0.00	0.00	0.00	0.00	0.00	0.00	0.00	0.00	0.00	0.00	0.00	0.00	0.00	0.00	0.00	0.00	0.00	0.00
MgO	0.00	0.00	0.00	0.00	0.00	0.00	0.00	0.00	0.00	0.03	0.00	0.00	0.00	0.00	0.00	0.00	0.00	0.00	0.00	0.00	0.00	0.00	0.00	0.00	0.00	0.00	0.00	0.00	0.00	0.00
CaO	4.63	4.53	4.47	4.77	4.74	4.66	4.58	5.05	4.91	5.19	5.00	4.77	4.73	4.71	4.78	4.79	4.83	4.79	4.60	4.19	5.52	5.06	3.10	4.68	4.94	4.78	4.94	5.90	5.52	4.75
Na2O	9.22	9.12	8.79	9.27	9.27	9.35	9.22	9.15	9.28	9.04	8.87	9.23	9.33	9.47	9.34	9.39	9.24	9.34	9.41	9.69	8.80	8.82	9.97	9.28	9.08	8.93	8.84	8.55	8.73	9.21
K2O	0.05	0.01	0.12	0.04	0.05	0.03	0.01	0.04	0.04	0.04	0.05	0.02	0.09	0.09	0.07	0.08	0.08	0.06	0.11	0.12	0.04	0.04	0.13	0.01	0.12	0.20	0.09	0.01	0.00	0.01
P2O5	0.05	0.06	0.07	0.01	0.02	0.01	0.01	0.15	0.00	0.00	0.00	0.01	0.07	0.06	0.07	0.07	0.06	0.08	0.06	0.07	0.00	0.00	0.04	0.05	0.01	0.00	0.00	0.01	0.03	0.07
Total	100.68	101.26	99.82	100.58	100.27	100.94	99.34	100.72	101.42	100.57	99.74	99.84	101.27	101.31	101.41	101.47	101.44	101.33	101.38	101.39	101.09	99.86	99.71	100.40	100.81	100.41	99.91	101.26	101.33	100.12
Si	2.80	2.84	2.75	2.78	2.76	2.79	2.78	2.78	2.78	2.75	2.74	2.78	2.79	2.79	2.79	2.79	2.78	2.78	2.80	2.82	2.75	2.77	2.86	2.79	2.77	2.76	2.76	2.72	2.76	2.78
Al	1.20	1.16	1.27	1.21	1.24	1.20	1.22	1.21	1.22	1.24	1.26	1.21	1.21	1.21	1.21	1.21	1.22	1.22	1.20	1.18	1.25	1.23	1.15	1.21	1.23	1.25	1.25	1.29	1.25	1.20
Ti	0.00	0.00	0.00	0.00	0.00	0.00	0.00	0.00	0.00	0.00	0.00	0.00	0.00	0.00	0.00	0.00	0.00	0.00	0.00	0.00	0.00	0.00	0.00	0.00	0.00	0.00	0.00	0.00	0.00	0.00
Fe	0.00	0.00	0.00	0.01	0.00	-0.01	0.00	0.00	-0.01	0.01	0.00	0.00	-0.01	-0.01	-0.01	-0.01	-0.01	-0.01	-0.01	-0.01	-0.01	-0.01	0.00	0.01	-0.01	-0.01	-0.01	0.00	-0.01	0.01
Mn	0.00	0.00	0.00	0.00	0.00	0.00	0.00	0.00	0.00	0.00	0.00	0.00	0.00	0.00	0.00	0.00	0.00	0.00	0.00	0.00	0.00	0.00	0.00	0.00	0.00	0.00	0.00	0.00	0.00	0.00
Mg	0.00	0.00	0.00	0.00	0.00	0.00	0.00	0.00	0.00	0.00	0.00	0.00	0.00	0.00	0.00	0.00	0.00	0.00	0.00	0.00	0.00	0.00	0.00	0.00	0.00	0.00	0.00	0.00	0.00	0.00
Ca	0.22	0.21	0.21	0.23	0.22	0.22	0.22	0.24	0.23	0.25	0.24	0.23	0.22	0.22	0.22	0.22	0.23	0.22	0.22	0.20	0.26	0.24	0.15	0.22	0.23	0.23	0.23	0.28	0.26	0.23
Na	0.79	0.77	0.76	0.79	0.80	0.80	0.80	0.78	0.79	0.77	0.76	0.79	0.79	0.80	0.79	0.80	0.78	0.79	0.80	0.82	0.75	0.76	0.86	0.79	0.78	0.76	0.76	0.73	0.74	0.79
K	0.00	0.00	0.01	0.00	0.00	0.00	0.00	0.00	0.00	0.00	0.00	0.00	0.01	0.01	0.00	0.00	0.00	0.00	0.01	0.01	0.00	0.00	0.01	0.00	0.01	0.01	0.01	0.00	0.00	0.00
An	0.22	0.22	0.22	0.22	0.22	0.22	0.22	0.23	0.23	0.24	0.24	0.22	0.22	0.21	0.22	0.22	0.22	0.22	0.21	0.19	0.26	0.24	0.15	0.22	0.23	0.23	0.23	0.28	0.26	0.22
Ab	0.78	0.78	0.78	0.78	0.78	0.78	0.78	0.76	0.77	0.76	0.76	0.78	0.78	0.78	0.78	0.78	0.77	0.78	0.78	0.80	0.74	0.76	0.85	0.78	0.76	0.76	0.76	0.72	0.74	0.78
Or	0.00	0.00	0.01	0.00	0.00	0.00	0.00	0.00	0.00	0.00	0.00	0.00	0.00	0.00	0.00	0.00	0.00	0.00	0.01	0.01	0.00	0.00	0.01	0.00	0.01	0.01	0.01	0.00	0.00	0.00
Oxygen	8	8	8	8	8	8	8	8	8	8	8	8	8	8	8	8	8	8	8	8	8	8	8	8	8	8	8	8	8	8

Table C2. Trace element composition of garnet

Specimen UM04

Spot number	Y89	1SE	La139	1SE	Ce140	1SE	Pr141	1SE	Nd146	1SE	Sm147	1SE	Eu153	1SE	Gd157	1SE	Tb159	1SE	Dy163	1SE	Ho165	1SE	Er166	1SE	Tm169	1SE	Yb172	1SE
UM04_1	226	4	0.0	0.0	0.0	0.0	0.0	0.0	0.1	0.1	1.4	0.2	0.3	0.0	9.2	0.8	3.5	0.1	33.1	1.1	8.5	0.3	28.4	0.6	4.9	0.2	32.6	1.2
UM04_2	248	3	0.0	0.0	0.0	0.0	0.0	0.0	0.1	0.1	1.5	0.2	0.3	0.0	9.2	0.8	4.0	0.2	38.3	1.1	9.2	0.3	29.4	0.9	4.7	0.2	36.8	1.1
UM04_3	456	7	0.0	0.0	0.0	0.0	0.0	0.0	0.0	0.0	1.4	0.2	0.1	0.0	9.0	0.7	4.7	0.1	63.0	1.8	15.8	0.5	58.2	1.5	9.1	0.3	74.4	2.0
UM04_4	815	12	0.0	0.0	0.0	0.0	0.0	0.0	0.0	0.0	0.7	0.1	0.2	0.0	8.0	0.6	5.8	0.2	91.9	1.3	27.6	0.5	107.1	1.7	18.0	0.3	144.9	3.0
UM04_5	865	11	0.0	0.0	0.0	0.0	0.0	0.0	0.1	0.1	0.6	0.1	0.3	0.0	8.5	0.6	6.3	0.2	92.7	1.9	29.5	0.7	116.1	2.0	20.7	0.5	151.6	3.1
UM04_6	718	11	0.0	0.0	0.0	0.0	0.0	0.0	0.1	0.1	0.8	0.1	0.4	0.1	7.8	0.5	5.6	0.2	85.3	1.8	25.1	0.5	86.2	2.2	14.4	0.3	105.3	2.1
UM04_7	458	6	0.0	0.0	0.0	0.0	0.0	0.0	0.0	0.0	0.9	0.2	0.3	0.1	11.4	0.6	5.3	0.2	64.7	1.4	15.9	0.3	56.3	1.3	9.2	0.2	70.8	1.7
UM04_8	297	4	0.0	0.0	0.0	0.0	0.0	0.0	0.1	0.0	1.1	0.1	0.3	0.1	9.9	0.4	4.3	0.1	44.3	1.1	10.6	0.3	36.4	0.9	6.5	0.2	45.1	1.0
UM04_9	227	3	0.0	0.0	0.0	0.0	0.0	0.0	0.2	0.1	1.3	0.2	0.2	0.0	10.7	0.5	4.1	0.1	36.2	1.0	8.1	0.2	29.2	0.8	4.8	0.2	34.3	1.0
UM04_10	226	4	0.0	0.0	0.0	0.0	0.0	0.0	0.0	0.0	1.5	0.2	0.3	0.0	11.7	0.8	3.5	0.1	36.4	1.0	8.7	0.3	29.1	0.6	4.9	0.2	30.6	0.8

Specimen UM05

Spot number	Y89	1SE	La139	1SE	Ce140	1SE	Pr141	1SE	Nd146	1SE	Sm147	1SE	Eu153	1SE	Gd157	1SE	Tb159	1SE	Dy163	1SE	Ho165	1SE	Er166	1SE	Tm169	1SE	Yb172	1SE
UM05_1	277	4	0.0	0.5	0.0	0.0	0.0	0.0	0.0	0.0	0.3	0.1	0.2	0.0	7.3	0.4	3.5	0.2	39.3	1.1	10.5	0.3	37.3	1.0	7.0	0.2	55.1	1.4
UM05_2	145	2	0.0	0.5	0.0	0.0	0.0	0.0	0.0	0.5	0.5	0.1	0.4	0.1	4.3	0.4	1.6	0.1	18.0	0.6	4.2	0.2	16.9	0.5	2.8	0.1	23.9	0.7
UM05_3	93	2	0.0	0.5	0.0	0.0	0.0	0.0	0.2	0.1	0.6	0.1	0.5	0.1	3.3	0.3	1.0	0.1	8.2	0.3	2.6	0.1	10.2	0.4	2.2	0.1	17.4	0.6
UM05_4	132	2	0.0	0.5	0.0	0.0	0.0	0.0	0.1	0.0	0.5	0.1	0.7	0.1	3.1	0.3	1.0	0.1	11.6	0.4	3.5	0.1	17.5	0.7	3.6	0.2	33.1	1.1
UM05_5	88	2	0.0	0.5	0.0	0.0	0.0	0.0	0.1	0.0	0.2	0.1	0.7	0.1	1.4	0.2	0.6	0.0	6.5	0.4	2.0	0.1	8.8	0.4	2.1	0.1	20.7	0.8
UM05_6	529	7	0.0	0.5	0.0	0.0	0.0	0.0	0.0	0.5	0.1	0.0	0.3	0.0	2.7	0.2	1.8	0.1	28.9	0.6	12.3	0.3	79.6	2.0	24.3	0.8	271.0	6.5
UM05_7	831	19	0.0	0.5	0.0	0.0	0.0	0.0	0.0	0.0	0.2	0.1	0.4	0.1	3.6	0.3	2.5	0.1	43.9	1.2	18.7	0.7	122.0	4.8	36.7	1.9	414.0	22.5
UM05_8	259	3	0.0	0.5	0.0	0.0	0.0	0.0	0.0	0.5	0.4	0.1	0.7	0.1	3.7	0.3	1.5	0.1	16.7	0.5	5.5	0.2	30.6	0.7	8.0	0.2	75.2	1.5
UM05_9	101	8	0.0	0.0	0.1	0.0	0.0	0.0	0.1	0.0	0.3	0.1	0.5	0.1	2.1	0.3	0.7	0.1	8.5	0.8	2.8	0.2	13.9	1.4	2.6	0.2	27.0	2.9
UM05_10	138	6	0.0	0.5	0.0	0.0	0.0	0.0	0.0	0.5	0.6	0.1	0.5	0.1	4.1	0.3	1.2	0.1	12.4	0.7	4.3	0.2	19.7	1.1	4.2	0.3	40.3	2.9
UM05_11	149	3	0.0	0.5	0.0	0.0	0.0	0.0	0.0	0.5	0.4	0.1	0.4	0.1	4.6	0.3	1.5	0.1	15.4	0.5	4.4	0.2	19.6	0.8	4.1	0.2	33.0	1.4
UM05_12	296	4	0.0	0.5	0.0	0.0	0.0	0.0	0.0	0.5	0.5	0.1	0.1	0.0	7.2	0.5	3.5	0.1	38.5	0.8	10.9	0.2	40.4	1.1	8.0	0.3	62.9	1.7

Specimen UM07

Spot number	Y89	1SE	La139	1SE	Ce140	1SE	Pr141	1SE	Nd146	1SE	Sm147	1SE	Eu153	1SE	Gd157	1SE	Tb159	1SE	Dy163	1SE	Ho165	1SE	Er166	1SE	Tm169	1SE	Yb172	1SE
UM07_1	232	9	0.0	0.0	0.0	0.0	0.0	0.0	0.2	0.0	1.4	0.1	0.3	0.0	3.6	0.2	4.0	0.2	36.0	1.4	8.1	0.3	23.2	0.9	3.3	0.2	20.2	0.8
UM07_2	112	4	0.0	0.0	0.0	0.0	0.0	0.0	0.3	0.0	1.7	0.1	0.4	0.0	3.2	0.2	2.7	0.1	19.7	0.8	3.8	0.1	10.3	0.4	1.5	0.1	9.1	0.4
UM07_3	135	5	0.0	0.0	0.0	0.0	0.0	0.0	0.3	0.0	1.4	0.1	0.4	0.0	3.6	0.2	3.2	0.2	22.9	0.9	4.6	0.2	12.6	0.5	1.8	0.1	11.3	0.4
UM07_4	188	7	0.0	0.0	0.0	0.0	0.0	0.0	0.2	0.0	1.3	0.1	0.4	0.0	3.9	0.3	4.2	0.2	32.3	1.3	6.1	0.2	17.0	0.7	2.4	0.1	15.2	0.6
UM07_5	326	12	0.0	0.0	0.0	0.0	0.0	0.0	0.2	0.0	1.2	0.1	0.4	0.0	4.5	0.3	5.8	0.3	51.9	2.1	10.6	0.4	29.3	1.1	4.2	0.2	28.3	1.1
UM07_6	1212	46	0.0	0.0	0.0	0.0	0.0	0.0	0.1	0.0	0.8	0.0	0.3	0.0	4.0	0.3	8.3	0.4	130.5	5.3	38.6	1.5	122.2	4.8	18.3	1.0	124.0	4.9
UM07_7	2214	84	0.0	0.0	0.0	0.0	0.0	0.0	0.1	0.0	0.6	0.0	0.2	0.0	3.3	0.2	7.7	0.4	157.0	6.4	65.2	2.5	281.6	11.1	47.8	2.5	340.0	13.5
UM07_8	2798	107	0.0	0.0	0.0	0.0	0.0	0.0	0.1	0.0	0.2	0.0	0.1	0.0	1.2	0.1	3.4	0.2	101.4	4.2	80.2	3.1	720.2	28.7	257.5	13.8	3150.6	126.5
UM07_9	2788	107	0.0	0.0	0.0	0.0	0.0	0.0	0.0	0.0	0.2	0.0	0.1	0.0	1.3	0.1	3.8	0.2	121.9	5.1	94.9	3.7	834.7	33.5	273.8	14.9	3045.9	123.6
UM07_10	2657	107	0.0	0.0	0.0	0.0	0.0	0.0	0.1	0.0	0.4	0.0	0.2	0.0	3.0	0.3	6.9	0.4	170.7	7.5	87.4	3.6	448.9	19.0	86.8	5.1	662.3	28.5
UM07_11	1875	76	0.0	0.0	0.0	0.0	0.0	0.0	0.1	0.0	0.5	0.0	0.2	0.0	3.7	0.3	7.7	0.4	154.1	6.8	61.0	2.5	251.3	10.8	41.8	2.5	293.8	12.8
UM07_12	566	23	0.0	0.0	0.0	0.0	0.0	0.0	0.2	0.0	1.1	0.1	0.4	0.0	5.6	0.5	7.4	0.4	81.7	3.7	18.4	0.8	52.4	2.3	7.9	0.5	52.6	2.3
UM07_13	315	13	0.0	0.0	0.0	0.0	0.0	0.0	0.2	0.0	1.2	0.1	0.4	0.0	5.3	0.5	5.7	0.3	49.9	2.3	10.1	0.4	28.0	1.2	4.1	0.3	28.6	1.3
UM07_14	198	8	0.0	0.0	0.0	0.0	0.0	0.0	0.2	0.0	1.4	0.1	0.4	0.0	5.0	0.5	4.3	0.3	34.2	1.6	6.6	0.3	18.1	0.8	2.6	0.2	17.7	0.8
UM07_15	135	6	0.0	0.0	0.0	0.0	0.0	0.0	0.3	0.0	1.4	0.1	0.4	0.0	4.5	0.5	3.1	0.2	23.5	1.1	4.7	0.2	12.8	0.6	1.8	0.1	11.8	0.5
UM07_16	113	5	0.0	0.0	0.0	0.0	0.0	0.0	0.3	0.0	1.4	0.1	0.3	0.0	4.2	0.4	2.5	0.2	19.5	0.9	4.0	0.2	11.4	0.5	1.6	0.1	10.3	0.5
UM07_17	114	5	0.0	0.0	0.0	0.0	0.0	0.0	0.2	0.0	1.5	0.1	0.3	0.0	4.1	0.4	2.4	0.2	19.4	0.9	4.0	0.2	11.2	0.5	1.5	0.1	10.0	0.5

Table C2. Trace element composition of garnet

Specimen UM08

Spot number	Y89	1SE	La139	1SE	Ce140	1SE	Pr141	1SE	Nd146	1SE	Sm147	1SE	Eu153	1SE	Gd157	1SE	Tb159	1SE	Dy163	1SE	Ho165	1SE	Er166	1SE	Tm169	1SE	Yb172	1SE
UM08_1	499	6	0.0	0.0	0.0	0.0	0.0	0.0	0.0	0.0	0.3	0.1	0.2	0.0	5.8	0.4	3.0	0.1	44.7	1.5	17.3	0.4	84.5	1.5	18.0	0.4	164.4	3.0
UM08_2	415	7	0.0	0.0	0.0	0.0	0.0	0.0	0.0	0.0	0.4	0.1	0.2	0.0	5.9	0.4	2.8	0.1	35.2	0.9	13.1	0.3	60.9	1.1	13.9	0.4	127.8	2.1
UM08_3	368	6	0.0	0.0	0.0	0.0	0.0	0.0	0.1	0.1	0.3	0.1	0.4	0.0	4.9	0.4	2.5	0.1	31.9	0.6	10.6	0.3	47.9	1.3	11.5	0.2	109.8	2.0
UM08_4	308	4	0.0	0.0	0.0	0.0	0.0	0.0	0.0	0.0	0.4	0.1	0.3	0.0	5.3	0.5	2.2	0.1	27.8	0.8	8.2	0.2	34.5	0.9	7.2	0.2	68.3	1.5
UM08_5	194	8	0.0	0.0	0.0	0.0	0.0	0.0	0.1	0.1	0.6	0.1	0.6	0.0	2.9	0.3	1.2	0.1	15.0	0.7	5.0	0.2	24.1	1.0	5.7	0.3	67.0	3.2
UM08_6	115	2	0.0	0.0	0.1	0.0	0.0	0.0	0.1	0.1	1.0	0.2	0.7	0.1	4.1	0.3	1.1	0.1	9.0	0.4	2.8	0.1	11.8	0.4	2.8	0.1	30.2	0.8
UM08_7	120	2	0.0	0.0	0.0	0.0	0.0	0.0	0.2	0.1	0.7	0.1	0.6	0.1	3.8	0.3	1.2	0.1	10.7	0.4	2.6	0.1	12.8	0.4	3.0	0.1	31.8	1.0
UM08_8	98	1	0.0	0.0	0.0	0.0	0.0	0.0	0.1	0.1	0.8	0.1	0.6	0.1	4.0	0.5	0.9	0.1	9.2	0.4	2.6	0.1	10.7	0.3	2.5	0.1	22.9	0.7
UM08_9	202	3	0.0	0.0	0.0	0.0	0.0	0.0	0.1	0.1	0.5	0.1	0.3	0.0	6.0	0.5	2.3	0.1	20.9	0.6	5.1	0.2	18.1	0.5	3.4	0.1	30.2	1.0
UM08_10	376	7	0.0	0.0	0.0	0.0	0.0	0.0	0.2	0.1	0.6	0.1	0.3	0.1	5.7	0.4	2.7	0.1	36.4	0.9	12.1	0.4	50.2	1.0	10.0	0.3	78.7	2.1

Specimen UM09

Spot number	Y89	1SE	La139	1SE	Ce140	1SE	Pr141	1SE	Nd146	1SE	Sm147	1SE	Eu153	1SE	Gd157	1SE	Tb159	1SE	Dy163	1SE	Ho165	1SE	Er166	1SE	Tm169	1SE	Yb172	1SE
UM09_1	42	9	0.0	0.0	0.0	0.0	0.0	0.0	0.2	0.0	1.5	0.3	1.0	0.3	8.0	1.4	2.5	0.5	11.4	1.9	1.8	0.4	4.2	1.1	0.5	0.1	4.2	1.1
UM09_2	137	29	0.0	0.0	0.0	0.0	0.0	0.0	0.4	0.1	2.5	0.5	1.6	0.4	13.7	2.4	5.8	1.3	37.7	6.3	6.0	1.4	12.6	3.3	1.5	0.3	8.3	2.2
UM09_3	205	43	0.0	0.0	0.0	0.0	0.0	0.0	0.4	0.1	2.7	0.5	1.7	0.4	16.0	2.8	6.9	1.5	49.4	8.1	8.6	2.0	20.5	5.3	2.3	0.4	14.2	3.6
UM09_4	249	52	0.0	0.0	0.0	0.0	0.0	0.0	0.7	0.1	3.6	0.6	1.8	0.4	21.4	3.7	8.7	1.8	54.3	8.8	10.6	2.4	25.1	6.3	2.8	0.5	15.2	3.8
UM09_5	215	44	0.0	0.0	0.0	0.0	0.0	0.0	0.9	0.2	3.8	0.7	1.2	0.3	16.8	2.8	5.4	1.1	37.4	6.0	7.9	1.8	22.6	5.6	2.7	0.5	16.3	4.0
UM09_6	73	13	0.0	0.0	0.0	0.0	0.0	0.0	0.7	0.1	3.3	0.5	1.0	0.2	10.0	1.5	2.5	0.5	14.6	2.1	2.8	0.6	7.0	1.6	0.9	0.1	5.9	1.3
UM09_7	97	18	0.0	0.0	0.0	0.0	0.0	0.0	0.6	0.1	2.6	0.4	0.9	0.2	11.5	1.7	3.3	0.6	19.9	2.8	3.7	0.7	8.8	2.0	1.1	0.2	7.7	1.7
UM09_8	153	27	0.0	0.0	0.0	0.0	0.0	0.0	0.5	0.1	2.4	0.4	0.7	0.1	13.6	2.0	5.0	0.9	31.9	4.5	5.9	1.2	15.0	3.3	1.9	0.3	12.7	2.7
UM09_9	295	52	0.0	0.0	0.0	0.0	0.0	0.0	0.4	0.1	2.0	0.3	0.6	0.1	16.7	2.4	7.5	1.3	55.0	7.6	11.1	2.2	27.6	5.9	3.7	0.6	24.1	5.1
UM09_10	713	124	0.0	0.0	0.0	0.0	0.0	0.0	0.2	0.0	1.5	0.2	0.4	0.1	16.1	2.3	10.8	1.9	110.9	15.1	25.3	4.8	66.3	14.0	9.0	1.4	61.9	13.0
UM09_11	2073	355	0.0	0.0	0.0	0.0	0.0	0.0	0.1	0.0	0.9	0.1	0.3	0.1	12.2	1.7	11.7	2.0	191.5	25.7	70.0	13.1	257.2	53.3	37.8	5.6	275.2	56.6
UM09_12	2147	362	0.0	0.0	0.0	0.0	0.0	0.0	0.1	0.0	0.6	0.1	0.2	0.0	7.8	1.1	8.3	1.4	166.5	22.0	80.8	14.9	370.5	75.5	69.2	10.1	564.3	114.1
UM09_13	2404	369	0.0	0.0	0.0	0.0	0.0	0.0	0.1	0.0	0.4	0.1	0.2	0.0	7.3	0.9	7.8	1.2	171.3	20.7	88.9	14.9	472.9	87.5	103.6	13.8	886.3	162.6
UM09_14	2387	361	0.0	0.0	0.0	0.0	0.0	0.0	0.1	0.0	0.5	0.1	0.2	0.0	7.1	0.9	7.9	1.2	168.5	20.0	92.5	15.3	523.0	95.2	102.2	13.4	1006.7	181.9
UM09_15	2412	360	0.0	0.0	0.0	0.0	0.0	0.0	0.1	0.0	0.4	0.1	0.2	0.0	6.6	0.8	7.7	1.2	169.0	19.8	88.5	14.4	514.8	92.3	113.9	14.8	1034.4	184.0
UM09_16	2312	340	0.0	0.0	0.0	0.0	0.0	0.0	0.0	0.0	0.5	0.1	0.2	0.0	7.2	0.9	8.3	1.2	161.4	18.6	91.6	14.7	439.0	77.5	92.7	11.9	787.9	138.0
UM09_17	1895	275	0.0	0.0	0.0	0.0	0.0	0.0	0.1	0.0	0.8	0.1	0.2	0.0	11.1	1.3	11.0	1.6	179.4	20.4	71.8	11.4	265.9	46.3	42.1	5.3	304.5	52.6
UM09_18	1615	231	0.0	0.0	0.0	0.0	0.0	0.0	0.1	0.0	0.9	0.1	0.3	0.0	10.9	1.3	10.7	1.6	168.0	18.9	60.9	9.5	193.2	33.1	29.2	3.6	201.9	34.3
UM09_19	223	31	0.0	0.0	0.0	0.0	0.0	0.0	0.3	0.1	2.4	0.3	0.8	0.1	16.2	1.9	7.2	1.0	45.6	5.1	7.9	1.2	18.8	3.2	2.3	0.3	15.4	2.6
UM09_20	214	28	0.0	0.0	0.0	0.0	0.0	0.0	0.4	0.1	2.4	0.3	0.7	0.1	16.1	1.8	6.3	0.9	41.1	4.2	7.6	1.1	18.8	2.9	2.2	0.3	15.4	2.4
UM09_21	101	13	0.0	0.0	0.0	0.0	0.0	0.0	0.4	0.1	2.6	0.3	0.7	0.1	12.6	1.4	3.5	0.5	20.9	2.1	3.8	0.5	9.1	1.4	1.2	0.1	7.4	1.1
UM09_22	58	7	0.0	0.0	0.0	0.0	0.0	0.0	0.7	0.1	2.7	0.3	0.7	0.1	8.7	0.9	2.3	0.3	12.2	1.2	2.3	0.3	5.4	0.8	0.7	0.1	4.1	0.6
UM09_23	79	10	0.0	0.0	0.0	0.0	0.0	0.0	0.8	0.1	3.4	0.4	0.9	0.1	10.3	1.1	2.5	0.3	15.3	1.5	2.8	0.4	7.1	1.1	0.8	0.1	4.9	0.7
UM09_24	263	33	0.0	0.0	0.0	0.0	0.0	0.0	0.7	0.1	3.5	0.4	1.4	0.2	19.9	2.1	8.3	1.1	55.8	5.5	10.2	1.4	24.6	3.7	2.8	0.3	15.0	2.2
UM09_25	156	20	0.0	0.0	0.0	0.0	0.0	0.0	0.4	0.1	2.7	0.3	1.6	0.2	14.9	1.6	6.5	0.8	42.6	4.2	7.0	1.0	15.1	2.3	1.7	0.2	10.2	1.5
UM09_26	39	5	0.0	0.0	0.0	0.0	0.0	0.0	0.2	0.0	2.1	0.2	1.1	0.2	9.4	1.0	2.7	0.3	11.3	1.1	1.7	0.2	3.9	0.6	0.5	0.1	4.2	0.6
UM09_27	44	5	0.0	0.0	0.1	0.0	0.0	0.0	0.1	0.0	1.4	0.2	0.8	0.1	7.5	0.8	2.3	0.3	11.4	1.1	1.9	0.3	4.6	0.7	0.7	0.1	5.9	0.9

NIST610

Spot number	Y89	1SE	La139	1SE	Ce140	1SE	Pr141	1SE	Nd146	1SE	Sm147	1SE	Eu153	1SE	Gd157	1SE	Tb159	1SE	Dy163	1SE	Ho165	1SE	Er166	1SE	Tm169	1SE	Yb172	1SE
run1																												
NIST610_1	504	5	446	4	449	4	447	5	436	3	460	6	467	4	467	5	444	5	483	6	495	4	506	5	489	5	509	6
NIST610_2	495	5	434	4	453	4	444	3	439	4	458	4	460	4	462	5	441	3	483	5	487	4	490	5	482	4	493	4
NIST610_3	492	5	441	5	456	4	446	4	447	5	470	5	463	4	467	7	449	5	487	5	490	5	492	5	489	5	505	6
NIST610_4	489	6	447	4	469	4	441	4	449	5	470	7	440	4	468	6	448	6	482	6	480	6	466	6	483	6	484	6
NIST610_5	498	5	440	5	461	3	439	4	446	5	476	4	444	4	467	5	450	4	479	5	480	5	468	4	485	4	487	5
NIST610_6	493	6	454	4	466	3	449	3	455	4	483	4	451	4	475	5	461	4	478	4	484	4	476	4	488	4	504	4
NIST610_7	496	4	449	3	459	3	445	3	447	5	480	4	444	3	468	6	459	3	480	5	479	4	473	4	483	4	495	4
NIST610_8	483	6	438	5	460	3	435	4	450	6	477	5	430	4	438	6	449	4	470	6	470	6	470	6	475	6	491	6
NIST610_9	485	4	442	4	458	3	439	3	444	5	471	5	429	4	445	6	452	4	467	5	462	3	470	5	480	4	490	6
NIST610_10	488	5	448	3	458	4	444	3	450	5	477	6	448	3	456	6	457	4	485	5	479	5	482	4	479	5	487	4
NIST610_11	473	6	432	4	457	4	442	3	440	3	461	4	441	4	449	6	447	3	472	5	470	5	474	5	470	3	477	4
NIST610_12	494	5	450	4	465	3	451	4	451	4	487	5	460	3	468	5	462	4	488	4	486	4	485	4	483	4	492	5

Table C2. Trace element composition of garnet

Spot number	Y89	1SE	La139	1SE	Ce140	1SE	Pr141	1SE	Nd146	1SE	Sm147	1SE	Eu153	1SE	Gd157	1SE	Tb159	1SE	Dy163	1SE	Ho165	1SE	Er166	1SE	Tm169	1SE	Yb172	1SE
run2																												
NIST610_01	511	19	468	24	476	26	474	24	470	19	483	19	462	21	520	31	474	23	510	20	496	18	487	18	475	23	520	19
NIST610_02	509	19	467	24	466	25	473	24	471	19	479	18	463	21	506	30	473	23	509	20	492	18	480	18	469	23	514	19
NIST610_03	508	19	475	24	473	26	471	23	476	19	485	19	467	21	506	31	470	22	511	20	489	18	483	18	468	23	519	19
NIST610_04	523	20	517	28	508	29	504	27	490	21	493	20	458	23	465	36	500	26	519	22	512	20	499	20	487	27	512	21
NIST610_05	536	21	503	28	502	29	498	27	485	21	490	20	468	24	462	37	493	26	523	22	508	20	504	21	478	27	511	21
NIST610_06	518	23	480	31	475	31	465	29	465	22	482	23	453	27	491	55	461	28	505	25	516	23	514	24	492	34	527	25
NIST610_07	538	24	502	33	492	32	483	30	476	23	501	24	477	29	516	59	477	30	524	26	527	24	523	25	509	36	551	27
NIST610_08	525	23	493	33	480	32	473	30	470	23	500	24	474	29	522	62	477	30	524	26	516	24	521	25	502	36	553	27

Spot number	Y89	1SE	La139	1SE	Ce140	1SE	Pr141	1SE	Nd146	1SE	Sm147	1SE	Eu153	1SE	Gd157	1SE	Tb159	1SE	Dy163	1SE	Ho165	1SE	Er166	1SE	Tm169	1SE	Yb172	1SE
run3																												
NIST610_01	482	58	491	67	466	55	446	49	454	55	482	50	478	63	442	44	473	58	453	43	495	65	454	65	452	48	508	72
NIST610_02	474	57	502	69	473	56	449	49	459	56	473	49	503	66	450	45	476	59	445	42	488	64	472	67	439	46	499	71
NIST610_03	463	56	449	62	456	54	434	47	450	55	444	46	471	62	422	42	433	54	437	42	433	57	444	64	418	44	462	66
NIST610_04	388	52	414	63	387	50	409	49	373	51	406	47	409	60	375	41	410	56	381	40	413	60	371	59	384	45	409	65
NIST610_05	438	59	430	66	455	59	405	49	410	56	429	50	431	64	408	46	406	56	417	45	411	61	387	63	389	46	430	69
NIST610_06	460	73	481	86	470	71	452	63	452	73	473	64	478	83	434	57	470	75	428	53	481	83	443	85	447	62	473	90
NIST610_07	419	67	404	73	416	64	386	55	396	65	431	59	424	74	388	51	407	66	401	51	408	72	383	74	400	56	409	79
NIST610_08	500	96	494	107	484	88	450	76	467	91	472	76	509	107	440	69	474	91	459	69	475	100	465	108	431	71	505	117
NIST610_09	491	95	535	117	488	90	499	85	476	94	509	83	538	114	455	73	515	101	446	68	519	111	482	114	475	80	538	126
NIST610_10	434	102	464	122	427	93	427	87	418	100	446	87	446	114	416	80	433	101	409	75	448	116	410	118	412	83	459	131
NIST610_11	445	106	447	119	437	97	420	87	433	105	438	87	459	119	412	81	431	102	426	79	438	115	418	122	411	84	441	128
NIST610_12	456	110	443	120	464	104	424	89	430	106	445	90	449	119	429	85	438	105	445	84	445	118	445	132	423	88	472	139

Table C3. Monazite U-Th-Pb geochronology data and trace elements

IGNEOUS SPECIMENS

GG10

Analysis #	Comment	207Pb/206Pb	2 SE %	207Pb/235U	2 SE %	206Pb/238U	2 SE %	208Pb/232Th	2 SE %	207Pb/206Pb Age (Ma)	2 SE abs.	207Pb/235U Age (Ma)	2 SE abs.	206Pb/238U Age (Ma)	2 SE abs.	208Pb/232Th Age (Ma)	2 SE abs.
UM10_1		0.0514	1.74	0.0237	3.04	0.0033	2.63	0.0011	2.78	258.7	39.9	23.8	0.7	21.5	0.6	21.5	0.6
UM10_2		0.0500	1.77	0.0227	3.15	0.0033	2.59	0.0011	2.53	196.9	41.1	22.8	0.7	21.2	0.5	21.3	0.5
UM10_3		0.0478	1.65	0.0207	3.06	0.0031	2.78	0.0012	2.99	91.3	39.0	20.8	0.6	20.2	0.6	24.1	0.7
UM10_4		0.0477	1.72	0.0206	3.24	0.0031	2.66	0.0012	3.13	83.2	40.7	20.7	0.7	20.2	0.5	25.0	0.8
UM10_5		0.0498	1.79	0.0258	2.82	0.0038	2.48	0.0012	2.61	185.5	41.8	25.8	0.7	24.2	0.6	23.9	0.6
UM10_6		0.0494	1.67	0.0239	2.86	0.0035	2.55	0.0010	2.87	167.8	39.1	24.0	0.7	22.6	0.6	20.6	0.6
UM10_7		0.0491	1.72	0.0221	2.53	0.0033	2.20	0.0011	2.25	154.7	40.4	22.2	0.6	21.0	0.5	21.4	0.5
UM10_8		0.0546	2.07	0.0263	2.92	0.0035	2.46	0.0011	2.49	395.5	46.3	26.3	0.8	22.5	0.6	22.6	0.6
UM10_9		0.0474	1.87	0.0219	2.81	0.0034	2.65	0.0011	2.66	67.9	44.5	22.0	0.6	21.6	0.6	21.7	0.6
UM10_10		0.0512	1.82	0.0215	3.45	0.0031	3.12	0.0010	3.18	248.7	42.0	21.6	0.7	19.6	0.6	19.8	0.6
UM10_11		0.0577	3.20	0.0324	5.55	0.0041	5.63	0.0009	5.64	519.6	70.2	32.3	1.8	26.2	1.5	18.9	1.1
UM10_12		0.0478	1.83	0.0219	3.37	0.0033	2.89	0.0011	2.89	88.2	43.4	22.0	0.7	21.4	0.6	21.3	0.6
UM10_13		0.0509	2.00	0.0224	3.47	0.0032	3.00	0.0011	2.70	238.1	46.1	22.5	0.8	20.5	0.6	21.3	0.6
UM10_14		0.0472	1.81	0.0210	3.72	0.0032	3.49	0.0011	3.63	61.7	43.1	21.1	0.8	20.8	0.7	22.5	0.8
UM10_15		0.0577	1.99	0.0271	3.41	0.0034	2.75	0.0011	3.01	517.3	43.7	27.1	0.9	21.9	0.6	23.2	0.7
UM10_16		0.0528	1.75	0.0229	3.38	0.0031	3.27	0.0011	3.19	318.7	39.9	23.0	0.8	20.2	0.7	22.4	0.7
UM10_17		0.0580	1.91	0.0282	5.10	0.0035	5.10	0.0011	3.87	531.6	41.8	28.3	1.4	22.7	1.2	22.0	0.9
UM10_18		0.0648	2.17	0.0304	3.87	0.0034	3.05	0.0011	3.14	766.9	45.8	30.4	1.2	21.9	0.7	21.5	0.7
UM10_19		0.0554	1.79	0.0255	4.06	0.0033	3.94	0.0011	3.88	427.0	39.9	25.6	1.0	21.5	0.8	21.5	0.8
UM10_20		0.0791	2.98	0.0413	4.11	0.0038	2.77	0.0011	2.71	1173.4	59.1	41.1	1.7	24.4	0.7	21.3	0.6
UM10_21		0.0489	1.74	0.0231	3.95	0.0034	3.58	0.0010	3.66	144.9	40.7	23.2	0.9	22.0	0.8	21.1	0.8
UM10_22		0.0501	1.74	0.0232	3.72	0.0034	3.36	0.0010	3.47	197.9	40.4	23.3	0.9	21.6	0.7	20.4	0.7
UM10_23		0.0519	2.24	0.0239	2.79	0.0033	2.00	0.0010	2.17	281.4	51.4	24.0	0.7	21.5	0.4	19.2	0.4
UM10_24		0.0687	6.27	0.0535	9.31	0.0056	5.13	0.0023	12.98	891.2	129.4	52.9	4.9	36.3	1.9	46.1	6.0
UM10_25		0.0488	1.72	0.0222	3.56	0.0033	3.14	0.0011	3.15	140.0	40.3	22.3	0.8	21.2	0.7	22.1	0.7
UM10_26		0.0480	1.83	0.0211	3.47	0.0032	3.09	0.0010	3.21	99.3	43.2	21.2	0.7	20.5	0.6	20.2	0.7
UM10_27		0.0514	1.78	0.0240	4.70	0.0034	4.17	0.0011	4.58	261.0	40.8	24.1	1.1	21.8	0.9	21.2	1.0
UM10_28		0.0539	1.81	0.0251	3.52	0.0034	3.34	0.0010	3.30	368.9	40.9	25.2	0.9	21.8	0.7	21.0	0.7
UM10_29		0.0483	1.88	0.0223	3.09	0.0033	2.71	0.0011	2.71	112.9	44.5	22.4	0.7	21.6	0.6	21.3	0.6
UM10_30		0.0558	1.95	0.0263	2.53	0.0034	2.24	0.0011	2.35	445.0	43.3	26.4	0.7	22.0	0.5	21.3	0.5
UM10_31		0.1275	16.87	0.0601	19.02	0.0034	4.97	0.0012	7.13	2063.8	297.4	59.3	11.3	22.0	1.1	24.2	1.7
UM10_32		0.0662	3.43	0.0317	7.81	0.0035	6.57	0.0010	7.09	812.6	71.7	31.6	2.5	22.3	1.5	20.8	1.5
UM10_33		0.0513	2.21	0.0220	3.53	0.0031	2.45	0.0010	4.04	256.4	50.9	22.1	0.8	20.0	0.5	20.0	0.8
UM10_34		0.0532	1.78	0.0235	3.17	0.0032	2.92	0.0010	2.85	336.2	40.3	23.6	0.7	20.7	0.6	20.8	0.6
UM10_35		0.0560	1.79	0.0253	3.76	0.0033	3.16	0.0011	3.40	453.9	39.8	25.3	1.0	21.1	0.7	21.6	0.7
UM10_36		0.0633	2.05	0.0297	3.88	0.0034	3.32	0.0010	3.34	717.3	43.6	29.8	1.2	21.9	0.7	20.7	0.7
UM10_37		0.0573	2.13	0.0238	3.30	0.0030	2.75	0.0010	2.76	501.7	46.9	23.9	0.8	19.4	0.5	20.0	0.6
UM10_38		0.0549	1.83	0.0242	4.12	0.0032	3.81	0.0010	3.44	406.8	40.9	24.2	1.0	20.6	0.8	20.7	0.7
UM10_39		0.0540	1.90	0.0240	2.69	0.0032	2.54	0.0011	2.60	369.7	42.9	24.1	0.6	20.8	0.5	21.5	0.6
UM10_40		0.0569	2.01	0.0253	3.89	0.0032	3.49	0.0010	3.46	488.7	44.4	25.4	1.0	20.8	0.7	21.2	0.7

Table C3. Monazite U-Th-Pb geochronology data and trace elements

IGNEOUS SPECIMENS

GG12

Analysis #	Comment	207Pb/206Pb	2 SE %	207Pb/235U	2 SE %	206Pb/238U	2 SE %	208Pb/232Th	2 SE %	207Pb/206Pb Age (Ma)	2 SE abs.	207Pb/235U Age (Ma)	2 SE abs.	206Pb/238U Age (Ma)	2 SE abs.	208Pb/232Th Age (Ma)	2 SE abs.
UM12_1		0.0567	6.30	0.0247	10.34	0.0032	4.76	0.0009	4.77	480.4	139.1	24.7	2.6	20.3	1.0	18.1	0.9
UM12_2		0.0499	1.77	0.0213	4.01	0.0031	3.62	0.0010	3.89	191.2	41.2	21.4	0.9	19.9	0.7	20.8	0.8
UM12_3		0.0512	1.78	0.0228	3.38	0.0032	3.19	0.0010	3.47	250.5	40.9	22.9	0.8	20.8	0.7	20.4	0.7
UM12_4		0.0506	1.77	0.0220	3.20	0.0032	3.00	0.0011	2.60	222.8	41.0	22.1	0.7	20.3	0.6	21.4	0.6
UM12_5		0.0513	1.86	0.0226	3.02	0.0032	2.93	0.0010	3.08	253.2	42.7	22.7	0.7	20.6	0.6	21.2	0.7
UM12_6		0.0592	5.22	0.0269	6.65	0.0033	3.41	0.0009	3.41	573.0	113.5	27.0	1.8	21.3	0.7	19.0	0.6
UM12_7		0.0493	1.70	0.0214	2.81	0.0032	2.37	0.0011	2.51	161.5	39.8	21.5	0.6	20.3	0.5	21.5	0.5
UM12_8		0.0507	1.67	0.0220	3.26	0.0032	2.83	0.0011	3.05	225.1	38.7	22.1	0.7	20.3	0.6	22.1	0.7
UM12_9		0.0514	1.87	0.0219	4.53	0.0031	4.25	0.0010	4.22	259.2	42.9	22.0	1.0	19.9	0.8	21.1	0.9
UM12_10		0.0547	1.84	0.0242	3.55	0.0032	3.04	0.0011	2.90	398.8	41.2	24.3	0.9	20.7	0.6	22.7	0.7
UM12_11		0.0583	4.62	0.0260	6.86	0.0032	3.48	0.0011	3.55	542.7	101.0	26.1	1.8	20.8	0.7	21.8	0.8
UM12_12		0.0628	3.72	0.0278	5.47	0.0032	4.38	0.0011	4.38	702.6	79.3	27.9	1.5	20.7	0.9	21.7	1.0
UM12_13		0.1897	9.26	0.1712	13.89	0.0065	10.38	0.0039	23.38	2739.7	152.4	160.4	22.3	42.1	4.4	78.4	18.3
UM12_14		0.2178	4.47	0.1297	6.25	0.0043	3.33	0.0013	6.45	2964.3	72.1	123.8	7.7	27.8	0.9	26.2	1.7
UM12_15		0.0533	2.26	0.0243	4.55	0.0033	3.40	0.0010	3.48	339.7	51.1	24.4	1.1	21.3	0.7	21.0	0.7
UM12_16		0.0531	1.76	0.0235	3.10	0.0032	2.78	0.0011	2.76	333.6	39.9	23.6	0.7	20.7	0.6	21.6	0.6
UM12_17		0.0570	2.21	0.0248	4.20	0.0032	3.56	0.0011	3.72	492.2	48.8	24.9	1.0	20.3	0.7	21.3	0.8
UM12_18		0.0505	1.68	0.0215	3.09	0.0031	2.55	0.0010	2.51	218.6	38.8	21.6	0.7	19.9	0.5	20.6	0.5
UM12_19		0.0521	1.75	0.0231	3.77	0.0032	3.50	0.0010	3.39	287.6	40.0	23.1	0.9	20.7	0.7	21.0	0.7
UM12_20		0.0517	1.84	0.0231	3.26	0.0032	3.01	0.0010	3.03	273.2	42.2	23.2	0.8	20.9	0.6	20.9	0.6
UM12_21		0.0531	2.16	0.0239	3.32	0.0033	2.91	0.0011	2.83	332.7	49.0	24.0	0.8	21.0	0.6	21.8	0.6
UM12_22		0.0536	1.77	0.0238	3.52	0.0032	3.50	0.0010	3.27	355.6	39.9	23.8	0.8	20.7	0.7	21.2	0.7
UM12_23		0.0507	1.83	0.0221	3.17	0.0032	2.53	0.0011	2.52	226.5	42.3	22.2	0.7	20.4	0.5	21.4	0.5
UM12_24		0.3427	12.89	0.3236	13.90	0.0069	5.81	0.0032	10.08	3674.9	196.7	284.6	39.6	44.0	2.6	63.6	6.4
UM12_25		0.0615	2.90	0.0279	5.30	0.0033	3.71	0.0010	3.99	657.0	62.3	28.0	1.5	21.2	0.8	20.8	0.8
UM12_26		0.0509	1.68	0.0225	3.66	0.0032	3.51	0.0011	3.42	237.1	38.8	22.6	0.8	20.6	0.7	22.0	0.8
UM12_27		0.0519	1.80	0.0226	3.80	0.0032	3.08	0.0011	3.23	280.0	41.3	22.7	0.9	20.4	0.6	21.5	0.7
UM12_28		0.0568	1.86	0.0267	3.23	0.0034	3.32	0.0011	3.32	484.7	41.0	26.8	0.9	21.9	0.7	21.5	0.7
UM12_29		0.0510	1.87	0.0239	4.21	0.0034	3.60	0.0011	3.68	239.0	43.2	24.0	1.0	21.9	0.8	21.6	0.8
UM12_30		0.0955	9.42	0.0449	11.48	0.0034	4.71	0.0011	6.12	1537.4	177.1	44.6	5.1	21.9	1.0	23.2	1.4
UM12_31		0.0721	5.17	0.0318	5.52	0.0032	4.69	0.0010	5.63	989.2	105.2	31.8	1.8	20.6	1.0	20.4	1.2
UM12_32		0.1095	4.80	0.0521	9.30	0.0034	8.58	0.0012	8.39	1791.9	87.5	51.6	4.8	22.2	1.9	24.7	2.1
UM12_33		0.0577	2.74	0.0256	4.07	0.0032	2.81	0.0011	2.86	519.6	60.2	25.6	1.0	20.7	0.6	21.5	0.6
UM12_34		0.0530	1.75	0.0238	3.63	0.0033	3.46	0.0011	3.43	329.6	39.7	23.9	0.9	20.9	0.7	22.0	0.8
UM12_35		0.0528	1.69	0.0238	3.39	0.0033	3.45	0.0011	3.16	321.3	38.3	23.8	0.8	21.0	0.7	22.0	0.7
UM12_36		0.0520	1.75	0.0232	3.33	0.0032	2.79	0.0011	2.87	286.3	40.0	23.3	0.8	20.8	0.6	21.4	0.6
UM12_37		0.0499	1.96	0.0242	3.09	0.0035	2.62	0.0011	2.75	192.2	45.7	24.3	0.8	22.7	0.6	21.7	0.6
UM12_38		0.0521	2.04	0.0251	3.96	0.0035	3.52	0.0011	3.66	290.8	46.7	25.1	1.0	22.5	0.8	21.6	0.8
UM12_39		0.0522	2.08	0.0245	4.62	0.0034	3.88	0.0010	3.81	294.8	47.6	24.5	1.1	21.9	0.8	20.8	0.8
UM12_40		0.0510	1.93	0.0236	3.22	0.0034	2.86	0.0010	3.09	239.5	44.6	23.7	0.8	21.6	0.6	21.2	0.7

Table C3. Monazite U-Th-Pb geochronology data and trace elements

METAMORPHIC SPECIMENS

UM05

Analysis #	Comment	207Pb/206Pb	2 SE %	207Pb/235U	2 SE %	206Pb/238U	2 SE %	208Pb/232Th	2 SE %	207Pb/206Pb Age (Ma)	2 SE abs.	207Pb/235U Age (Ma)	2 SE abs.	206Pb/238U Age (Ma)	2 SE abs.	208Pb/232Th Age (Ma)	2 SE abs.
UM05A_M2_1		0.2056	4.66	0.1020	5.11	0.0037	3.05	0.0010	3.49	2864.0	75.7	98.6	5.0	23.5	0.7	19.9	0.7
UM05A_M2_2		0.1909	3.35	0.0911	4.33	0.0035	2.53	0.0010	2.85	2746.0	55.1	88.5	3.8	22.4	0.6	19.3	0.5
UM05A_M2_3		0.3980	6.41	0.2690	11.33	0.0049	5.45	0.0011	3.78	3890.0	96.5	241.0	27.3	31.7	1.7	21.3	0.8
~~UM05A_M2_4~~	~~Excluded (matrix)~~	~~0.6680~~	~~6.13~~	~~1.0700~~	~~12.31~~	~~0.0115~~	~~9.77~~	~~0.0015~~	~~8.96~~	~~4665.0~~	~~88.3~~	~~734.0~~	~~90.4~~	~~73.7~~	~~7.2~~	~~30.5~~	~~2.7~~
~~UM05A_M3_1~~	~~Excluded (matrix)~~	~~0.7280~~	~~2.44~~	~~2.7200~~	~~9.41~~	~~0.0268~~	~~9.54~~	~~0.0042~~	~~11.13~~	~~4799.0~~	~~34.9~~	~~1327.0~~	~~124.8~~	~~171.0~~	~~16.3~~	~~83.6~~	~~9.3~~
~~UM05A_M3_3~~	~~Excluded (matrix)~~	~~0.4660~~	~~4.48~~	~~0.3620~~	~~4.85~~	~~0.0056~~	~~3.95~~	~~0.0011~~	~~5.33~~	~~4135.0~~	~~66.5~~	~~314.0~~	~~15.2~~	~~35.8~~	~~1.4~~	~~23.2~~	~~1.2~~
UM05A_M5_1		0.1450	2.99	0.0662	3.62	0.0033	2.41	0.0010	2.90	2287.0	51.4	65.1	2.4	21.1	0.5	19.2	0.6
~~UM05A_M14_1~~	~~Excluded (matrix)~~	~~0.6210~~	~~3.62~~	~~0.8890~~	~~10.32~~	~~0.0103~~	~~7.62~~	~~0.0014~~	~~6.77~~	~~4555.0~~	~~52.5~~	~~640.0~~	~~66.0~~	~~66.3~~	~~5.1~~	~~27.6~~	~~1.9~~
UM05A_M18_1		0.4140	3.40	0.3000	4.77	0.0053	3.96	0.0011	3.63	3959.0	50.9	266.0	12.7	33.8	1.3	22.2	0.8
~~UM05A_M8_1~~	~~Excluded (matrix)~~	~~0.5700~~	~~13.05~~	~~0.7200~~	~~18.17~~	~~0.0092~~	~~5.71~~	~~0.0015~~	~~10.37~~	~~4420.0~~	~~190.3~~	~~548.0~~	~~99.5~~	~~58.8~~	~~3.4~~	~~30.1~~	~~3.1~~
~~UM05A_M8_2~~	~~Excluded (matrix)~~	~~0.3830~~	~~6.40~~	~~0.2430~~	~~8.47~~	~~0.0046~~	~~4.38~~	~~0.0010~~	~~4.52~~	~~3835.0~~	~~96.6~~	~~220.0~~	~~18.6~~	~~29.7~~	~~1.3~~	~~19.8~~	~~0.9~~

UM07

Analysis #	Comment	207Pb/206Pb	2 SE %	207Pb/235U	2 SE %	206Pb/238U	2 SE %	208Pb/232Th	2 SE %	207Pb/206Pb Age (Ma)	2 SE abs.	207Pb/235U Age (Ma)	2 SE abs.	206Pb/238U Age (Ma)	2 SE abs.	208Pb/232Th Age (Ma)	2 SE abs.
UM07A_M1_1		0.0815	1.96	0.0348	2.76	0.0031	2.42	0.0010	2.85	1231.0	38.5	34.8	1.0	19.9	0.5	19.3	0.5
UM07A_M1_2		0.0840	2.51	0.0351	3.18	0.0030	2.46	0.0009	2.81	1302.0	48.8	35.0	1.1	19.4	0.5	18.9	0.5
~~UM07A_M1_3~~	~~Excluded (matrix)~~	~~0.0993~~	~~4.04~~	~~0.0423~~	~~4.49~~	~~0.0031~~	~~2.64~~	~~0.0010~~	~~3.17~~	~~1609.0~~	~~75.3~~	~~42.1~~	~~1.9~~	~~19.9~~	~~0.5~~	~~19.8~~	~~0.6~~
UM07A_M1_4		0.0884	2.14	0.0381	2.96	0.0032	2.34	0.0010	2.80	1393.0	41.0	38.0	1.1	20.3	0.5	19.4	0.5
UM07A_M1_5		0.0933	2.79	0.0391	3.45	0.0031	2.50	0.0009	2.91	1487.0	52.7	39.0	1.3	19.7	0.5	19.1	0.6
UM07A_M1_6		0.0875	2.34	0.0384	3.28	0.0032	2.60	0.0010	2.97	1373.0	45.0	38.2	1.3	20.5	0.5	20.2	0.6
UM07A_M1_7		0.0874	2.44	0.0367	3.60	0.0031	2.61	0.0010	3.01	1364.0	46.9	36.6	1.3	20.0	0.5	19.2	0.6
UM07A_M1_8		0.0956	2.37	0.0409	3.35	0.0031	2.49	0.0010	3.03	1543.0	44.7	40.7	1.4	20.1	0.5	20.0	0.6
UM07A_M1_9		0.0883	2.05	0.0389	3.00	0.0032	2.38	0.0010	2.82	1386.0	39.4	38.7	1.2	20.5	0.5	20.1	0.6
UM07A_M1_10		0.0890	2.40	0.0396	3.42	0.0032	2.55	0.0010	2.93	1398.0	46.1	39.4	1.3	20.9	0.5	19.9	0.6
UM07A_M1_11		0.0882	2.42	0.0387	3.48	0.0032	2.46	0.0010	2.99	1381.0	46.5	38.5	1.3	20.3	0.5	19.8	0.6
UM07A_M2_1		0.1310	7.74	0.0609	9.73	0.0034	3.07	0.0010	3.36	2060.0	135.8	59.8	5.8	21.9	0.7	20.7	0.7
UM07A_M2_2		0.1496	5.50	0.0684	8.43	0.0033	4.64	0.0010	4.40	2337.0	94.2	67.2	5.7	21.5	1.0	19.6	0.9
UM07A_M2_3		0.0955	2.65	0.0410	3.01	0.0032	2.57	0.0010	2.94	1532.0	49.8	40.8	1.2	20.4	0.5	19.6	0.6
UM07A_M2_4		0.1650	10.38	0.0750	13.48	0.0032	5.08	0.0009	4.91	2520.0	174.7	73.3	9.9	20.7	1.1	17.7	0.9
UM07A_M2_5		0.1450	9.06	0.0639	8.99	0.0033	3.31	0.0009	3.63	2270.0	155.9	62.8	5.6	21.5	0.7	18.4	0.7
UM07A_M2_6		0.1860	6.58	0.0877	9.90	0.0034	4.29	0.0010	3.55	2690.0	108.6	85.3	8.4	22.1	0.9	20.8	0.7
UM07A_M2_7		0.0998	2.47	0.0433	3.42	0.0032	2.59	0.0010	2.88	1623.0	46.0	43.1	1.5	20.4	0.5	19.7	0.6
UM07A_M2_8		0.0972	4.91	0.0408	4.84	0.0030	3.28	0.0010	3.91	1585.0	91.9	40.6	2.0	19.3	0.6	20.1	0.8
UM07A_M2_9		0.0861	3.94	0.0362	5.88	0.0031	3.07	0.0009	3.30	1333.0	76.1	36.1	2.1	19.8	0.6	18.8	0.6
~~UM07A_M3_1~~	~~Excluded (matrix)~~	~~0.2560~~	~~4.86~~	~~0.1359~~	~~5.46~~	~~0.0039~~	~~3.45~~	~~0.0012~~	~~3.20~~	~~3216.0~~	~~76.8~~	~~129.3~~	~~7.1~~	~~25.2~~	~~0.9~~	~~23.3~~	~~0.7~~
~~UM07A_M3_3~~	~~Excluded (matrix)~~	~~0.6260~~	~~3.75~~	~~0.8320~~	~~7.72~~	~~0.0095~~	~~4.67~~	~~0.0020~~	~~4.87~~	~~4569.0~~	~~54.3~~	~~613.0~~	~~47.3~~	~~60.9~~	~~2.8~~	~~40.1~~	~~2.0~~
UM07A_M3_4		0.0826	2.04	0.0354	2.93	0.0031	2.53	0.0010	2.97	1258.0	39.9	35.3	1.0	20.3	0.5	20.2	0.6
UM07A_M3_5		0.1819	3.34	0.0899	4.38	0.0036	2.65	0.0010	3.18	2673.0	55.3	87.4	3.8	22.9	0.6	20.6	0.7
UM07A_M4_1		0.0900	2.39	0.0393	3.16	0.0032	2.61	0.0010	2.96	1420.0	45.6	39.1	1.2	20.3	0.5	19.2	0.6
UM07A_M4_2		0.0928	2.61	0.0414	2.83	0.0033	2.52	0.0010	2.86	1484.0	49.4	41.2	1.2	21.0	0.5	20.2	0.6
UM07A_M4_3		0.0990	3.02	0.0434	3.99	0.0032	2.36	0.0010	2.97	1607.0	56.3	43.1	1.7	20.5	0.5	20.1	0.6
UM07A_M4_4		0.0904	2.38	0.0394	3.23	0.0032	2.67	0.0009	3.03	1436.0	45.4	39.2	1.3	20.4	0.5	18.9	0.6
UM07A_M4_5		0.0973	2.97	0.0445	3.54	0.0033	2.37	0.0010	3.03	1573.0	55.6	44.2	1.6	21.4	0.5	20.2	0.6
UM07A_M4_6		0.0919	2.72	0.0397	3.62	0.0031	2.39	0.0010	3.01	1460.0	51.7	39.5	1.4	20.1	0.5	19.2	0.6
UM07A_M4_7		0.0872	2.84	0.0389	3.46	0.0032	2.71	0.0010	2.99	1366.0	54.7	38.7	1.3	20.7	0.6	19.7	0.6
~~UM07A_M5_1~~	~~Excluded (matrix)~~	~~0.7350~~	~~2.31~~	~~2.7000~~	~~18.26~~	~~0.0264~~	~~16.41~~	~~0.0035~~	~~13.62~~	~~4815.0~~	~~33.0~~	~~1310.0~~	~~239.2~~	~~168.0~~	~~27.6~~	~~70.7~~	~~9.6~~
~~UM07A_M6_1~~	~~Excluded (matrix)~~	~~0.1348~~	~~6.37~~	~~0.0571~~	~~6.61~~	~~0.0031~~	~~3.17~~	~~0.0010~~	~~3.56~~	~~2160.0~~	~~111.0~~	~~56.3~~	~~3.7~~	~~19.7~~	~~0.6~~	~~19.9~~	~~0.7~~
~~UM07A_M6_2~~	~~Excluded (matrix)~~	~~0.1499~~	~~6.53~~	~~0.0700~~	~~7.28~~	~~0.0034~~	~~3.29~~	~~0.0012~~	~~4.14~~	~~2300.0~~	~~111.8~~	~~68.6~~	~~5.0~~	~~22.0~~	~~0.7~~	~~23.9~~	~~1.0~~
~~UM07A_M6_3~~	~~Excluded (matrix)~~	~~0.1152~~	~~3.23~~	~~0.0495~~	~~4.15~~	~~0.0031~~	~~3.00~~	~~0.0009~~	~~3.41~~	~~1873.0~~	~~58.1~~	~~49.1~~	~~2.0~~	~~19.8~~	~~0.6~~	~~19.2~~	~~0.7~~
~~UM07A_M6_4~~	~~Excluded (matrix)~~	~~0.1386~~	~~4.24~~	~~0.0575~~	~~4.47~~	~~0.0031~~	~~2.66~~	~~0.0010~~	~~3.06~~	~~2216.0~~	~~73.6~~	~~56.7~~	~~2.5~~	~~19.8~~	~~0.5~~	~~20.7~~	~~0.6~~
~~UM07A_M7_2~~	~~Excluded (matrix)~~	~~0.5390~~	~~8.82~~	~~0.5500~~	~~10.91~~	~~0.0076~~	~~7.79~~	~~0.0012~~	~~4.80~~	~~4340.0~~	~~129.2~~	~~444.0~~	~~48.4~~	~~48.6~~	~~3.8~~	~~25.2~~	~~1.2~~
~~UM07A_M7_3~~	~~Excluded (matrix)~~	~~0.5180~~	~~11.66~~	~~0.4810~~	~~14.28~~	~~0.0068~~	~~12.44~~	~~0.0011~~	~~7.97~~	~~4290.0~~	~~171.3~~	~~398.0~~	~~56.8~~	~~43.9~~	~~5.5~~	~~21.9~~	~~1.7~~
UM07A_M7_4		0.1088	3.22	0.0481	3.70	0.0032	2.56	0.0010	3.00	1779.0	58.7	47.7	1.8	20.9	0.5	19.6	0.6
UM07A_M7_5		0.0943	2.86	0.0405	3.57	0.0032	2.72	0.0010	3.04	1506.0	53.9	40.3	1.4	20.6	0.6	19.8	0.6
~~UM07A_M7_6~~	~~Excluded (overlapp~~	~~0.1108~~	~~3.42~~	~~0.0488~~	~~4.20~~	~~0.0032~~	~~2.66~~	~~0.0010~~	~~2.90~~	~~1812.0~~	~~62.1~~	~~48.4~~	~~2.0~~	~~20.5~~	~~0.5~~	~~19.3~~	~~0.6~~
UM07A_M7_7		0.0976	2.09	0.0437	3.02	0.0033	2.90	0.0010	3.29	1581.0	39.1	43.4	1.3	21.2	0.6	19.9	0.7
UM07A_M7_8		0.1083	5.87	0.0450	5.08	0.0031	3.09	0.0009	3.75	1750.0	107.2	44.7	2.3	20.2	0.6	18.7	0.7
UM07A_M7_9		0.0908	2.28	0.0393	3.24	0.0032	2.92	0.0010	3.36	1443.0	43.4	39.1	1.3	20.3	0.6	19.8	0.7

Table C3. Monazite U-Th-Pb geochronology data and trace elements

Analysis #	Comment	207Pb/206Pb	2 SE %	207Pb/235U	2 SE %	206Pb/238U	2 SE %	208Pb/232Th	2 SE %	207Pb/206Pb Age (Ma)	2 SE abs.	207Pb/235U Age (Ma)	2 SE abs.	206Pb/238U Age (Ma)	2 SE abs.	208Pb/232Th Age (Ma)	2 SE abs.
UM07A_M7_10		0.1011	2.97	0.0460	4.01	0.0033	2.67	0.0011	3.02	1645.0	55.1	45.6	1.8	21.5	0.6	21.4	0.6
UM07A_M8_1		0.0846	3.56	0.0360	5.13	0.0031	3.14	0.0010	3.39	1295.0	69.0	35.9	1.8	20.0	0.6	19.4	0.7
UM07A_M8_2		0.0819	2.25	0.0336	3.54	0.0030	2.75	0.0009	3.22	1238.0	44.0	33.5	1.2	19.4	0.5	19.0	0.6
UM07A_M8_3		0.0797	2.29	0.0335	3.25	0.0031	2.74	0.0010	3.16	1186.0	45.2	33.5	1.1	19.9	0.5	19.8	0.6
UM07A_M8_4		0.0861	2.46	0.0360	3.65	0.0031	3.02	0.0009	3.45	1335.0	47.6	35.9	1.3	19.9	0.6	18.7	0.6
UM07A_M8_5		0.0885	2.61	0.0382	3.51	0.0032	3.13	0.0010	3.47	1388.0	50.0	38.1	1.3	20.3	0.6	20.1	0.7
UM07A_M8_6		0.0791	2.40	0.0329	2.99	0.0031	2.85	0.0010	3.37	1169.0	47.6	32.8	1.0	19.7	0.6	19.6	0.7
UM07A_M8_7		0.0857	2.27	0.0354	4.43	0.0030	3.44	0.0009	3.76	1333.0	44.0	35.3	1.6	19.3	0.7	18.7	0.7
UM07A_M8_8		0.0784	2.64	0.0317	3.58	0.0029	2.46	0.0009	2.99	1150.0	52.3	31.7	1.1	18.8	0.5	18.4	0.6
~~UM07A_M8_9~~	~~Excluded (matrix)~~	~~0.2240~~	~~10.35~~	~~0.1200~~	~~15.96~~	~~0.0037~~	~~5.75~~	~~0.0010~~	~~5.67~~	~~2990.0~~	~~166.2~~	~~114.0~~	~~18.2~~	~~23.8~~	~~1.4~~	~~21.0~~	~~1.2~~
UM07A_M8_10		0.0950	2.47	0.0418	3.50	0.0032	2.88	0.0010	3.34	1529.0	46.6	41.6	1.5	20.8	0.6	20.1	0.7
~~UM07A_M8_11~~	~~Excluded (matrix)~~	~~0.0825~~	~~2.75~~	~~0.0357~~	~~3.67~~	~~0.0031~~	~~2.97~~	~~0.0010~~	~~3.23~~	~~1249.0~~	~~53.8~~	~~35.6~~	~~1.3~~	~~20.2~~	~~0.6~~	~~19.8~~	~~0.6~~
UM07A_M8_12		0.0770	2.24	0.0319	3.09	0.0030	2.98	0.0010	3.32	1116.0	44.6	31.8	1.0	19.5	0.6	19.5	0.6
UM07A_M8_13		0.0849	2.19	0.0360	3.01	0.0031	2.42	0.0010	2.85	1315.0	42.5	36.1	1.1	19.8	0.5	19.3	0.5
UM07A_M8_14		0.0915	2.45	0.0389	3.46	0.0031	2.74	0.0010	3.44	1464.0	46.6	38.8	1.3	20.3	0.6	19.7	0.7
UM07A_M10_1		0.0938	2.41	0.0417	3.50	0.0032	2.65	0.0010	3.20	1499.0	45.5	41.4	1.5	20.7	0.5	20.2	0.6
UM07A_M10_2		0.2000	7.12	0.1060	9.64	0.0038	4.18	0.0010	3.74	2790.0	116.2	101.9	9.8	24.6	1.0	20.4	0.8
UM07A_M10_3		0.2450	9.88	0.1340	12.84	0.0040	4.72	0.0010	4.96	3130.0	156.8	127.0	16.3	25.6	1.2	20.8	1.0
UM07A_M10_4		0.1253	2.87	0.0574	3.57	0.0033	2.63	0.0010	3.02	2034.0	50.7	56.7	2.0	21.5	0.6	20.3	0.6
UM07A_M10_5		0.1073	4.12	0.0473	4.87	0.0032	2.51	0.0010	2.93	1737.0	75.5	46.9	2.3	20.9	0.5	19.9	0.6
UM07A_M10_6		0.1407	5.69	0.0647	6.50	0.0034	2.81	0.0010	3.06	2217.0	98.5	63.6	4.1	21.8	0.6	19.5	0.6
UM07A_M11_1		0.1025	2.59	0.0455	3.86	0.0032	2.86	0.0010	3.23	1664.0	48.0	45.1	1.7	20.7	0.6	19.8	0.6
UM07A_M11_2		0.0943	3.54	0.0411	4.38	0.0032	3.18	0.0009	3.61	1501.0	66.7	40.9	1.8	20.5	0.7	18.6	0.7
~~UM07A_M11_3~~	~~Excluded (matrix)~~	~~0.0915~~	~~2.93~~	~~0.0406~~	~~3.78~~	~~0.0032~~	~~2.88~~	~~0.0010~~	~~3.28~~	~~1449.0~~	~~55.7~~	~~40.4~~	~~1.5~~	~~20.8~~	~~0.6~~	~~20.0~~	~~0.7~~
UM07A_M11_4		0.1371	4.57	0.0609	4.86	0.0032	3.29	0.0009	3.62	2180.0	79.4	60.0	2.9	20.7	0.7	18.5	0.7
UM07A_M11_5		0.0912	2.27	0.0405	3.57	0.0032	3.35	0.0010	3.58	1460.0	43.3	40.3	1.4	20.6	0.7	19.8	0.7
UM07A_M11_6		0.0895	2.30	0.0399	3.13	0.0033	2.80	0.0010	3.19	1411.0	44.0	39.8	1.2	21.1	0.6	20.3	0.6
UM07A_M12_1		0.0887	2.32	0.0397	3.20	0.0032	2.65	0.0010	3.13	1393.0	44.4	39.5	1.3	20.8	0.6	20.5	0.6
UM07A_M12_2		0.0879	2.92	0.0387	3.69	0.0032	3.05	0.0010	3.39	1380.0	56.1	38.5	1.4	20.4	0.6	20.4	0.7
UM07A_M12_3		0.0969	5.62	0.0420	6.51	0.0031	3.04	0.0010	3.32	1550.0	105.4	41.7	2.7	20.2	0.6	19.4	0.6
UM07A_M12_4		0.1370	8.13	0.0565	8.56	0.0031	4.08	0.0009	5.06	2140.0	141.4	55.7	4.8	19.9	0.8	17.9	0.9
UM07A_M12_5		0.1450	5.20	0.0667	6.75	0.0033	2.80	0.0010	3.32	2272.0	89.5	65.5	4.4	21.3	0.6	19.4	0.6
UM07A_M12_6		0.1119	4.65	0.0478	5.80	0.0031	2.77	0.0009	3.20	1840.0	84.3	47.4	2.7	19.9	0.5	19.2	0.6
UM07A_M12_7		0.0922	2.72	0.0407	3.56	0.0032	2.72	0.0010	3.04	1479.0	51.6	40.5	1.4	20.9	0.6	19.8	0.6
UM07A_M12_8		0.1215	4.47	0.0538	5.75	0.0032	3.48	0.0010	3.86	1981.0	79.7	53.2	3.1	20.8	0.7	20.6	0.8
UM07A_M12_9		0.0903	3.06	0.0419	4.96	0.0033	3.90	0.0010	3.98	1441.0	58.4	41.7	2.1	21.1	0.8	20.2	0.8
UM07A_M12_10		0.0883	2.14	0.0384	3.14	0.0032	2.96	0.0010	3.17	1386.0	41.1	38.2	1.2	20.3	0.6	19.7	0.6
UM07A_M12_11		0.0896	2.03	0.0396	3.63	0.0032	3.08	0.0010	3.36	1413.0	38.9	39.4	1.4	20.6	0.6	19.8	0.7
UM07A_M12_12		0.0950	2.30	0.0408	3.76	0.0032	3.08	0.0010	3.27	1531.0	43.3	40.6	1.5	20.4	0.6	20.2	0.7
UM07A_M12_13		0.0951	3.61	0.0416	4.34	0.0032	2.99	0.0010	3.19	1518.0	67.9	41.4	1.8	20.5	0.6	20.3	0.6
UM07A_M13_1		0.1537	3.69	0.0768	5.22	0.0036	2.76	0.0011	3.38	2393.0	62.7	75.0	3.9	22.9	0.6	21.4	0.7
UM07A_M13_2		0.0826	1.86	0.0364	3.25	0.0032	2.83	0.0010	3.19	1262.0	36.4	36.3	1.2	20.6	0.6	20.6	0.7
UM07A_M13_3		0.1017	4.61	0.0457	5.62	0.0033	3.37	0.0010	3.75	1634.0	85.4	45.3	2.5	20.9	0.7	19.6	0.7
~~UM07A_M13_4~~	~~Excluded (matrix)~~	~~0.2930~~	~~5.95~~	~~0.1840~~	~~9.45~~	~~0.0045~~	~~6.07~~	~~0.0014~~	~~6.43~~	~~3421.0~~	~~92.3~~	~~171.0~~	~~16.2~~	~~29.2~~	~~1.8~~	~~27.6~~	~~1.8~~
UM07A_M13_6		0.1470	7.60	0.0720	10.06	0.0035	4.20	0.0010	4.07	2270.0	130.3	70.4	7.1	22.6	1.0	20.8	0.8
~~UM07A_M13_7~~	~~Excluded (matrix)~~	~~0.5290~~	~~9.17~~	~~0.5320~~	~~17.97~~	~~0.0073~~	~~10.54~~	~~0.0013~~	~~7.39~~	~~4310.0~~	~~134.5~~	~~430.0~~	~~77.3~~	~~46.6~~	~~4.9~~	~~27.0~~	~~2.0~~
UM07A_M13_8		0.0915	2.54	0.0414	3.33	0.0033	2.97	0.0010	3.30	1452.0	48.4	41.2	1.4	21.1	0.6	20.6	0.7
~~UM07A_M15_1~~	~~Excluded (matrix)~~	~~0.5410~~	~~3.92~~	~~0.5810~~	~~5.38~~	~~0.0078~~	~~4.21~~	~~0.0015~~	~~3.41~~	~~4354.0~~	~~57.4~~	~~465.0~~	~~25.0~~	~~50.3~~	~~2.1~~	~~30.4~~	~~1.0~~
UM07A_M15_2		0.1368	5.42	0.0606	7.21	0.0032	3.29	0.0010	3.26	2191.0	94.3	59.6	4.3	20.7	0.7	19.3	0.6
UM07A_M15_3		0.0952	3.51	0.0427	4.04	0.0032	2.95	0.0010	3.36	1518.0	66.0	42.5	1.7	20.7	0.6	20.7	0.7
UM07A_M15_4		0.1019	4.23	0.0474	6.04	0.0033	3.67	0.0010	3.65	1649.0	78.3	47.1	2.8	20.9	0.8	19.7	0.7
UM07A_M20_1		0.0811	2.36	0.0354	3.46	0.0032	3.18	0.0010	3.46	1219.0	46.4	35.4	1.2	20.8	0.7	20.2	0.7
UM07A_M20_2		0.0824	2.75	0.0366	4.08	0.0032	2.77	0.0010	3.07	1248.0	53.9	36.5	1.5	20.8	0.6	20.3	0.6
UM07A_M20_3		0.0808	2.37	0.0363	3.25	0.0033	2.87	0.0010	3.14	1211.0	46.6	36.2	1.2	20.9	0.6	20.2	0.6
UM07A_M20_4		0.0864	2.55	0.0389	3.46	0.0032	3.17	0.0010	3.48	1348.0	49.3	38.8	1.3	20.9	0.7	20.0	0.7
UM07A_M20_5		0.2219	3.75	0.1256	5.77	0.0041	3.96	0.0011	4.32	2990.0	60.3	120.0	6.9	26.4	1.0	21.2	0.9
UM07A_M20_6		0.0944	2.14	0.0431	3.43	0.0033	2.75	0.0010	3.10	1519.0	40.3	42.8	1.5	21.4	0.6	19.8	0.6
UM07A_M20_7		0.0894	2.30	0.0411	3.74	0.0033	2.96	0.0010	3.33	1414.0	44.1	40.9	1.5	21.5	0.6	20.2	0.7
UM07A_M20_8		0.0876	2.53	0.0391	3.45	0.0033	2.67	0.0010	3.15	1376.0	48.6	38.9	1.3	21.1	0.6	20.0	0.6
UM07A_M21_1		0.0939	3.25	0.0421	4.94	0.0032	3.42	0.0010	3.99	1513.0	61.5	42.1	2.1	20.9	0.7	20.8	0.8
UM07A_M21_2		0.2020	11.46	0.1080	15.87	0.0037	4.80	0.0010	4.28	2760.0	186.8	103.0	16.3	23.6	1.1	21.0	0.9

Table C3. Monazite U-Th-Pb geochronology data and trace elements

UM09

Analysis #	Comment	207Pb/206Pb	2 SE %	207Pb/235U	2 SE %	206Pb/238U	2 SE %	208Pb/232Th	2 SE %	207Pb/206Pb Age (Ma)	2 SE abs.	207Pb/235U Age (Ma)	2 SE abs.	206Pb/238U Age (Ma)	2 SE abs.	208Pb/232Th Age (Ma)	2 SE abs.
~~UM09_M1_1~~	~~Excluded (matrix)~~	~~0.4750~~	~~7.69~~	~~0.4220~~	~~15.30~~	~~0.0064~~	~~9.39~~	~~0.0016~~	~~9.59~~	~~4160.0~~	~~113.8~~	~~356.0~~	~~54.5~~	~~41.3~~	~~3.9~~	~~32.7~~	~~3.1~~
~~UM09_M1_2~~	~~Excluded (matrix)~~	~~0.1560~~	~~6.54~~	~~0.0735~~	~~8.80~~	~~0.0034~~	~~3.19~~	~~0.0010~~	~~3.87~~	~~2390.0~~	~~111.1~~	~~71.9~~	~~6.3~~	~~21.8~~	~~0.7~~	~~20.5~~	~~0.8~~
UM09_M3_1		0.1026	2.59	0.0493	3.81	0.0035	3.01	0.0011	3.57	1665.0	47.9	48.9	1.9	22.3	0.7	23.0	0.8
UM09_M3_2		0.1073	2.43	0.0525	3.65	0.0035	3.28	0.0011	3.61	1754.0	44.4	51.9	1.9	22.8	0.7	22.5	0.8
UM09_M3_3		0.1238	2.33	0.0598	4.34	0.0034	3.46	0.0010	3.80	2008.0	41.4	58.9	2.6	22.2	0.8	21.2	0.8
UM09_M3_4		0.1142	3.25	0.0552	3.98	0.0035	3.33	0.0011	3.63	1866.0	58.6	54.5	2.2	22.3	0.7	21.5	0.8
UM09_M3_5		0.1315	3.10	0.0651	3.67	0.0036	3.67	0.0011	3.93	2115.0	54.3	64.0	2.3	23.0	0.8	22.0	0.9
UM09_M5_1		0.1000	1.91	0.0461	3.28	0.0033	3.25	0.0010	3.60	1626.0	35.5	45.7	1.5	21.3	0.7	21.0	0.8
UM09_M5_2		0.1020	2.27	0.0490	3.16	0.0035	3.05	0.0011	3.40	1656.0	42.1	48.6	1.5	22.6	0.7	21.9	0.7
UM09_M5_3		0.1103	1.95	0.0486	3.68	0.0031	3.45	0.0010	3.82	1803.0	35.4	48.1	1.8	20.2	0.7	19.6	0.7
UM09_M6_1		0.1573	3.79	0.0784	4.78	0.0036	3.01	0.0011	3.24	2436.0	64.3	76.6	3.7	23.2	0.7	22.6	0.7
UM09_M7_1		0.1237	3.41	0.0625	5.20	0.0036	3.32	0.0011	3.71	2000.0	60.5	61.5	3.2	23.0	0.8	22.1	0.8
UM09_M7_2		0.2190	9.22	0.1250	11.38	0.0042	3.92	0.0012	4.06	2930.0	148.6	119.0	13.5	26.7	1.0	24.0	1.0
~~UM09_M8_1~~	~~Excluded (matrix)~~	~~0.1277~~	~~3.46~~	~~0.0637~~	~~4.83~~	~~0.0036~~	~~3.44~~	~~0.0012~~	~~4.06~~	~~2060.0~~	~~61.1~~	~~62.7~~	~~3.0~~	~~23.1~~	~~0.8~~	~~23.4~~	~~0.9~~
~~UM09_M8_2~~	~~Excluded (matrix)~~	~~0.2940~~	~~4.61~~	~~0.1890~~	~~7.67~~	~~0.0047~~	~~3.94~~	~~0.0014~~	~~3.63~~	~~3432.0~~	~~71.6~~	~~175.0~~	~~13.4~~	~~30.3~~	~~1.2~~	~~29.2~~	~~1.1~~
UM09_M8_3		0.1164	4.98	0.0569	5.80	0.0035	3.19	0.0011	3.45	1877.0	89.6	56.1	3.3	22.7	0.7	22.0	0.8
~~UM09_M8_4~~	~~Excluded (matrix)~~	~~0.1118~~	~~5.52~~	~~0.0527~~	~~5.15~~	~~0.0035~~	~~3.73~~	~~0.0012~~	~~4.42~~	~~1815.0~~	~~100.1~~	~~52.1~~	~~2.7~~	~~22.5~~	~~0.8~~	~~23.3~~	~~1.0~~
UM09_M9_1		0.1523	2.58	0.0773	3.69	0.0037	3.04	0.0011	3.26	2379.0	44.1	75.5	2.8	23.6	0.7	22.2	0.7
UM09_M9_2		0.1455	3.04	0.0725	4.47	0.0036	3.27	0.0011	3.48	2285.0	52.3	71.0	3.2	23.1	0.8	21.8	0.8
UM09_M10_1		0.1325	2.88	0.0627	3.90	0.0034	2.83	0.0011	3.19	2125.0	50.3	61.7	2.4	22.2	0.6	21.4	0.7
UM09_M10_2		0.1392	3.69	0.0671	5.45	0.0035	3.94	0.0011	4.12	2205.0	63.9	65.9	3.6	22.7	0.9	22.8	0.9
UM09_M10_3		0.1091	3.98	0.0536	4.73	0.0035	3.02	0.0011	3.31	1779.0	72.5	53.0	2.5	22.7	0.7	21.4	0.7
UM09_M10_4		0.1413	5.81	0.0641	7.00	0.0033	2.91	0.0010	3.41	2224.0	100.4	63.0	4.4	21.3	0.6	20.1	0.7
UM09_M10_5		0.0991	2.66	0.0447	3.72	0.0033	3.42	0.0010	3.71	1601.0	49.6	44.4	1.6	21.1	0.7	20.6	0.8
~~UM09_M11_2~~	~~Excluded (matrix)~~	~~0.1552~~	~~3.53~~	~~0.0761~~	~~4.66~~	~~0.0035~~	~~3.30~~	~~0.0010~~	~~3.23~~	~~2402.0~~	~~60.1~~	~~74.4~~	~~3.5~~	~~22.6~~	~~0.7~~	~~20.8~~	~~0.7~~
~~UM09_M11_4~~	~~Excluded (matrix)~~	~~0.1609~~	~~2.97~~	~~0.0781~~	~~5.02~~	~~0.0035~~	~~3.51~~	~~0.0010~~	~~3.65~~	~~2475.0~~	~~50.2~~	~~76.9~~	~~3.9~~	~~22.3~~	~~0.8~~	~~20.5~~	~~0.7~~
~~UM09_M11_5~~	~~Excluded (matrix)~~	~~0.1653~~	~~4.03~~	~~0.0891~~	~~4.91~~	~~0.0040~~	~~3.64~~	~~0.0013~~	~~3.98~~	~~2508.0~~	~~67.7~~	~~86.6~~	~~4.3~~	~~25.4~~	~~0.9~~	~~25.5~~	~~1.0~~
~~UM09_M11_6~~	~~Excluded (matrix)~~	~~0.1340~~	~~3.95~~	~~0.0634~~	~~5.72~~	~~0.0034~~	~~3.54~~	~~0.0011~~	~~3.91~~	~~2136.0~~	~~69.0~~	~~62.4~~	~~3.6~~	~~22.0~~	~~0.8~~	~~21.5~~	~~0.8~~
~~UM09_M12_1~~	~~Excluded (matrix)~~	~~0.1200~~	~~3.73~~	~~0.0523~~	~~5.01~~	~~0.0032~~	~~3.98~~	~~0.0011~~	~~4.78~~	~~1954.0~~	~~66.7~~	~~51.8~~	~~2.6~~	~~20.6~~	~~0.8~~	~~21.3~~	~~1.0~~
~~UM09_M12_2~~	~~Excluded (matrix)~~	~~0.0898~~	~~1.95~~	~~0.0404~~	~~3.18~~	~~0.0033~~	~~3.10~~	~~0.0010~~	~~3.41~~	~~1418.0~~	~~37.2~~	~~40.3~~	~~1.3~~	~~21.2~~	~~0.7~~	~~20.9~~	~~0.7~~
~~UM09_M12_3~~	~~Excluded (matrix)~~	~~0.1260~~	~~3.07~~	~~0.0646~~	~~4.08~~	~~0.0037~~	~~3.83~~	~~0.0011~~	~~4.02~~	~~2035.0~~	~~54.2~~	~~63.6~~	~~2.6~~	~~23.7~~	~~0.9~~	~~23.1~~	~~0.9~~
UM09_M12_4		0.1159	2.74	0.0571	3.88	0.0036	3.10	0.0011	3.29	1887.0	49.3	56.3	2.2	23.1	0.7	21.7	0.7
~~UM09_M12_5~~	~~Excluded (matrix)~~	~~0.2808~~	~~3.46~~	~~0.1740~~	~~6.63~~	~~0.0044~~	~~3.93~~	~~0.0013~~	~~4.09~~	~~3362.0~~	~~54.0~~	~~162.5~~	~~10.8~~	~~28.6~~	~~1.1~~	~~25.6~~	~~1.0~~
~~UM09_M12_6~~	~~Excluded (matrix)~~	~~0.3810~~	~~5.41~~	~~0.2330~~	~~6.74~~	~~0.0047~~	~~4.94~~	~~0.0013~~	~~6.35~~	~~3833.0~~	~~81.7~~	~~212.0~~	~~14.3~~	~~29.9~~	~~1.5~~	~~26.0~~	~~1.7~~
~~UM09_M13_1~~	~~Excluded (matrix)~~	~~0.7100~~	~~7.16~~	~~2.9000~~	~~34.54~~	~~0.0292~~	~~30.54~~	~~0.0054~~	~~37.12~~	~~4760.0~~	~~102.8~~	~~1340.0~~	~~462.8~~	~~185.0~~	~~56.5~~	~~109.0~~	~~40.5~~
UM09_M13_2		0.0848	2.10	0.0408	3.56	0.0035	3.32	0.0011	3.46	1307.0	40.8	40.6	1.4	22.4	0.7	22.0	0.8
UM09_M13_3		0.0843	1.76	0.0389	2.89	0.0034	2.85	0.0010	3.21	1297.0	34.2	38.7	1.1	21.6	0.6	21.0	0.7
UM09_M13_4		0.0971	2.52	0.0463	3.81	0.0035	3.07	0.0010	3.46	1564.0	47.3	45.9	1.7	22.4	0.7	21.1	0.7
UM09_M13_5		0.0926	2.08	0.0446	3.53	0.0035	3.21	0.0011	3.46	1476.0	39.4	44.3	1.6	22.6	0.7	22.0	0.8
UM09_M13_6		0.0829	2.13	0.0382	3.51	0.0033	2.80	0.0010	3.11	1269.0	41.6	38.1	1.3	21.3	0.6	20.8	0.6
UM09_M13_7		0.1131	2.56	0.0543	4.19	0.0034	2.87	0.0010	3.30	1858.0	46.4	53.7	2.3	21.9	0.6	20.6	0.7
UM09_M14_1		0.1521	2.99	0.0788	4.53	0.0037	3.36	0.0011	3.52	2370.0	51.0	76.9	3.5	23.9	0.8	22.0	0.8
UM09_M14_2		0.1192	2.61	0.0592	3.93	0.0036	2.89	0.0011	3.23	1946.0	46.7	58.3	2.3	23.4	0.7	21.8	0.7
UM09_M14_3		0.1058	2.29	0.0515	4.03	0.0035	2.76	0.0011	3.12	1724.0	42.1	50.9	2.0	22.6	0.6	21.6	0.7
UM09_M14_4		0.1185	2.20	0.0599	3.75	0.0037	3.62	0.0011	3.89	1929.0	39.3	59.1	2.2	23.5	0.8	22.4	0.9
UM09_M14_5		0.1010	2.37	0.0473	3.40	0.0034	2.95	0.0011	3.20	1644.0	44.0	46.9	1.6	22.0	0.6	21.3	0.7
UM09_M14_6		0.1056	2.62	0.0505	3.42	0.0035	2.69	0.0011	3.19	1718.0	48.1	50.0	1.7	22.5	0.6	21.4	0.7
UM09_M14_7		0.1285	3.52	0.0614	5.13	0.0035	3.98	0.0010	4.11	2069.0	61.9	60.5	3.1	22.5	0.9	21.1	0.9
~~UM09_M15_1~~	~~Excluded (inclusior~~	~~0.1740~~	~~7.02~~	~~0.1050~~	~~10.67~~	~~0.0043~~	~~5.05~~	~~0.0014~~	~~5.41~~	~~2560.0~~	~~117.0~~	~~100.7~~	~~10.7~~	~~27.7~~	~~1.4~~	~~27.8~~	~~1.5~~
~~UM09_M15_4~~	~~Excluded (matrix)~~	~~0.1319~~	~~3.44~~	~~0.0651~~	~~4.74~~	~~0.0036~~	~~3.05~~	~~0.0010~~	~~3.27~~	~~2111.0~~	~~60.2~~	~~64.0~~	~~3.0~~	~~23.2~~	~~0.7~~	~~21.0~~	~~0.7~~
~~UM09_M15_5~~	~~Excluded (matrix)~~	~~0.1561~~	~~3.88~~	~~0.0772~~	~~6.53~~	~~0.0036~~	~~5.85~~	~~0.0011~~	~~6.65~~	~~2407.0~~	~~65.8~~	~~75.4~~	~~4.9~~	~~23.4~~	~~1.4~~	~~22.6~~	~~1.5~~
UM09_M15_6		0.0947	1.97	0.0459	3.12	0.0035	3.01	0.0011	3.32	1520.0	37.1	45.6	1.4	22.6	0.7	22.2	0.7
UM09_M15_7		0.1019	2.04	0.0501	3.12	0.0035	2.97	0.0011	3.34	1656.0	37.7	49.6	1.5	22.8	0.7	21.8	0.7
UM09_M15_8		0.0917	2.09	0.0444	3.18	0.0035	2.95	0.0011	3.00	1468.0	39.7	44.2	1.4	22.3	0.7	21.8	0.7
UM09_M15_9		0.0897	1.87	0.0441	3.75	0.0035	3.37	0.0011	3.83	1416.0	35.7	43.8	1.6	22.7	0.8	22.3	0.9
UM09_M15_10		0.0893	1.79	0.0427	3.45	0.0035	2.97	0.0011	3.42	1413.0	34.3	42.4	1.5	22.3	0.7	21.7	0.7
~~UM09_M15_11~~	~~Excluded (inclusior~~	~~0.0897~~	~~1.95~~	~~0.0456~~	~~3.31~~	~~0.0037~~	~~3.33~~	~~0.0011~~	~~3.51~~	~~1417.0~~	~~37.2~~	~~45.2~~	~~1.5~~	~~23.9~~	~~0.8~~	~~22.9~~	~~0.8~~
~~UM09_M15_12~~	~~Excluded (matrix)~~	~~0.1130~~	~~3.20~~	~~0.0479~~	~~4.82~~	~~0.0030~~	~~4.13~~	~~0.0009~~	~~4.29~~	~~1856.0~~	~~57.8~~	~~47.5~~	~~2.3~~	~~19.6~~	~~0.8~~	~~19.2~~	~~0.8~~

bdl - below detection limit

Table C3. Monazite U-Th-Pb geochronology data and trace elements

METAMORPHIC SPECIMENS

UM05

Analysis #	Si	Sr	Y89	Zr90	La139	Ce140	Pr141	Nd146	Sm147	Eu153	Gd157	Tb159	Dy163	Ho165	Er166	Tm169	Yb172	Lu175
UM05A_M2_1	120000	79	13700	38	104000	254000	24700	94000	17300	1005	12100	1450	5250	630	825	62.1	156	13
UM05A_M2_2	36200	78.6	15000	35	103900	257000	24800	97700	19800	1020	14100	1570	5430	646	873	68.3	207	14.8
UM05A_M2_3	46000	74	11600	53	108000	253000	23700	90800	16700	1090	12700	1360	5190	556	736	57.5	171	11.9
~~UM05A_M2_4~~	~~8000000~~	~~690~~	~~7900~~	~~17~~	~~92000~~	~~221000~~	~~20900~~	~~87000~~	~~12200~~	~~1300~~	~~9700~~	~~1180~~	~~3950~~	~~401~~	~~510~~	~~45~~	~~250~~	~~41~~
~~UM05A_M3_1~~	~~3280000~~	~~321~~	~~9000~~	~~19~~	~~87000~~	~~229000~~	~~24100~~	~~79000~~	~~15000~~	~~1360~~	~~10900~~	~~1100~~	~~4200~~	~~445~~	~~540~~	~~46~~	~~150~~	~~8~~
~~UM05A_M3_3~~	~~790000~~	~~122~~	~~11500~~	~~64~~	~~103000~~	~~287000~~	~~26000~~	~~90000~~	~~17600~~	~~1180~~	~~13300~~	~~1500~~	~~4950~~	~~525~~	~~790~~	~~64~~	~~165~~	~~12.7~~
UM05A_M5_1	38300	48.2	12700	64	119000	285000	26100	102600	17100	1105	13400	1460	4950	586	790	60.8	169	12.4
~~UM05A_M14_1~~	~~720000~~	~~129~~	~~9300~~	~~26~~	~~90600~~	~~248000~~	~~23500~~	~~84000~~	~~15600~~	~~1270~~	~~11300~~	~~1160~~	~~4210~~	~~486~~	~~611~~	~~44.8~~	~~168~~	~~10.6~~
UM05A_M18_1	172000	166	14700	34	127000	252000	26300	100000	18200	1160	13000	1540	5480	658	920	67.6	195	16.6
~~UM05A_M8_1~~	~~1090000~~	~~178~~	~~12200~~	~~10~~	~~102000~~	~~240000~~	~~25100~~	~~91000~~	~~16000~~	~~840~~	~~11400~~	~~1290~~	~~4870~~	~~480~~	~~740~~	~~69~~	~~166~~	~~8.1~~
~~UM05A_M8_2~~	~~255000~~	~~124~~	~~13500~~	~~10.2~~	~~114000~~	~~307000~~	~~27700~~	~~93400~~	~~19400~~	~~1300~~	~~12900~~	~~1420~~	~~5070~~	~~609~~	~~798~~	~~63.6~~	~~191~~	~~13.9~~

UM07

Analysis #	Si	Sr	Y89	Zr90	La139	Ce140	Pr141	Nd146	Sm147	Eu153	Gd157	Tb159	Dy163	Ho165	Er166	Tm169	Yb172	Lu175
UM07A_M1_1	8100	85.1	14300	58	93000	237000	24000	78200	15300	1550	10400	1360	5420	627	930	69.5	189	12
UM07A_M1_2	26300	80	14100	51	107000	281000	26600	89500	15900	2010	11400	1400	5440	644	953	74.2	214	13.9
~~UM07A_M1_3~~	~~83000~~	~~51.1~~	~~10300~~	~~39~~	~~96000~~	~~263000~~	~~24700~~	~~84000~~	~~13900~~	~~2150~~	~~8700~~	~~1010~~	~~3930~~	~~485~~	~~780~~	~~59.5~~	~~143~~	~~11.8~~
UM07A_M1_4	18100	80.4	12400	2600	85000	252000	21100	75600	14700	1430	10500	1340	5070	534	813	61.1	174	12.4
UM07A_M1_5	8000	52.4	10700	60	102000	244000	23300	83000	13400	2100	8920	1100	4070	501	744	56	147	10.5
UM07A_M1_6	18300	75	11900	59	110000	294000	26600	91500	16400	1900	10800	1440	5160	628	869	60.6	161	11.9
UM07A_M1_7	15700	79	11800	60	105000	258000	25500	91000	15000	1720	10700	1250	4860	594	849	60.5	166	11
UM07A_M1_8	65000	89.7	13900	42	99000	258000	23200	86500	15900	1350	11800	1380	5300	606	836	61.8	170	12.1
UM07A_M1_9	29800	84.3	13100	56	85900	231000	19900	76300	13700	1160	10850	1300	5020	592	865	61.8	170	11.1
UM07A_M1_10	22400	98	15500	47	97700	248000	21700	83500	16100	1130	12100	1530	5640	689	941	68.2	180	12.7
UM07A_M1_11	4100	68.1	14800	67	136000	328000	30300	109000	19100	2580	12200	1470	5430	719	936	79.7	219	13
UM07A_M2_1	33000	65.5	10600	49	104000	301000	24600	85800	13300	2630	9920	1120	4060	493	708	59.2	158	9.4
UM07A_M2_2	240000	173	11600	28	106000	277000	23800	94700	15200	2970	9300	1190	4040	508	800	57	143	12.1
UM07A_M2_3	7300	68.8	12600	58	113000	290000	27200	90000	16700	2060	9730	1260	4710	584	758	61.8	163	11.1
UM07A_M2_4	154000	122	10800	35	114000	286000	23600	94000	15600	3390	10200	1160	3940	472	707	59.2	156	15.7
UM07A_M2_5	128000	165	13000	1200	109000	277000	23700	92000	16200	2540	10400	1240	4600	531	780	67.6	172	13
UM07A_M2_6	296000	96	11200	27	80200	243000	19600	79000	13000	1300	9180	1090	4120	464	681	57.7	153	10.7
UM07A_M2_7	28000	74.3	11600	330	99000	255000	23500	82000	13700	1940	10400	1230	4470	520	740	58.5	149	10.5
UM07A_M2_8	170000	84	12900	21	105000	266000	25800	97000	17800	2010	11500	1340	5140	595	822	59.3	158	11.9
UM07A_M2_9	49000	109	14000	59	107800	281000	24600	92400	16600	2000	10860	1300	5060	619	855	64.5	174	11.4
~~UM07A_M3_1~~	~~179000~~	~~68~~	~~9200~~	~~21.5~~	~~96000~~	~~263000~~	~~20000~~	~~77600~~	~~12600~~	~~2200~~	~~8270~~	~~910~~	~~3370~~	~~414~~	~~621~~	~~48.9~~	~~127~~	~~10.1~~
~~UM07A_M3_3~~	~~930000~~	~~164~~	~~10000~~	~~11.6~~	~~108000~~	~~276000~~	~~26100~~	~~91000~~	~~16800~~	~~3370~~	~~9200~~	~~1050~~	~~4230~~	~~484~~	~~666~~	~~54~~	~~160~~	~~13.5~~
UM07A_M3_4	17100	76.2	14400	50	100000	275000	24400	84600	15800	1610	11800	1360	5490	629	810	65.6	179	12
UM07A_M3_5	47800	109	14600	59	106000	271000	22600	86300	18100	1410	12800	1520	5550	672	903	70.9	187	12.9
UM07A_M4_1	6700	69.2	12600	62	105000	273000	25100	84100	15200	1840	10460	1280	4830	564	781	58	148	12.2
UM07A_M4_2	64500	63.3	11100	50	102000	259000	24300	93000	14500	1830	9900	1230	4570	551	765	58.2	151	9.7
UM07A_M4_3	31000	78.6	13700	51	116000	309000	26700	99000	16100	1950	11800	1430	5000	586	910	61.8	173	10.8
UM07A_M4_4	30000	91	14200	38	97000	259000	22700	84000	15700	1470	12000	1510	5710	627	890	66	166	13
UM07A_M4_5	bdl	74.9	13700	45	116000	304000	24900	92500	16000	1940	11500	1360	5000	648	796	60	178	12.3
UM07A_M4_6	48400	108	16500	48	97800	273000	22100	84400	16300	1370	12900	1730	6220	735	1000	73.3	198	13.6
UM07A_M4_7	2200	79	13700	71	100000	262000	24000	84100	15100	1590	11200	1490	5200	621	889	60.2	171	10.7
~~UM07A_M5_1~~	~~155000~~	~~340~~	~~11500~~	~~26~~	~~105000~~	~~332000~~	~~27700~~	~~95000~~	~~16300~~	~~2490~~	~~10500~~	~~1200~~	~~4470~~	~~550~~	~~830~~	~~62.9~~	~~164~~	~~12.7~~
~~UM07A_M6_1~~	~~98000~~	~~44.6~~	~~15900~~	~~34~~	~~121000~~	~~312000~~	~~25400~~	~~95000~~	~~16500~~	~~3970~~	~~10000~~	~~1160~~	~~4280~~	~~615~~	~~1300~~	~~149~~	~~605~~	~~56.6~~
~~UM07A_M6_2~~	~~238000~~	~~61.2~~	~~15700~~	~~34~~	~~110000~~	~~291000~~	~~23800~~	~~84000~~	~~14700~~	~~3480~~	~~8640~~	~~1010~~	~~4020~~	~~605~~	~~1240~~	~~159~~	~~661~~	~~63.7~~
~~UM07A_M6_3~~	~~12400~~	~~39.1~~	~~16700~~	~~44~~	~~116000~~	~~299000~~	~~23300~~	~~90000~~	~~15300~~	~~3660~~	~~9400~~	~~1110~~	~~4300~~	~~686~~	~~1380~~	~~179~~	~~770~~	~~72~~
~~UM07A_M6_4~~	~~73000~~	~~47.7~~	~~18400~~	~~50~~	~~101700~~	~~268000~~	~~23100~~	~~81300~~	~~14400~~	~~3430~~	~~9200~~	~~1052~~	~~4540~~	~~662~~	~~1520~~	~~198~~	~~926~~	~~96.4~~
~~UM07A_M7_2~~	~~550000~~	~~202~~	~~15800~~	~~510~~	~~127000~~	~~355000~~	~~29600~~	~~130000~~	~~19600~~	~~4010~~	~~12400~~	~~1310~~	~~4890~~	~~510~~	~~890~~	~~64~~	~~193~~	~~12~~

Table C3. Monazite U-Th-Pb geochronology data and trace elements

Analysis #	Si	Sr	Y89	Zr90	La139	Ce140	Pr141	Nd146	Sm147	Eu153	Gd157	Tb159	Dy163	Ho165	Er166	Tm169	Yb172	Lu175
~~UM07A_M7_3~~	~~520000~~	~~143~~	~~11100~~	~~27~~	~~145000~~	~~275000~~	~~27700~~	~~91000~~	~~17200~~	~~3390~~	~~9800~~	~~1120~~	~~3310~~	~~481~~	~~800~~	~~52~~	~~134~~	~~14.5~~
UM07A_M7_4	24500	48	9580	58	110000	271000	25700	88200	14700	2460	9060	990	3910	446	656	55.2	154	10
UM07A_M7_5	9900	72.9	11500	52	107200	270000	23500	96500	15500	1920	10500	1200	4640	567	762	59.6	154	9.9
~~UM07A_M7_6~~	~~16300~~	~~73.6~~	~~13400~~	~~60~~	~~130000~~	~~327000~~	~~29200~~	~~105700~~	~~17700~~	~~2520~~	~~11900~~	~~1380~~	~~5210~~	~~626~~	~~910~~	~~65.1~~	~~194~~	~~12.7~~
UM07A_M7_7	14400	91.2	13900	50	105000	270000	22400	88000	15500	1140	11600	1480	5370	615	855	58.2	163	10.5
UM07A_M7_8	7200	63.5	10900	53	115000	292000	24200	83000	17300	2250	10700	1190	4440	520	719	59.1	179	8.4
UM07A_M7_9	15700	69.4	14900	61	113000	283000	25100	89000	16300	1750	11900	1450	5370	663	866	65.5	169	10.4
UM07A_M7_10	99000	102	16000	46	111000	263000	24300	98000	18600	1070	14100	1640	5890	733	1060	79.9	210	13.2
UM07A_M8_1	9200	103	13400	49	98700	242000	22800	82000	14800	1230	12100	1570	6210	678	960	70.1	189	12.1
UM07A_M8_2	17600	89.1	15700	57	108900	297000	26400	88600	16400	1500	12570	1700	6420	729	1025	77.1	214	14.7
UM07A_M8_3	4700	74.8	13300	75	97000	243000	23400	77600	15300	1660	11000	1450	5510	670	990	73	189	11.7
UM07A_M8_4	10800	96.3	13100	60	96000	271000	21700	79300	16300	1090	11500	1440	5460	645	902	71.9	186	14
UM07A_M8_5	9300	84.7	14800	46	97800	263000	20600	84300	16400	1240	12200	1450	5370	672	980	69.4	180	12.9
UM07A_M8_6	700	73	13900	54	105000	268000	23700	85000	16300	1520	11300	1380	5630	641	860	67.7	179	12.9
UM07A_M8_7	4900	66.7	12200	55	101500	273000	24600	87200	14800	1580	10980	1410	5160	629	828	61.8	166	10.6
UM07A_M8_8	39600	79	15000	40	111000	304000	25300	101000	18700	2010	12800	1620	6020	715	960	73.9	192	11.8
~~UM07A_M8_9~~	~~106000~~	~~106~~	~~13900~~	~~43~~	~~125000~~	~~316000~~	~~26000~~	~~99000~~	~~18000~~	~~2740~~	~~11300~~	~~1350~~	~~4830~~	~~588~~	~~892~~	~~64.8~~	~~182~~	~~12.4~~
UM07A_M8_10	14500	99	14100	43	106000	260000	24200	85000	15800	1070	13500	1540	5590	708	970	78	198	13.5
~~UM07A_M8_11~~	~~3900~~	~~73.7~~	~~14300~~	~~51~~	~~113000~~	~~273000~~	~~25200~~	~~88100~~	~~17100~~	~~1740~~	~~11500~~	~~1460~~	~~5890~~	~~666~~	~~968~~	~~75.3~~	~~187~~	~~11.8~~
UM07A_M8_12	3700	83	13200	76	98000	260000	25000	86700	16400	1580	12200	1490	5740	645	931	72	196	13.4
UM07A_M8_13	6300	100	13300	51	99000	247000	23300	83300	15800	1230	12300	1580	5960	700	960	74.8	196	11.2
UM07A_M8_14	8100	94	13600	36	102000	257000	21700	83700	14800	1080	11200	1420	5370	601	930	69.3	181	11.1
UM07A_M10_1	42200	96.9	14500	40	100100	246000	21500	77300	15900	1060	12400	1450	5630	673	936	69.7	186	11.5
UM07A_M10_2	12000	112	12900	50	91000	239000	22500	83300	16200	1310	12100	1430	5310	648	873	62.8	162	10.9
UM07A_M10_3	6900	135	12600	51	88700	243000	22300	75400	15400	1370	11400	1360	5010	599	870	60.7	173	11.4
UM07A_M10_4	23100	75.6	11200	35	104000	265000	22500	82900	15500	1590	10550	1310	4870	558	815	59.4	145	8.8
UM07A_M10_5	10000	49.6	10600	41	101000	250000	22500	81800	14300	2010	8650	1050	3940	469	685	52.6	141	9
UM07A_M10_6	25100	57.3	12500	1400	118000	304000	24000	94700	16200	2880	10500	1220	4570	560	855	71.3	186	12.9
UM07A_M11_1	35000	113	16300	57	106000	288000	25300	90000	16200	1540	13400	1690	6380	700	940	71	190	12.8
UM07A_M11_2	13100	102	14400	51	100000	248000	21100	81700	15600	1400	11800	1470	5670	662	950	70.9	187	12.4
~~UM07A_M11_3~~	~~34900~~	~~92~~	~~17700~~	~~113~~	~~105000~~	~~281000~~	~~24100~~	~~91000~~	~~16800~~	~~1720~~	~~12400~~	~~1550~~	~~6040~~	~~765~~	~~1270~~	~~120~~	~~410~~	~~57~~
UM07A_M11_4	65000	140	16800	13	119000	299000	27100	110000	19700	2730	14300	1700	6440	754	1090	78	223	18.1
UM07A_M11_5	50000	73.7	11500	40	94000	286000	23700	82500	15000	1660	10800	1390	5030	612	815	62.5	165	11.9
UM07A_M11_6	5600	91	13200	55	108000	286000	24500	88000	16100	1830	11200	1350	5460	653	880	64.4	182	11.7
UM07A_M12_1	34000	98.9	16500	70	106700	256000	25900	87800	17800	1230	13600	1520	5570	658	1050	74.6	201	14.5
UM07A_M12_2	65000	92.6	16000	46	109000	287000	23200	88000	16300	1570	13400	1550	5890	743	1016	77.7	195	13
UM07A_M12_3	6700	72.1	13900	51	112000	322000	28700	101000	17100	2350	11300	1360	5600	619	930	71	176	14.4
UM07A_M12_4	97000	99	11600	39	121000	324000	26700	93000	16900	2500	11500	1190	4910	618	790	64.1	155	12
UM07A_M12_5	30000	61	11600	48	121000	342000	27700	100700	17900	3250	10300	1225	4210	538	839	66.6	185	14
UM07A_M12_6	24600	51.6	11800	57	120000	318000	27800	93300	17800	2770	10270	1174	4410	534	815	63.8	166	13.1
UM07A_M12_7	2300	80.5	16000	50	100000	267000	24700	79200	14600	1760	11600	1320	5140	579	850	57.8	161	13.6
UM07A_M12_8	175000	63.1	11900	37	108000	281000	22100	87000	15000	2300	10100	1190	4240	516	722	62.1	154	12.8
UM07A_M12_9	130000	79.4	12900	57	93400	235000	22700	81000	14700	1180	11300	1340	4760	614	764	60.6	152	11.3
UM07A_M12_10	6100	67.5	12300	55	103000	268000	21200	86800	14400	1770	10200	1240	4780	579	810	62	177	12.4
UM07A_M12_11	8700	93	13100	34	117000	304000	26000	95000	16800	1770	12500	1570	6190	692	980	68.7	181	14.4
UM07A_M12_12	4400	51.6	12000	62	114000	316000	26700	92800	15400	2520	9910	1220	4640	584	820	63.3	185	13.3
UM07A_M12_13	4500	48.1	10600	55	106000	278000	24300	79900	15600	2230	9050	1041	4160	540	728	55.1	156	11.5
UM07A_M13_1	28500	93	12800	44	99000	280000	21900	82400	15700	1000	11700	1360	5120	614	831	63.3	174	12
UM07A_M13_2	11300	76.5	12900	57	96200	274000	20700	74100	15400	745	11800	1300	4940	609	876	62.8	169	13.7
UM07A_M13_3	26000	63.9	12700	31	112000	314000	26900	89000	16100	2110	11100	1320	5000	571	890	64.9	176	16.4
~~UM07A_M13_4~~	~~93000~~	~~192~~	~~13200~~	~~46~~	~~93000~~	~~277000~~	~~20600~~	~~78700~~	~~16000~~	~~752~~	~~11700~~	~~1230~~	~~4470~~	~~497~~	~~666~~	~~53~~	~~125~~	~~10.8~~
UM07A_M13_6	24400	58.1	13600	75	111000	308000	25700	89000	17100	2600	10600	1130	4170	525	755	57	185	14.3
~~UM07A_M13_7~~	~~268000~~	~~175~~	~~12100~~	~~14~~	~~128000~~	~~345000~~	~~32000~~	~~117000~~	~~20500~~	~~3350~~	~~11000~~	~~1200~~	~~4610~~	~~610~~	~~920~~	~~78~~	~~173~~	~~14.8~~
UM07A_M13_8	16300	88.7	12600	68	103400	256000	22900	87500	15000	1390	11220	1520	5340	616	863	59.9	157	12.6
~~UM07A_M15_1~~	~~138000~~	~~152~~	~~13600~~	~~32~~	~~143000~~	~~332000~~	~~30200~~	~~99000~~	~~17800~~	~~3350~~	~~10200~~	~~1210~~	~~4740~~	~~549~~	~~790~~	~~65.9~~	~~178~~	~~15.7~~

Table C3. Monazite U-Th-Pb geochronology data and trace elements

Analysis #	Si	Sr	Y89	Zr90	La139	Ce140	Pr141	Nd146	Sm147	Eu153	Gd157	Tb159	Dy163	Ho165	Er166	Tm169	Yb172	Lu175
UM07A_M15_2	90000	49	12200	27	128500	316000	27500	102000	16700	2850	10130	1220	4690	557	824	60.1	187	16.9
UM07A_M15_3	66000	53.1	11800	40	109000	293000	23600	83300	14900	1780	9730	1160	4510	522	770	62.2	166	10.5
UM07A_M15_4	17200	86	12700	54	112000	271000	26000	88600	16400	1630	11300	1350	5300	617	851	65.6	172	12.2
UM07A_M20_1	4800	67.5	12400	36	109000	278000	26300	91400	16200	1810	10100	1360	4800	616	867	70.4	179	13.1
UM07A_M20_2	20100	66.5	13300	60	103500	268000	25000	85000	15600	1620	10480	1310	5080	605	884	68.7	191	11.5
UM07A_M20_3	2300	69.6	13100	63	119000	274000	25300	91000	16200	1840	11150	1380	5180	642	928	67.6	195	13
UM07A_M20_4	8200	89.6	14200	56	90500	248000	21800	77800	14200	1037	12090	1600	5880	706	990	71.5	200	13.8
UM07A_M20_5	9500	84.3	13100	54	96000	256000	21200	90000	16000	1330	10900	1380	5330	612	872	58.1	166	11.4
UM07A_M20_6	7000	95.8	12100	60	89700	228000	20700	83600	14800	1050	11600	1330	5110	618	827	63.8	169	11.1
UM07A_M20_7	6900	89.6	12900	58	90000	239000	20100	74600	14200	1000	11100	1350	5140	627	890	69.4	172	11.4
UM07A_M20_8	200	57.9	11300	51	114000	277000	25000	89000	14800	1890	9420	1200	4660	556	806	64.5	154	12.6
UM07A_M21_1	61000	65.7	11700	27	99700	262000	24200	87000	15500	1760	10300	1230	4800	570	870	61.1	152	11.8
UM07A_M21_2	101000	114	14100	25	105000	268000	25200	87500	16700	2060	11250	1420	5420	599	908	66.5	191	12.5

UM09

Analysis #	Si	Sr	Y89	Zr90	La139	Ce140	Pr141	Nd146	Sm147	Eu153	Gd157	Tb159	Dy163	Ho165	Er166	Tm169	Yb172	Lu175
~~UM09_M1_1~~	~~310000~~	~~400~~	~~6600~~	~~21~~	~~129000~~	~~349000~~	~~30400~~	~~114000~~	~~22500~~	~~3980~~	~~15000~~	~~1000~~	~~2270~~	~~298~~	~~470~~	~~34.4~~	~~185~~	~~25.3~~
~~UM09_M1_2~~	~~262000~~	~~88.9~~	~~3700~~	~~9.4~~	~~113300~~	~~247000~~	~~25900~~	~~99570~~	~~20200~~	~~3090~~	~~10770~~	~~739~~	~~1740~~	~~198~~	~~283~~	~~33~~	~~151~~	~~11.9~~
UM09_M3_1	2500	53.4	4630	49	116000	225000	26100	89600	17000	3050	10300	859	2460	253	306	24	57.2	5.27
UM09_M3_2	3600	75.7	5940	34	126000	249000	27500	102000	19900	3320	12000	1040	3050	329	448	29.4	71.8	6.46
UM09_M3_3	12100	110	4260	53	143000	319000	31900	117000	23900	3690	12400	1050	2330	232	302	24.4	74	7.7
UM09_M3_4	3500	67.9	4970	37	120000	265000	27400	94100	20800	3390	12300	1060	2990	263	339	22	63	5.1
UM09_M3_5	27000	85	5040	64	121000	254000	26200	103000	21100	3350	12900	1090	2770	273	358	31	99	11.8
UM09_M5_1	5500	81.5	4600	30	117000	262000	27300	105000	20800	3200	12060	946	2400	229	345	34.4	148	15.9
UM09_M5_2	3900	91.4	4400	43	110700	269000	27800	98600	21400	3080	12700	980	2150	210	303	29	116	12.8
UM09_M5_3	8700	85	5340	41	118000	255000	25100	96000	21200	3190	12600	940	2320	212	356	33.9	163	18.4
UM09_M6_1	195000	90	4180	21	131000	274000	29200	118000	19600	1250	11400	860	2210	234	283	18.6	33	5.4
UM09_M7_1	16800	93	2890	60	109000	248000	24600	87100	20500	2770	13300	918	1940	161	164	9.9	30.6	3.67
UM09_M7_2	61000	103	3640	35	108000	235000	25800	98000	21000	3020	13300	930	2170	177	230	25.1	77	6.8
~~UM09_M8_1~~	~~13600~~	~~106~~	~~3110~~	~~55~~	~~104700~~	~~230000~~	~~26400~~	~~88000~~	~~18500~~	~~3040~~	~~11500~~	~~827~~	~~1930~~	~~163~~	~~197~~	~~13.1~~	~~38.9~~	~~3.59~~
~~UM09_M8_2~~	~~126000~~	~~112~~	~~3830~~	~~21.9~~	~~104000~~	~~254000~~	~~23700~~	~~87800~~	~~20400~~	~~2890~~	~~11400~~	~~814~~	~~2000~~	~~189~~	~~286~~	~~23.2~~	~~90~~	~~11.1~~
UM09_M8_3	8300	82.1	2650	45	123000	236000	28000	101000	20500	3170	11300	752	1610	128	164	11.6	35.7	4.2
~~UM09_M8_4~~	~~21500~~	~~184~~	~~3180~~	~~53~~	~~99900~~	~~218000~~	~~25000~~	~~83000~~	~~17100~~	~~2550~~	~~10300~~	~~744~~	~~1690~~	~~153~~	~~220~~	~~21.5~~	~~77~~	~~8.6~~
UM09_M9_1	42900	95	1120	34	129000	264000	23300	90000	20200	3160	9700	653	1050	54.7	60.5	2.4	9.6	1.47
UM09_M9_2	19100	82	1180	41	110000	261000	26400	95200	20500	3590	10800	632	919	49.4	55.1	2.46	10	1.62
UM09_M10_1	57000	83.2	2750	31	117000	256000	23100	98000	18600	3160	10300	769	1640	148	190	18.2	68	9.7
UM09_M10_2	160000	74.7	4090	20	102000	249000	23900	96000	18200	3250	11100	868	1980	190	280	21.7	84	10.6
UM09_M10_3	bdl	64.1	4620	42	123900	261000	28400	93500	20000	3460	12170	1172	2870	253	263	15.7	35.3	3.47
UM09_M10_4	21700	85.5	5170	36	126000	269000	26900	104400	21400	3430	12940	1106	2760	266	328	26.6	102.3	13.1
UM09_M10_5	11200	72.1	5140	49	108800	252000	26500	95800	19100	3100	13110	1026	2630	252	351	27.7	108	13.6
~~UM09_M11_2~~	~~31300~~	~~72.5~~	~~8000~~	~~26~~	~~121000~~	~~282000~~	~~25900~~	~~102000~~	~~20000~~	~~3970~~	~~11000~~	~~1040~~	~~3450~~	~~437~~	~~730~~	~~91~~	~~380~~	~~40.5~~
~~UM09_M11_4~~	~~9500~~	~~71.6~~	~~10300~~	~~70~~	~~108000~~	~~249000~~	~~23500~~	~~89100~~	~~20000~~	~~4030~~	~~11900~~	~~1170~~	~~3930~~	~~514~~	~~940~~	~~113~~	~~478~~	~~53.6~~
~~UM09_M11_5~~	~~89000~~	~~65.8~~	~~8700~~	~~57~~	~~106000~~	~~276000~~	~~25900~~	~~107000~~	~~20100~~	~~4310~~	~~11700~~	~~1110~~	~~4130~~	~~472~~	~~870~~	~~98~~	~~431~~	~~45.2~~
~~UM09_M11_6~~	~~18500~~	~~64.6~~	~~5650~~	~~28~~	~~107000~~	~~251000~~	~~24100~~	~~89400~~	~~19100~~	~~3480~~	~~9400~~	~~910~~	~~2560~~	~~274~~	~~470~~	~~53.1~~	~~209~~	~~22.1~~
~~UM09_M12_1~~	~~95000~~	~~80~~	~~5010~~	~~14.2~~	~~108000~~	~~270000~~	~~23900~~	~~103000~~	~~20200~~	~~3090~~	~~10300~~	~~849~~	~~2080~~	~~218~~	~~359~~	~~35.7~~	~~155~~	~~19~~
~~UM09_M12_2~~	~~44200~~	~~93~~	~~9600~~	~~42~~	~~121000~~	~~284000~~	~~27700~~	~~116000~~	~~24300~~	~~4180~~	~~13600~~	~~1430~~	~~4370~~	~~472~~	~~685~~	~~51.3~~	~~162~~	~~15~~
~~UM09_M12_3~~	~~50800~~	~~80~~	~~3930~~	~~32~~	~~114000~~	~~265000~~	~~24500~~	~~105000~~	~~20900~~	~~3500~~	~~11700~~	~~970~~	~~2160~~	~~209~~	~~276~~	~~22.8~~	~~72~~	~~8.1~~
UM09_M12_4	6200	67.9	3930	44	119000	278000	27300	95000	20400	3550	11800	1005	2530	227	271	16.5	52.5	5.39
~~UM09_M12_5~~	~~111000~~	~~94~~	~~4970~~	~~58~~	~~108000~~	~~268000~~	~~21500~~	~~96000~~	~~19200~~	~~3580~~	~~11400~~	~~940~~	~~2440~~	~~201~~	~~269~~	~~26.4~~	~~82~~	~~10.3~~
~~UM09_M12_6~~	~~450000~~	~~94~~	~~7600~~	~~14~~	~~90000~~	~~235000~~	~~23600~~	~~100000~~	~~19800~~	~~3380~~	~~10900~~	~~1070~~	~~3020~~	~~336~~	~~566~~	~~61.7~~	~~243~~	~~21.6~~
~~UM09_M13_1~~	~~750000~~	~~81~~	~~910~~	~~9~~	~~62000~~	~~133000~~	~~14500~~	~~51800~~	~~9700~~	~~1670~~	~~5000~~	~~284~~	~~530~~	~~35~~	~~73~~	~~12.2~~	~~96~~	~~35~~
UM09_M13_2	3000	75	5080	46	105300	233000	25100	87300	17900	2710	13230	1224	2980	220	193	7.8	17.5	2.6
UM09_M13_3	4500	100.1	6460	27	105300	234000	22300	85200	17300	2830	15260	1438	3760	292	266	13.5	23.7	2.8
UM09_M13_4	8400	85.9	4130	36	105400	244000	23400	90700	18200	3190	12900	1131	2670	200	158	7.26	15.6	1.63

Table C3. Monazite U-Th-Pb geochronology data and trace elements

Analysis #	Si	Sr	Y89	Zr90	La139	Ce140	Pr141	Nd146	Sm147	Eu153	Gd157	Tb159	Dy163	Ho165	Er166	Tm169	Yb172	Lu175
UM09_M13_5	26000	81	4330	33	113000	241000	26300	93500	17900	3430	12060	1150	2420	178	150	7.8	19.4	1.82
UM09_M13_6	8500	94.2	6360	37	125000	279000	27000	99000	20800	3650	15800	1480	3620	279	242	11.8	21	2.59
UM09_M13_7	24700	84.5	2880	53	115700	274000	26200	95500	20000	3360	11260	923	1880	122	106	5.28	13.2	1.84
UM09_M14_1	22100	104	4370	51	135000	329000	30800	108000	26700	4110	14200	1310	2780	237	236	12.9	34.9	3.1
UM09_M14_2	5500	79	4510	18.6	103000	247000	24300	92000	20400	3460	12400	1130	2850	236	235	11.8	28.2	3.27
UM09_M14_3	3800	88.4	4800	23	116000	246000	25600	93800	20400	3730	12800	1180	3130	269	283	14.1	29.7	3.47
UM09_M14_4	8200	67.2	3930	32	102000	241000	24100	85900	18800	3350	11000	948	2460	201	220	11.8	31.1	2.78
UM09_M14_5	1300	81.1	5460	29	109900	264000	26600	90700	19600	3590	13100	1240	3360	290	276	15.3	32.5	3.13
UM09_M14_6	10700	77	5400	40	98000	242000	20800	82800	18200	3280	12600	1100	2870	233	244	14.1	39.6	3.44
UM09_M14_7	2200	87.4	4400	72	109000	255000	24400	97000	18500	3490	12500	1100	2810	214	226	11.2	34.6	4.4
~~UM09_M15_1~~	~~bdl~~	~~96~~	~~3940~~	~~23~~	~~51200~~	~~146000~~	~~12100~~	~~44000~~	~~9600~~	~~1040~~	~~8400~~	~~760~~	~~2000~~	~~200~~	~~217~~	~~14.3~~	~~40.4~~	~~5.46~~
~~UM09_M15_4~~	~~46700~~	~~82.7~~	~~4570~~	~~28~~	~~128000~~	~~279000~~	~~26900~~	~~110000~~	~~22900~~	~~3710~~	~~13110~~	~~1060~~	~~2720~~	~~216~~	~~240~~	~~19.1~~	~~57~~	~~7.4~~
~~UM09_M15_5~~	~~54000~~	~~74~~	~~4940~~	~~16~~	~~84000~~	~~222000~~	~~22700~~	~~86700~~	~~19200~~	~~2840~~	~~10800~~	~~990~~	~~2600~~	~~222~~	~~284~~	~~29.1~~	~~76~~	~~10.3~~
UM09_M15_6	600	76.3	4070	51	101200	250000	27100	89500	19100	2850	12700	1100	2600	198	188	9.1	19.5	2.39
UM09_M15_7	3700	91.4	3130	59	123000	285000	29300	106300	22600	3170	12900	940	2070	146	156	9.1	24.4	2.97
UM09_M15_8	300	89.1	6040	44	104300	254000	24500	100600	20900	2850	14700	1320	3310	304	319	18.7	58	6.6
UM09_M15_9	8100	132	10800	27	114000	238000	28900	93000	21500	2200	18600	1750	4640	472	520	29.6	62.1	5.22
UM09_M15_10	3600	109	8100	66	115000	247000	24800	100000	21800	2510	17400	1580	4450	389	410	20.9	48.7	4.07
~~UM09_M15_11~~	~~5100~~	~~120~~	~~8600~~	~~65~~	~~100000~~	~~249000~~	~~24400~~	~~91000~~	~~18600~~	~~1880~~	~~17300~~	~~1590~~	~~4240~~	~~424~~	~~470~~	~~25.3~~	~~55.4~~	~~4.01~~
~~UM09_M15_12~~	~~25000~~	~~77.3~~	~~10400~~	~~43~~	~~122000~~	~~260000~~	~~24400~~	~~102000~~	~~21700~~	~~3470~~	~~14400~~	~~1530~~	~~4730~~	~~465~~	~~756~~	~~81.9~~	~~299~~	~~36.9~~

bdl - below detection limit

Table C4. Modal proportions* (%) of minerals

Mineral	UM04	UM05	UM07	UM08	UM09
Quartz	35	39	33	55	45
Biotite	16	12	18	10	16
Muscovite	22	26	24	14	1
Feldspar	12	12	8	16	12
Garnet	2	2	3	1	5
Staurolite	10	6	12	0	16
Sillimanite	-	-	-	-	2
Accessory min.	3	3	2	4	3
	100	100	100	100	100

*Graphite not included

Table C5. Temperature and pressure estimates for metamorphic specimens.

Specimen UM04

Ti-in-biotite

Analysis number	Temp.	Location
3 / 1 .	588	Matrix
3 / 2 .	570	Matrix
3 / 3 .	545	Matrix
3 / 4 .	571	Matrix
3 / 5 .	583	Matrix
3 / 6 .	588	Matrix
3 / 7 .	553	Matrix
3 / 9 .	575	Matrix
3 / 10 .	582	Matrix
3 / 12 .	599	Matrix
3 / 13 .	593	Matrix
3 / 16 .	444	Matrix
3 / 17 .	570	Matrix
3 / 19 .	584	Matrix
5 / 1 .	608	Near garnet
5 / 2 .	603	Near garnet
5 / 3 .	576	Near garnet
5 / 4 .	581	Near garnet
5 / 5 .	567	Near garnet
5 / 6 .	581	Near garnet
5 / 7 .	574	Near garnet
5 / 8 .	567	Near garnet
5 / 10 .	573	Near garnet
5 / 11 .	594	Near garnet
5 / 12 .	477	Near garnet
5 / 16 .	540	Near garnet
5 / 18 .	517	Near garnet

Garnet-biotite

Max. temp.	Location
569	Near garnet

Garnet-biotite-muscovite-plagioclase

Max. pressure	Location
4.4	Near garnet

Specimen UM05

Ti-in-biotite

Analysis number	Temp.	Location
1 / 1 .	561	Matrix
1 / 2 .	578	Matrix
1 / 6 .	555	Matrix
1 / 10 .	540	Matrix
12 / 2 .	557	Matrix
12 / 6 .	549	Matrix
12 / 9 .	575	Matrix
12 / 12 .	516	Matrix
6 / 6 .	480	Near garnet
6 / 7 .	459	Near garnet
6 / 8 .	438	Near garnet
10 / 1 .	566	Near garnet
10 / 2 .	547	Near garnet
10 / 4 .	554	Near garnet
10 / 5 .	543	Near garnet
10 / 7 .	567	Near garnet

Garnet-biotite

Max. temp.	Location
563	Near garnet

Garnet-biotite-muscovite-plagioclase

Max. pressure	Location
5.2	Near garnet

Specimen UM07

Ti-in-biotite

Analysis number	Temp.	Location
1 / 1 .	537	Matrix
1 / 2 .	513	Matrix
1 / 3 .	537	Matrix
1 / 4 .	539	Matrix
1 / 5 .	518	Matrix
1 / 6 .	543	Matrix
1 / 7 .	534	Matrix
1 / 9 .	525	Matrix
1 / 10 .	578	Matrix
1 / 11 .	586	Matrix
1 / 12 .	573	Matrix
1 / 13 .	582	Matrix
5 / 6 .	559	Matrix
5 / 8 .	521	Matrix
5 / 10 .	530	Matrix
3 / 3 .	543	Near garnet
7 / 2 .	578	Near garnet
7 / 3 .	587	Near garnet
7 / 4 .	584	Near garnet
7 / 6 .	476	Near garnet
7 / 9 .	530	Near garnet
9 / 15 .	523	Near garnet
9 / 17 .	553	Near garnet

Garnet-biotite

Max. temp.	Location
579	Near garnet

Garnet-biotite-muscovite-plagioclase

Max. pressure	Location
5.2	Near garnet

Specimen UM08

Ti-in-biotite

Analysis number	Temp.	Location
1 / 1 .	565	Matrix
1 / 3 .	562	Matrix
1 / 4 .	565	Matrix
1 / 6 .	625	Matrix
3 / 1 .	564	Matrix
3 / 2 .	580	Matrix
3 / 3 .	592	Matrix
3 / 6 .	567	Matrix
3 / 8 .	565	Matrix
3 / 9 .	526	Matrix
3 / 11 .	511	Matrix
6 / 7 .	548	Matrix
6 / 10 .	548	Matrix
6 / 11 .	584	Matrix
6 / 12 .	575	Matrix
6 / 13 .	569	Matrix
6 / 15 .	555	Matrix
10 / 2 .	558	Matrix
6 / 2 .	546	Near garnet
6 / 3 .	569	Near garnet

Garnet-biotite

Max. temp.	Location
562	Near garnet

Garnet-biotite-muscovite-plagioclase

Max. pressure	Location
5.0	Near garnet

Specimen UM09

Ti-in-biotite

Analysis number	Temp.	Location
1 / 1 .	631	Near garnet
1 / 2 .	631	Near garnet
1 / 4 .	634	Near garnet
1 / 5 .	636	Near garnet
1 / 6 .	632	Near garnet
1 / 7 .	637	Near garnet
1 / 9 .	628	Near garnet
1 / 10 .	545	Near garnet
1 / 11 .	568	Near garnet
1 / 13 .	555	Near garnet
1 / 14 .	582	Near garnet
1 / 15 .	562	Near garnet
2 / 2 .	597	Near garnet
2 / 5 .	592	Near garnet
2 / 6 .	592	Near garnet
2 / 7 .	617	Near garnet
2 / 8 .	617	Near garnet
2 / 10 .	618	Near garnet
9 / 4 .	627	Near garnet
9 / 12 .	623	Near garnet
9 / 13 .	639	Near garnet
4 / 2 .	620	Matrix
4 / 3 .	614	Matrix
4 / 4 .	602	Matrix
4 / 5 .	645	Matrix
4 / 6 .	633	Matrix
4 / 7 .	628	Matrix
4 / 8 .	626	Matrix
4 / 9 .	629	Matrix
4 / 10 .	631	Matrix
7 / 1 .	644	Matrix
7 / 2 .	641	Matrix
7 / 4 .	625	Matrix
7 / 5 .	637	Matrix
7 / 6 .	637	Matrix
7 / 7 .	645	Matrix
7 / 8 .	648	Matrix
7 / 9 .	644	Matrix
7 / 10 .	643	Matrix
7 / 11 .	648	Matrix

Garnet-biotite

Max. temp.	Location
615	Near garnet

Garnet-biotite-muscovite-plagioclase

Max. pressure	Location
5.3	Near garnet

Table C6. Whole rock XRF analysis (wt. %)

Oxide	UM04	UM05	UM07	UM08	UM09
SiO_2	63.64	59.47	61.69	69.87	64.38
TiO_2	1.08	1.17	1.18	0.85	1.25
Al_2O_3	17.25	18.7	16.96	12.86	13.94
Fe_2O_3	6.99	5.35	9.18	5.67	13.99
MnO	0.04	0.08	0.05	0.13	0.14
MgO	1.7	1.27	1.35	1.16	1.32
CaO	1.11	1.59	0.82	1.99	0.65
Na_2O	1.16	1.78	1.15	2.18	1.21
K_2O	3.11	3.5	3.13	1.16	1.74
P_2O_5	0.13	0.12	0.14	0.18	0.16
S	0.05	0.01	0.05	0.01	0.01
Total	96.26	93.04	95.71	96.05	98.79